Assessment of Vehicle Fire Development in Road Tunnels for Smoke Control Ventilation Design

by

Cheong Mun Kit

Supervised by

Dr. Michael Spearpoint
and
Associate Professor Charley Fleischmann

August 2009

A thesis submitted in partial fulfilment of the requirements for the PhD Degree in Fire Engineering

Department of Civil and Natural Resources Engineering
University of Canterbury
Private Bag 4800
Christchurch, New Zealand

Abstract

A fire in road tunnel can be dangerous and lead to serious consequences if not addressed appropriately. In a tunnel fire incident, creating a smoke free path for motorist evacuation and facilitating fire fighters to access the fire is critical for fire and rescue operations. A means of achieving this is to use ventilation fans to blow sufficient air down the tunnel ensuring no back-layering of smoke occurs upstream of the fire. The airflow necessary for such operation is known as the critical velocity which is a function of a number of factors includes; heat release rate, tunnel geometry, tunnel gradient etc. Among these parameters, the heat release rate is the most difficult to identify as this value is dependent on the types of vehicles, number of vehicles involved, the type of cargo and the quantity of cargo carried by these vehicles. There are also other factors such as the influence of ventilation condition, tunnel geometry and the use of legislation (to restrict hazardous vehicles entering in tunnel) that could affect the heat release rate in a tunnel fire. The number of possible fire scenarios is numerous.

Based on current practise, fire size selection for most tunnel ventilation design often references various guidelines such as NFPA 502, BD78/99 or the PIARC technical committee report. The heat release rate, particularly for goods vehicle recommended by the guidelines varies from 20 to 30 MW. However, recent fire tests conducted in the Runehamar tunnel experiments indicate a higher heat release rate. These experiments suggest that heat release rate guidelines for goods vehicles might be underestimated. An ideal means to estimate the heat release rate in the tunnel is to use the oxygen consumption calorimetry technique. However, this approach is generally expensive, logistically complicated to perform and it is often not feasible to conduct such tests for a tunnel project at the initial design stage simply because the structure and systems are not ready for such activities.

This research thesis presents an approach to establish a design fire in a road tunnel particularly the peak heat release rate for emergency tunnel ventilation system design. The analysis consists of two stages; stage one involves the use of a probabilistic approach (risk analysis) to identify the potential cause and type of vehicle which could result in a tunnel fire. Findings from the risk analysis are used in stage two in which Computational Fluid

Dynamics (CDF) modelling is used to establish the heat release rate in the tunnel considering factors such as fuel load, ventilation condition, tunnel geometry and ignition location. The Fire Dynamics Simulator (FDS 4.0.7), a CFD model of fire-driven fluid flow is used for the analysis and an urban road tunnel project in Singapore is used to illustrate this methodology.

Other topic related to this research work includes the reconstruction for the Runehamar tunnel fire test using numerical approach to calibrate the FDS simulation model. The used of Probabilistic Bayesian approach and CFD approach using FDS to estimate the heat release rate in the tunnel is also investigated in this thesis. The effect of vehicle fire spread in road tunnel and numerical simulation of road tunnel fires using parallel processing is presented. Preliminary work in using FDS5 for tunnel simulation work is discussed as part of the research work in this project.

Acknowledgments

I would like to acknowledge the valuable assistance and support of the following people and organisation I have received throughout this research project:

My supervisors, Dr Mike Spearpoint and Associate Professor Charley Fleischmann for their patience, guidance and invaluable advice throughout the development of this project.

My employer, the Land Transport Authority (LTA) of Singapore for providing me a scholarship grant to pursue the PhD in Fire Engineering degree.

Mr Leong Kwok Weng and Mr Melvyn Thong for their ongoing encouragement and support on my pursuit of a PhD degree.

My colleagues in the LTA, Eddie Teo and Chun Hui in helping me to gather information I have requested for this project. Boon Hui in providing constructive feedback on my research work.

Major Yeo Geok Kuan from the Singapore Civil Defence Force for providing the vehicle fire statistics data for Singapore.

Computer manager Brandon Hutchison, HPC support consultant Colin John McMurtrie for providing me the technical support and librarian Christine McKee in assisting me to source information related to my research work.

Dr. Haukur Ingason from SP Technical Research Institute of Sweden for providing the test results and photographs for the Runehamar fire experiments.

Chuang Y J from National Taiwan University of Science and Technology for providing information for the 3.49 Ton truck fire test.

The New Zealand Fire Service Commission for their continued support of the Fire Engineering programme at the University of Canterbury.

Yoke Yin and Matthew Kwek for proof reading this thesis.

My family for all the support they had given me during the course of this programme.

List of Publications and Tunnel Projects Portfolio

The thesis is based on the following papers:

1) Cheong M K, Thong M, Soh L T, Sng C H, See C S, published as "Keeping Track" in *Fire Prevention & Fire Engineers Journal*, pp. 14-16, October 2007.

2) Cheong M K, Spearpoint M J, Fleischmann C M, published as "Design Fires for Vehicles in Road Tunnel", in the *7th International Conference on Performance-Based Codes and Fire Safety Design Methods*, Auckland New Zealand, pp. 229 - 240, April 2008.

3) Cheong M K, Spearpoint M J, Fleischmann C M, published as "Using Peak Heat Release Rate to Determine the Fire Risk Level of Road Tunnels" in *Journal of Risk and Reliability,* Vol 222, number 4, pp.595 – 604, 2008.

4) Cheong M K, Fleischmann C M, Spearpoint M J, published as "Calibrating an FDS Simulation of Goods Vehicle Fire Growth in a Tunnel Using the Runehamar Fire Experiment" in *Journal of Fire Protection Engineering*, Vol 19 No 3, pp. 177-196, August 2009.

5) Cheong M K, Spearpoint M J, Fleischmann C M, published as "Comparison of Statistical and Numerical Approach to Estimate Heat Release Rate in Road Tunnel Fires", in *Fire Technology*, August 2009.

6) Cheong M K, Spearpoint M J, Fleischmann C M and M Thong, published as "The Effect of Road Tunnel Ventilation on the Separation of Vehicles to Minimise Fire Spread", 13th International Symposium on Aerodynamics and Ventilation of Vehicle Tunnels, New Brunswick, New Jersey, USA, BHR Group Conference, pp. 199 – 210, 13th to 15th May 2009.

In addition to the above papers included in this thesis, others papers the author has been involved in includes:

7) Steven Lai, C W Wong, Tony Tay, K C Lim and M K Cheong, published as "The Use of Tunnel Pressurization Scheme for Smoke Control", in *Tunnel International Management Journa*l, Vol 8 Issue, December 2005.

8) L W Lim and M K Cheong, published as "Single Tunnel Ventilation Shaft for Underground Stations", in *Tunnel International Management Journa*l, Vol 9 Issue, March 2006.

The road and rail tunnel projects the author has been involved in includes:

i) The Kallang Paya Lebar (KPE) Tunnel in Singapore, a 9 km long dual three lanes road tunnel.

ii) The Fort Canning Tunnel in Singapore, a 350 m long three lanes road tunnel.

iii) The Woodsville Vehicular Interchange in Singapore *(Feasibility stu*dy), 250 m long (3 tube) two lanes road tunnel.

iv) The Marina Coastal Expressway (MCE) in Singapore (*Feasibility study*), 3.5 km long dual four lanes road tunnel.

v) The North South Expressway in Singapore, 16 km long dual three lane road tunnel.

vi) The Circle line in Singapore, 33.3 km long with 29 stations and an underground depot, rail project.

vii) The North South Extension Line in Singapore, 1.5 km long rail tunnel with 1 station.

viii) The Down Town Line 2 in Singapore, 16.6 km long rail tunnel with 12 stations and a depot.

ix) The Down Town Line 3 in Singapore, 19.1 km long rail tunnel with 15 stations.

Table of Contents

List of Figures

List of Tables

Nomenclature

Symbol	Description	Unit
A	Pre-exponential factor	m/s
A	Surface area of fire	m^2
A_T	Tunnel cross-sectional area	m^2
A_f	Horizontal burning area of the fuel	m^2
C	Empirical constant	-
C_{nc}	Natural convection coefficient	-
c	Specific heat	kJ/kgK
c_p	Specific heat of ambient air at constant pressure	kJ/kgK
D	Equivalent circular diameter	m
D_i	Diffusion coefficient of species *i*	-
D^*	Characteristic fire diameter	m
E_A	Activation energy	kJ/kmol
Fr	Froude number	-
f	External force vector (excluding gravity)	-
g	Acceleration due to gravity	m/s^2
grade	Tunnel gradient	%
H	Height	m
H_{eff}	Effective heat of combustion	MJ/kg
h	Enthalpy	J
I	Radiation intensity	W/m^2
κ	Absorption coefficient	-
k	Multiplicative factor	-
k	Thermal conductivity	W/mK
L	Characteristic length	m
M	Molecular weight	kg/kmol
$\dot{m}$	Mass loss rate	kg/s
$\dot{m}''$	Mass loss rate per square meter	kg/m^2s
$\dot{m}_a$	Mass flow rate for air	kg/s

Symbol	Description	Unit
p	Pressure	Pa
Pr	Prandtl number	-
$\dot{Q}$	Heat release rate	W or kW or MW
$\dot{Q}_{vent}$	Heat release rate of fire subject to ventilation	W or kW or MW
$\dot{Q}_{open}$	Heat release rate of fire in open space	W or kW or MW
$\dot{q}_c^{"}$	Convective heat flux	kW/m^2
$\dot{q}_{cr}^{"}$	Critical heat flux	kW/m^2
$\dot{q}_r^{"}$	Radiative heat flux	kW/m^2
Re	Reynolds number	-
T	Temperature	°C or K
T_f	Average temperature near fire site	°C or K
t	Time	s
u	Vector describing the velocity in the u, v and w directions	-
V	Velocity	m/s
V_c	Critical velocity	m/s
W_T	Width of the tunnel	m
W_F	Width of the fire object	m
x	Vector position in the x, y and z directions	-
Y_i	Mass fraction	-
Y_F^I	Fuel mass fraction in the fuel stream	-
Z	Mixture fraction	-

Greek symbol	Description	Unit
ψ	HRR enhancement coefficient	-
ρ	Density	kg/m^3
δ	Thickness	m
χ	Combustion efficiency factor	-
χ_{rad}	Radiative loss fraction	-
τ	Viscous stress tensor	Pa
R	Universal gas constant	kJ/kmolK
v	Stoichiometric coefficients	-
Φ	Dissipation function	-
ϕ	Stoichiometric combustion	-
σ	Stefan-Boltzmann's constant ($5.67x10^{-11}$)	kW/m^2K^4
ΔH_{eff}	Effective heat of combustion	kJ/kg or MJ/kg
ΔH_o	Heat release rate per unit mass of oxygen consumed	kJ/kg or MJ/kg
ΔH_v	Heat of vaporization	kJ/kg or MJ/kg

List of superscripts	Description	Unit
$\dot{}$	Per unit time	s^{-1}
$'$	Per unit length	m^{-1}
$''$	Per unit area	m^{-2}
$'''$	Per unit volume	m^{-3}

List of subscripts	Description
∞	Ambient
a	Property of air
CO	Property of carbon monoxide
CO_2	Property of carbon dioxide
cr	Critical value
eff	Effective

List of subscripts	Description
F	Fuel
g	Gas
i	Chemical species
ig	Ignition
int	Initial
max	Maximum value
min	Minimum value
O_2	Property of oxygen
P	Products
$peak$	Peak value
$rad\ or\ r$	Radiative
sur	Surface
t	Tunnel

List of Abbreviations	Description
ABS	ACRYLONITRILE BUTADIENE STYRENE
AC	Alternating current
AID	Automatic incident detector
BD	British Design
CCTV	Closed Circuit Television
CETU	Centre d'Etudes des Tunnels
CPU	Central processing unit
CTE	Central Expressway Tunnel, Singapore
CFD	Computational fluid dynamics
DC	Direct current
DNS	Direct Numerical Simulation
ETA	Event tree analysis
EPDM	ETHYLENE PROPYLENE DIENE RUBBER
FDS	Fire Dynamics Simulator
FHWA	Federal Highway Administration

List of Abbreviations	Description
FMEA	Failure mode and effect analysis
FTA	Fault tree analysis
GPS	Global Positioning System
HGV	Heavy good vehicles
HRR	Heat release rate
HRRPUA	Heat release rate per unit area
HTDP	Hazmat Transport Driver Permit
HTV	Hazmat Transport Vehicle
HTVTS	Hazmat Transport Vehicle Tracking System
ITPMS	Integrated traffic and plant management system
ISO	International Organization for Standardization
LES	Large Eddy Simulation
LGV	Light goods vehicle
LTA	Land Transport Authority, Singapore
LUS	Lane used signal
MPI	Messaging Passing Interface
MVU	Mobile ventilation unit
NA	Not available
NEA	National Environment Authority, Singapore
NFPA	National Fire Protection Association
NIST	National Institute of Standards and Technology
NR	Not required
n/a	Not applicable
PIARC	Permanent International Association of Road Congresses
PC	Polycarbonate
PE	Polyethylene
PP	Polypropylene
PS	Polystyrene
PUR	Polyurethane

List of Abbreviations	Description
PWRI	Public Works Research Institute
RTE	Radiative Transport Equation
RTV	Road Tunnel Ventilation
ROP	Report of Progress
SBF	Surface Burning Factor
SCDF	Singapore Civil Defence Force
SES	Subway Environment Simulation
SFPE	Society of Fire Protection Engineers
SPF	Singapore Police Force
SURS	SINGAPORE UNDERGROUND ROAD SYSTEM, SINGAPORE
UK	United Kingdom
USA	United States of America
USFA	U.S. Fire Administration
VHGV	Very heavy good vehicles
VMS	Variable message signal

Chapter 1:
INTRODUCTION

1.1 Background

A road tunnel is an enclosed facility through which road vehicles such as motorcycles, cars, vans, buses and trucks could travel. It is usually constructed to overcome obstacles such as mountains and above-ground structural developments or to facilitate vehicles crossing under the sea or river (Bendelius 2003). The type of tunnel constructed is determined by the obstacle it seeks to overcome, for example there are mountain tunnels, urban tunnels or underwater tunnels.

An efficient road system is an essential element for access yet also a greedy occupant of space and a major source of noise pollution (PIARC 1987). The restrictions imposed by the local geography and the intensive use of land in countries where land is scarce would mean that the only available space for improved transportation systems is underground (Carvel and Beard 2005). In the past few years, more underground road tunnels of increasingly greater length have been built in Singapore. It seems likely that this process will continue. With more road tunnels being built and an increasing volume of traffic using them, it becomes important to establish a quantified picture of fire behaviour in tunnels and to better understand the risks involved.

The use of tunnel ventilation system to control smoke movement in tunnels are common in most road tunnel designs. The operation of the tunnel ventilation is critical as its primary purpose during a fire emergency is to control the movement of smoke and heated gas away from the fire and to provide a tenable environment along the egress path allowing safe evacuation of motorists. The secondary purpose is to facilitate fire fighters to access the fire location by providing a clear path to the fire site (Bendelius 2003). This means that either the smoke stratification must be kept intact, leaving clear and breathable air underneath the smoke layer or to completely push the smoke to one side of the fire (PIARC 1999). There are several methods in controlling smoke movement in an event of a tunnel fire (NFPA 502 2004). The risk of having a fire in a tunnel and designing an effective tunnel ventilation system through providing sufficient airflow to achieve tenable conditions at the egress path is dependent on many parameters such as heat release rate

(HRR), tunnel geometry, gradient of the tunnel, operation (whether bi-directional traffic is required) (Bendelius 2003) and legislation (whether vehicles carrying dangerous goods are allowed to access the tunnel, e.g. petrol tankers). Among these parameters, the heat release rate is the primary parameter for tunnel ventilation design and is the most difficult to identify as this value is dependent on the types of vehicles and the associated loads the vehicle is carrying. Very often, the cargos carried by these goods vehicles varies considerably, therefore it is difficult to quantify the exact value of HRR for a goods vehicle traversing a tunnel.

A major risk factor is the use of tunnel by heavy goods vehicles carrying loads with substantial energy content and yet not a great deal of research has been carried out to determine how these heavy goods vehicles affect the development and spread of fires in tunnel. A fire from a heavy goods vehicle could result in a dangerous situation both to other vehicles, people in the tunnel and the fire fighters if the fire starts to spread to other vehicles (Ingason and Lonnermark 2004).

Legislation is another factor that would affect the heat release rates in a road tunnel fire. In order to enhance the fire safety in tunnels; some countries like Singapore (Traffic Act 2006), Netherlands, Switzerland, France (urban tunnel only) and United Kingdom (Dartford, Mersey and Tyne tunnel only) have forbidden vehicles transporting dangerous goods such as liquid fuels in a road tunnel (OECD / PIARC 2006).

In a country like Singapore, a Hazmat Transport Vehicle Tracking System (HTVTS) is also implemented as part of the national effort to enhance the fire safety in a road tunnel. All local and foreign vehicles carrying bulk petroleum and toxic materials are tracked and monitored by the Singapore Civil Defence Force (SCDF). Vehicles carrying hazardous materials that attempt to enter a road tunnel will be stopped by the Traffic Police (SCDF 2005). This legislation has a direct effect on reducing the degree of fire risk in tunnels.

The heat release rate for various types of fires proposed by the PIARC technical committee reports (PIARC 1987), NFPA 502 (2004), BD78/99 have generally been used for the design of tunnel ventilation systems. The heat release rates for the various types of vehicle fire range from 2.5 MW to 5 MW for cars to 20 MW to 100 MW for goods vehicles.

However, recent fire tests conducted in the Runehamar Tunnel showed that larger vehicles (HGV) with burning goods may cause higher peak HRR (approx 66.4 to 201.9 MW) outputs (Ingason 2006a). These tests seriously hinted that previous data regarding heavy goods vehicles might have been underestimated.

Generally, a tunnel fire has a complex flow behavior because the physical phenomenon is affected by the geometry and ventilation condition including the chemical reaction of the fuel (Lee and Ryou 2006). Full-scale tests are carried out by researchers with the aim of obtaining new knowledge about the fire development in a tunnel. These tests provide valuable information on the design of smoke control systems in the tunnel but are generally very expensive and limited. Another limitation is that most of these test programmes were performed in abandoned tunnels. For a road application, extrapolations are often necessary because of the reduced cross-section and its different shape (i.e. horse shoe instead of rectangular shape (PIARC 1999)). It should be noted that the results obtained in full-scale tests are also dependent on test conditions such as air velocity and geometry. An observation has been made in the EUREKA test that the variation of longitudinal air velocity will result in different heat release rates (Ingason and Lonnermark 2005). In a research project by Carvel et al (2005), it was found that differences in tunnel width and ventilation condition can influence the HRR of a fire. However, ventilation conditions in a tunnel may have a far more dramatic influence on the HRR than the tunnel geometry (Carvel et al 2001).

1.2 Initiative for the Research

As previously mentioned, one of the most important parameters concerning a fire in a tunnel is its heat release rate. Heat release rate is defined as the enthalpy change per unit time as a result of conversion of the chemical energy of a fuel to heat in a combustion process (Bryant et al 2003). The peak heat release rate is so important that it has been described as a key predictor in fire hazard (Babrauskas 2002) particularly in the area of tunnel ventilation design. Observations from different research work and fire tests on tunnel fires shows that the heat release rate in a tunnel is affected by the ventilation

condition, geometry and fuel load. Up unit now, there have been very few extensive studies carried out on the relationship between these parameters.

The relatively low number of tunnel fire tests conducted to-date does not allow a general conclusion to be drawn on appropriate credible vehicle design fires for road tunnel ventilation design because of the huge cost required in such test programmes. In addition, factors such as tunnel geometry, ventilation condition, fuel load can vary from tunnel to tunnel. The complexity of these factors suggested that credible vehicle design fires should be analysed on an individual tunnel basis.

In this project, an attempt will be made to use Fire Dynamic Simulator 4.07 (FDS); a computational fluid dynamics (CFD) model developed by the National Institute of Standards and Technology (NIST) to predict fire growth and flame spread in a tunnel. FDS is used because it is a CFD tool that many fire engineers use. There is completed work as well as on-going work to validate FDS for use in a wide variety of fire problems (McGrattan and Hamins 2002). The on-going effect at NIST and elsewhere to validate FDS has evaluated the model's ability to predict the transport of heat and exhaust products from a fire through an enclosure. Recently, validation effort has moved beyond transport issues in considering fire growth and flame spread phenomena (McGrattan 2005), this can be seen from the work elsewhere (Hietaniemi et al 2004); (Floyd 2002); (Kashef et al 2002); (Hostikka and McGrattan 2001) and many more mentioned in the FDS technical reference guide. Last but not least, the FDS program is available in the public domain which can be downloaded from the NIST website. The analysis for this research project will be based on an urban road tunnel project in Singapore because the author is involved in the design and development stage for this project. Information on the tunnel geometry, ventilation mode and expected traffic fleet and type of vehicle accessing through this tunnel is available to the author. As fuel load is expected to be an important factor that could affect the fire size, the issue of allowing dangerous goods vehicles in the tunnel is not considered in this analysis in view of the implementation of HTVTS. A detailed discussion on HTVTS is covered in chapter 5 of this thesis.

From a research perspective, this thesis could provide another source of valuable information towards understanding the behaviour of fire in tunnel when different tunnel

geometry and ventilation conditions are applied. The HRR predicted in this project can also be used as a guide for future road tunnel project with similar geometry, ventilation condition and traffic mix in formulating evacuation and fire fighting strategies.

1.3 Objective of this Research

The objective of this research project is to formulate a methodology to establish a credible fire (heat release rate) in a road tunnel considering factors such as tunnel geometry, ventilation condition and fuel load. The work for this research project involved a combination of probabilistic and deterministic approaches. A risk based probabilistic analysis approach is used to identify the possible fire scenarios followed by a deterministic approach using FDS 4.07 to quantify the estimated fire size in the tunnel. The context of this research work is related to identifying the peak heat release rate so that this information can be used for tunnel ventilation smoke control design. It is acknowledged that in other contexts, the design fire may be related to issues such as fire detection or evacuation where fire development at the growth phase of the fire is critical; or structural fire resistance where the burning and decay phases are important. However these are not the focus of this research work although there are similarities across the various contexts.

The tasks in achieving the objective are:

i) Understand the causes of vehicle fire in road tunnel.

ii) Identify potential fire scenarios in a road tunnel using a quantitative risk assessment approach by incorporating statistical data on traffic fleet, fire incident data such as faulty vehicle, acts of carelessness, intentional fires, fires arising from collision and legislation.

iii) Perform numerical simulation work under free burning conditions using FDS 4.07. This is part of the model calibration process to ensure the FDS modelling approach used would produce similar results as compared to an actual fire experiment.

iv) Perform numerical simulation work by calibrating the FDS tunnel simulation model based on Runehamar tunnel fire test. This is a similar objective to task (iii) except it is performed in a tunnel environment.

v) Perform numerical simulation of fire in an urban road tunnel in Singapore (case study) using FDS 4.07 to quantify potential fire size and fire curve considering fuel load, tunnel geometry and ventilation condition. The work from this study would enable similar modelling approach to be used for other tunnel design applications by changing the tunnel geometry, ventilation condition and fuel load.

vi) Explore the impact of vehicle fire spreading from one vehicle to another (upstream and downstream of the fire) for scenarios using longitudinal ventilation air flow in the tunnel.

vii) Compare the method formulated by Carvel based upon experimental data using a Bayesian methodology to produce a probability distribution of fire size for goods vehicles. Results from the Carvel method will be compared with the FDS 4.07 simulated results to examine if there is any significant difference in the heat release rate value using these two approaches.

viii) Explore the pros and cons of using high performance computing for FDS simulation work.

ix) The launch of FDS 5 has inspired this project to do preliminary simulations using FDS 5.0.3 to estimate the heat release rate in the Runehamar tunnel fire experiment.

1.4 Limitations of this research

A risk analysis approach followed by numerical simulation of a light goods vehicle (LGV) and a heavy goods vehicle (HGV) considering tunnel geometry and air velocity in the tunnel is performed to establish the heat release rate in the tunnel.

It is acknowledged by the author that parameters such as tunnel cross section, tunnel air velocity could have an effect on the heat release rate in the tunnel and different tunnels might yield different heat release rate estimates. Therefore, for the purpose of this research project, an urban road tunnel in Singapore is used as a basis for this study to narrow down the scope of the analysis.

The cost of setting up a full-scale fire test is expensive and requires significant facilities, equipment and the relevant authority's approval. Due to the lack of resources, a full-scale fire test has not been conducted to verify the simulation results. However, a simulation model for the Runehamar tunnel was built and simulated to calibrate the modelling approach.

The material properties of the fuel load (example wood and plastic) are extracted from the Cone Calorimeter test data and used for the FDS simulation. Thermal properties such as thermal conductivity and specific heat are assumed to be constant. The burning behaviour of the materials in the fire scenario is assumed to be similar to that of the small-scale fire tests.

Further details of the limitations of the modelling approach are given in Chapter 16.

1.5 Structure of Thesis

This thesis consists of sixteen chapters of which seven chapters have been published or submitted to journals or as conference proceedings. Although these papers were written to address different issues related to the overall research outcome, there is some repetition in the content of these papers. In particular, the introduction, so as to provide essential background information on the research works to the readers of the journal / conference paper. Chapters in the thesis that were taken from the author's journal papers during his research work often include additional information that was not included in the original journal paper submission. These additional materials include range of substantial HRR curves based on different tunnel conditions, calculations to determine various input

parameters used for the numerical simulations and FDS input files. This additional information is meant to provide readers of this thesis with a more in-depth knowledge of the author's research work.

The thesis commences by providing reader the initiative and objective of this research work followed with a brief introduction on the ventilation system concept used in road tunnel design. A brief outline on some of the international standards used for tunnel ventilation design will be presented proceeding with an introduction on the fire size adopted in some road tunnel projects around the world.

The literature review in chapter 3 provides an overview to the reader the fire tests experiments conducted in tunnel based on different types of vehicles. The fire test experiments conducted in a non-tunnel environment such as in a test laboratory or open space will also be covered in this chapter. Various types of ventilation systems for tunnel ventilation design and the effect of different tunnel geometry; ventilation condition and fuel load based on various research studies will be discussed.

Chapter 4 presents the history of tunnel fire incident that have occurred internationally and the statistics on vehicle fires in Singapore. The regulation of tunnel access and Hazmat Transport Vehicle Tracking System (HTVTS) will be discussed in chapter 5.

A brief introduction on the urban tunnel in Singapore is covered in chapter 6 to provide the reader with the information needed for the case study presented in chapter 8 and 11.

Chapter 7 outlines the governing equations and assumptions used in FDS providing an appreciation on the concept behind fire modelling.

In chapter 8, the probabilistic risk assessment approach will be used to identify and define the fire scenarios for the case study tunnel.

FDS 4.07 will be used to reconstruct the SP laboratory pallets fire tests (free burning) and tunnel fire test conducted in the Runehamar tunnel. The purpose of this exercise is to calibrate the fuel model setup in FDS for subsequent simulations run on tunnel fire design

applications. Comparison of the FDS simulated results versus experimental values and the differences in grid size, boundary condition used in the simulation will be discussed in chapter 9 and 10.

Chapter 11 will discuss the simulation setup and the simulated results for the 2 lane and 3 lane urban road tunnel in Singapore. Various tunnel geometies and ventilation conditions used in this tunnel will be highlighted.

The findings on the effect of vehicle fire spread in the case study tunnel is presented in chapter 12.

Chapter 13 compares the results using Bayesian methodology with FDS 4.07 to examine if there is any significant difference in the heat release rate value.

The discussion on advantages and limitations of using higher performance computing are covered in chapter 14.

Preliminary findings on the simulated results using FDS 5.0.3 are discussed in chapter 15.

Discussion on the recommendations and conclusions for this research project are provided in chapter 16.

Chapter 2:
TUNNEL VENTILATION SYSTEM AND DESIGN CONCEPTS

This chapter provides an introduction to the various ventilation system concepts usually employed in the ventilation of road tunnels followed with a brief discussion on the recommendations for the choice of heat release rate from various standards. The use of fire models as an analytical tool for the design of road tunnel environments is also presented in this chapter with the last section summarising the design fire size adopted in various road tunnel designs.

2.1 Tunnel ventilation operation mode

Generally, the design of the tunnel ventilation system consists of three different operation modes (normal, congestion and emergency mode). Normal operation mode is where the tunnel fans are off and the recirculation of air within the tunnel is through the vehicle piston effect. The pollution concentration in the tunnel is less than the design pollution concentration limit. As traffic in the tunnel increases with a slow down in traffic movements, the amount of CO (carbon monoxide) and the temperature in the tunnel will increase. When this happens, the sensors in the tunnel will trigger the operation of the tunnel fans to dilute the CO concentration. This is known as the congestion mode. In the event of a fire, the operation of the tunnel fans will create a longitudinal air velocity higher than the critical velocity for preventing back layering of smoke thus allowing motorists trapped upstream of the fire to evacuate (Figure 2.1). This is defined as the emergency mode. As the objective of the project is to establish the credible vehicle fire size in a tunnel, subsequent discussion will be focused on the emergency operation mode.

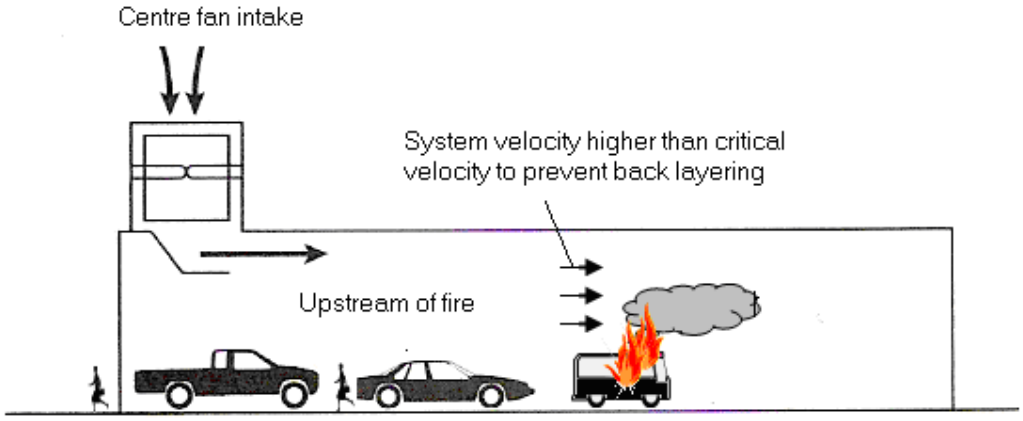

Figure 2.1: Emergency fan operating mode

2.2 Tunnel ventilation system concepts

The heat release rate for fire scenarios is also related to the purpose of the ventilation design which is influenced by the construction and operating cost (PIARC 1999). In addition, the mode of the tunnel ventilation operation (normal, congestion or emergency) at the time of the fire incident could also have an impact on the fire size as the burning rate of the fire is dependent on the amount of air supplied to the fire (fuel control or ventilation control) due to the ventilation system in the tunnel.

Ventilation is necessary in most road tunnels (except for a short tunnel which is ventilated naturally - i.e. no fans) to control smoke and heated gases that are generated during a tunnel fire. The primary objective for controlling smoke movement in the tunnel is to provide safe evacuation and the secondary purpose is to facilitate fire fighters in accessing the fire site (NFPA 502 2004). The approach used for smoke control varies depending on the type of ventilation system being used and if the tunnel is serving bidirectional or unidirectional traffic flow.

Systems used for mechanical ventilation can be categorized into longitudinal and transverse. Longitudinal systems are sub-categorized into jet-fan-based ventilation systems and longitudinal ventilations with saccardo nozzle. For the transverse system, the sub-categories are full-transverse systems, semi-transverse supply systems and semi-transverse exhaust systems.

From the Memorial Tunnel Fire Ventilation Test Program (Bechtel and Brinckerhoff 1995), it is known that different ventilation strategies can yield different effectiveness in smoke and heat management. The following sub-sections discuss the various ventilation system concepts usually employed in the ventilation of road tunnels.

2.2.1 Jet-fan-based ventilation system

The jet-fan ventilation system (Figure 2.2) employs a series of axial fans mounted at the ceiling level of the tunnel producing a high discharge thrust and velocity which induces additional airflow within the tunnel. This system can only be used in unidirectional tunnels as smoke and heat will be discharged from the exiting portal (Bendelius 2003).

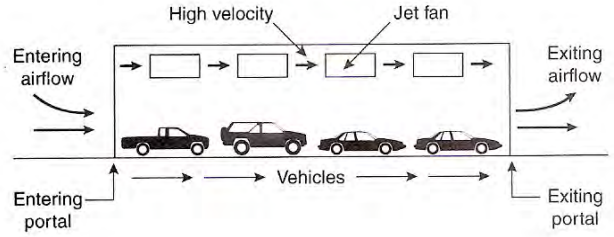

Figure 2.2: Jet fan longitudinal system (reproduced from Bendelius (2003))

2.2.2 Longitudinal ventilation with Saccardo nozzles

This is a system (Figure 2.3) in which air is introduced into or removed from the tunnel at a limited number of points such as at the portal or a shaft (Bendelius 2003). In long tunnels, exchanging vitiated air for fresh air through a shaft may be a better solution than a larger number of jet fans (PIARC 1995).

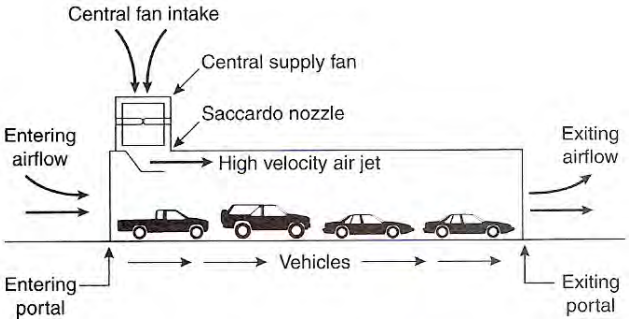

Figure 2.3: Longitudinal with Saccardo Nozzle (reproduced from Bendelius (2003))

2.2.3 Full transverse ventilation system

A full transverse system has both supply and exhaust throughout the length of the tunnel (Figure 2.4). The major portion of the smoke is discharged through a stack. This system can be used in either bidirectional or unidirectional trafficked flow tunnel (Bendelius 2003).

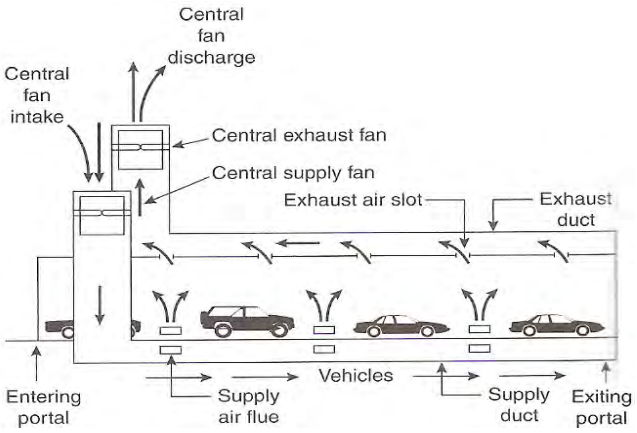

Figure 2.4: Full transverse system (reproduced from Bendelius (2003))

2.2.4 Semi transverse supply / exhaust ventilation

Semi transverse ventilations are those that have only supply (Figure 2.5) or exhaust ducts (Figure 2.6). The exhaust from the tunnel is discharged at the portal for semi transverse supply or through the exhaust stack for semi transverse exhaust (Bendelius 2003).

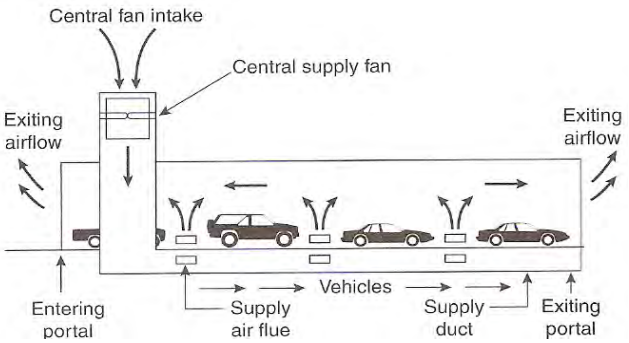

Figure 2.5: Semi transverse supply system (reproduced from Bendelius (2003))

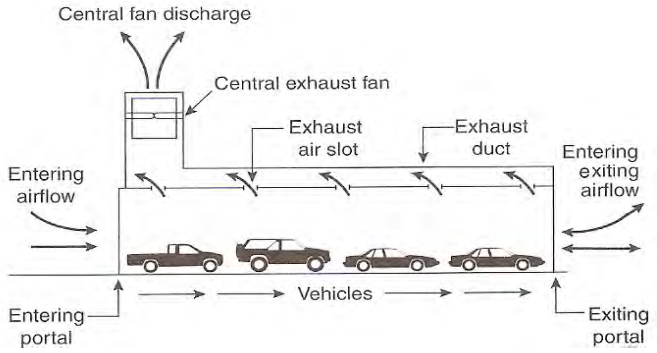

Figure 2.6: Semi transverse exhaust system (reproduced from Bendelius (2003))

2.3 Worldwide road tunnel fire safety standards / guidelines

2.3.1 Heat release rate recommendation from road tunnel fire safety standards

In a road tunnel, the vehicle fire load is either unknown or inconsistent. It is often dependent on the traffic flow in the tunnel. In some countries, working groups from fire brigades, regulators, tunnel owners, and consultants are looking at the recommended choice of heat release rate for road tunnel application (PIARC 1999). Table 2.1 shows the heat release rate recommended in standards and committees related to tunnel fire design.

Standards / Guidelines	**NFPA 502 (2004)**	**NFPA 502 (2008)**	**BD 78/99**	**CETU**	**PIARC**
Fire Load	**Fire heat release rate (MW)**	**Fire heat release rate (MW)**	**Fire heat release rate (MW)**	**Fire heat release rate (MW)**	**Fire heat release rate (MW)**
Passenger Car	5	5 -10	5	-	2.5
Bus	20	20 – 30	20	-	20
Van	-	-	15	15	15
Goods Truck	20 - 30	70 - 200	30 - 100	30	20 – 30
Tankers	100	200 - 300	-	200	-
Source	(NFPA 502 2004)	(NFPA 502 2008)	(BD 1999)	(Hall 2006)	(PIARC 1999)

Table 2.1: Recommended heat release rate from various standards and committee

From Table 2.1, one can see that the heat release rate for light weight vehicles and buses are fairly consistent among these standards. However, the recommended heat release rate for heavy goods vehicles and tankers varies significantly. One reason may be due to inconsistent fire loads on these heavy goods vehicles and the lack of actual fire test data to establish these values.

2.4 Fire model as an analytical tools for road tunnel design

For longitudinal ventilation design, one of the tunnel ventilation design requirements is to ensure no smoke backlayering (Figure 2.7) occurs at the upstream of the fire. At low tunnel airflow where buoyancy induced flow from the fire is not overcome, this will result in the spread of smoke and hot gases in a direction opposite to the forced ventilation which is often termed as "backlayering"

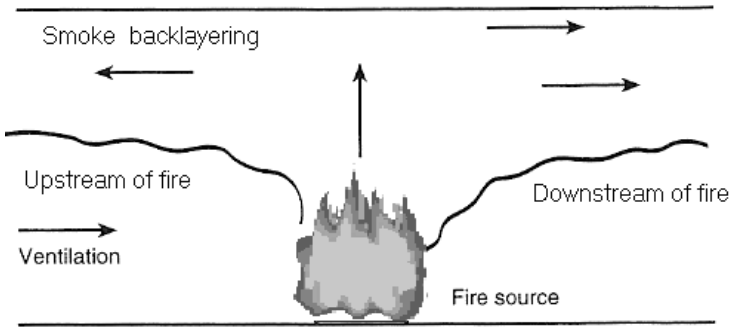

Figure 2.7: Under ventilated fire causing Backlayering

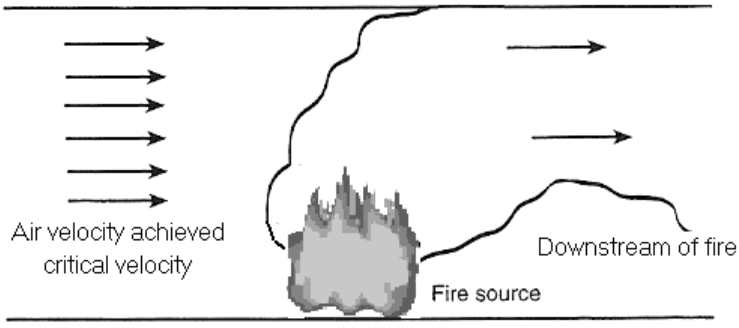

Figure 2.8: Sufficiently ventilated to achieve critical velocity

A feasible approach to control smoke is pushing it through the tunnel portal thereby creating a smoke free path for motorists trapped upstream to evacuate. The airflow necessary for such operation is known as the critical velocity (Figure 2.8). The critical velocity is a function of a number of factors which include the heat release rate, tunnel gradient and tunnel geometry. The theoretical critical velocity calculation is obtained from the following relationships (Bechtel and Brinckerhoff 1995):

$$V_c = K_1 K_g \left(\frac{gHQ}{\rho c_p A_T T_f} \right)^{1/3} \qquad \text{Equation 2.1}$$

$$K_1 = Fr_c^{-1/3} \qquad \text{Equation 2.2}$$

$$K_g = 1 + 0.0374(grade)^{0.8} \qquad \text{Equation 2.3}$$

$$T_f = \frac{Q}{\rho c_p A_T V_c} + T \qquad \text{Equation 2.4}$$

The use of a tunnel ventilation system has played an important role in most road tunnel projects. It is important to investigate how a suitable tenable environment can be secured at the time of tunnel fire. This analysis can be performed by the use of a road tunnel ventilation software tool (one dimensional model) such as Subway Environment Simulation (SES) (Brinckerhoff and Douglas 1997), Road Tunnel Ventilation (RTV) (IDA 2005), TUNVEN (FHWA 1980) or CFD tool (field model) such as FDS (McGrattan and Forney 2005), Fluent (Fluent 2008), CFX (CFX 2008), Phoenics (Phoenics 2008), Solvent (Solvent 2008), Jasmine (BRE 2008) to establish the conditions in the road tunnel. Very often, in the conceptual and preliminary stage of the tunnel design, a one dimensional model is used to establish the appropriate tunnel fan size to ensure that airflow in the tunnel can meet the critical velocity. The design of the tunnel ventilation system is considered acceptable if the design air velocity in the tunnel (system airflow) is higher than the calculated critical velocity to prevent smoke backlayering at the fire site (Figure 2.9). The advantage of the one dimensional model is its ability to provide bulk results

(example average values for air temperature and airflow) for the entire tunnel network system which may be a few kilometres in length. Using a field model for this type of analysis can be very time consuming and expensive. However, a field model is able to provide detailed results including temperature, smoke profiles, velocity (Figure 2.10), visibility and heat release rate, and therefore ideally suited for road tunnel analysis (Bendelius 2003).

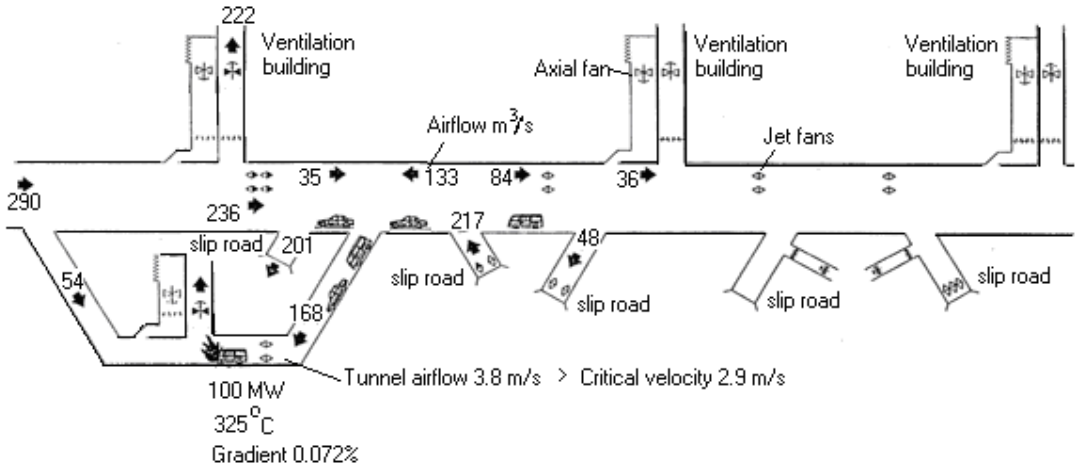

Figure 2.9: A schematic diagram showing the airflow and temperature simulated using a one dimensional model (SES)

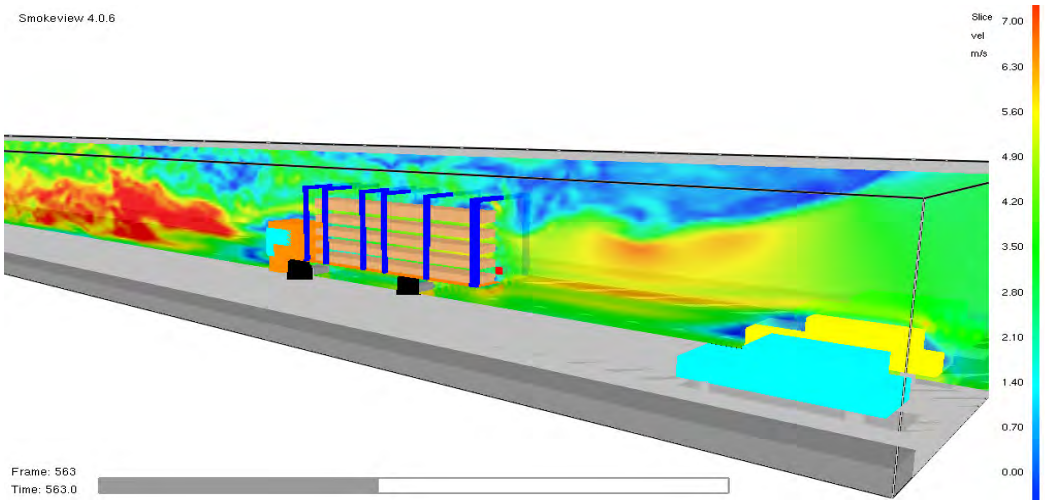

Figure 2.10: A diagram showing the air velocity simulated using a field model (FDS)

2.5 Tunnel slope and super-critical velocity

Due to buoyancy effects, smoke from a fire in a tunnel with no slope will naturally tend to propagate in both directions. In a tunnel with considerable slope, one influence during a fire can be due to the chimney effect (Riess et al 2001). If the ventilation is operating, the smoke will tend to be driven in the direction of the airflow (PIARC 1999).

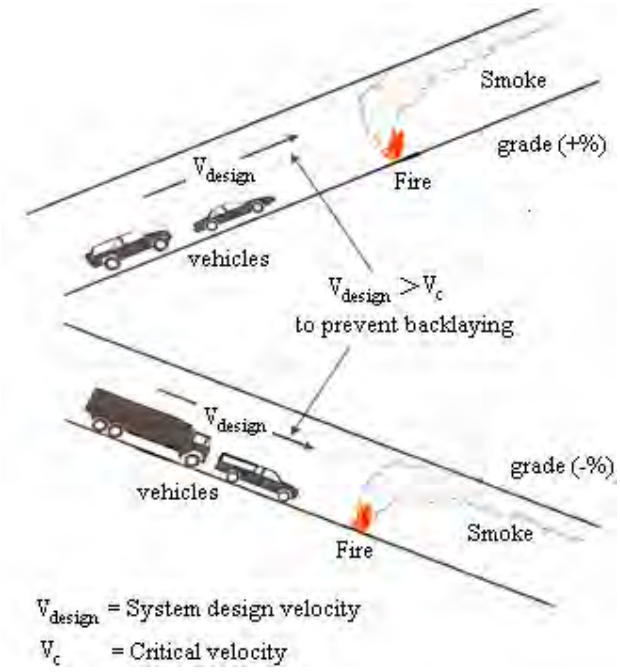

Figure 2.11: Slope determination

According to Atkinson (1996), the design methods for smoke control systems are based on results from study of methane-rich roof layers experiment to predict the critical velocity in sloping tunnel. Equation 2.5 shows the correlation factor used in the US Department of Transport Subway Environment Simulation Program.

$$V(grade) = V(0)\left[1 + 0.0374(grade)^{0.8}\right] \qquad \text{Equation 2.5}$$

where:

grade = the tangent of the angle of slope expressed as a percentage

V(0) = the critical velocity in a corresponding horizontal tunnel

As previously discussed in section 2.4, depending on the gradient of the tunnel, a downhill sloped tunnel could have an indirect effect on the critical velocity resulting in the need to provide a higher system design velocity to prevent backlayering. The provision of a higher airflow in the tunnel could indirectly affect the heat release rate. However, according to PIARC (1999), it has been found from computer simulation that the velocity increases with heat release rate but levels off at certain point as the heat release rate increases further (Figure 2.12).

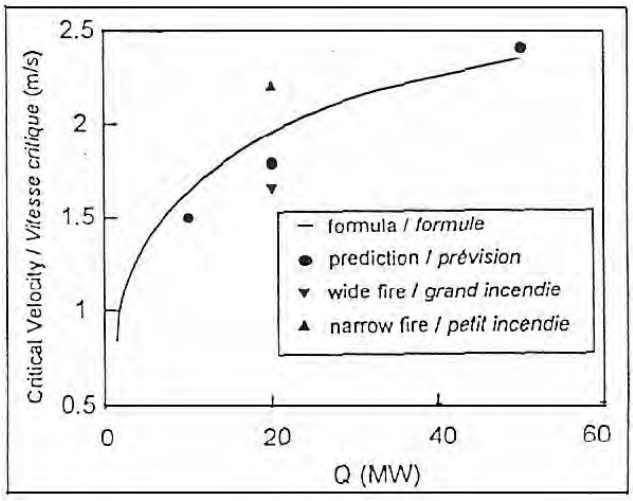

Figure 2.12: Predicted critical velocity Vs Heat release rate (reproduced from PIARC 1999)

A similar finding has also been mentioned by Wu (2007) where the heat release rate is increased to a certain level, the intermittent flames would occupy the upper part of the tunnel. The intermittent flames have a feature of constant flow speed resulting buoyancy force in the backlayering become insensitive to the heat release rate. This behaviour is defined as super-critical velocity. To limit the scope of this research work, the behaviour of super-critical velocity will not be investigated.

2.6 Design fire adopted by various road tunnel projects

For design purposes, the choice of a design fire often corresponds to the traffic flow expected for a particular tunnel. This is because the material which burns in a road tunnel mostly comes from the vehicles involved. They include elements of the vehicles such as the seats, tyres, plastic materials in the finishing, fuel tank and the cargo goods, principally for goods vehicles. This latter can be extremely varied and leads to many different sorts of fires (PIARC 1995). Recommendations from various standards are often used as a base in incorporating the expected traffic flow of the particular tunnel to determine the design fire. The different peak HRR values adopted for the design of emergency tunnel ventilation systems for some road tunnels ranges from 20 MW to 150 MW is as shown in Table 2.2.

Country	Road Tunnel	Design Fire (MW)	Reference
Australia	Eastern Distributor, Sydney	50 MW fanned to 100 MW	(Parson 2000)
Australia	Lane Cove Tunnel	50 MW	(Holliday 2002)
Belgium	Cointe Tunnel	150 MW	(Jacques and Seynhaeve 2006)
Canada	L-H-La Fontaine Tunnel	20 MW	(Kashef et al 2006)
China	Guangzhou Kang Wang Tunnel	20 MW	(Wong pers.comm.)
China	Shanxi Qiling Zhong Nan Mountain Tunnel	30 MW	(Wong pers.comm.)
China	Xiamen Xiang'an Tunnel	20 MW	(Wong pers.comm.)
China	Shanghai Xin Jin Road Tunnel	20 MW	(Wong pers.comm.)
China	Shanghai Fuxing East Road Tunnel	20 MW	(Wong pers.comm.)
China	Shanghai Yanan Road Tunnel	20 MW	(Wong pers.comm.)
HKSAR, China	Route 3, Tai Lam Tunnel	20 MW fanned to 40 MW (bus) 50 MW fanned to 100 MW (Oil Tankers)	(Parson 2000)

Country	Road Tunnel	Design Fire (MW)	Reference
HKSAR, China	Route 3, Tai Lam Tunnel	20 MW fanned to 40 MW (bus) 50 MW fanned to 100 MW (Oil Tankers)	(Parson 2000)
HKSAR, China	Western Harbour Crossing	100 MW	(Wong pers.comm.)
Singapore	CTE Tunnel	100 MW	(Philips 1991)
Singapore	Singapore Underground Road System (SURS)	100 MW	(Parson 2000)
Singapore	Fortcanning Tunnel	100 MW	(Luk 2004)
Singapore	Woodsville Vehicular Interchange	100 MW	(Cheong & Lim 2005)
Singapore	Marina Coastal Expressway Tunnel	200 MW	(Ng and Gong 2007)
South Korea	Neundong Tunnel	50 MW fanned to 100 MW	(Parson 2000)
Egypt	El Azhar Road Tunnel	100 MW	(Welburn and Nettancourt, 2002)
USA	Ted Williams Tunnel	20 MW	(Levy et al 2000)

Table 2.2: Peak HRR values adopted by some road tunnel projects

2.7 Conclusion drawn from above discussion

This chapter had provided a brief introduction on the various ventilation systems and design concepts adopted for road tunnel design. Through the above discussion, the heat release rate is an important parameter that can affect the tunnel ventilation design. It is worth mentioning that there are also other factors such as tunnel geometry, ventilation condition and the type of fuel load that could affect the heat release rate in the tunnel. These will be further examined in chapter 3 (Literature review) of this report.

Chapter 3:
LITERATURE REVIEW

The literature review in this report consists of three parts. Part one and two is a report on the fire test programmes that had been conducted internationally in a tunnel and relevant non-tunnel environments. Part three outlines the impact of tunnel geometry ventilation conditions and fuel load on the heat release rate in the tunnel.

3.1 Tunnel fire test experiments– HRR for vehicles

Large scale fire testing has been carried out to obtain acceptable verification in realistic scale and it provide the basis for the technical standards and guidelines used for tunnel design today. To date, a dozen or so large scale fire test programmes have been carried out (Ingason 2006). Some of these fire tests will be discussed in the following sections.

3.1.1 PWRI Tunnel fire experiments, 1980 (Japan)

The Japanese Public Works Research Institute (PWRI) carried out sixteen full-scale fire tests in a 700m-long fire gallery and eight fire tests in a 3.3 km long tunnel. The fire load consisted of pools of petrol, passenger cars and buses. The main observation derived from this study was that the heat release rate of a fire increased at higher longitudinal ventilation velocities; for example, the HRR of a petrol pool fire was 4 MW at 1-2 m/s and 6 MW at 4 m/s (Carvel and Marlair 2005).

3.1.2 Large-scale fire tests – EUREKA 499 project "Firetun" – 1990 to 1992 (Norway)

From 1990 to 1992, a series of fire test programmes was conducted by EUREKA 499 (a collaborative project between Austria, Switzerland, Germany, France, Italy, Sweden, Norway, UK and Finland) to measure the smoke generation, optical density, gas concentration and heat release rate of burning vehicles. These fire tests were conducted in a 2.3 km long abandoned mining tunnel in Norway (Ingason et al 1994). The HRRs of a bus and a simulated truck are discussed below.

School bus fires

An approximately 25-35 years old Volvo school bus with 85 seats was burnt in a copper-mine tunnel. The test was carried out without any forced ventilation (Ingason et al 1994). The heat release curve is as shown in Figure 3.1.

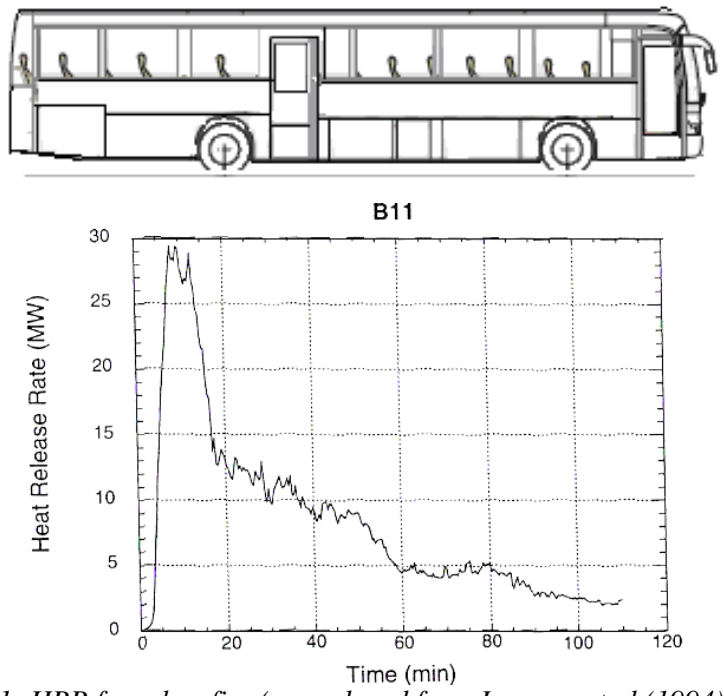

Figure 3.1: HRR for a bus fire (reproduced from Ingason et al (1994))

Simulated truck fires

This test was conducted using a simulated truck load in an abandoned mining tunnel in Norway. The fuel load consisted of 2212 kg of densely packed cribs, 310 kg of plastic mixed with wood cribs and 332 kg of rubber tyres placed at the top of the wood stacks. The length, breath and height of the simulated truck were 2.4 m, 2.4 m and 2.2 m respectively (Ingason et al 1994). The heat release curve for this test is as shown in Figure 3.2.

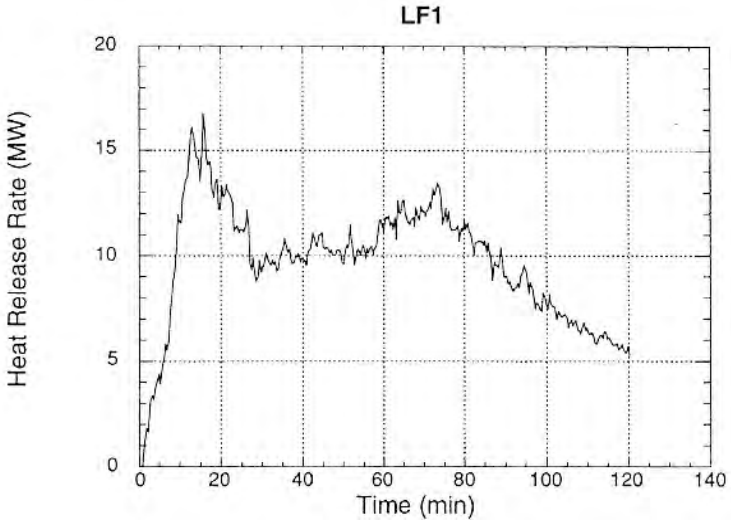

Figure 3.2: HRR for simulated truck (reproduced from Ingason et al (1994))

Wood Crib test without forced ventilation

The test was conducted in the tunnel using 950 kg of wood crib with a density of 500 kg/m^3. The size of each wood crib was around 0.04 m thick, 0.04 m wide and 0.8 m long. The wood cribs were piled into a stack measuring 3.2 m long, 0.8 m wide and 2.4 m high, by volume 30% of wood and 70% of air. The test was carried out without any forced ventilation (Ingason et al 1994). The heat release rate curve measured in this experiment is shown in Figure 3.3.

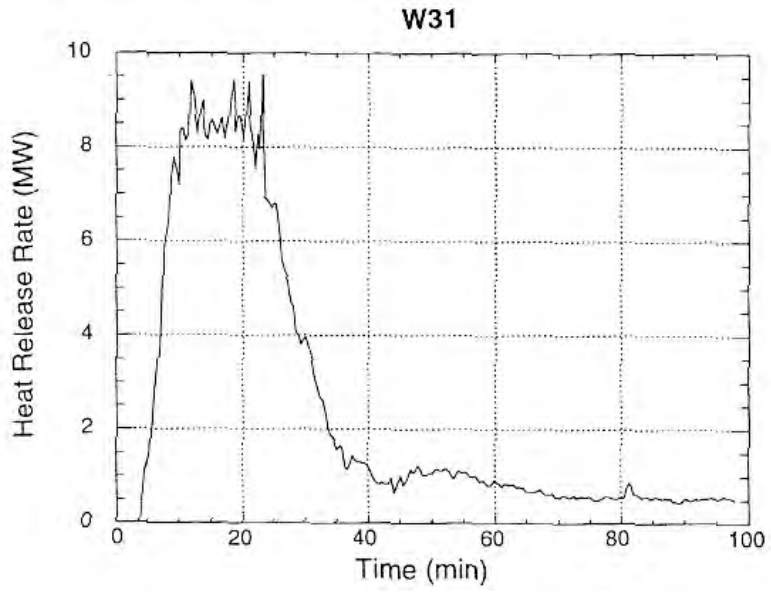

Figure 3.3: HRR for wood crib without forced ventilation (reproduced from Ingason et al (1994))

Wood Crib test with forced ventilation

This test was similar to the previous fire test where 950 kg wood cribs were used for the experiment except with an average air velocity of 2.9 m/s introduced into the tunnel. An axial flow fan type PSC, 450 kW was placed at the entrance to create a longitudinal airflow in the tunnel. There were no changes in temperature and velocity upstream of the tunnel which meant that all the heat and smoke was blown in the direction of airflow (Ingason et al 1994). The heat release rate recorded is presented in Figure 3.4.

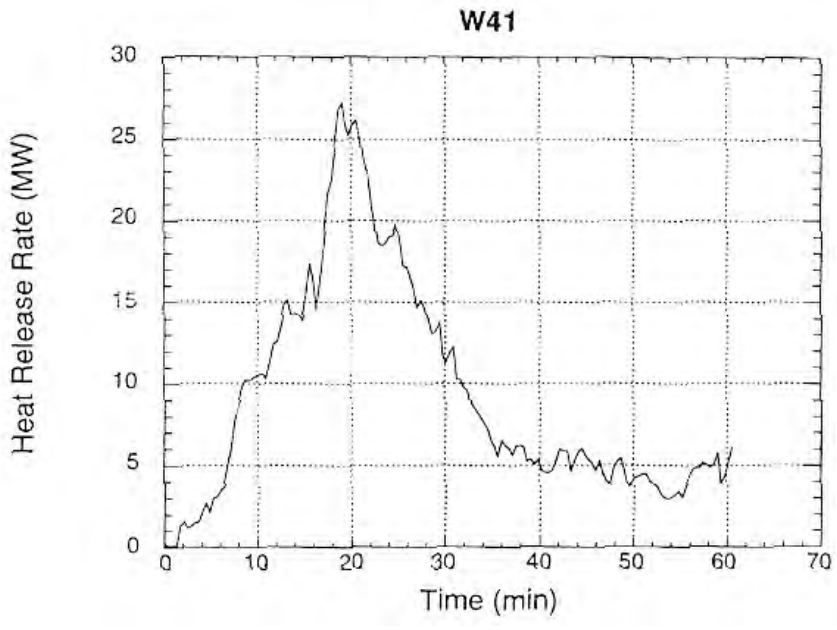

Figure 3.4: HRR for wood crib with forced ventilation (reproduced from Ingason et al (1994))

Car fires (Prime mover)

The vehicle used for this test was a Renault Espace people mover (Figure 3.5). Generally, the vehicle is fully equipped except that two rear seats had been removed and replaced with an equivalent fire-load of foam material. The fuel tank contained approximately 30 litres of petrol and the air velocity in the tunnel was about 0.4 m/s (EUREKA 1995).

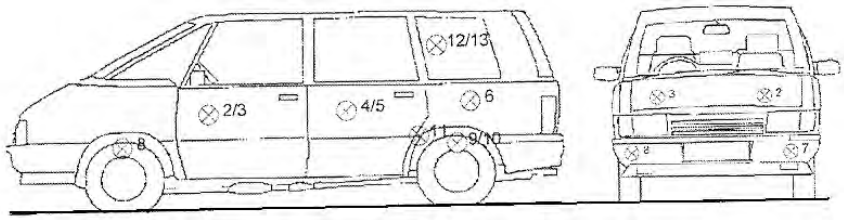

Figure 3.5: A Renault Espace People Mover

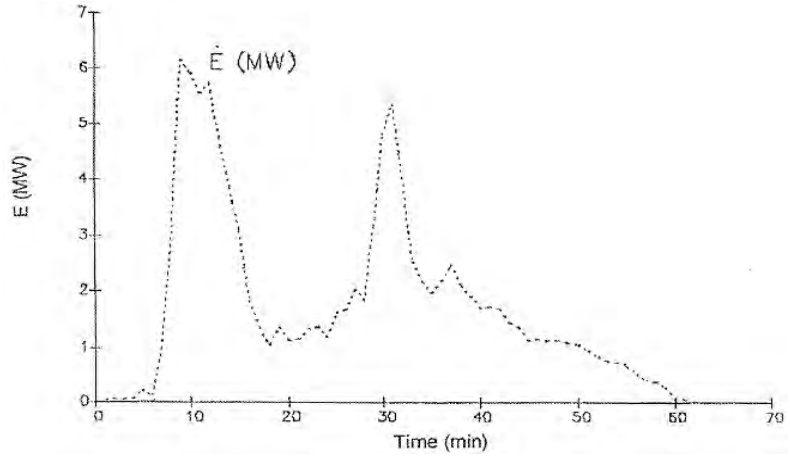

Figure 3.6: HRR for Car fire People mover (reproduced from EUREKA (1995))

Heavy goods vehicle fires

A Leyland DAF 310ATi type tractor (3.96 m long) unit and a double axial trailer (12.2 m long) with twin axles at the rear was used for this test. The trailer had a steel chassis, a 35 mm thick timber board flooring with a sheet metal bulkhead at the front giving open side and top. The side tilts were made of aluminium panels on the lower edge. Tarpaulin made of reinforced synthetic fibre was positioned by hooks attached to the side tilts. The material used to construct the cabin and trailer together with the cargo furniture placed inside the trailer made up the total fire load for this test. A description of the furniture on the trailer is tabulated in Table 3.1 (EUREKA 1995).

Item	No	Weight (kg)	Construction
Mattresses, single	4	-	Cotton padding, textile cover polythene wrapping
Mattresses, double	4	155	Timber frame, man-made fibre textiles, plastic wrapping
Divan beds	12	230	As above
Headboards, single	7	107	Chipboard or hardboard panels, fibre filling, textile
Headboards, double	6	-	Wrapping
Chairs	25	592	Timber frame, fibre filling
Settees	19	754	Urethane, textile wrapping
Settees	2	76	Polystyrene frame, urethane
Cushions	20	80	Urethane, acrylic fibre
Total weight		1994	

Table 3.1: Description of furniture in trailer (reproduced from EUREKA (1995))

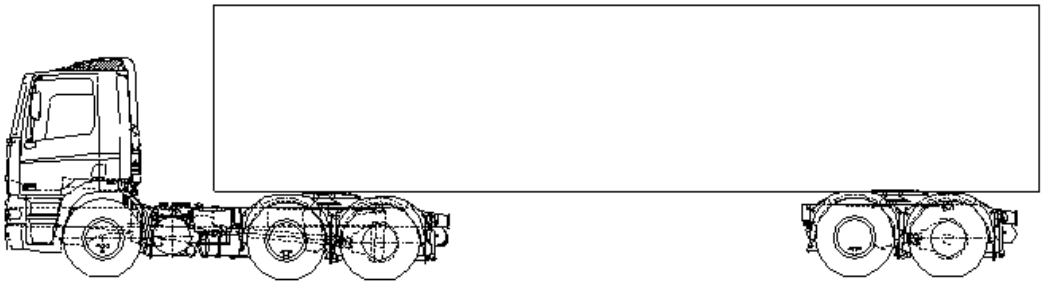

Figure 3.7: A tractor with a trailer

The airflow in the tunnel was around 6 m/s. As the test progressed, a decision was made to turn off the fan between 13.5 to 16.5 minutes when the fire appeared to be burning fiercely. The measurement showed the decrease in heat release rate when the ventilation was turned off during this period. The test result for the HRR is as shown in Figure 3.9.

Figure 3.8: Fire test involving a heavy goods vehicle (reproduced from Hack (2002))

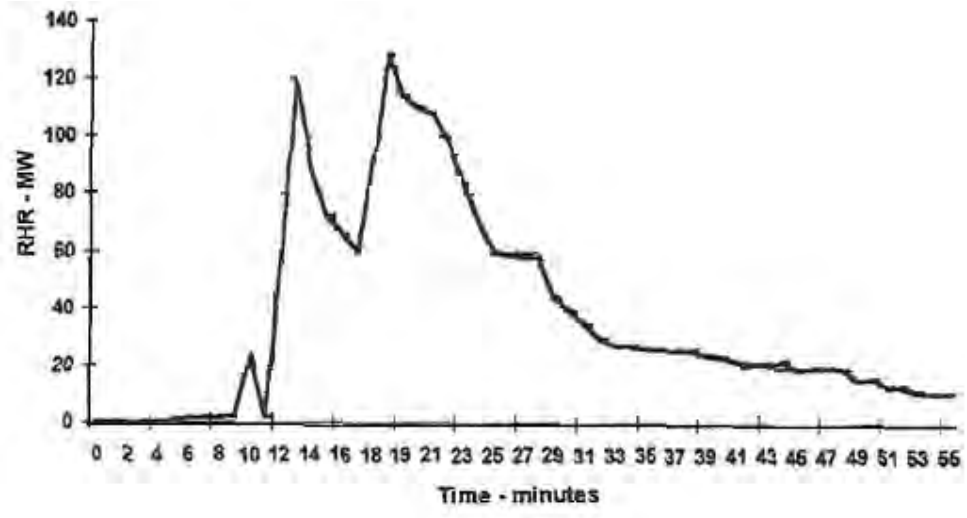

Figure 3.9: HRR for Heavy goods vehicle (reproduced from EUREKA (1995))

3.1.3 Large-scale fire tests in the Second Benelux Tunnel (Netherlands)

The tests were conducted in the recently built Second Benelux tunnel near Rotterdam. The tunnel has a rectangular cross section with a height of 5.1 m, a width of 9.8 m and a length of 840 m. A total of fourteen full-scale fire tests were carried out in this test programme. Several types of fires sources were used: fuel pans, cars, a van and covered truck loads (Lemaire and Kenyon 2006). The car fire tests and the covered truck loads fire tests will be discussed in the following sections.

Car Fires

The influence of forced ventilation on the development of fire within cars was explored in this fire test programme. Two car fire tests, one without ventilation and another at 6 m/s ventilation were carried out with the ignition source at the front of the car. It was found that longitudinal ventilation at 6 m/s has a significant effect on the fire development. One explanation is because fire spread slower in the upwind direction due to the higher airflow (6m/s) resulting in lower heat release rate for Fire Test 7 as compared to the test without ventilation (Fire Test 6). The heat release rate for Fire Test 7 is about 1 to 2 MW for half an hour before a peak of 5 MW occurs followed by linearly decay to 1 MW (Lemaire and Kenyon 2006).

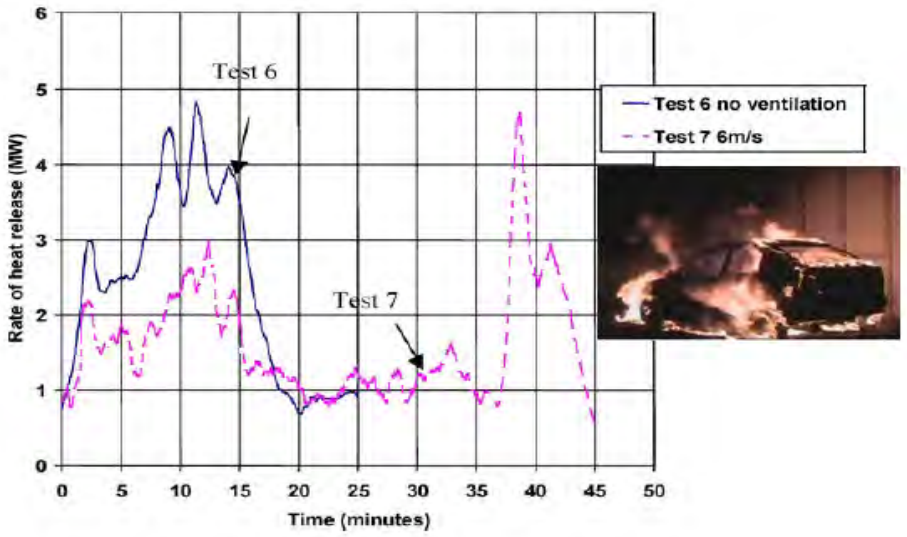

Figure 3.10: HRR of a car fire (reproduced from Lemaire and Kenyon (2006))

Small trucks fires

The covered truck loads fire tests consisted of 800 kg of wooden pallets (4 piles with 9 pallets each) with four tyres placed on top and a metal frame with a tarpaulin to simulate a small truck. The dimensions of the fuel load measured was about 2.4 m wide, 4.5 m long and 2.5 m high. The ventilation velocity varied from no ventilation to 6 m/s (Lemaire and Kenyon 2006). Figure 3.11 shows the HRR for the simulated truck based on various ventilation conditions.

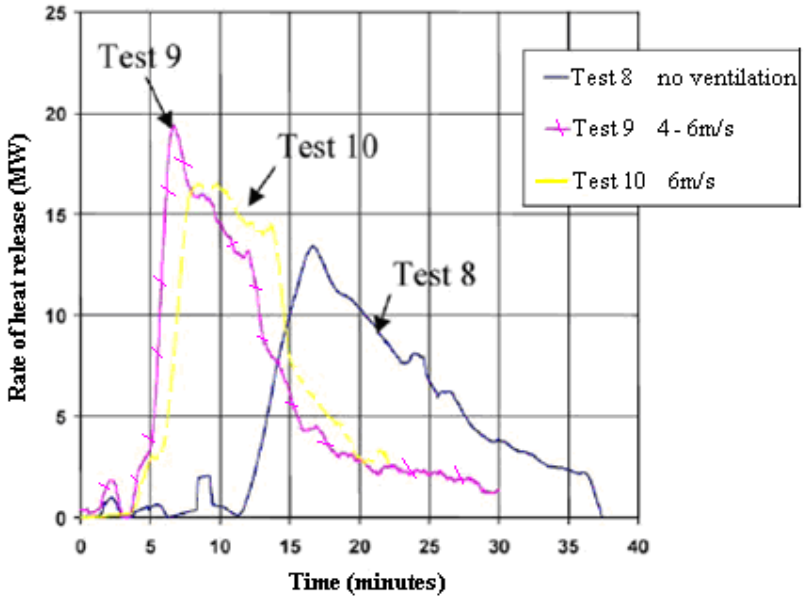

Figure 3.11: HRR of a small truck fire (reproduced from Lemaire and Kenyon 2006)

3.1.4 The Memorial Tunnel fire ventilation test program, 1993-1995 (USA)

The objective of The Memorial Tunnel Fire Ventilation Test Program was to determine the effectiveness of various ventilation system configurations, ventilations rates and operating modes in the management of the spread of smoke and heat for tunnel fires of varying intensities (Bechtel and Brinckerhoff 1995).

A total of 98 full-scale fire ventilation tests were conducted in the decommissioned two lane Memorial Tunnel at West Virginia with fire sizes of 10, 20, 50 and 100 MW involving different airflow capacities in conjunction with a series of alternative configurations including:

i) Full Transverse Ventilation
ii) Partial Transverse Ventilation
iii) Partial Transverse Ventilation with Single Point Extraction
iv) Partial Transverse Ventilation with Oversized Exhaust Ports
v) Point Supply and Point Exhaust Operation
vi) Natural Ventilation
vii) Longitudinal Ventilation with Jet Fans

Figure 3.12: Memorial Tunnel test site (reproduced from Bechtel and Brinckerhoff (1995))

As the subject of this research is based on the longitudinal ventilation with jet fans system (see chapter 6), only the result for the longitudinal ventilation with jet fans system will be discussed in this section.

The purpose of these tests was to examine the ability of a longitudinal ventilation system using jets fans to manage smoke and heat under the influence of various fire sizes and response times. There were 15 tests performed involving the longitudinal ventilation system with jet fans (Figure 3.13). The fire sizes of 10, 20, 50 and 100 MW were conducted in these fire tests.

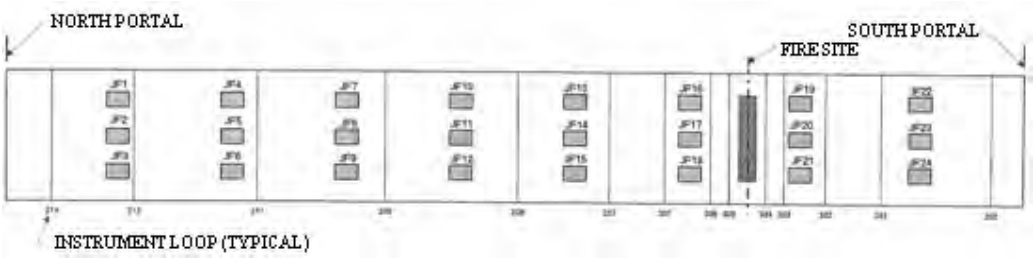

Figure 3.13: Tunnel plan showing jet fans arrangement (reproduced from Bechtel and Brinckerhoff (1995))

The findings drawn from these tests are presented below (Bechtel and Brinckerhoff):

i) The longitudinal ventilation system using jet fans was able to provide a positive means of smoke control for fire size ranging from 10 to 100 MW.

ii) The theoretical relationship (Equation 2.1 to Equation 2.4) between the minimum tunnel air velocity required to prevent backlayering seemed to over predict the air velocity requirements for fire sizes 50 MW and 100 MW.

iii) The fire tests data shown in Figure 3.14 suggest that air velocities of 2.54 m/s (500 fpm) to 2.95 m/s (580fpm) were sufficient to prevent backlayering for fires sizes from 10 to 100 MW. However, the air velocities are also dependent on the tunnel cross section area and grade as shown in previous chapter 2, Equation 2.1 to 2.4 (Bechtel and Brinckerhoff 1995).

iv) At least one group of jet fans closest to the fire site are at risk of being damaged by the exposure to high temperature. Table 3.2 shows the air temperature at the fans caused by various fire sizes.

v) As the hot smoke layer can spread quickly (490 to 580 m) during the initial 2 minutes of a fire, the time interval between the onset of a fire and activation of fans should be minimized.

vi) The operation of fans can disrupt the thermal stratified smoke layers, this effect is minimised by operating fans located either far upstream or downstream of the fire site.

Fire Size (MW)	Air Temperature at the Fans	Fan Temperatures	
		Motor Bearings	Motor Windings
20	204°C	114°C	106°C
50	334°C	178°C	138°C
100	677°C	-	198°C

Note: - no data provided

Table 3.2: Air temperature at the fans caused by various fire sizes (Bechtel and Brinckerhoff 1995)

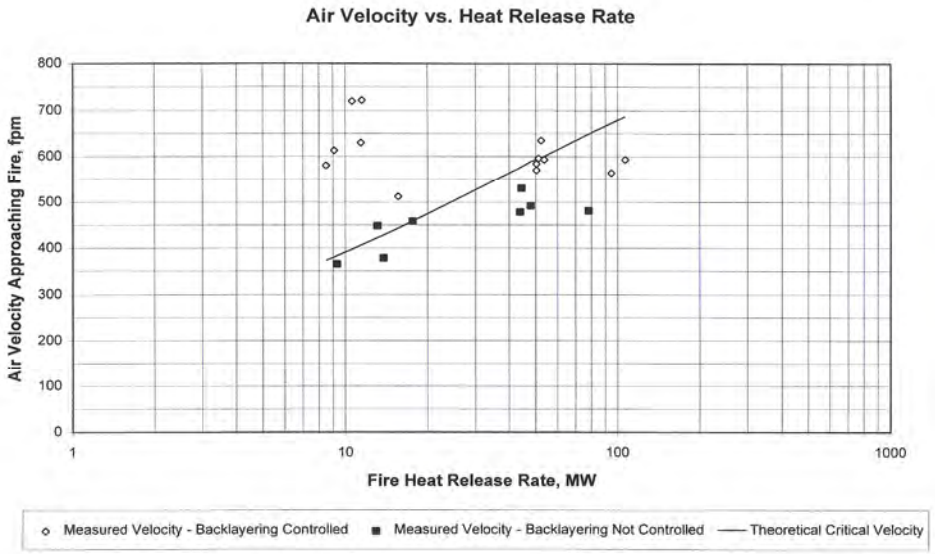

Figure 3.14: Air Velocity Vs HRR (Bechtel and Brinckerhoff 1995)

3.1.5 Large scale fire tests in Runehamar Tunnel, 2003 (Norway)

In 2003, large scale fire tests involving semi-trailer cargos were conducted in the Runehamar tunnel in Norway. This is an abandoned tunnel with a slope varying from 0.5% and 1% with a cross-sectional area of about 6 m high by 9 m wide and 1.6 km long (Figure 3.15). A total of four tests with mass ratio approximately 80% cellulose and 20% plastic materials were performed in a semi-trailer mock-up (Figure 3.16). The description of the fire load used in the tests and the HRR are presented in Table 3.3 and Figure 3.17 respectively (Lönnermark A., and Ingason H 2005). Details of these fire tests are presented in the following sections.

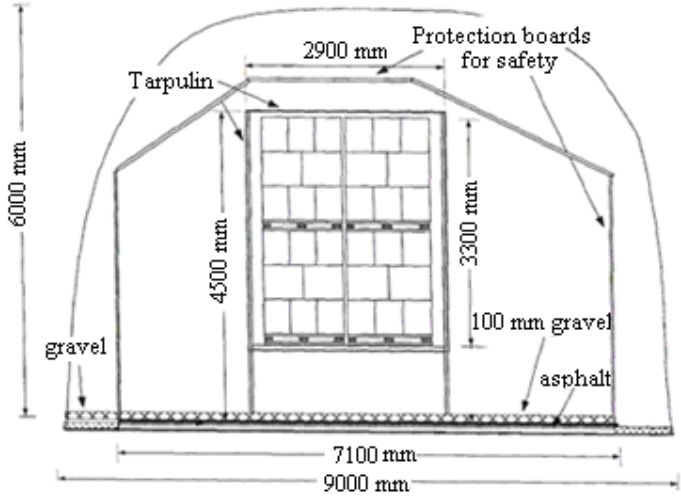

Figure 3.15: Tunnel Cross section (reproduced from Lönnermark and Ingason 2005)

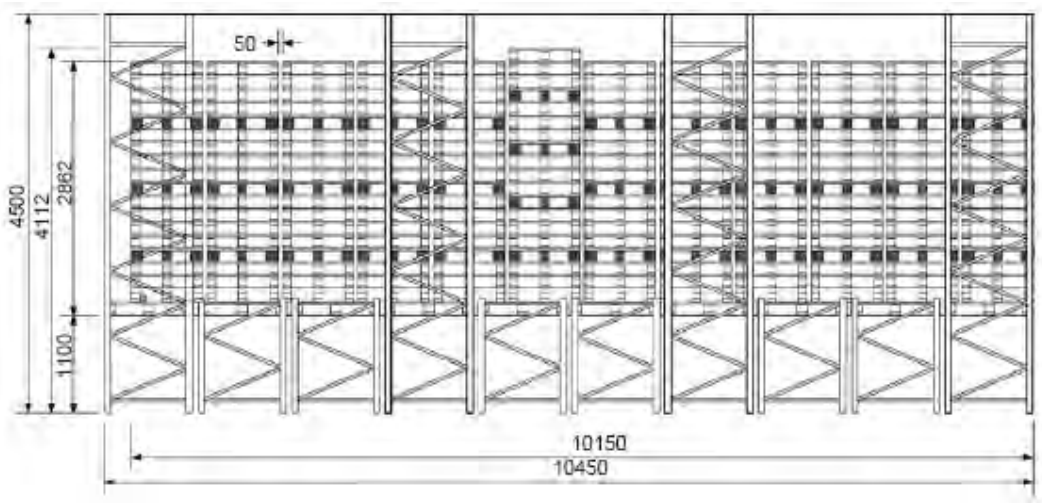

Figure 3.16: Semi-trailer set-up for T1(reproduced from Lönnermark and Ingason 2005)

One factor that significantly affects the size of the fire is the type of commodity carried by the goods vehicle on fire. Swedish statistics identify 24 different groups of commodities commonly transported on Swedish roads and the combustible commodity can be apportioned by mass ratio into four different categories as cellulosic material (42% by mass), miscellaneous commodity inclusive of packaging material (28%), food product (17%) and oil product (13%). From the above information, one can see that the two largest categories are cellulosic and miscellaneous commodity. According to Ingason and Lonnermark (2005), discussions with professional goods transport agents indicate that a mass ratio of 80% - 85% cellulose material with 15% - 20% plastics is a reasonable division between these two categories. The commodities used in the Runehamar tunnel fire tests consisted of four different materials and each represented materials commonly found in the cargo of heavy goods vehicle. The type of commodities used for the fire tests are shown in Table 3.3.

Test No.	Description	Total mass (kg)	Mass ratio of plastic
Test 1	Wood pallets and plastic (PE) pallets	11010	18 %
Test 2	Wood pallets and mattresses (PUR)	6930	18 %
Test 3	Furniture + rubber tyres	8550	18 % (tyres not included)
Test 4	Plastic cups (PS) in cardboard boxes on wood pallets	2850	19 %

Table 3.3: Description of fire load (Ingason and Lonnermark 2005)

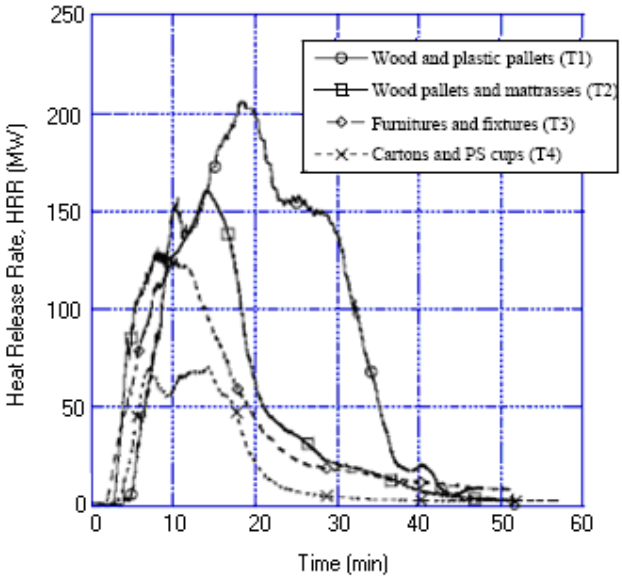

Figure 3.17: Fire test HRR (reproduced from Ingason and Lonnermark 2005)

The detailed description of the fire load, theoretical calorific value, peak heat release rate and photograph of fire tests is shown in Table 3.4 and Figure 3.18 respectively.

Description of fire load	Theoretical calorific value (GJ)	Linear fire growth rate / (R – linear regression coefficient) (MW/min)	Peak heat release rate (MW)
Test 1 360 wood pallets 20 wood pallets 74 PE plastic pallets	247	20.1 (0.996)	201.9
Test 2 216 wood pallets 240 PUR mattresses	135	26.3 (0.992)	156.6
Test 3 Furniture and fixtures plastic wood cabinet doors upholstered PUR arm rest upholstered sofas stuffed animals plastic potted plant wood toy house plastic toys 10 large rubber tyres	179	16.4 (0.998)	118.6
Test 4 600 corrugated paper cartons 1800 poly-styrene (PS) cups 40 wood pallets	62	16.9 (0.996)	66.4

Table 3.4: Description of fire load used in large-scale fire test (Ingason and Lonnermark 2005)

Test 1

Fuel load | Fire development after 5 minutes | Fire development after 30 minutes

Test 2

Fuel load | Fire development after 5 minutes | Fire development after 30 minutes

Test 3

Fuel load | Fire development after 5 minutes | Fire development after 30 minutes

Test 4

Fuel load | Fire development after 5 minutes | Fire development after 30 minutes

Figure 3.18: Photographs of Runheamar Fire Tests ((reproduced from Promat (2007a))

The four tests with different mixtures of commodity in the HGV-trailer cargo show that the fire growth rate appeared to be relatively linear for all the tests (linear regression coefficient R found to be very high >0.99). Findings from these fire tests found that the wood pallets and mattresses in Test 2 yield the fastest fire growth rate (26.3 MW/min) followed by wood and plastic pallets (Test 1 – 20.1 MW/min). The growth rate for Test 3 and 4 were found to be similar (16.4 to 16.9 MW/min). In terms of heat release rate, the peak HRR is in the range of 66.4 to 201.9 MW with wood and plastic pallets commodity (Test 1) having the highest peak HRR (201.9 MW).

3.2 Non-tunnel fire test experiments – HRR for vehicles

In addition to the above-mentioned experiments, a number of other experiments have been conducted to estimate the HRR of vehicles in a non-tunnel environment.

3.2.1 Fire test involving private cars, 1994 (Finland)

Three full scale fire experiments on a Ford Taunus 1.6, Datsun 160J sedan and Datsun 180B sedan passenger cars were conducted by VTT Technical Research Centre of Finland (Mangs & Keski-Rahkonen 1994). The aim of the research was to determine a realistic car fire scenario in an open car park. The cars were ignited either from the passenger cabin or beneath the engine. The heat release rate was measured by means of oxygen consumption calorimetry, the schematic of the car fire experiment configuration and the measured heat release rate is shown in Figure 3.19.

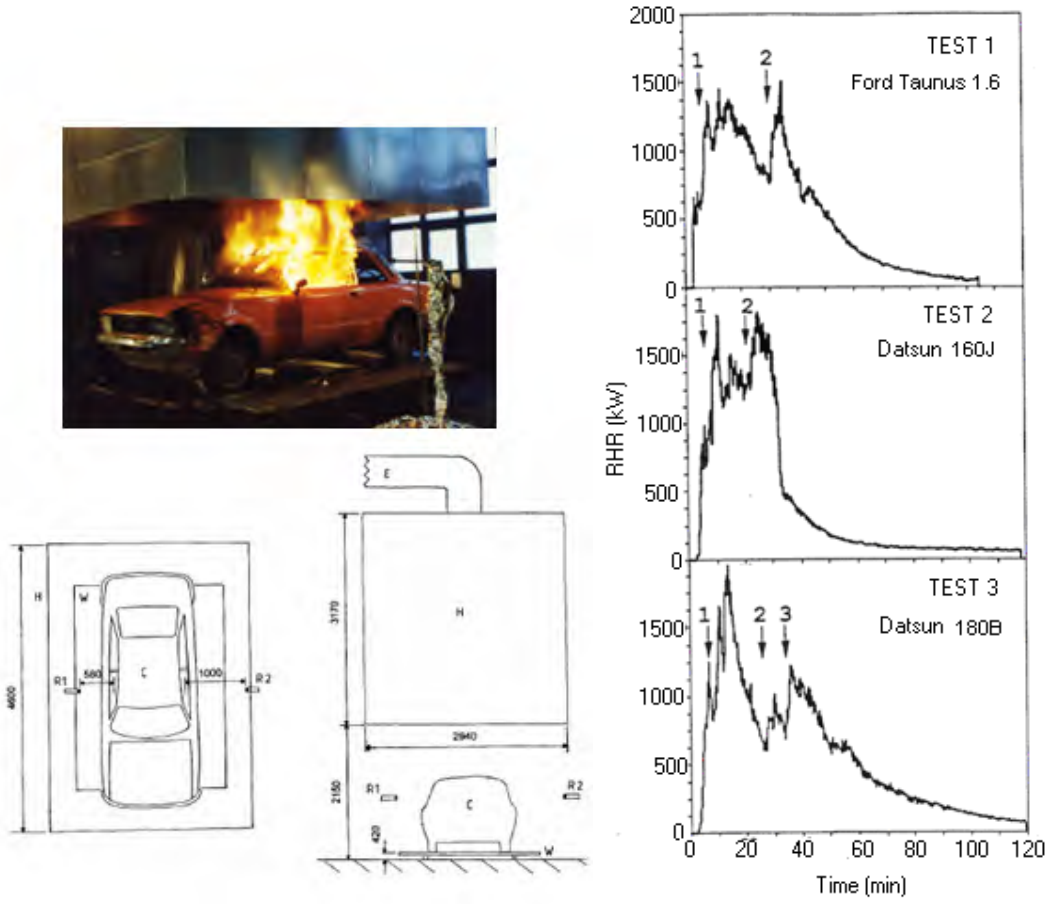

Figure 3.19: HRR Cars (reproduced from (Mangs & Keski-Rahkonen 1994))

3.2.2 Fire test involving private motor vehicle, 1991 (UK)

A full-scale fire test for private motor vehicles under instrumented calorimeter hoods were conducted by Fire Research Station in 1991. Two tests were carried out in this test programme, an Austin Maestro 1.3L (seat ignition) and a Citroen BX (engine ignition) in a closed canopy (Figure 3.20). A total heat output of at least 8.5 MW and peak heat output of 4.5 MW was captured for the Austin Maestro and Citroen respectively (Figure 3.21).

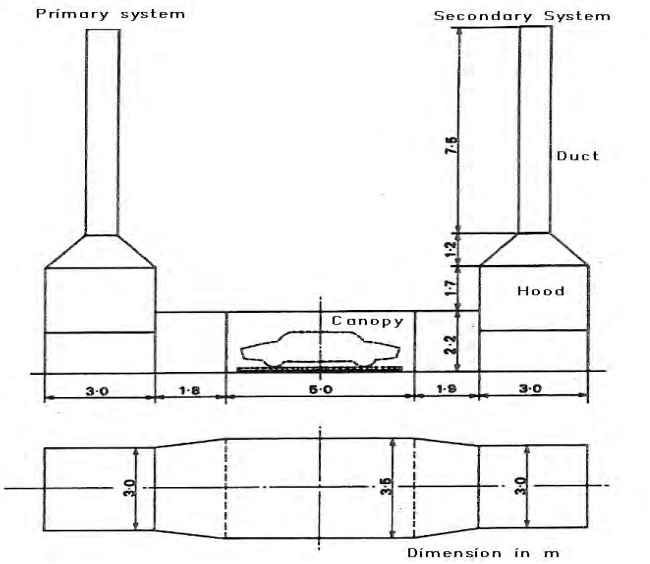

Figure 3.20: Canopy configuration (reproduced from (Shipp and Spearpoint 1995))

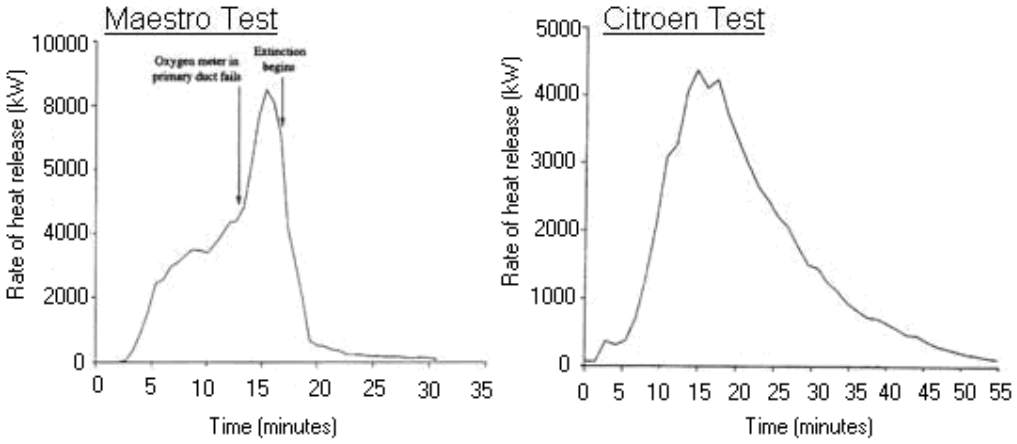

Figure 3.21: HRR Cars (reproduced from (Shipp and Spearpoint 1995))

According to Shipp and Spearpoint (1995), the findings from these experiments indicate that the heat release rate (4.5 MW and 8.5 MW) are significantly higher compared to past car fire tests conducted by Mangs and Keski-Rahkonen (1.5 MW and 2 MW). The difference in peak heat release rate could be due to materials used by the manufacturer of different vehicles, the ventilation condition and the heat feedback mechanisms conducted for these tests.

3.2.3 Fire test involving minivan, 1999 (USA)

Two fire tests involving a minivan were conducted in the NIST large fire research facility in December 1999 using calorimetry. In the first test, paper was ignited in the passenger compartment with its window closed. The fire extinguished itself due to the lack of oxygen. The second test was conducted using 2 litres of gasoline in the passenger compartment with the windows open. The measured heat release rate is shown in Figure 3.22, the peak HRR for this test was 2.4 MW (Stroup et al 2001).

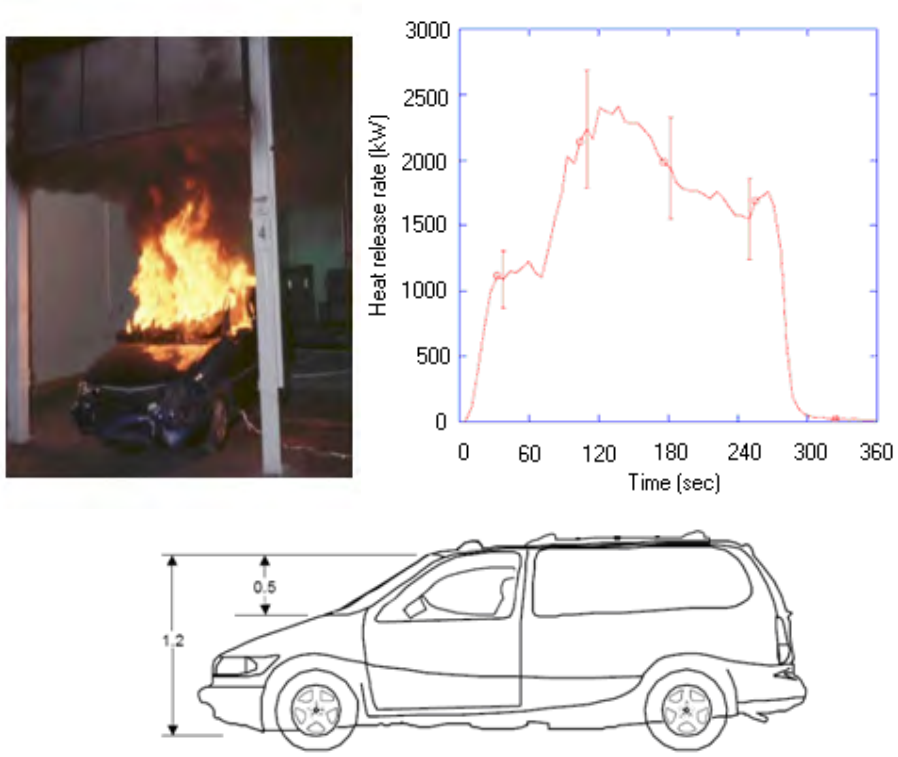

Figure 3.22: HRR Minivan (reproduced from (Stroup et al 2001))

3.2.4 Fire test on ignition of post crash vehicle fire (USA)

A series of fire tests to examine the ignition mechanism of post crash vehicle fires were carried out by General Motors. A summary of these fire tests are tabulated in Table 3.5 and the details covered in this section are mainly referenced from Part 3, Part 4, Part 6, Part 7 Part 9, Part 10, Part 12 and Part 13 of "Evaluation of Motor Vehicle Fire Initiation and Propagation" by General Motors.

Summary of post crash vehicle fire test

Test	Vehicle description	Ignition mechanism	Ignition location	Time of extinguishment after ignition	Source
Part 3	1996 Dodge Caravan Sport	An electrical igniter was used to ignite the battery and power distribution centre housing	Engine compartment	11 minutes	(Santrock 2000)
Part 4	1996 Plymouth Voyager	Gasoline pool under test vehicle by allowing gasoline flow out of a hole in the filler tube and a hand-held propane torch to ignite gasoline	Under body of vehicle	215 seconds	(Santrock 2001)
Part 6	1997 Chevrolet Camaro	Gasoline pool under test vehicle by using a gasoline delivery system to deliver liquid gasoline under the test vehicle and a hand-held propane torch to ignite gasoline	Under body of vehicle	210 seconds	(Santrock 2001a)
Part 7	1997 Chevrolet Camaro	A propane torch installed in engine compartment so that flames can impinged on the HVAC module of the dash panel	Engine compartment	16 minutes	(Santrock 2002)

Test	Vehicle description	Ignition mechanism	Ignition location	Time of extinguishment after ignition	Source
Part 9	1998 Ford Explorer	Gasoline was pumped continuously during test from an external reservoir onto the ground under the test vehicle. A propane torch was used to ignite the gasoline	Rear under body of vehicle	170 seconds	(Santrock 2002a)
Part 10	1998 Ford Explorer	Gasoline was pumped continuously during test from an external reservoir onto the ground under the test vehicle. A propane torch was used to ignite the gasoline	Mid -Under body of vehicle	250 seconds	(Santrock 2002b)
Part 12	1998 Honda Accord	Gasoline was pumped continuously during test from an external reservoir onto the top of the fuel tank. Liquid gasoline flowed to onto the floor under the test vehicle. A propane torch was used to ignite the gasoline	Under body of vehicle	155 seconds	(Santrock 2003)

Test	Vehicle description	Ignition mechanism	Ignition location	Time of extinguishment after ignition	Source
Part 13	1998 Honda Accord	Power steering fluid aerosol was sprayed from a hand-held oil mister through a flame of a propane torch toward the windshield washer fluid reservoir of the test vehicle and ignited methanol vapour in the windshield washer fluid reservoir.	Engine compartment	27 minutes	(Santrock 2003a)

Table 3.5: A summary of fire tests carried out by General Motors

The crash tested vehicles were prepared at the General Motors Technical Centre in Warren and transported to the Factory Mutual Test Center in West Gloucester for the fire test. During the tests, measurements on temperature, heat flux, gaseous combustion products, and heat release rate of the vehicles were recorded using thermocouples, flame thermometers, fire products collector and FITR gas analysis. The test vehicle was placed in a fluid containment pan and the fire products collector was above the test vehicle. Figure 3.23 illustrates the experimental setup for the test.

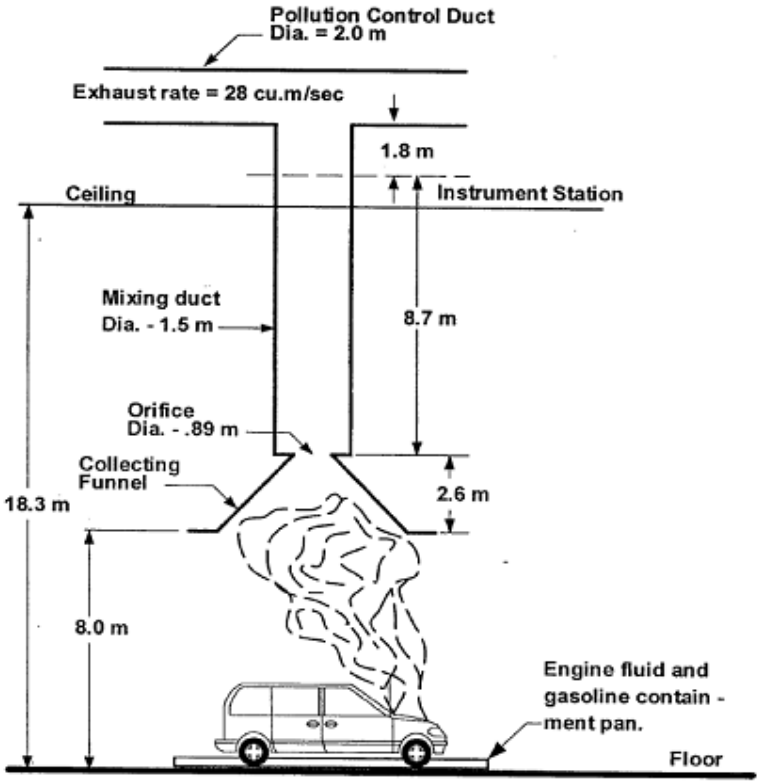

Figure 3.23: Experimental setup for the fire test (reproduced from Santrock (2000))

The intent of the test was to allow the flames to spread into the passenger compartment sufficiently so that the fire path could be determined while allowing physical evidence to be preserved. This physical evidence would be lost if the test allowed the vehicle to burn completely. Therefore, certain criteria were established to determine the appropriate time to extinguish the fire.

The measured heat release rate and photographs for each of these fire tests are shown in Figure 3.24 to Figure 3.31.

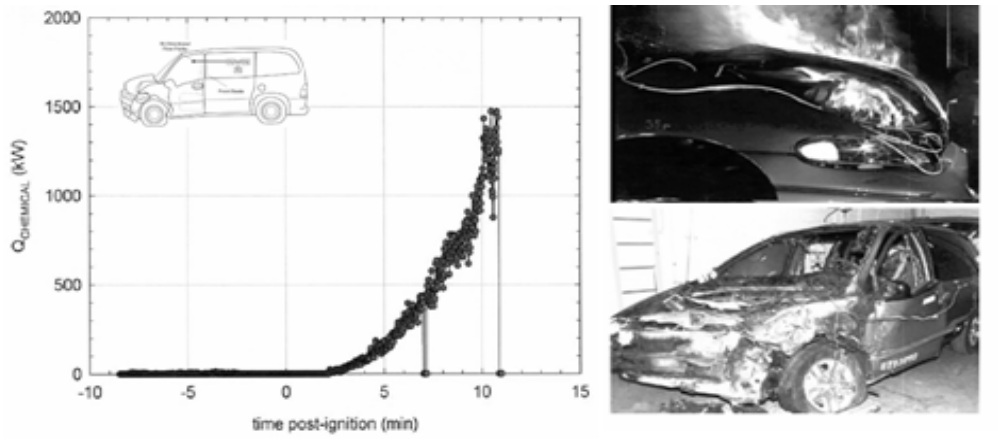

Figure 3.24: HRR and photograph for Test Part 3 (reproduced from Santrock (2000))

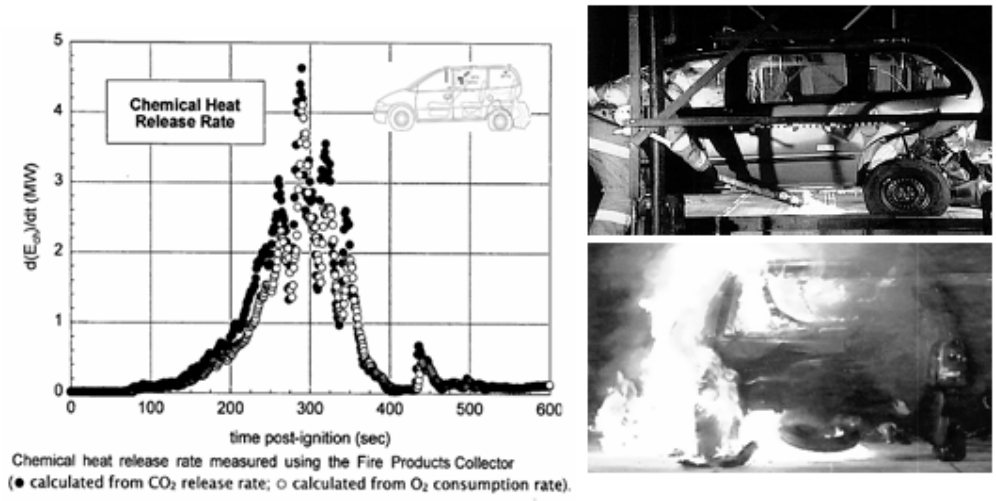

Figure 3.25: HRR and photograph for Test Part 4 (reproduced from Santrock (2001))

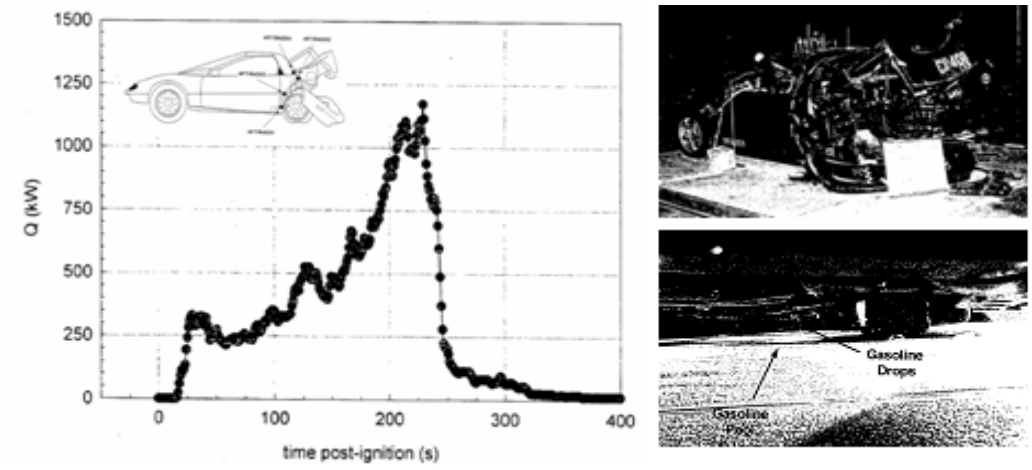

Figure 3.26: HRR and photograph for Test Part 6 (reproduced from Santrock (2001a))

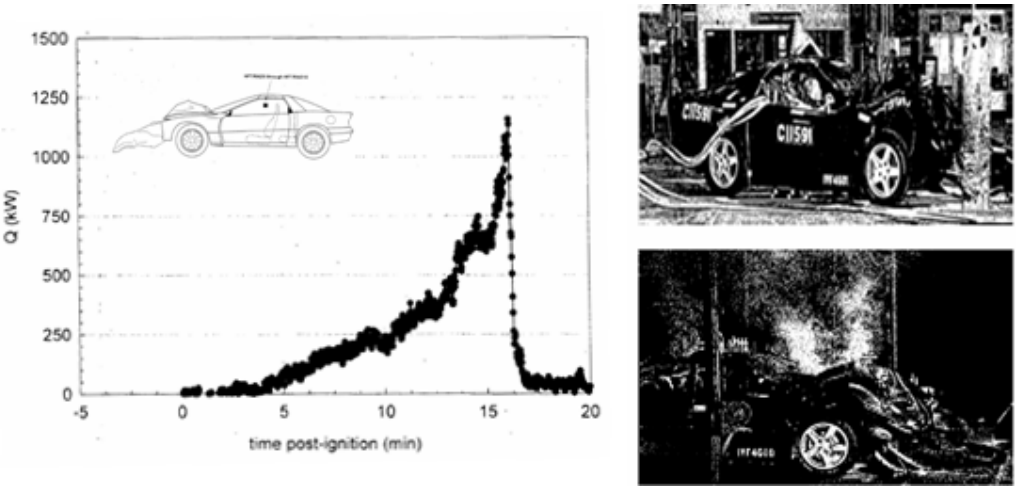

Figure 3.27: HRR and photograph for Test Part 7 (reproduced from Santrock (2002))

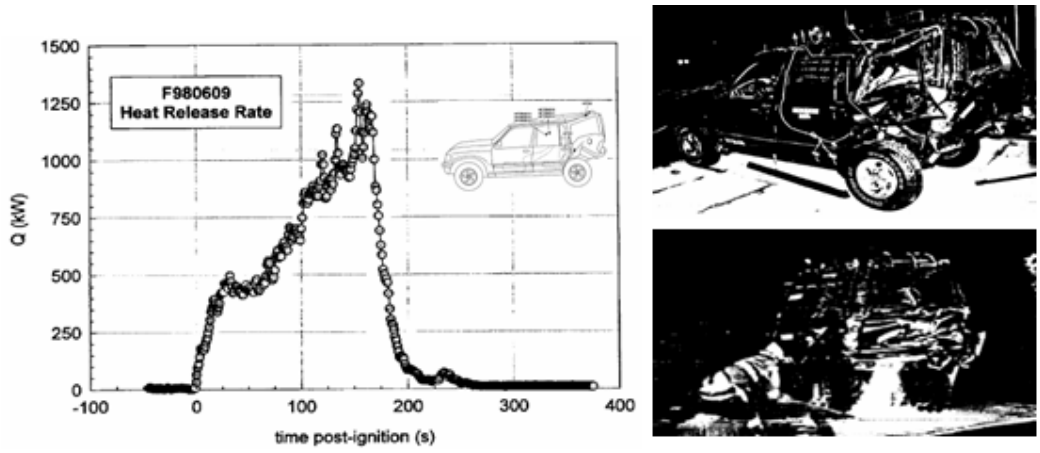

Figure 3.28: HRR and photograph for Test Part 9 (reproduced from Santrock (2002a))

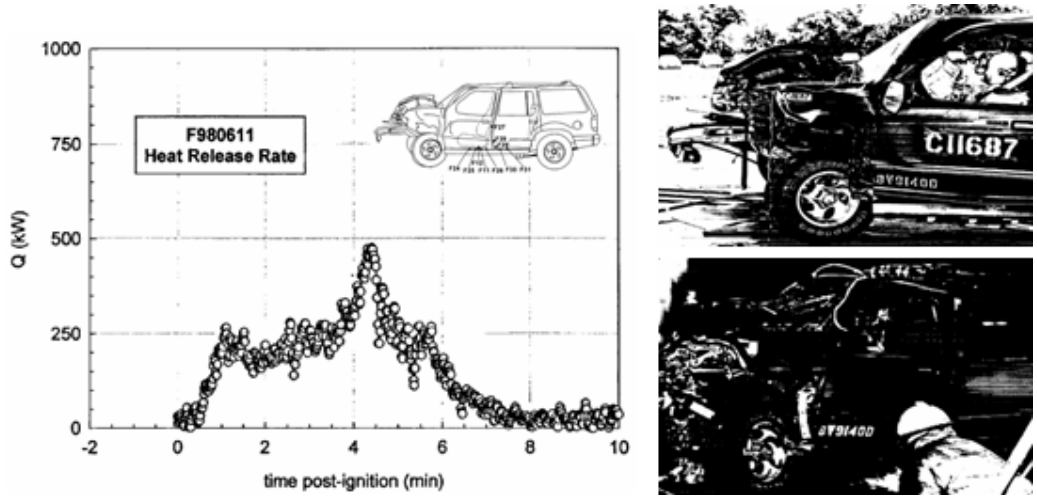

Figure 3.29: HRR and photograph for Test Part 10 (reproduced from Santrock (2002b))

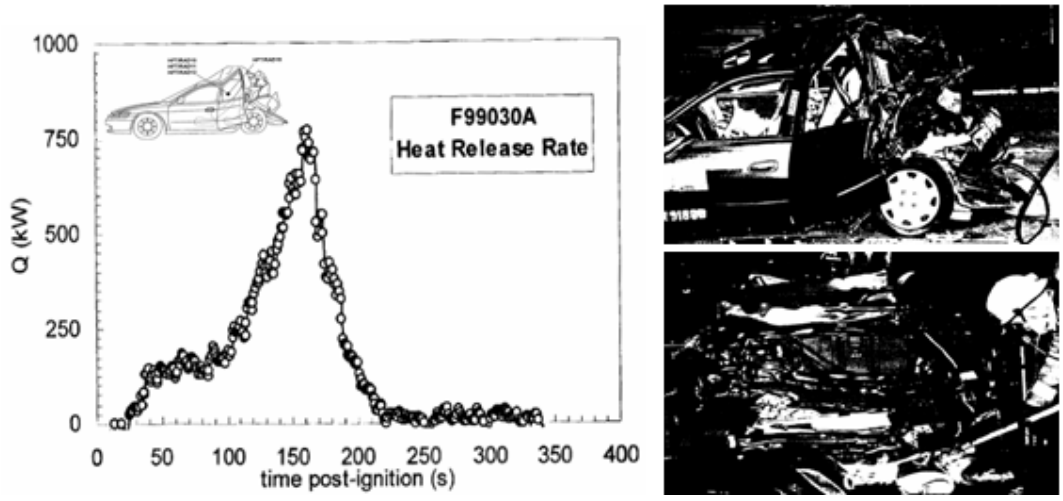

Figure 3.30: HRR and photograph for Test Part 12 (reproduced from Santrock (2003))

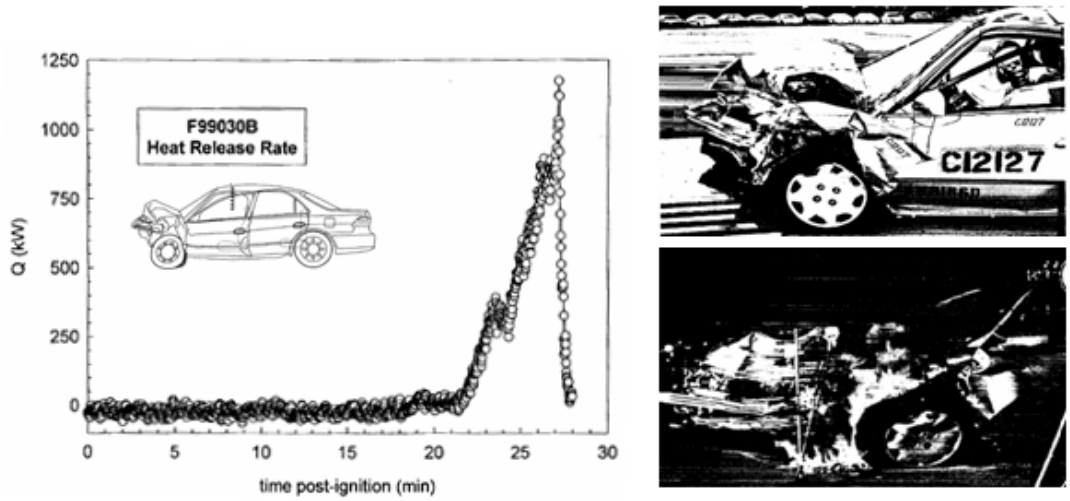

Figure 3.31: HRR and photograph for Test Part 13 (reproduced from Santrock (2003a))

3.2.5 Fire test involving motor scooters, 2005 (Taipei)

There were a series of fire tests conducted on motor scooters using a 10 MW large-scale fire products collectors in Taiwan. The heat release rate for the 125 cc motorcycle was estimated to be 1.22 MW (Figure 3.33) (Chen et al. 2005).

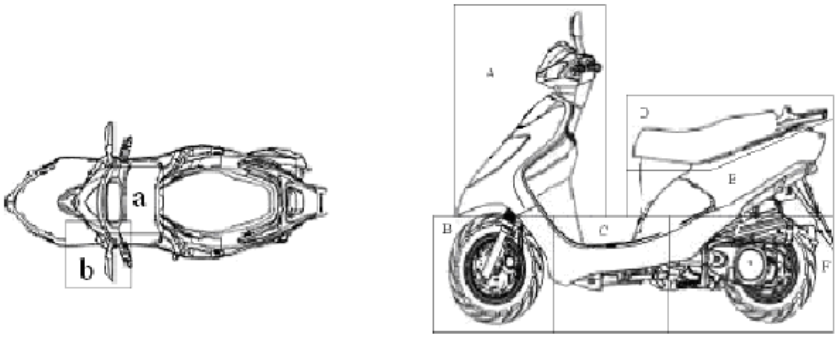

Figure 3.32: Scooter used for the fire test (reproduced from Chen et al. (2005))

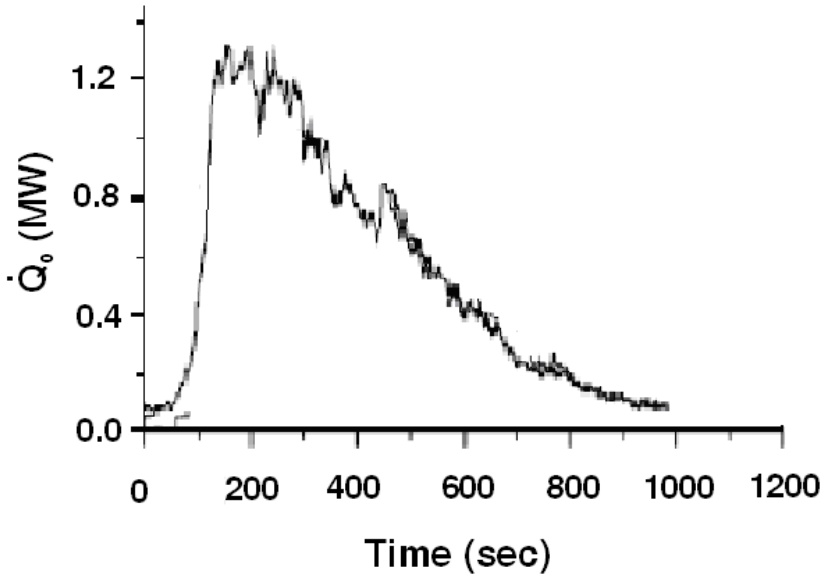

Figure 3.33: HRR Scooter (reproduced from Chen et al. (2005))

3.2.6 Fire test involving 3.49 Ton Truck with goods, 2006 (Taiwan)

Five full scale fire experiments on a 3.49 ton truck with goods were conducted by the National Taiwan University of Science and Technology under a free burning condition (Figure 3.34). The variables in these tests were the type of goods materials (plastic barrels and wood pallets), the ignition location (on the vehicle seats and at the bottom centre of the goods) and the use of fire-resistant blanket with iron trough to compartment the fire (Chuang et al 2006), Table 3.6 and Figure 3.35 provide a summary of the peak HRR and test conditions used in these fire experiments.

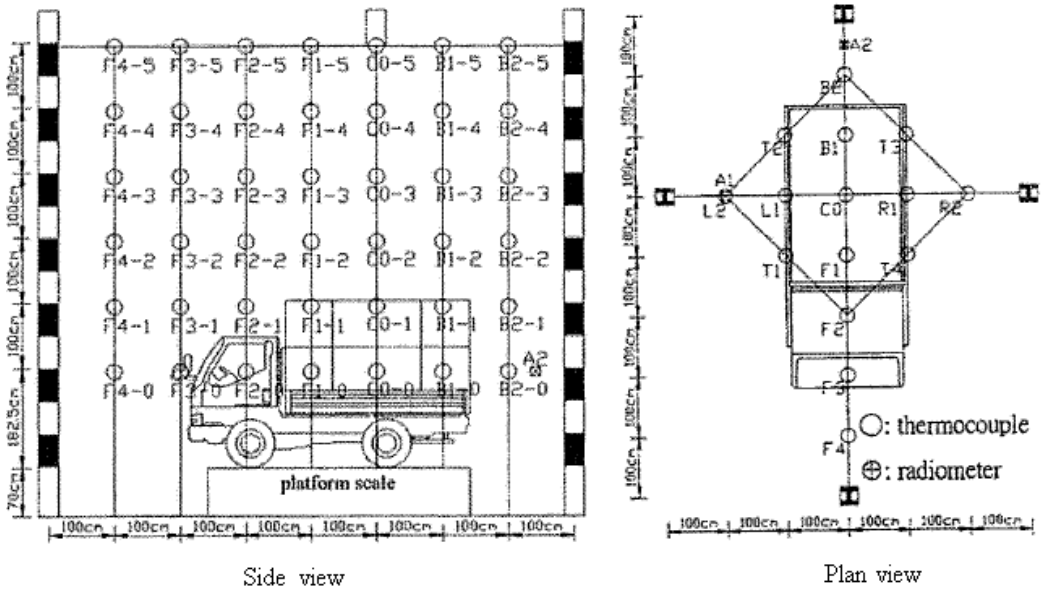

Figure 3.34: Fire test configuration (reproduced from Chuang et al (2006))

Test No	Iron trough	Blanket	Ignition position	Goods	Peak HRR (MW)
1	No	No	Bottom centre of goods	890 kg wood pallets	23.38
2	No	No	Seat surface	890 kg wood pallets	20.92
3	No	No	Bottom centre of goods	452 kg plastic barrels	47.47
4	Yes	Yes	Bottom centre of goods	890 kg wood pallets	-
5	Yes	Yes	Bottom centre of goods	452 kg plastic barrels	-

Table 3.6: Peak HRR and test condition (reproduced from Chuang et al (2006))

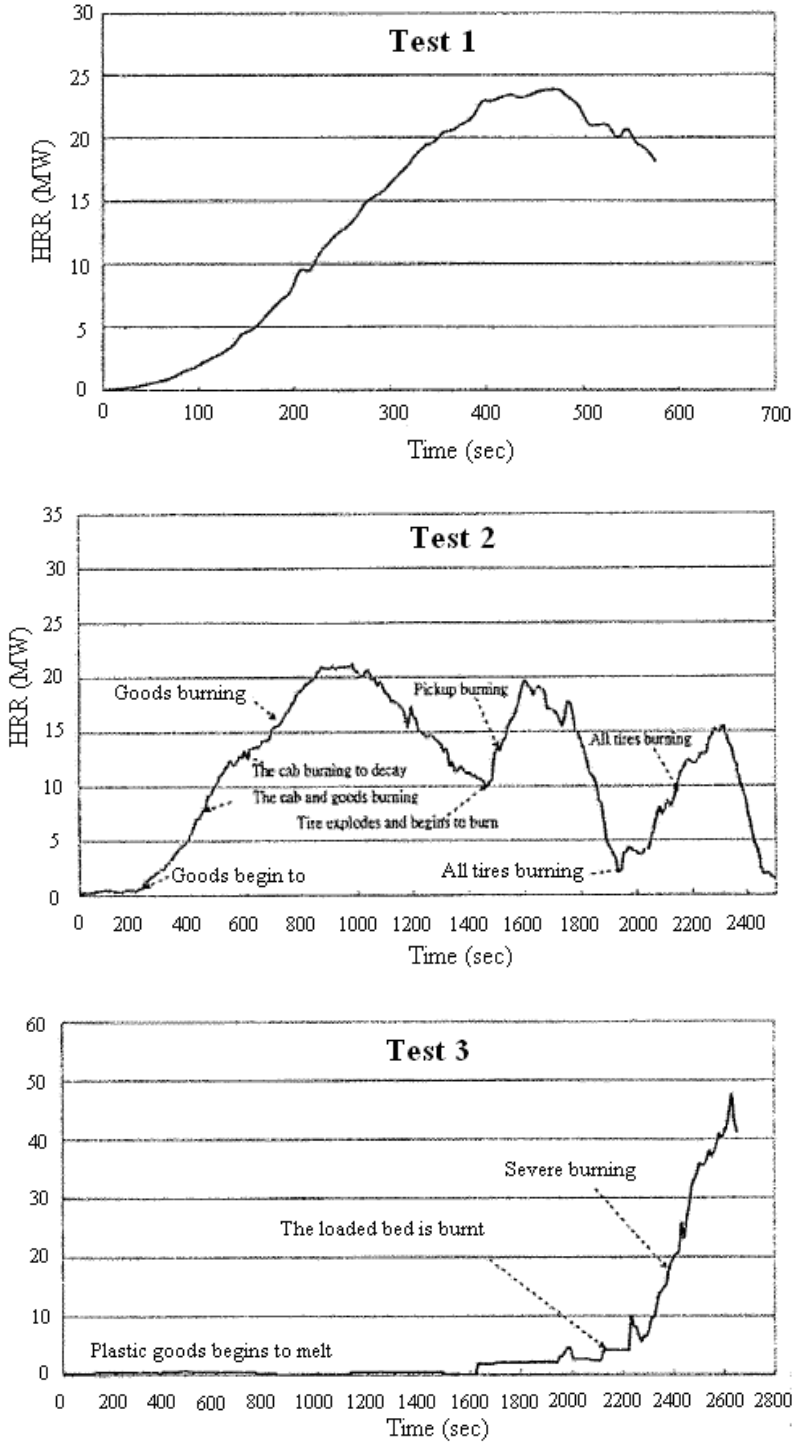

Figure 3.35: HRR 3.49Ton Truck with goods (reproduced from Chuang et al (2006))

From the above experiments depending on the type of goods, the peak HRR of a 3.49 Ton truck with goods can vary between 20.92 MW to 47.47 MW with a fast to ultra-fast growth rate.

3.3 Studies relevant to this research project

3.3.1 Tunnel geometry and ventilation condition

Forced ventilation systems can affect fires in tunnels in many ways. In some situations, increasing the airflow in tunnels may cause a reduction in the severity of the fire; however, in other situations, increasing the airflow will cause the fire to engulf a vehicle more rapidly, resulting in a substantial increase in the heat release rate of the fire (Jagger and Grant 2005).

At Heriot-Watt University, research projects were carried out to estimate the influence of longitudinal ventilation on fire size in tunnels. The estimates were based upon experimental data using a Bayesian methodology producing a probability distribution of fire size for an HGV, car and pool fire (Carvel et al 2004a).

The influence of tunnel geometry and ventilation condition on fire in tunnels can be described as:

$$Q_{vent} = k\psi Q_{open} \qquad \text{Equation 3.1}$$

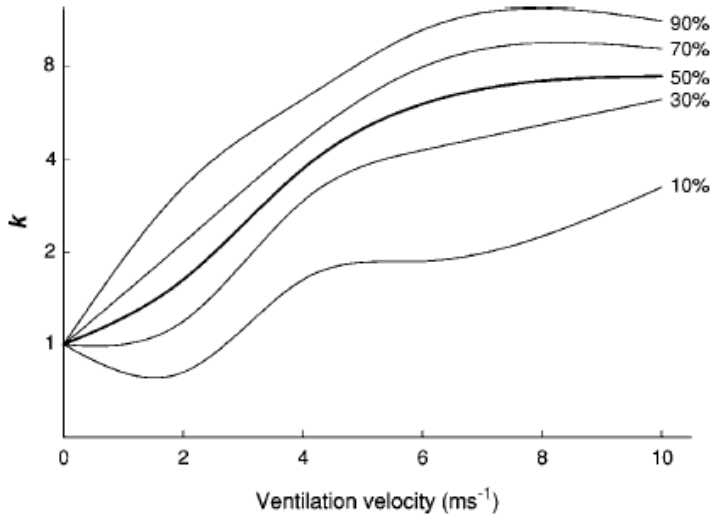

Figure 3.36: Probability percentile graph for HGV fire in tunnel (Carvel et al 2004a)

According to Carvel et al (2004a), in a situation where airflow is not restricted, a wider tunnel is safer as the HRR of the fire is less in a wider tunnel as compared with a narrow tunnel of the same height. However, it is important to note that the ventilation condition in the tunnel may have a bigger influence on the heat release rate than the tunnel geometry. It is important to consider both geometry and ventilation condition when making a design fire estimate.

From the fire tests mentioned above, it has been observed that the ventilation condition in the tunnel does affect the heat release rate. The large-scale fire tests conducted in Norway (refer to section 3.1.2) using wood cribs with (Figure 3.4) and without ventilation (Figure 3.3) illustrated that there is a substantial difference in heat release rate when the ventilation condition in the tunnel varies.

The fire test conducted in the EUREKA 499 on a Leyland DAF 310ATi type tractor with a trailer is another example of the influence of ventilation on heat release rate (refer to section 3.1.2). From the fire test measurements shown in Figure 3.9, there is a decrease in heat release rate when the ventilation was cut off between 13.5 to 16.5 minutes (EUREKA 1995). The result from this test showed that there is a significant difference in maximum heat release rate when the ventilation conditions in the tunnel are varied.

A fire test with truck loads consisting of 800 kg of wooden pallets, four tyres placed on top and a metal frame with a tarpaulin to simulate a small truck was performed in the Second Benelux Tunnel with various tunnel velocities (refer to section 3.1.3). Observations by Lemaire and Kenyon (2006) indicated that the fire growth with ventilation is about 2 to 3 times faster than the fire development without ventilation and the peak heat output for ventilated fire is about 1.2 to 1.5 times higher than a non-ventilated fire (Figure 3.11).

Another two tests were performed in the same tunnel as mentioned above; a car fire test with no ventilation and another with 6 m/s ventilation were conducted. It was found that at 6 m/s, the fire spread is not accelerated compared to the test without ventilation. The heat release rate is about 1 to 2 MW for half an hour before a peak of 5 MW occurs followed by decay linearly to 1 MW (Lemaire and Kenyon 2006). It is interesting to see that in this test

(Figure 3.10), fire spread to the rear of the car is delayed due to the ventilation in the driving direction resulting in lower heat release rate at the first half an hour of the fire development (Figure 3.37). From these tests, it is worthwhile to note that the location of fire ignition will affect the behaviour of the fire development as ventilation could cause an accelerated fire spread if the fire originates in the rear of a vehicle and delay the fire spread if fire occurred at the front of the vehicle (direction of airflow from rear to front of the vehicle).

Figure 3.37: Fire development of a car fire after 10 minutes. (reproduced from (Lemaire and Kenyon 2006))

3.3.2 Fuel load

One of the factors to consider when designing a road tunnel is the unknown nature of the potential fire load. In other transportation tunnels such as rail tunnels, the potential fire load can be reasonably estimated in view that the train and the passenger load is controlled by the operating agency. This is not the case for the typical road tunnel as an innocent looking truck may not necessarily be classified as hazardous cargo but may be carrying a load that is capable of supporting a fast-growing fire (Bendelius 2003).

A compartment fire is usually defined as either fuel-controlled or ventilation controlled. In the growth phase (pre-flashover stage) where there is sufficient oxygen for combustion, the fire is dependent on the flammability and amount of fuel. The fire is defined as fuel controlled. As burning progresses, the fire will continue to develop up to a point at which interaction with compartment become significant (flashover), resulting in the rapid

increase of heat release rate and temperature. The period after flashover is called the fully developed phase, during this period the heat release rate is dictated by the oxygen flow through the openings and the fire is said to be ventilation controlled. The mode of combustion (whether the fire is fuel-controlled or ventilation control) can be estimated using the equation as shown in Equation 3.2 (Ingason 2005).

$$\phi = 3000 \frac{\dot{m}_a}{\dot{Q}} \qquad \text{Equation 3.2}$$

where:

$\dot{m}_a$ = the mass flow rate of air supply (kg/s)

$\dot{Q}$ = the heat release rate (kW).

If $\varnothing$ (air-to-fuel mass ratio) is greater than 1 the fire is considered fuel-controlled. The last phase is the decay phase where the fire has consumed most of the fuel and the heat release rate will diminish. The different phase of a typical compartment fire is shown in Figure 3.38.

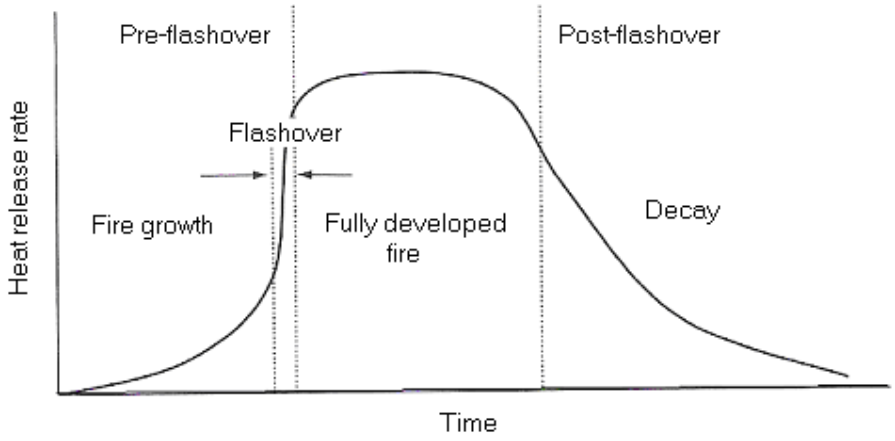

Figure 3.38: Different phases of a compartment fire (reproduced from Ingason (2005))

According to Ingason (2005) tunnels are often equipped with mechanical ventilation and the majority of fire in tunnels are often fuel controlled. Tunnel fires are not likely to grow to conventional 'flashover' (temperature in the compartment reaches 500–600^{o}C or

radiation to the floor of the compartment is 15 to 25 kW/m^2) due to large heat losses from the fire to the surrounding walls and the lack of containment of hot fire gases. Thus their burning rate would not be controlled by the rate of air supply to the fire. For such fires the burning rate and heat output is dependent on the amount of fuel in the tunnel.

A recent full scale fire test conducted by the Swedish National Testing and Research Institute SP in a road tunnel (Runehamar) in Norway showed that a fire in a heavy goods vehicle loaded with ordinary mixed goods can create a heat release rate between 66.4 to 201.9 MW. If a heavy goods vehicle carrying loads with substantial energy content catches fire in a tunnel, the fire can be extremely intense and burn for a long period of time. A discussion of this fire test taken from Ingason and Lonnermark (2003) is presented in section 3.1.5

3.4 Conclusion drawn from specific studies

The recent fire test programmes and research work that has been carried out by various researchers in the area of tunnel fires has greatly improved our understanding of tunnel fire behaviour. This work has provided invaluable insight and allowed development of better fire protection measures and ways to mitigate these incidents.

The above studies mentioned in this chapter highlighted the importance of tunnel conditions such as tunnel geometry; ventilation condition; fuel load and location of fire ignition on heat release rate in a tunnel fire. In this research project, the effect on tunnel geometry and ventilation condition affecting the heat release rate will be examined. As the fuel load in the tunnel varies depending on the type of vehicles and the goods it is carrying, a risk analysis approach is adopted to address these issues.

Chapter 4:
STATISTIC ON VEHICLES FIRES IN SINGAPORE AND INTERNATIONAL FIRE INCIDENTS IN ROAD TUNNELS

The causes of vehicle fires are discussed in this chapter followed by an update on the vehicle fire statistics in Singapore. A history of tunnel fire incidents that have occurred internationally is also presented in this chapter.

4.1 Vehicles Fires

Vehicle fires have been occurring for as long as people have been using automobiles. A broken fuel line resulting in a spray of petroleum on a hot engine, overheating of a braking system and electrical spark malfunctioning are all possible causes of vehicle fire (Lee 2001). There is also a possibility of vehicle fire due to deliberate acts such as arson and collision. According to USFA (1999), the causes of a vehicle fire generally fall under the following four categories; the result of a faulty vehicle, the result of an act of carelessness such as discarded cigarettes on the upholstery, the result of arson or the aftermath of a collision.

There are many factors that could contribute to the cause of a fire hazard in a motor vehicle. Lee (2001) has provided a range of possible causes of a vehicle fire due to faulty vehicle, act of carelessness and arson. A few of these fire scenarios will be discussed in the subsequent section.

Engine and the fuel system fire (Lee 2001)

The engine is the heart of the vehicle. It converts heat into motion when the engine is started. The gasoline or diesel in the fuel tank is drawn through a filter system into the carburettor or direct injectors mounted on the engine top. Mixing of gasoline and air occurs and the mixture is fed into the engine cylinders. For the gasoline to burn as energy, it must be vaporized. The problem arises when the connection from the fuel line to the carburettor is a poorly fitted. When gasoline flows and collects on top of the hot manifold, it can give off vapours resulting in a fire in the presence of an ignition source.

Exhaust system fire (Lee 2001)

Some vehicle fire incidents are related to the emission control system (e.g. catalytic converter – Figure 4.1) connected to the vehicle's exhaust. Waste products are removed from the car's engine when the gases enter the exhaust pipe, the muffler and out to the rear tail pipe. A device known as the catalytic converter is used to hold a chemical substance

while the exhaust gases passes through; the reaction of the chemical substance with the hydro-carbon exhaust converts them into water and carbon dioxide through further burning of the pollutants. The temperature of the exterior converter can be very high due to the reaction that occurs inside the catalytic converter. A heat shield is often provided to protect the under body of the vehicle.

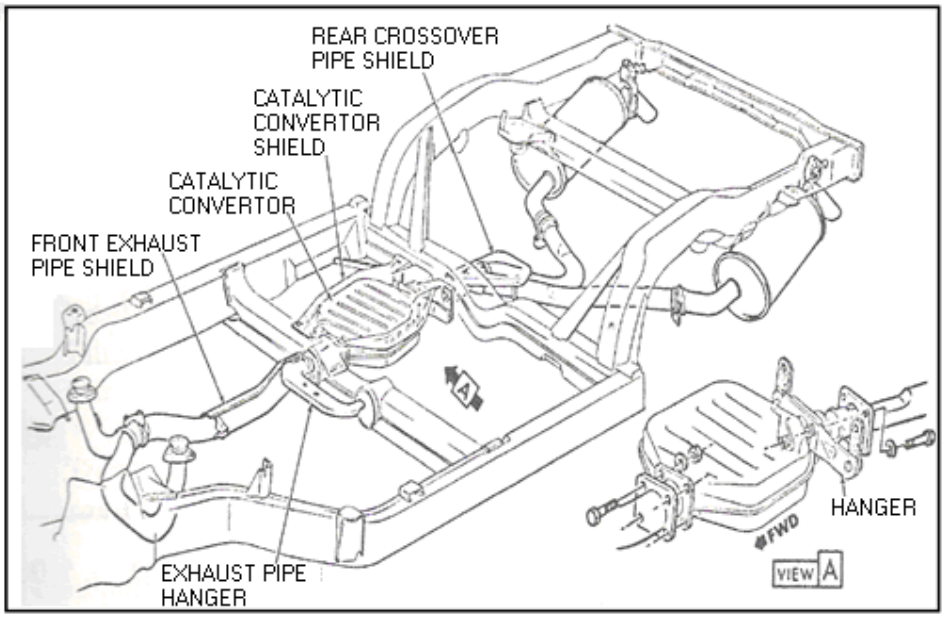

Figure 4.1: Catalytic converter location in exhaust system (reproduced from Lee (2001))

An example of vehicle fire hazard can be due to poor repair work or improperly positioning the catalytic converter too close to the underside of the vehicle body. If the normal design clearance on a proper vehicle assembly is not followed, the carpeting at the rear end of the vehicle is likely to catch fire.

Friction and tyre fire (Lee 2001)

In the presence of flammables such as petroleum or oil, a fire can occur if sparks are produced when parts are rubbed together. An example would be a fire caused by brake fluid spilling on the brake lining.

From Lee (2001), tyre fires are encountered more frequently in buses and heavy goods vehicles. The internal heat of the tyres increases when these tyres operate under stress of

frequent stop and go driving caused by the road surface friction. When their ignition temperature is reached, the tyres catch fire.

Turbo charger fire (Lee 2001)

The function of a turbo charger is to increase the engine power output allowing the vehicle to move faster by increasing the amount of fuel and air delivered to its engine cylinders. For this to work, a small turbine wheel is mounted in the exhaust system where flow of gases can cause the turbine to spin and drive a compressor in the intake manifold. This allows the compressor to force more air and fuel into the engine cylinders allowing a higher power output. However, the nature of this design often results in the turbocharger to operate at extremely high temperature. In the event where there are flammable materials in its proximity due to fuel leakage or faulty fuel line, a fire may occur.

Electrical system fire (Lee 2001)

The battery in the vehicle provides the flow of electric current and boots the voltage required to fire the spark plugs for engine ignition. In addition, it provides the electrical energy to operate headlights, interior lights signals, horn and other electrical accessories. The alternator is a generator which produces alternating current (AC) by connecting it to the belt of the engine crankshaft when the engine is operating. A voltage regulator is used to control electric output from the alternator to prevent the battery from overcharging. The rectifier converts the AC current to direct current (DC) to charge the battery.

During charging, electrolysis separates each water molecule into two parts hydrogen and one part oxygen within a storage battery. For continuous charging over a long period of time, the mixture in the ullage space may remain hydrogen rich. Generally there is small vent hole in the battery to allow hydrogen to escape into the surrounding air. Hydrogen can be extremely flammable when mixed with oxygen with an ignition temperature of approximately 579^{o}C.

The alternators can be another source of a vehicle fire. Connectors used in these units can develop high resistance if they are not properly connected. The heat output generated from the high resistance may cause melting resulting in a fire.

Smoldering material on upholstery (Lee 2001)

The result of an act of carelessness such as discarded cigarettes on the upholstery could lead to a fire occurring in a vehicle. According to Lee (2001), there is an experiment conducted where a lighted cigarette was placed on the seat cushion with the vehicle doors closed. Flames could be observed in the area where the cigarette was placed and shortly after, the seats and the entire passenger compartment were fully engulfed in flames.

Arson fire (Lee 2001) & (Kocsis 2002)

Arson is a serious offence and often results in substantial financial losses and environmental damage. The motives of an arsonist can be grouped into six categories. A profit motive; where the offender could benefit from an insurance claim on the property destroyed by the fire. Animosity crime; by using fire as a tool for revenge. Crime concealment; an attempt to destroy evidence from another crime. Vandalism; an abnormal fire-setting behaviour. Personality disorders and political objectives; where arson is committed to achieve political goals such as terrorism (Kocsis 2002). Details on the used of materials that are easily obtainable and not leaving trace of hydrocarbon related with accelerated fire by arson can be find in Lee (2001).

4.2 Vehicles Fires Statistic in Singapore

From the statistics provided by the Singapore Civil Defence Force (SCDF 2006a), there was a total of 4916, 5039 and 4702 fire incidents in Singapore within the years 2004, 2005 and 2006 respectively. Of the 4702 cases of fire which occurred in 2006, 161 cases were due to vehicle-related fires. Fire involving vehicles contributed to about 3.4 % of the total fires in Singapore from January to December 2006. Similar figures (3.3 % for 2004 and 3.6 % for 2005) relating to vehicle fire in Singapore have been observed in the past few years. Table 4.1 and Figure 4.2 is a breakdown of genuine fire calls during the period from January 2004 to December 2006.

Fire Description	**Jan – Dec 2004**	**Jan – Dec 2005**	**Jan –Dec 2006**
Residential Premises	3210	3056	2957
Non-Residential Premises	681	635	610
Non Building			
Vegetation	500	800	651
Rubbish (in open space)	231	241	216
Vehicles	177	168	161
Others (bus stop, tentage, canvas and vessels)	117	139	107
Total	4916	5039	4702

Table 4.1: Breakdown of genuine fire calls (SCDF 2005a) & (SCDF 2006a)

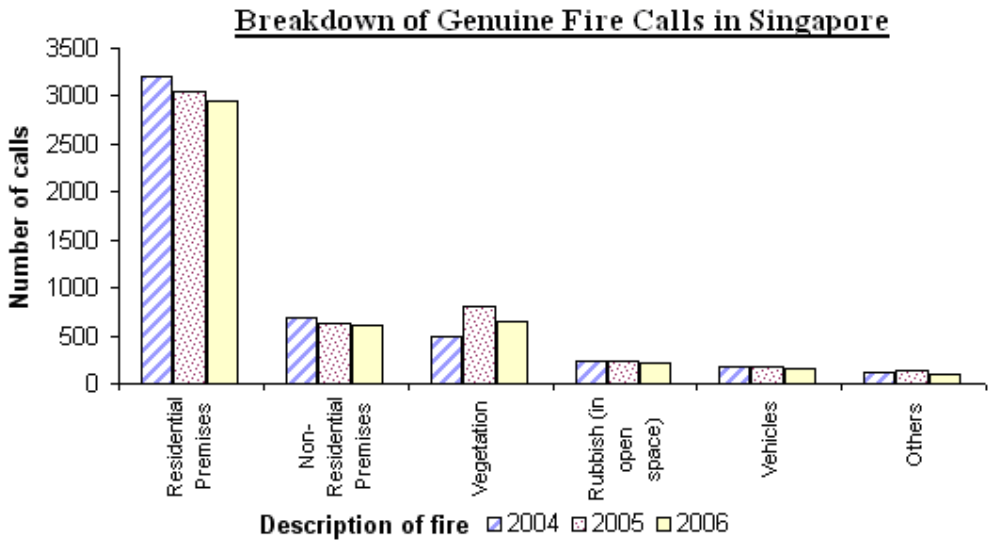

Figure 4.2: Breakdown of genuine fire calls (SCDF 2005a) & (SCDF 2006a)

Generally, a fire in a tunnel will occur due to the tunnel structure, system provisions in the tunnel or the vehicles and their goods that pass through the tunnel (FHA 1984). The trend of tunnel fire incident from past international tunnel fire incidents compiled in Appendix A of this thesis suggests that the cause of fire will continue to be originated from the vehicles (example: engine fire, brake overheating, electrical fault). To analyse the impact of vehicle fire, a breakdown on the causes of vehicle fire obtained from SCDF (2006b) is tabulated in Table 4.2 and Figure 4.3.

Cause of vehicle fire	2004	2005	2006
Overheating	55	62	59
Electrical Fault	76	63	55
Incendiary / Arson	56	59	54
Others*	32	21	24

Others include naked lights, spark, dropped lights and collision*

Table 4.2: Breakdown of vehicle fire incident in Singapore (SCDF 2006b)

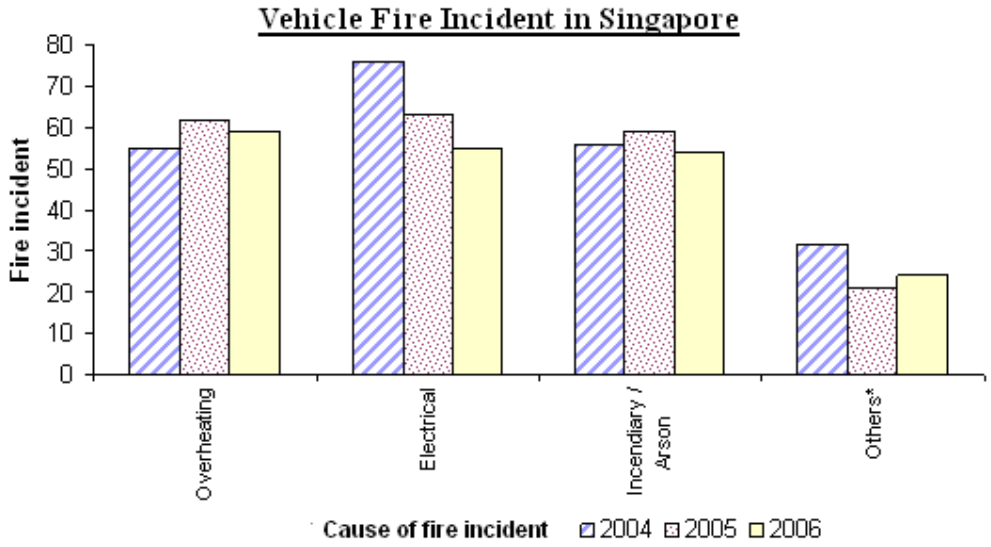

Figure 4.3: Breakdown of vehicle fire incident in Singapore (SCDF 2006b)

Past international tunnel fire incidents have shown that faulty vehicle, the act of carelessness and collision resulting in a fire were the main causes of tunnel fires (Appendix A). As the subject for this analysis is based on a road tunnel in Singapore, the vehicle fire statistics taken from the Singapore Civil Defence Force (SCDF) will be used for the quantitative risk analysis work as described in chapter 8.

From the statistical data shown in Figure 4.3, the cause of vehicle fire is mainly due to overheating or electrical (faulty vehicle) followed by arson (intentional); carelessness or collision (others). From the statistics, the number of vehicle fire incidents arising from the above causes were fairly consistent over the past few years (2004 to 2006).

4.3 History of Fire Incidents in Road Tunnel

The catastrophic tunnel fires in Europe have placed a focus on fire spread and fire development in tunnels. The need for a better understanding of fire development in such fires has become apparent (Ingason 2003). The most likely type of fire scenario can be determined from consideration of the items most commonly ignited and the ignition source from relevant fire incident statistics (ISO 13387-2 1999). Based on the information gathered from PIARC (1995), Carvel and Marlair (2005), Lonnermark (2005) and Johnson and Barber (2007), a list of fire incident is compiled and summarised in Appendix A.

From past tunnel fire incidents compiled in Appendix A, vehicle fault due to mechanical (engine fire, brake overheating, tyre fire, gear box and fuel tank leakage) or electrical (motor fire, short circuits) caused almost 48% of the tunnel fires. 28% of fires were due to collision and a minority of 1% were caused intentionally (Suicidal car crash). As the causes of fire reported in some tunnel fire incidents were not identified, the remaining 22% were categorised as unknown. There may also be some tunnel fire incidents that the author may not be aware of and hence not included in this compilation. The above compilation provides a general awareness of the magnitude and seriousness of tunnel fire.

Using the information from Appendix A, the trends on fire causes in tunnels and the types of vehicle most likely involved in a tunnel fire is presented in Figure 4.4 and Figure 4.5 respectively. It is evident that the largest share of vehicles involved in a tunnel fire is heavy vehicles followed by buses, cars and motorcycles. As mentioned by Reilly (2005), the factors that affect fire incidents are also dependent on the traffic mode and flow in the tunnel.

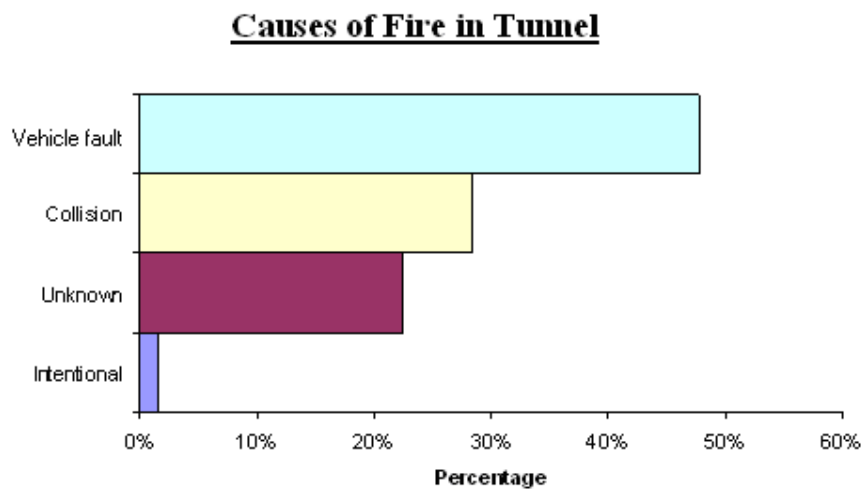

Figure 4.4: Causes of fire in tunnel (data base on Appendix A)

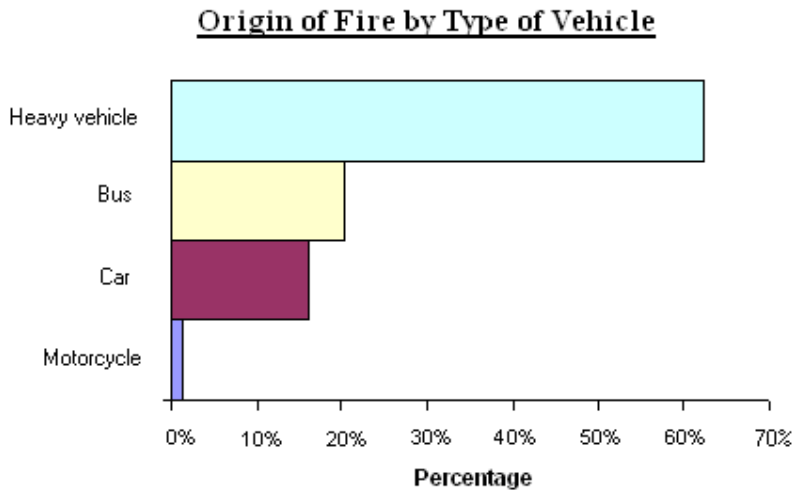

Figure 4.5: Origin of fire by type of vehicle (data base in Appendix A)

This chapter provides an insight on the trend of a fire and characterise the nature of fire problem in tunnels for the subsequent analysis work in this project. The detailed analysis work will be discussed in chapter 8 of this report.

Chapter 5:
TUNNEL ACCESS REGULATION AND HAZMAT TRANSPORT VEHICLE TRACKING SYSTEM IN SINGAPORE

Cheong M K, Thong M, Soh L T, Sng C H, See C S. Published as "Keeping Track" in *Fire Prevention & Fire Engineers Journal*, pp. 14-16, October 2007.

The regulation on vehicle access in Singapore road tunnel and the use of Hazmat Transport Vehicle Tracking System (HTVTS) is discussed in this chapter.

5.1 Tunnel Restrictions in Singapore

The transport of hazardous materials (hazmat) through a road tunnel can be a dangerous activity, with a fire or toxic spillage from the vehicles carrying the material having the potential to cause a significant incident involving multiple casualties. One way of reducing the risk is to prohibit or restrict vehicles that carry hazmat from entering and using tunnels. However, the introduction of such restrictions and the use of control measures will be ineffective unless accompanied by strict enforcement.

In Singapore, there are regulations prohibiting vehicles carrying hazmat from entering road tunnels. To ensure the rules are followed, a Hazmat Transport Vehicle Tracking System (HTVTS) has been introduced by the Singapore Civil Defence Force (SCDF). The move is part of a security and fire safety programme developed by authorities in the country. Its main aim is to prevent a terrorist incident involving the use of hazmat in a tunnel, although there are also benefits in terms of improving safety management on the road network and enhancing fire and life safety standards in tunnels. A comprehensive road network is critical both in sustaining economic activities and in providing better links for the public. However, in a country like Singapore, where land is scarce, there is an important balance to be struck in the development of the road network, since more land being used for road above ground means less land for other developments. In addition, the last decade has seen an increase in the number of vehicles in Singapore (LTA 2006). The authorities in Singapore therefore face a challenge in meeting the needs of a growing city that expects high standards in infrastructure, while at the same time keeping major arterial road that run through key business districts relatively free-flowing.

Tunnel Restrictions

In the past few years, more underground road tunnels of increasingly greater length have been built in Singapore. It seems likely that this process will continue. Road tunnels are generally built to overcome an obstacle such as structural above-ground development, or a facilitate vehicles crossing under a sea or river. They can provide better links for motorists

and can help to ease congestion in developed areas where improving the road network above ground is not feasible.

However, with an increasing reliance on road tunnels, it is necessary to put in place controls to ensure that fire and safety risk are minimised. As multi-fatality tunnel fires, such as the Mont Blanc tunnel blaze in March 1999 in which 41 people died, illustrates, the physical damage and economic consequences of a tunnel fire, not to mention the safety implications, can be very serious. Vehicles transporting hazmat through tunnels pose particular risks – for example, the leakage of petroleum from a tanker due to a rupture can result in fire and cause hazardous material and fumes being released into the enclosed tunnel space.

One method of controlling the risks is to restrict vehicles carrying hazmat from using the tunnel. Indeed, in Singapore, there are regulatory requirements limiting the type of vehicles that can access tunnel, as well as measures to enforce these regulations. In particular, the Road Traffic Act 2006 prohibits hazmat vehicles from entering road tunnels. These restrictions serve to reduce the fuel available for a major tunnel fire. However, restricting hazardous materials and placing controls on the actions of drivers will be ineffective unless accompanied by strict enforcement.

The rules and regulatory requirements for vehicles using tunnels vary considerably among countries. In Singapore, the Road Traffic Act 2006 (Chapter 276, Sections 114 and 140) and the Fire Safety (Petroleum and Flammable Materials) Regulations 2005 define the type of vehicles that are not allowed to access the tunnel. In addition, the SCDF's Circular No 4 outlines the measures for enforcing these regulations (SCDF 2005).

For example, the Road Traffic Act prohibits the following vehicles from accessing road tunnels:

i) *vehicles carrying any of the substances or articles set out in the Third Schedule of the Act - generally this includes dangerous goods such as flammable liquids or hazardous substances*

ii) *vehicles whose overall height (including any load) is 4.5m or above*

iii) vehicles whose overall width (including any load) exceeds 2.5 m

iv) vehicles whose overall length (including any load) exceeds 13 m

v) trailers conveying a standard container

vi) tanker carrying diesel fuel

To support this legislation, government agencies in Singapore have adopted a range of practical measures to minimise the risks. These include:

a) education drivers about the danger of the materials being transported

b) installing safety features and warning signs on vehicles, and carrying out regular inspections and reliability checks.

c) providing designated approved travel routes for vehicles carrying hazmat, which avoid road tunnels

5.2 HazMat Transport Vehicle Tracking System (HTVTS) in Singapore

The vehicle tracking system known as HTVTS has been introduced to ensure that vehicles carrying hazmat do not use road tunnels, in line with the regulations. The system is part of a wider effort to enhance security and fire safety in Singapore, particularly to prevent hazmat being used in a terrorist attack.

On 1 July 2005, the SCDF implemented Phase 1 of HTVTS. Under the system, all transport vehicles carrying bulk quantities of petroleum or non-petroleum flammable

material in excess of three metric tonnes need to be installed with Global Positioning System (GPS) tracking devices and alarm units. The vehicles can then be monitored by SCDF in real time using the GPS technology (Figure 5.1). The system can locate the exact position of these vehicles while they are on the move. In the event of any breach in transportation rules, such as deviation from approved routes or times, an alarm installed in the vehicle will sound and the system will alert the SCDF control centre. The centre will also be notified if there is an unauthorised removal or tampering of the tracking devices (SCDF 2006).

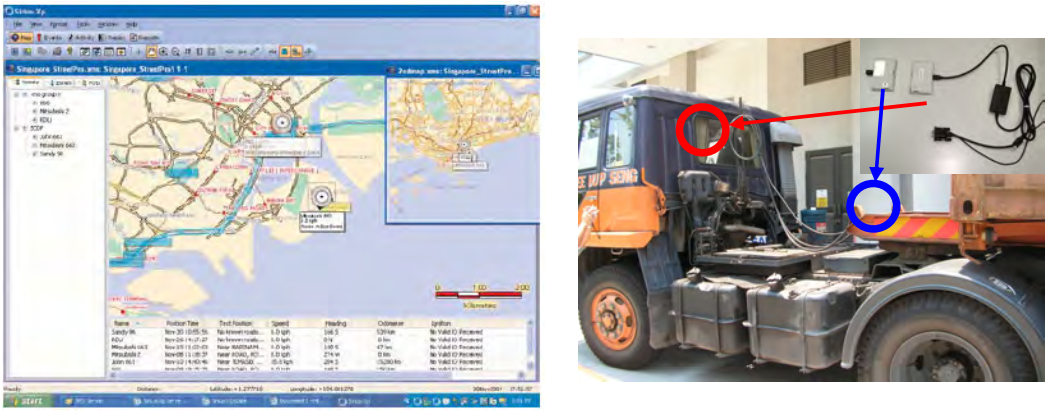

Figure 5.1: GPS to monitors HazMat vehicles and vehicle tracking devices

In addition, all local foreign registered vehicles that carrying petroleum and other flammable materials – such as road tankers, prime movers, trailer and lorries – are subject to a transport licensing scheme. To obtain a transportation licence, the vehicle has to undergo a third-party inspection to meet required safety standards and also has to be tested and certified by a professional engineer on a yearly basis. The driver of the licensed vehicle is required to hold a valid Hazmat Transport Driver Permit at all times when transporting petroleum and flammable materials. He must also attend a one-day hazmat transport driver course, conducted at the Civil Defence Academy, and pass the test at the end of the course before being issued with the permit, which is valid for two years.

All vehicles monitored by the HTVTS are required to display the approved orange-coloured vehicle registration plate (Figure 5.2) and to adhere to the approval routes and hours of transportation.

Figure 5.2: Orange colour vehicle plate (reproduced from (HTVTS 2006))

System Violations

Vehicles transporting hazmat are monitored by the duty officer at the SCDF control centre. In the event of any violation detected by the system, such as deviation from the approved routes, the alarm fitted in the vehicle will trigger the horn and hazard warning lights. The SCDF officer will then contact the registered company, which will required to contact the driver immediately and take corrective action (Figure 5.3).

Monitoring system *Control room* *SCDF officers*

Figure 5.3: Using GPS to monitors HazMat vehicles

The driver of the vehicle is required to stop by the road and contact SCDF for verification and to explain his reasons for deviating from the designated routes or times. In the event of the vehicle not stopping or the driver not being contactable within 2 minutes, the SCDF officer will inform the Singapore Police Force to dispatch their personnel to investigate the cause of the deviation.

In addition to investigating violations, routine checks are conducted by SCDF, in conjunction with Singapore's National Environment Authority (NEA) and Land Transport Authority (LTA), to enforce the rules.

There are currently around 660 vehicles installed with GPS tracking devices in Singapore SCDF (2007). Foreign hazmat vehicles entering from Malaysia are also required to rent the portable tracking devices when they cross at the border checkpoint. The tracking devices are fitted by SCDF personnel at the checkpoint (HTVTS 2006).

To date, the HTVTS has been effective in detecting vehicles that have deviated from the approved routes. The number of violations is not high and none have led to a catastrophic incident. A summary of the HTVTS violation detected is shown in Table 5.1.

Type of offence	**Jul to Dec 2005**	**Jan to Jun 2006**
Transportation along non-approved routes	48	28
Transportation with insufficient fire extinguishers on the vehicle	36	-
Transportation with no "Emergency Information Panel" and warning labels on the vehicle	32	-
Transportation (above 3 MT) without tracking device on the vehicle	10	2
Transportation without valid licence on the vehicle	15	58
Transportation beyond approved transporting hours	-	3
Transportation without HazMat Transport Driver Permit (HTDP)	9	16
Overnight parking (with LPG)	29	29
Supply of petroleum to non-licensed vehicle / premises	-	9
Total	179	145

Table 5.1: Type of HTVTS violation (SCDF 2006)

Phase 2 of the HTVTS implementation began in April 2007. In addition to monitoring the movement of hazmat vehicles using the GPS tracking devices, a strategy has been developed to fit immobiliser systems in hazmat vehicles. The immobiliser can be activated remotely, when necessary, in the event of a violation. It controls the throttle of the vehicle, restricting the fuel injection to the engine and forcing the driver to slow down and stop. The vehicle speed is reduced to 10 – 15 km/hr before coming to a gradual stop. SCDF and

police personnel are then dispatched to the incident. Prior to the activation of the immobiliser system, the vehicle's horn and hazard warning lights are automatically turned on to alert motorists so as to avoid any accidents. A flow chart showing the operation of the immobiliser system is shown in Figure 5.4.

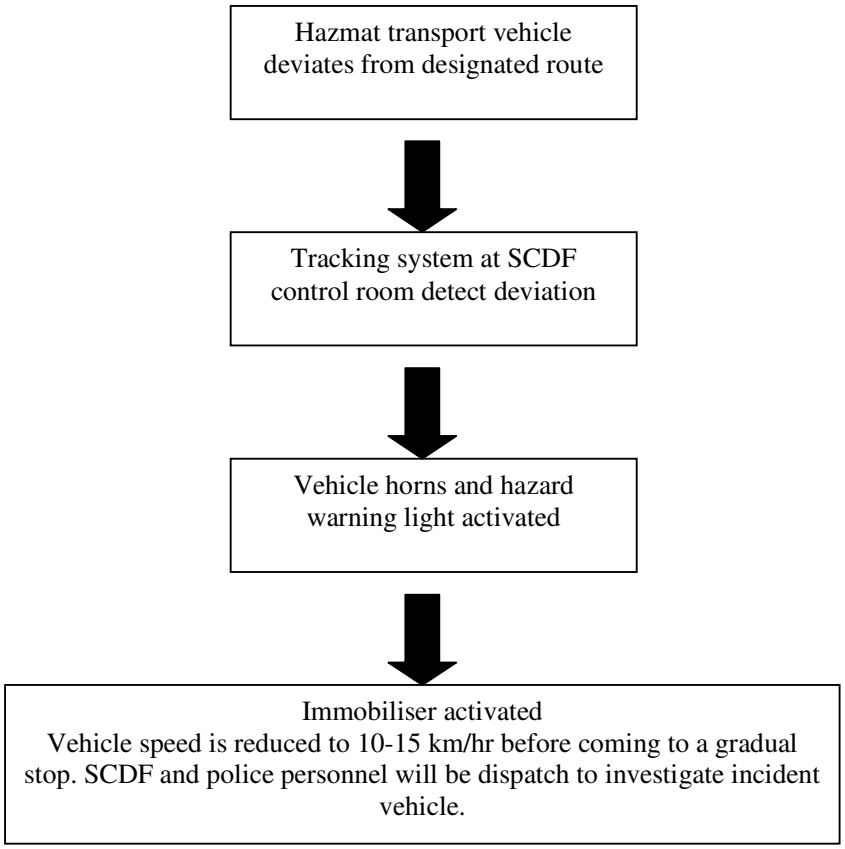

Figure 5.4: Operation of the immobiliser in Phase 2 HTVTS

The HTVTS is proving effective in minimising the risk of hazmat being used in a terrorist attack in Singapore, while also enhancing fire and life safety in road tunnels. In addition, Phase 2 of the system has further strengthened the requirement of the Road Traffic Act for a more effective management of vehicles carrying hazmat on Singapore roads.

Chapter 6:
THE URBAN ROAD TUNNEL IN SINGAPORE

This chapter describes the concepts and principles of the fire and life safety measures of an urban road tunnel in Singapore which is used as a subject for the analysis. An introduction to the system provisions and discussion on vehicle access rights in Singapore tunnels is also presented in this chapter. The concepts and regulations discussed in this chapter will be used for the later risk analysis work and FDS modelling work.

6.1 The Urban Road Tunnel in Singapore

The urban road tunnel in Singapore is a 9 km long motorway constructed as a dual-three lane tunnels connecting the main tunnel to the above ground road network through the tunnel slip roads. A schematic of the tunnel layout is shown in Figure 6.1.

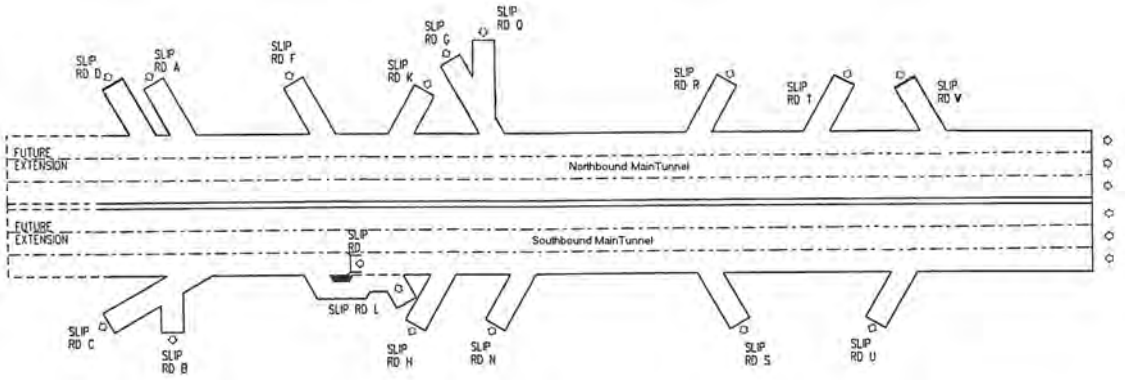

Figure 6.1: Tunnel layout

It consists of ventilation buildings (Figure 6.2) built along the tunnel alignment to house the mechanical and electrical equipment such as tunnel ventilation fans, electrical switchboards and generators.

The entire tunnel is manned by the control centres using

- Automatic incident detector (AID) system to detect accidents
- Linear detector system to detect fire
- CCTV cameras to view the conditions in the tunnel
- Integrated Traffic and Plant Management System (ITPMS)
- Tunnel ventilation system
- Tunnel fire alarm system and strobe lights
- Variable message sign (VMS)
- Radio re-broadcast system
- Lane use signal (LUS)
- Emergency telephone

The fire safety features in this tunnel are shown in Figure 6.2.

Tunnel Jet fans

Ventilation building

Escape staircase to above ground

Green arrow tunnel is open

Flashing Amber cross lane closure ahead get ready to change lane

Red cross lane is closed to traffic

Escape staircase

Cross passage door

Variable message sign (VMS) and lane use sign (LUS)

Emergency (SOS) phone

Hydrant, hosereel, call point beacan light , fire alarm, fire extinguisher

Fire engine cross passage door

Tunnel operation control centre (OCC)

Figure 6.2: Fire safety feature in tunnel

6.2 Tunnel geometry

The tunnel generally consists of two types of tunnel section (Main tunnel and slip road) (Figure 6.1). In the main tunnel (Figure 6.3), the southbound traffic is separated from the northbound traffic by a centre dividing wall. Cross passage doors are provided at 100 m intervals to expedite the evacuation of motorists in the event of a tunnel fire. For each direction of the carriageway, there is a 2.4 m wide shoulder and three 3.6 m wide traffic lanes with a tunnel structural height of approximately 6 m high (Parson 2001).

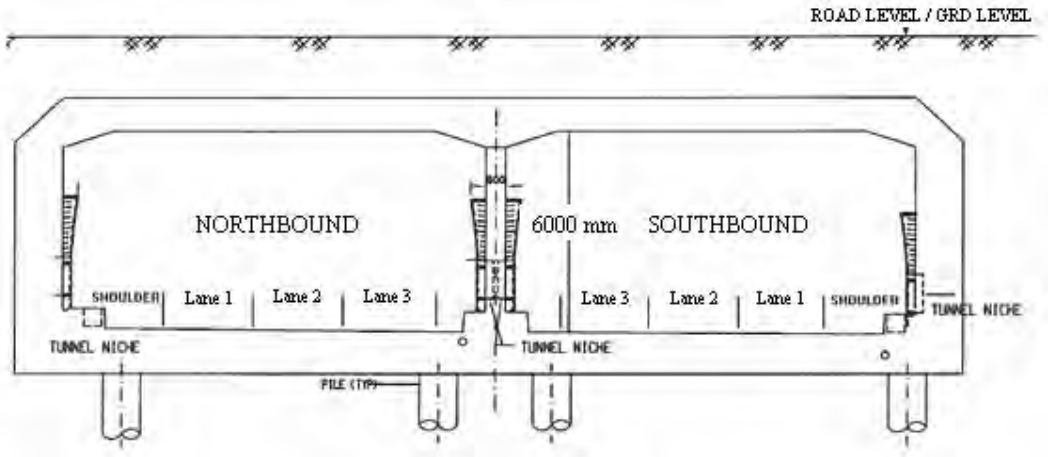

Figure 6.3: Dual three lane main tunnel

The slip road is used by vehicles to access and exit the main tunnels. The slip road (Figure 6.4) consists of two 3.6 m wide traffic lane and staircases connected to open ground are provided at 100 m intervals to facilitate motorists' evacuation in the event of a fire occurring on the slip road (Parson 2001).

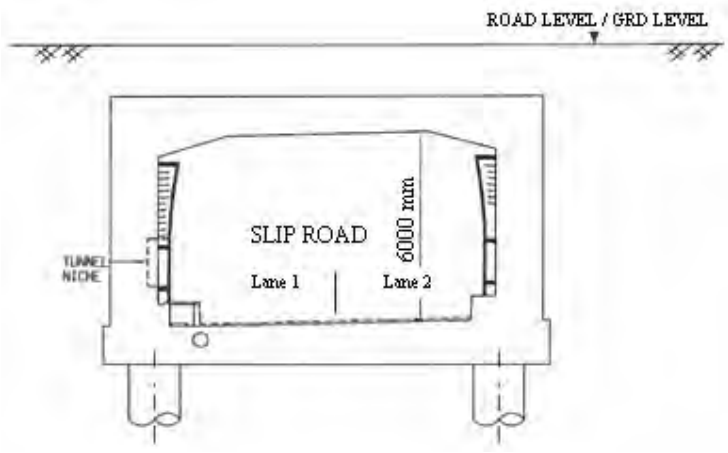

Figure 6.4: Two lane slip road

6.3 Fire incident respond and traffic management in tunnel

An Integrated Traffic and Plant Management System (ITPMS) is also in place to divert traffic above ground away from the exit slip roads allowing vehicles downstream of the fire site to be quickly driven away in the event of a fire. The following section discusses the fire incident respone adopted for the tunnel:

Fire incident detection

Prompt detection of a fire in the tunnel is an important factor in preventing a catastrophic fire incident from occurring. The detection criterion is set at 30 to 60 seconds and automatic incident detector (AID) and linear heat detector are provided (Parson 2001).

Verification of fire incident

When an incident occurrs, it is important that the tunnel operator is able to quickly assess the situation and respond to the problem immediately. Real time information of events occurring in the tunnel is important to the tunnel operator and CCTVs and emergency telephones installed in the tunnel provide the means to verify the severity of the tunnel fire. A 60 second time line is allocated to verify and identify a fire in the tunnel (Parson 2001).

Respone to fire incident

Upon confirmation of a tunnel fire, depending on the tunnel condition, appropriate respone measure includes closure of tunnel by a variable message signal (VMS) to stop additional vehicles from entering the tunnel. Vehicles already in the tunnel will be directed to the nearest exit and vehicles down stream of the fire will be able to drive away. Strobe lights and variable message signs are installed along the tunnel to inform motorists trapped upstream of the fire to evacuate the tunnel. Radio re-broadcast with break-in facilities is also provided to broadcast messages to the motorists. Pre-programmed messages will be broadcast to advise motorists of an incident in the tunnel and motorists in both the incident and non-incident tunnel would be able to receive the message (Parson 2001). The ventilation fans will be turned on to create a longitudinal airflow to prevent backlayering of smoke to the vehicles trapped upstream of the fire. This will create a smoke-free path

for the motorists trapped upstream of the fire to evacuate safely through the cross passage doors. Radio channels used by the emergency services are supported in the tunnel. The tunnel operator will also provide information to the fire service (SCDF) such as the best direction to approach the fire location (Parson 2001). Figure 6.5 illustrates the incident management process when a fire occurs in the tunnel.

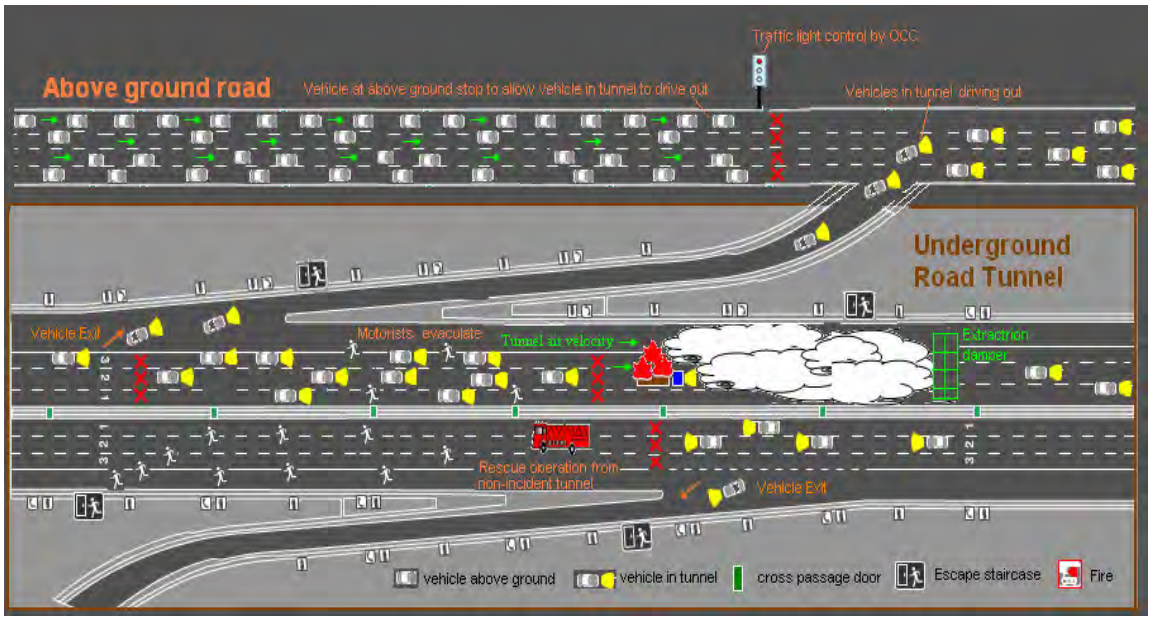

Figure 6.5: Incident management process in the event of a tunnel fire

6.4 Tunnel ventilation system

The traffic in this tunnel is uni-directional and a longitudinal ventilation system is adopted for the tunnel ventilation design. The airflow in the tunnel varies depending on the location of the tunnel and the tunnel fan operation mode. In normal operating mode, the tunnel fans are off. Whenever there is a traffic congestion in the tunnel leading to a build-up of carbon monoxide (CO), temperature and low visibility (due to emissions from vehicles), the sensors in the tunnel will be triggered and the tunnel fans will be subsequently turned on. In the event of a fire, traffic downstream of the fire site will be able to drive away while traffic upstream of the fire site may be trapped. The tunnel will be ventilated and smoke from the incident vehicles will be released to the atmosphere via exhaust stacks in the ventilation buildings (Figure 6.6). The operation of the tunnel ventilation fans is critical as

it will prevent the spread of smoke and heat to the trapped motorists upstream of the fire site. Sufficient airflow is necessary upstream of the fire site to prevent smoke backlayering so that a smoke-free path can be achieved allowing trapped motorists to evacuate to the non-incident tunnel section.

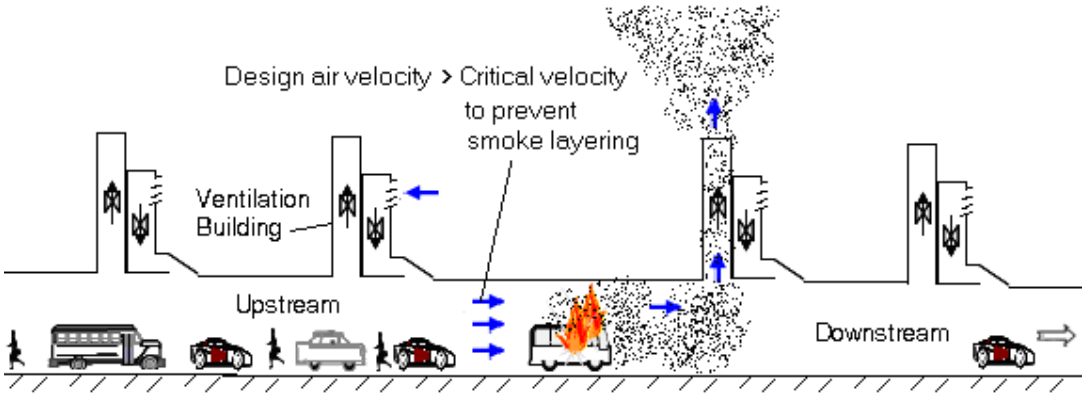

Figure 6.6: Smoke control and evacuation strategy in tunnel

The design air velocity in the tunnel to achieve critical velocity varies depending on the cross sectional area and gradient of the tunnel. The tunnel air velocity varies from 1.7 m/s to 5.2 m/s. These air flows are based on the tunnel ventilation design airflow for this tunnel. Various fire event scenarios considering detection time, operator reaction time and time required for the change of fan operational mode is shown in Figure 6.7 and Figure 6.8. Criteria based on NFPA 502 which requires the tunnel ventilation fans to operate from standstill to full rotational speed within 60 seconds or reversible fans completing full rotational reversal within 90 seconds are considered in the following fire events scenarios.

Normal to emergency ventilation mode	Time after ignition	Detector & fan operation status
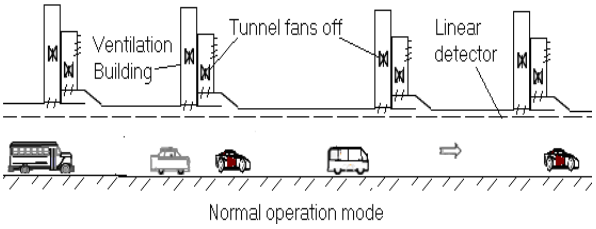	0 sec	No fire detected / Fan off
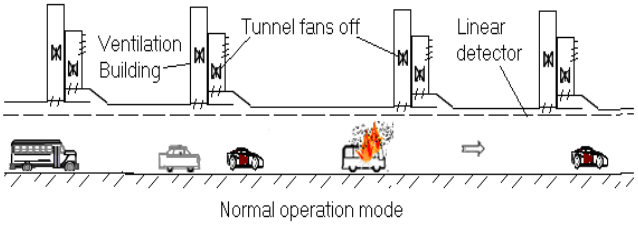	60 sec	Fire detected / Fan off
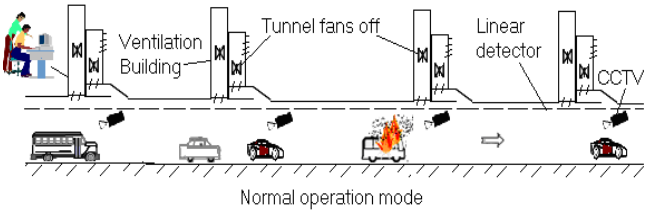	120 sec Verification	Fire detected / Fan off
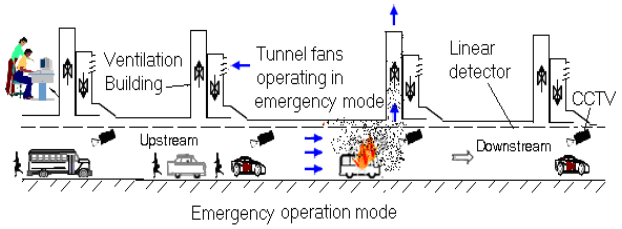	300 sec Respond	Fire detected / Fan operating in emergency mode
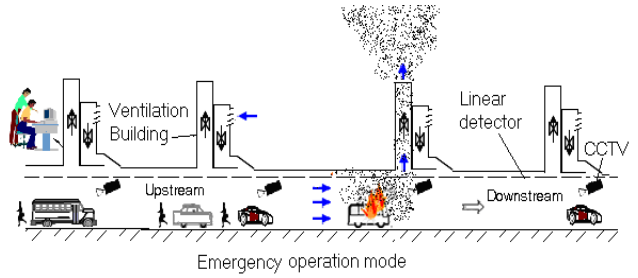	360 sec Respond	Fire detected / Fan operating in emergency mode at full rotational speed

Figure 6.7: Tunnel ventilation fans operation mode (normal to emergency)
(Information on the time of each event is taken from (Parson 2001))

Congestion to emergency ventilation mode	Time after ignition	Detector & fan operation status
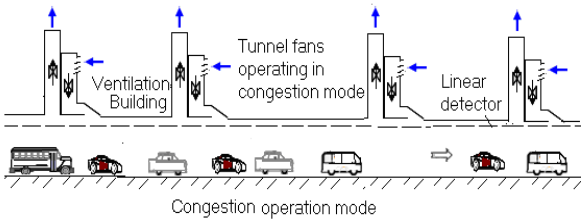	0 sec	No fire detected / Fan operating in congestion mode
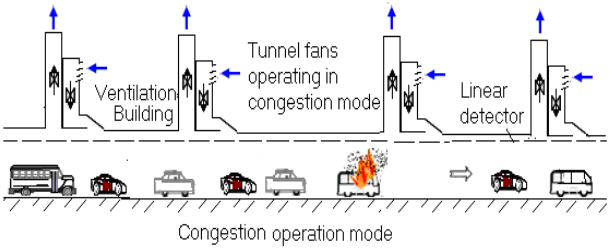	60 sec	Fire detected / Fan operating in congestion mode
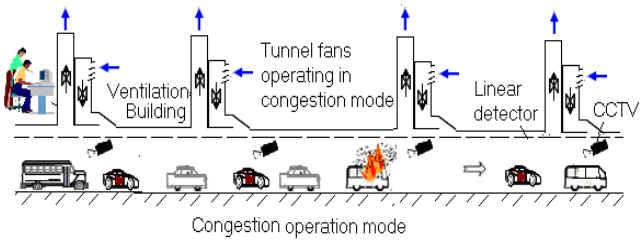	120 sec Verification	Fire detected / Fan operating in congestion mode
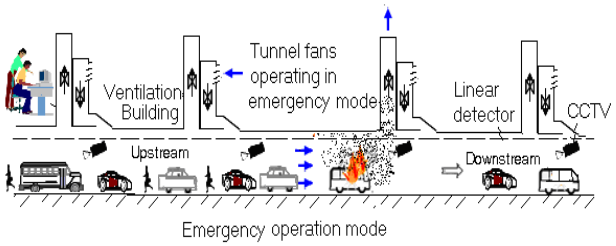	300 sec Respond	Fire detected / Fan operating in emergency mode
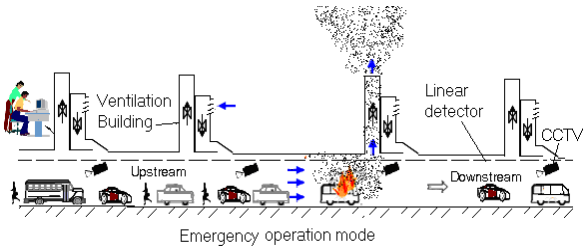	390 sec Respond	Fire detected / Fan operating in emergency mode at full rotational speed

Figure 6.8: Tunnel ventilation fans operation mode (congestion to emergency)

(Information on the time of each event is taken from (Parson 2001))

An example of a fire scenario showing the tunnel ventilation fans operating sequence is presented in Figure 6.9.

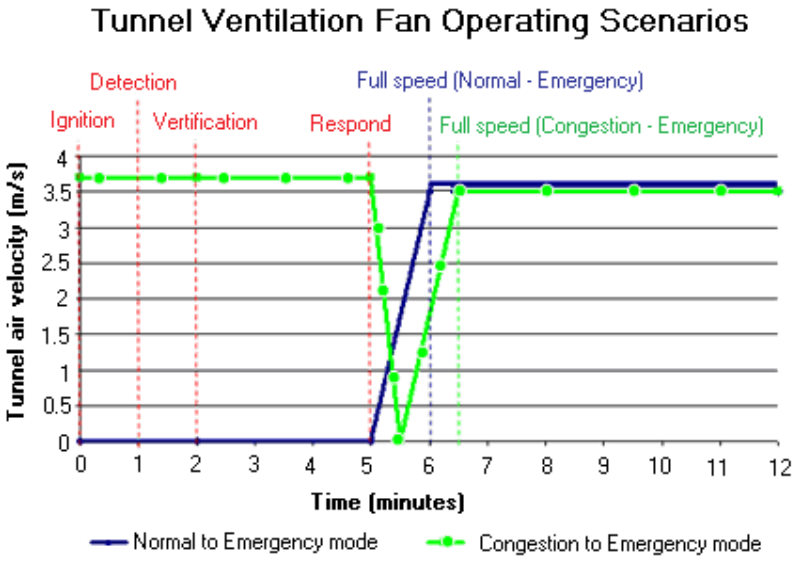

Figure 6.9: Examples of tunnel ventilation fans operating scenarios

6.5 Vehicle access right in Singapore road tunnel

According to (LTA 2006), vehicle types are classified into cars, taxis, motorcycles, buses and goods vehicles (Figure 6.10 and Figure 6.11). Under goods vehicles, they are further categorized into light goods vehicles (LGV), heavy goods vehicles (HGV) and very heavy goods vehicles (VHGV). The classification of goods vehicles are according to their laden weight where goods vehicles less than 3.5 tonne are categorized as LGV, vehicles with laden weight between 3.5 tonne to 16 tonne are HGV (example rigid truck) and vehicles more than 16 tonne laden weight are identified as VHGV (example tractor with trailer). As has been discussed in chapter 5, vehicles more than 13 m are prohibited from entering the tunnel and generally VHGV falls under this category.

From the Singapore road traffic act (Chapter 276, section 114 and 140), it is regulated that vehicles carrying dangerous goods such as flammable liquid or material and toxic substances, vehicles whose overall height (including any load) is 4.5 metres or more, overall width (including any load) exceeding 2.5 metres, overall length (including any load)

exceeding 13 metres, trailers conveying a standard container and tankers carrying diesel fuel (Figure 6.11) are prohibited in road tunnels.

Based on the above regulation, the types of vehicles that are allowed into the tunnel are motorcycles/scooters, cars, taxis, buses, LGV and HGV. From the observations of truck manufacturers, it is found that the length of most LGV and HGV varies between 4 m to 10 m and their width generally less than 2.5 m. Therefore if these goods vehicles do not carry any flammable or dangerous goods, they would be allowed to access the tunnel.

Figure 6.10: Types of vehicles allowed in tunnel

*Figure 6.11: Types of vehic*les not allowed in tunnel

6.6 Hazmat Tracking System

As mentioned in the previous sections, vehicles carrying hazardous materials in Singapore are not allowed to enter tunnels. The restriction on hazardous materials and placing controls on driver's action will be ineffective unless accompanied by vigorous enforcements. With the implementation of Hazmat Tracking System, this allows SCDF to track and remotely disable the engine of a Hazmat Transport Vehicle (HTV) in the event of a violation. Therefore the scenario of a hazardous goods vehicle entering a tunnel and resulting in a fire will not be considered in the analysis for this project.

Chapter 7:
FIRE DYNAMICS SIMULATOR (FDS)

This chapter provides a brief description of the assumptions and governing equations associated with the model used in FDS. The background theory of the numerical equations, prediction of fire growth and flame spread in FDS will be discussed. Most of the relevant materials for the discussion in this chapter are obtained from the FDS Version 4 technical reference guide (McGrattan 2005) and Cox (1995).

7.1 Hydrodynamics Model

FDS is a Computational Fluid Dynamics (CFD) model which solves numerically a form of the Navier-stoke equations for low-speed, thermally-driven flow with an emphasis on smoke and heat transport from fires. The partial derivatives of the conservation equations of mass, momentum and energy are approximated as finite difference and the solution is updated over time on a three-dimensional, rectilinear grid. Turbulence is treated as a Direct Numerical Simulation (DNS), in which the dissipative terms are computed directly, or as a Large Eddy Simulation (LES) technique to represent unsolved, sub-grid scale motion. The selection of using a DNS or LES turbulence model is dependent on the objective of the calculation and the resolution of the computational grid (McGrattan 2005). In view of practical reasons due to grid resolutions and computational power available, the LES turbulence model approach was used for this research project.

The conservation equations for mass, momentum, energy and species coupled with the equation of state are used in FDS. Each of these equations will be discussed in the following sections.

7.1.1 Conservation of mass

The conservation of mass is written as:

$$\frac{\partial \rho}{\partial t} + \nabla \rho u = 0 \qquad \text{Equation 7.1}$$

The first term represents the density change with time while u in the second term is the velocity vector in the u, v and w directions. This equation describes that the rate of mass storage within the control volume due to change in density is balanced by the net rate of inflow. At steady flow, it states that mass flow in is equal to mass flow out (Cox 1995).

7.1.2 Conservation of momentum

The conservation of momentum is written as:

$$\frac{\partial}{\partial t}(\rho u) + \nabla puu = -\nabla p + \rho f + \nabla \tau_{ij} \qquad \text{Equation 7.2}$$

The equation for conservation of momentum is derived from Newton's second law of motion. This is also known as the Navier Stoke equation which states that the sum of forces acting on a fluid element is equal to its rate of change of momentum (Cox 1995). The first two terms on the left-hand side of the equation define the rate of change of momentum and the terms on the right-hand side of the equation are the forces acting upon it where p represents pressure, τ_{ij} is the stress tensor acting on the fluid and f in the momentum equation consists of gravity plus other forces such as drag exerted by liquid droplets (McGrattan 2005).

7.1.3 Conservation of energy

The conservation of energy is written as:

$$\frac{\partial}{\partial t}(\rho h) + \nabla \rho hu = \frac{\partial p}{\partial t} + \dot{q}''' - \nabla q + \Phi \qquad \text{Equation 7.3}$$

The energy equation is derived from the first law of thermodynamics where the rate of change of energy within the control volume is equal to the rate of heat added to the control volume minus the rate at which work is done within the control volume (Abbott and Basco 1989). The term on the left is the net rate of energy accumulation within the control volume while the term on the right-hand side of the equation represent the heat release rate per unit volume from a chemical reaction ($\dot{q}'''$), the conductive and irradiative heat flux (∇q) and the dissipation function (Φ), the rate at which kinetic energy is transferred to thermal energy due to the viscosity of the fluid (McGrattan, 2005).

7.1.4 Equation of state

The equation of state is written as:

$$p = \frac{\rho RT}{M} = \rho TR\sum\left(Y_i / M_i\right) \qquad \text{Equation 7.4}$$

According to Abbott and Basco (1989), thermodynamics is the study of the equilibrium states of matter. In general, the state of a given mass of fluid in the control volume in an equilibrium state is specified by two parameters such as the density (ρ) and the pressure (p). If any two of the properties is fixed, the relationship between the other properties such as temperature can be determined. Equation 7.4 shows the equation of state used in FDS.

7.1.5 Conservation of species

The conservation of species is written as:

$$\frac{\partial \rho Y_i}{\partial t} + \nabla \rho Y_i u = \nabla \rho D_i \nabla Y_i + \dot{m}_i''' \qquad \text{Equation 7.5}$$

where fluid consists of a mixture of species, the transport equations for each species will need to be solved. The equations have the form as illustrated in Equation 7.5 where Y_i is the mass of the *ith* species, D_i is the diffusion coefficient of species i into the mixture and $\dot{m}_i'''$ is the production rate of the species i (McGratten 2001).

7.2 Combustion model

7.2.1 Mixture fraction combustion model

The two types of combustion models used in FDS are DNS and LES. The choice is dependent on the resolution of the computational grid. DNS calculation is available in FDS where a global one-step finite rate chemical reaction with the diffusion of fuel and oxygen can be modelled directly. In cases where grid is not fine enough to resolve the diffusion of fuel and oxygen, LES approach; a mixture fraction-based combustion model is used.

In a fire scenario, the actual chemical rate processes that control the combustion energy release rate are often unknown. Even if they are known, with the present computer resources, placing detailed description of the combustion process is beyond reach in view of the spatial and temporal resolution limits imposed. Therefore, the model adopted is based on the assumption that the combustion is mixing-controlled (McGratten 2005).

The combustion model based on mixture fraction involves infinitely fast chemistry kinetics. The general form of the combustion reaction is:

$$v_F Fuel + v_O O_2 \rightarrow \sum_i v_{P,i} \text{Pr} oducts \qquad \text{Equation 7.6}$$

The number v_i are the stoichiometric coefficient for the overall combustion process that react fuel “F” with oxygen “O” to produce the products “P”.

The assumption that the combustion is mixing-controlled implies that all species of interest can be described in terms of mixture fraction Z(x,t). The mixture fraction Z is defined as:

$$Z = \frac{sY_F - (Y_O - Y_O^\infty)}{sY_F^I + Y_O^\infty}; s = \frac{v_O M_O}{v_F M_F} \qquad \text{Equation 7.7}$$

where Y_F^I is the fraction of fuel in the fuel system, M_F is the fuel molecular weight and M_O is the oxygen molecular weight. By design, the value of Z varies from 1 in a region containing only fuel and Z = 0 where oxygen mass fraction takes on un-depleted ambient value Y_O^∞.

The mixture fraction satisfies the conservation law

$$\rho \frac{DZ}{Dt} = \nabla . \rho D \nabla Z \qquad \text{Equation 7.8}$$

The assumption where infinitely fast chemistry kinetics means that the reactions that consume fuel and oxidizer occur so rapidly that the fuel and oxidizer cannot co-exist and fuel and oxidizer simultaneously vanish defining a flame surface as:

$$Z_f = \frac{Y_O^\infty}{sY_F^I + Y_O^\infty} \qquad \text{Equation 7.9}$$

The above assumption leads to the "state relation" between oxygen mass fraction Y_O and Z as shown in Equation 7.10

$$Y_O(Z) = \begin{cases} Y_O^\infty (1 - Z/Z_f) & Z < Z_f \\ 0 & Z > Z_f \end{cases} \qquad \text{Equation 7.10}$$

An example illustrating the state relations between species of a typical fire base on wood is shown in Figure 7.1.

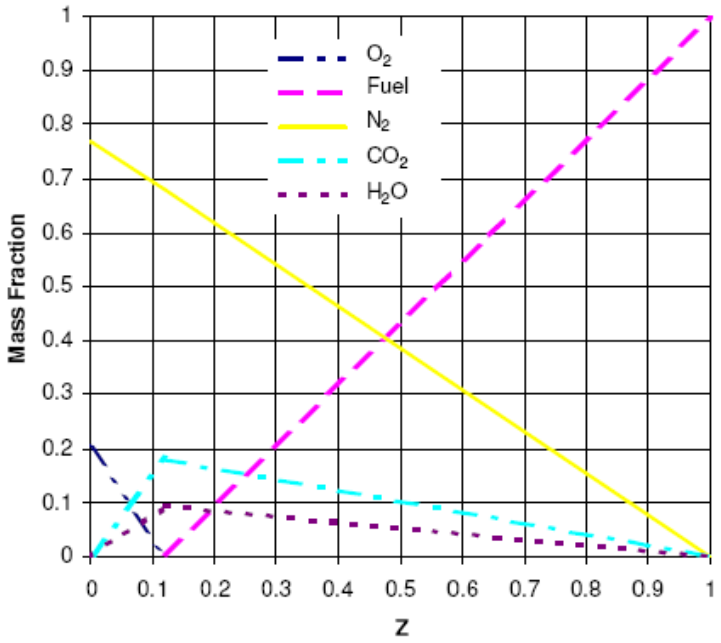

Figure 7.1: State relations for wood (reproduced from Yun (2006))

An expression for the heat release rate per unit volume can be derived based on Huggett's relationship oxygen consumption, where ΔH_O is the heat release rate per unit mass of oxygen consumed (about 13.1 MJ/kg for most fuels), and $\dot{m}_O'''$ is the mass burning rate based on oxygen consumption rate.

$$\dot{q}''' = \Delta H_{O2} \dot{m}_O''' \qquad \text{Equation 7.11}$$

7.2.2 Enhancement to the mixture fraction model

The mixture fraction model described in the previous section has several limitations, both numerical and physical. The numerical limitations are related to the grid resolution. When coarse grids are used, the accuracy of the fuel transport and combustion process is diminished resulting in the fire not being adequately resolved and an under-estimated heat release rate. To address the issue, an improvement to estimate the flame height is to use different values of Z to define the combustion region (McGratten 2005):

$$\frac{Z_f, eff}{Z_f} = \min\left(1, C\frac{D^*}{\delta x}\right) \qquad \text{Equation 7.12}$$

where C is an empirical constant (0.6 is used for all fire scenarios), δx is the nominal grid size and D^* is the characteristic fire diameter given as:

$$D^* = \left(\frac{\dot{Q}}{\rho_\infty c_p T_\infty \sqrt{g}}\right)^{\frac{2}{3}} \qquad \text{Equation 7.13}$$

Another issue with the coarse numerical grid is that a disproportionate amount of the combustion energy is released near the edge of the burning region. When a coarse grid is used and to prevent too much of the energy from being released too close to the burning region, there is a maximum bound imposed on the heat release rate per unit area of flame sheet. An analysis based on Heskestad's correlation (Equation 7.14) is used (McGratten 2005):

$$\frac{H}{D} = 3.7Q^{*2/5} - 1.02 \quad ; \; A = \pi r\sqrt{r^2 + h^2} \qquad \text{Equation 7.14}$$

where A is the conical in shape surface area, H is the flame height

Where a coarse grid is used and the surface area of a real flame is larger than that of a cone, the upper bound estimate will prevent too much energy from being released too close to the fire but high enough not to interfere with the calculation when the grid is well-resolved.

In terms of the physical limitation, McGratten (2005) mentions that simulations involving large-scale well-ventilated fires, the use of mixture fraction approach which assumed fuel and oxygen burn instantaneously when mixed would be a good assumption. However, if a fire is in an under-ventilated compartment, or if a suppression agent such as water is introduced, the fuel and oxygen may mix but may not burn. In addition, a shear layer with high strain rate would separate the fuel system from oxygen supply and prevent

combustion from occurring. A simple model for flame extinction has been introduced in FDS where the mixture fraction continues to be used to track the fuel mixing with the surrounding air but also to assess if it is more or less likely to support combustion. Figure 7.2 shows the oxygen-temperature phase space to determine whether combustion is allowed or not allowed to take place. In the situation where the gas environment falls in the "No Burn" zone, the state relation as shown in Figure 7.2 will no longer be valid for values of Z below stoichiometric, since now some fuel may be mixed with other combustion products.

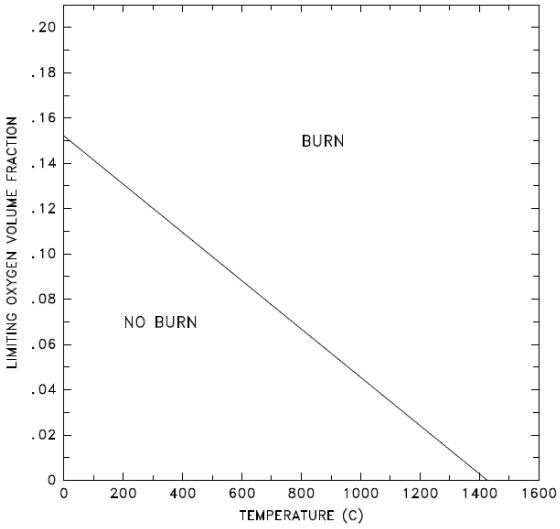

Figure 7.2: Oxygen-temperature phase space showing where combustion is allowed and not allowed to take place (reproduced from McGratten (2005))

7.3 Thermal radiation model

From McGratten (2005), the Radiative Transport Equation (RTE) for a non-scattering gas is used to compute the radiative heat flux.

$$s.\nabla I_\lambda(x,s) = \kappa(x,\lambda)\left[I_b(x) - I_\lambda(x,s)\right] \qquad \text{Equation 7.15}$$

where $I_b\,(x)$ is the source term given by planck function, $I_\lambda(x,s)$ is the radiation intensity at wavelength λ, s is the direction vector of the intensity and $\kappa(x)$ is the absorption

coefficient. In view of practical simulations, the radiation spectrum is divided into relatively small bands with a separate RTE derived for each band (Equation 7.16) and the total intensity is calculated by summing over all the bands (Equation 7.17).

$$s.\nabla I_n(x,s) = \kappa_n(x)\left[I_{b,n}(x) - I_n(x,s)\right] \ , \ n = 1....N \qquad \text{Equation 7.16}$$

$$I(x,s) = \sum_{n=1}^{N} I_n(x,s) \qquad \text{Equation 7.17}$$

In most large-scale fire scenarios, soot is the most important combustion product controlling the thermal radiation from a fire. As the radiation spectrum of soot is continuous, it is reasonable to assume that the gas behaves as a grey medium. The spectral dependence is grouped into one absorption coefficient where N is equal to 1 and the source term as

$$I_b(x) = \frac{\sigma.T(x)^4}{\pi} \qquad \text{Equation 7.18}$$

In calculations of limited spatial resolution for the source term, treatment in the neighbourhood of the flame sheet is required because temperature can smear out over a grid cell and therefore a considerably lower value is expected for a particular point in a diffusion flame. As it is dependent on the temperature raised to the fourth power, this will affect the radiation heat flux calculation in the simulation. In areas outside the flame zone, there is greater confidence in the computed temperature (*T*) and the source term can assume its value there.

$$\kappa I_b = \begin{cases} \kappa\sigma T^4/\pi & \textit{Outside flame zone} \\ \max(\chi_r \dot{q}'''/4\pi, \kappa\sigma T^4/\pi) & \textit{Inside flame zone} \end{cases} \qquad \text{Equation 7.19}$$

The equations to calculate the source term are shown in Equation 7.19 where $\dot{q}'''$ is the HRR per unit volume, χ_r is the local fraction of that energy emitted as thermal radiation, σ is the Stefan-Boltzmann constant and κ is the absorption coefficient where a sub-model know as RACAL is implemented in FDS (McGratten 2005).

7.4 Thermal boundary condition

There are a few ways in which the thermal boundary condition can be prescribed in FDS. By heating the surface allowing it to burn or the burning rate is prescribed as a burner. The type of thermal boundary used is dependent on the objective of the simulation analysis. Some of the thermal boundary conditions relevant to this project are discussed as follow:

7.4.1 Convective heat transfer to walls

The convective heat flux performed in an LES simulation is obtained from a combination of natural and forced convection correlations as shown in Equation 7.20 (McGratten 2005).

$$\dot{q}_c'' = h\ \Delta T \qquad \text{W/m}^2 \qquad \text{Equation 7.20}$$

where:

$$h = \max\left[C_{nc} \left|\Delta T\right|^{\frac{1}{3}},\ \ \frac{k}{L} 0.037\, \text{Re}^{\frac{4}{5}}\, \text{Pr}^{\frac{1}{3}} \right] \text{ --- W/m}^2\text{/K}$$

$\triangle T$ is the difference between the wall and the gas temperature, C_{nc} is the natural convection coefficient, L is a characteristic length related to the size of the physical obstruction, k is the thermal conductivity of the gas and the Reynolds Re and Prandtl Pr numbers are based on the gas flowing past the obstruction.

7.4.2 Pyrolysis Model

There are sub-models available in FDS for ignition and surface flame spread. Users are allowed to prescribe the heat release rate per unit area (HRRPUA) on the surface line or let the burning rate be predicted based on the fuel's thermal properties and its heat of vaporization (McGratten and Forney 2006).

The rate of pyrolysis depends on whether the HRRPUA or the heat of vaporization modelling approach is adopted by the user. If HRRPUA is adopted, the surface of the object will start to burn when it reaches its ignition temperature while for the heat of vaporization approach; the burning rate of the object is a function of the energy feedback from the fire via convection and radiation (McGratten and Forney 2006). The HRRPUA modelling approach is used for this project.

Where the surface material is assumed to be thermally thick, a one-dimensional heat conduction equation for the material temperature *T (x,t)* is applied in the direction *x* pointing into the solid (the point $x = 0$ represents the surface). The equation is written as (McGratten 2006):

$$\rho_s c_s \frac{\partial T_s}{\partial t} = \frac{\partial}{\partial x}\left(k_s \frac{\partial T_s}{\partial x} \right) \quad ; \qquad -k \frac{\partial T_s}{\partial x}(0,t) = \dot{q}_c'' + \dot{q}_r'' - \dot{m}'' \Delta H_v \qquad \text{Equation 7.21}$$

where ρ_s, c_s and k_s are the temperature dependent density, specific heat and conductivity of the materials respectively; $\dot{q}_c''$ is the convective and q_r'' is the (net) radiative heat flux at the surface, $\dot{m}''$ is the mass loss rate of fuel and ΔH_v is the heat of vaporization. An assumption is made where fuel pyrolysis takes place at the surface therefore the heat required to vaporize the fuel is extracted from the incoming energy flux (McGratten 2006). An Arrhenius expression as shown in Equation 7.22 is used for the pyrolysis rate:

$$\dot{m}'' = A \rho_s e^{-E_A / \Re T} \qquad \text{Equation 7.22}$$

where *A* is the pre-exponential factor E_A is the activation energy and *R* is the universal gas constant. The *A* and E_A parameters are often not readily accessible for real fuels (McGratten and Forney 2005) and the mass flux critical (kg/m^2/s) and ignition temperature (^{o}C) is used instead for this research work.

For surface material assumed to be thermally-thin, its temperature is assumed uniform across its width, *T (t)* is affected by gains and losses due to convection, radiation and

pyrolysis. The thermal lag of the material is a function of the product of its density, specific heat and thickness δ. This expression is shown in Equation 7.23.

$$\frac{\partial T_s}{\partial t} = \frac{\dot{q}_c'' + \dot{q}_r'' - \dot{m}'' \Delta H_v}{\rho_s c_s \delta} \qquad \text{Equation 7.23}$$

The convective and radiative fluxes are summed over the front and back surfaces of the thin fuel. The individual value of ρ_s c_s and δ are grouped together as a product and the pyrolysis rate for thermally-thin fuel is as shown in Equation 7.22. The pyrolysis rate for a thermally-thin fuel is the same as for thermally-thick (McGratten 2006).

In this work, the burning object is assumed to be a homogenous solid that burns at the surface. Burning behaviour where the material burns internally, leaving char in the wake of a pyrolysis front that progresses into the material is not considered in the simulation. The rate at which liquid fuel evaporates and burns is also not considered in the analysis.

Chapter 8:
FIRE RISK ANALYSIS

Cheong M K, Spearpoint M J, Fleischmann C M, published as "Using Peak Heat Release Rate to Determine the Fire Risk Level of Road Tunnels" to *Journal of Risk and Reliability,* Vol 222, number 4, pp. 595 – 604, 2008.

A wide range of fire incidents can occur in a road tunnel, for example a fire in the cargo compartment of a goods vehicle; carelessness due to discarded smoker's materials or loss of vehicle control and a crash resulting in a multiple vehicle fire. The number of possible fire scenarios is numerous so for design applications, rather than attempting to analyse every possible event using a deterministic approach, a preliminary analysis using a quantitative risk assessment approach should be considered. This chapter presents a risk assessment methodology to identify the possible fire scenarios that can occur in a road tunnel in order to specify design fire requirements for smoke control systems. The analysis considers factors such as legislation, vehicle fuel load, traffic mix in the tunnel, vehicle accident rate and the causes of vehicle ignition.

8.1 Introduction

Fire incidents have occurred ever since road tunnels have been used as part of transportation networks and events have often led to multiple causalities (Carvel and Marlair 2005). Although there is no universally accepted definition of risk (Elms 2004), it is commonly defined as the product of likelihood of the events and its consequences (AS/NZ 4360 2004a) such that

$$Fire\ Risk = Probability \times Consequence \qquad \text{Equation 8.1}$$

For road tunnel fires, the probability component of the risk analysis depends on the likelihood of the various causes of fire. The consequence component can be obtained from the fire growth characteristics where the combustible material available as fuel may come from the tunnel structure such as the unlikely case of having combustible insulation or lining materials, the combustible elements of systems and services in the tunnel or more likely the vehicles and their goods that pass through the tunnel.

This chapter presents an approach to determining the fire risk level of a road tunnel using quantitative risk assessment by incorporating statistical data on traffic fleet and vehicle fire incident data. The chapter focuses on identifying credible design fire scenarios with higher fire risk levels so that they can be used for subsequent analysis involving tunnel smoke control design rather than being directly applicable to the risk analysis of injury or death. The fire risk level established from this approach can then be used as gauging criteria to identify potential tunnel fire scenarios thereby enabling further deterministic analysis work using computer modelling to establish the heat release rate in the tunnel. The use of computer modelling to obtain the fire size will be discussed in chapter 10 and 11.

8.2 Fire risk analysis

The first step in the analysis is to define the context and goals such that stakeholders (designers, tunnel operator, approving authority and fire service etc.) are aware of the risk involved. It involves identifying aspects of design and operation that are within or outside

the scope of the analysis. In this work a Fault Tree Analysis (FTA) technique is then used to identify the potential fire risk. Figure 8.1 shows the overall approach which involves the use of a probabilistic approach coupled with deterministic approach to establish a design fire for road tunnel smoke control design. A probabilistic approach can be used to identify the fuel load as it relates to the vehicle mix expected in the tunnel and the likely causes of ignition that have the greatest impact on the risk. Numerical modelling to determine the design fire size can then be carried out for different tunnel geometries and ventilation velocities for the identified fuel loads and ignition conditions.

It should be recognised that it is not possible to design a smoke control system for every potential fire that might occur in a tunnel. Depending on the length and usage of a particular tunnel it is feasible that in an extreme case up to several tens or hundreds of vehicles could be involved in a severe collision. The cost and practicality to design for such events is beyond what might be considered a reasonable worst case. Thus the selection of the design fire scenario is best made on the basis of a risk analysis and the peak rate of heat release becomes the critical consequence component in this analysis. In many tunnel smoke control system designs the peak rate of heat release is chosen without proper regard for the effect of the tunnel characteristics on the fire growth or the traffic mix expected to use the tunnel. Often the rate of heat release for a single vehicle fire taken from an experiment published in the literature and it is unlikely to account for the specific conditions within the tunnel being designed, the regulatory environment in place or the likely vehicle usage during the operation of the tunnel (Biollay et al 1999). The selection does not always consider whether such a vehicle is likely to enter the tunnel or whether a multiple vehicle collision scenario might be a more credible event. The type of vehicles allowed access to the tunnel is an important consideration when analysing the fire risk level. As vehicles on the road can vary from motorcycles to heavy goods vehicles or even a petrol tanker, the magnitude of their heat release rate in the event of a fire can vary significantly, restricting certain vehicles from entering the tunnel is therefore an effective means to reduce the tunnel fire risk.

Numerical modelling would aid in the determination of the heat release rate for a specific tunnel design but it is not practical to simulate every possible event through modelling simply because of the time it would take to run all of the simulations. Therefore before

performing any detailed numerical modelling work to establish the design peak heat release rate it is necessary to know the general fire risk and thus identify the fuel load to be included in the modelling. This is achieved by first performing a fire risk analysis to identify the credible fire scenarios in the tunnel by gathering information on the vehicle population of each vehicle category, the motor vehicle accident rate and the causes of vehicle fire incident; the probability of a faulty vehicle resulting in fire, probability of a careless act resulting in fire, probability of intentional act resulting in fire and probability of vehicle fire due to motor vehicle accident.

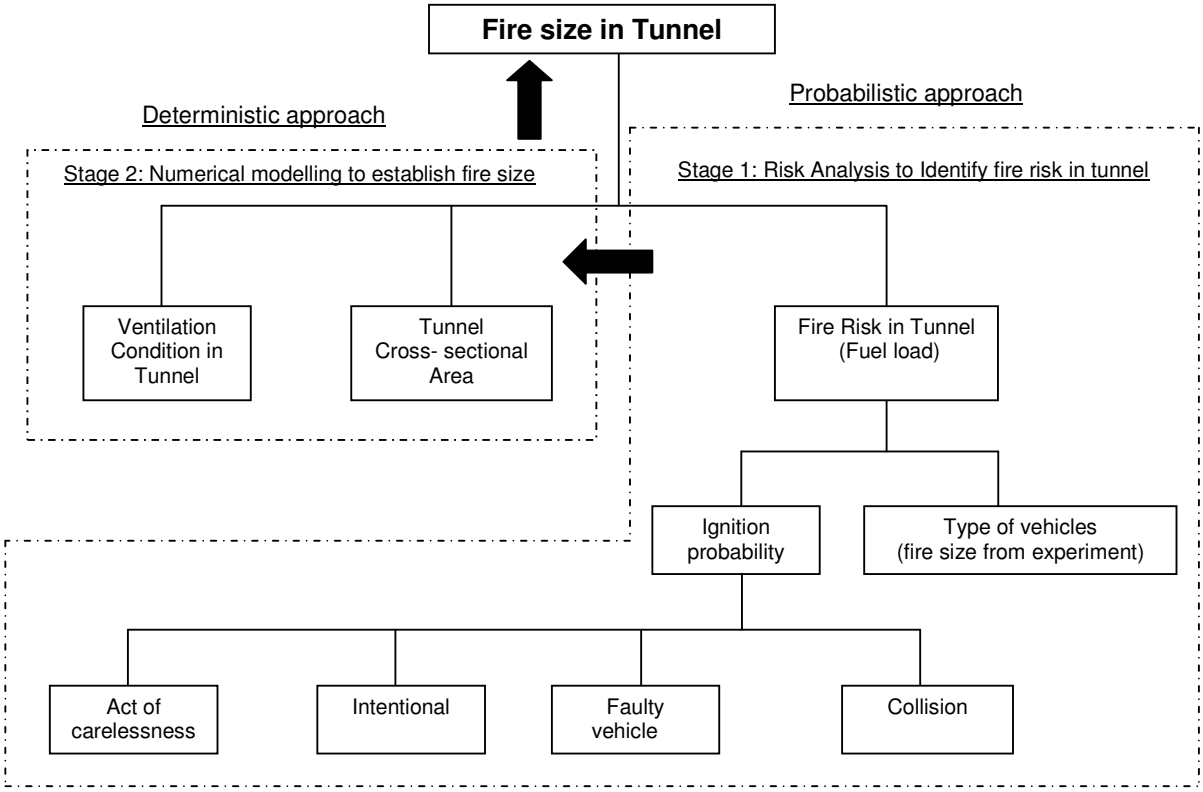

Figure 8.1: Approach to estimate fire size in tunnel.

8.2.1 Causes of vehicle fire

According to USFA (1999), the causes of a vehicle fire can be divided into four categories; the result of faulty vehicle, the result of an act of carelessness, the result of arson and the aftermath of a collision. From past international tunnel fire incidents compiled by Carvel and Marlair (2005), it appears that the causes of road tunnel fire will continue to originate from the vehicle itself. A damaged fuel line resulting in a spray of flammable fuel on a hot

engine, overheating of braking systems and sparks are all possible causes of vehicle fire. Careless acts include causes such as dropped lights, naked lights and discarded cigarettes on upholstery. According to Kocsis (2002), intentional acts can be grouped into six categories: a profit motive, animosity crime, crime concealment, vandalism, personality disorders (including suicides) and political objectives such as terrorism. Collision is an incident in which a vehicle impacts into anything that causes damage to itself, other vehicles or the tunnel facilities. Vehicle collisions could involve either single or multiple vehicles of various types.

8.2.2 Heat release rate of vehicles

The heat release rate of vehicle fire plays an important role in the risk analysis as a higher heat release rate would contribute to a higher fire risk level. The literature contains heat release rate data obtained from large-scale vehicle fire experiments conducted in tunnel and non-tunnel environments. Results from these experiments have shown that the heat release rate can vary from 1.24 MW to 202 MW (refer to Table 8.1). Reasons for this variation are due to the vehicle type; experimental geometry and procedure; material and quantity of the fuel package and ventilation conditions.

Full-scale vehicle fire experiments conducted in tunnels often have different cross-sectional areas. The effect of re-radiation will have an effect on the fire size as tunnels with a smaller cross-sectional area tend to yield a higher heat release rate value as compared to tunnels with a larger cross-sectional area (Carvel et al 2004a). Another major influence on the rate of heat release is the ventilation condition in the tunnel. Depending on the critical velocity in the tunnel (the minimum velocity to prevent backlayering of smoke), the design velocities are often different from one tunnel to another. It has been observed from tunnel fire experiments that tunnels with higher airflow tend to fan the fire resulting in higher heat release rates and this burning enhancement likely due to the improved mixing at higher velocities (Ingason et al 1994). The material, quantity and geometry of fuel package used in the experiment will also affect the heat release rate. This is especially true for goods vehicles as the fire size is often dominated by the characteristics of the fuel package that is burning.

The fire test programmes carried out by various researchers have provided valuable information to engineers and tunnel designers on the magnitude of a fire in the tunnel. Depending on the type of vehicle fires, tunnel geometry and ventilation condition, the heat release rate value obtained through these large scale experiments allows fire engineers to make a preliminary estimation of a design fire. A summary of the peak heat release rate obtained from these experimental studies is shown in Table 8.1.

Type of vehicle / Test series	Peak HRR (MW)	Testing location	Reference
Motorcycle / Scooter			
Scooter	1.24	Laboratory	Chen et al (2005)
Motorcar			
1.6 Ford Taunus	1.5	Laboratory	Mangs & Keski-Rahkonen (1994)
Datsun 160J sedan	1.8	Laboratory	Mangs & Keski-Rahkonen (1994)
Datsun 180B sedan	2	Laboratory	Mangs & Keski-Rahkonen (1994)
Dodge Caravan Sport (Engine fire)	1.5[a]	Laboratory	Santrock (2000)
Plymouth Voyaer (Under body fire)	4.8 [a]	Laboratory	Santrock (2001)
Chevrolet Camaro (Under body fire)	1.2 [a]	Laboratory	Santrock (2001a)
Chevrolet Camaro (Engine fire)	1.2 [a]	Laboratory	Santrock (2002)
Ford Explorer (Rear under body fire)	1.35 [a]	Laboratory	Santrock (2002a)
Ford Explorer (Mid under body fire)	0.5 [a]	Laboratory	Santrock (2002b)
Honda Accord (Under body fire)	0.8 [a]	Laboratory	Santrock (2003)
Honda Accord (Engine fire)	1.2 [a]	Laboratory	Santrock (2003a)
Austin Maestro	8.5	Canopy	Shipp & Spearpoint (1995)
Citroen BX	4.3	Canopy	Shipp & Spearpoint (1995)
Renault Espace People Mover u = 0.4 m/s	6	Tunnel	EUREKA (1995)
Opel Kadett with u = 6 m/s	4.7	Tunnel	Lemair and Kenyon (2006)
Bus			
Volvo Bus with u = 0.3 m/s	29.7	Tunnel	Ingason et al (1994)

Goods Vehicle			
Trailer with 10 ton load of wood and plastic, u = 3 m/s	201.9	Tunnel	Ingason & Lonnermark (2005)
Trailer with 6.3 ton load of wood and mattresses , u = 3 m/s	156.6	Tunnel	Ingason & Lonnermark (2005)
Trailer with 8.3 ton load of furniture and rubber , u = 3 m/s	118.6	Tunnel	Ingason & Lonnermark (2005)
Trailer with 2.9 ton load of plastic cup in cardboard boxes on wood pallets,u = 3 m/s	66.4	Tunnel	Ingason & Lonnermark (2005)
Leyland DAF 310ATi Tractor with 2 Ton of furniture, u = 3-6 m/s	125	Tunnel	EUREKA (1995)
Simulated small truck with 0.8 Ton of wooden pallets, 4 tyres with tarpaulin, u =0, 4-6 m/s and 6 m/s.	13, 19, 16	Tunnel	Lemair and Kenyon (2006)
Simulated track with 2.8 Ton of rubber tyres, wood and plastic cribs, u = 0.7 m/s	17	Tunnel	Ingason et al (1994)

Note: a – The fire was extinguished during the experiment.
u – Air velocity in the tunnel (m/s)

Table 8.1: Heat release rate from various fire experiments

8.3 Application of the risk approach

8.3.1 The urban road tunnel in Singapore

An urban road tunnel in Singapore is used as an example of the application of the risk analysis approach. The following discussion provides a brief outline of the system provisions, the regulation of vehicle access rights in the Singapore road tunnel network and identifies the operational aspects relevant to the risk analysis. The tunnel is a 9 km tunnel constructed with dual-three lane roadways. There are six ventilation buildings built along the tunnel alignment to house the mechanical and electrical equipment such as tunnel ventilation fans, electrical switchboards and generators. The entire tunnel is managed by an operation control centre and fire safety systems such as a linear fire detection system, the longitudinal

ventilation system and audio visual systems to inform motorists to evacuate in the event of a fire are available.

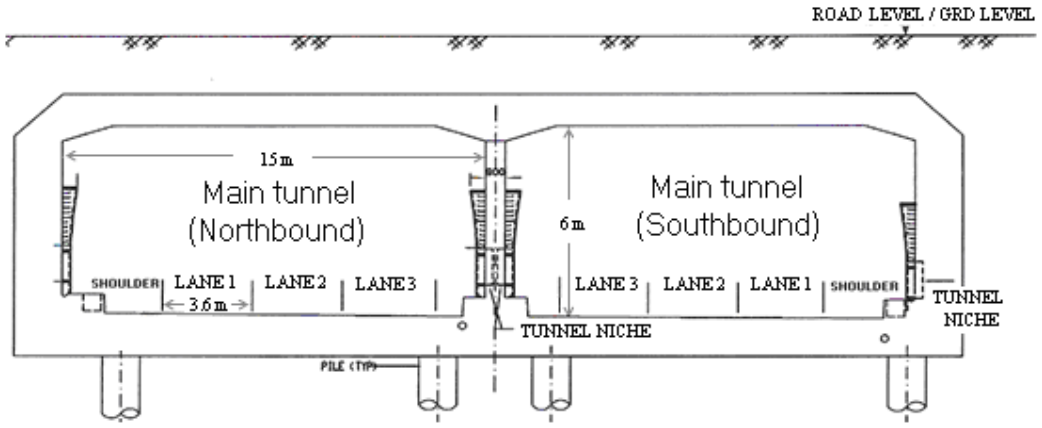

Figure 8.2: Cross section of the tunnel showing the tunnel dividing wall

The tunnel is bi-directional in which the northbound tunnel traffic is separated from the southbound tunnel traffic by a centre dividing wall (Figure 8.2). Cross passage doors are provided at 100 m intervals to expedite the evacuation of motorists. Airflows in the tunnel environment are dynamic and it is often not possible to maintain a single air velocity considering the tunnel cross sectional areas, gradients and the different operating modes such as normal traffic conditions, congested traffic conditions and emergency airflow conditions. Depending on the location in the tunnel and the operating mode, the design air velocity varies from 1.7 m/s to 5.2 m/s. In the event of a fire, the tunnel ventilation system will re-direct smoke and heat from the burning vehicle (or vehicles) and extract to the atmosphere via the exhaust stacks allowing motorists to evacuate from the incident tunnel as shown in Figure 8.3. The required critical velocities will be in the previously mentioned range depending on the specific tunnel conditions.

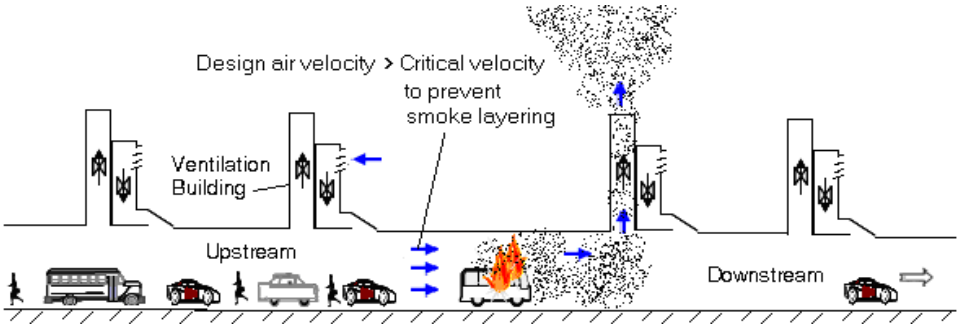

Figure 8.3: Smoke control and evacuation strategy in tunnel

8.3.2 Vehicle classification

In Singapore, vehicle types are classified into motorcycles, cars, buses and goods vehicles. Under goods vehicles, they are further categorized into light goods vehicles (LGV), heavy goods vehicles (HGV) and very heavy goods vehicles (VHGV). The classification of goods vehicles are according to their laden weight where goods vehicles less than 3.5 tonne are categorized as LGV, vehicles with laden weight between 3.5 tonne to 16 tonne are HGV (for example a rigid truck) and vehicles more than 16 tonne laden weight are identified as VHGV (for example a tractor with trailer) (LTA 2006). According to the Singapore Traffic Act (Traffic Act 2006), vehicles that are classified as VHGV and vehicles carrying hazardous goods such as flammable liquids or toxic substances are forbidden to enter road tunnels. Measures such as the Hazmat Transport Vehicle Tracking System (HTVTS); a GPS device that allows the Singapore Civil Defence Force to track and remotely disable the engine of vehicle carrying hazardous materials are in place to enforce these regulations (Chapter 5). Therefore the scenario of a hazardous goods vehicle entering the tunnel resulting in a fire is not considered in the urban tunnel risk analysis. Details of the projected vehicle traffic mix for the urban tunnel is shown in Table 8.2.

Vehicle description	Traffic mix %	Vehicle category	Percentage fleet by category
Motorcycle / Scooter	11.75	Motorcycle	11.75
Petrol Passenger Car	54.21	Car	56.76
Taxi	2.55		
Van	28.4	LGV	30.64
Light Goods Truck	2.24		
Medium Goods Truck	0.18	HGV	0.75
Heavy Goods Truck	0.57		
Omibus	0.03	Bus	0.1
School Bus	0.02		
Single-decker Bus	0.04		
Double-decker Bus	0.01		

Table 8.2: Tunnel traffic Mix for this project (Luk 2003)

8.3.3 Singapore vehicle fire and accident statistics

Databases are essential for many fire risk studies and in this work they are needed to identify the traffic statistics for the fire risk analysis. The fire incident reports from the Singapore Civil Defence Force (SCDF) showed that a total of 4916, 5039 and 4702 fire incidents occurred in Singapore in 2004, 2005 and 2006 respectively. Fire involving vehicles contributed to 161 (about 3.4%) of the total fires in Singapore between January 2006 and December 2006. Similar figures (3.3% for 2004 and 3.6 % for 2005) related to vehicle fires in Singapore has been observed. A detailed breakdown of the vehicle population in Singapore obtained from Land Transport Authority (LTA) (LTA 2006), the motor vehicle accident statistics obtained from the Singapore Traffic Police (Statistic 2006) and the causes of vehicle fire obtained from SCDF (SCDF 2006b) are shown in Figure 8.4 to Figure 8.6.

From 2004 to 2006, around 60% of vehicle fires in Singapore have occurred as a result of mechanical and electrical fault such as overheating, friction tyres, faulty fuel lines, faulty turbo charger or faulty electrical parts. The available data did not identify whether faults were more prevalent in one vehicle type over another and so the same probability has been used throughout the risk analysis. Although past statistics of vehicle fire due to carelessness in Singapore is lower than the other causes, the possibility of such events do exist and have been included in the risk analysis. When the types of intentional acts identified by Kocsis (2002) are considered it would seem that vandalism, personality disorders and political objectives are less probable since this urban tunnel is a monitored and controlled facility.

The probability of vehicle collisions is more difficult to assess from the available statistics. The SCDF data do not specifically deal with collisions as a single cause but combines with a number of other causes as indicated in Figure 8.5. Furthermore the data do not distinguish between a single vehicle collision with the tunnel structure and a multiple vehicle collision. The statistics also do not distinguish between vehicle types involved in a collision. This work therefore assumed the collision probability is constant regardless of the number and type of vehicles involved in a collision and also conservatively assumed

that the data for other causes was wholly due to collisions. The possible collision combinations (eg Car-Bus-HGV-HGV) that could occur in a multiple collision are numerous as the number of vehicles in the collision increases and combinations depend on the vehicle mix in the tunnel. Multiple vehicle collisions are considered in the risk analysis procedure however it would have been desirable to have had more detailed data so that probabilities could account for vehicle type, number and statistical contribution.

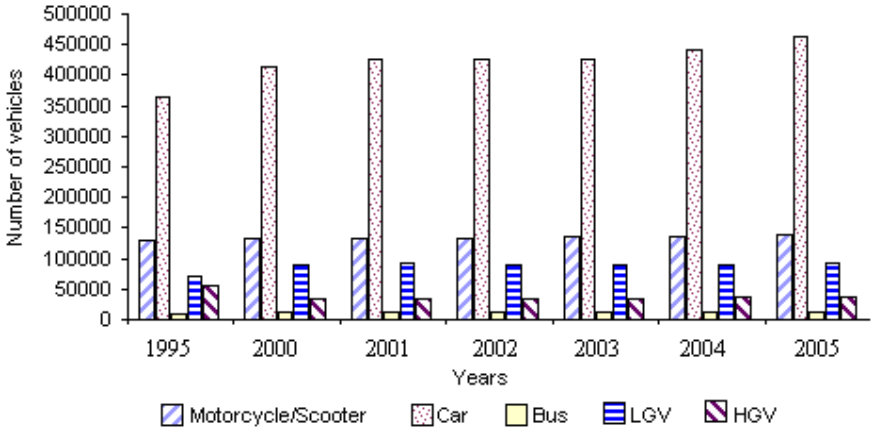

Figure 8.4: Motor vehicle population by vehicle type (LTA 2006)

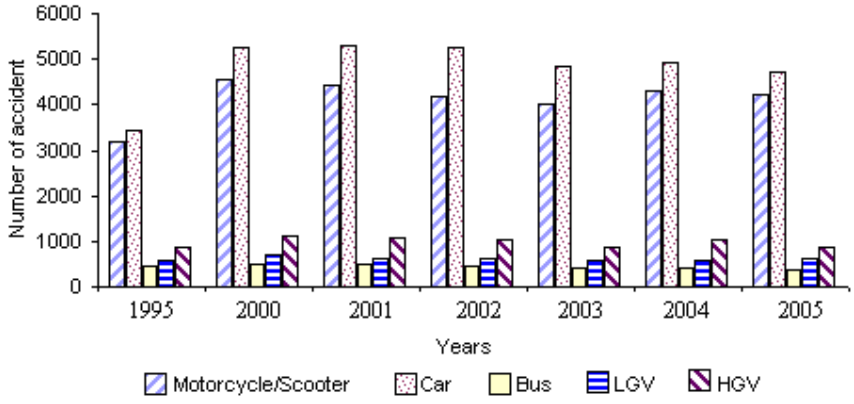

Figure 8.5: Number of motor vehicle accidents (Singstat 2006)

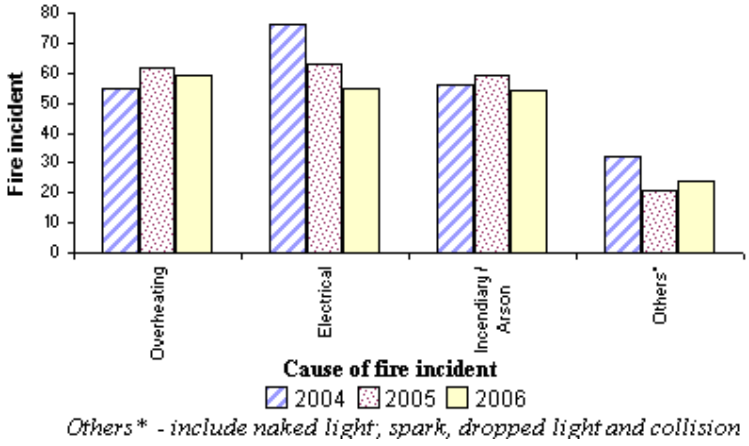

Figure 8.6: Vehicle fire incidents in Singapore (SCDF 2006b)

8.3.4 Selection of vehicle fire growth

The selection of the vehicle heat release rate is based on the data given in Table 8.1 and the selection criteria is based on the ventilation condition and fuel load closest to the urban tunnel condition. Based on these criteria Figure 8.7 shows the heat release rate curves used and the peak heat release rate values selected for the fire risk analysis; Scooter – 1.24 MW, Car – 4.7 MW, Bus – 29.7 MW, LGV – 16 MW, HGV – 201.9 MW

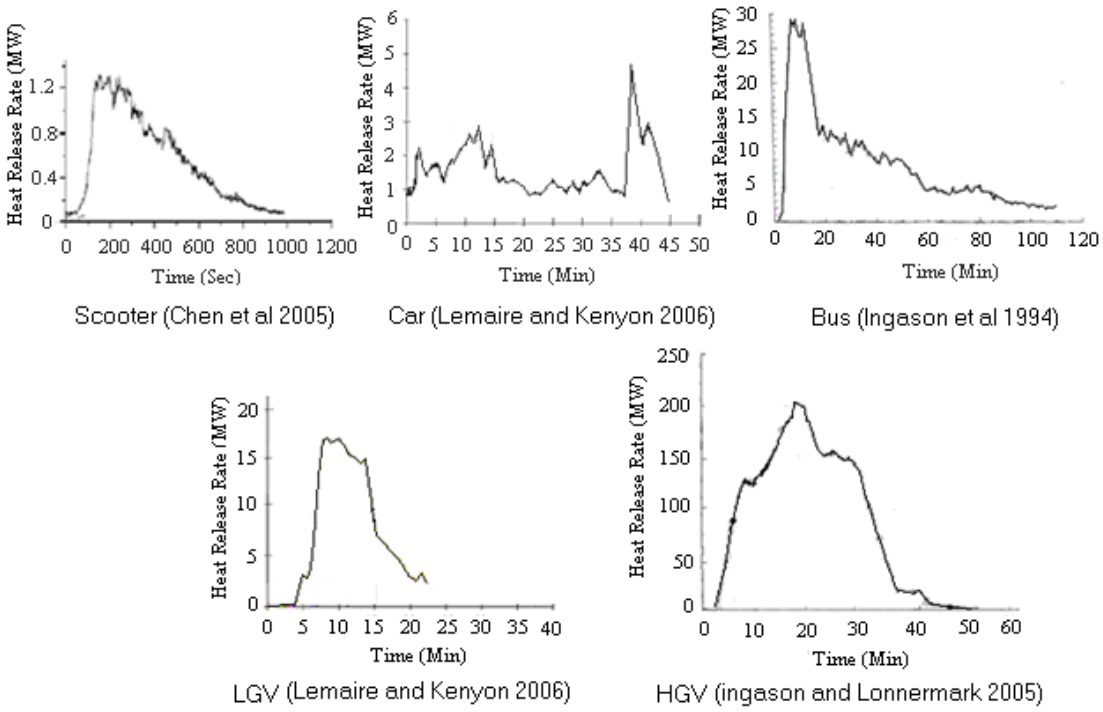

Figure 8.7: HRR curves from fire experiments selected for this tunnel analysis.

Heat release rates for fire scenarios involving multiple vehicles have not generally been reported in the literature. Given this state of current knowledge, the heat release rate used for a fire scenario involving multiple-vehicles collision assumes all incident vehicles ignite at the same time and the peak heat release rate is the sum of the individual vehicle heat release rates taken from the single vehicle fire experiments. Figure 8.8 shows typical heat release rate curves generated for vehicle fires involving multiple collisions using the heat release rate curves referred to in Figure 8.7. This concurrent ignition assumption is likely to produce a more conservative estimate of the heat release rate as compared to the situation in which fire propagates from one vehicle to another. More details of heat release rate curve for vehicles fire involving multiple collisions generated using the above approach can be found in Appendix B.

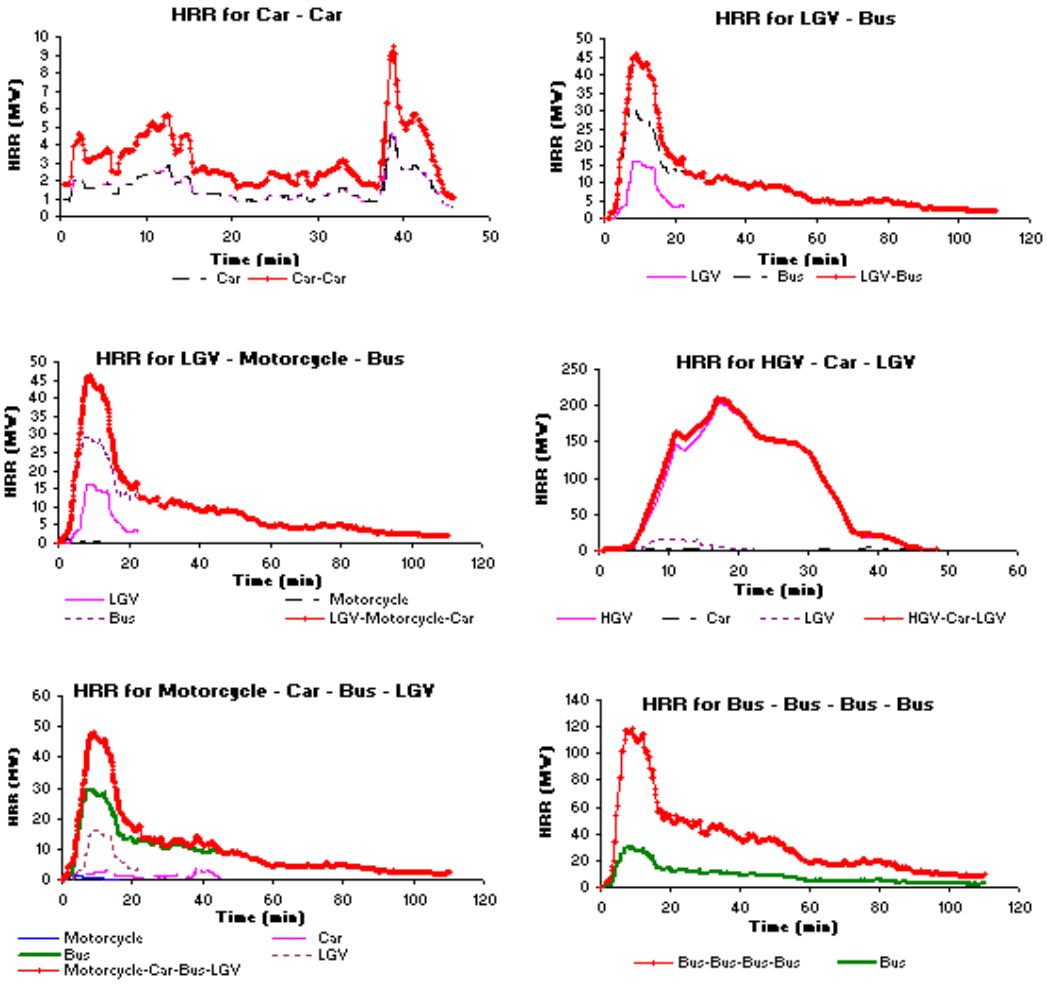

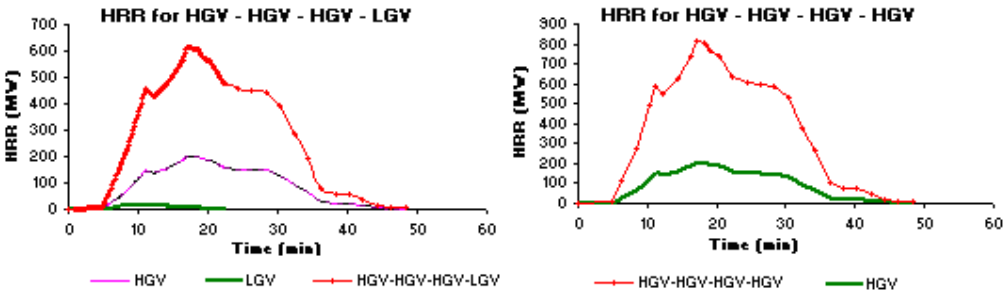

Figure 8.8: Heat release rate curve for vehicles fire involving multiple collisions

8.3.5 Tunnel fire risk

Figure 8.9 shows the fault tree logic diagram used to identify the fuel load in the urban tunnel. The analysis focused on the potential risk that could result in a fire based on fuel load by considering type and number of vehicles burning and the cause of ignition. Ignition causes include faulty vehicle, act of carelessness and intentional vehicle collision resulting in a fire. The cut-sets of each fire scenario that lead to fire risk in the tunnel can be determined from Figure 8.9. For example, the fire risk due to a faulty motorcycle is found from the motorcycle frequency in the urban tunnel multiplied by the frequency of motorcycle faults resulting in fire multiplied by the peak HRR of a motorcycle (i.e. branch A-B-P). Other risks are determined similarly from Figure 8.9.

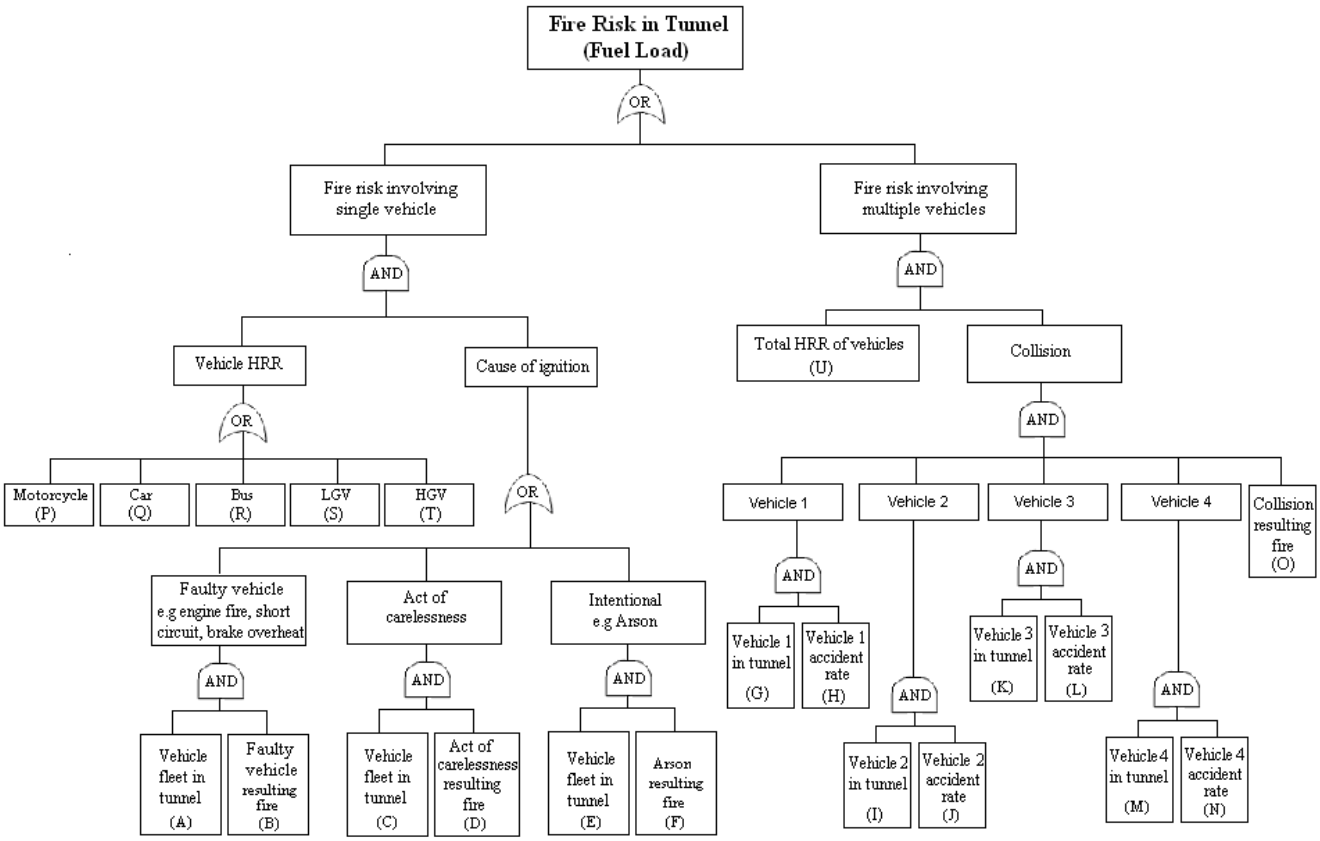

Figure 8.9: Fault tree logic diagram for fire risk in tunnel

Clearly a multiple vehicle fire has the potential to cause a high consequence event however this consequence needs to be combined with the likelihood of a particular multiple vehicle collision occurring. For example, the collision of several HGVs could lead to a significant rate of heat release but depends on the probability of these HGVs travelling in close proximity. This probability is a function of the traffic mix that is in the tunnel since the types of vehicles in a stream of traffic might generally be randomly interspersed. In view of the many possible vehicle collision configurations involving the types and number of vehicles involved, an event tree is used to supplement the analysis for vehicle collision resulting in a tunnel fire. The tunnel event tree analysis considers a total of up to a four-vehicle collision configuration.

Based on a collision configuration of up to four vehicles in combination, a total of 780 scenarios were generated using the event tree technique and these scenarios were further simplified to 125 scenarios in view of the repetition in the collision combinations (i.e. Bus – Car is the same as Car – Bus etc.). Table 8.4 shows the determination the fire risk level

in this tunnel due to collision which considers factors such as the type of vehicles, the traffic mix in the tunnel, the vehicle accident rate and the combined vehicle heat release rate.

Using the values in Table 8.2 and data from Figure 8.4 to Figure 8.6, the fire risk calculation considering vehicle fault, act of carelessness, intentional act and vehicle collision are shown in Tables 8.3 and 8.4. Using the '*Probability* x *Consequence*' approach, Table 8.3 uses the product of a type of vehicle in the tunnel, the probability of a cause of ignition and the selected peak HRR for a vehicle type to obtain the fire risk. The calculation of the fire risk from collision in Table 8.4 is a more complex procedure. It requires the determination of the probability of a vehicle type being present in the tunnel and accident rates for that vehicle type. These data were then used to determine the probability of combinations of vehicle types being involved in a collision. The combined vehicle collision probability, the probability that the collision would result in a fire and the total peak HRR of the vehicle combination (Figure 8.8) were multiplied together to obtain the fire risk. Vehicle accident rate were estimated from the motor vehicle statistics and although these statistics are not specific to road tunnels, they give the reasonable measure of the likelihood of a particular vehicle type being involved in an accident. For example, the total Singapore car population in 2005 is taken from Figure 8.4 and the number of cars involved in accidents in 2005 from Figure 8.5 so that the probability of car accident for year 2005 in Singapore is 4713 / 462966 = 1.02×10^{-2}. Similar calculations were performed for the other years and the average of these values was found to be 1.14×10^{-2}. Average accident rates were calculated for the other vehicle types in a similar manner. The probability of a vehicle collision causing a fire in the tunnel was determined from the average of the probabilities of a collision causing a fire in 2004, 2005 and 2006. For example, the number of vehicle fires due to other causes in 2006 was 24 and the total vehicle population was 771695 and therefore the probability is 24 / 771695 = 3.11×10^{-5} and the average of the 3 years of data was 3.47×10^{-5}. In view of the large number of scenarios involved for the vehicle collision analysis, only some of the vehicle collision results are presented in Table 8.4. The event tree and the complete list of the calculation results are shown in Appendix E & F.

Faulty Vehicle				
Type of vehicle	*Probability of vehicle type in tunnel*	*Probability of faulty vehicle resulting in fire*	*Peak HRR (MW)*	*Fire Risk*
M	0.1175	1.66×10^{-4}	1.24	2.42×10^{-5}
C	0.5676	1.66×10^{-4}	4.7	4.43×10^{-4}
B	0.0010	1.66×10^{-4}	29.7	4.93×10^{-6}
LGV	0.3064	1.66×10^{-4}	16	8.14×10^{-4}
HGV	0.0075	1.66×10^{-4}	201.9	2.51×10^{-4}
Act of Carelessness				
Type of vehicle	*Probability of vehicle type in tunnel*	*Probability of act carelessness resulting in fire*	*Peak HRR (MW)*	*Fire Risk*
M	0.1175	3.47×10^{-5}	1.24	5.06×10^{-6}
C	0.5676	3.47×10^{-5}	4.7	9.26×10^{-5}
B	0.0010	3.47×10^{-5}	29.7	1.03×10^{-6}
LGV	0.3064	3.47×10^{-5}	16	1.70×10^{-4}
HGV	0.0075	3.47×10^{-5}	201.9	5.25×10^{-5}
Intentional Act				
Type of vehicle	*Probability of vehicle type in tunnel*	*Probability of intentional act resulting in fire*	*Peak HRR (MW)*	*Fire Risk*
M	0.1175	7.58×10^{-5}	1.24	1.10×10^{-5}
C	0.5676	7.58×10^{-5}	4.7	2.02×10^{-4}
B	0.0010	7.58×10^{-5}	29.7	2.25×10^{-6}
LGV	0.3064	7.58×10^{-5}	16	3.72×10^{-4}
HGV	0.0075	7.58×10^{-5}	201.9	1.15×10^{-4}

Note: M – Motorcycle, C – Car, B – Bus, LGV – Light goods vehicle, HGV – Heavy goods vehicle
Probability of vehicle type in the urban tunnel at Singapore refer to Table 8.2
Probability of faulty vehicle, carelessness act and intentional act refer to Appendix C
Peak HRR refer to Appendix B

Table 8.3: Fire risk due to vehicle fault, carelessness and intentional act

Risk analysis due to collision

Collision											
Vehicle collision configuration	Vehicle 1		Vehicle 2		Vehicle 3		Vehicle 4		Probability vehicle collision resulting fire	Total vehicle HRR (MW)	Fire Risk Level
	Probability vehicle 1 in tunnel	Probability of vehicle 1 accident	Probability vehicle 2 in tunnel	Probability of vehicle 2 accident	Probability vehicle 3 in tunnel	Probability of vehicle 3 accident	Probability vehicle 4 in tunnel	Probability of vehicle 4 accident			
C	0.5676	1.14×10^{-2}	-	-	-	-	-	-	3.47×10^{-5}	4.7	1.06×10^{-6}
HGV	0.0075	2.64×10^{-2}	-	-	-	-	-	-	3.47×10^{-5}	201.9	1.39×10^{-6}
C-C	0.5676	1.14×10^{-2}	0.5676	1.14×10^{-2}	-	-	-	-	3.47×10^{-5}	9.4	1.37×10^{-8}
LGV-B	0.3064	7.02×10^{-3}	0.0010	3.53×10^{-2}	-	-	-	-	3.47×10^{-5}	45.7	1.20×10^{-10}
LGV-M-B	0.3064	7.02×10^{-3}	0.1175	3.08×10^{-2}	0.0010	3.53×10^{-2}	-	-	3.47×10^{-5}	46.2	4.41×10^{-13}
HGV-C-LGV	0.0075	2.64×10^{-2}	0.5676	1.14×10^{-2}	0.3064	7.02×10^{-3}	-	-	3.47×10^{-5}	210.1	2.01×10^{-11}
M-C-B-LGV	0.1175	3.08×10^{-2}	0.5676	1.14×10^{-2}	0.0010	3.53×10^{-2}	0.3064	7.02×10^{-3}	3.47×10^{-5}	48.4	2.99×10^{-15}
B-B-B-B	0.0010	3.53×10^{-2}	0.0010	3.53×10^{-2}	0.0010	3.53×10^{-2}	0.0010	3.53×10^{-2}	3.47×10^{-5}	118.8	6.40×10^{-21}
HGV-HGV-HGV-LGV	0.0075	2.64×10^{-2}	0.0075	2.64×10^{-2}	0.0075	2.64×10^{-2}	0.3064	7.02×10^{-3}	3.47×10^{-5}	615	3.56×10^{-16}
HGV-HGV-HGV-HGV	0.0075	2.64×10^{-2}	0.0075	2.64×10^{-2}	0.0075	2.64×10^{-2}	0.0075	2.64×10^{-2}	3.47×10^{-5}	807.6	4.31×10^{-17}

Note: M – Motorcycle, C – Car, B – Bus, LGV – Light goods vehicle, HGV – Heavy goods vehicle
Probability of vehicle type in the urban tunnel at Singapore refer to Table 8.2
Probability of collision refer to Appendix C- Table C6
Probability o f collision resulting fire refer to Appendix C- Table C5
Total vehicles peak HRR refer to Appendix B

Table 8.4: Fire risk due to vehicle collision selected data (Refer to Appendix F for full data)

The results from the 125 multiple vehicle collisions were plotted in descending order of fire risk as shown in Figure 8.10. It was found that the fire risk level reduces as the number of vehicles increases in a collision combination. Although the peak rate of heat release of a multiple vehicle collision increases with the number of vehicles, the probability of the combination occurring reduces hence reducing the risk as shown by the collision scenarios grouping by the number of vehicles involved. In view of this finding, it was decided not to consider vehicle collision configurations of more than four vehicles as the fire risk level continues to diminish when compared to a single or double vehicle collision.

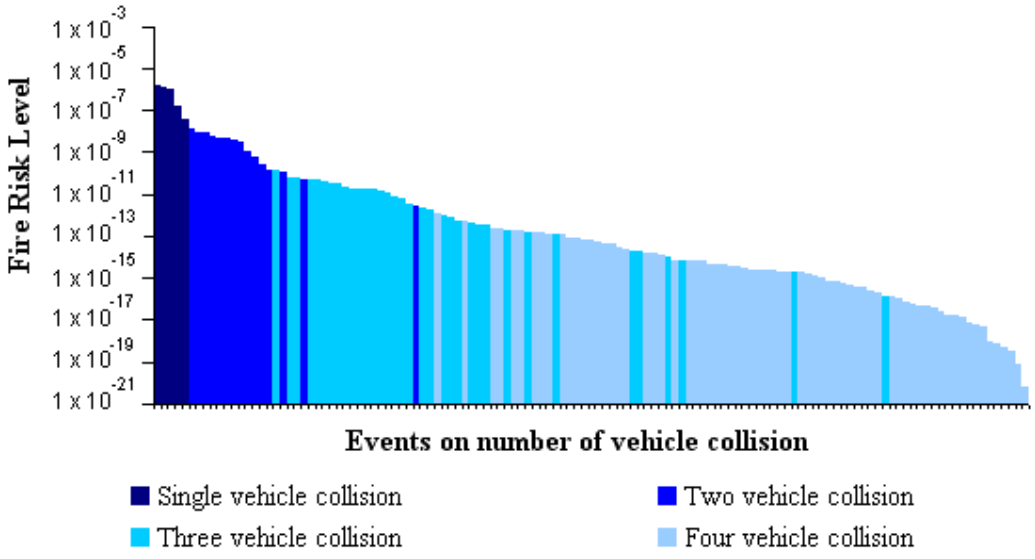

Figure 8.10: Fire risk level in the tunnel for this project

8.4 Discussion

Examining the causes of a vehicle fire due to faulty vehicle, act of carelessness and intentional act, (Tables 8.3 and 8.4) it can be seen that fire from a light goods vehicle (LGV) has a higher fire risk level in this tunnel as compared to other vehicle types. The reason is due to the higher number of LGVs expected in this tunnel and its high heat release rate relative to the smaller vehicles resulting in an overall higher fire risk. Although there are more motorcars expected in this urban tunnel, the fire risk is not as high compared to a LGV fire in view of their lower heat release rate. Similarly for HGV, while

the heat release rate of this vehicle with goods is significantly higher, the fire risk is low considering the small number of HGVs expected in the tunnel.

The analysis of vehicle fire resulting from collision shows that a single HGV fire has the highest fire risk level and a multiple collision involving four buses has the lowest fire risk. The possibility of a multiple bus collision in the urban road tunnel in Singapore is attributed to the low bus traffic expected and the relatively low bus accident rate in Singapore. A summary of the potential fire risk analysis for this is tabulated in Table 8.5.

Type of potential fire risk	*Vehicle fault*	*Act of carelessness*	*Intentional*	*Collision*
Maximum expose risk: Vehicles configuration:	8.14×10^{-4} Single LGV	1.70×10^{-4} Single LGV	3.72×10^{-4} Single LGV	1.39×10^{-6} Single HGV
Minimum expose risk: Vehicles configuration:	4.93×10^{-6} Single Bus	1.03×10^{-6} Single Bus	2.25×10^{-4} Single Bus	6.40×10^{-21} Bus-Bus-Bus-Bus

Table 8.5: Summary of potential fire risk in the urban road tunnel in Singapore

With the identification of the high fire risk scenarios complete, the fire engineer can investigate the effects on the design fire of the specific tunnel geometrical and ventilation conditions. Numerical models can be set up in which the fire load corresponding to the highest risk scenarios are specified; in the case of this tunnel they are a single LGV and a single HGV. The result from a numerical analysis then allows the expected reasonable worst case peak heat release rate to be specified for the smoke control design. An application of this analysis procedure is presented in chapter 11.

8.5 Conclusion

From this analysis, stakeholders are provided a measure of the potential fire risk that could occur in the tunnel. It also highlights the potential fire scenarios such as the number and types of vehicle fire that could occur in the tunnel, thereby enabling designers to consider these scenarios in their design analysis. The analysis of an urban road tunnel in Singapore found when collision events in which up to four vehicles involved are considered, a single HGV collision fire has the greatest fire risk level and a multiple collision involving four buses has the lowest fire risk. However a fire in a light goods vehicle (LGV) due to faulty vehicle gave the highest overall risk.

The authors recognise that there is a circular argument in this approach in that rate of heat release values from full-scale fire tests are used to establish the fire risk level and subsequently this is used to enable fire engineers to establish the design fire considering ventilation condition and tunnel geometry using a numerical approach. Additional results from full-scale vehicle fire experiments conducted in tunnels with differing geometries and ventilation rates would alleviate this circular argument. However it is obvious that the resources needed to conduct such experiments are well in excess of what is ever likely to be available. Nevertheless the risk analysis approach discussed in this chapter gives measure of the fire risk involved thereby providing direction in finding a reasonable worse case fire.

This methodology requires a substantial amount of data and collating sufficient statistical data such as vehicle fire incident data, traffic accident data and vehicle population data for the analysis is crucial. As each tunnel is unique, depending on the country and the location of the tunnel, results from the fire risk analysis finding can vary. This is because of the rules and regulations on vehicle access right which vary considerable among countries or states. There are tunnels where vehicle carrying hazardous materials are not allowed entry while other tunnels do not have such restriction. The legislation often plays an important role on the outcome of the fire risk analysis and it is important to consider such factors while performing fire risk analysis.

Chapter 9:
MODELLING THE SP LABORATORY PALLETS

This chapter discusses the approach using FDS 4.07 to model a stack of wood and plastic pallets burning under a free burning condition. The purpose of this work is to explore the feasibility of using a numerical tool to establish the heat release rate of a burning object. The tests conducted by SP's Fire Laboratory involving 16 wood pallets and 4 plastic pallets were used for the modelling subject. Details of the experiment setup and the modelling approach to reconstruct the SP laboratory pallets fire test are discussed in this chapter.

9.1 SP Laboratory Fire Experiments

A series of fire experiments involving wood pallets, plastic pallets, polyurethane mattresses and polystyrene cups were performed in the SP laboratory. The aim of these fire tests was to obtain preliminary estimate of the peak heat release rate and to gain knowledge of the fire development in these commodities on the Runehamar tunnel fire test (Ingason and Lonnermark, 2003).

The tests were carried out under a large industry calorimeter where the following commodities were stacked in two piles of pallets and burned in the SP laboratory (Ingason and Lonnermark, 2003):

1) 82 % wood pallets and 18 % plastic pallets (Figure 9.1)
2) 82 % wood pallets and 18 % PUR mattresses (Figure 9.1)
3) 81 % cardboard with 19 % PS cups (Figure 9.1)

Wood & Plastic Wood & PUR mattresses Cardboard & PS cups

Figure 9.1: Commodities setup (Ingason pers.comm)

From these experiments, it was found that the wood pallets and mattress has the fastest fire growth rate as compared with the other types of commodities. At the initial fire growth phase, the wood and plastic pallets had similar growth rate as the cardboard & PS cups. However, in terms of the heat release rate, the wood and plastic yielded the highest heat release rate value (7.75 MW), followed by wood and mattresses (6.96 MW) and cardboard & PS cups (3.96 MW). The heat release rate curve and photographs of these fire tests are shown in Figure 9.2 and 9.3 respectively (Ingason and Lonnermark, 2003).

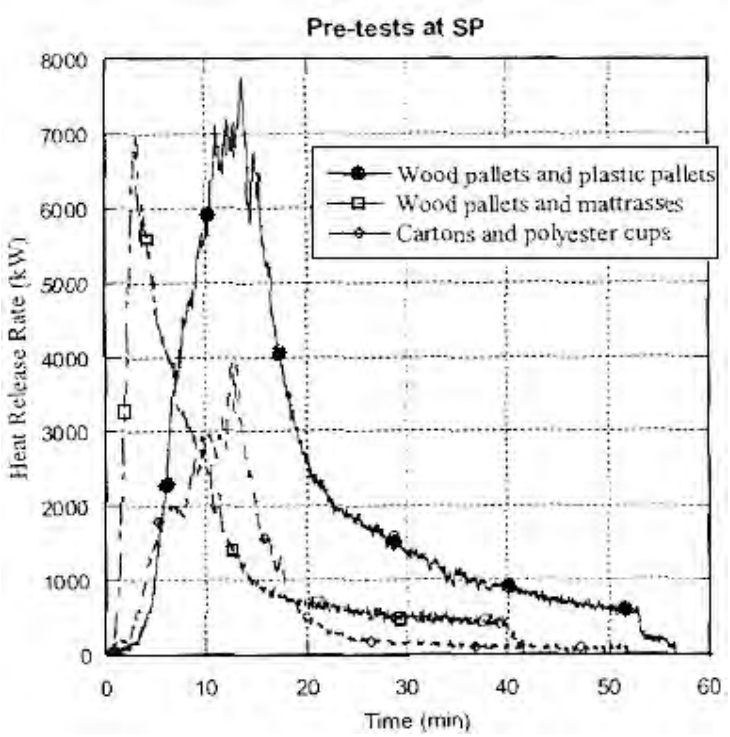

Figure 9.2: HRR curve recorded by SP laboratory (Ingason and Lonnermark 2003)

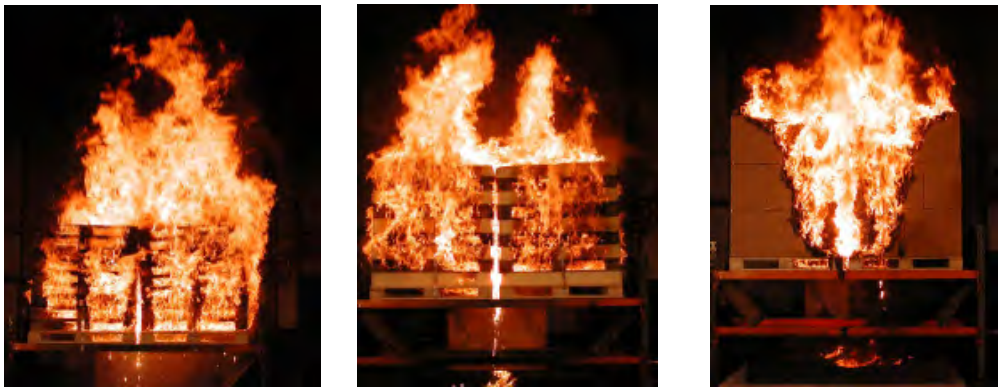

Wood & Plastic Wood & PUR mattresses Cardboard & PS cups

Figure 9.3: Commodities burned during the experiments (Ingason pers.comm)

9.2 Reconstruction of the SP wood and plastic pallets experiment using FDS

As part of this research objective, the goal is to examine the feasibility of using a numerical tool such as FDS to establish the heat release rate of a burning object. The SP

wood and plastic free burning experiment mentioned in section 9.1 was selected for the reconstruction because it has the highest heat release rate and these materials are commodities commonly transported on the roads (Lönnermark and Ingason 2005). Details of the modelling approach are described in the following section.

9.2.1 Layout of fuel package

The first step was to gather information on the type of fuel involved and their arrangement in the fire experiment. Information provided by Ingason (pers.comm) showed that a total of fourteen 1.2m x 0.8m x 0.15m wood pallets, two 1.2m x 1m x 0.15m wood pallets and four 1.2m x 0.8m x 0.15m plastic pallets were burned during the experiments. The arrangement of the fuel package layout is shown in Figure 9.4.

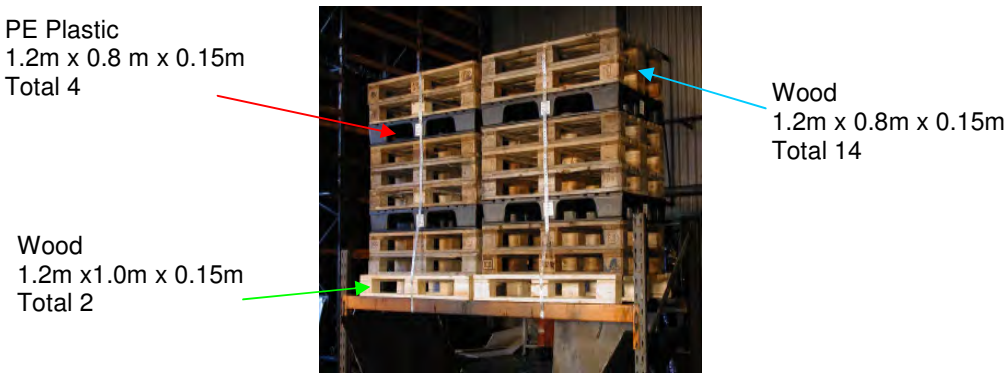

Figure 9.4: Fuel arrangement setup and fuel quantity (Ingason pers.comm)

9.2.2 Fuel package (Wood and Plastic Pallets)

There are three types of pallets used in this fire test ; 1.2 m x 0.8 m x 0.15 m wood pallet (Figure 9.5), 1.2 m x 1 m x 0.15 m wood pallets (Figure 9.6) and 1.2 m x 0.8 m x 0.15 m plastic pallets (Figure 9.7). The author has made certain assumptions based on pallets of similar dimensions in the fire test for the FDS modelling. According to White et al (2000), pallets of these ranges of dimensions are known as EURO pallets which are one of the few internationally recognized standard pallets commonly used in Europe.

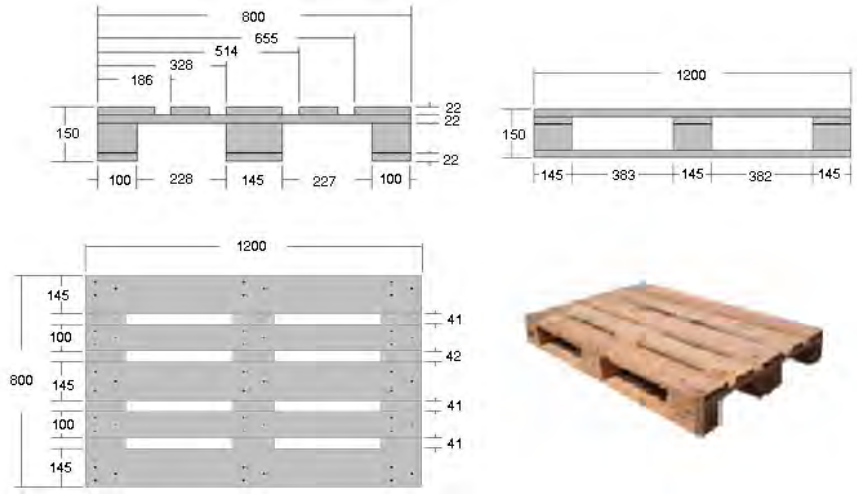

Note: Diagram dimensions are in mm

Figure 9.5: 1.2 m by 0.8 m by 0.15 m wood pallets (reproduced from (VTPL 2000))

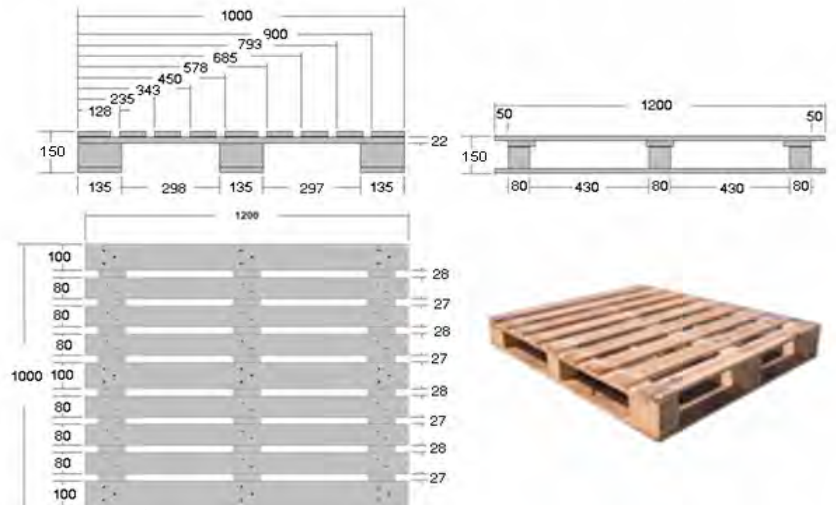

Note: Diagram dimensions are in mm

Figure 9.6: 1.2 m x 1 m wood pallet (reproduced from (VTPL 2000a))

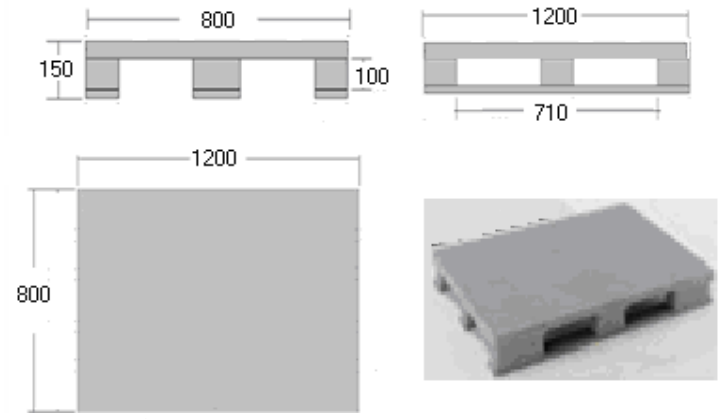

Note: Diagram dimensions are in mm

Figure 9.7: 1.2 m x 0.8 m plastic pallet (reproduced from Kaiserkraft (2006))

9.2.3 Hand calculation estimate

Prior to the FDS simulation, a hand calculation was performed to estimate the heat release rate using equation 9.1 (Karlsson and Quintiere, 2000).

$$Q = A_f \dot{m}'' \Delta H_{eff} \quad \text{---------- [9.1]}$$

As there are three types of pallets, the sum of the heat release rate of these pallets will be the calculated peak heat release rate for the experiment. Table 9.1 shows the mass loss rate, effective heat of combustion, burning area of the respective pallets used for the calculation.

Description	Number of pallets	Total horizontal burning area (m^2)	Mass loss rate ($kg/m^2 s$)	Effective heat of combustion (MJ/kg)
Wood pallets 1.2m x 0.8m x 0.15m	14	16.46	0.013[a]	11.5[c]
Wood pallets 1.2m x 1m x 0.15m	2	2.79	0.013[a]	11.5[c]
PE plastic pallets 1.2m x 0.8 x 0.15m	4	5.56	0.026[b]	38.4[d]

Note: a) Mass loss rate for wood (Drysdale 1998)
b) Mass loss rate for plastic (Tewarson 2006)
c) Effective heat of combustion wood (Thureson 1991)
d) Effective heat of combustion plastic (Tewarson 2006)

Table 9.1: Thermal properties for wood and plastic pallets

Using equation 9.1

Heat release rate (1.2m x 0.8m x 0.15m wood pallets) = 16.46 x 0.013 x 11.5 = 2.5 MW
Heat release rate (1.2m x 1m x 0.15m wood pallets) = 2.79 x 0.013 x 11.5 = 0.4 MW
Heat release rate (1.2m x 0.8m x 0.15m plastic pallets) = 5.56 x 0.026 x 38.4 = 5.6 MW
Therefore, the heat release rate for the 20 pallets is 2.5 + 0.4 + 5.6 = 8.5 MW
A heat release rate value of 8.5 MW was calculated. The experiment value together with the calculated value using equation 9.1 can be used as a cross check on the subsequent heat release rate estimate using FDS.

9.2.4 Simulation approach

The simulation was set up with the fuel package consisting of 16 wood pallets and 4 plastic pallets positioned on a rack in an open space with no wind conditions. The pallets were ignited using a heat source introduced at the rear of the bottom layer pallet for a few minutes before it was removed from the fuel package. The setup of the simulation is as shown in Figure 9.8.

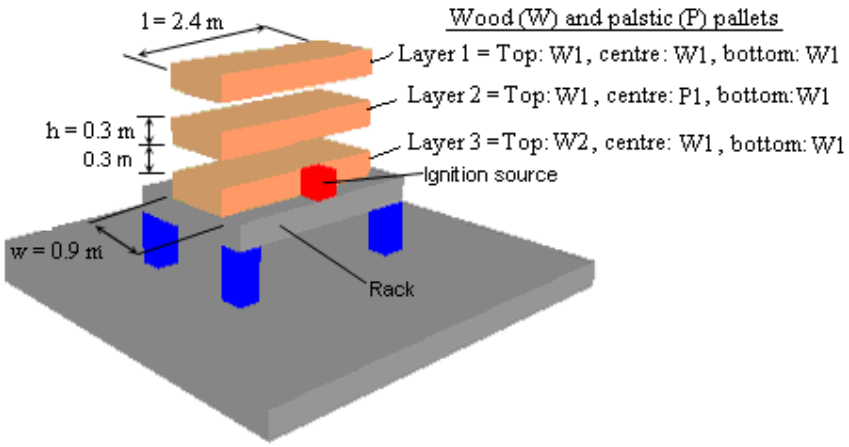

Note: W1 - wood pallet of 1.2m x 0.8m x 0.15m , W2 – wood pallet of 1.2m x 1m x 0.15m and P1 –plastic pallet of 1.2m x 0.8m x 0.15m.

Figure 9.8: Fuel arrangement model using FDS

Using FDS to model the exact dimension of each pallet would require a very fine grid size (0.01m) and computing this simulation with a workstation would involve a substantially long period of time making the simulation time impractical. To overcome this limitation, the modelling of the pallets was simplified and constructed as layer with each layer size 2.4m x 0.9m x 0.3m. The benefit of this approach enabled a larger grid size to be used which shortened the simulation time. The heat release rate can be estimated using the heat release rate per unit area from cone tests and input into FDS; a surface burning area factor is introduced to ensure the fuel load area model in the simulation is equivalent to the fuel load area used in the experiment.

A heat flux of 20 to 25 kW/m^2 was selected for the free burning simulation. Findings from Hopkins and Quintiere (1996) have shown that the net incident heat flux in a cone calorimeter (free burning condition) for nylon, polyethylene, polypropylene and PMMA

varies from 11 kW/m^2 to 28 kW/m^2 is obtained for irradiation level ranging from 0 to 90 kW/m^2. Generally a lower heat flux has been observed when burning occurs under a free burning condition. In view of the above reason, cone test data with heat flux as mentioned in this range were used when performing free burning simulation. Details of the wood and plastic thermal properties of the cone tests data used for the simulation under free condition are shown in Figure 9.9 and Table 9.2 respectively. The limitations of using this approach to estimate the heat release rate of the pallets is discussed in Chapter 16 of this thesis.

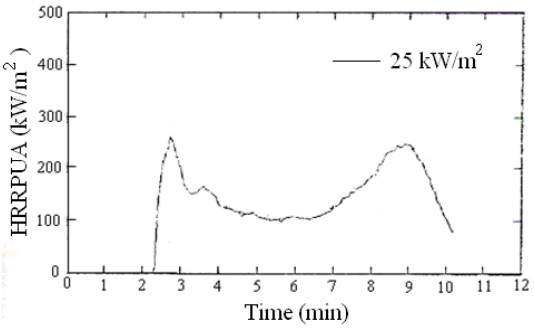

HRRPUA for wood exposed at 25 kW/m^2
(Thureson 1991)

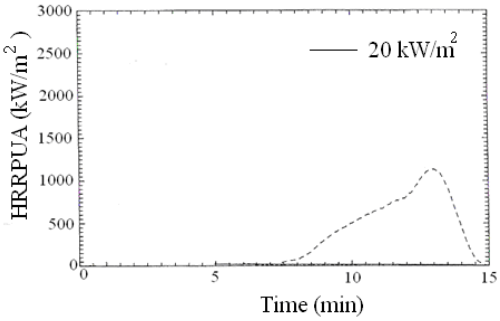

HRRPUA for polyethylene exposed at 20 kW/m^2
(Babrauskas and Grayson 1992)

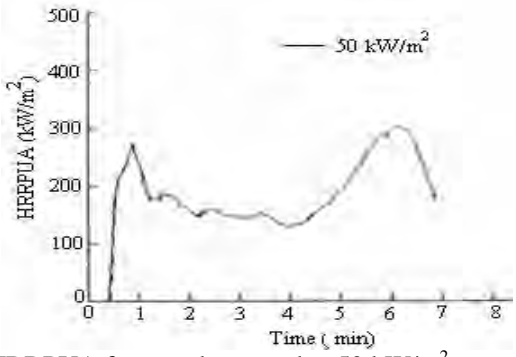

HRRPUA for wood exposed at 50 kW/m^2
(Thureson 1991)

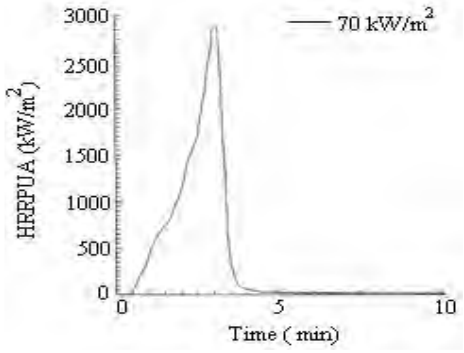

HRRPUA for polyethylene exposed at 70 kW/m^2
(Babrauskas and Grayson 1992)

Figure 9.9: Cone test data for wood and plastic - heat flux generated by cone

Material	Thermal conductivity (W/m/K)	Density (kg/m^3)	Ignition temperature (^oC)	Specific heat (kJ/kg/K)
Wood[a]	0.12	600	373	2.58
Polyethylene[b]	0.64	956	323	3

Note: a) Cone test data taken from (Thureson 1991)
b) Cone test data taken from (Babrauskas and Grayson 1992) and (Babrauskas 2003)

Table 9.2: Thermal properties for wood and plastic pallets

An example of the input parameters defining the fuel package for the FDS simulation is presented in Appendix H and calculation to determine the fuels thickness and their surface burning area factor for the FDS simulation is shown as follows:
Calculation to determine thickness and surface burning area factor for

i) (1.2m by 0.8m by 0.15m) wood pallets

Actual volume per (1.2m by 0.8m by 0.15m) wood pallets is 0.046 m^3 (Figure 9.5).
Actual volume for 14 of (1.2 m x 0.8 m x 0.15 m) wood pallets is
= number of wood pallets x volume of one wood pallet = 14 x 0.046 = 0.64 m^3.

Total area of (1.2m by 0.8m by 0.15m) wood pallets model in FDS (Figure 9.8) is
Layer 1 area: 2[(l x w)+(h x w)+(l x h)] = 2[(2.4 x 0.9)+(0.3 x 0.9)+(2.4 x 0.3)] = 6.3 m^2
Layer 2 area: 2[(l x w)] = 2[(2.4 x 0.9)] = 4.32 m^2
Layer 3 area: 2[(h x w)+(l x h)]+(l x w) = 2[(0.3 x 0.9)+(2.4 x 0.3)]+(2.4 x 0.9) = 4.14 m^2
Total area (1.2m by 0.8m by 0.15m) wood pallets model in FDS is 6.3 + 4.32 + 4.14 = 14.76 m^2

Therefore thickness used for simulation is

$$\frac{Actual\ pallets\ volume}{simulated\ \ area} = \frac{0.64}{14.76} = 0.043 \text{ m}$$

Actual area per (1.2m by 0.8m by 0.15m) wood pallet is 4.3 m^2 (Figure 9.5).

Actual area for 14 of (1.2 m x 0.8 m x 0.15 m) wood pallets is
= number of wood pallets x area of one wood pallet = 14 x 4.3 = 60.2 m^2.

Therefore the surface burning area factor used for simulation is

$$\frac{Actual\ pallets\ area}{simulated\ \ area} = \frac{60.2}{14.76} = 4$$

ii) (1.2m by 1.0m by 0.15m) wood pallets

Actual volume per (1.2m by 1.0m by 0.15m) wood pallets is 0.04 m^3. (Figure 9.6)
Actual volume for 2 of (1.2 m x 1.0 m x 0.15 m) wood pallets is
= number of wood pallets x volume of one wood pallet = 2 x 0.04 = 0.08 m^3.
Total area of (1.2m by 1.0m by 0.15m) wood pallets model in FDS (Figure 9.8) is
Layer 3 area: (l x w) = (2.4 x 0.9) = 2.16 m^2
Total area (1.2m by 1.0m by 0.15m) wood pallets model in FDS is 2.16 = 2.16 m^2
Therefore thickness used for simulation is

$$\frac{Actual\ pallets\ volume}{simulated\ area} = \frac{0.08}{2.16} = 0.037\ \text{m}$$

Actual area per (1.2m by 1.0m by 0.15m) wood pallet is 4.14 m^2 (Figure 9.6).

Actual area for 2 of (1.2 m x 1.0 m x 0.15 m) wood pallets is
= number of wood pallets x area of one wood pallet = 2 x 4.14 = 8.3 m^2.

Therefore the surface burning area factor used for simulation is

$$\frac{Actual\ pallets\ area}{simulated\ area} = \frac{8.3}{2.16} = 3.84$$

iii) (1.2m by 0.8m by 0.15m) plastic pallets

Actual mass for 1 PE plastic pallets is 23 kg (Kaiserkraft 2006)
Density for PE plastic is 956 kg/m^3. (Babrauskas 2003)

Actual volume per plastic pallet is $\frac{Mass}{Density} = \frac{23}{956} = 0.024\ m^3$.

Actual volume for 4 PE plastic pallets is
= number of PE pallets x volume of 1 PE pallet = 4 x 0.024 = 0.096 m^3.

Total area of PE pallets model in FDS is

Layer 2 area: 2[(h x w) + (l x h)] = 2[(0.3 x 0.9) + (2.4 x 0.3)] = 1.98 m^2 (Figure 9.8)

Total area PE pallets model in FDS is 1.98 m^2

Therefore thickness used for simulation is

$$\frac{Actual\ pallets\ volume}{simulated\ area} = \frac{0.096}{1.98} = 0.048 \text{ m}$$

Actual area per PE pallet is 4.1 m^2 (Figure 9.7).

Actual area for 4 of PE pallets is

= number of PE pallets x area of 1 PE pallet = 4 x 4.1 = 16.4 m^2.

Therefore the surface burning area factor used for simulation is

$$\frac{Actual\ pallets\ area}{simulated\ area} = \frac{16.4}{1.98} = 8.3$$

9.3 Sensitivity analysis

To replicate the heat release rate of the fire experiment, a series of simulations considering different domain, grid and heat flux were simulated and compared with the experimental value. In FDS only one reaction can be specified and wood was used for the reaction in the simulation because the majority of the fuel load is made up of wood.

The non-dimensional expression $D^* / \delta x$, where D^* is a characteristic fire diameter and δx is the nominal size of a mesh cell is used as a gauge to see what values worked well for the simulation model. Mesh sensitivity study by NUREG 2007 shows that the $D^* / \delta x$ values ranging from 4 to 16 were able to adequately resolve plume dynamics.

No	δx (m)	$\dot{Q}$ (kW)	D* (m)	$D^* / \delta x$
1	0.15	7750	2.17	14.5
2	0.3	7750	2.17	7.3

Note: ρ = 1.2 kg/m^3, C_p = 1.003 KJ/kgK, T_∞ = 293 K, g = 9.81 m/s^2

In view of the above study, grid sizes of 0.15 m and 0.3 m were selected for the sensitivity analysis. A tabulation of the simulations performed and the simulation results are shown in Table 9.3 and Figure 9.10 – 9.12 respectively.

Simulation No.	Heat flux[a] (kW/m^2)	Grid size (mm)	Domain Height (m)
SP 1	50-70	300	15
SP 2	20-25	300	15
SP 3	20-25	300	13.5
SP 4	20-25	150	15

Note: a) Cone data when exposed to a heat flux as shown by Figure 9.9

Table 9.3: Summary of the simulations performed on the burning pallets experiment

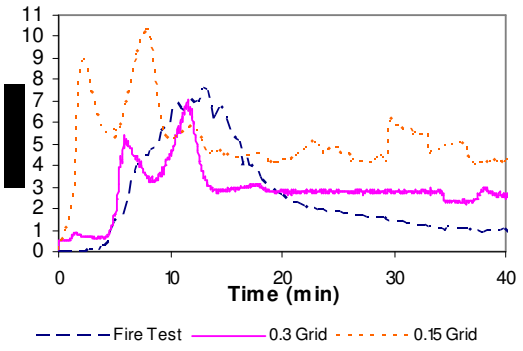

Figure 9.10: Grid sensitivity s/no SP2 & SP4

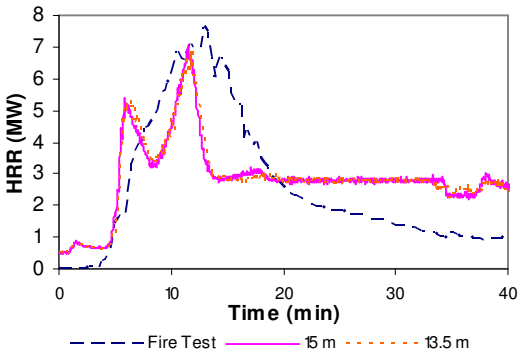

Figure 9.11: Domain sensitivity s/no SP2 & SP3

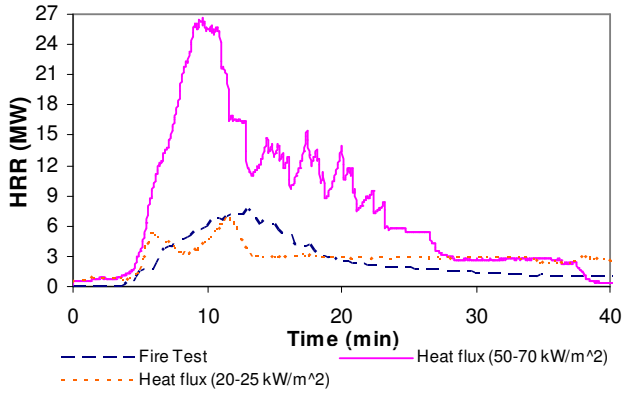

Figure 9.12: Different heat flux s/no SP1 & SP2

9.4 Discussion and Conclusion

The use of FDS for the fire re-construction of SP's Fire Laboratory involving 16 wood pallets and 4 plastic pallets demonstrates the possibility of using numerical approach to establish the heat release rate of a burning object. From Figure 9.13, a similar growth rate and peak heat release rate (8% different) was computed using FDS (i.e. with 0.3 m grid, 15 m domain height and 20-25 kW/m^2 cone data).

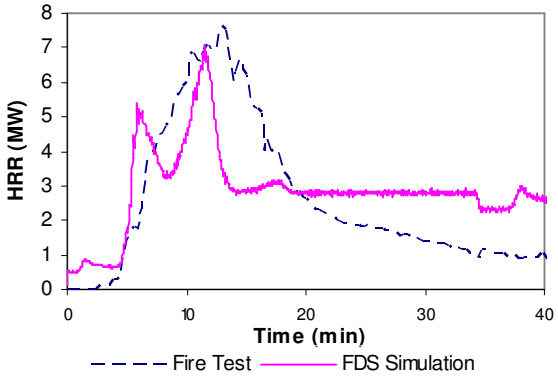

Figure 9.13: Heat release rate recorded from SP's Fire Laboratory Vs FDS simulation

Although similar burning behaviour at the growth phase was observed from the simulation, the current model is unable to capture the fire development during the decay phase. This could be due to the limitation in FDS where phenomena such as fuel collapse cannot be captured by the simulation.

Further work using this approach to establish heat release rate of a burning object is performed. The fire re-construction using FDS to estimate the heat release rate for the Runehamar tunnel fire experiment will be discussed in the next chapter.

Chapter 10:
CALIBRATING AN FDS SIMULATION OF GOODS VEHICLE FIRE GROWTH IN A TUNNEL USING THE RUNEHAMAR FIRE EXPERIMENT

Based on Cheong M K, Spearpoint M J, Fleischmann C M, published as "Calibrating an FDS Simulation of Goods Vehicle Fire Growth in a Tunnel Using the Runehamar Fire Experiment" to *Journal of Fire Protection Engineering*, Vol 19 No. 3, pp.177 – 196, August 2009.

As with any complex fuel assembly configuration, modelling a goods vehicle fire using FDS to estimate the heat release rate in a tunnel is a challenging task. The work presented in this chapter involves the use of heat release rate curve taken from the Runehamar tunnel fire experiment T1 to 'calibrate' the heat release rate curve predicted using FDS 4.0.7. It is not the intention of this work to adjust the input parameters in FDS to achieve the Runehamar tunnel fire test result. A logical approach is adopted where small scale cone tests data are input into the FDS simulation to examine if similar HRR estimate can be predicted using FDS. This work develops a simplified representation of burning wood and plastic pallets and illustrates that an FDS simulation is able to reproduce a reasonable estimate of the fire growth characteristics in the tunnel. This chapter considers the effects of the assumptions made to calibrate the simulations and then investigates how the fire growth might change if conditions were varied.

10.1 Introduction

The use of ventilation systems to control smoke movement is common in most road tunnel designs. The operation of the tunnel ventilation system is critical as its purpose during a fire emergency is to control the movement of smoke and heated gas away from the fire to provide a tenable environment along the egress path allowing for safe evacuation of motorists. The secondary purpose is to facilitate fire fighters access to the incident by providing a clear path to the fire site (Bendelius 2003). The risk of having a fire in a tunnel and designing an effective tunnel ventilation system through the provision of sufficient airflow to achieve tenable conditions in the egress path is dependent on multiple parameters including heat release rate (HRR), tunnel geometry, tunnel gradient, operation (whether bi-directional traffic is required) (Bendelius 2003) and legislation (whether vehicles carrying dangerous goods are allowed to access the tunnel, e.g. petrol tankers). Among these parameters, the heat release rate is the primary parameter for tunnel ventilation design and it is the most difficult to identify as this value is dependent on the types of vehicles and any associated loads carried by the vehicles. In current practice, the heat release rate for various types of fires proposed by the PIARC 1999 technical committee reports (PIARC 1999), NFPA 502 (NFPA 2004), BD78/99 (BD 1999) have generally been used for the design of tunnel ventilation systems. The heat release rates for the various types of vehicle fire range from 2.5 MW to 5 MW for passenger cars to 20 MW to 30 MW for heavy goods vehicles (HGV). However, recent fire experiments conducted in the Runehamar Tunnel showed that vehicles with burning goods may result in higher HRR (approx 66.4 to 201.9 MW peak) outputs (Ingason and Lonnermark 2005). These experiments seriously hinted that previous data regarding heavy goods vehicles might have been underestimated.

The purpose of this work is to present an approach using a CFD computer program, Fire Dynamics Simulator (FDS) to establish the heat release rate in a tunnel considering factors such as tunnel geometry, ventilation condition and fuel load. Obtaining the fire growth of any burning fuel package using a computer model is a difficult exercise. The recent

attempts to predict fire development prior to the Dalmarnock experiments (Rein et al 2007) has showed some of the very considerable difficulties involved in doing this. Amongst other things, the work described in this chapter involves a relatively complex 3-dimensional fuel package of varying material types which is also subject to a forced ventilation and re-radiation effects. Therefore this work does not attempt to predict the fire growth a priori but uses published experimental data taken from one of the Runehamar tunnel fire experiment to 'calibrate' the heat release rate curve predicted using FDS 4.0.7. Similar to modelling work discussed in (Rein et al 2007), 'calibrate' in this context refers to a process to establish a relationship between the experimental value with the numerical analysis by considering the modelling approach used, the fuel arrangement, grid size and domain length. The objective of this simulation is to develop a simplified representation of wood and plastic pallets burning in a tunnel to illustrate that the simulation is able to reproduce a reasonable approximation of the fire growth characteristics and investigate the sensitivity of the baseline 'calibrated' model setup. When sufficient confidence level is achieved from the simulation, a similar approach can be used to establish the heat release rate for a design application. The work discussed in this chapter is applicable to scenarios where a similar fuel arrangement to the Runehamar tunnel fire experiment is used for the simulation. Further calibration work would be necessary if other types of fuel materials or fuel arrangement setup were used for the numerical analysis.

10.2 The Runehamar Tunnel Experiment

In 2003, a programme of large-scale fire experiments was conducted in the Runehamar tunnel in Norway (Ingason & Lonnermark 2003a). This is an abandoned tunnel that has been closed down from traffic. It has previously been used for fire testing of various tunnel insulation materials. The Runehamar tunnel is dug into hard gneiss rock and is 1600 m in length, 9 m wide and 6 m high with a slope varying between 0.5 to 1 % (Lonnermark and Ingason 2005), the tunnel cross sectional area and photograph of this fire test are shown in Figure 10.1 and 10.2. A total of four fire experiments were performed using a semi-trailer mock up with different commodities as the fuel source. These commodities included wood pallets, polyethylene plastic pallets, cardboard cartons containing polystyrene cups,

polyurethane (PU) mattresses and furniture. The commodities used as fuel in the four experiments are shown and tabulated in Figure 10.3 and Table 10.1 respectively.

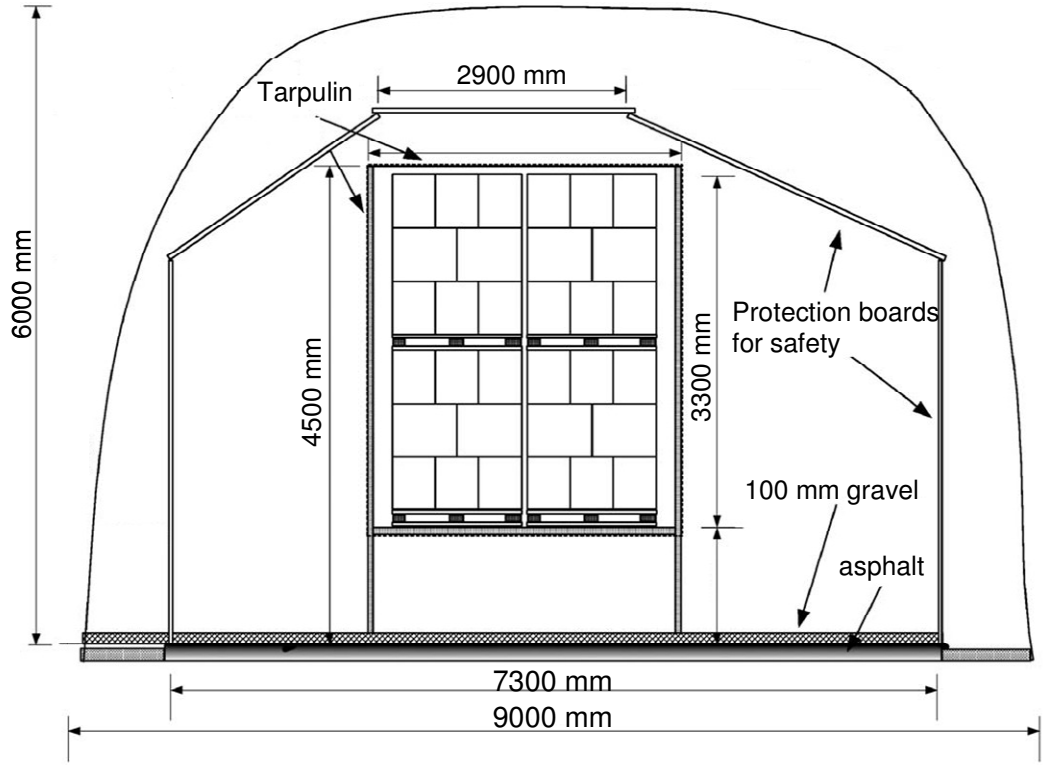

Figure 10.1: Cross section of Runehamar tunnel (Brekelmans & Bosch 2003)

Figure 10.2: Photographs of Runehamar tunnel fire test (Vegvesen 2006)

Figure 10.3: Photograph of fuel load used for the fire tests (Brekelmans & Bosch 2003)

Expt No.	Description of fuel load	Total weight (kg)	Theoretical calorific value (GJ)	Measured peak HRR (MW)
T1	360 wood pallets measuring 1.2 m x 0.8 m x 0.15 m 20 wood pallets measuring 1.2 m x 1 m x 0.15 m 74 PE plastic pallets measuring 1.2 m x 0.8 m x 0.15 m	11010	247	201.9
T2	Wood pallets measuring 1.2 m x 0.8 m x 0.15 m PU mattresses	6930	135	156.6
T3	Furniture and fixtures Ten large rubber tyres Polyester tarpaulin	8550	179	118.6
T4	Corrugated paper cartons Polystyrene (PS) cups, Wood pallets Polyester tarpaulin	2850	62	66.4

Table 10.1: Fuel load used for the Runehamar Tunnel fire experiments (Ingason and Lonnermark 2005)

The experiments were conducted by the SP Swedish National Testing and Research Institute. Measurements included gas temperature, visibility, thermal radiation and gas species. A sketch of the measuring station setup and overview of the measurement position in the tunnel is shown in Figure 10.4. The heat release rate was calculated using the oxygen consumption calorimetry technique for the data at the downstream station (Lonnermark and Ingason 2005). A mobile fan positioned at the tunnel entrance generated an air velocity of 3 m/s driving the fire gases in one direction enabling the heat release rate to be measured at the opposite end of the tunnel. The maximum heat release rate varying between 66.4 MW to 201.9 MW was recorded in these tests (Lonnermark and Ingason 2005); the HRR curves for the four experiments are shown in Figure 10.5.

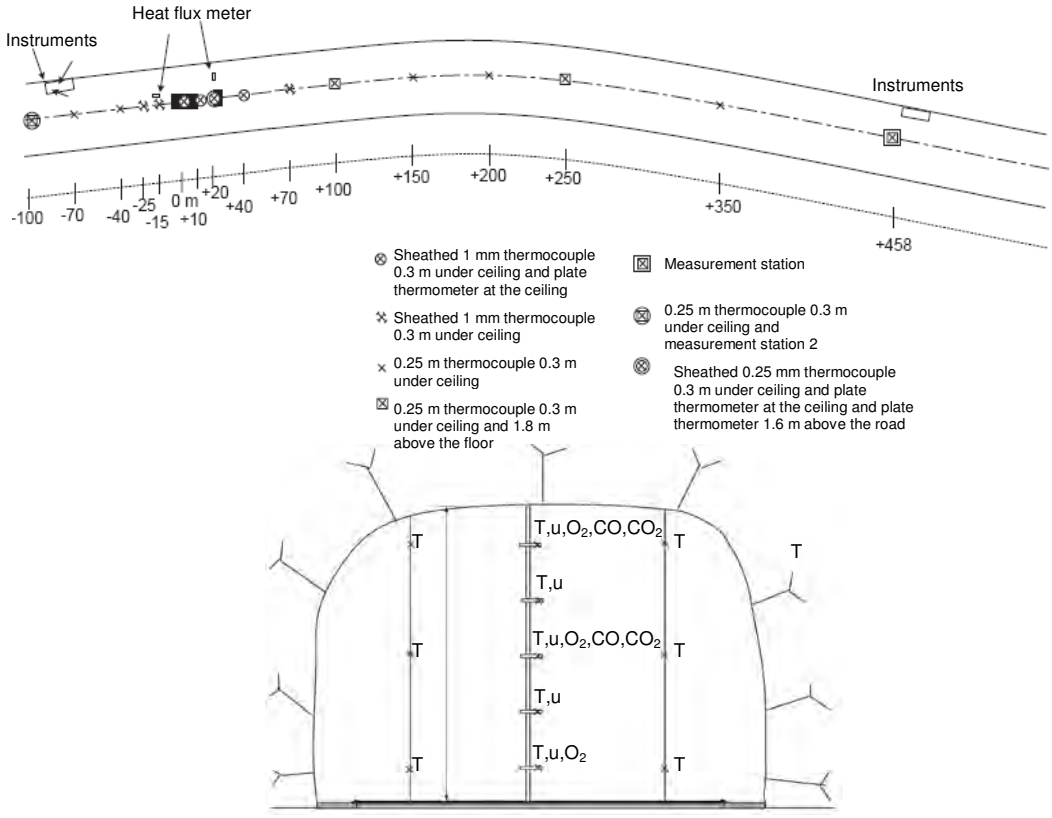

Note: T = gas temperature, u = gas velocity, CO_2 = carbon dioxide, CO = carbon monoxide, O_2 = oxygen, OD = visibility.

Figure 10.4: Measurement station used in the Runehamar Tunnel fire experiments (Ingason & Lonnermark 2005),(Lonnermark and Ingason 2005).

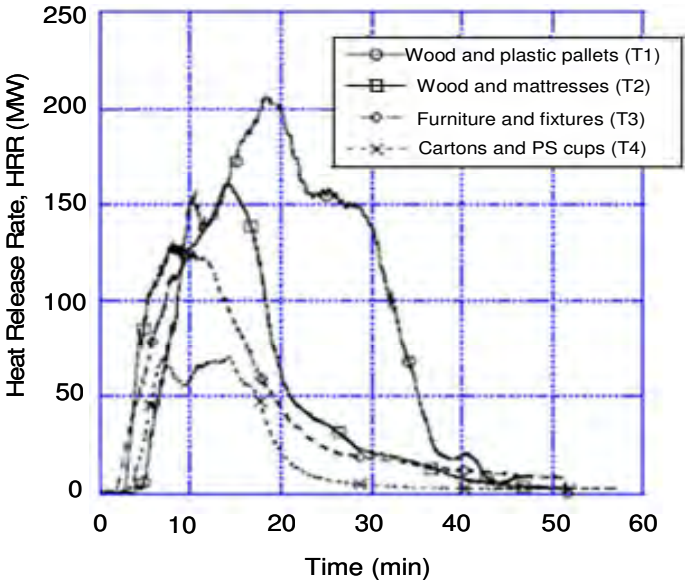

Figure 10.5: HRR recorded for the four Runehamar Tunnel fire experiments (Ingason & Lonnermark 2005)

10.3 Modelling of Fire Experiment T1

FDS model and stability criteria

For this work, FDS 4.0.7 was used for the calibration of the Runehamar tunnel fire experiment T1. The equations in FDS code include the conservation of mass, species, momentum, energy and equation of state where this is a set of partial differential equations to compute the density, three components of velocity, mass fraction, temperature and pressure (McGrattan 2005). In the Large Eddy Simulation turbulence model where the grid is not fine enough to resolve the diffusion of fuel and oxygen, a mixture fraction-based combustion model is used. Combustion is calculated from the mixing rate of fuel and oxidant where the chemical reaction between fuel and oxygen are taken to follow a single one-step stoichiometric reaction. The assumption that fuel and oxidizer cannot co-exist leads to the state relations between the oxygen mass fraction and mixture fraction (McGrattan 2005). In FDS, the total heat release rate is established using

$$\dot{Q} = \Delta H_{O2} \int_F -\dot{m}''_{O2} dA = \Delta H_{o2} \int_F \frac{dY_o}{dZ} \rho D \nabla Z dS \qquad \text{Equation 10.1}$$

As the conservation equations in FDS are coupled together, a change in the velocity will affect the density, mass fraction of the species or mixture fraction and so indirectly affect the heat release rate estimate. The velocity components in each grid cell will be a combination of any imposed external velocity, the effects of any combustion in neighbouring cells and the influence of obstructions.

According to McGrattan, FDS model solves numerically a form of the Navier-Stokes equation and discretises the domain using an explicit scheme. The domain is made up of a rectangular box that is divided into rectangular grid cells. To ensure that the results computed are numerically correct, the time step is constrained by the Courant-Friedrichs-Lewy (CFL) condition where:

$$\delta t \max = \left(\frac{u}{\delta x}, \frac{v}{\delta y}, \frac{w}{\delta z} \right) \leq 1 \qquad \text{Equation 10.2}$$

The velocities *u*, *v* and *w* are tested at each time step to ensure that the CFL condition is satisfied. If the above is greater than 1, the time step is set to 0.8 of its allowed maximum value and these velocities are recalculated and tested again. CFL is used to assess the solution to the equations and it cannot be updated with a time-step larger than 1 resulting in a parcel of fluid crossing a grid cell (McGrattan 2005). This process helps to enhance the stability of the simulation but can result in long computational times where a fine grid is used and/or a large domain is specified.

To achieve a more realistic simulation, the "Burn away" function in FDS was used to make an object disappear from the computational domain once its fuel had been exhausted and further details can be found in the FDS user guide (McGrattan and Forney 2005). However it is recognised that there are some important phenomena such as any change in the shape of fuel package after collapse of the fuel during the burning process cannot be captured by FDS. FDS is also limited in its ability to model the effects of solid materials like wood related to glowing effects of the material.

Tunnel conditions

To capture the effect of re-radiation, the geometry of the tunnel and the wall lining material were included in the simulation. The thermal conductivity, density and specific heat used for the fire board in the simulation were 0.48 W/m/K, 1440 kg/m^3 and 0.84 kJ/kg/K respectively (Drysdale 1998).

In the experiments, one of the considerations was to protect the tunnel with high temperature resistant fire board insulation as high thermal outputs were expected (Promat 2003). The provision of the fire board would also mean that the tunnel section was smaller and the effect of re-radiation was higher. Therefore, geometry details relating to the provision of the fire board was included in the simulation. A baseline domain size of 9.3 m (width) by 6.3 m (height) by 93 m (length) was selected for the simulations and Figure 10.6 provides the internal tunnel geometry and fire board dimensions used.

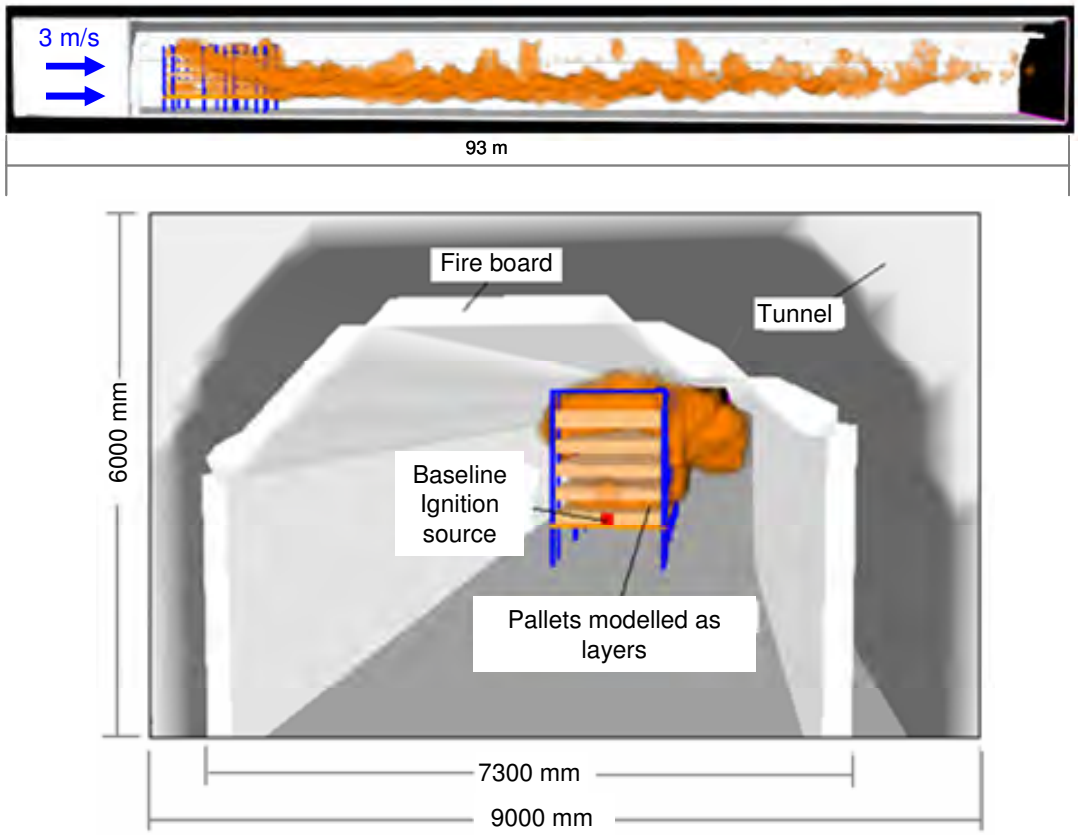

Figure 10.6: Cross section of the Runehamar tunnel showing the geometry set up for the simulations.

As the thermal properties of hard gneiss rock are not available, the thermal properties of concrete were used instead as a baseline. The concrete thermal conductivity, density and specific heat used for the simulation were 1.0 W/m/K, 2100 kg/m^3 and 0.88 kJ/kg/K respectively (Drysdale 1998).

To create a longitudinal airflow in the tunnel, an external forced ventilation boundary condition was provided at the upstream boundary of the tunnel section with the downstream boundary being open to the atmosphere. A baseline upstream uniform velocity of 3 m/s was appropriate to match the experiment.

Fuel geometry

According to Ingason and Lonnermark (2005), the commodities used for each fire experiment represent a specific category of material found in the cargo of semi-trailers. From the experimental results, fire experiment T1 had the greatest calorific value and the

highest peak heat release rate. Selecting experiment T1 for the calibration of the FDS modelling approach and subsequently using it for design fire simulation work provides a certain degree of conservativeness for tunnel fire hazard analysis.

Three types of pallets were used in the T1 experiment; 1.2 m x 0.8 m x 0.15 m wood pallets, 1.2 m x 1 m x 0.15 m wood pallets and 1.2 m x 0.8 m x 0.15 m polyethylene plastic pallets. According to White (2000), pallets of this range of dimension are known as EURO pallets which are one of the internationally recognised standard pallets commonly used in Europe. The authors have made certain assumptions concerning the modelling of the pallets for the Runehamar tunnel fire experiment using FDS. These assumptions include:

1) Dimensions for the wood and plastic pallets were based on EURO pallets.

2) The fuel package was modelled in layers consisting of 80% wood and 20% polyethylene (PE) plastic.

3) These wood or plastic pallets were modelled as a composite material by summing their mass and redistributing it into layers of rectangular elements equivalent to the size of the trailer. The advantage of this approach is that large scale fires with a complex fuel configuration can be simulated.

4) The thermal properties for wood and polyethylene were taken from cone calorimeter tests. The cone test data for wood taken from Thureson (1991) and polyethylene taken from Babrauskas and Grayson (1992) were used in the simulation. Cone test data based on a heat flux of 50 – 70 kW/m^2 were used in this simulation (an enclosure environment) because in a vehicle fire test performed by Shipp and Spearpoint (1995) in an enclosed environment, it has been observed that the heat flux can reach a peak of 50 – 80 kW/m^2. In view of the above reason and given the available cone test data from Thureson (1991) and Babrauskas and Grayson (1992), a heat flux of 50 – 70 kW/m^2 was used for this simulation. Figures 10.7 and 10.8 show the heat release rate per unit area (HRRPUA) cone test data at specified exposure heat fluxes for wood and polyethylene that were used in

the FDS simulations. The wood and polyethylene thermal conductivity, density, ignition temperature and specific heat are tabulated in Table 10.2.

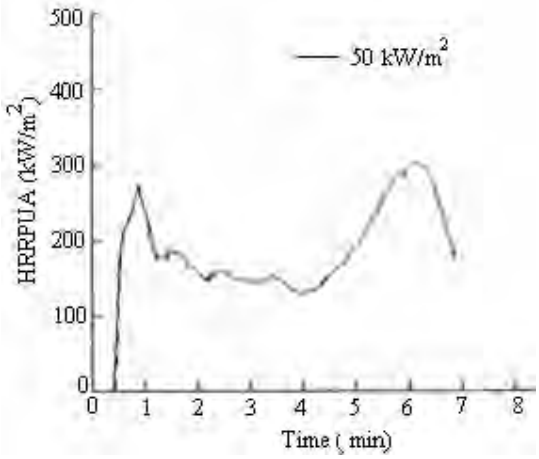

Figure 10.7: HRRPUA for plywood exposed at 50 kW/m^2(Thureson 1991).

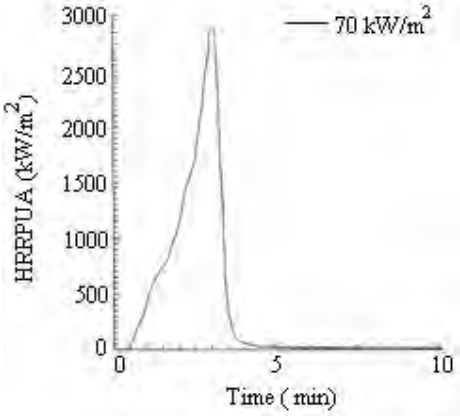

Figure 10.8: HRRPUA for plastic exposed at 70 kW/m^2 (Babrauskas and Grayson 1992)

Material	**Thermal conductivity (W/m/K)**	**Density (kg/m^3)**	**Ignition temperature (^{o}C)**	**Specific heat (kJ/kg/K)**	**HRRPUA (kW/m^2)**
Wood[a]	0.12	600	373	2.58	Figure 10.7
Polyethylene[b]	0.64	956	323	3.00	Figure 10.8

Note: a) Cone test data taken from Thureson (1991)
b) Cone test data taken from Babrauskas and Grayson (1992) and Babrauskas (2003)

Table 10.2: Cone test data for wood and polyethylene

In the T1 fire experiment, a total of 454 pallets were used and fuel load was set up in the proportion by mass ratio of 80% wood and 20% plastic. The arrangement of the wood and plastic pallets burned in the experiment is shown in Figure 10.9.

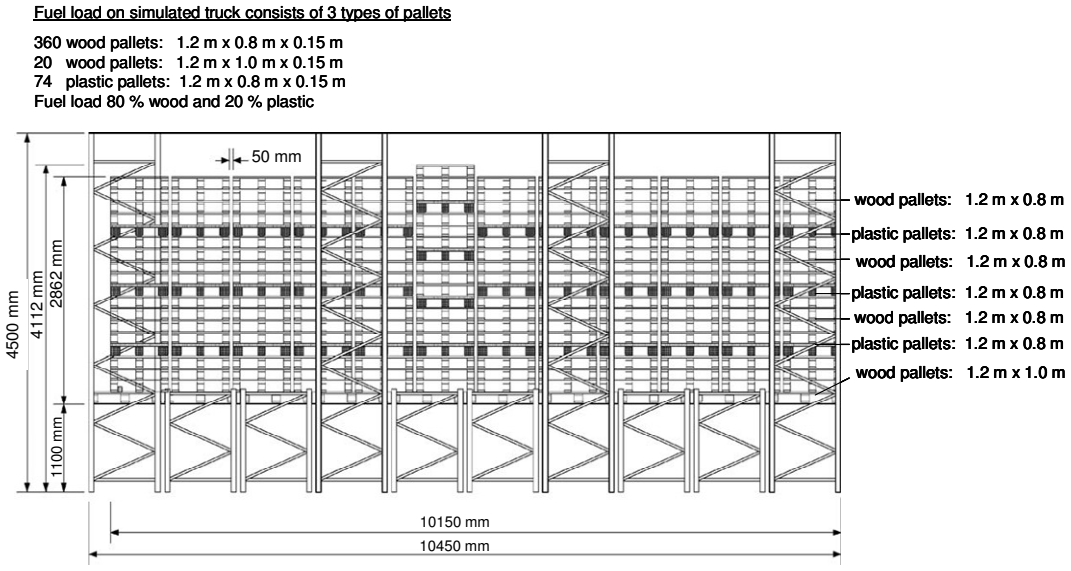

Figure 10.9: Pallet fuel load burned in the T1 Runehamar experiment

In setting up calculation in the FDS simulation, it is necessary to specify geometry in the space and apply boundary conditions to the objects modelled. An object in the FDS simulation is defined as an obstruction (OBST) which can heat up, burn and conduct heat depending on the type of boundary condition specified. Details of various types of boundary conditions are discussed in the FDS user guide (McGrattan and Forney 2005). The time dependent boundary condition was used in this work to estimate the heat release rate for the Runehamar tunnel fire experiment. Burning histories based on heat release rate per unit area taken from cone calorimeter tests were used. When the burning of an obstruction commences, the heat release rate per unit area was ramped up where 'T' is the time in seconds and 'F' indicates the fraction of the heat release rate per unit area (Figure 10.10) to match the data obtained in the appropriate cone calorimeter test.

FDS input parameters for wood material	Remarks
&SURF ID = 'WOOD PALLETS 1.2 X 1'	
FYI = 'PLYWOOD ORDINARY'	
KS = 0.12	Refer to Table 10.2
DENSITY = 600	Refer to Table 10.2
C_P = 2.58	Refer to Table 10.2
DELTA = 0.013	With the pallet mass or volume identify, the thickness can be established
BURN_AWAY = .TRUE.	To make object disappear once fuel is exhausted
TMPIGN = 373	Refer to Table 10.2
BACKING = 'INSULATED'	
HRRPUA = 421.6	[SBF × cone test peak HRRPUA = 310 × 1.36 = 421.6]
RAMP_Q = 'GAP1'	Refer to Figure 10.7
&RAMP ID='GAP1',T= 0.0,F=0 /	Refer to Figure 10.7
&RAMP ID='GAP1',T= 68.0,F=0.85 /	Refer to Figure 10.7
&RAMP ID='GAP1',T= 120.0,F=0.53 /	Refer to Figure 10.7
&RAMP ID='GAP1',T= 180,F=0.48 /	Refer to Figure 10.7
&RAMP ID='GAP1',T= 240,F=0.4 /	Refer to Figure 10.7
&RAMP ID='GAP1',T= 300,F=0.64 /	Refer to Figure 10.7
&RAMP ID='GAP1',T= 383,F=1 /	Refer to Figure 10.7
&RAMP ID='GAP1',T= 420,F=0.54 /	Refer to Figure 10.7

Figure 10.10: FDS input file extract showing an example of the material property Specification

One of the constraints of this modelling approach is the limitation in the available computational capability. Considering the complexity of the pallet construction it was not feasible to model an exact physical representation of each pallet as a substantial number of grid cells, each of the order of 0.01 m or smaller, would be required to capture the geometrical detail resulting in huge computational run times. Therefore to overcome this limitation, the geometry of the pallets was simplified into layers.

From an examination of the pallet arrangement in the experiment it can be seen that for every 4 layers of wood pallets there is a layer of plastic pallets. This stacking arrangement is repeated for three times followed by a single layer of wood pallets contributing a total of 360 wood pallets (1.2 m x 0.8 m), 20 wood pallets (1.2 m x 1 m) and 74 polyethylene pallets (1.2 m x 0.8 m). The simulation model was constructed using five layers each having dimensions with a multiple of 0.15 m to maintain volumes similar to the actual fire experiment. Considering the plastic pallets are sandwiched between every four layers of wood pallets, the fuel package arrangement in the simulation was specified to mimic the fuel arrangement in a similar way to the experiment.

For this type of modelling approach, it is important to ensure the fuel package surface area in the simulation is equivalent to the fuel package area used in the fire experiments. However, it is often not possible to equate a simulated fuel package surface area with the actual fuel area if a simplified fuel geometry is constructed in the simulation. A surface burning factor (SBF) is introduced here to overcome this shortfall. The surface burning factor is established by dividing the surface area of the gross bounding volume of an actual pallet fuel package by the fuel package area modelled in the simulation. This SBF value is multiplied by the heat release rate per unit area from the cone test data and subsequently used in the simulation. Details of the calculation required to establish the surface burning factor and thickness of the fuel used in the Runehamar simulation is presented in Appendix I.

An illustration to determine the surface burning factor for layer 5 (20 wood pallets) is shown as follows:

- The total surface area for layer 5 in the FDS simulation is (9.9 m × 2.7 m × 2) + (9.9 m × 0.3 m × 2) + (2.7 m × 0.3 m × 2) = 61.02 m^2;
- Bounding volume surface area per actual wood pallet (1.2 m by 1 m by 0.15 m) = 4.14 m^2;
- Total bounding volume surface area for 20 actual pallets is 20 × 4.14 = 82.8 m^2;
- Therefore the surface burning rate factor used for the FDS simulation is $\frac{82.8}{61.02} = 1.36.$

The baseline arrangement of the fuel load layout modelled in the simulation is shown in Table 10.3 and Figure 10.11. The 'centre' properties for each layer refer to the vertical faces of the layer as defined by the FDS input file.

Layer	Pallet dimensions (Number of pallets)	Top	Centre	Bottom
		SBF/Material/Thickness	SBF/Material/Thickness	SBF/Material/Thickness
1	1.2 m x 0.8 m x 0.15 m (154 pallets)	10.24 / wood / 0.109 m	10.24 / wood / 0.109 m	10.24 / wood / 0.109 m
2	1.2 m x 0.8 m x 0.15 m (74 pallets)	5 / plastic / 0.03 m	5 / plastic / 0.03 m	7.27 / wood / 0.077 m

3	1.2 m x 0.8 m x 0.15 m (103 pallets)	7.27 / wood / 0.077 m	7.27 / wood / 0.077 m	7.27 / wood / 0.077 m
4	1.2 m x 0.8 m x 0.15 m (103 pallets)	5 / plastic / 0.03 m	7.27 / wood / 0.077 m	7.27 / wood / 0.077 m
5	1.2 m x 1.0 m x 0.15 m (20 pallets)	1.36 / wood / 0.013 m	1.36 / wood / 0.013 m	1.36 / wood / 0.013 m

Table 10.3: Re-distribution of plastic and wood pallets for baseline FDS simulation

Based on the fuel load arrangement shown in Table10.3, the SBF for layer 1 to 5 varies from 1.36 to 10.24. As the fuel quanity of each layer is associated with the SBF, layer with more pallets will have a higher SBF. This approach indirectly accounts for the amount of energy consumed in each layer. To minic the buring behaviour for experiment T1, the plastic material is swapped among layers to establish the HRR curve that resembles the HRR curve from fire experiment T1.

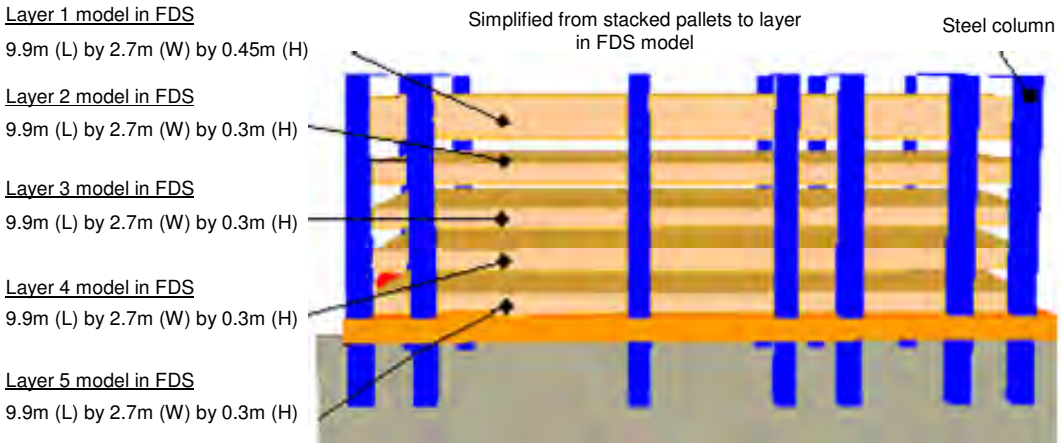

Figure 10.11: Representation of the fuel load pallets model for the Runehamar experiment

10.4 Simulation Results and Comparisons

Baseline simulations run for the Runehamar tunnel experiment T1 were based on conditions described earlier. Observations from the EUREKA (Ingason et al 1994) fire experiments and studies by Carvel et al. (2004a) have shown that ventilation condition, tunnel geometry, fuel configuration and even the location of ignition can affect the burning characteristics of a fire. The effect on the simulated fire growth of these parameters and the FDS representation of the Runehamar tunnel experiment T1 were investigated as part of the computational analysis.

The thermal properties of granite were used to examine if varying the tunnel material properties affected the simulation results. Granite with thermal conductivity, density and specific heat of 2.85 W/m.K, 2640 kg/m^3, 0.82 kJ/kg.K (DiNenno 2002) respectively were used to replace the concrete properties selected for the baseline. Results from simulations using these two types of material did not vary by more than 2.3% and therefore material data for concrete was considered reasonable for the simulations.

The experimental results and the simulated results using FDS are presented in Figure 10.12 to 10.16 for comparison. The effect of grid size, domain length and fuel load configuration were investigated to select what were appropriate ‘calibration’ values. Although the airflow in the fire experiment was provided at 3 m/s, different air velocities were simulated to examine the impact of varying the airflow in the tunnel and its effect on the heat release rate curve. The location of the ignition source was also changed to observe the impact on the heat release rate curve. Table 10.4 shows a summary of the simulations conducted around the Runehamar tunnel fire experiment T1.

Simulation no.	Ignition location	Grid size (mm)	Domain length (m)	Tunnel air flow (m/s)	Fuel arrangement
1	Upstream	150	93	3	Fuel arrangement 1[a]
2	Upstream	300	36	3	Fuel arrangement 1[a]
3	Upstream	300	87	3	Fuel arrangement 1[a]
4	Upstream	300	93	3	Fuel arrangement 1[a]
5	Upstream	300	102	3	Fuel arrangement 1[a]
6	Upstream	300	93	3	Fuel arrangement 2[b]
7	Upstream	300	93	3	Fuel arrangement 3[c]
8	Upstream	300	93	1	Fuel arrangement 1[a]
9	Upstream	300	93	1.5	Fuel arrangement 1[a]
10	Downstream	300	93	3	Fuel arrangement 1[a]

Note: a) Fuel arrangement 1: Refer to Table 10.3
b) Fuel arrangement 2: Plastic pallets positioned in layer 3
c) Fuel arrangement 3: Plastic pallets positioned in layers 2 & 4

Table 10.4: Summary of the FDS simulations performed around the Runehamar tunnel fire experiment

Figure 10.12 shows the simulation results performed on the 300 mm and 150 mm grid sizes. As described earlier, the pallets were modelled as 300 mm thick layers therefore using a grid size larger than 300 mm was not sufficient to capture the burning behaviour of the objects. Simulations using the 150 mm grid required almost 40 days to complete and limitations on computational power and available run times meant that finer grids could not be investigated. Results from the two grid size simulations show a considerable difference which cannot be easily explained particularly as they show that the 300 mm grid gave a more favourable result than the 150 mm grid. It would be typical to expect that the numerical solution will approach the 'exact' solution as finer grids are used but in this case there is no exact HRR for a burning goods vehicle. If the fire experiment were to be repeated under the same conditions it is inevitable that the HRR curve would be different. According to Beard (2008), the peak HRR recorded in the Runehamar fire experiment has been estimated to be around 59th percentile of possible results. Ideally replications of the fire experiments should be undertaken which would yield a distribution HRR data for comparison. Unfortunately such data are not available because of the cost and complexity of doing this. Clearly what is important is that the grid size has a significant influence on

the simulation results and it is only through a calibration process that an appropriate grid can be determined. For this calibration exercise a 300 mm grid is found to give a reasonable match with the experiment where the simulated peak heat release rate of 190 MW compares to the experimental result of 201.9 MW.

Domain sensitivities were performed to ensure that the flame extension was captured in the simulation. Tunnel lengths of 36 m, 87 m, 93 m and 102 m were simulated. Visual inspections of the flame extension using Smokeview; a software tool designed to visualise the numerical calculations computed using FDS (Forney and McGrattan 2004) (Figure 10.6) and a comparison of the HRR results shown in Figure 10.13 indicate a domain length of 36 m was not appropriate whereas 93 m is sufficient to capture the flame extension for this analysis.

Three fuel configurations were simulated to examine if there was any significant effect on the fire development. Fuel arrangement 1 was used as the baseline and is described in Table 10.3. Fuel arrangement 2 had the plastic pallets only positioned in layer 3 whereas fuel arrangement 3 had the plastic pallets positioned in layers 2 and 4. From the simulation results shown in Figure 10.14, it appears that these fuel package arrangements do have an affect on the HRR. Comparing the simulated fuel arrangement layouts with the Runehamar tunnel fire experiment T1, in terms of the growth rate and peak heat release rate, fuel arrangement 1 has the closer resemblance to the HRR curve from T1 although arrangement 2 gave very similar results. Therefore fuel arrangement 1 was used as the baseline for the other simulation analysis work.

The influence of ventilation on fire in tunnels was investigated. For illustration purposes, velocities of 1 m/s, 1.5 m/s and 3 m/s were performed similar to ventilation velocities that might be expected from a tunnel smoke control system and Figure 10.15 indicates there is an increase in the peak heat release rate as the air velocity in the tunnel increases similar to previous experimental observations (Ingason et al 1994),(Carvel et al. 2004a). The total simulated energy release at 3 m/s was found to be 257 GJ compared with the theoretical 247 GJ experimental value (Table 10.1). It is also clear that the total energy released increases with velocity and one reason for the enhanced burning may be due to the provision of additional oxygen to the fire improving the mixing in the flames.

The effect of ignition location (rear and front of the trailer, Figure 10.17) where ignition occurred at the base of fuel stack adjacent to the upper surface of the platform and midway across the lateral extent of the fuel was also studied to examine fire development using longitudinal ventilation in the tunnel. Examination of the fire simulations number 4 and 10 (Figure 10.16) shows the location of the ignition source can affect fire development. The results show that in the presence of tunnel air flow that a fire ignited at the upstream of the trailer spreads faster and yields a slightly higher heat release rate as compared to fire ignited at the downstream end of the trailer. Conversely, if the ignition occurs at the downstream end of the fuel load there will be a delay in the fire development. Similar findings have been observed in the large scale fire tests in Second Benelux Tunnel (Lemaire and Kenyon 2006).

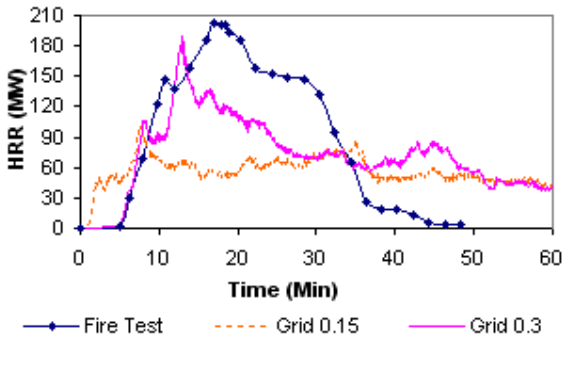

Figure 10.12: Grid sensitivity (simulations 1 and 4)

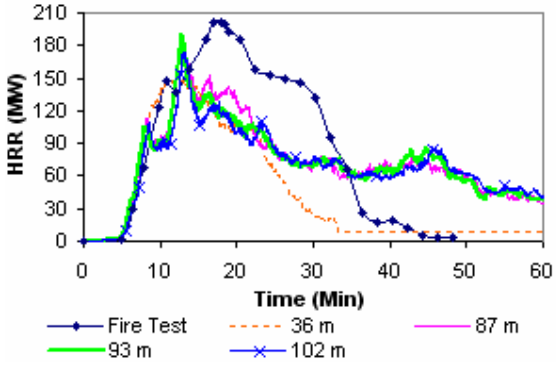

Figure 10.13: Domain length sensitivity (simulations 2,3,4 and 5)

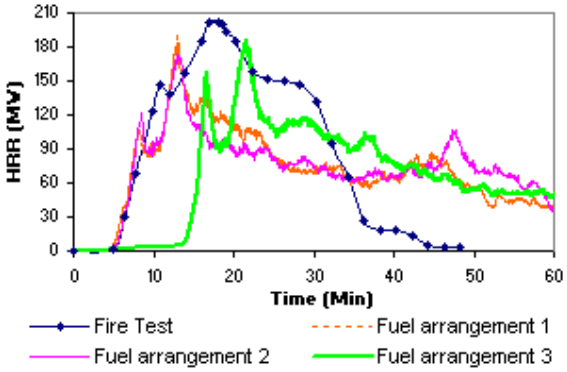

Figure 10.14: Different fuel arrangement (simulations 4,6 and 7)

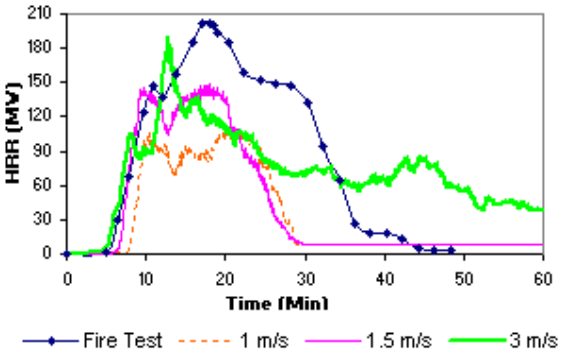

Figure 10.15: Different tunnel airflow (simulations 4,8 and 9)

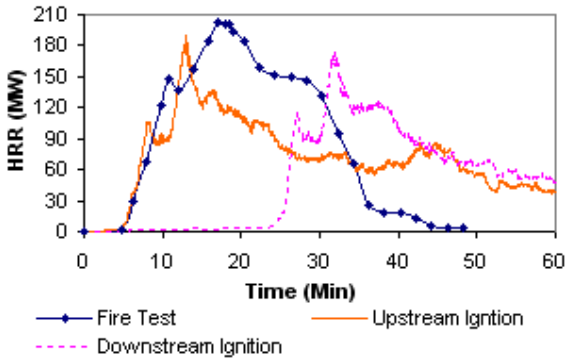

Figure 10.16: Different ignition location (simulations 4 and 10)

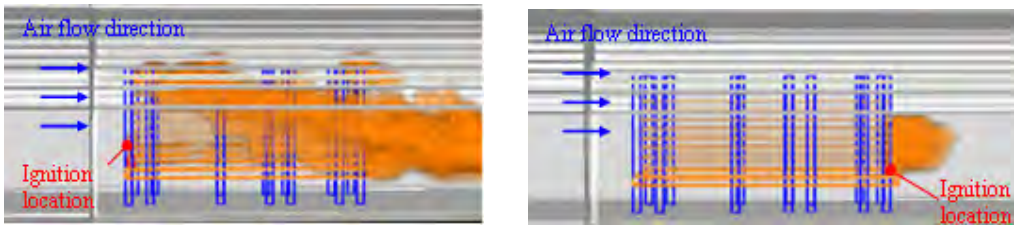

Time 800 sec: Upstream ignition at 3 m/s Time 800 sec: Downstream ignition at 3 m/s

Figure 10.17: Effect of ignition location on fire behaviour

The chronology of the Runehamar tunnel fire experiment T1 at 0, 5 and 30 minute intervals are shown in Figure 10.18. Photographs taken from the experiment are compared with the snap shots taken from the Runehamar tunnel simulation number 4. Although the simulation was able to simulate the growth rate history and peak heat release rate, as expected, phenomena such as collapse of the fuel package during the burning process was not captured. The detailed discussion on the limitation of using this approach to estimate the heat release rate of the pallets is covered in Chapter 16 of this thesis.

Photograph of fire experiment T1 **Snap shot from FDS simulation**

Fuel load at time 0

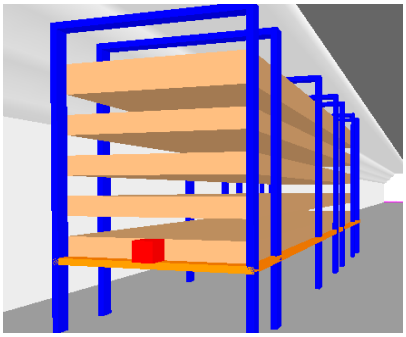

Fuel load at time 0

Fire development after 5 minutes

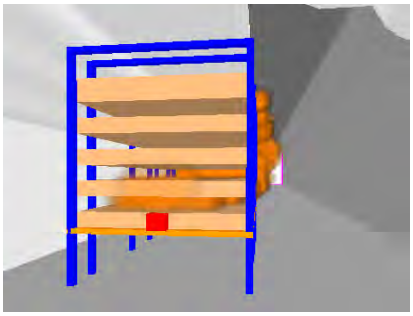

Fire development after 5 minutes

Fire development after 30 minutes

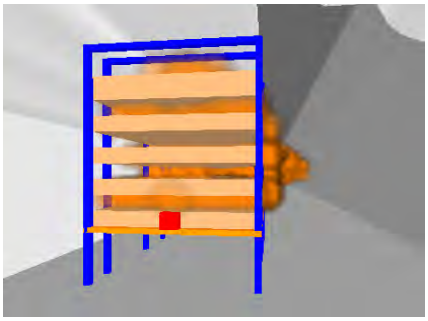

Fire development after 30 minutes

Figure 10.18: Runehamar tunnel fire events from actual test and FDS simulation (photographs reproduced from Promat 2007b)

10.5 Findings

The following findings were obtained when comparing the FDS fire growth curve with the heat release rate in the Runehamar tunnel fire experiment T1:

1. Using a grid size of 300 mm for the simulations was appropriate for the following reasons:

   i) The simulations based on a 300 mm grid produce fairly consistent predictions in terms of the growth phase of the fire development as compared with the actual fire experiment.

   ii) From Figure 10.12, the 300 mm grid size provides a closer resemblance in terms of its peak HRR and fire curve as compared with the 150 mm grid size.

   iii) Depending on the computer speed, a typical workstation (Pentium IV, 1 GB RAM) could take more than 39 days to simulate the fire using a grid size of 150 mm in order to provide results compared with 5 days for the 300 mm grid.

2. The domain sensitivity shown in Figure 10.13 illustrates that it is important to define an appropriate domain size for the simulation. A computational domain which is not large enough may not capture all the flame extension produced from the combustion resulting in a lower heat release rate output estimated from the simulation.

3. It is important to ensure the fuel package surface area model in the simulation is equivalent to the fuel package area used in the fire experiments. This can be achieved by introducing a 'surface burning factor' in the simulation as illustrated in this work.

4. To establish the heat release rate in a tunnel, it is important to capture the details of the tunnel geometry and air velocity in the simulation as the effect of re-radiation and ventilation conditions in the tunnel are likely to affect the fire development.

5. Depending on the airflow velocity, the fire development in tunnels can vary substantially. Tunnel airflow direction and the ignition location can have a significant effect in delaying or accelerating the propagation of the fire during the initial stages of the fire development. The location of the ignition source at both

upstream and downstream of the fire may need to be considered when establishing a design fire for a tunnel.

10.6 Conclusions

A calibrated simulation of the Runehamar tunnel fire experiment T1 using FDS 4.0.7 demonstrates that the model is able to capture much of the detail of the fire growth rate and peak heat release rate compared to the experimental result. Although simulation results using this modelling approach look favourable, the current approach has only focused on the modelling of wood and plastic pallets in a trailer. A similar exercise would need to be performed if other commodities (e.g paper cartons, mattresses) with a different fuel arrangement was used for an FDS simulation. Other simulation parameters such as a SBF, the grid size and domain length would need to be re-examined as these modelling assumptions can affect the heat release rate estimate. This work has particularly noted that:

i) The modelling of a complex fire scenario in a CFD model such as FDS is challenging task. Calibrating simulations against experimental data is a useful approach which then allows the effect of varying parameters outside of the original experiments to be investigated.

ii) Although similar growth rate history and peak heat release rate were produced from the simulations (Figure 10.19), the current model is unable to simulate phenomena such as collapse of the fuel package.

iii) The results from the FDS model show that airflow in the tunnel will have a significant effect on the heat release rate where a higher airflow yields higher heat release rate.

iv) The location of the ignition source will affect the fire growth characteristics of a goods vehicle burning in a tunnel. A fire originating at the upstream end of the fuel package accelerates the fire spread as compared to fire ignition occurring at the downstream end of the fuel package.

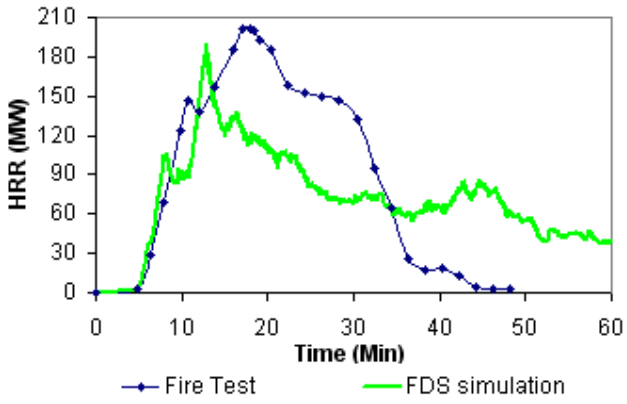

Figure 10.19: Heat release rate recorded from Runehamer fire test Vs FDS simulation

Additional Comments:

The following text was not included in the original paper because of subsequent additional work carried out by the author.

10.7 Radiation Distribution on Surface

In large-scale fires, radiative transport can be an important parameter in affecting the rate of flame spread on the fuels surface. The multidimensional combustion within the domain consists of highly non-isothermal and non-homogeneous medium where the radiative properties of the medium can greatly complicate the modelling of the heat transfer within a burning environment (Karlsson and Quintiere 2000).

In FDS, the Radiative Transport Equation (RTE) for an absorbing and scattering medium as shown in equation 7.15 is used. The equation consists of the source term, the radiation intensity at a specific wavelength, the direction vector of the intensity and the absorption coefficient. The spectral calculations are performed by dividing the wavelength spectrum into several bands and a separate RTE is derived for each band. To obtain the discretized form of the RTE, the unit sphere is divided into a finite number of solid angles. The discretized RTE is derived by integrating equation 7.15 over the grid cell and the control angle. A narrow-band model, Rad-Cal is combined with FDS for the computation where during the simulation absorption coefficient is found by table-lookup (McGrattan 2005).

The equations to calculate the radiation intensity in FDS are shown in Equation 10.13 where $\dot{q}'''$ is the HRR per unit volume, χ_r is the local fraction of that energy emitted as thermal radiation, σ is the Stefan-Boltzmann constant, κ is the absorption coefficient and T is the temperature (McGratten 2005).

$$\kappa I = \begin{cases} \kappa\sigma T^4/\pi & \textit{Outside flame zone} \\ \max(\chi_r \dot{q}'''/4\pi, \kappa\sigma T^4/\pi) & \textit{Inside flame zone} \end{cases} \qquad \text{Equation 10.3}$$

The following work attempts to examine the calibration model used in this chapter to see if there is any concern on the radiation banding or star-like pattern where propagation of flame spread on the fuel surface would be affected. Radiation banding in this context refers to pattern of high and low intensity radiation zone that occurs on the surface which can be an artefact produced in FDS. If the radiation is correctly modelled, one would expect the distribution of the heat flux decreases when the measurement is taken at a distance further away from the heat source as shown in Figure 10.20a. In the example shown in Figure 10.20b where 1 dimensional banding occurs, one would notice a series of peaks and troughs in the radiation distribution occur where sign of radiation intensity reduces when measurement taken at a distance further away from the heat source are not observed. When the effect of banding is projected in the x and y axis on a surface object, a star-like pattern will be developed.

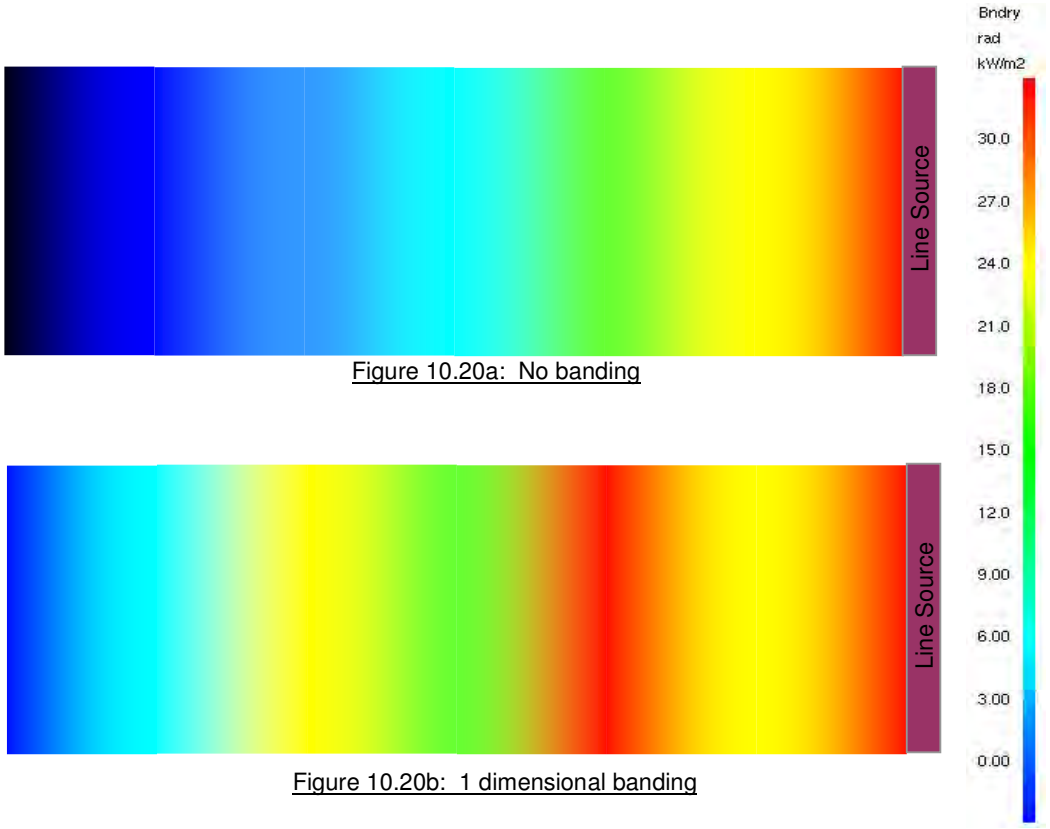

Figure 10.20a: No banding

Figure 10.20b: 1 dimensional banding

Figure 10.20: Examples of radiation banding
(please note that the coloured scale reproduced is representative of the visualisation method used by Smokeview to indicate heat flux profiles over surfaces.)

For the fire reconstruction work in this chapter; once the fire is fully developed, it is difficult to determine whether the effect of radiation banding (if any) is a result of the combustion or if it is due to the modelling limitation. In order to isolate this uncertainty, the investigation work in this section looks at the early stages of the fire development around the ignition burner. A sensitivity analysis by varying the number of solid angles 100 (default value in FDS) and 300 was also performed to see if this would affect the simulation results.

The Runehamar tunnel model as previously discussed in this chapter is used with an air velocity of 3 m/s introduced at one end of the tunnel. The simulation setup for this study is shown in Figure 10.21.

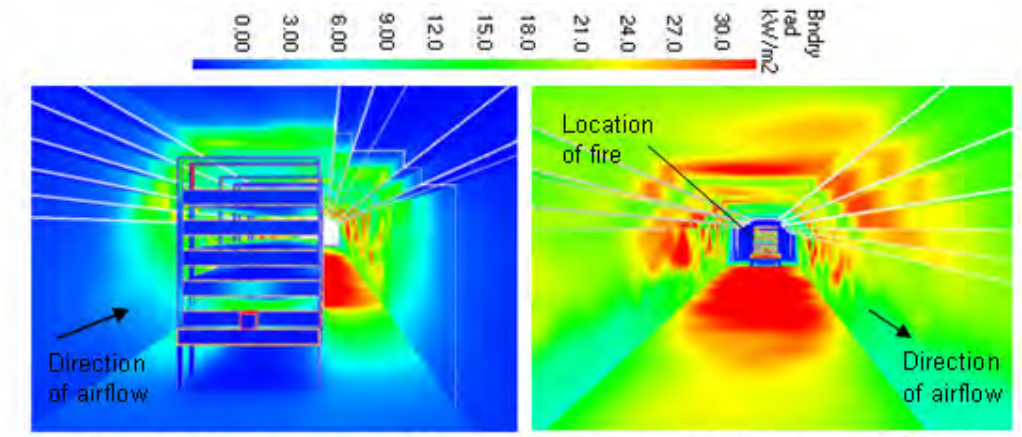

Figure 10.21a; Downstream of fire *Figure 10.21b; Upstream of fire*

Figure 10.21: Model setup

Number radiation angles = 100, Grid = 0.3 m Number radiation angles = 300, Grid = 0.3 m

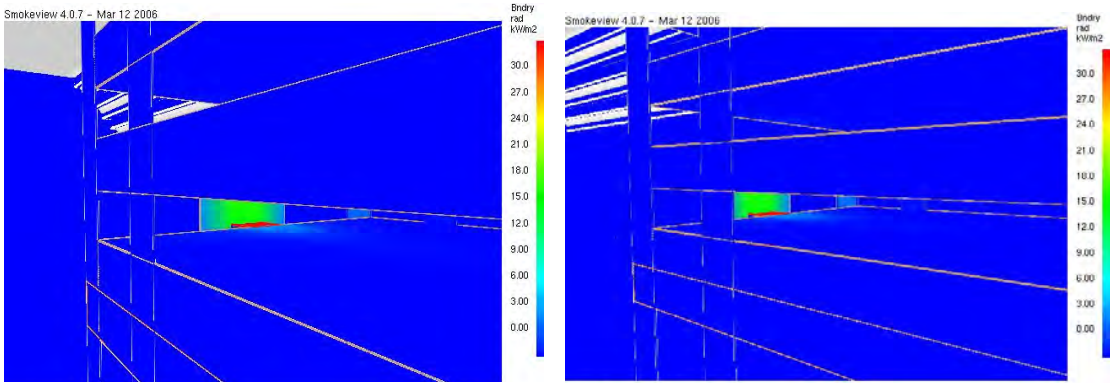

Figure 10.22a: Simulation time at 0 sec

Figure 10.22: Radiation heat flux on fuel surface

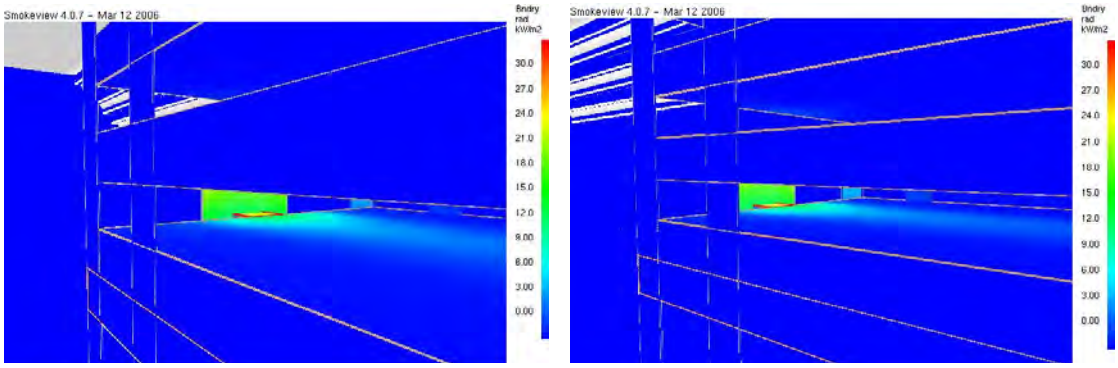

Figure 10.22b: Simulation time at 60 sec

Number radiation angles = 100, Grid = 0.3 m Number radiation angles = 300, Grid = 0.3 m

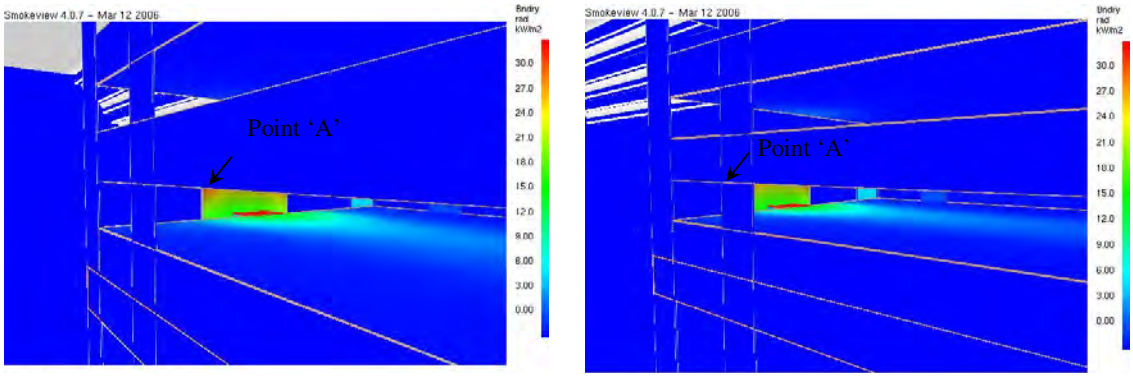

Figure 10.22c: Simulation time at 120 sec

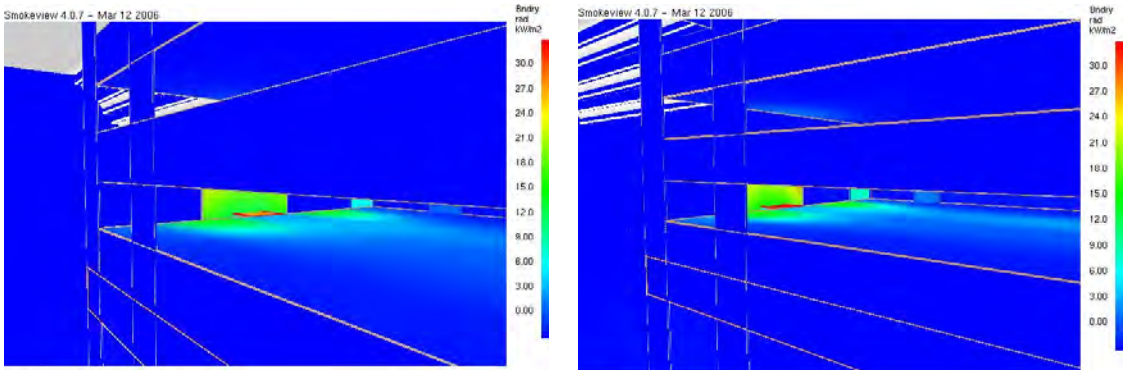

Figure 10.22d: Simulation time at 180 sec

Figure 10.22: Radiation heat flux on fuel surface

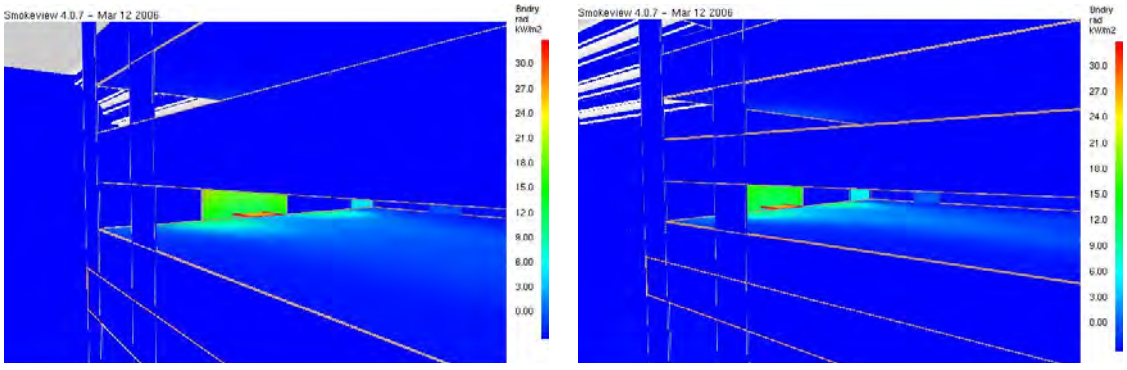

Figure 10.22e: Simulation time at 240 sec

Number radiation angles = 100, Grid = 0.3 m Number radiation angles = 300, Grid = 0.3 m

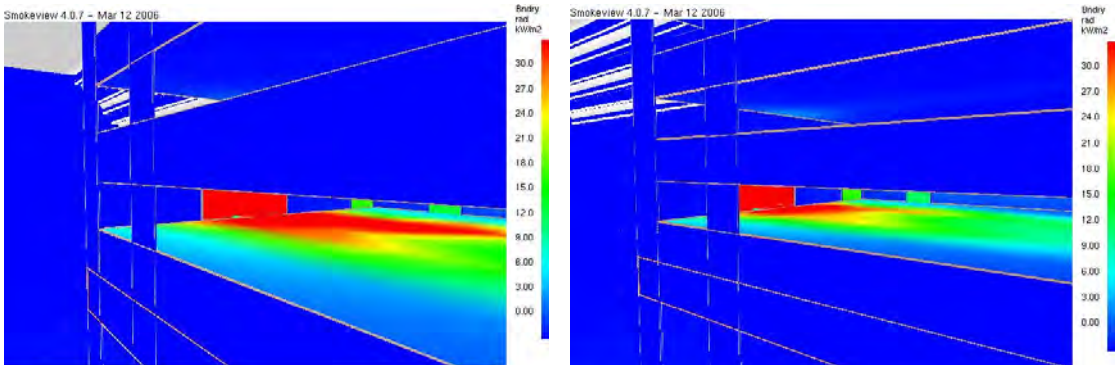

Figure 10.22f: Simulation time at 300 sec

Figure 10.22: Radiation heat flux on fuel surface

Figure 10.22 shows the snap-shot view of the surface radiation heat flux on the pallets layer at 1-minute intervals over a period of 5 minutes of the fire development. It has been observed that there is no sign of radiation banding occurs around the ignition burner and the distribution of radiation flux on the fuel surfaces seems one would expect where the radiation intensity reduces when the measurement is taken at a distance further away from the ignition burner (Figure 10.22). At 120 sec of the simulation results (Figure 10.22c), it appears that there is a localised area (point 'A') where higher radiation heat flux is observed at a location further away from the ignition burner. The higher radiation flux is due to the effect of flame extension near point 'A' resulting in the above simulation outcome.

There is also no significant difference between the two simulations performed with the number of solid angles increasing from 100 to 300 (Figure 10.22). The computed heat release rate graph for 100 and 300 number of radiation angles is shown in Figure 10.23.

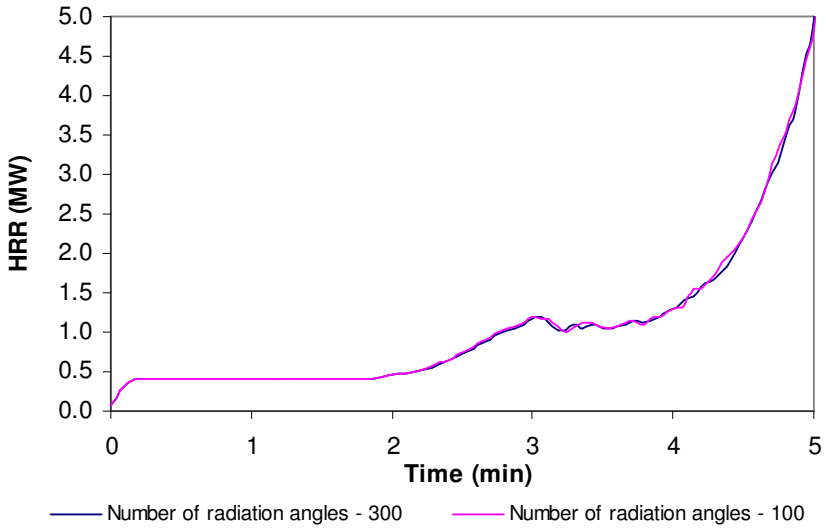

Figure 10.23: HRR for 100 and 300 number of radiation angles

From the above study, it appears that there is no major concern on the radiation banding or star-like pattern where propagation of flame spread on the fuel surface would be affected. However, the mechanism of flame spread is highly complicated due to the complex combustion dynamics and fluid mechanics sub-processes involved. These include heat transfer, combustion, turbulence and the effect of soot. For each of these processes, it involves a number of models and it is difficult to isolate what is going on with the radiation. Although an effort has made to isolate some of this process by examining the fire at the early phase of the development, it would be beneficial to perform more work to address some of the issues as mentioned above in future research work.

Chapter 11:
NUMERICAL SIMULATION OF A GOODS VEHICLE FIRE IN TUNNEL

Cheong M K, Spearpoint M J, Fleischmann C M, published as "Design Fires for Vehicles in Road Tunnel", in the 7th International Conference on Performance-Based Codes and Fire Safety Design Methods, Auckland New Zealand, pp. 229 - 240, April 2008.

This chapter covers the materials presented in the above paper; it provides an outline on the modelling approach used to establish the heat release rate in an urban road tunnel taking into consideration the quantity of the fuel load, tunnel geometry, ventilation condition in the tunnel and the location of the ignition. FDS 4.07, a computational fluid dynamics program, is used for the analysis. The simulation approach to predict the heat release rate for a heavy goods vehicle (HGV) or a light goods vehicle (LGV) in the tunnel is similar to the approach described in chapter 10 for the Runehamar tunnel except different sizes of the fuel load were used and materials in the truck cabin such as the vehicle's seat, internal panels, tyres etc were included in these simulation analyses. The simulation analyses in this chapter also build-on the information and analysis performed and discussed in chapters 6 and 8.

11.1 Quantity and type of fuel load

The first step is to determine a credible fire scenario in the tunnel. Risk analysis performed in chapter 8 had identified two types of potential fire scenarios that would likely occur in this tunnel. These scenarios are fire due to vehicle fault (e.g. engine fire, brake overheating, electrical fault) in a single light goods vehicle (LGV) and a single heavy goods vehicle (HGV) collision resulting in a fire. Therefore, these two scenarios are used as a basis for subsequent FDS simulation. A summary of the risk analysis finding is reproduced in the table below for easy reference.

Types of potential fire risk	*Vehicle fault*	*Act of carelessness*	*Intentional*	*Collision*
Maximum expose risk:	8.14×10^{-4}	1.70×10^{-4}	3.72×10^{-4}	1.39×10^{-6}
Number of vehicles involved :	Single LGV	Single LGV	Single LGV	Single HGV

Light goods vehicle (LGV)

Heavy goods vehicle (HGV)

Figure 11.1: Risk analysis findings

Past fire tests conducted in Second Benelux Tunnel and Runehamar tunnel indicated that the fire size for a LGV and a HGV is around 16 MW (at a ventilation air velocity of 6 m/s) and 203 MW (at a ventilation air velocity of 3 m/s) respectively. Considering the scenarios of a single light goods vehicle or a single heavy goods vehicle fire and from the calculation shown in Table 11.1, when a fire occurs in this study, it is more likely to be fuel-controlled rather than ventilation-controlled as the tunnel ventilation fans will generate a high flow

rate. For such fires, the burning rate and heat output is dependent on the amount of fuel available for burning which is related to the size of the goods vehicle.

Calculations to determine combustion mode in tunnel

Calculation for main tunnel	**Calculation for slip road**
Tunnel section: typical main tunnel Cross section area: 90 m^2 Air velocity in tunnel (v): 3.1 m/s Air density (ρ): 1.2 kg/m^3 $\phi = 3000\frac{\dot{m}_a}{Q}$ Equation 11.1 (Ingason 2005) where ϕ: stoichiometric combustion $\phi > 1$ the fire is fuel-controlled $\dot{m}_a$: mass flow rate air (kg/s) Q : HRR (kW) $\dot{m}_a = \rho \times v \times area$ $\dot{m}_a = 1.2 \times 3.1 \times 90 = 334.8 kg/s$ By setting ϕ = 1 and using Equation 11.1 $Q = 3000\frac{334.8}{1} = 1004400 kW$ to obtain a ventilation-controlled fire.	Tunnel section: typical slip road Cross section area: 55.8 m^2 Air velocity in tunnel (v):1.7 m/s Air density (ρ): 1.2 kg/m^3 $\phi = 3000\frac{\dot{m}_a}{Q}$ Equation 11.1 (Ingason 2005) where ϕ: stoichiometric combustion $\phi > 1$ the fire is fuel-controlled $\dot{m}_a$: mass flow rate air (kg/s) Q : HRR (kW) $\dot{m}_a = \rho \times v \times area$ $\dot{m}_a = 1.2 \times 1.7 \times 55.8 = 113.8 kg/s$ By setting ϕ = 1 and using Equation 11.1 $Q = 3000\frac{113.8}{1} = 341400 kW$ to obtain a ventilation-controlled fire.

Table 11.1: Calculation to determine combustion mode in tunnel

According to LTA (2006), vehicle types are classified into cars, taxis, motorcycles, buses and goods vehicles. Under goods vehicles, they are further categorized into light goods vehicles (LGV), heavy goods vehicles (HGV) and very heavy goods vehicles (VHGV). The classification of goods vehicles are according to their laden weight where goods vehicles less than 3.5 tonne are categorized as LGV, vehicles with laden weight between 3.5 tonne to 16 tonne are HGV (example rigid truck) and vehicles more than 16 tonne laden weight are identified as VHGV (example tractor with trailer). It has been discussed in chapter 5 that vehicles more than 13 m are prohibited from entering the tunnel and generally VHGV falls under this category. Thus VHGV is not considered in the simulation

analysis as they are not allowed to enter the tunnel. Further analysis work will be focused on LGV and HGV.

In a goods vehicle fire, the main component that could sustain combustion is the commodities on the vehicle and the vehicle itself. The following sections provide an approach in establishing the type and quantity of material used for the FDS simulation.

11.1.1 Establish the commodities and quantity in goods vehicle

The amount of fuel load a goods vehicle can carry is dependent on the goods vehicle category. Goods vehicle of higher category are generally larger in size and is capable of carrying larger loads. Although goods vehicles are categorized according to their laden weight, the dimensions of a LGV or a HGV varies from one vehicle to another, depending on the manufacturer. To address this issue, a common goods vehicle by make on the Singapore road were selected for this analysis. The common deck dimensions used in an LGV and HGV are shown in Table 11.2.

Light goods vehicle (LGV)
Deck dimensions: 3.1 m (length) by 1.69 m (width)
Heavy goods vehicle (HGV)
Deck dimensions: 8.2 m (length) by 2.4 m (width)

Table 11.2: Goods vehicle deck dimension for LGV and HGV

There is also a requirement in Singapore where heavy goods vehicle with height more than 4.5 m is not allowed to enter the tunnel (Traffic Act 2006) and for light goods vehicle, the maximum canopy installation height should not be more than 3.2 m (LTA Veh Eng 2007). Given the above requirements, the simulation model construction for a LGV or a HGV inclusive of the fuel load is based on dimensions shown in Figure 11.2 and Figure 11.3 respectively.

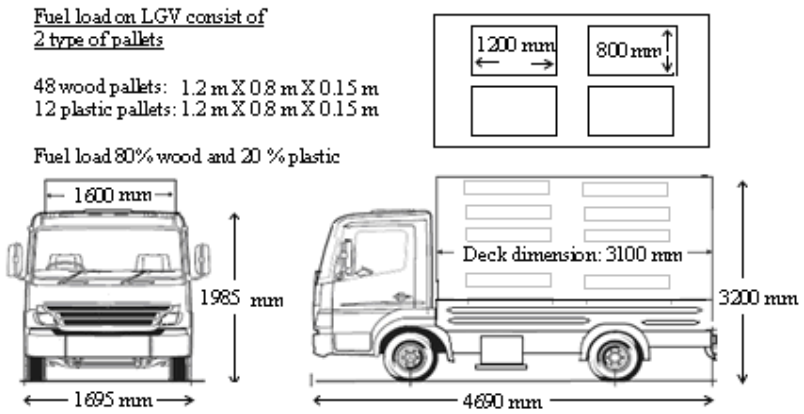

Figure 11.2: LGV carrying wood and plastic pallets

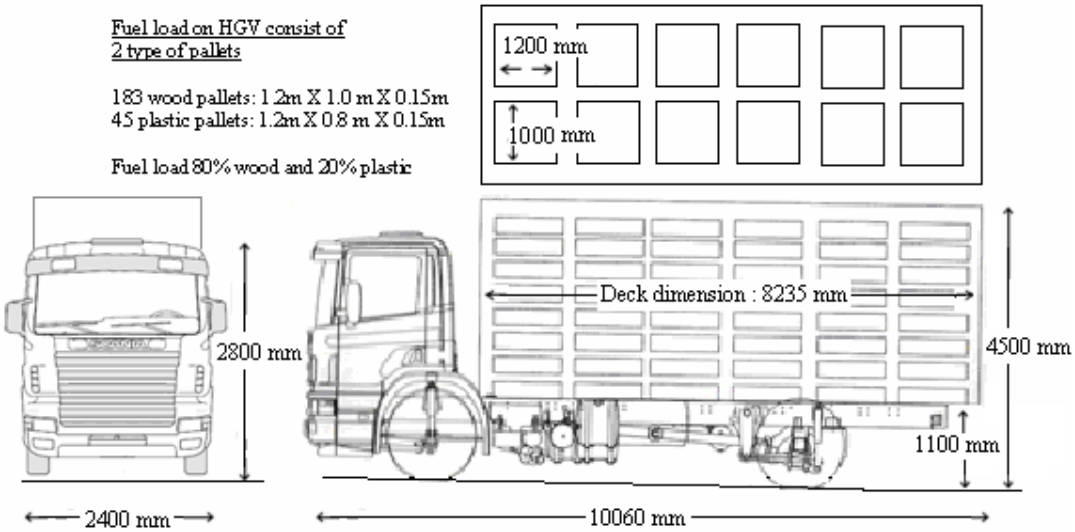

Figure 11.3: HGV carrying wood and plastic pallets

Another factor that affects the heat release rate is the type of cargo / commodity (e.g. wood, plastic) selected for the simulation. The type of cargo and the quantity carried by goods vehicles transversing the tunnel varies considerably. As information on commodities transported by road in Singapore is not available, data from other countries such as Sweden was used instead. Like Sweden, Singapore is a well developed country where the daily necessity products are similar in nature; therefore it is a reasonable assumption to use data from this county for this analysis.

According to Ingason and Lonnermark (2003), Swedish statistics have identified 24 different groups of commodities commonly transported on Swedish roads, these combustible commodities can be apportioned by mass ratio into four different categories:

cellulose materials - 42%, packaging material - 28%, food product - 17% and oil product - 13% and discussion with professional goods transport agents indicated that a mass ratio of 80 – 85% cellulose material and 15 - 20% plastic would be a reasonable division among these categories.

Gathering the above information, the types of commodities by mass ratio selected for the simulation is 80% wood and 20% plastic with the quantity of commodities dependent on the amount of pallets a goods vehicle (depending on vehicle category – e.g. LGV or HGV) can carry. The following sections describe the process of establishing the quantity of combustible fuel for the simulation.

11.1.2 Commodities fuel load thickness and surface burning factor used in FDS simulation

This section explains the approach to establish the thickness and surface burning factor for the goods vehicle simulation. It presents the calculation for an HGV. A similar approach is adopted for an LGV and the detailed calculation for an LGV is attached in Appendix K.

The deck dimensions (allowable cargo space) for a HGV is approximately 8.2 m (L) by 2.4 m (W) by 3.4 m (H). An HGV of this size is able to carry around 228 pallets and by using a mass ratio of 80 % wood and 20 % plastic, the fuel load used for the FDS simulation for a HGV consists of 183 wood pallets (1.2 m × 1 m × 0.15 m) and 45 plastic pallets (1.2 m × 0.8 m × 0.15 m) (Figure 11.4).

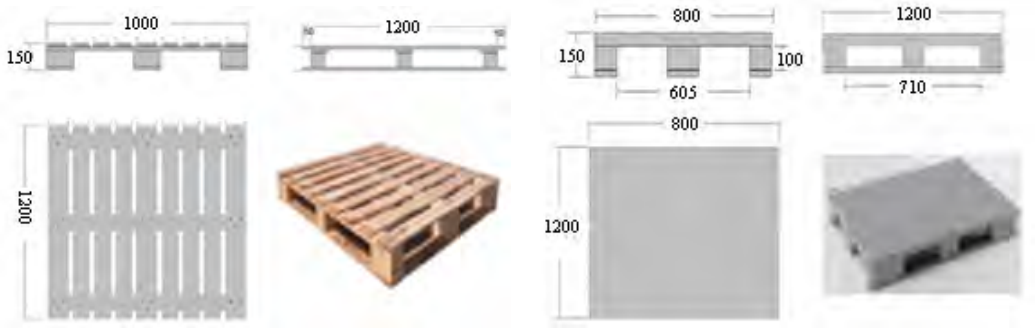

1.2m by 1.0m by 0.15m wood pallets (reproduced from (*VTPL* 2000a))

1.2m by 0.8m by 0.15m plastic pallets (reproduced from (Kaiserkraft 2006))

Figure 11.4: Wood and plastic pallets dimensions

To simplify the modelling of wood and plastic pallets, these pallets are modelled as multiple layers in the simulation (Figure 11.5). The re-distribution of plastic and wood pallets for the HGV simulation model is as follows:

HGV simulation

Layer	Pallet dimensions (Number of pallets)	Top SBF/Material/Thickness	Centre SBF/Material/Thickness	Bottom SBF/Material/Thickness
1	1.2 m x 1.0 m x 0.15 m (60 pallets)	6.12 / wood / 0.059 m	6.12 / wood / 0.059 m	6.12 / wood / 0.059 m
2	1.2 m x 0.8 m x 0.15 m (45 pallets)	5 / plastic / 0.029 m	5 / plastic / 0.029 m	4.51 / wood / 0.043 m
3	1.2 m x 1.0 m x 0.15 m (41 pallets)	4.51 / wood / 0.043 m	4.51 / wood / 0.043 m	4.51 / wood / 0.043 m
4	1.2 m x 1.0 m x 0.15 m (41 pallets)	5 / plastic / 0.029	4.51 / wood / 0.043 m	4.51 / wood / 0.043 m
5	1.2 m x 1.0 m x 0.15 m (41 pallets)	4.51 / wood / 0.043 m	4.51 / wood / 0.043 m	4.51 / wood / 0.043 m

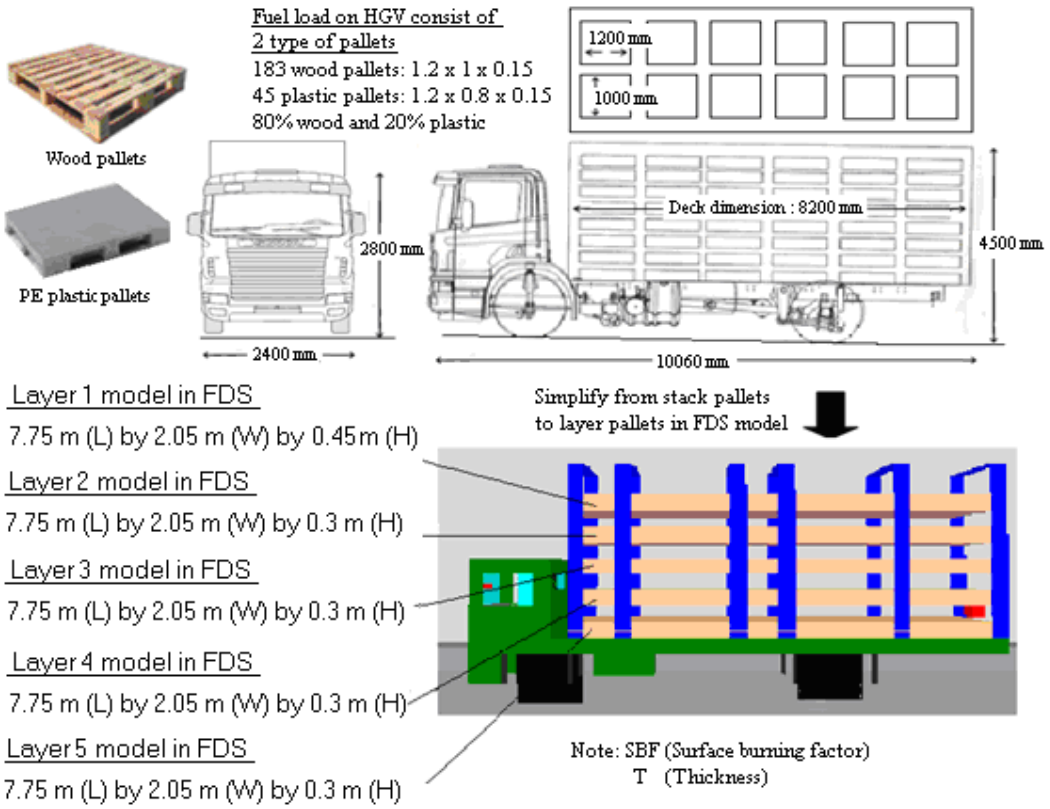

Figure 11.5: Dimensions for heavy goods vehicle (HGV)

Calculations to determine thickness and surface burning factor for layer 1 pallets (HGV)

Layer 1 – based on layer with 60 pallets

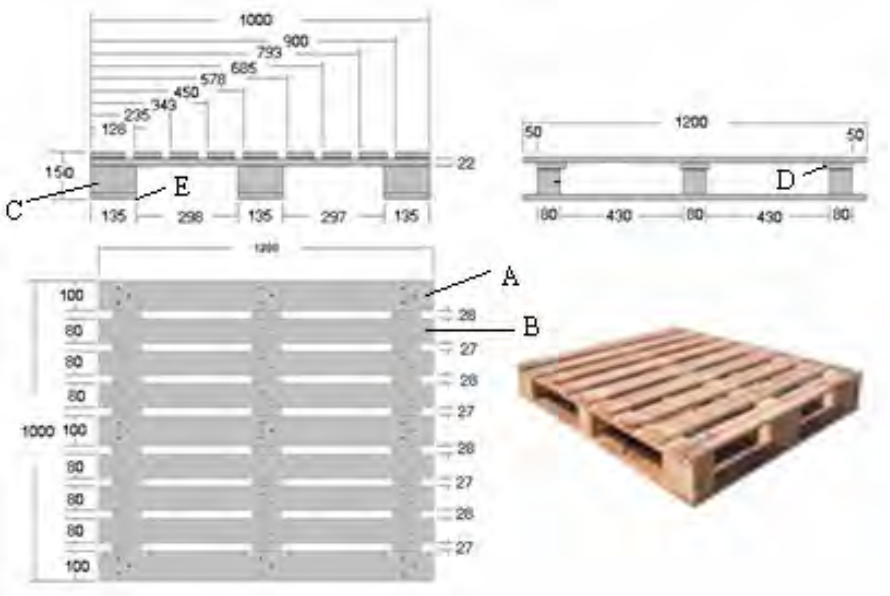

Figure 11.6: 1.2m by 1m by 0.15m wood pallets

Plank	*Number of planks*	*Total area (m^2)*	*Total volume (m^3)*
A	*3*	*0.82*	*0.008*
B	*6*	*1.37*	*0.013*
C	*9*	*0.33*	*0.008*
D	*3*	*0.67*	*0.005*
E	*3*	*0.95*	*0.009*

Total area per pallet = 0.82+1.37+0.33+0.67+0.95=4.14 m^2

Total volume per pallet = 0.008+0.013+0.008+0.005+0.009=0.04 m^3

Volume per actual wood pallet (1.2m by 1.0m by 0.15m) is 0.04 m^3.

Total volume for 60 actual pallets is $60 \times 0.04 = 2.4$ m^3.

The total area model for layer 1 in the simulation is

$(7.75\text{m} \times 2.05\text{m} \times 2)+(7.75\text{m} \times 0.45\text{m} \times 2)+(2.05\text{m} \times 0.45\text{m} \times 2) = 40.6$ m^2.

Therefore the thickness used for the FDS simulation is $\frac{2.4}{40.6} = 0.059$ m.

Area per actual wood pallet (1.2m by 1.0m by 0.15m) is 4.14 m^2.

Actual total area for 60 pallets is $60 \times 4.14 = 248.4$ m^2

Therefore the burning rate factor used for the FDS simulation is $\frac{248.4}{40.6} = 6.12$

Calculations to determine thickness and surface burning factor for layer 2 pallets (HGV)

Layer 2 – based on layer with 45 pallets

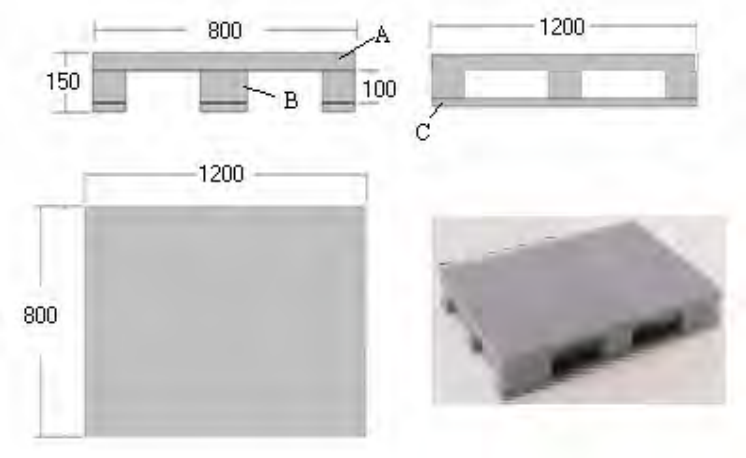

Figure 11.7: 1.2m by 0.8m by 0.15m plastic pallets

Plank	*Number of planks*	*Total area (m^2)*
A	*1*	*2.02*
B	*9*	*1.037*
C	*2*	*0.598*
D	*1*	*0.428*

Total area per pallet = 2.02+1.037+0.598+0.428=4.1 m^2

Mass for 1 pallet of PE plastic is 23 kg. (kaiserkraft 2006)

Density for PE plastic is 956 kg/m^3. (Babrauskas 2003)

Volume per actual plastic pallet is $\frac{mass}{density} = \frac{23}{956} = 0.024\,\mathrm{m}^3$

Total volume for 45 actual pallets is 45 × 0.024 = 1.08 m^3.

The total area model for layer 2 in the simulation is

(7.75m × 2.05m × 2)+(7.75m × 0.3m × 2)+(2.05m × 0.3m × 2) = 37.66 m^2.

Therefore the thickness used for the FDS simulation is $\frac{1.08}{37.66} = 0.029$ m.

Area per actual plastic pallet (1.2m by 0.8m by 0.15m) is 4.1 m^2.

Actual total area for 45 pallets is 45 × 4.1 = 185 m^2.

Therefore the surface burning factor used for layer 2 is $\frac{185}{37.66} = 5$

Calculations to determine thickness and surface burning factor for layer 3 pallets (HGV)

Layer 3 – based on layer with 41 pallets

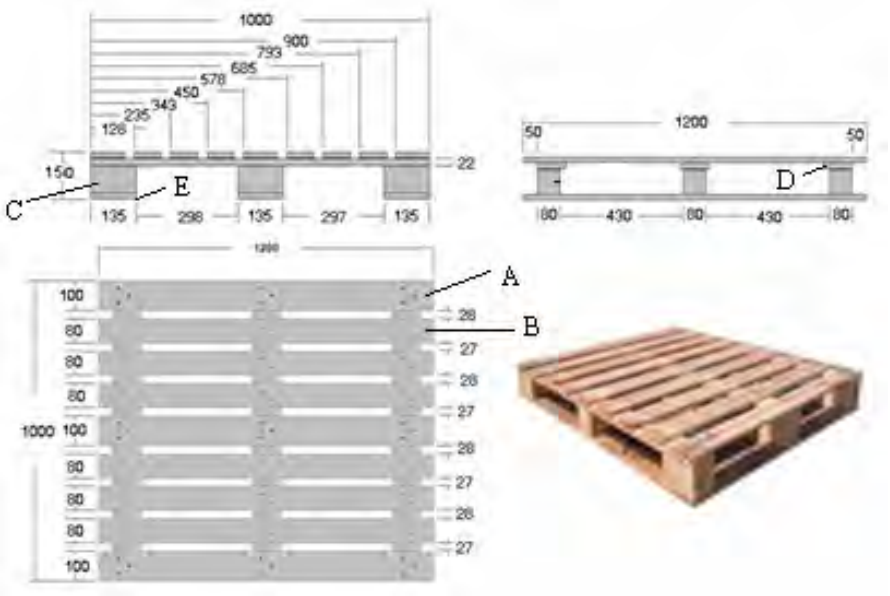

Figure 11.8: 1.2m by 1m by 0.15m wood pallets

Plank	*Number of planks*	*Total area (m^2)*	*Total volume (m^3)*
A	*3*	*0.82*	*0.008*
B	*6*	*1.37*	*0.013*
C	*9*	*0.33*	*0.008*
D	*3*	*0.67*	*0.005*
E	*3*	*0.95*	*0.009*

Total area per pallet = 0.82+1.37+0.33+0.67+0.95=4.14 m^2

Total volume per pallet = 0.008+0.013+0.008+0.005+0.009=0.04 m^3

Volume per actual wood pallet (1.2m by 1.0m by 0.15m) is 0.04 m^3.

Total volume for 41 actual pallets is 41 × 0.04 = 1.64 m^3.

The total area model for layer 1 in the simulation is

(7.75m × 2.05m × 2)+(7.75m × 0.3m × 2)+(2.05m × 0.3m × 2) = 37.66 m^2.

Therefore the thickness used for the FDS simulation is $\frac{1.64}{37.66} = 0.043$m.

Area per actual wood pallet (1.2m by 1.0m by 0.15m) is 4.14 m^2.

Actual total area for 41 pallets is 41 × 4.14 = 169.74 m^2

Therefore the burning rate factor used for the FDS simulation is $\frac{169.74}{37.66} = 4.51$

Calculations to determine thickness and surface burning factor for layer 4 pallets (HGV)

Layer 4 – based on layer with 41 pallets

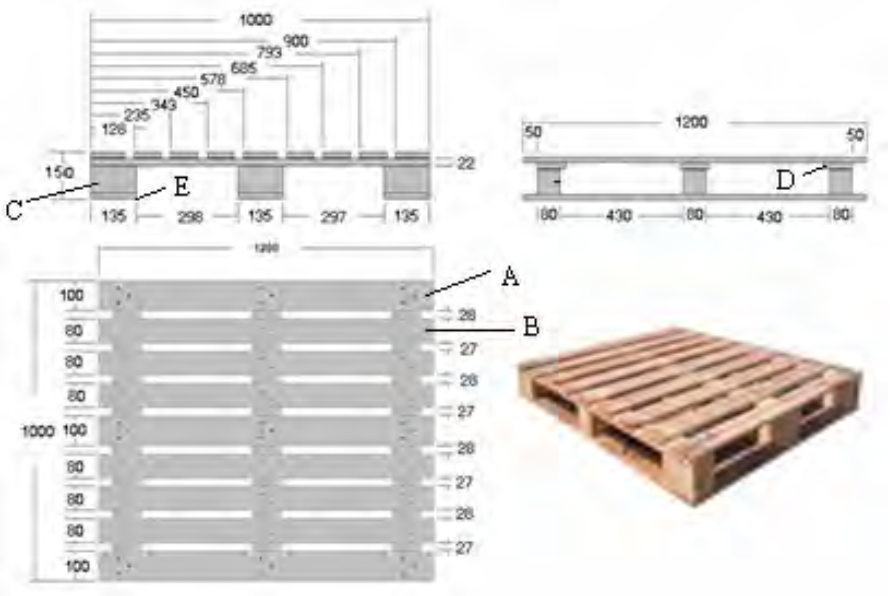

Figure 11.9: 1.2m by 1m by 0.15m wood pallets

Plank	*Number of planks*	*Total area (m^2)*	*Total volume (m^3)*
A	*3*	*0.82*	*0.008*
B	*6*	*1.37*	*0.013*
C	*9*	*0.33*	*0.008*
D	*3*	*0.67*	*0.005*
E	*3*	*0.95*	*0.009*

Total area per pallet = 0.82+1.37+0.33+0.67+0.95=4.14 m^2

Total volume per pallet = 0.008+0.013+0.008+0.005+0.009=0.04 m^3

Volume per actual wood pallet (1.2m by 1.0m by 0.15m) is 0.04 m^3.

Total volume for 41 actual pallets is 41 × 0.04 = 1.64 m^3.

The total area model for layer 1 in the simulation is

(7.75m × 2.05m × 2)+(7.75m × 0.3m × 2)+(2.05m × 0.3m × 2) = 37.66 m^2.

Therefore the thickness used for the FDS simulation is $\frac{1.64}{37.66} = 0.043$m.

Area per actual wood pallet (1.2m by 1.0m by 0.15m) is 4.14 m^2.

Actual total area for 41 pallets is 41 × 4.14 = 169.74 m^2

Therefore the burning rate factor used for the FDS simulation is $\frac{169.74}{37.66} = 4.51$

Calculations to determine thickness and surface burning factor for layer 5 pallets (HGV)

Layer 5 – based on layer with 41 pallets

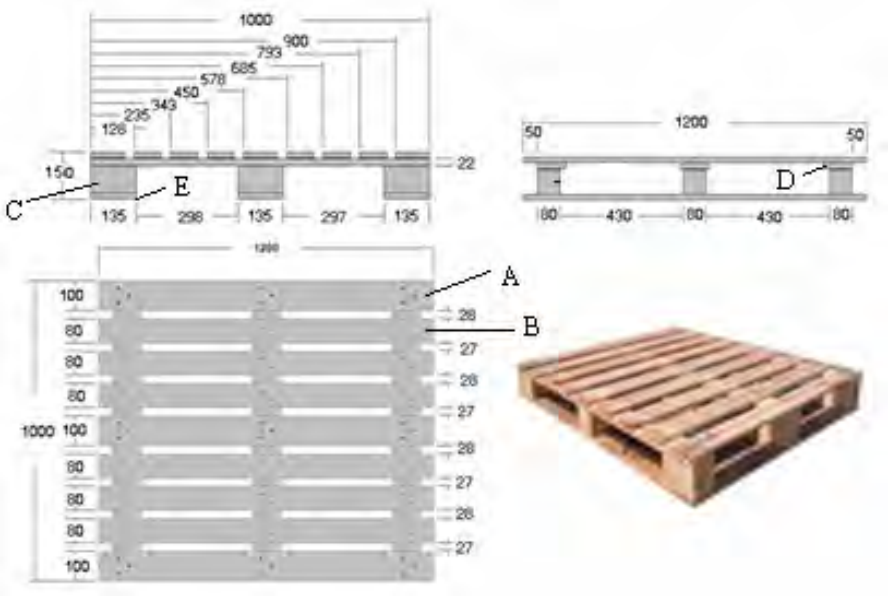

Figure 11.10: 1.2m by 1m by 0.15m wood pallets

Plank	*Number of planks*	*Total area (m^2)*	*Total volume (m^3)*
A	*3*	*0.82*	*0.008*
B	*6*	*1.37*	*0.013*
C	*9*	*0.33*	*0.008*
D	*3*	*0.67*	*0.005*
E	*3*	*0.95*	*0.009*

Total area per pallet = 0.82+1.37+0.33+0.67+0.95=4.14 m^2

Total volume per pallet = 0.008+0.013+0.008+0.005+0.009=0.04 m^3

Volume per actual wood pallet (1.2m by 1.0m by 0.15m) is 0.04 m^3.

Total volume for 41 actual pallets is 41 × 0.04 = 1.64 m^3.

The total area model for layer 1 in the simulation is

(7.75m × 2.05m × 2)+(7.75m × 0.3m × 2)+(2.05m × 0.3m × 2) = 37.66 m^2.

Therefore the thickness used for the FDS simulation is $\frac{1.64}{37.66} = 0.043$m.

Area per actual wood pallet (1.2m by 1.0m by 0.15m) is 4.14 m^2.

Actual total area for 41 pallets is 41 × 4.14 = 169.74 m^2

Therefore the burning rate factor used for the FDS simulation is $\frac{169.74}{37.66} = 4.51$

11.1.3 Establishing goods vehicle fuel load

Components of the vehicle chassis and truck cabin are another source of fuel that can be involved in a fire (Figure 11.11). In a goods vehicle, the combustible item includes tyres, mud guard, bumper, seats, instrument panel, cabin internal lining etc.

Specifications from truck manufacturers are used to identify the types of material for the construction of goods vehicles. In view of the vast number of different materials involved, only the major materials are considered for the FDS simulation. Figure 11.12 and Table 11.3 shows an example of the materials used in a heavy goods vehicle construction and the material schedule used for the FDS simulation. For material vehicle specification on light goods vehicle, refer to Appendix L.

Heavy goods vehicle chassis with cabin

Internal of a heavy goods vehicle cabin

Light goods vehicle chassis with cabin

Internal of a light goods vehicle cabin

Figure 11.11: Main component of a HGV and LGV

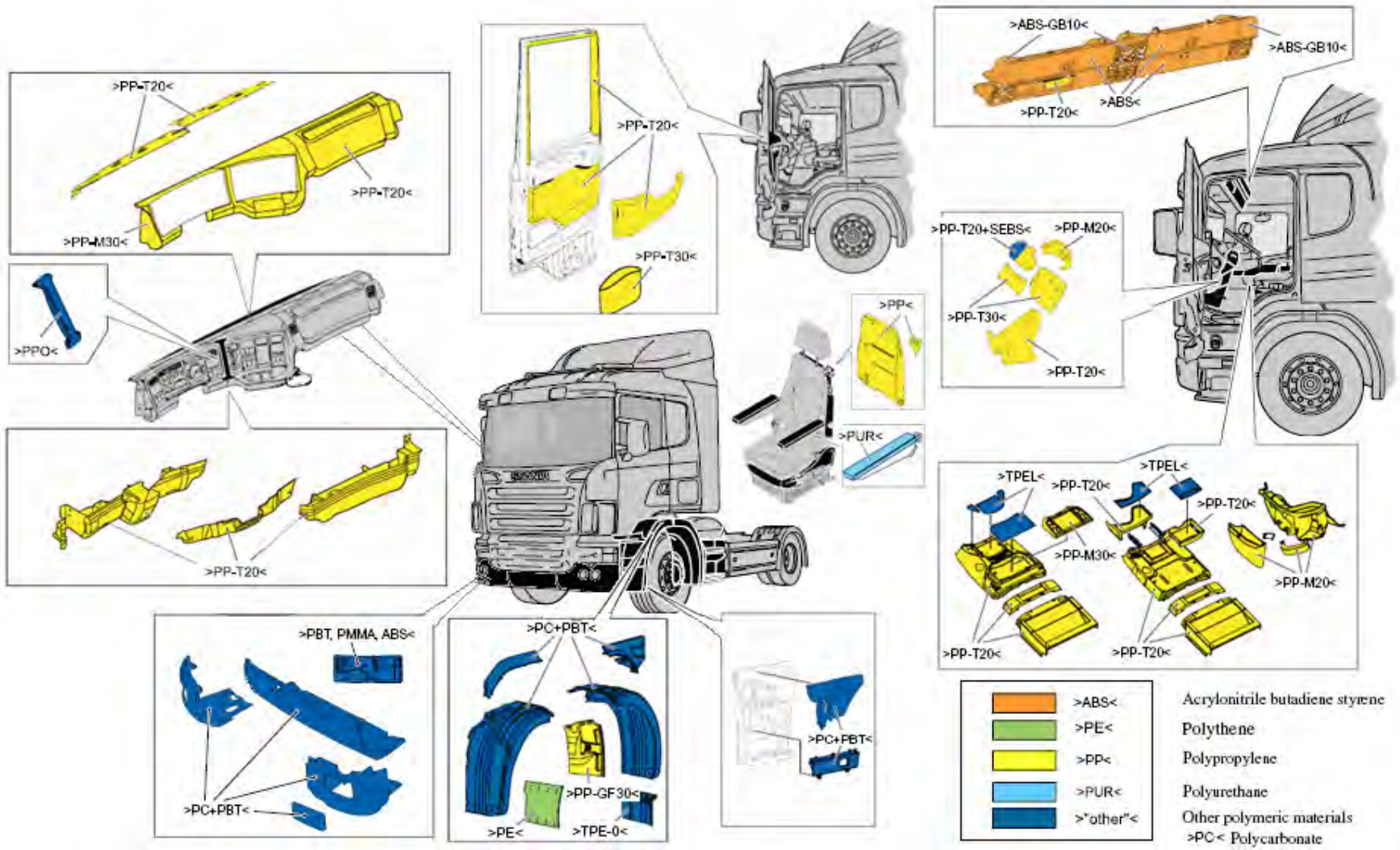

Figure 11.12: Material used in a goods vehicle construction (Scania 2005)

Heavy goods vehicle (HGV) material schedule

Parts Description	Material	Thickness (mm)
Vehicle - Vehicle seat	PUR - Polyurethane	50 [a]
Vehicle - Storage compartment	ABS - Acrylonitrile butadiene styrene	3 [a]
Vehicle - Cabin internal panel trim	PP - Polypropylene	3 [a]
Vehicle - Instrument panel	PP - Polypropylene	3 [a]
Vehicle - Bumper cover	PC - Polycarbonate	5 [a]
Vehicle - Tyres	EPDM – Ethylene propylene diene rubber	45 [a]
Vehicle - Mud guard	PC - Polycarbonate	5 [a]
Cargo - Plastic Pallets	PE - Polyethylene	29 [b]
Cargo - Wood Pallets	Wood	42 and 56 [b]

Note - a: Thickness of material measured from a heavy goods vehicle
b: Refer to section 11.1.2

Table 11.3: HGV material schedule used for FDS simulation

11.2 Thermal properties used for the simulations

A modelling approach based on heat release rate per unit area is used for the simulations. Thermal properties from cone test data taken from Thureson (1991), Babrauskas and Grayson (1992) and Babrauskas (2003) for PUR (Polyurethane), ABS (Acrylonitrile butadiene styrene), PP (Polypropylene), PC (Polycarbonate), EPDM (Ethylene propylene diene rubber), PE (Polyethylene) and wood are used for the simulation analysis. The thermal properties for these materials are summarised in Table 11.4.

Material	Thermal conductivity (W/m/K)	Density (kg/m^3)	Ignition temperature (^oC)	Specific heat (kJ/kg/K)	HRRPUA (Cone test) (kW/m^2)
PUR (Polyurethane)	0.034 [a]	20 [a]	272 [b]	1.4 [a]	Figure 11.13 [m]
ABS (Acrylonitrile butadiene styrene)	0.17 [c]	1050 [c]	414 [d]	1.48 [e]	Figure 11.14 [m]
PP (Polypropylene)	0.38 [b]	900 [b]	305 [b]	6.27 [b]	Figure 11.15 [m]
PC (Polycarbonate)	0.2 [f]	1190 [f]	497 [b]	2.06 [f]	Figure 11.16 [m]
EPDM (Ethylene propylene diene rubber)	0.3 [g]	860 [h]	369 [i]	2.18 [j]	Figure 11.17 [m]
PE (Polyethylene)	0.64 [b]	956 [b]	323 [b]	3 [b]	Figure 11.18 [m]
Wood	0.12 [k]	600 [l]	373 [b]	2.58 [n]	Figure 11.19 [l]

Reference: a - (Drysdale 1998), b - (Babrauskas 2003), c – (Goodfellow 2007), d – (Fleischmann 2006), e - (Tangram 2007), f – (Tewarson 2006), g – (Ismat 2000), h – (Chanda et al 1987), i - (Appendix M), j - (Nate Hoyt 2007), k - (Nisted 1991), l – (Thureson 1991), n - (Incropera and DeWitt 2002), m - (Babrauskas and Grayson 1992)

Table 11.4: Material thermal properties for FDS simulation

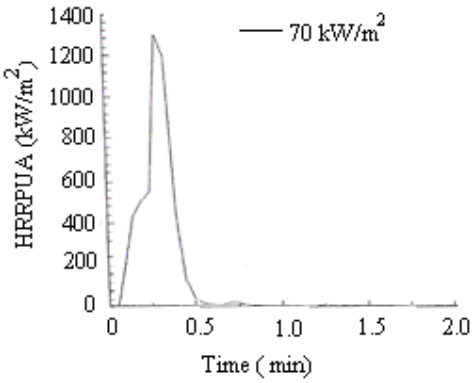

Figure 11.13: HRRPUA for PUR (Babrauskas and Grayson 1992)

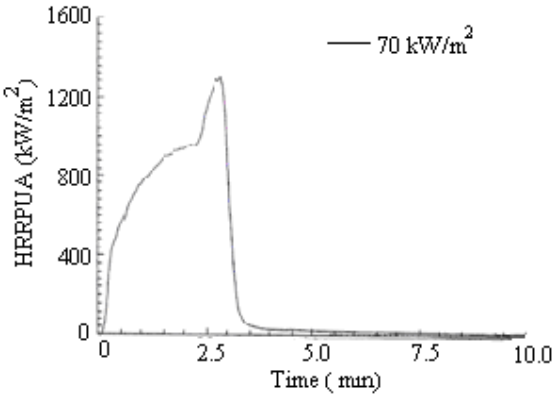

Figure 11.14: HRRPUA for ABS (Babrauskas and Grayson 1992)

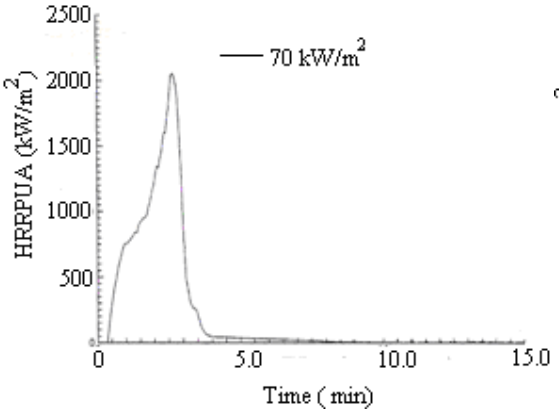

Figure 11.15: HRRPUA for PP (Babrauskas and Grayson 1992)

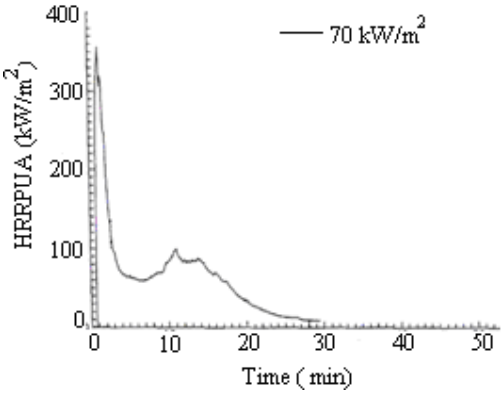

Figure 11.16: HRRPUA for PC (Baauskas and Grayson 1992)

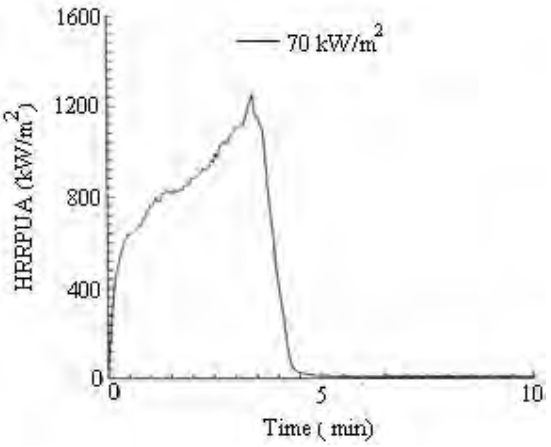

Figure 11.17: HRRPUA for EPDM (Babrauskas and Grayson 1992)

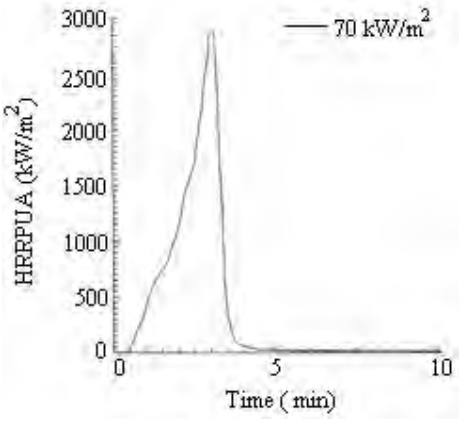

Figure 11.18: HRRPUA for PE (Babrauskas and Grayson 1992)

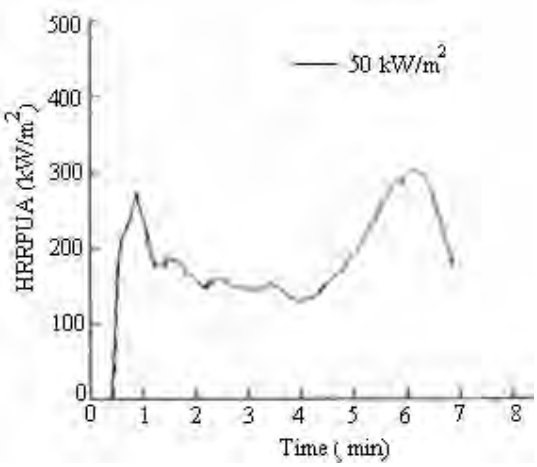

Figure 11.19: HRRPUA for wood (Thureson 1991)

11.3 Fire incident respond and traffic management in tunnel

Over the past few years, there have been several major tunnel fire incidents (e.g. St Gotthard tunnel fire, the Mont Blanc tunnel fire and the Tauern tunnel fire) in Europe that resulted in a high number of fatalities and property loss. The factors that contributed to these high consequences (high heat release rate) are partly due to the goods carried by the vehicle, the effect of ventilation in the tunnel which might enhance burning due to improved mixing at higher velocities, the proficiency of tunnel operators in terms of fire incident response; their ability to divert traffic in the tunnel and a strategy that allows fire fighters quick access to the fire site to fight the fire. During the initial stage of the fire development, it is important for tunnel operators to divert traffic allowing vehicles downstream of the fire to drive out. This allows motorists downstream the fire to escape and also limit the amount of combustible fuel (e.g. vehicles, goods carried by vehicles) in the tunnel, thereby reducing the effect of flame spread.

As discussed in chapter 6, the tunnel for this project is monitored by an automatic incident detector (AID) and linear heat detector (Parson 2001). When a fire incident occurs, the tunnel operator is able to assess the situation through the CCTV and emergency telephone installed in the tunnel. Upon confirmation of a tunnel fire, the tunnel will be closed and variable message signal (VMS) is used to inform and stop motorists from entering the tunnel. A radio re-broadcast system will also be used as a separate means to inform

incoming motorists from entering the tunnel. Vehicles already in the tunnel will be directed to the nearest exit and vehicles downstream of the fire will be driven away. The ventilation fans will be turned on to create a longitudinal airflow to prevent backlayering of smoke to the vehicles trapped upstream of the fire. This will create a smoke-free path for the motorists trapped at the upstream of the fire to evacuate safely through the cross passage doors. The tunnel operator will also provide information to the fire service the best direction to approach the fire location (Parson 2001). An overall picture of the fire incident management strategy used in the event of a tunnel fire is presented in Figure 11.20. In view of the fire strategy management system in place, the majority of the simulations are performed with no traffic downstream of the fire.

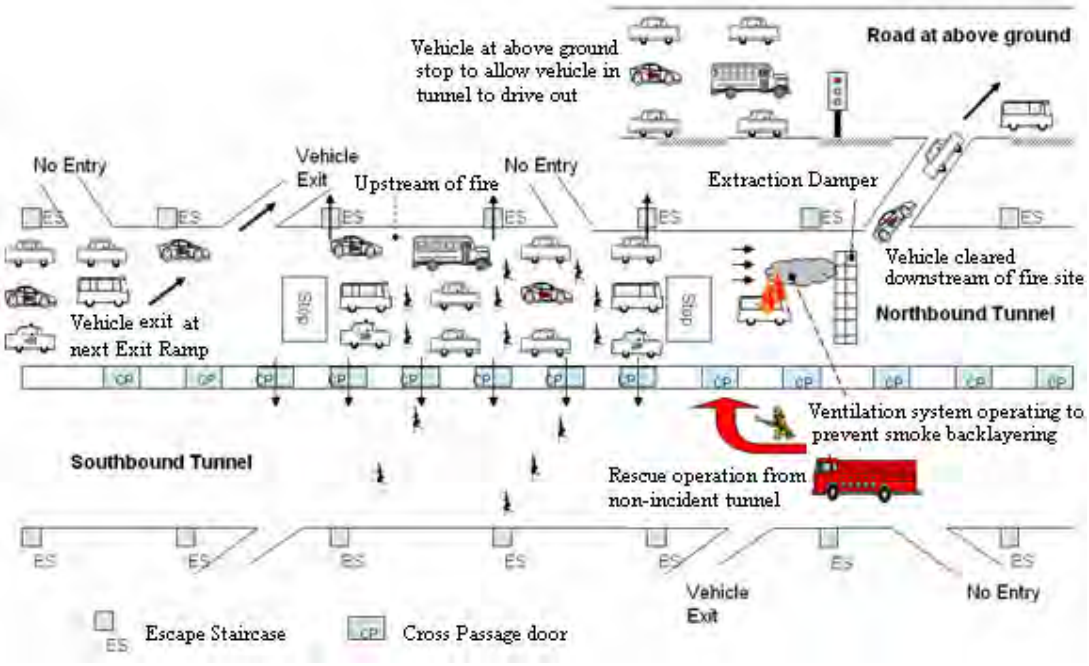

Figure 11.20: Fire incident respond and traffic management in tunnel

11.4 Tunnel geometry

Tunnel geometry is another factor which can affect the heat release rate. Due to re-radiation effects a tunnel, tunnel with smaller cross sectional area tends to produce higher heat release as compared to tunnel with a bigger cross sectional area. However, the situation can be reversed when there is no ventilation provision in the tunnel. Without the

supply of air, the condition can change to a ventilation controlled situation in view of smaller space that hinders combustion of the fuel.

In this project, there are two types of tunnel section (Main tunnel and slip road). The main tunnel (Figure 11.21) is a 3 lane carriageway with a 2.4 m shoulder to facilitate fire appliances to reach the incident scene in the event of a fire. The main tunnel cross section is approximately 15 m in width and 6 m in height.

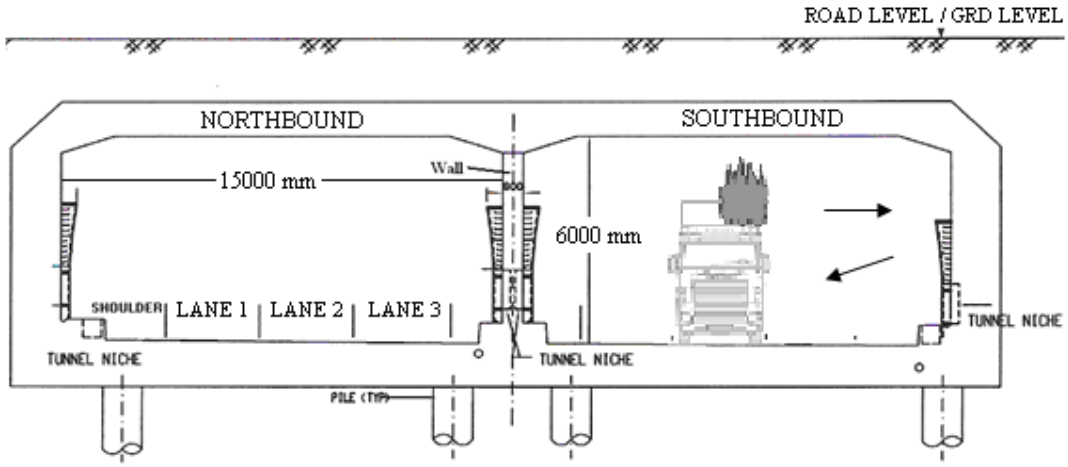

Figure 11.21: Typical Cross-section for Main Tunnel

The slip road (Figure 11.22) is the connection link between the main tunnel and the above ground road network. It is a two lane vehicle tunnel with a cross sectional area of approximately 9.3 m in width and 6 m in height.

The simulation for this tunnel has considered the effect of different cross sectional area along the tunnel alignments to ensure that the above phenomena are captured in the analysis.

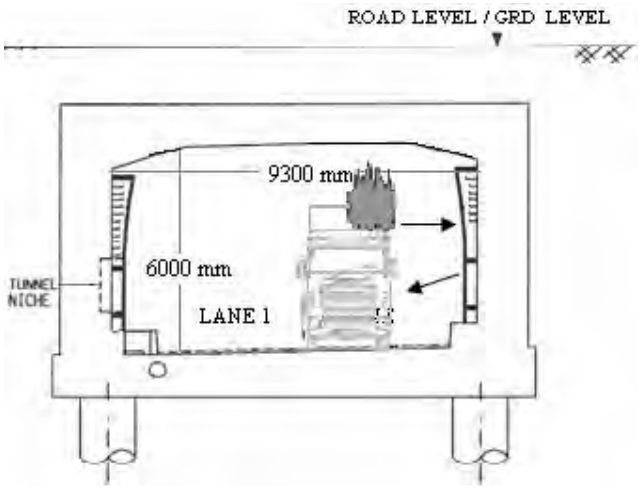

Figure 11.22: Typical Cross-section for 2-Lane Slip Road

11.5 Ventilation condition

The velocity in the tunnel can vary depending on location of the tunnel and the mode of the tunnel ventilation. In a tunnel fire incident, the ventilation condition in the tunnel is changing, particularly at the early stage of the fire incident (change of ventilation mode to facilitate motorist's evacuation and fire service fire fighting). There may be instances where the tunnel fans are operating in a congestion mode due to traffic congestion and a fire occurs in the tunnel or a normal mode where the tunnel fans are turned off and a there is a tunnel fire. The operation modes of the above mentioned events are different resulting in a different airflow at different moments in time. These changes in airflow may have an effect on the heat release rate in the tunnel. Scenarios considering the detection time, operator reaction time and time required for the change of fan operational mode were considered in the simulation (Figure 6.7 and Figure 6.8). Criteria based on NFPA 502 where the tunnel ventilation fans operate from standstill to full rotational speed within 60 seconds or reversible fans completing full rotational reversal within 90 seconds is captured in the simulations. Examples of the tunnel ventilation fans operating scenarios are shown in Figure 11.23.

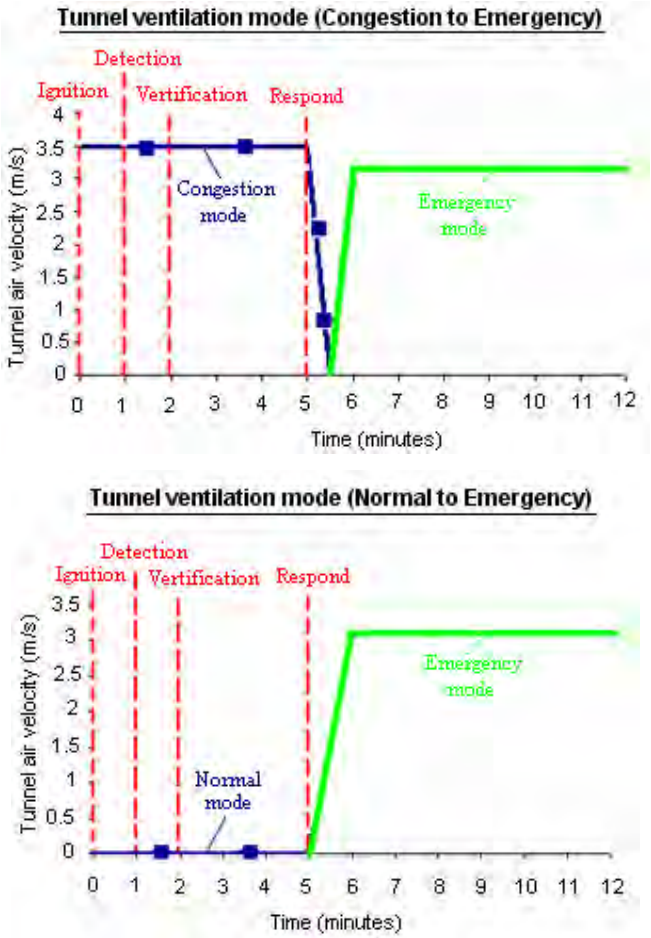

Figure 11.23: Examples of tunnel ventilation fans operating scenarios

11.6 Location of fire ignition

The literature review in chapter 3 and the analysis work in chapter 10 have found that the location of fire ignition could affect the heat release rate curve. Fire spread to the rear of the vehicle is delayed due to the ventilation in the driving direction resulting in lower heat release rate at the initial phase of the fire development. Fire ignition at the front and rear of the goods vehicles were simulated to consider this factor. Figure 11.24 shows the location of the fire ignition used for the simulation analysis.

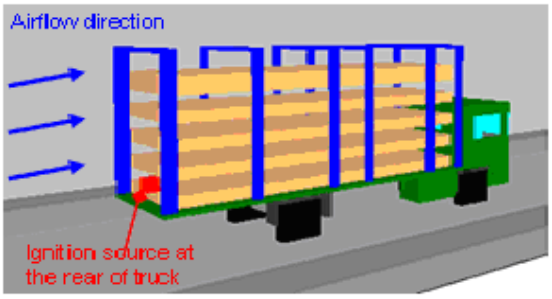

Rear of vehicle

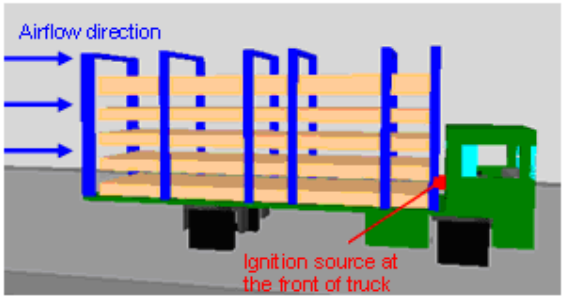

Front of vehicle

Figure 11.24: Location of ignition source

11.7 LGV and HGV fire simulation models

LGV and HGV simulation models for this project were constructed using FDS 4.07. Scenarios discussed in sections 11.1 to 11.6 are considered in the simulations. These factors include the tunnel geometry (slip road and main tunnel), ventilation condition (tunnel ventilation operational mode), fuel quantity (vehicle and its goods) and material properties of the combustible fuel.

To predict the heat release rate for goods vehicle fire, there are generally two fuel component groups to be considered. The vehicle itself and the goods on the vehicle, the LGV and HGV are simulated based on the material generally used in a goods vehicle and the commodities are based on a fuel ratio of 80% wood and 20% plastic (refer to section 11.1 – 11.2). All the materials defined for the HGV or LGV are combustible in the simulation.

The effect of re-radiation will have an effect on the fire size, such that a tunnel with smaller cross-sectional area tends to yield higher heat release rate as compared to a tunnel with larger cross-sectional area. In an urban tunnels, it is common to have different cross-sectional areas (e.g. slip road and main tunnel) along the tunnel alignment to facilitate vehicle entry and exit. Different cross-sectional area is considered in the simulations analysis.

Transient simulations are performed by considering events of fire detection, operator response (e.g. operating the tunnel fans) and fans start up time (example: Figure 11.23) in the simulation.

To capture the burning behaviour of the truck cabin, the effect of glass breakage is also modelled in the simulation. Snapshots of the LGV and HGV model are shown in Figure 11.25 and Figure 11.26 respectively. Details of the FDS input parameters are shown in Appendix N & O.

Simulation model of a LGV (Light goods vehicle)

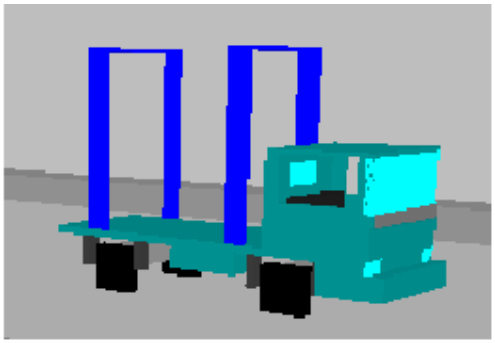

Light goods vehicle without goods

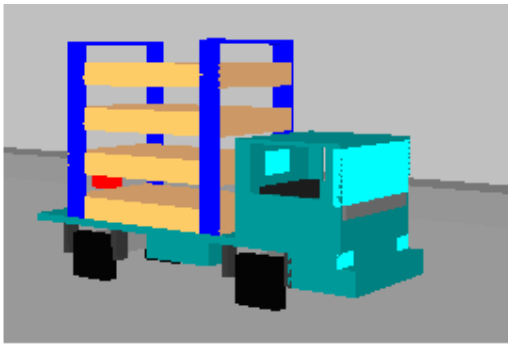

Light goods vehicle with goods

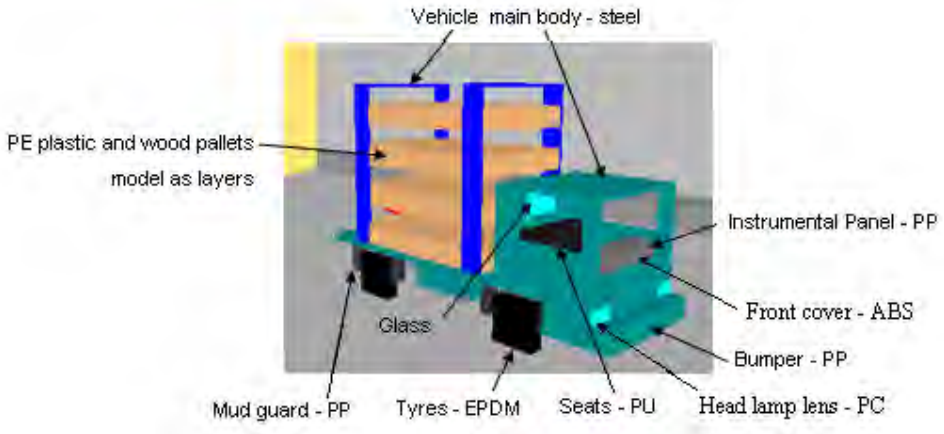

Material defined for light goods vehicle simulation

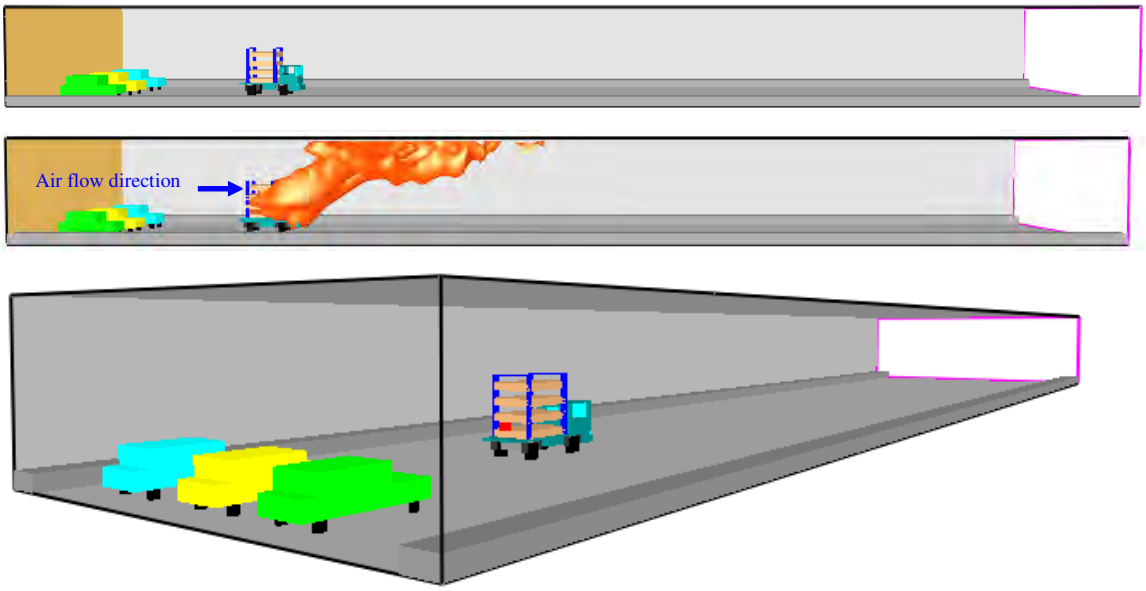

Figure 11.25: Snapshot of LGV in the main tunnel

Simulation model of a HGV (Heavy goods vehicle)

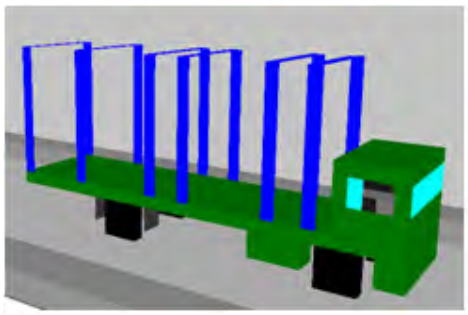

Heavy goods vehicle without goods

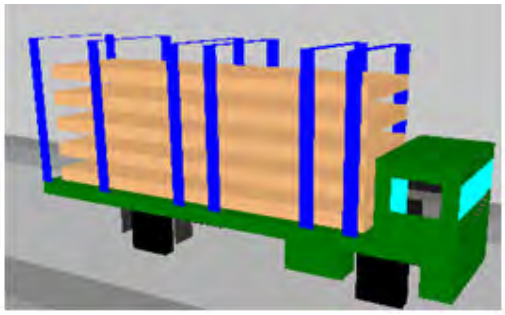

Heavy goods vehicle with goods

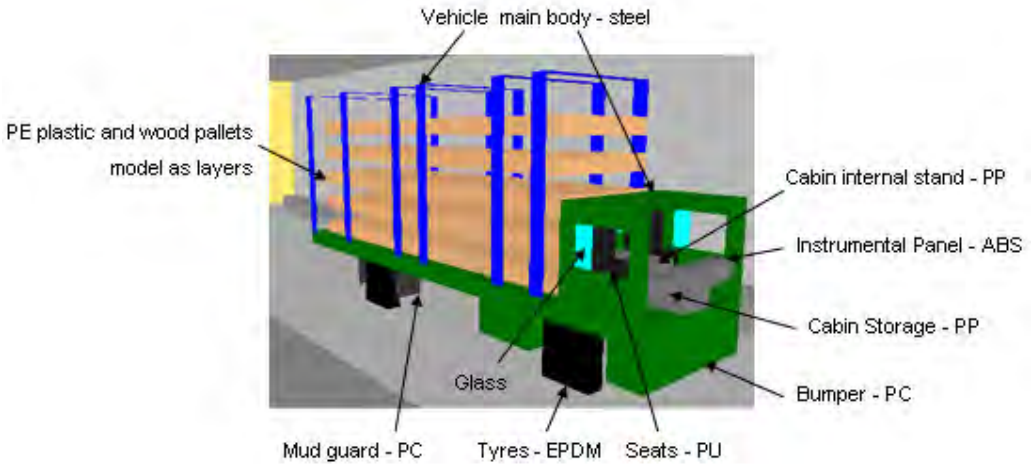

Material defined for heavy goods vehicle simulation

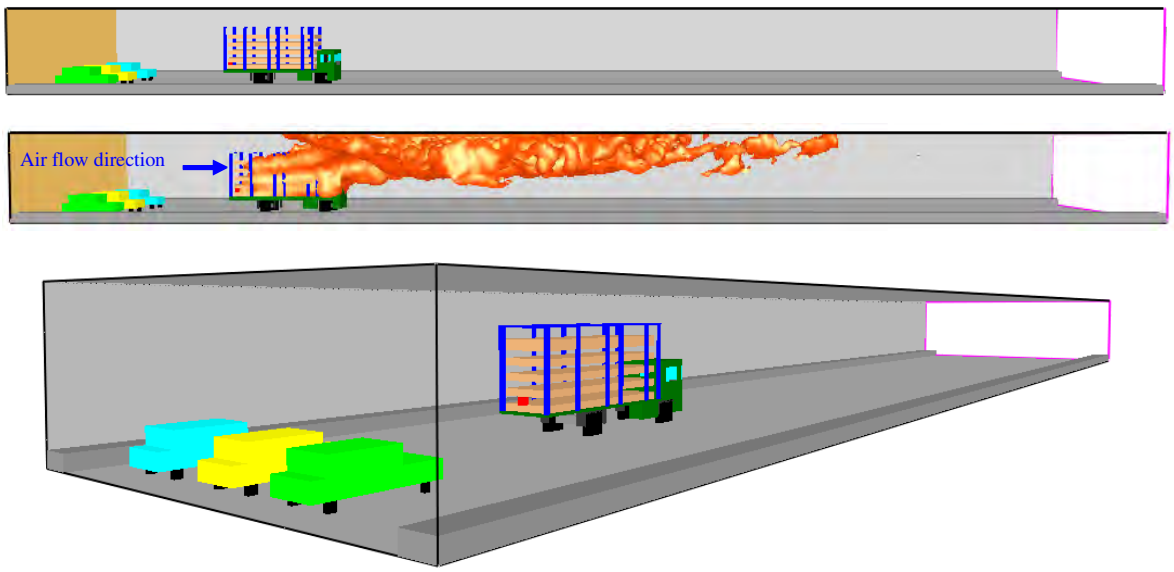

Figure 11.26: Snapshot of HGV in the main tunnel

11.8 Modelling limitations

One of the limitations is that the petrol in the fuel tank is not included in the simulation. In a vehicle collision, there is a possibility of a fuel tank rupture resulting in liquid fuel spilling onto the incident and neighbouring vehicles. The flow rate from the ruptured fuel tank can vary depending on the opening of the damaged fuel tank. The area of the resulting patch of liquid fuel on the road tunnel surface is related to the flow rate of the ruptured fuel tank. When the flammable liquid fuel ignites, the heat release rate would vary depending on the diameter of the pool fire on the surface of the road tunnel. Based on the above conditions, the number of scenarios involved can be numerous. There are also other factors such as gradient in the tunnel which can affect the direction and flow of the spillage. When the liquid fuel burns, the flaming liquid fuel may be flowing down slope and this is different from the approach used to model a solid material fire for this study. A new simulation approach considering the liquid fuel movement while burning is beyond the scope of this study. However, as this tunnel project is provided with a drainage system that is protected by detectors and automatic foam systems at the petrol interceptors. When such an event occurs, the drainage system is designed to quickly capture the spilled petrol so that its spreads will be limited and indirectly reducing the fire risk due to fuel tank rupture.

Another assumption made in the simulation is it assumed the burning behaviour of materials in a tunnel fire is similar to a small-scale fire experiment as Cone Calorimeter data are used as input for the FDS simulation. The thermal properties such as the specific heat and thermal conductivity are constant.

11.9 Tunnel simulation results

A summary of the simulations conducted using FDS 4.07 is tabulated in Table 11.5. The heat release rate curves are presented in Figure 11.27 to Figure 11.57

S/no	Type of fuel load [a]	Location of tunnel [b] / tunnel area (m^2)	Ventilation operation mode [c]	Tunnel air flow [c] (m/s)	Ignition location [d]	Grid size (mm)	Domain length (m)
1	LGV without goods	Slip road / 55.8	Normal to Emergency	0 – 2.9	Vehicle cabin	300	84
2	HGV without goods	Slip road / 55.8	Normal to Emergency	0 – 2.9	Vehicle cabin	300	84
3	LGV with goods	Slip road / 55.8	Normal to Emergency	0 – 2.9	Rear of vehicle	150	84
4	LGV with goods	Slip road / 55.8	Normal to Emergency	0 – 2.9	Rear of vehicle	300	84
5	LGV with goods	Slip road / 55.8	Normal to Emergency	0 – 2.9	Rear of vehicle	300	102
6	LGV with goods	Slip road / 55.8	Normal to Emergency	0 – 2.9	Front of vehicle	300	84
7	LGV with goods	Slip road / 55.8	Normal to Emergency	0 – 5.2	Rear of vehicle	300	84
8	LGV with goods	Slip road / 55.8	Normal to Emergency	0 – 1	Rear of vehicle	300	84
9	LGV with goods	Slip road / 55.8	Congestion to Emergency	5.6 – 2.9	Rear of vehicle	300	84
10	LGV with goods	Slip road / 55.8	Congestion to Emergency	3.4 – 5.2	Rear of vehicle	300	84
11	LGV with goods	Main tunnel / 90	Normal to Emergency	0 - 3.1	Rear of vehicle	150	84
12	LGV with goods	Main tunnel / 90	Normal to Emergency	0 - 3.1	Rear of vehicle	300	84
13	LGV with goods	Main tunnel / 90	Normal to Emergency	0 - 3.1	Rear of vehicle	300	102

Table 11.5 continue from next page

S/no	Size of fuel load [a]	Location of tunnel [b] / tunnel area (m^2)	Ventilation operation mode [c]	Tunnel air flow [c] (m/s)	Ignition location [d]	Grid size (mm)	Domain length (m)
14	LGV with goods	Main tunnel / 90	Normal to Emergency	0 - 3.1	Front of vehicle	300	84
15	LGV with goods	Main tunnel / 90	Normal to Emergency	0 – 1	Rear of vehicle	300	84
16	LGV with goods	Main tunnel / 108	Normal to Emergency	0 – 4.6	Rear of vehicle	300	84
17	LGV with goods	Main tunnel / 90	Congestion to Emergency	3.5 – 3.1	Rear of vehicle	300	84
18	LGV with goods	Main tunnel / 108	Congestion to Emergency	3.2 – 4.6	Rear of vehicle	300	84
20	HGV with goods	Slip road / 55.8	Normal to Emergency	0 – 2.9	Rear of vehicle	150	93
21	HGV with goods	Slip road / 55.8	Normal to Emergency	0 – 2.9	Rear of vehicle	300	93
22	HGV with goods	Slip road / 55.8	Normal to Emergency	0 – 2.9	Rear of vehicle	300	102
23	HGV with goods	Slip road / 55.8	Normal to Emergency	0 – 2.9	Front of vehicle	300	93
24	HGV with goods	Slip road / 55.8	Normal to Emergency	0 – 1	Rear of vehicle	300	93
25	HGV with goods	Slip road / 55.8	Normal to Emergency	0 – 5.2	Rear of vehicle	300	93
26	HGV with goods	Slip road / 55.8	Congestion to Emergency	5.6 – 2.9	Rear of vehicle	300	93
27	HGV with goods	Slip road / 55.8	Congestion to Emergency	3.4 – 5.2	Rear of vehicle	300	93
28	HGV with goods	Main tunnel / 90	Normal to Emergency	0 - 3.1	Rear of vehicle	150	93
29	HGV with goods	Main tunnel / 90	Normal to Emergency	0 - 3.1	Rear of vehicle	300	93
30	HGV with goods	Main tunnel / 90	Normal to Emergency	0 - 3.1	Rear of vehicle	300	102

Table 11.5 continue from next page

S/no	Size of fuel load [a]	Location of tunnel [b] / tunnel area (m^2)	Ventilation operation mode [c]	Tunnel air flow [c] (m/s)	Ignition location [d]	Grid size (mm)	Domain length (m)
31	HGV with goods	Main tunnel / 90	Normal to Emergency	0 - 3.1	Front of vehicle	300	93
32	HGV with goods	Main tunnel / 90	Normal to Emergency	0 - 1	Front of vehicle	300	93
33	HGV with goods	Main tunnel / 108	Normal to Emergency	0 – 4.6	Rear of vehicle	300	93
34	HGV with goods	Main tunnel / 90	Congestion to Emergency	3.5 – 3.1	Rear of vehicle	300	93
35	HGV with goods	Main tunnel / 108	Congestion to Emergency	3.2 – 4.6	Rear of vehicle	300	93

Note: a) Refer to section 11.1 and 11.2 on size of fuel load
b) Refer to section 11.4 on tunnel geometry
c) Details of the various tunnel ventilation modes are discussed in section 11.5
d) Refer to section 11.6 for location of ignition source

Table 11.5: Summary of the fire scenarios to be simulated

11.9.1 Simulated heat release rate curve

Single LGV and HGV fire without goods in the tunnel (slip road)

Although no fire test was conducted on a truck cabin fire, a study from EUREKA and others (1995) claimed that the cabin furnishings and other attachments on a truck vehicle were of the same order as those found in a medium-sized car. Depending on the type and year of the car, estimates made in connection with car fires tests had shown that this value is around 4.3 to 8.5 MW (Ship and Spearpoint 1995). An attempt has been made to estimate the heat release rate of a light goods truck (without goods) and a heavy good truck (without goods) using a numerical approach. This work would hopefully provide some useful information on the magnitude of a truck cabin fire without goods on the vehicle.

Single LGV and HGV fire without goods in the tunnel (slip road)

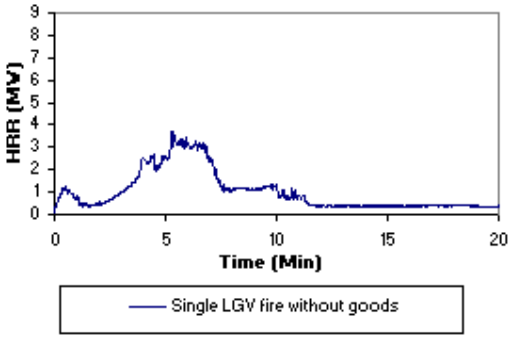

Figure 11.27: LGV fire without goods s/no 1 (LGV, ignition: cabin, area: 55.8 m^2, 0 - 2.9m/s)

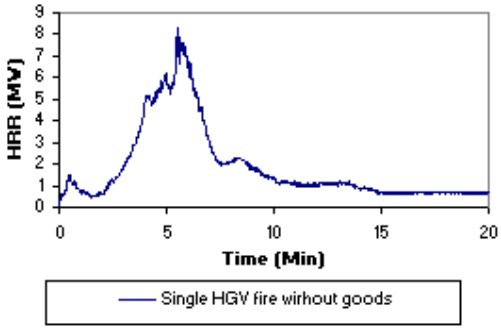

Figure 11.28: HGV fire without goods s/no 2 (HGV, ignition: cabin, area: 55.8 m^2, 0 – 2.9m/s)

The simulations were performed in a 2 lane tunnel with cross sectional area of 9.3 m (width) and 6 m (high). The material of the truck cabin was discussed in section 11.1 and 11.2. A 2.9 m/s air velocity were provided at one end of the tunnel section. Simulations results from FDS showed the heat release rate of a LGV and HGV fire (without goods) is around 3.7 and 8.3 MW respectively. From the simulation results (Figure 11.29), a cabin vehicle fire without goods can produce a fast to ultra-fast growth rate.

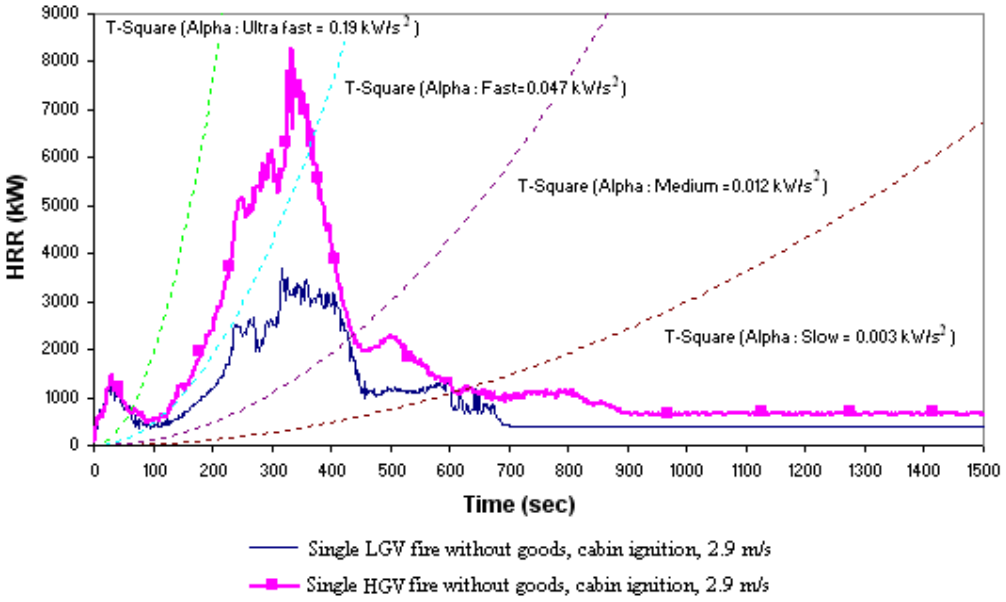

Figure 11.29: Comparing LGV and HGV heat release rate with different fire growth rate

Slip road and main tunnel, light goods vehicle (LGV)

This section presents the FDS results simulated for the slip road and main tunnel involving a light goods vehicle fire. Velocities varying from 1 m/s to 5.6 m/s were considered in these simulations. The effect of ignition location (front or rear vehicle fire) on vehicle fire size was also investigated.

Slip road, light goods vehicle (LGV)

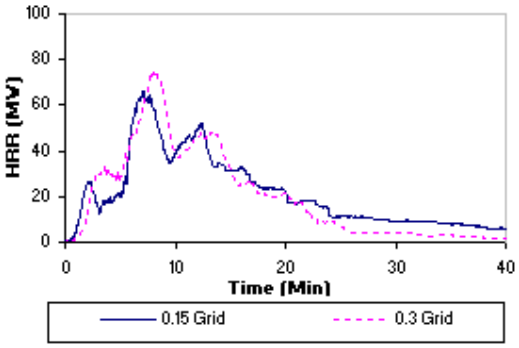

Figure 11.30: Grid sensitivity s/no 3 & 4 (LGV, ignition: rear, area: 55.8 m^2, 0 – 2.9m/s)

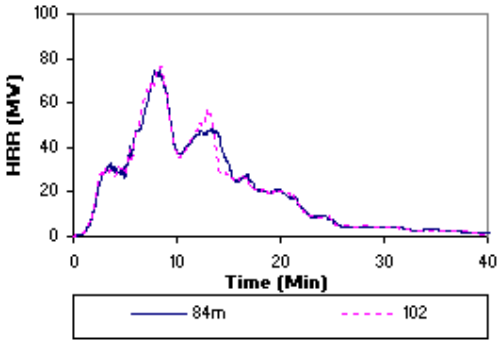

Figure 11.31: Domain sensitivity s/no 4 & 5 (LGV, ignition: rear, area: 55.8 m^2, 0 – 9m/s)

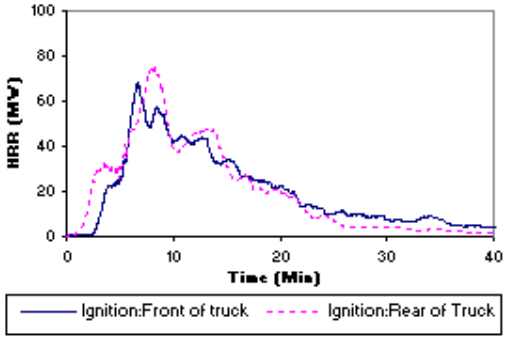

Figure 11.32: Ignition location s/no 4 & 6 (LGV, ignition: varies, area: 55.8 m^2, 0 – 2.9m/s)

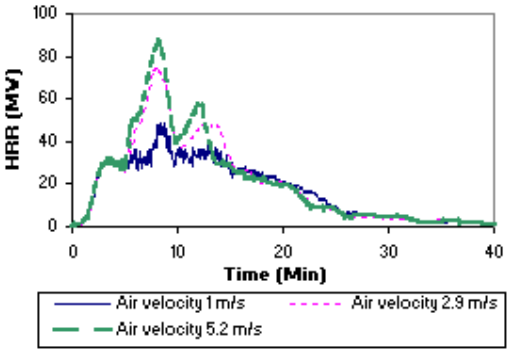

Figure 11.33: Different airflow s/no 4, 7 & 8 (LGV, ignition: rear, area: 55.8 m^2, (varies m/s)

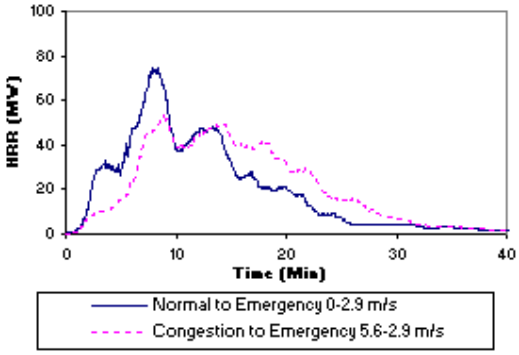

Figure 11.34: Operation mode s/no 4 & 9 (LGV, ignition: rear, area: 55.8m^2, velocity: varies)

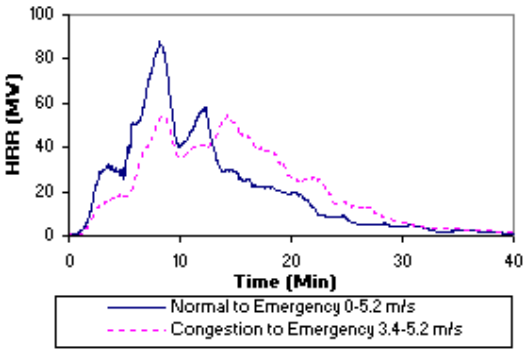

Figure 11.35: Operation mode s/no 7 &10 (LGV, ignition: rear, area: 55.8m^2, velocity: varies m/s)

Main tunnel, light goods vehicle (LGV)

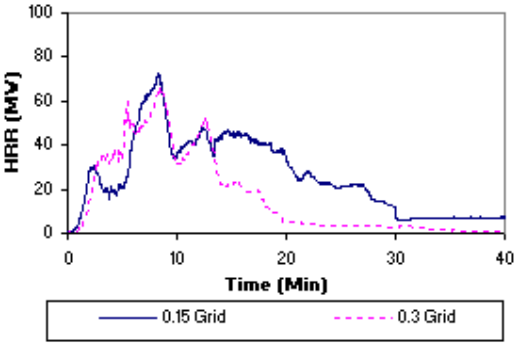

Figure 11.36: Grid sensitivity s/no 11&12 (LGV, ignition: rear, area: 90 m^2, 3.1m/s)

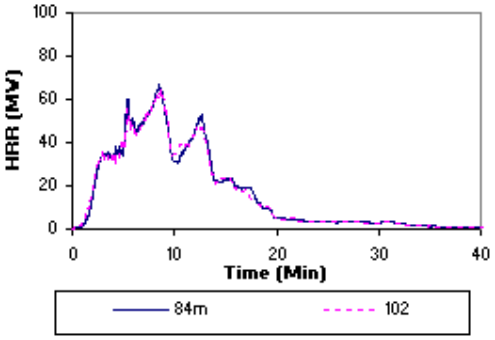

Figure11.37: Domain sensitivity s/no12&13 (LGV, ignition: rear, area: 90m^2, 3.1m/s)

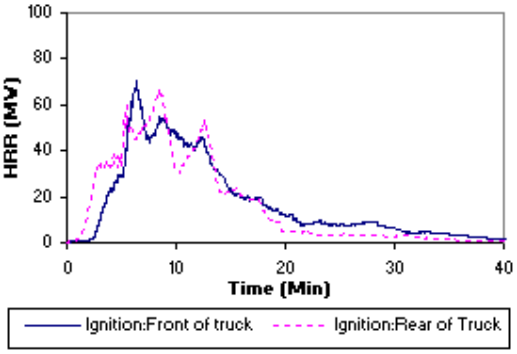

Figure 11.38: Ignition location s/no 12 & 14 LGV, ignition: varies, area: 90 m^2, 0 - 3.1m/s)

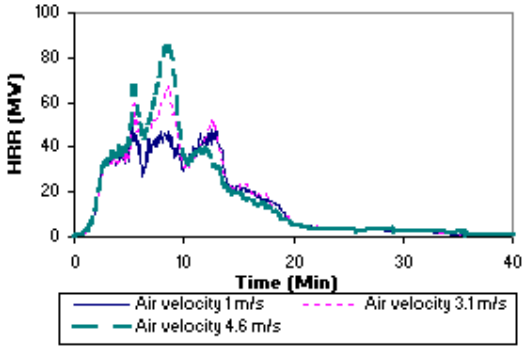

Figure 11.39: Different airflow s/no 12, 15 & 16 (LGV, ignition: rear, area: 90 m^2, varies m/s)

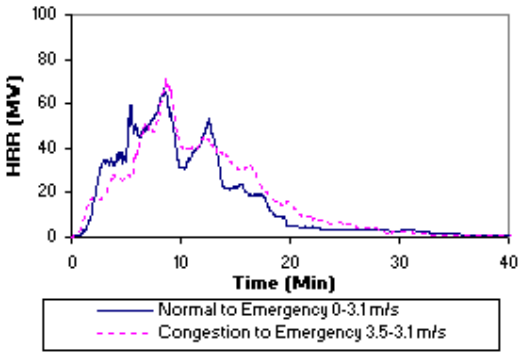

Figure 11.40: Operation mode s/no 12 & 17 (LGV, ignition: rear, area: 90 m^2, varies m/s)

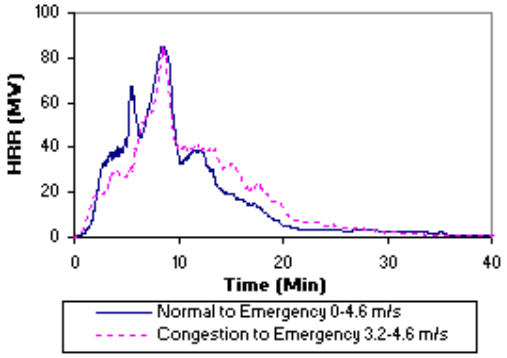

Figure 11.41: Operation mode s/no 16 & 18 (LGV, ignition: rear, area: 108 m^2, varies m/s)

The simulation results (Figure 11.30 to 11.43) showed that:

i) When fire ignites at the front of the vehicle, a delay on the fire development at the growth phase has been observed (Figure 11.32 and 11.38) as compared to scenario with fire igniting at the rear of the vehicle.

ii) Increasing the air velocity in the tunnel will result in an increase in heat release rate (Figure 11.33 and 11.39).

iii) Operating the tunnel at a higher air velocity in the early stage of the fire development can provide a cooling effect resulting in lower heat release rate (Figure 11.34 and 11.40).

iv) Operating the tunnel ventilation at the early stage of the fire development helps to reduce the severity of the fire during the growth phase (Figure 35 and 41).

v) Fire growth rate (α = 0.45 kW/m^2) greater than the standard Ultra-fast growth has been observed for a goods vehicle fire in a two and three lane tunnel (Figure 11.42 and 11.43).

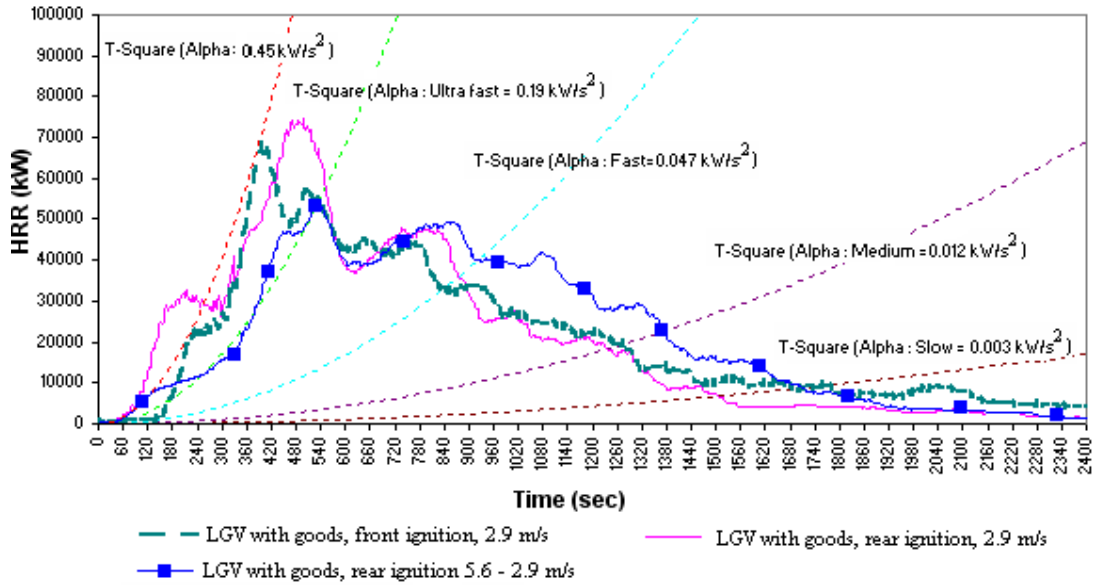

Figure 11.42: Comparing LGV heat release rate with different growth rate in a 2 lane tunnel

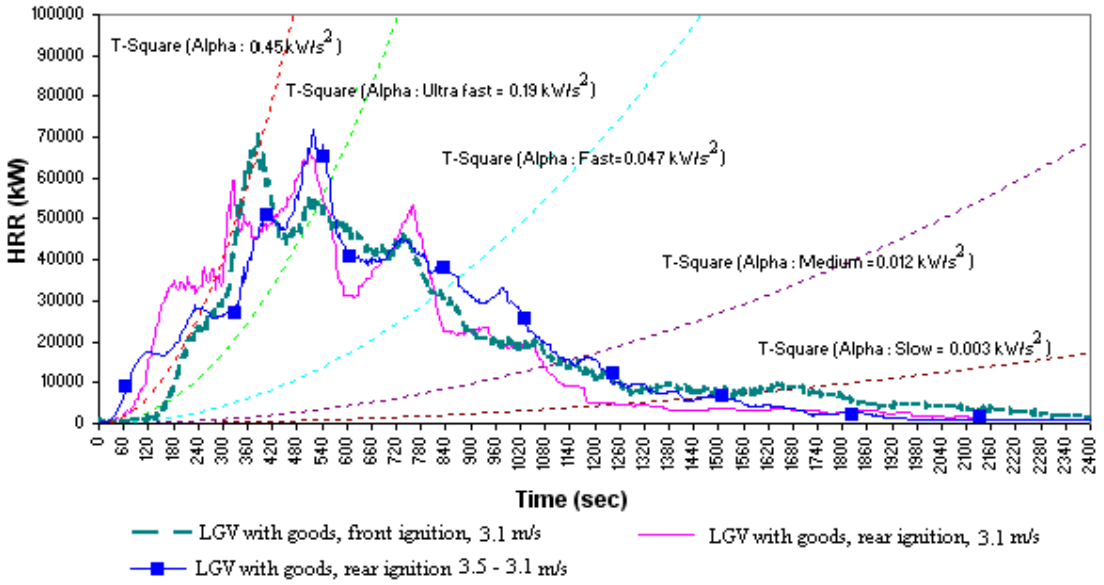

Figure 11.43: Comparing LGV heat release rate with different growth rate in a 3 lane tunnel

Slip road and main tunnel, heavy goods vehicle (HGV)

A series of simulations involving HGV were performed in the slip road and main tunnel. Similar air velocity and tunnel geometry performed on the LGV were used for these analyses.

Slip road, heavy goods vehicle (HGV)

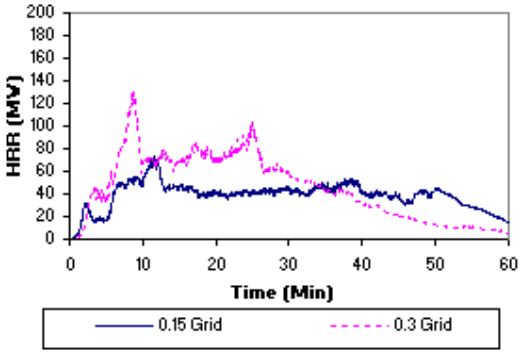

Figure 11.44: Grid sensitivity s/no 20 & 21 (HGV, ignition: rear, area: 55.8m^2, 0 – 2.9m/s)

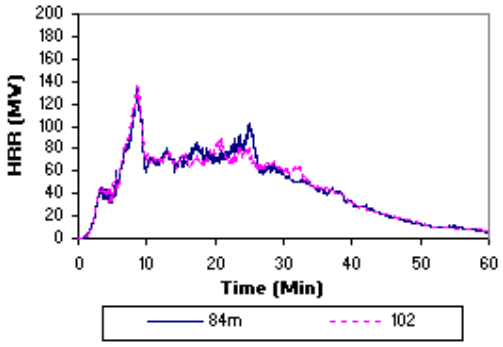

Figure 11.45: Domain sensitivity s/no 21 & 22 (HGV, ignition: rear, area: 55.8m^2, 0 – 2.9m/s)

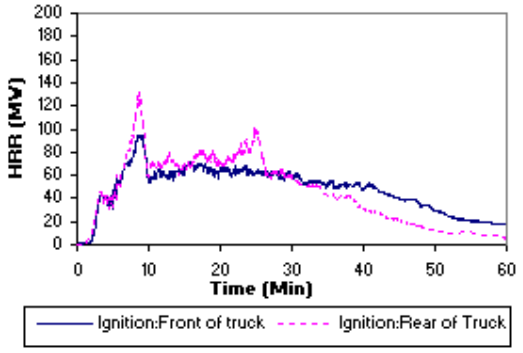

Figure 11.46: Ignition location s/no 21 & 23 (HGV, ignition: varies, area: 55.8 m^2, 0 – 2.9m/s)

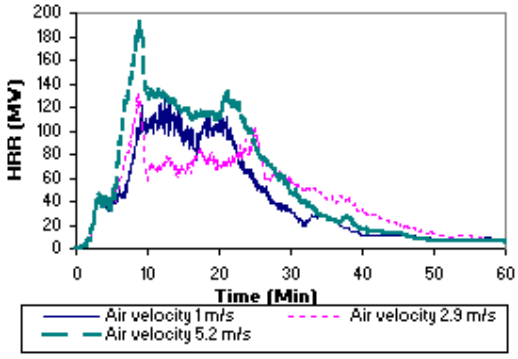

Figure 11.47: Different airflow s/no 21, 24 & 25 (HGV, ignition: rear, area: 55.8m^2, varies m/s)

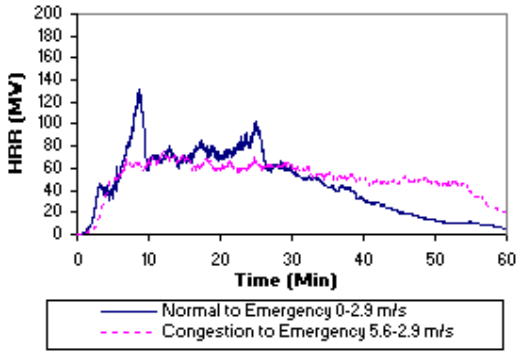

Figure 11.48: Operation mode s/no 21 & 26 (HGV, ignition: rear, area: 55.8m^2, varies m/s)

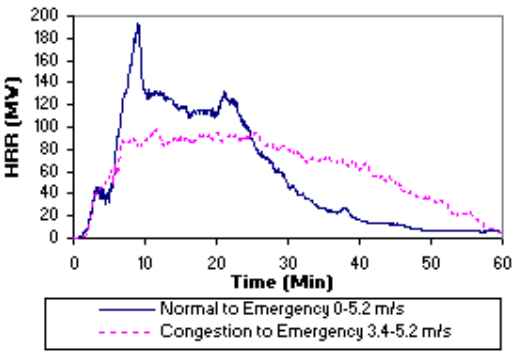

Figure 11.49: Operation mode s/no 25 & 27 (HGV, ignition: rear, area: 55.8m^2, varies m/s)

Main tunnel, heavy goods vehicle (HGV)

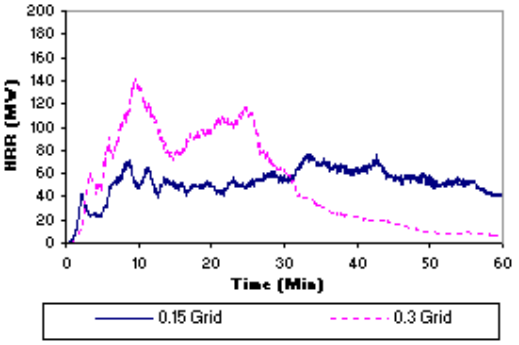

Figure 11.50: Grid sensitivity s/no 28 & 29 (HGV, ignition: rear, area: 90 m^2, 0 – 3.1m/s)

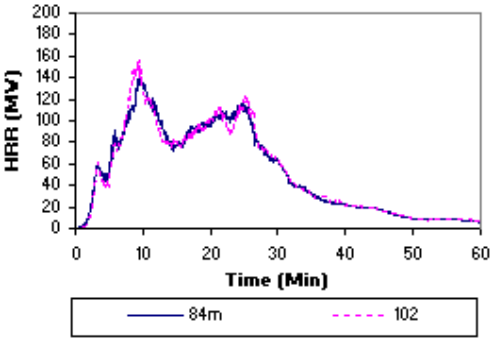

Figure 11.51: Domain sensitivity s/no 29 & 30 (HGV, ignition: rear, area: 90 m^2, 0 – 3.1m/s)

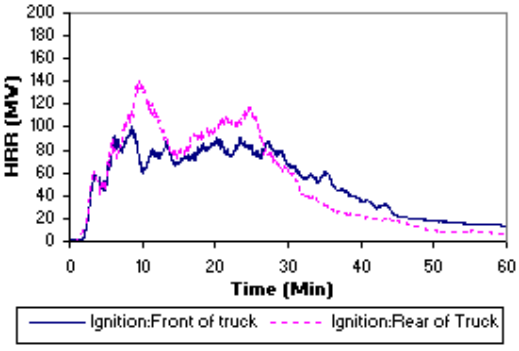

Figure 11.52: Ignition location s/no 29 & 31 (HGV, ignition: varies, area: 90 m^2, 0 – 3.1m/s)

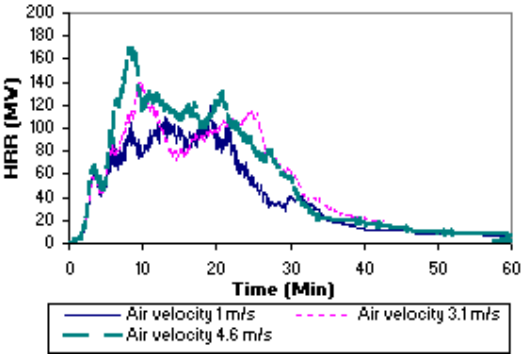

Figure 11.53: Different airflow s/no 29, 32 & 33 (HGV, ignition: rear, area: 90m^2, varies m/s)

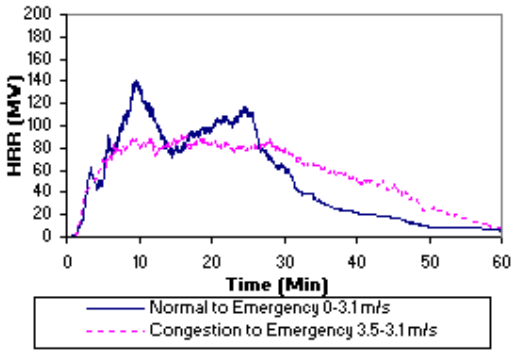

Figure 11.54: Operation mode s/no 29 & 34 (HGV, ignition: rear, area: 90 m^2, varies m/s)

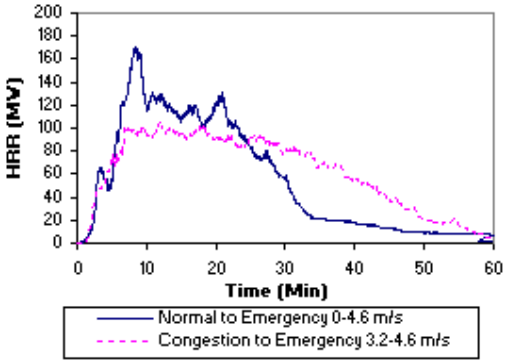

Figure 11.55: Operation mode s/no 33 & & 35 (HGV, ignition: rear, area: 108 m^2, varies m/s)

The simulation results (Figure 11.44 to 11.57) showed that:

i) A lower heat release rate has been observed when the fire ignites at the front of the vehicle as compared to a scenario where the fire ignites at the rear of the vehicle (Figure 11.46 and 11.52).

ii) There is an increase in peak heat release rate when air velocity in the tunnel increases (Figure 11.47 and 11.53).

iii) Operating the tunnel at a higher air velocity in the early stage of the fire development provides a cooling effect and helps to reduce the severity of the fire during the growth phase (Figure 49 and 55).

iv) Ultra-fast fire growth rate (α = 0.45 kW/m^2) has been observed for a HGV fire in a two and three lane tunnel (Figure 11.56 and 11.57).

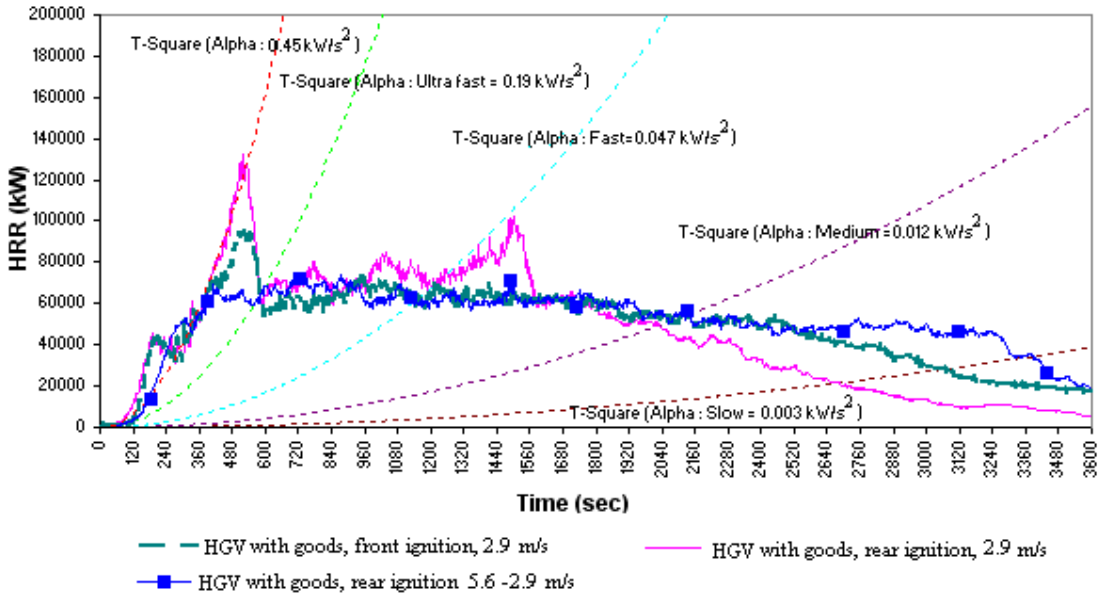

Figure 11.56: Comparing HGV heat release rate with different growth rate in a 2 lane tunnel

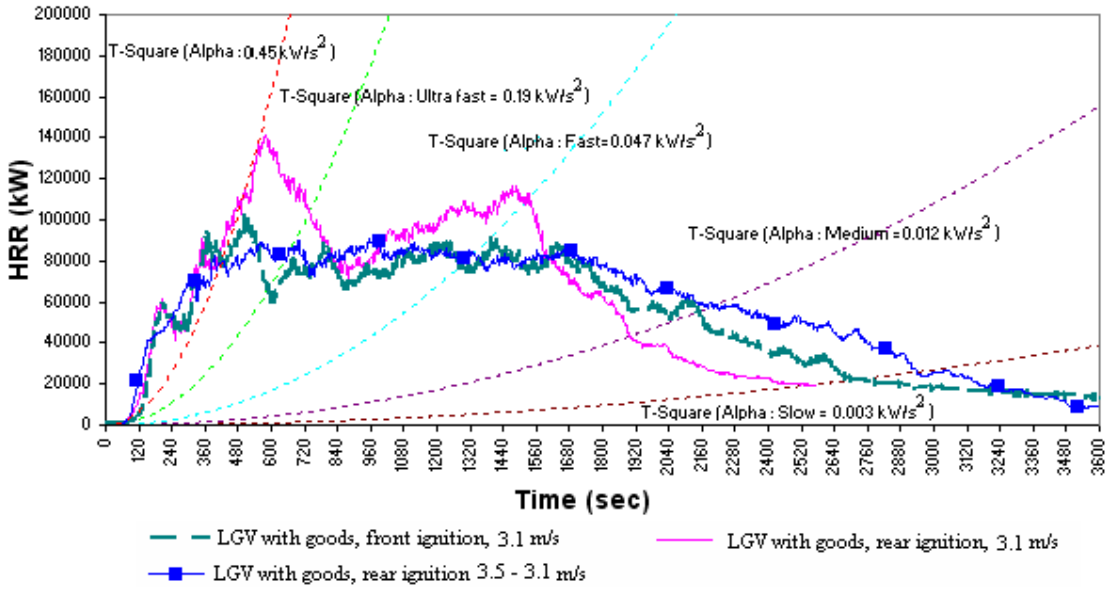

Figure 11.57: Comparing HGV heat release rate with different growth rate in a 3 lane tunnel

11.10 Discussions on the simulations

Table 11.6 & Table 11.7 presents a summary of the predicted peak heat release rate considering factors such as fuel load (HGV or LGV loaded with 80% wood; 20% plastic), tunnel geometry, ventilation condition, location of ignition source and the traffic condition in the tunnel. Details of each of the parameters affecting the heat release rate are discussed in this section. The author would like to remind the reader that the fire scenarios in Table 11.6 and 11.7 were established based on the risk analysis discussed in chapter 8 where a single LGV or a single HGV have been identified as the potential fire risk that could occur for this tunnel project. When establishing the heat release rate in another tunnel, a risk analysis process will have to be conducted prior to any detailed CFD simulation work.

Predicted peak HRR value for a single LGV

S/no	Size of fuel load	Location of tunnel / tunnel area (m^2)	Tunnel air flow (m/s)	Ignition location	Predicted peak HRR (MW)
1	LGV without goods	Slip road / 55.8	0 – 2.9	Rear of vehicle	3.7
4	LGV with goods	Slip road / 55.8	0 – 2.9	Rear of vehicle	75
6	LGV with goods	Slip road / 55.8	0 – 2.9	Front of vehicle	68
7	LGV with goods	Slip road / 55.8	0 – 5.2	Rear of vehicle	88
8	LGV with goods	Slip road / 55.8	0 – 1	Rear of vehicle	49
9	LGV with goods	Slip road / 55.8	5.6 – 2.9	Rear of vehicle	54
10	LGV with goods	Slip road / 55.8	3.4 – 5.2	Rear of vehicle	55
12	LGV with goods	Main tunnel / 90	0 – 3.1	Rear of vehicle	67
14	LGV with goods	Main tunnel / 90	0 – 3.1	Front of vehicle	70
15	LGV with goods	Main tunnel / 90	0 – 1	Rear of vehicle	50
16	LGV with goods	Main tunnel / 108	0 – 4.6	Rear of vehicle	85
17	LGV with goods	Main tunnel / 90	3.5 – 3.1	Rear of vehicle	72
18	LGV with goods	Main tunnel / 108	3.2 – 4.6	Rear of vehicle	85

Table 11.6: Summary of predicted peak HRR value for a single LGV for this project

Predicted peak HRR value for a single HGV

S/no	Size of fuel load	Location of tunnel / tunnel area (m^2)	Tunnel air flow (m/s)	Ignition location	Predicted peak HRR (MW)
2	HGV without goods	Slip road / 55.8	0 – 2.9	Rear of vehicle	8.3
21	HGV with goods	Slip road / 55.8	0 – 2.9	Rear of vehicle	132
23	HGV with goods	Slip road / 55.8	0 – 2.9	Front of vehicle	95
24	HGV with goods	Slip road / 55.8	0 – 1	Rear of vehicle	126
25	HGV with goods	Slip road / 55.8	0 – 5.2	Rear of vehicle	193
26	HGV with goods	Slip road / 55.8	5.6 – 2.9	Rear of vehicle	75
27	HGV with goods	Slip road / 55.8	3.4 – 5.2	Rear of vehicle	99
29	HGV with goods	Main tunnel / 90	0 – 3.1	Rear of vehicle	141
31	HGV with goods	Main tunnel / 90	0 – 3.1	Front of vehicle	101
32	HGV with goods	Main tunnel / 90	0 – 1	Rear of vehicle	119
33	HGV with goods	Main tunnel / 108	0 – 4.6	Rear of vehicle	170
34	HGV with goods	Main tunnel / 90	3.5 – 3.1	Rear of vehicle	91
35	HGV with goods	Main tunnel / 108	3.2 – 4.6	Rear of vehicle	104

Table 11.7: Summary of predicted peak HRR value for a single HGV for this project

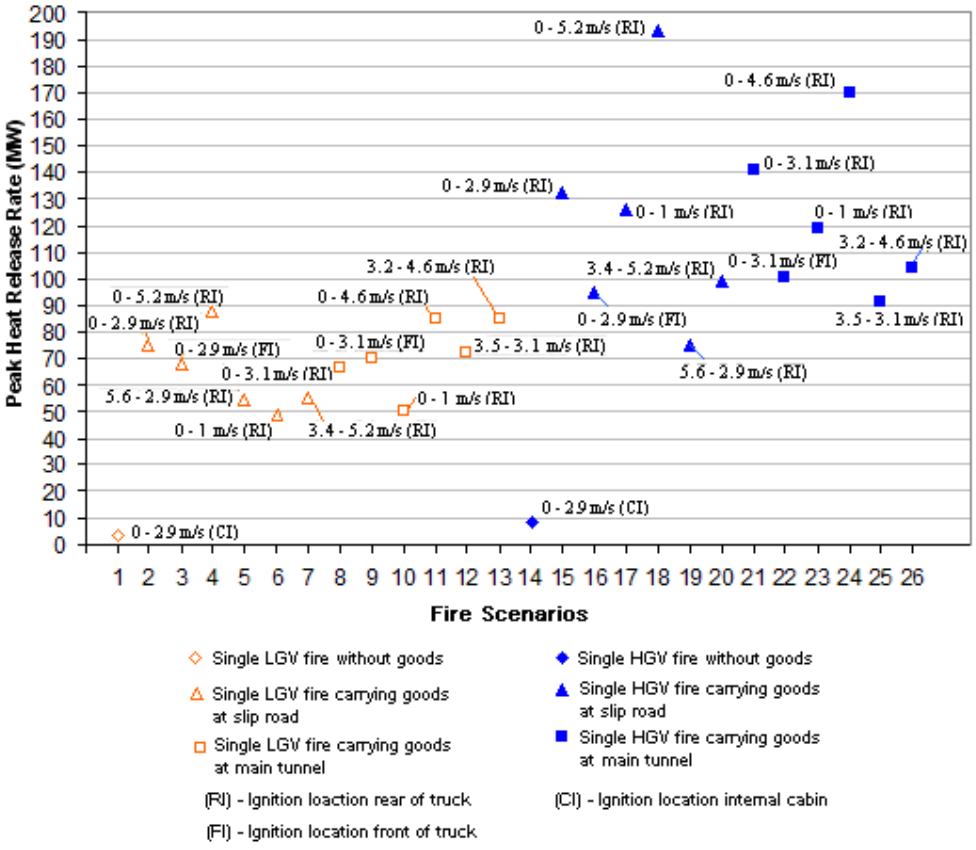

Figure 11.58: Predicted peak heat release rate

It has been observed in Figure 11.58 that the heat release rate for this tunnel project varies from 49 MW to 88 MW for a single LGV fire with goods and 75 MW to 193 MW for a single HGV fire with goods. From the above analysis, we can see that the quantity of fuel load can significantly affects the fire size in the tunnel. An HGV generally has a much higher heat release rate as compared with an LGV because an HGV usually carries a larger quantity of fuel than an LGV.

Another important observation made is higher airflow in the tunnel would generally yield higher heat release rate. This can be seen from fire scenarios no 12 and 15 (LGV), fire scenarios no 29 and 32 (HGV) where increasing the air velocity by another 2 m/s would result in a higher peak heat release rate of approximately 17 MW and 22 MW respectively (Figure 11.59 and Figure 11.60).

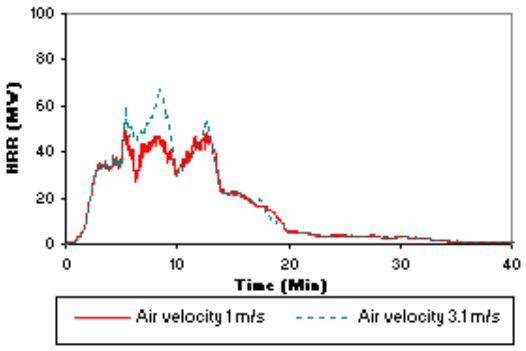

Figure 11.59: Varying air velocity (LGV)

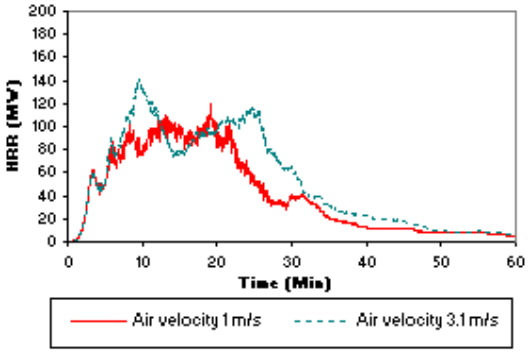

Figure 11.60: Varying air velocity (HGV)

Close examination of fire scenarios no 21 and 23 shows that the location of the ignition source could have an effect on fire development. From Figure 11.61, it has been observed that with the aid of the air flow in the tunnel; fire ignited at the rear of the vehicle seems to spread faster as compared to fire ignited at the front of the vehicle and yielding higher heat release rate.

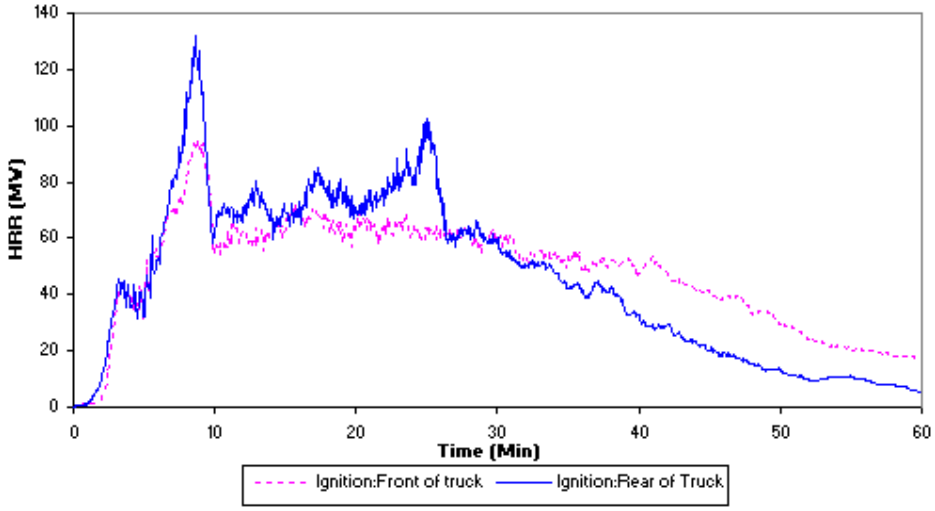

Ignition: Rear of the truck **Ignition: Front of the truck**

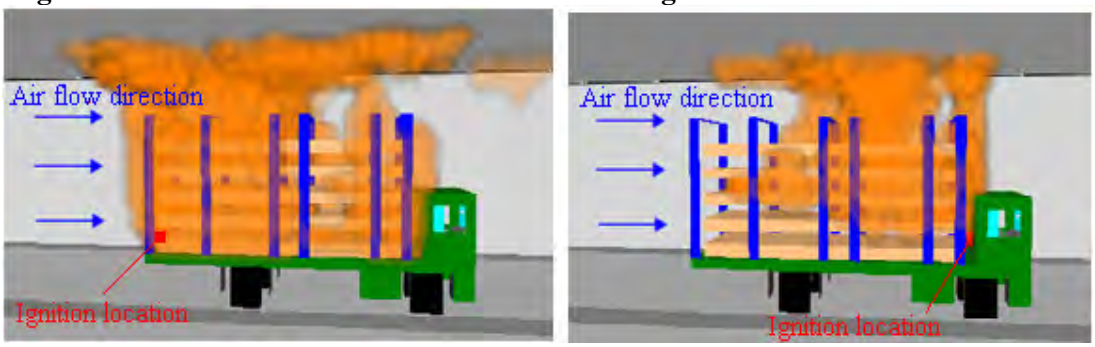

Figure 11.61: Time = 162 sec at 2.9 m/s (HGV)

11.11 Conclusion from simulations analysis

The above numerical analysis has drawn the following conclusions:

When a single LGV or single HGV fire occurs in the tunnel, it is more likely to be fuel controlled rather than ventilation controlled due to the high flow rate generated by the tunnel ventilation fans.

The heat release rate can varies from 49 MW to 88 MW for a single LGV fire and 75 MW to 193 MW for a single HGV fire. The fire size varies depending on factors such as tunnel geometry, ventilation condition and ignition location of the fire.

The quantity of fuel load can significantly affect the fire size in the tunnel. A LGV would have a much lower heat release rate as compared with HGV because the amount of goods carried is determined by laden weight of the goods vehicle.

The ventilation condition in the tunnel could have a significant impact on the heat release rate. Generally, a higher air velocity in the tunnel would result in a higher heat release rate.

With the aid of the tunnel air flow, a fire igniting at the rear of the vehicle appears to spread faster as compared to a fire igniting at the front of the vehicle yielding a higher heat release rate.

Chapter 12:
THE EFFECT OF ROAD TUNNEL VENTILATION ON THE SEPARATION OF VEHICLES TO MINIMISE FIRE SPREAD

Cheong M K, Spearpoint M J, Fleischmann C M and M Thong, published as "The Effect of Road Tunnel Ventilation on the Separation of Vehicles to Minimise Fire Spread", 13th International Symposium on Aerodynamics and Ventilation of Vehicle Tunnels, New Brunswick, New Jersey, USA, BHR Group Conference, pp. 199 – 210, 13th to 15th May 2009.

The fire safety measures in a road tunnel often includes a ventilation system to create safe egress conditions upstream of the fire by forcing heat and smoke away from vehicles and their occupants. Vehicle to vehicle fire spread in a road tunnel can be a major hazard particularly where vehicles downstream of a fire cannot be driven out. This chapter examines the minimum separation distance between different types of vehicle so that the probability of a catastrophic tunnel fire as a result of secondary ignitions is minimised.

Computational Fluid Dynamics simulations using Fire Dynamics Simulator (FDS 4.07) are used to calculate the heat flux received by downstream vehicles. Ignition criteria determined from typical materials used in vehicles are used to establish the likelihood of ignition at different separation distances. The analysis is based on fires occurring in a light goods vehicle (LGV) and a heavy goods vehicle (HGV) which are commonly found in road tunnels in Singapore. Scenarios involving a petrol tanker fire or a fire in a vehicle carrying hazardous materials were not considered in view of the HAZMAT tracking system available in Singapore (refer to chapter 5).

The simulation results showed that a minimum separate distance of 160 m and 55 m for heavy goods vehicle and light goods vehicle respectively is required. The results from this work allow tunnel operators to strategise their emergency procedures if a fire should arise.

12.1 Introduction

For a road tunnel emergency ventilation design adopting the longitudinal ventilation system concept, when a fire occurs in a uni-directional tunnel the activation of the ventilation system will direct smoke away from the flow of oncoming traffic (Figure 12.1). Motorists upstream of the fire can evacuate through the nearest emergency exit and vehicle downstream of the fire can drive out of the tunnel (Bendelius 2003). For this scheme to work, a road traffic management system is critical to ensure there are no traffic hold-ups in the downstream flow direction of the tunnel and at the exit portal. Without proper traffic management in place, vehicles downstream may be held up by a traffic jam resulting heat and smoke reaching these vehicles. This may increase the potential for secondary vehicle ignition which may then lead to a more severe fire and compromise the safe evacuation of motorists.

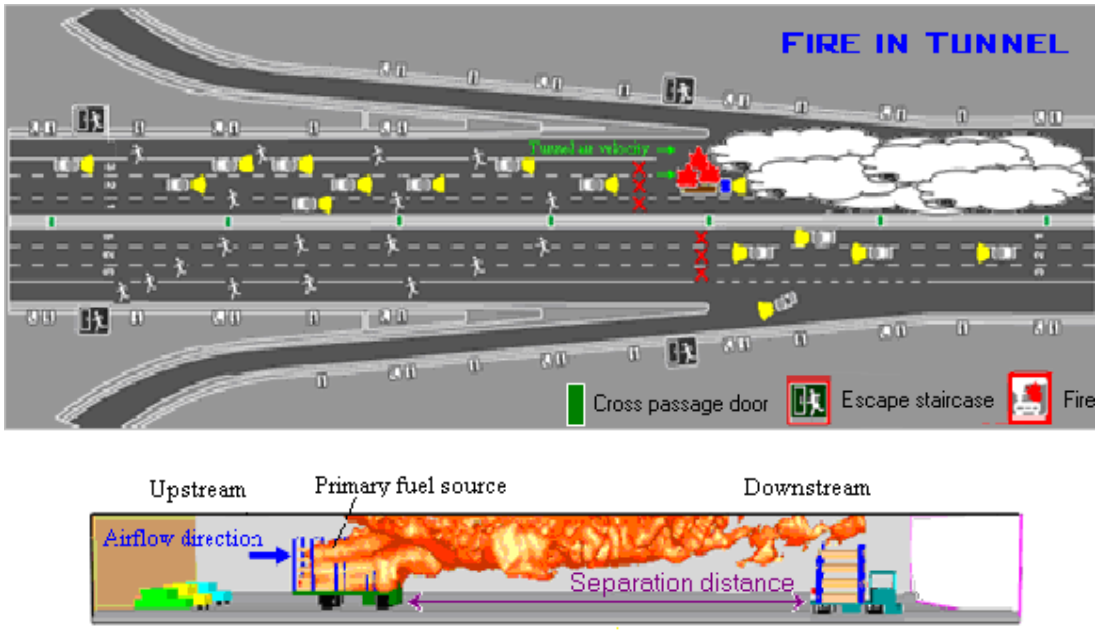

Figure 12.1: Effect of force ventilation on flame spread

Studies by Carvel et al. (2004) and fire experiments conducted in the EUREFIC study (EUREKA 1995) show that the use of forced ventilation can enhanced the heat release rate in the tunnel. The Runehamar tunnel fire tests conducted by the Swedish National Testing and Research Institute have also shown that a goods vehicle fire in the tunnel where a fuel load consisting of ordinary mixed goods such as wood pallets, plastic pallets, paper cartons,

furniture etc can generate peak heat releases in the order of 66.4 MW to 201.9 MW (Ingason and Lonermark 2005). The intensity of these fires with the effect of forced ventilation can enhance the likelihood of fire spread between vehicles resulting in higher heat releases and devastating consequences.

Various options can be explored to reduce the risk of a catastrophic fire in a tunnel. At the design level, this includes the use of fire suppression system to control the fire size of the incident vehicles (Liu et al. 2007). From a tunnel operational aspect, solutions include compartmentalising the goods vehicle cargo deck with fire rating material (Ingason and Lonermark 2004); imposing safe fire separation distances between vehicles while driving in tunnel; and during the event of a tunnel fire, ensuring minimum fire separation between vehicles through traffic management procedures. The work in this chapter focuses on the examination of the appropriate safe fire separation distance required to prevent vehicle fire spread in the tunnel through the use of computer simulation.

12.2 Methodologies

According to the work conducted by Carvel et al. (2005) on fire size and fire spread in tunnels, the fire severity in a the tunnel is affected by the heat release rate, air ventilation velocity in the tunnel, tunnel geometry and vehicles separation distance.

The enhancement of flame spread by radiant heat can be significant to the fire development in the incident tunnel. On exposure to sufficiently high radiant heat, the surface temperature of the combustible solids will increase resulting in the likelihood of a second ignition to the vehicles downstream of the fire. The work in this chapter is to vary these parameters to investigate the minimum vehicle separation to prevent a catastrophic tunnel fire incident.

Vehicle Heat Release Rate

LGV and HGV fires have been simulated to investigate the effect of fire spread by different vehicle categories using Fire Dynamics Simulator (FDS 4.07). The equations in FDS the code include the conservation of mass, species, momentum, energy and equation of state where this is a set of partial differential equations to compute the density, three

components of velocity, mass fraction, temperature, pressure heat flux and heat release rate (McGrattan and Forney 2005). A Large Eddy Simulation (LES) turbulence model is used for this analysis. The heat release rate of the vehicle is estimated using the heat release rate per unit area from cone calorimeter tests (ISO 5660 2002) and a surface burning factor is incorporated in the simulation to ensure that the fuel load area modelled in the simulation is equivalent to the fuel load carried by a good vehicle. More details of the modelling approach to establish the heat release rate in the tunnel are discussed in chapter 10 and 11. For this study, the fire is ignited at the rear of a goods vehicle carrying an 80% wood and 20% plastic mixed fuel load similar to the Runehamar experiments. The analysis also considers the effect of flame spread in a two lane and a three lane tunnel where dimension of 9.3 m width by 6 m height (2 lane tunnel) and 15 m width by 6 m height (3 lane tunnel) have been used with the fire source located at the centre of the tunnel. The air ventilation velocity in the tunnel can vary depending on the tunnel location and the design velocity can vary from one tunnel to another. For this analysis, the focus is on an urban tunnel in Singapore where the design tunnel velocity varies from 2.9 m/s to 5.2 m/s. A total of 8 simulations were performed, details of these simulations are tabulated in Table 12.1 and the heat release rate curves are presented in Figure 12.2.

S/no	Fuel load	Location of tunnel / tunnel area (m^2)	Tunnel air flow (m/s)	Simulation results
1	LGV[a]	2 lane tunnel / 55.8	2.9	Figure 12.2a
2	LGV[a]	2 lane tunnel / 55.8	5.2	Figure 12.2a
3	LGV[a]	3 lane tunnel / 90	3.1	Figure 12.2b
4	LGV[a]	3 lane tunnel / 90	4.6	Figure 12.2b
5	HGV[b]	2 lane tunnel / 55.8	2.9	Figure 12.2c
6	HGV[b]	2 lane tunnel / 55.8	5.2	Figure 12.2c
7	HGV[b]	3 lane tunnel / 90	3.1	Figure 12.2d
8	HGV[b]	3 lane tunnel / 90	4.6	Figure 12.2d

Note: 300 mm grid size is used for the above simulations
(a) - LGV carrying 48 wood pallets and 12 plastic pallets
(b)- HGV carrying 183 wood pallets and 45 plastic pallets

Table 12.1: Simulation schedule used for the Singapore urban road tunnel

From the computer simulation results shown in Figure 12.2, it can be seen that higher peak heat release rate are with the aid of higher air flows in the tunnel. This has also been observed in tunnel fire experiments where tunnels with higher airflow tend to fan the fire resulting in a higher heat release rate (Ingason et al 1994).

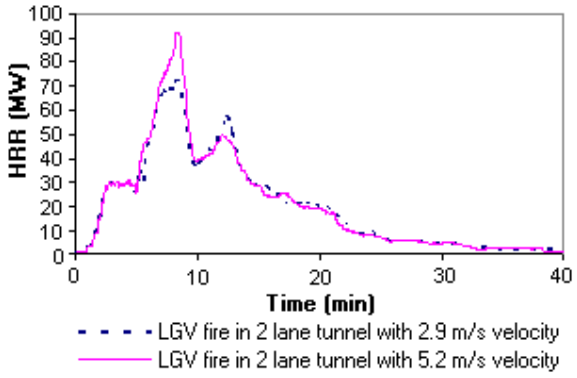

Figure 12.1a

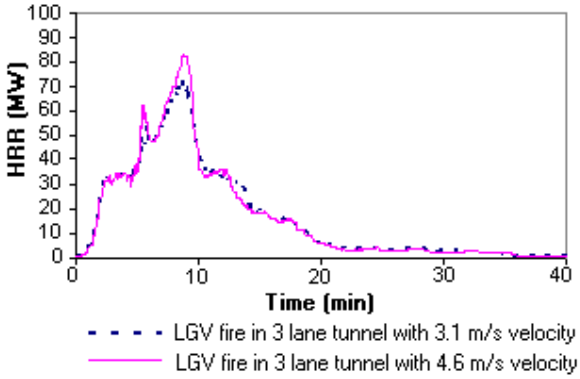

Figure 12.1b

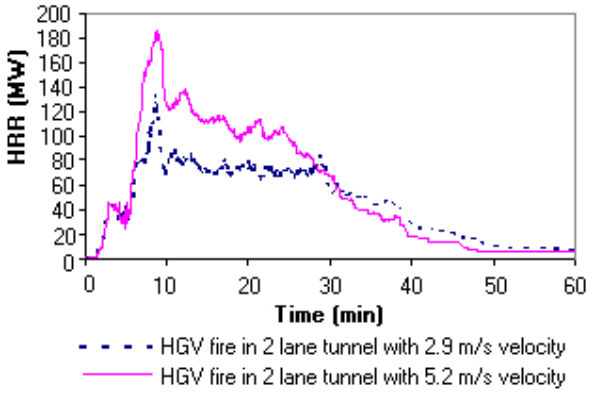

Figure 12.1c

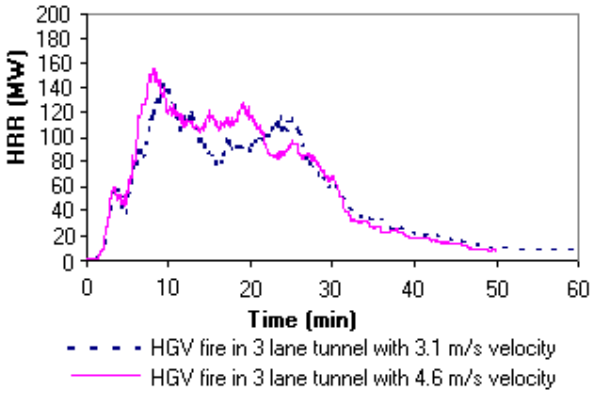

Figure 12.1d

Figure 12.2: Simulated LGV and HGV heat release rate using FDS

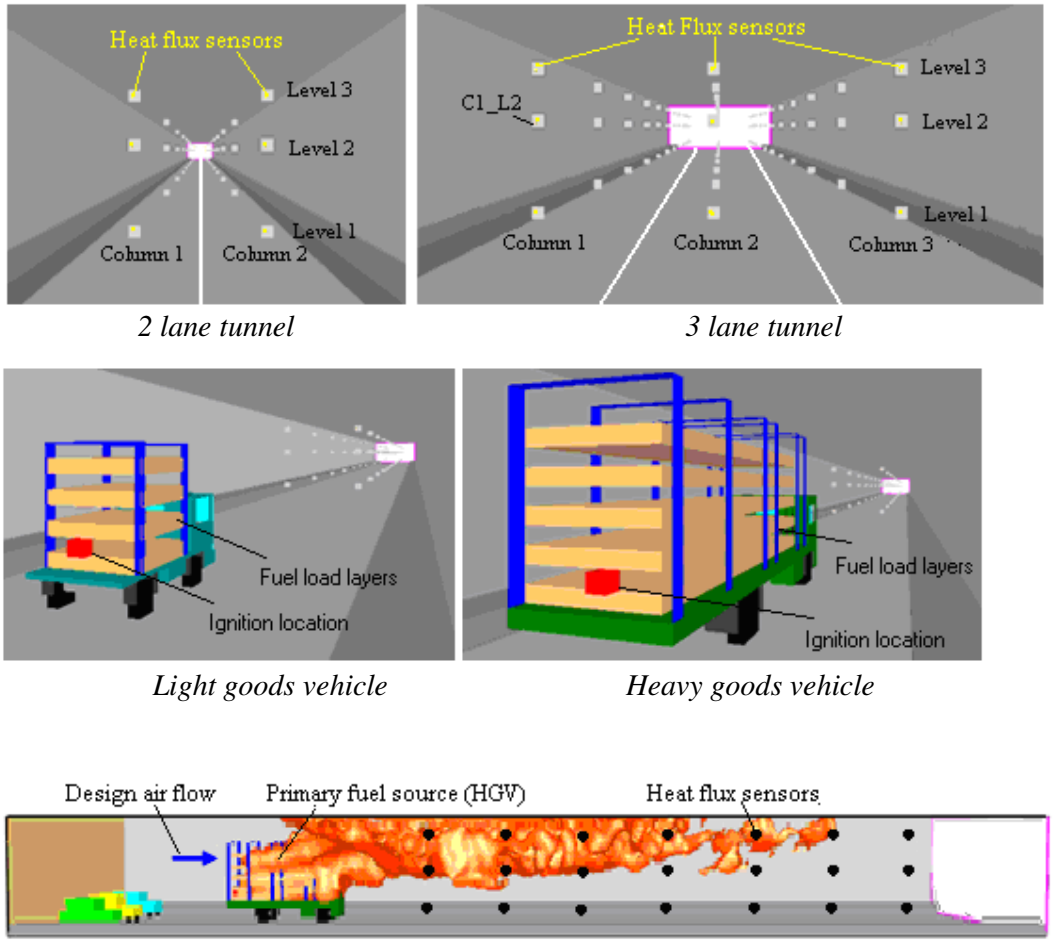

Figure 12.3: FDS model setup

Virtual sensors are positioned at every 10 m downstream of the fire to capture the heat flux level. The placing of the heat flux sensors is based on the average height of typical vehicles where level 1 (1.3 m from road level) represents the average height for automobile, level 2 (3.1 m from road level) represents the average height for an LGV and level 3 (.3 m from road level) represents the average height for an HGV. Each column of sensors are provided in the two lane tunnel and similarly three columns of sensors are positioned in a plane in the three lane tunnel. Details of the FDS model set up is shown in Figure 12.3.

Ignition criteria

There are two criteria suggested by Donaldson et al (2005) to identify ignition. These include ignition temperature and heat flux. Although there are other works by Beard and Carvel (2005) to identify fire spread, heat flux is used as a criterion for ignition because it is more convenient to consider from an engineering view point in which there must be a heat flux incident upon a solid object for ignition to occur, rather than the temperature to which its surface must rise. Another reason to use a heat flux criterion is because minimum heat flux ignition information for plastic and wood materials used or carried by vehicles are available in the literature (Table 12.2). By identifying the minimum heat flux needed for ignition for the various vehicle parts the minimum separate distance between fire location and the vehicle downstream can be established.

Material	Minimum heat flux for ignition (kW/m^2)	
	Piloted	Auto-ignition
Acrylonitrile butadiene styrene (ABS) [a]	< 20	-
Polycarbonate (PC) [b]	15	47
Polyethylene (PE) [a]	17	-
Polypropylene (PP) [a]	11	-
Polyurethane (PU) [a]	< 10 to 16	-
Ethylene propylene diene rubber (EPDM) [b]	20 to 23	-
Wood [a]	12	20

Source: a) – Donaldson et al. 2005
b) – SFPE engineering guide 2002

Table 12.2: Minimum heat flux for ignition

The materials shown in Table 12.2 are the materials commonly used by vehicle manufacturers for the construction of an automobile (Scania 2005). The minimum ignition heat flux for these materials varies from 10 kW/m^2 to 23 kW/m^2. This information provides an ideal range of heat fluxes in which vehicle ignition could occur and enable fire engineers or designers to use as a criteria to determine ignition and eventually use this criteria to determine the minimum separation distance needed between vehicles downstream of a fire.

12.3 Simulation results and discussion

Figure 12.4 to 12.7 shows the heat flux level in a 2 lane and 3 lane tunnels with an operating airflow varying from 2.9 m/s to 5.2 m/s. The simulation results indicate that heat flux in the tunnel decreases with the increase in vehicle separation distance. Based on a 10 kW/m^2 heat flux criteria, the required separation distance required can vary from 30 m to 160 m. A summary of the findings are tabulated in Table 12.3.

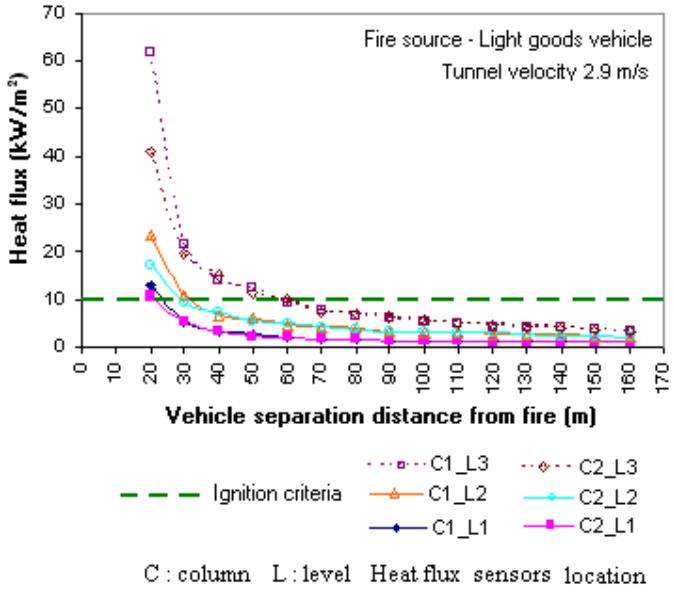

Figure 12.4a: LGV fire in a 2 lane tunnel heat flux level at receiving surface

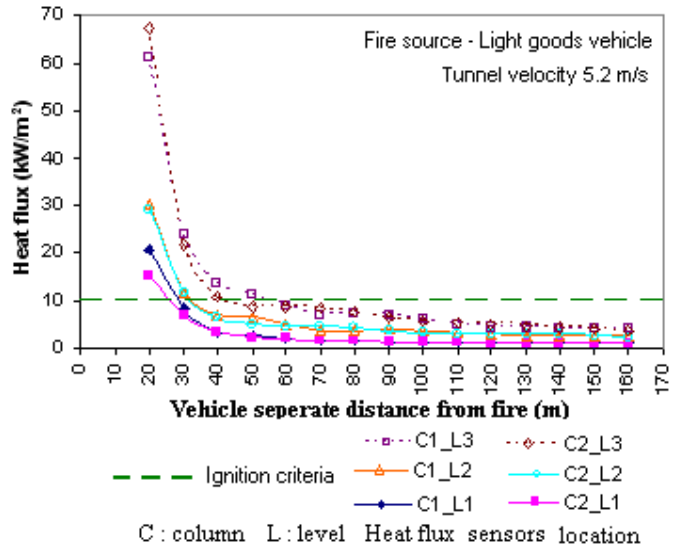

Figure 12.4b: LGV fire in a 2 lane tunnel heat flux level at receiving surface

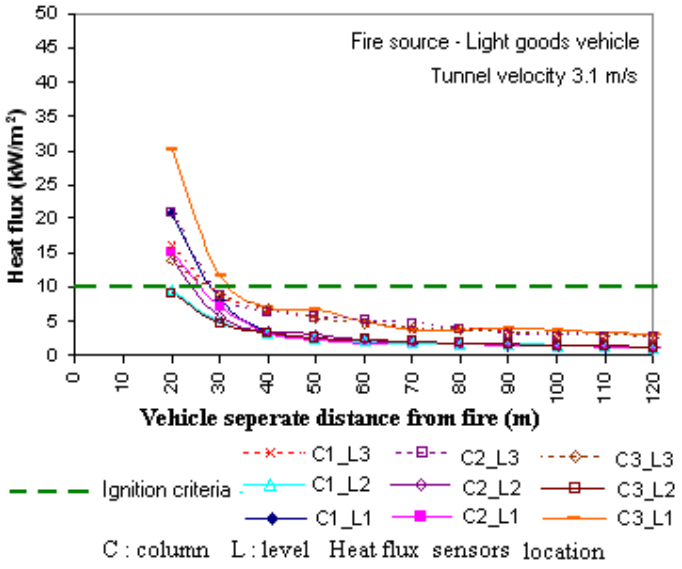

Figure 12.5a: LGV fire in a 3 lane tunnel heat flux level at receiving surface

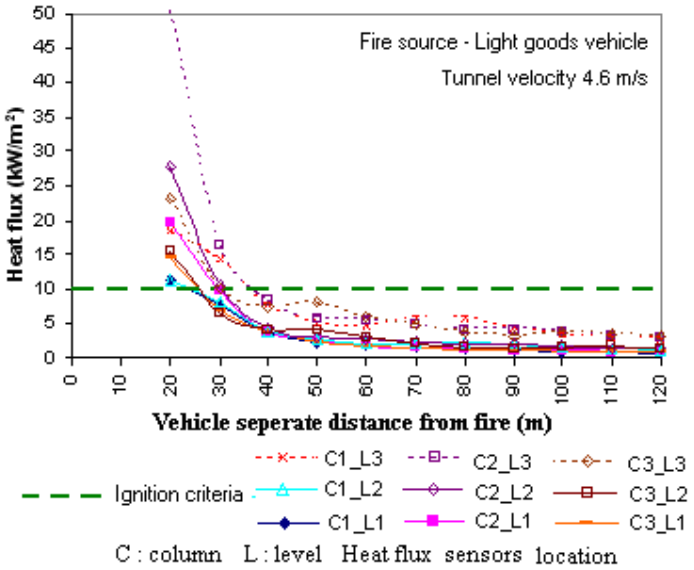

Figure 12.5b: LGV fire in a 3 lane tunnel heat flux level at receiving surface

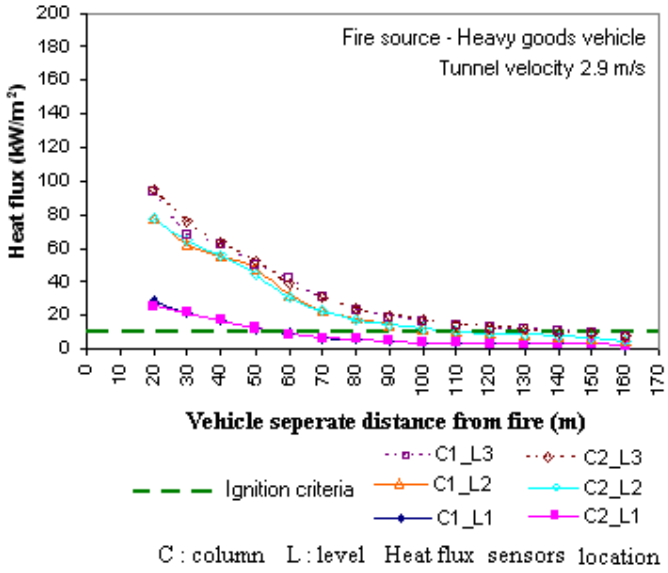

Figure 12.6a: HGV fire in a 2 lane tunnel heat flux level at receiving surface

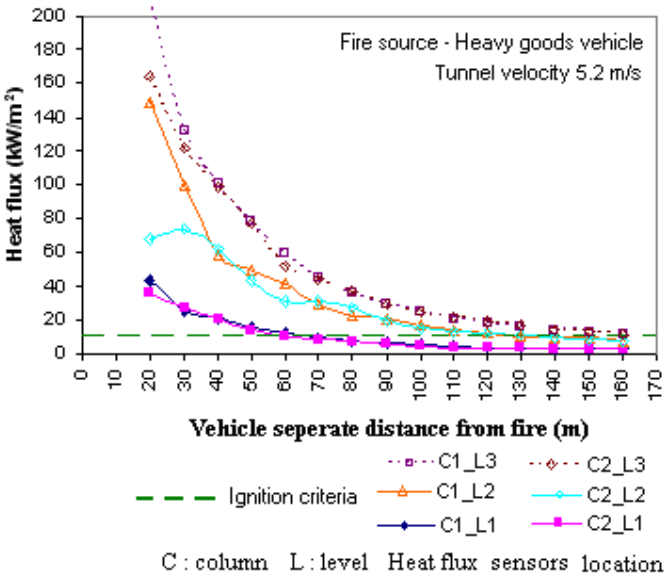

Figure 12.6b: HGV fire in a 2 lane tunnel heat flux level at receiving surface

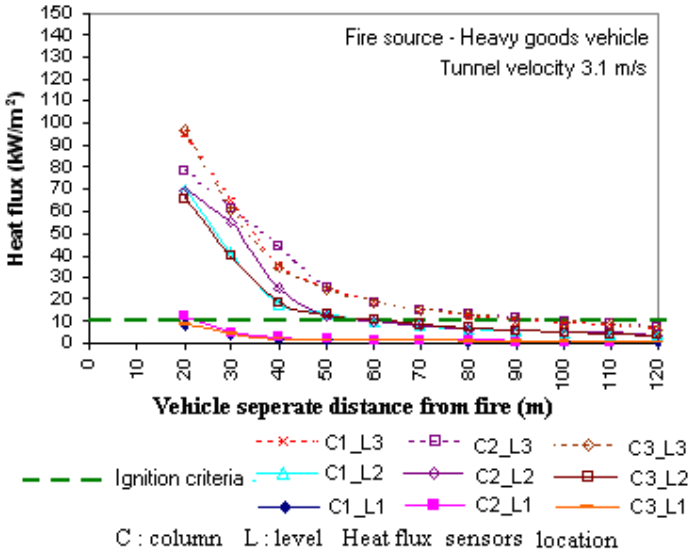

Figure 12.7a: HGV fire in 3 lane tunnel heat flux level at receiving surface

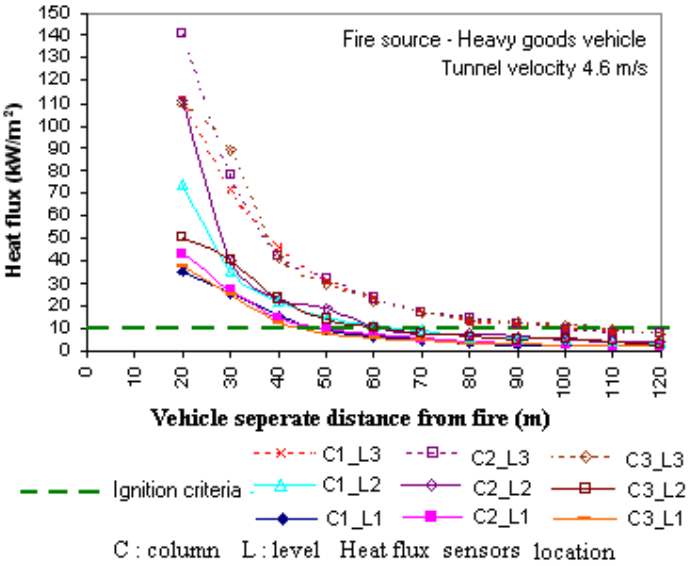

Figure 12.7b: HGV fire in 3 lane tunnel heat flux level at receiving surface

From Table 12.3, it can be observed that fire intensity (i.e. HGV or LGV fire) play an important role on the effect of fire spread in tunnel. Longer separation distance (approximately 1 to 2 times longer) are required for an HGV fire as compared to an LGV fire.

S/no	Primary fuel source by vehicle type [a]	FDS predicted peak HRR (MW)	Type of tunnel / tunnel area (m^2)	Tunnel air flow (m/s)	Vehicle minimum separate distance from fire (m) [b]
1	LGV	75	2-lane tunnel / 55.8	2.9	50
2	LGV	93	2-lane tunnel / 55.8	5.2	55
3	LGV	73	3-lane tunnel / 90	3.1	30
4	LGV	83	3-lane tunnel / 90	4.6	38
5	HGV	133	2-lane tunnel / 55.8	2.9	140
6	HGV	186	2-lane tunnel / 55.8	5.2	160
7	HGV	143	3-lane tunnel / 90	3.1	100
8	HGV	155	3-lane tunnel / 90	4.6	100

Note: a – refer to figure 3
b - vehicles minimum separate distance from fire is based on 10 kW/m^2 criteria

Table 12.3: Summary of vehicle separate distance from fire to prevent ignition

The simulations also show that a higher heat flux is observed at the upper level portion of the tunnel section as compared to the lower level (Figure 12.4 to 12.7). This is because when the vehicle is burning, fire plume will impinge on the tunnel ceiling and in the presence of forced ventilation, the flame will be pushed along the airflow direction with flame spreading along the tunnel soffit. This implies that for vehicles located downstream of the fire, the chances of an HGV igniting is higher as compared to a private car in view of its higher vehicle height.

Increasing the air velocity can affect vehicle fire spread in the tunnel. Comparing the HGV fire simulation results with a tunnel air velocity of 2.9 m/s and 5.2 m/s (Figure 12.6a and 12.6b) at a vehicle separation distance of 20 m from the fire source the maximum heat flux level of 95 kW/m^2 and 210 kW/m^2 were estimated respectively. The increase in heat flux level is partly attributed to the increase in heat release rate and partly due to the longer flame extension. It is likely that the higher airflow tends to improve the mixing between the fresh air and combustible gases leading to a burning enhancement. At the same time the higher air velocity increases the flame extension down the tunnel. The increase in heat release rate and the closer proximity of flames leads to a higher incident heat flux to a target as the forced ventilation increases. Similar trends where increasing the air velocity results in a higher heat flux level has also been observed in other simulations conducted in

this study (Table 12.3). In general a greater separation distance from the fire is required when the velocity in the tunnel increases.

12.4 Conclusion

Heat flux results to determine separation distances between the fire and vehicles downstream in a two and three lane road tunnel are presented. The simulation results showed that a minimum separation distance of 55 m for LGV and 160 m for HGV is generally required to prevent vehicles downstream from igniting. The computer simulations show that the required separation distance increases with increasing forced airflow velocity. This study provides an estimate on the separation distance required thereby allowing tunnel operators to strategise their emergency operating procedure if such situation arises.

Chapter 13:
A COMPARISON OF BAYESIAN AND FIRE DYNAMICS SIMULATOR APPROACH TO ESTIMATE HEAT RELEASE RATE IN ROAD TUNNEL FIRES

Cheong M K, Spearpoint M J, Fleischmann C M, published as "A Comparison of Statistical and Computational Fluid Dynamics Approach to Estimate Heat Release Rate in Road Tunnel Fires", to *Fire Technology*, August 2009.

Computational tools such as one-dimensional modes or Computational Fluid Dynamics (CFD) have been used for the fire safety design of road tunnels. However, most of these analyses are performed using a specified fire source where the heat release rate (HRR) in the tunnel is fixed by the user and the influences of ventilation conditions and tunnel geometry are not considered. For a more realistic estimate, models need to incorporate these factors in their input. This chapter discusses the use of a statistical approach previously developed by other researches (Carvel and Beard 2005) and the use of a CFD approach to estimate the HRR in a road tunnel fire. As an application example, fire scenarios in which a light goods vehicle carrying wooden pallets are used to compare the estimation of the HRR using these two methods.

13.1 Introduction

The use of a ventilation system to control smoke movement during fire is common in most tunnel designs. Its primary objective is to create a smoke free path for motorist evacuation and to facilitate fire-fighter access for fire and rescue operations. The airflow necessary for such operation is known as the critical velocity. The critical velocity is a function of a number of factors which includes the heat release rate (HRR), tunnel gradient and tunnel geometry (Bechtel and Brinckerhoff 1995). In a longitudinal ventilation design, the performance of the system is considered acceptable if the system design velocity is higher than the calculated critical velocity. One dimensional analytical tools such as Subway Environmental Simulation (SES) (Parson and Douglas 1997), Road Tunnel Ventilation (RTV) (IDA 2005) or TUNVEN (FHWA 1980) can be used to establish the required system design velocity. The use of these tools often requires input of the tunnel layout, fan capacity and heat release rate of a design fire.

From a fire analysis and life safety point of view, it is clear that the design fire plays an important part in the ventilation design as inappropriate selection could result in a system that is under-designed. Conversely, stakeholders such as the developer, tunnel designer and tunnel operator want a tunnel system that is safe but not over-designed which would otherwise result in a project which is unsuitable for commercial financing. Events such as multiple vehicle collisions resulting in several tens or hundreds of vehicles involved in a catastrophic fire incident are not cost effective and practical to design for as a reasonable worse case. Therefore selecting scenarios is best made on the basis of risk analysis and details of identifying such scenarios are discussed in chapter 8. Based on current practice, fire size selection for most tunnel ventilation designs often reference various guidelines such as NFPA 502 (NFPA 2008), BD78/99 (BD 1999) or the PIARC technical committee report (PIARC 1999). The peak heat release rate for goods vehicles recommended by these guidelines varies from 20 to 200 MW. The upper heat release rate limit recommended is based on the recent fire tests conducted in the Runehamar tunnel fire experiment (66.4 MW to 201.9 MW) (Ingason and Lonnermark 2005).

Each tunnel is unique in terms of design airflow, tunnel geometry and vehicle traffic conditions so that in the event of a fire, the heat release rate can vary from one tunnel to another. Although the ideal means to determine heat release rate might be to conduct fire experiments using the oxygen consumption calorimetry technique, this approach is generally expensive, time consuming and logistically complicated to perform (Ingason 2006). It is also noted that the heat release rate results obtained from fire experiments are dependent on conditions in the tunnel which may not reflect those conditions for which the ventilation system has been designed. The peak heat release rate can vary depending on the tunnel velocity (Ingason et al 1994) and tunnel geometry available during a specific experiment.

The use of computer simulation models for the fire safety design of tunnels has been increasing over the past few years. This increase has been attributed to many factors including the complexity of tunnel networks, the need for a better understanding of fire behaviour in tunnels because heat and toxic combustion products cannot be dissipated out of the tunnel as compared an open environment and the advancement of computer technology with increased availability of inexpensive computer workstations. While using computer modelling in fire safety design enables designers to build a computational model that represents the system for analysis of fire dynamics, smoke movement and to test performance of their design, most of these models require the input of heat release rate by the user.

This chapter compares two methodologies to estimate the heat release rate in a tunnel considering tunnel geometry and ventilation conditions. A statistical approach, which is a simple and quick calculation method, is compared to a numerical approach using Fire Dynamics Simulator 4.0.7 (FDS4). The discussion in this work evolves around the estimating the heat release rate involving a single light goods vehicle (LGV) fire carrying wooden pallets and factors that could possibly affect the analysis.

13.2 Methodologies

13.2.1 Statistical Approach

The statistical approach developed at Heriot-Watt University considers the interaction of forced ventilation, tunnel cross-section and fire size. The method allows for a rapid assessment of the peak HRR of a vehicle fire in a road tunnel that includes the effects of the tunnel conditions. Experimental data were used to produce a probability distribution of fire size for heavy goods vehicles (HGV), cars and a range of pool fire sizes (Carvel and Beard 2005). The peak heat release rate in a tunnel is established from an equation in the form of (Carvel et al 2004a):

$$\dot{Q}_{vent} = \kappa\psi \dot{Q}_{open} \qquad \text{Equation 13.1}$$

where $\dot{Q}_{vent}$ is the heat release rate in the tunnel (MW) and $\dot{Q}_{open}$ is the heat release rate of a similar fire in the open space (MW). The parameter ψ is the heat release rate enhancement coefficient representing the difference between open air conditions and re-radiating conditions in a tunnel. The relationship for ψ is

$$\psi = 24\left(\frac{W_F}{W_T}\right)^3 + 1 \qquad \text{Equation 13.2}$$

where W_F is the width of the fuel (m) and W_T is the width of the tunnel (m). κ represents the difference between a fire subject to natural ventilation and forced ventilation conditions in a tunnel. κ is presented as probability percentile graphs which vary depending on the type of fuel burning. According to Carvel et al (2004a), the probability distribution for κ are categorised into HGVs, medium sized pool fires and large pool fires (Figure 13.1). For example, 50% of all fires have a κ value of 4 at 4 m/s for HGV fires.

Fuel quantity and type are important factors in estimating the peak heat release rate so that this chapter and associated work in chapter 11 makes the distinction between HGVs and

LGVs considering different goods vehicle classifications based on vehicle tonnage. It is recognised that the term HGV has been used by Carvel et al to categorise the probability distributions for κ with regard to a goods vehicle fire. However, the distinction between HGV and LGV is not explicitly noted by Carvel et al (2004a) and it is assumed that goods vehicles in general are considered as HGVs for the selection of the κ value. An LGV fire is used in this chapter because the statistical approach requires the peak HRR data from an experiment carried out an the open air environment. Documented HGV fire experiments in the open are not available in the literature and so HRR data from a 3.49 ton LGV free burning fire is used.

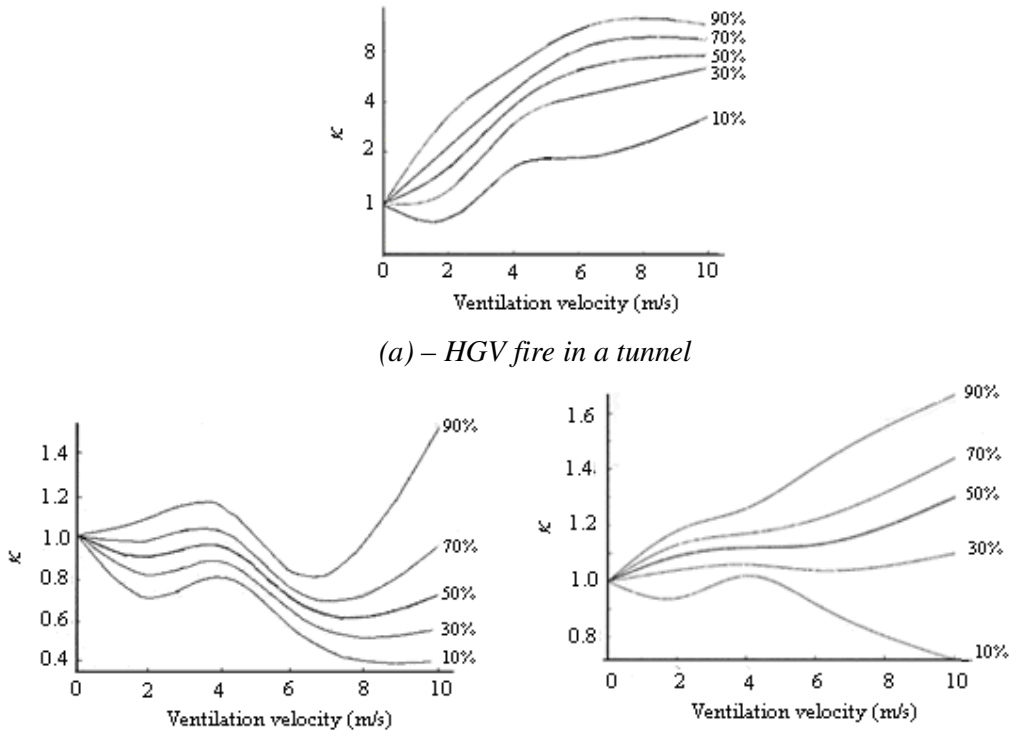

(a) – HGV fire in a tunnel

(b) – medium pool fire in a tunnel

(c) – large pool fire in a tunnel

Figure 13.1: Probability percentage graph for HGV, medium and large pool fire in tunnel (Carvel et al 2004a)

13.2.2 Numerical Approach using Fire Dynamics Simulator

Fire Dynamics Simulator (FDS) is a computational fluid dynamics (CFD) code developed by the National Institute of Standards and Technology (NIST). FDS solves a form of the Navier-Stokes equations appropriate for low-speed, thermally driven flows for the purpose of estimating output quantities in the gas phase such as temperature, velocity, pressure and global output quantities such as energy flux, heat release rate etc (McGrattan 2005). Although FDS version 5 was released during the course of the analysis discussed here, FDS4 has been used for this work for the reasons that follow. Extensive work had already been completed using FDS4 to match a simulated fire development with experimental data. Even at the time of writing new releases of FDS5 have been regularly appearing and so it was not possible to select a fixed release to work with. According to McGrattan et al (2008), there have been a number of enhancements to FDS5 compared to FDS4. The most relevant to this research are the changes to the gas phase combustion. FDS5 allows a multi-step reaction schemes to describe local extinction, CO production, among various other phenomena. FDS4 uses a single gas phase reaction.

The two ways of designating a fire in an FDS simulation is the heat release rate per unit area (HRRPUA) or the heat of vaporization approach where the burning rate of the fuel is depends on the net heat feedback to the surface (McGrattan 2005). For this study, heat release rate in the tunnel is determined using the heat release rate per unit area from cone calorimeter tests reported in the literature. Materials were modelled as composites by summing their mass and redistributing them into layers of rectangular boxes with an equivalent size. When using this modelling approach, it was important to ensure the fuel package surface area in the simulation was equivalent to the fuel package area in an actual tunnel fire scenario. This was achieved by dividing the actual fuel package area over the fuel package area modelled in the simulation to establish a surface burning factor (SBF). The SBF value was multiplied by the peak heat release rate per unit area from cone calorimeter test data.

As with any complex fuel assembly configuration, modelling a goods vehicle fire using FDS to estimate the heat release rate in a tunnel is a challenging task. The predominant factor which affects the heat release rate of a goods vehicle is the type of commodity (e.g. wood, plastic) carried. Components of the vehicle chassis and truck cabin are another

source of fuel load. Combustible items include tyres, mud guards, bumpers, seats, the instrument panel, cabin internal lining etc.

To enhance the confidence in using FDS to estimate the initial fire growth and peak heat release rate, work to develop a simplified representation of a mixture of wood and plastic pallets burning in the tunnel was undertaken and illustrated that it was possible to reproduce a reasonable estimate of the fire characteristics using one of the Runehamar tunnel fire experiments as discussed in chapter 10. Although similar growth rate history and peak heat release rate were produced from the simulation, the current model is unable to simulate phenomena such as collapse of the fuel package. This is observed in the decay phase of the fire development (Figure 13.2). More details of the modelling approach in a tunnel environment using FDS4 are discussed chapter 10. Preliminary simulations using the same inputs to FDS5 showed sufficient differences between the rate of heat release results that a similar calibration process that was used for FDS4 would need to be repeated if FDS5 was to be used.

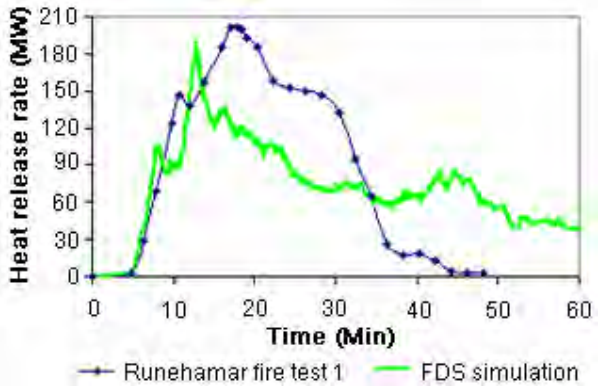

Figure 13.2: Comparison of FDS and Runehamar fire experiment.

13.3 Estimation of HRR in a Road Tunnel

This section illustrates the use of the statistical and numerical approaches to estimate the heat release rate in a road tunnel. A sensitivity study on the effect of air velocity and tunnel geometry on heat release rate is performed. As heat release rate information in an open space environment is required for the statistical approach, a free burning fire test of a light

goods vehicle conducted by Chuang et al (2007) is used. For comparison purposes, similar fuel quantity and material properties are used for the FDS4 simulations.

13.3.1 The 3.49 ton truck fire experiment

A total of five full scale fire experiments on 3.49 ton trucks carrying various cargo loads, ignition locations and the use of fire resistant blanket have been conducted by the National Taiwan University of Science and Technology under free burning conditions. Table 13.1 and Figure 13.3 provide a summary of these fire experiments.

Test No	Fire blanket	Ignition position	Goods carried	Peak HRR
1	No	Bottom centre of goods	890 kg wood pallets	23.38 MW
2	No	Seat surface	890 kg wood pallets	20.92 MW
3	No	Bottom centre of goods	452 kg plastic barrels	47.47 MW
4	Yes	Bottom centre of goods	890 kg wood pallets	-
5	Yes	Bottom centre of goods	452 kg plastic barrels	-

- Not available

Table 13.1: HRR 3.49 Ton truck with goods in free burning conditions Chuang et al (2007)

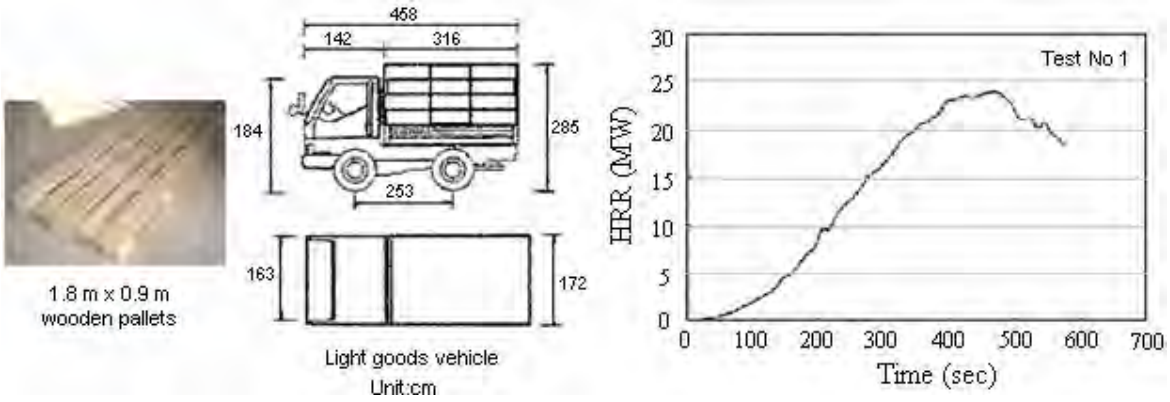

Figure 13.3: HRR of 3.49 Ton truck with goods reproduced from Chuang et al (2007)

Test No. 1 was an approximately 1.7 m wide light goods vehicle loaded with 70 wood pallets of dimensions 1.8 m x 0.9 m and total mass of 890 kg (Chuang et al 2007). The experiment excluded the use of the fire blanket, ignition was within the pallets and the peak HRR was reported. Verification work on using FDS4 to estimate heat release rate

from the ignition and burning of wood pallets has been performed in chapter 10, therefore information on Test No 1 is used to establish the heat release rate in a tunnel for this work. Unfortunately measurement of the test ended prematurely due to scale recording interference so that information after 575 s was not recorded. Since the statistical approach relies on having the peak free burning HRR there might be a concern that the heat release rate recorded in Test No 1 was not the peak HRR.

A simple hand calculation was performed for wood pallets of the above mentioned quantity to estimate the likely peak HRR. The HRR per unit area of a stack of wood pallets $\dot{Q}''$ can be determined from the equations reported by Babrauskas (2002) such that

$$\dot{Q}'' = 919(1 + 2.14h_p)(1 - 0.03M) \qquad \text{Equation 13.3}$$

where M is the moisture content for wood, using a typical value of 10% (Cholin 2003) since the experimental value was not reported; h_p is height of pallets = 2.85 m – 0.75 m (LGV deck height) = 2.1 m thus $\dot{Q}'' = 919(1 + 2.14 \times 2.1)(1 - 0.03 \times 10) \approx 3534$ kW/m^2.

The total peak HRR is found from

$$\dot{Q}_{open} = \dot{Q}'' \times A_f \qquad \text{Equation 13.4}$$

where A_f is the horizontal burning area of the fuel = 5.2 m^2 [refer to Figure 13.3]; $\dot{Q}_{open}$ is free burning heat release rate (MW) therefore $\dot{Q}_{open} = 3534 \times 5.2 \approx 18.4$ MW.

In a report from the EUREKA project (EUREKA 1995), it was suggested that the heat release rate of truck cabin furnishings and other attachments to a truck were in the order of what would be obtained from a medium sized car. Depending on the type of the car, estimates from car fires tests have shown that this value varies from 1.5 to 2.4 MW under free burning conditions (Mangs & Keski-Rahkonen 1994a) (Stroup et al 2001). By summing the above two results, the peak heat release of a LGV fire is estimated to be 21 MW. This is a reasonably close estimate to the peak recorded in the Test No. 1 fire

experiment and suggests that the maximum fire size had been captured prior to the loss of data recording.

13.3.2 Calculation methods

The following scenario is used as a case study to determine the expected peak heat release rate using the two methods. The scenario involves the same LGV as described above but this time it is assumed to be located in a road tunnel. The tunnel operates with a longitudinal ventilation system to control smoke movement during a fire incident. Depending on the location of the tunnel, the design airflow in this tunnel has values of 2, 3, 4 and 5 m/s. The LGV is either on a slip road section of the tunnel (9.3 m wide by 6 m high two lane tunnel) or in the main tunnel (15 m wide by 6 m high three lane tunnel). A summary of the scenarios performed for this study is shown in Figure 13.4.

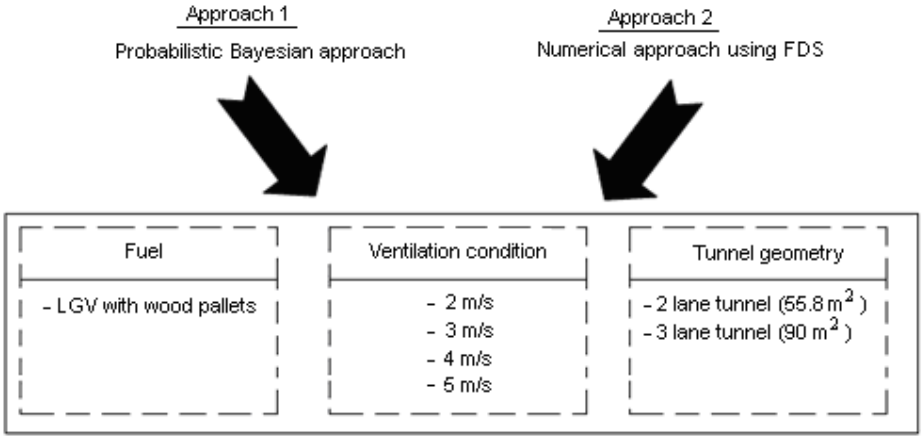

Figure 13.4: Scenarios setup

Approach 1: Probabilistic Bayesian approach

As reported by Chuang et al (2007) $\dot{Q}_{open}$ = 23.38 MW for Test No. 1, so that the heat release rate of the LGV is obtained by first determining the heat release rate enhancement coefficient ψ using Equation 13.2 followed by Equation 13.1 to establish the peak heat release rate in the tunnel. With an air velocity of 3 m/s, Figure 13.1(a) is used to obtain κ values of 4.8, 3.4, 2.6, 1.8 and 1.2 for 90%, 70%, 50%, 30% and 10% cumulative probabilities respectively. This analysis process is repeated by varying the velocities, tunnel widths and the probabilistic percentages. A summary of the results is shown in Table 13.2.

Scenario	Velocity (m/s)	Peak HRR (MW) from probabilistic Bayesian values				
		90%	**70%**	**50%**	**30%**	**10%**
2 lane tunnel 9.3 m x 6 m (55.8 m^2)	2	90	61	45	32	16
	3	127	90	69	48	32
	4	170	117	100	83	45
	5	212	170	133	98	48
3 lane tunnel 15 m x 6 m (90 m^2)	2	82	55	41	29	15
	3	116	82	63	43	29
	4	154	106	92	75	41
	5	193	154	121	89	43

Table 13.2: Estimated peak HRR using probabilistic Bayesian approach.

From the above analysis, depending on the air velocity and tunnel geometry, the heat release rate for a LGV carrying 890 kg of wood pallets in the tunnel can vary from 16 to 212 MW (in the two lane tunnel) and 15 to 193 MW (in the three lane tunnel). As expected, it can be seen that in Table 13.2 that the heat release rate increases with an increase in the tunnel ventilation velocity and generally a tunnel with smaller cross-sectional area tends to result in higher heat release rates as compared to a tunnel with larger cross-sectional section area due to re-radiation effects.

The FDS simulation of the LGV followed a similar approach as used for the Runehamar fire experiment. The numerical solution was obtained using a grid size of 0.3 m where grid and domain sensitivity was performed. As previously, it was not possible to model the wood pallets in FDS to a high level of detail so they were represented by layers of rectangular boxes in which the HRRPUA obtained from cone calorimeter tests was adjusted with an appropriate SBF. The materials and their thermal properties used for the simulation are shown in Table 13.3 and in Figures 13.5 and 13.6. Figure 13.5 is an example of the material properties input for the FDS simulation.

Material	Thermal conductivity (W/mK)	Density (kg/m^3)	Ignition temperature (^oC)	Specific heat (kJ/kgK)	SBF
PUR (Polyurethane)	0.034 [a]	20 [a]	272 [b]	1.4 [a]	1
ABS (Acrylonitrile butadiene styrene)	0.17 [c]	1050 [c]	414 [d]	1.48 [e]	1
PP (Polypropylene)	0.38 [b]	900 [b]	305 [b]	6.27 [b]	1
PC (Polycarbonate)	0.2 [f]	1190 [f]	497 [b]	2.06 [e]	1
EPDM (Ethylene propylene diene rubber)	0.3 [g]	860 [h]	369 [i]	2.18 [j]	1
Wood	0.12 [k]	600 [l]	373 [b]	2.58 [n]	10.3

Note: Refer to cone test data shown in Figure 13.6 used for FDS simulation

Reference: a - (Drysdale 1998), b - (Babrauskas 2003), c – (Goodfellow 2007), d – (Fleischmann 2006), e - (Tangram 2007), f – (Tewarson 2006), g – (Ismat 2000), h – (Chanda et al 1987), i - (Appendix M), j - (Nate Hoyt 2007), k - (Nisted 1991), l – (Thureson 1991), n - (Incropera and DeWitt 2002)

Table 13.3: Material thermal properties used for FDS simulation.

AN EXAMPLE OF THE MATERIAL PROPERTIES INPUT FILE USED IN FDS4
****

FDS input parameters for wood material	Remarks
&SURF ID = 'WOOD'	
FYI = 'WOOD'	
KS = 0.12	Refer to Table 13.3
DENSITY = 600	Refer to Table 13.3
C_P = 2.58	Refer to Table 13.3
DELTA = 0.034	Thickness of the material
BURN_AWAY = .TRUE.	To make object disappear once fuel is exhausted
TMPIGN = 373	Refer to Table 13.3
BACKING = 'INSULATED'	
HRRPUA = 3193	[SBF × cone test peak HRRPUA = 10.3 × 310 = 3193]
RAMP_Q = 'GAP1'/	Refer to Figure 13.6
&RAMP ID='GAP1',T= 0.0,F=0 /	Refer to Figure 13.6
&RAMP ID='GAP1',T= 68.0,F=0.85 /	Refer to Figure 136
&RAMP ID='GAP1',T= 120.0,F=0.53 /	Refer to Figure 13.6
&RAMP ID='GAP1',T= 180,F=0.48 /	Refer to Figure 13.6
&RAMP ID='GAP1',T= 240,F=0.4 /	Refer to Figure 13.6
&RAMP ID='GAP1',T= 300,F=0.64 /	Refer to Figure 13.6
&RAMP ID='GAP1',T= 383,F=1 /	Refer to Figure 13.6
&RAMP ID='GAP1',T= 420,F=0.54 /	Refer to Figure 13.6

Figure 13.5: Material definition for light goods vehicle simulation.

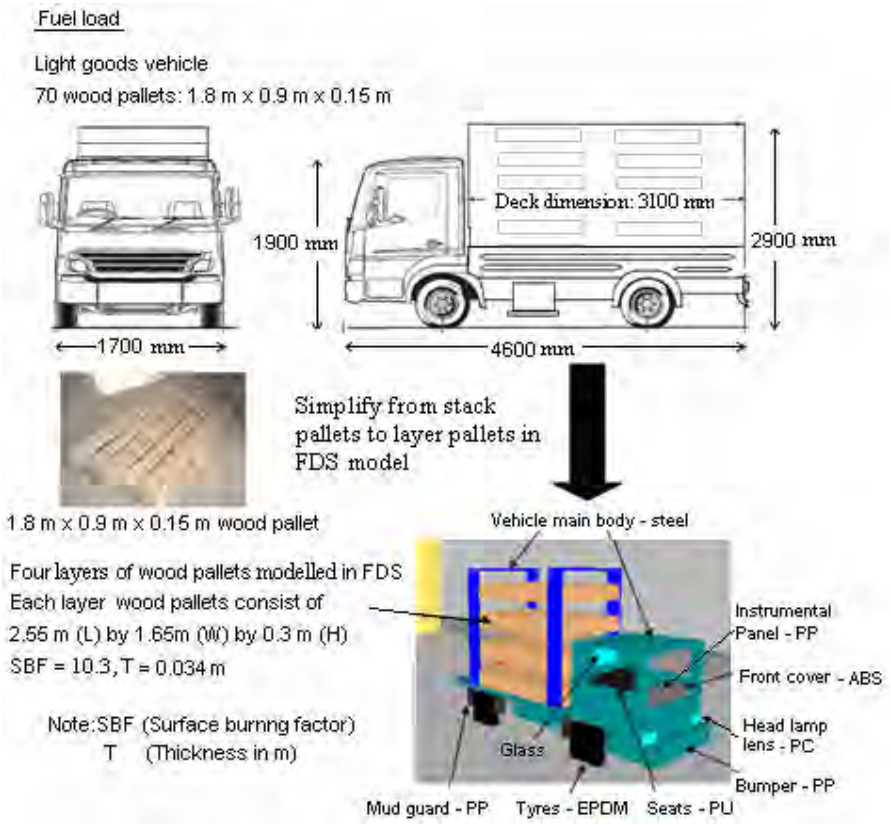

Figure 13.5: Material definition for light goods vehicle simulation.

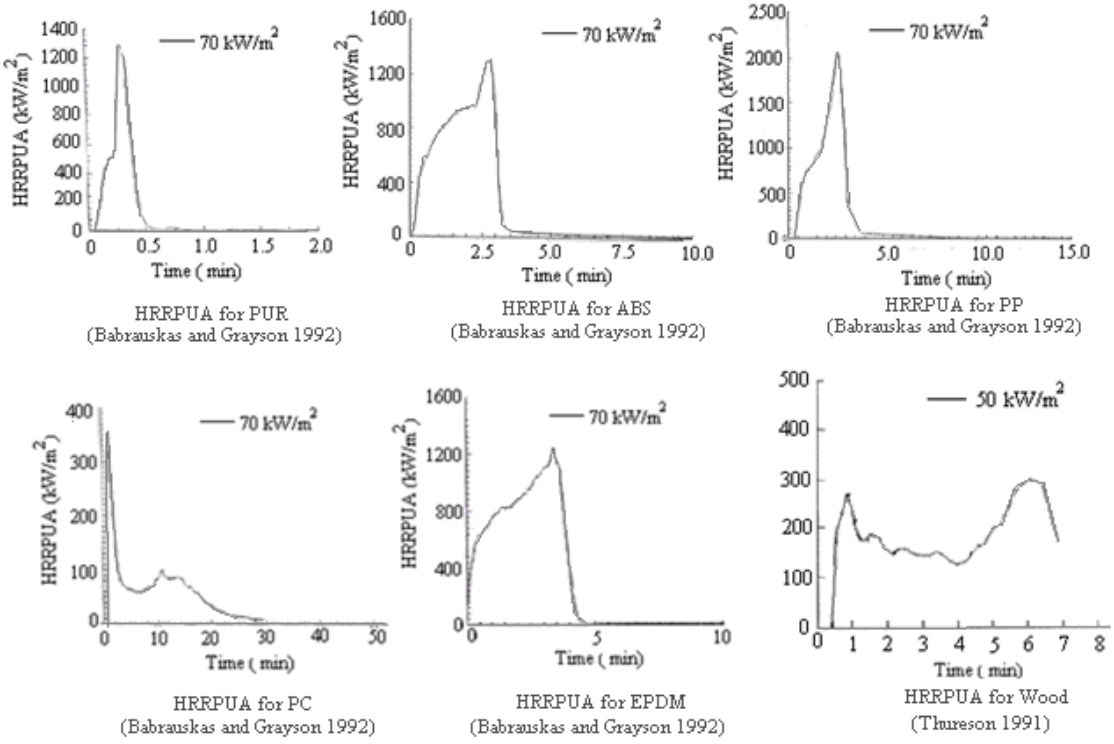

Figure 13.6: Cone test data at specified exposure heat fluxes used for FDS simulations.

A total of eight simulations, four in a two lane tunnel and four in a three lane tunnel with air velocity of 2, 3, 4 and 5 m/s with fire ignited in the pallets at the rear of the vehicle were simulated. The heat release rate curves using FDS4 are presented in Figures 13.7 and in Table 13.4. Results from the FDS simulations show that the peak heat release rate of LGV fire carrying wood pallets can vary from 68 MW to 101 MW. It has also been observed that the severity of the fire increases in terms of peak heat release rate with an increase tunnel air velocity. The re-radiation effects in the tunnel also affect the heat release rate where in general, a lower peak release rate was obtained in the wider tunnel as compared to the narrow tunnel. This difference is particularly distinct in scenarios with tunnels operating at the higher air flows (4 or 5 m/s).

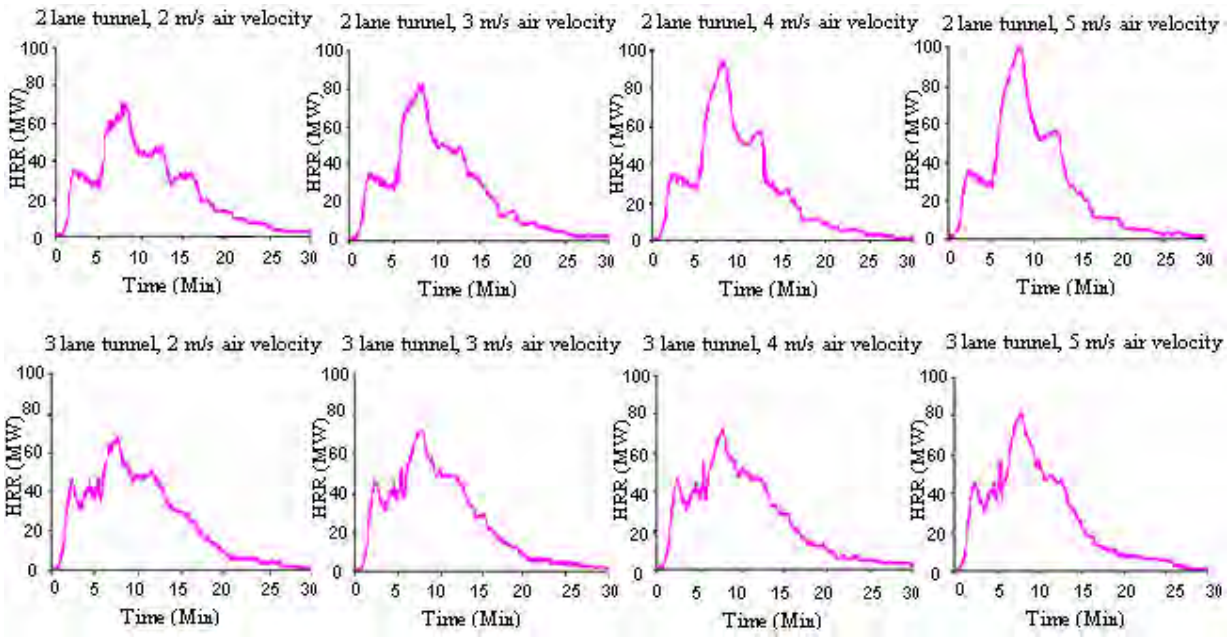

Figure 13.7: Heat release rate curves predicted using FDS4.

Scenario	Air velocity in tunnel			
	2 m/s	**3 m/s**	**4 m/s**	**5 m/s**
2 lane tunnel 9.3 m x 6 m (55.8 m^2)	71 MW	83 MW	94 MW	101 MW
3 lane tunnel 15 m x 6 m (90 m^2)	68 MW	72 MW	73 MW	82 MW

Table 13.4: FDS4 predicted peak HRR for rear ignition of LGV.

13.3.3 Comparison of results

The results from the FDS simulations consistently fall within the range of values obtained from the statistical approach (Figures 13.8 and 13.9). The results computed from both approaches show the same dependency on air velocity and tunnel dimensions. Although it is encouraging to see similar heat release rate trend estimates it is more difficult to determine which might be the more appropriate for design purposes. The statistical approach provides a very wide range of peak heat release values particularly as the tunnel air velocity increases. At the lower tunnel air velocities the FDS simulations are at the higher end of the statistical results but at higher tunnel air velocities the simulations are at the lower end. If the trends were extended to higher velocities then it is possible that the FDS results would no longer be within the range obtained from the statistical method but such velocities would be outside of those that would be used in practice for typical tunnel designs. A designer or regulator might find the range of peak HRRs suggested by the statistical method too wide for practical use. However the FDS results are only for a specific deterministic case and do not include any indication of the possible variability.

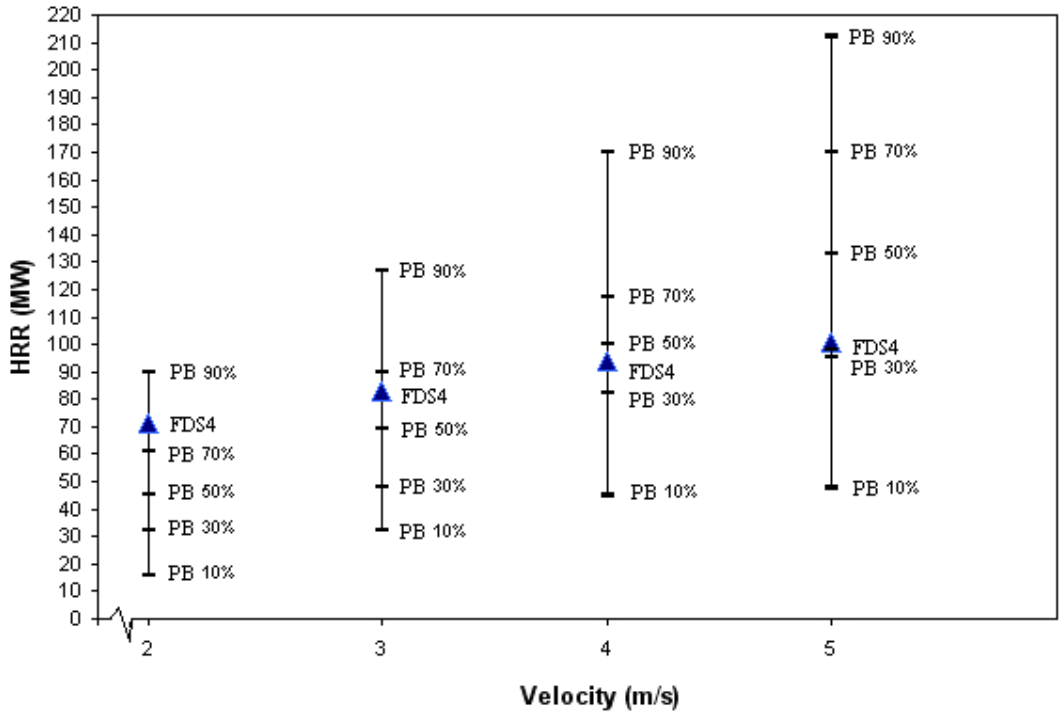

Figure 13.8: HRR estimate for LGV fire using Probabilistic Bayesian and FDS (2 lane tunnel).

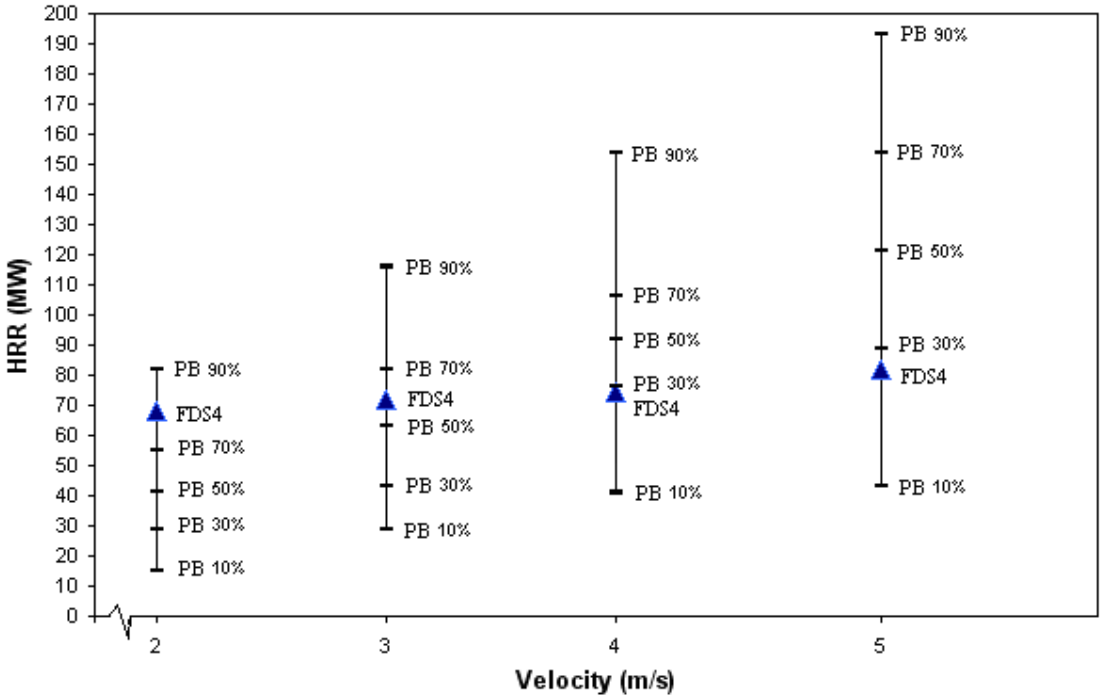

Figure 13.9: HRR estimate for LGV fire using Probabilistic Bayesian and FDS (3 lane tunnel).

13.4 Discussion

As already noted by Carvel et al (2004a), the statistical approach is empirical based on a small number of experimental fires involving cars, wooden cribs and pool fires. It is unfortunate that data for the burning of goods vehicles in tunnels or in the open air is so sparse. Only a single appropriate open air experiment has been identified for an LGV and no data for an HGV has been found in the literature. This lack of data makes it difficult to investigate the likely variability that might be obtained from similar experiments and the sensitivity of the FDS simulation method.

Variations in the results are subject to aleatoric and epistemic uncertainties that could affect the outcome of the heat release rate estimate. Aleatoric uncertainty includes the moisture content of the wood resulting in variability between the heat release rate data obtained in the LGV fire experiment and cone calorimetry data used as input to the FDS simulations. Clearly it is unlikely that the same HRR history would be obtained from repeated experiments even if everything could be arranged to be exactly the same.

However it would be expected that material properties would vary between experiments and conditions might be altered for the same fuel arrangement, for example, the ignition location could be different in the full-scale experiments. There is also the need to select appropriate small-scale test data that appropriately represent the materials used in the full-scale experiments.

At the full-scale, aleatoric uncertainty could be investigated by conducting further goods vehicle experiments. At small-scale, aleatoric uncertainty can be handled by collecting more cone calorimeter data. Material properties could be used to create probability distributions as input into numerical simulations, therefore allowing a range of heat release rate outputs similar to the probabilistic statistical approach. Unfortunately, the concept of using probability distribution input data for numerical computation, particularly CFD, to produce a probability distribution output would require extensive set of cone calorimetry data, material property data and huge computational resources which are beyond the limits of this work.

The effect of ignition location in the simulation of the LGV fire was performed with the fire ignited at the front of the vehicle to compare the effect of ignition location on fire development and compared to the similar simulation in which ignition was at the rear of the vehicle (Figure 13.7, two lane tunnel at 3 m/s). Examination of the two fire simulations (Figure 13.10) shows that in the presence of tunnel air flow, there is a delay in the fire development during the growth phase with fire ignited at the front of the vehicle as compared to fire ignited at the rear. This is because when the fire is ignited at the front of the vehicle, fire spread to the rear of the vehicle is delayed due to the effect of opposed tunnel wind flow. However the peak heat release rates from the two simulations are essentially the same and do not contribute appear to significantly contribute to aleatoric uncertainty.

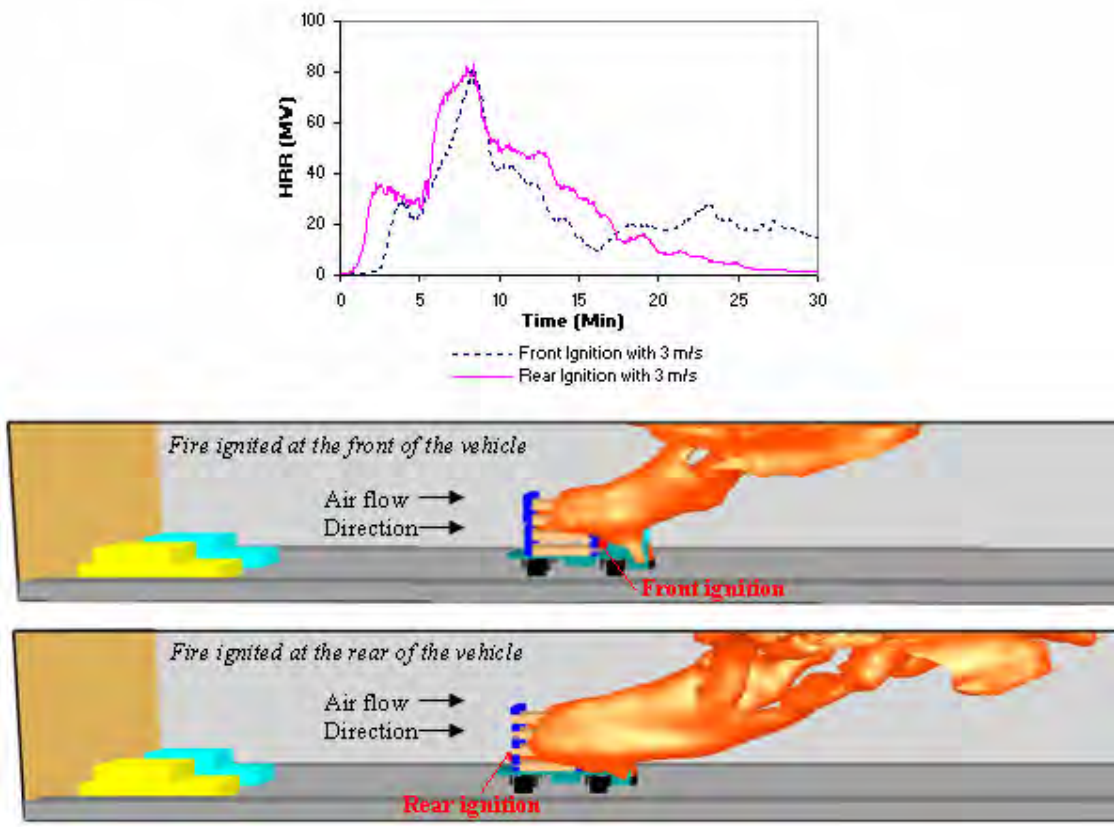

Figure 13.10: Heat release rate estimate for front and rear ignition using FDS4

Epistemic uncertainty includes the extent of modelling assumptions and any limitations in the numerical code used for the simulations; the modelling of wood pallets in layers to represent the burning behaviour and phenomena such as collapse of the wood pallets in the simulation which is not captured by FDS. Epistemic uncertainty can be reduced through further refinement of the simulation modelling approach and improving on the computational algorithms. It might be expected that further releases of FDS could address some of these uncertainties however if would require the simulation modelling approach used here for the pallets to be fully re-assessed.

Using the statistical method requires the selection of a probability value and this selection will need to reflect the level of risk that is acceptable to the stakeholders. Having peak heat release rates that could vary by a factor of four or more may make it difficult for the stakeholders to agree on what might be an appropriate design fire. Carvel et al (2004a) do not provide any recommendation for what might be an appropriate choice for the

probability and it is not the purpose of this chapter to suggest what should be used. From tunnel ventilation design perspective, comparing the heat release rate estimated using statistical curves at 10% and 90% results in an increase of 25-50% in the airflow needed to maintain the critical velocity with a corresponding increase in cost. Clearly selecting the higher probability values gives a more conservative result compared with the FDS simulations. However without having experimental data for the tunnel scenarios considered it is not possible to determine which method gives a more realistic result for the peak heat release rate.

13.5 Conclusion

This chapter provides a description of the use of empirical statistical approach and a numerical approach using FDS4 to provide an estimate on the heat release rate of a LGV in a road tunnel. From the above illustration, it is clear that the ventilation condition in the tunnel is an important parameter to consider when analysing fire growth behaviour. The magnitudes of the peak heat release intensify as tunnel air velocity increases. The selection of most design fires for road tunnel applications are generally based on the traffic flow expected for a particular tunnel and selection is made based on recommendations from road tunnel standards or guidelines to identify vehicle heat release rate. However, regardless of the means to establish heat release rate, principal parameters such as fuel load, ventilation condition and tunnel geometry should be assessed when evaluating design fires for road tunnel design.

Carvel et al (2004a) are of the opinion that their statistical approach will hold for HGVs but also recognise that more experimental data is needed to test the relationship. It would appear from this analysis that the wide range and substantially higher peak HRR obtained from the statistical method, particularly at the greater ventilation velocities, are not replicated in the FDS simulations. Further full-scale experimental data of burning goods vehicles, further evaluation of the statistical method and additional FDS simulations may provide a better match between appraches.

As in any methodology, there are advantages and disadvantages between the two approaches. The statistical approach using the empirical equation developed by Carvel et al. provides a fast means of establishing the heat release rate while a substantial amount of simulation run time and computational resources are required to use the numerical approach. An initial assessment of potential design fires is important in tunnel fire design because it is often common to have various design velocities and tunnel geometries along a tunnel alignment. In contrast, the numerical approach provides details of the fire growth and does not rely on having heat release rate data from an experiment in an open environment. However relevant material properties are required and the modelling still relies on certain assumptions being appropriate.

In conclusion, the choice of using the statistical approach or the CFD approach depends on the objective, the information available, the time available, the degree of detail required and the availability of computational resources to analyse the problem. Designers should be aware that these methods may result in quite different results depending on the scenario and the selection of parameters.

Chapter 14:
NUMERICAL SIMULATION OF ROAD TUNNEL FIRES USING PARALLEL PROCESSING

With longer and wider road tunnel projects being implemented around the world the demand to solve larger computational fluid dynamics simulation problems arise from their complexity. The need to understand the fire behaviour by considering the dynamics of tunnel air movement often strains the ability of single processor computer systems to handle such applications. Parallel processing becomes an attractive option to overcome this limitation. This chapter examines the use of parallel processing techniques in Fire Dynamics Simulator (FDS4.07) simulations. Aspects concerning the computed heat release rate using different mesh boundary arrangements at the fire location and within the flame extension were investigated. Improvements in the efficiency of computation run times and an example of parallel processing for tunnel fire analysis work are presented in this chapter.

14.1 Parallel processing for CFD simulations

Using computational fluid dynamics (CFD) techniques to analyse fire and smoke behaviour in tunnels has become increasingly popular over the past few years (Rhodes 2005). Tunnel fire simulations allow designers to assess the conditions in the tunnel by extracting information such as air velocity, air temperature, visibility, radiation heat flux and carbon monoxide concentration. Simulations can be used to verify tunnel ventilation performance by examining the system design velocity to determine whether sufficient airflow is provided to achieve the critical velocity to prevent smoke back-layering. Evacuation strategies in terms of number of cross passage doors and escape staircase provisions can be assessed. Evacuation analysis can be used to obtain movement times and evacuation paths can be assessed in conjunction with the simulated tunnel conditions.

The use of CFD techniques for research analysis or design applications often requires a substantial amount of computational power and simulation run time. Although the performance capabilities of a typical office personal computer or desktop workstation have improved significantly over the past decades, there is a continual demand for higher computation capability to compute complex CFD problems in a reasonable time period. Time is often a limitation when performing such a task using a desktop workstation. The application of parallel processing to provide high performance computational CFD work is emerging as an alternative to overcome this limitation (Paprzycki and Stpiczynski 2005).

The parallel computing concept utilises several processors to work on a single simulation task by dividing the problem into “multiple meshes” (multiple computational domains) (McGrattan and Forney 2005) and these meshes are simultaneously computed by several processors so that a shorter overall runtime can be achieved. Another advantage of parallel processing is its ability to perform simulation work involving large domains without the need to compromise on the use of fine grids to solve highly calculation intensive problems (Barney 2007). With sufficient computational resources, the ability to simulate large complex CFD problems in a reasonable time frame is feasible.

Typically, CFD simulations involve a huge number of calculations to obtain a numerical solution. There are several parallel computing architectures available to achieve shorter computation run times. These include the use of computer clusters such as the Beowulf cluster where a group of personal computers are connected to each other on a private system network with open source software infrastructure (Beowulf 2007) or using a high end computation platform such as a Supercomputer.

An example of parallel processing involving Fire Dynamics Simulator Version 4.0.7 (FDS4) to investigate fire in the World Trade Center Towers was conducted by McGrattan et al. (2005). The work in this chapter presents the findings on the use of parallel processing techniques within FDS4 to predict the heat release rate (HRR) of a vehicle fire in a tunnel. The objective is to investigate the limitations of using parallel processing techniques for FDS4 simulations and to examine the amount of computational time that might be saved as compared to using a single processor. All of the simulations performed in this chapter were carried out using the University of Canterbury Supercomputer (UCSC).

14.2 UCSC Computing Facility

The UCSC facility is used by researchers who require advanced computing capability (Figure 14.1). The UCSC setup allows users to solve large complex computational problems which are not possible using a conventional workstation. In view of the number of CPUs available, it provides concurrency where users can perform multiple runs at the same time which further reduces simulation run time on tasks that require sensitivity analysis.

Figure 14.1: The UCSC room with p5-575 case opened to show fans, memory and processors.

The building block for the UCSC system is the IBM system p5^{TM} 575 node which utilizes the IBM chip technology. Each of the ten symmetric multiprocessing (SMP) nodes consists of 8 dual core power5 processors and 32 GB or 64 GB of memory. Each p5-575 server can support up to 256 GB of DDR2 memory and provides a sustained memory bandwidth of 105.5 GB/sec (McMurtrie 2006). The ten node P5 system with 160 processors provides a theoretical peak performance of over one teraflop per second or 10^{12} floating point instructions (UCSC 2007). Software packages such as the Parallel Environment for support of the Messaging Passing Interface (MPI) and batch job scheduling system (Load leveller) are installed to allow users to run more jobs in less time by matching the job processing needs based on the available resources in the system. An example showing the load leveller status and schematic of the operation set-up for the UCSC is shown in Figure 14.2.

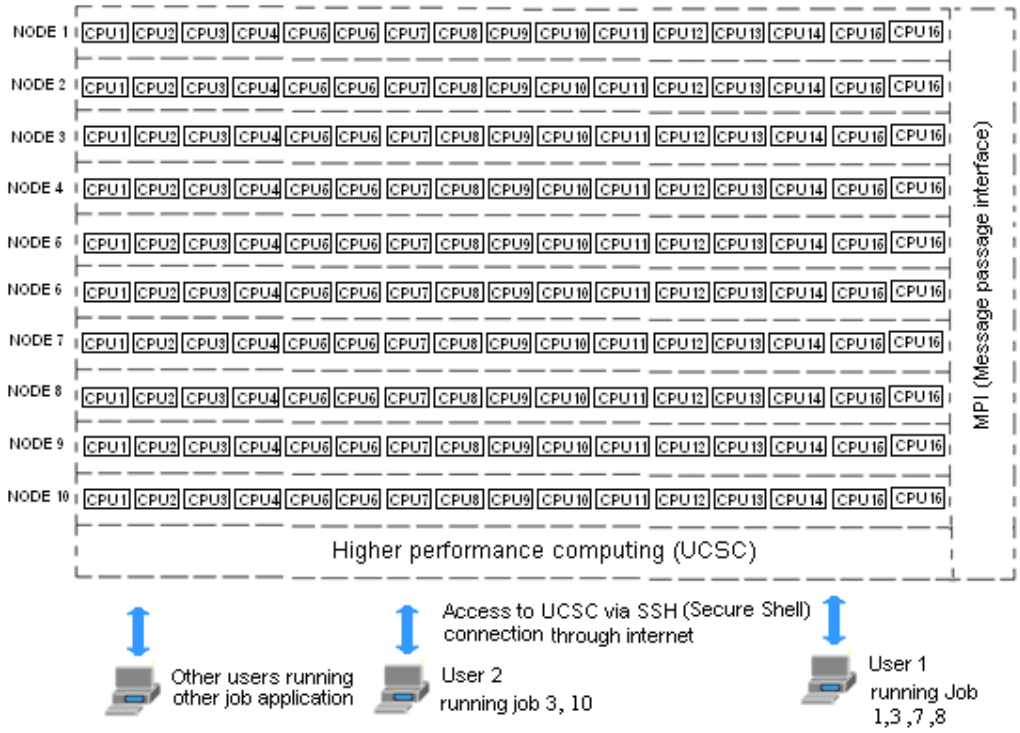

(a)

LoadLeveler job queue

Job Task	Users	Number of mesh	Running on	Job State
Job 1	User 1	2	Node 1 – CPU 1 to CPU 2	Running
Job 2	User 2	4	Node 1 – CPU 3 to CPU 6	Running
Job 3	User 1	5	Node 1 – CPU 7 to CPU 11	Running
Job 4	User 3	5	Node 1 – CPU 12 to CPU 16	Running
Job 5	User 3	8	Node 2 – CPU 1 to CPU 8	Running
Job 6	User 4	3	Node 2 – CPU 9 to CPU 11	Running
Job 7	User 1	1	Node 2 – CPU 12	Running
Job 8	User 1	3	Node 2 – CPU 13 to CPU 15	Running
Job 9	User 3	6	Node 3 – CPU 1 to CPU 6	Running
Job 10	User 2	20	Node 4 – CPU 1 to CPU 16 Node 5 – CPU 1 to CPU 4	Running
Job 11	User 4	3	Node 5 – CPU 5 to CPU 7	Running
Job 12	User 5	7	Node 5 – CPU 8 to CPU 14	Running
Job 13	User 6	2	Node 5 – CPU 15 to CPU 16	Running
Job 14	User 6	5	Node 6 – CPU 1 to CPU 5	Running
Job 15	User 7	7	Node 6 – CPU 6 to CPU 12	Running
Job 16	User 8	30	-	Waiting

Status of UCSC job queue

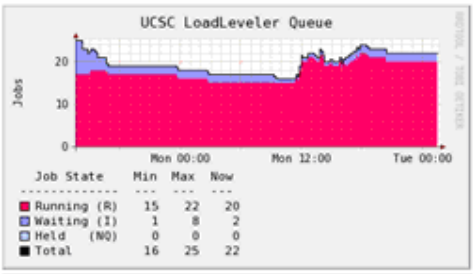

Overall CPU utilization

(b)

Figure 14.2: The UCSC system; (a) schematic setup;(b) example job tasks issued to UCSC

The 64 bit FDS4 an open source code is also available in the system to allow users to perform fire related CFD simulation work. Wood pallets were chosen for the initial simulation to verify the computed results using the 64 bit and 32 bit FDS4 version because

wood pallets were used as the main fuel source for subsequent simulation analysis. Initial verification tests found that the computed simulation result for heat release rate using the UCSC 32 bit compiled version, UCSC 64 bit compiled version and PC 32 bit compiled version produced similar simulation results (Figure 14.3) and subsequent simulations were carried out using the UCSC 64 bit compiled version of the FDS4.0.7 code.

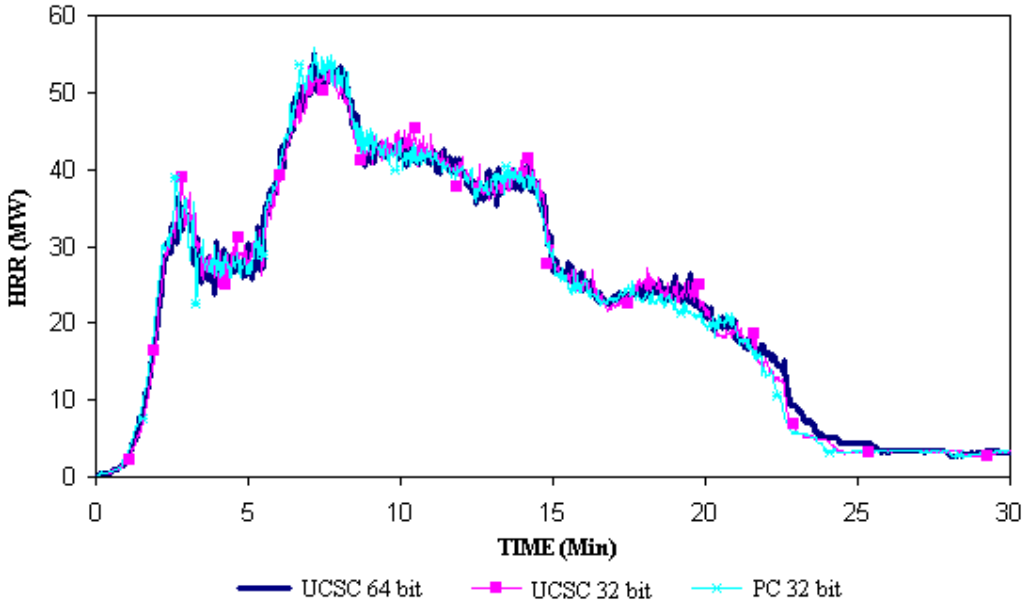

Figure 14.3: FDS simulation results using 32bit and 64bit compiled version

14.3 Using parallel processing techniques with FDS to estimate HRR

In this work, a light goods vehicle (LGV) carrying 80% wood and 20% plastic was simulated in a two lane tunnel. Work in chapter 8 has identified the type of vehicle in a road tunnel that could result in a higher fire risk. Details of the material thermal properties, information on the cone calorimeter tests data and the modelling approach to estimate the HRR are discussed in chapters 10 and 11. An air velocity of 2.9 m/s was provided at one end of the tunnel and the simulation time is set to 25 min (Figure 14.4a). Material specifications from a truck manufacturer (Mitsubishi 2004) and typical pallets were used to identify the type of materials for the construction of the LGV and pallets for the simulation (Figure 14.4b). The heat release rate was determined using the heat release rate per unit area data from cone calorimeter tests and input into the FDS4; the heat release rate

per unit area was adjusted in the simulation using a surface burning factor to ensure the fuel load area model in the simulation is equivalent to the fuel load area used for a LGV fire carrying wood and plastic pallets.

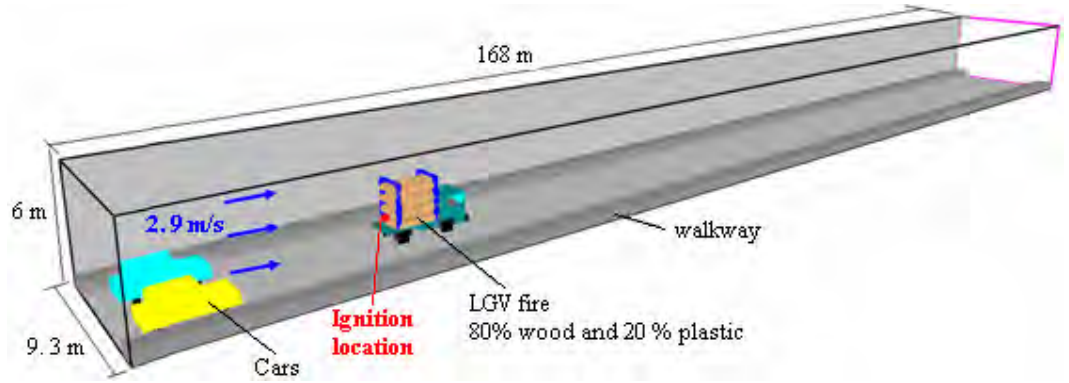

(a)

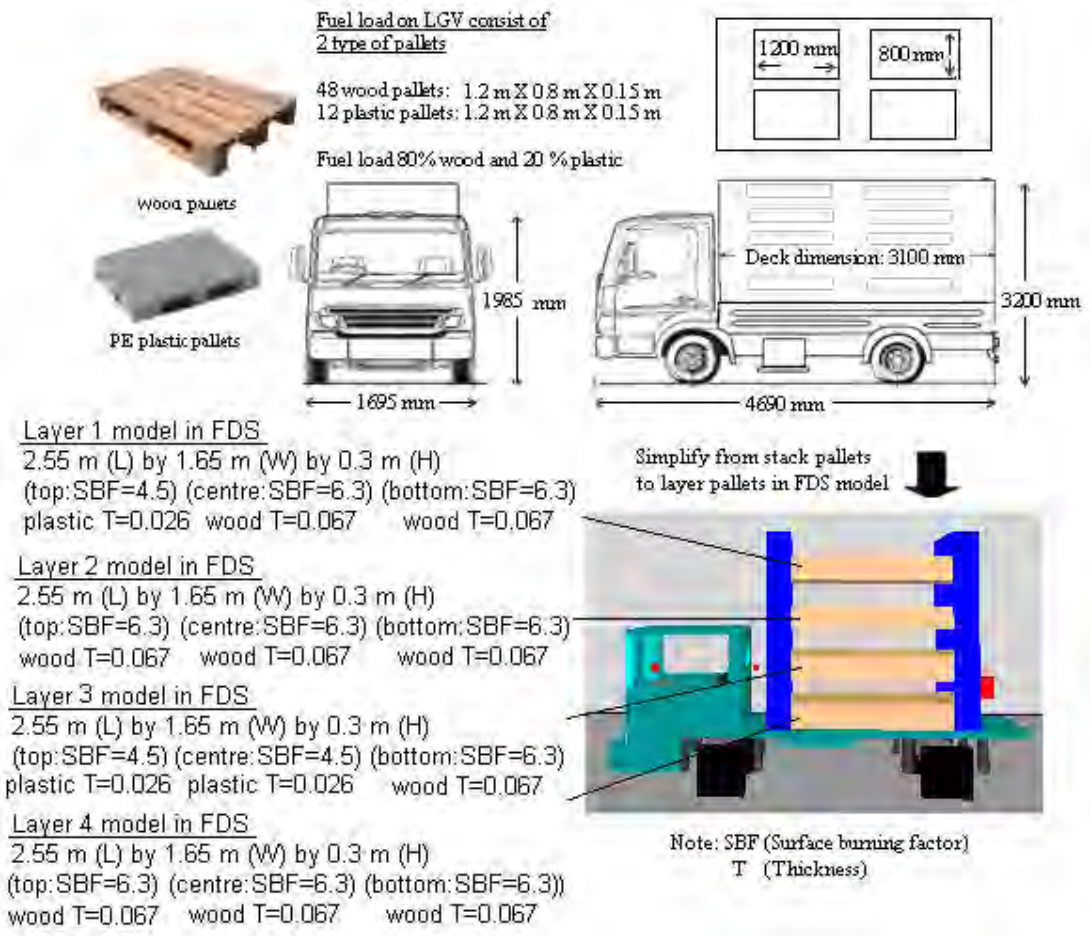

(b)

Figure 14.4: (a) FDS model setup; (b) Material define for light goods vehicle simulation

To run FDS4 using the parallel processing approach, the computation domain needed to be broken up into multiple meshes so that each processor received one mesh to work on (McGrattan and Forney 2005). Command line instructions "PDIM" and "Grid" specifying the size and grid characteristics of each domain were required in the FDS input file, the values for "PDIM" and "Grid" dependent on the number of domains specified in the simulation. Meshes should be entered from the finest to the coarsest if a different grid size is used amongst meshes. On the time line command instruction "SYNCHRONIZE=.TRUE." was set to ensure that time steps in all meshes were the same.

An example of multiple mesh command used in a 3 mesh tunnel model with dimensions of 9.3m width, 168m length and 6m high is shown below:

****An example of multiple mesh command for parallel computing - FDS input file *****

Mesh 1
&GRID IBAR=31,JBAR=190,KBAR=20/ 0.3 grids
&PDIM XBAR0=0,XBAR=9.3,YBAR0=0,YBAR=57,ZBAR=6/
Mesh 2
&GRID IBAR=31,JBAR=190,KBAR=20/ 0.3 grids
&PDIM XBAR0=0,XBAR=9.3,YBAR0=57,YBAR=114,ZBAR=6/
Mesh 3
&GRID IBAR=31,JBAR=180,KBAR=20/ 0.3 grids
&PDIM XBAR0=0,XBAR=9.3,YBAR0=114,YBAR=168,ZBAR=6/

SIMULATION TIME
&TIME TWFIN=1500, SYNCHRONIZE=.TRUE./

****

14.4 Simulation schedule

A total of 7 simulations were performed to investigate computational run time and to verify computational results obtained using a single mesh over multiple meshes. These simulations were also used to analyse the effect of using multiple-mesh arrangements in FDS4 to obtain heat release rate. Each mesh is assigned to an individual processor. The work included performing simulations with:

i) Tunnel model using a single mesh with homogeneous grid.

ii) Tunnel model using multiple meshes with homogeneous grid.

iii) Tunnel model using multiple meshes with coarse grid in regions where temporal and spatial gradients of key quantities are small.

Table 14.1 summaries the simulations carried out. All simulations performed in this work had an overall domain size of 9.3 m (width), 168 m (length) and 6 m (height) with an air velocity of 2.9 m/s blowing at one end of the tunnel. All simulations were performed using the same fuel package (LGV carrying pallets) and with the same external boundary conditions. The first, second and third simulations were performed using a single mesh, two meshes and three meshes (MP1, MP2 and MP3) with all the flame extension captured within a mesh. Simulations involved placing different mesh boundaries at critical positions such as at the fire location (MP5) and through the flame extension (MP4) were performed to investigate the effect of mesh boundaries on the computational results. The implication on heat release rate in tunnel when using coarse grid at the downstream of the fire was carried in MP6. The last simulation (MP7) was to apply computer scaling to explore if more processors would reduce computational run time in FDS4.

No	Number of meshes / CPUs	Mesh 1		Mesh 2		Mesh 3	
		Grid size (x,y,z)	Domain size (x,y,z)	Grid size (x,y,z)	Domain size (x,y,z)	Grid size (x,y,z)	Domain size (x,y,z)
MP1	1	0.3m, 0.3m, 0.3m	0 - 9.3m, 0 - 168m, 0 - 6m	-	-	-	-
	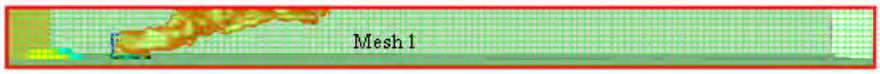						
MP2	2	0.3m, 0.3m, 0.3m	0 - 9.3m, 0 - 84m, 0 - 6m	0.3m, 0.3m, 0.3m	0 - 9.3m, 84 - 168m, 0 - 6m	-	-
							
MP3	3	0.3m, 0.3m, 0.3m	0 - 9.3m, 0 - 60m, 0 - 6m	0.3m, 0.3m, 0.3m	0 - 9.3m, 60 - 120m, 0 - 6m	0.3m, 0.3m, 0.3m	0 - 9.3m, 120 - 168m, 0 - 6m
							
MP4	3	0.3m, 0.3m, 0.3m	0 - 9.3m, 0 - 21m, 0 - 6m	0.3m, 0.3m, 0.3m	0 - 9.3m, 21 - 93m, 0 - 6m	0.3m, 0.3m, 0.3m	0 - 9.3m, 93 - 168m, 0 - 6m
	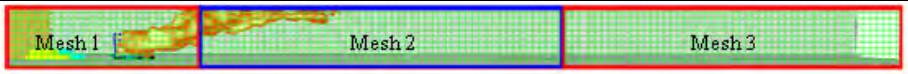						
MP5	3	0.3m, 0.3m, 0.3m	0 - 9.3m, 0 - 18m, 0 - 6m	0.3m, 0.3m, 0.3m	0 - 9.3m, 18 - 93m, 0 - 6m	0.3m, 0.3m, 0.3m	0 - 9.3m, 93 - 168m, 0 - 6m
	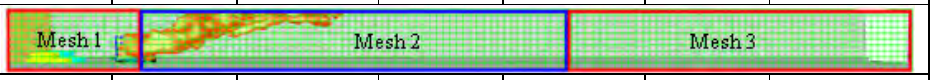						
MP6	2	0.3m, 0.3m, 0.3m	0 - 9.3m, 0 - 84m, 0 - 6m	0.3m, 0.6m, 0.3m	0 - 9.3m, 84 - 168m, 0 - 6m	-	-
							

No	Number of meshes / CPUs	Mesh 1		Mesh 2 to Mesh 9 (each mesh)	
		Grid size (x,y,z)	Domain size (x,y,z)	Grid size (x,y,z)	Domain size (x,y,z)
MP7	9	0.3m, 0.3m, 0.3m	0 - 9.3m, 0 - 84m, 0 - 6m	0.3m, 0.3m, 0.3m	9.3m, 10.5m, 6m
	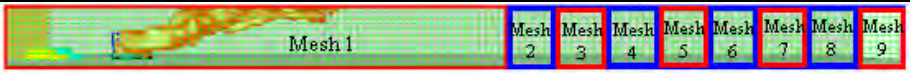				

Table 14.1: Multiple meshes simulation schedule

14.5 SIMULATION RESULTS

14.5.1 Mesh boundary locations

The simulation results shown in Figure 14.5 indicate no significant difference in the HRR curve when flame extension is captured within a single mesh (MP1 and MP3). However, placing mesh boundaries at critical locations such as at the fire source or cutting through the flame extension gave different computational results. This is evident from the simulations performed with the domain configuration setups in MP4 and MP5. From Figure 14.5, it is observed that a higher heat release rate in the growth phase of the fire development has been computed with mesh boundaries placed near the fire source when compared to simulations with all flame extension captured within a mesh. As highlighted by McGrattan and Forney (2005), one reason for this is due to the exchange of information across mesh boundaries not being as accurate as cell to cell exchange within a mesh. The above example demonstrates that it is important to capture all the flame extension within a mesh when using parallel processing techniques in FDS4.

.

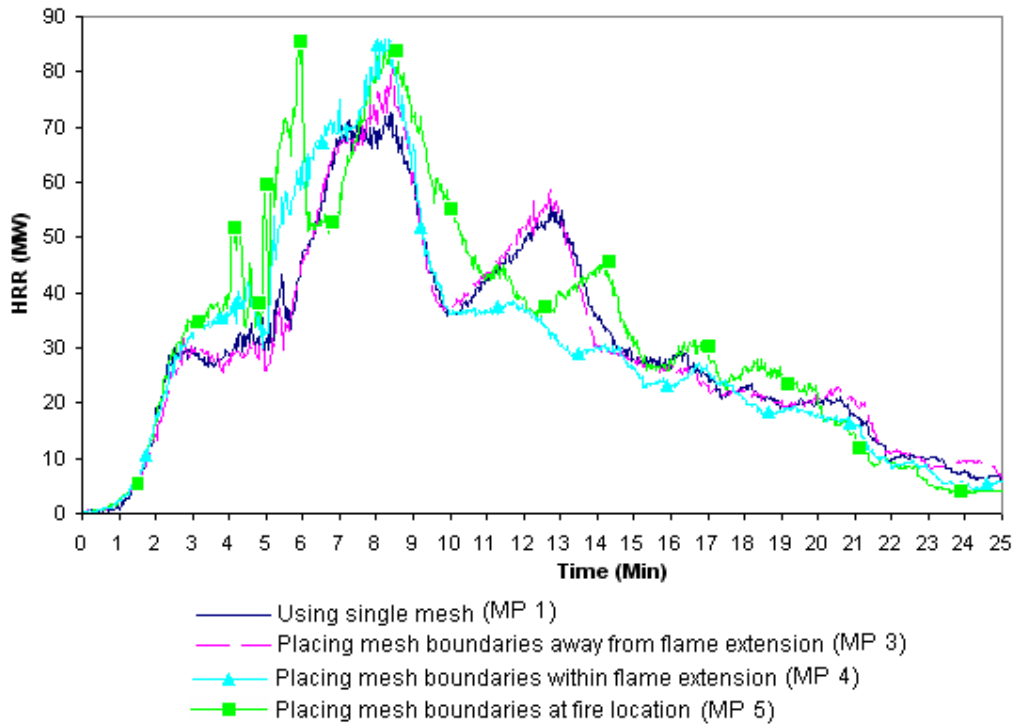

Figure 14.5: Effect of putting mesh boundaries at fire location

14.5.2 Multiple processors

The second aspect of this chapter is to examine the claim on computer scaling in reducing simulation run time. The following series of simulations compared simulation results and computational run times of the LGV fire in a two lane tunnel performed using a single mesh with 1 CPU (MP1), 2 meshes with 2 CPU (MP2), 3 meshes with 3 CPU (MP3) and 9 meshes with 9 CPU (MP7). To ensure the overall fire behaviour computed for the multiple meshes was similar to the single mesh, the simulations were performed with all the flame extension captured within a single mesh as shown in MP1, MP2, MP3 and MP7. Generally there is a reduction in the computational time as more CPU resources are allocated for a job. This is evident from the computational time shown in Figure 14.6 for MP 1, MP 2 and MP 3. However, it is observed in MP7 that this simulation does not produce a shorter computation run time as compared to the previous three simulations. The processors computing meshes 2 to 9 were idling most of the time in view of the smaller domain size assigned for the computation as compared to mesh 1. The larger domain size for mesh 1 was necessary to ensure that all the flame extension was captured to yield an appropriate HRR prediction. The processors computing the other meshes with smaller domain size were not ready to be updated by the computational information from mesh 1 which required a longer run time. The computation time from MP7 was only marginally less than that obtained from MP1 and significantly greater than the other simulations.

.

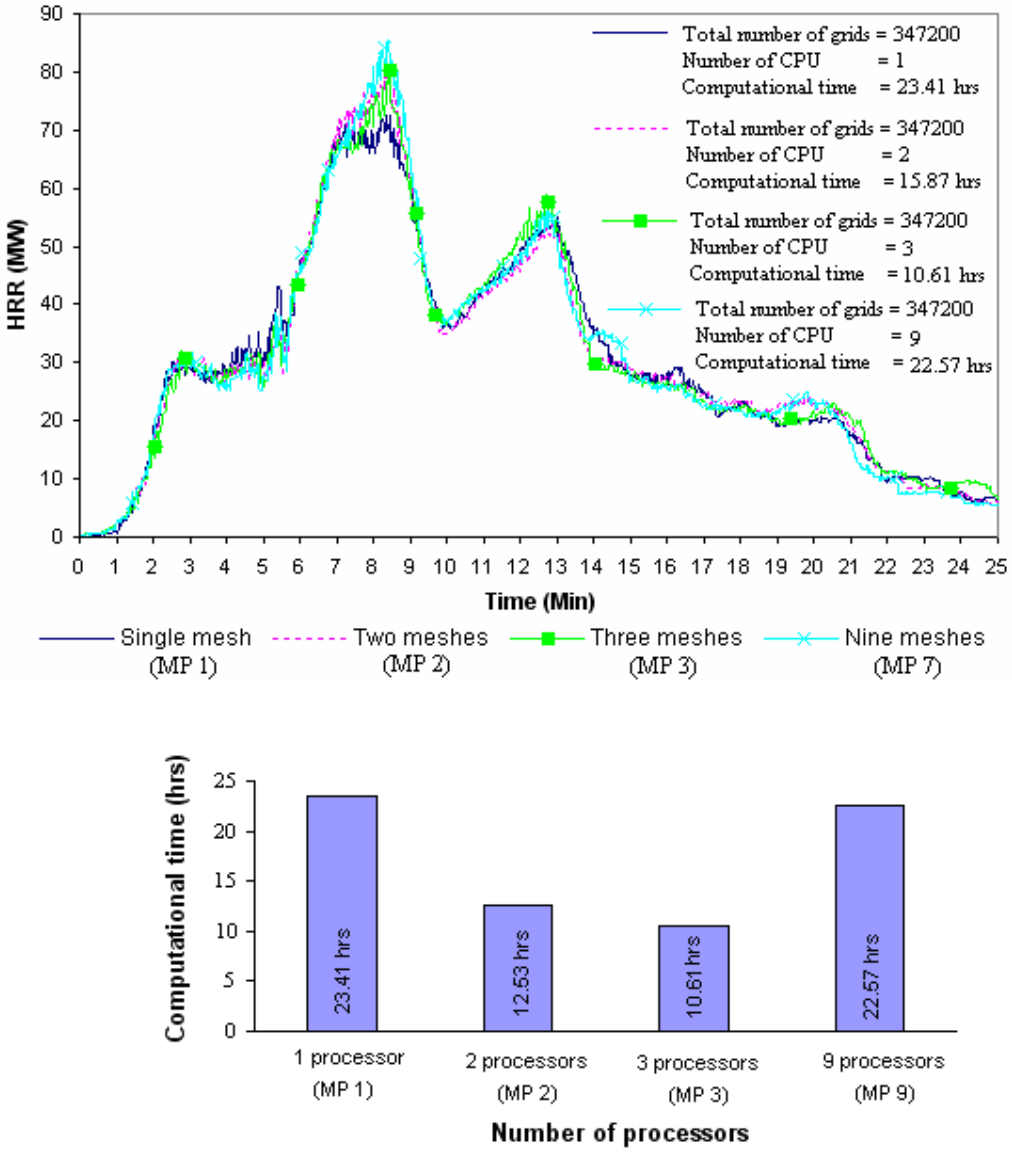

Figure 14.6: Simulation results using meshes

The benefits of using multiple processors can be further illustrated in a tunnel design application (Figure 14.7). The simulated tunnel is a 660 m long by 30.6m wide and 6 m high and using a grid size of 0.3 m, approximately 4.5 millions grid cells were required for this simulation. Time duration of the simulation was set to 30 minutes.

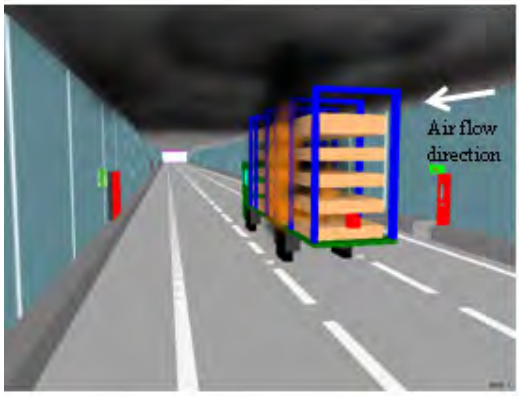

(a) - Using FDS to verify tunnel ventilation performance

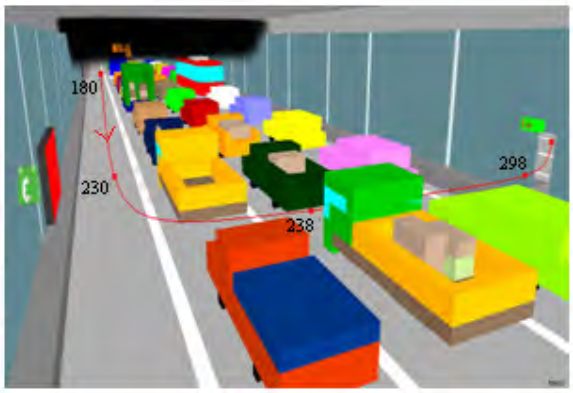

(b) - Evacuation path locus in FDS

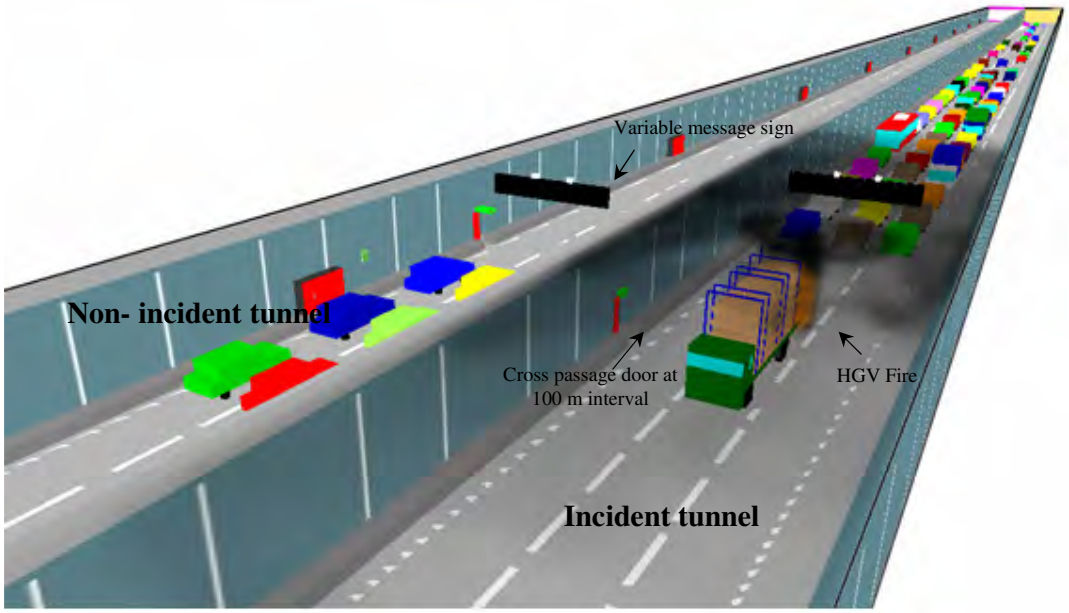

(c) - Using FDS to assess tenable condition in tunnel ventilation performance

Figure 14.7: Tunnel design application

Considering the domain size, grid size and time duration of the simulation involved, performing such job task using a single-computer system would be computationally taxing and inefficient as substantially long computational run time would be required. A scaling exercise using the UCSC was performing using different quantities of CPUs to compute this model, all the simulations performed were based on the same input parameters. Results in Figure 14.8 show that the computational time reduces significantly with increase in CPUs utilisation.

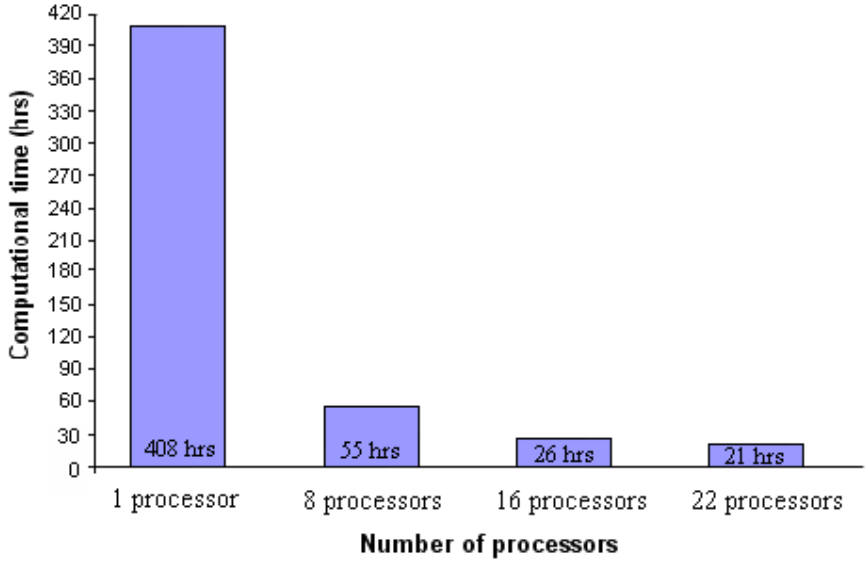

Figure 14.8: Computational time using different number of CPUs

14.5.3 Grid specification

The third part of the study was to use a coarse grid in regions where temporal and spatial gradients are small to investigate if this would affect the global heat release rate computed using FDS4. In most numerical solutions, the use of finer grids will generally provide a better computed solution however this would also mean that the grid size will decrease resulting in a longer computational time. Here a coarser computational grid at the downstream end of a tunnel fire was explored to see if there was any significant difference to the HRR value and the computational time as compared to a simulation where finer grid cells were used.

Simulation MP2 consisting of 2 domains with mesh 2 grid with y = 0.3 m and MP6 with similar setup except with y = 0.6 m for mesh 2. The computations showed that grid variation had small effect on the HRR results and the computational time has improved by 26% when the coarser grid was used at the downstream end of the tunnel fire (Figure 14.9).

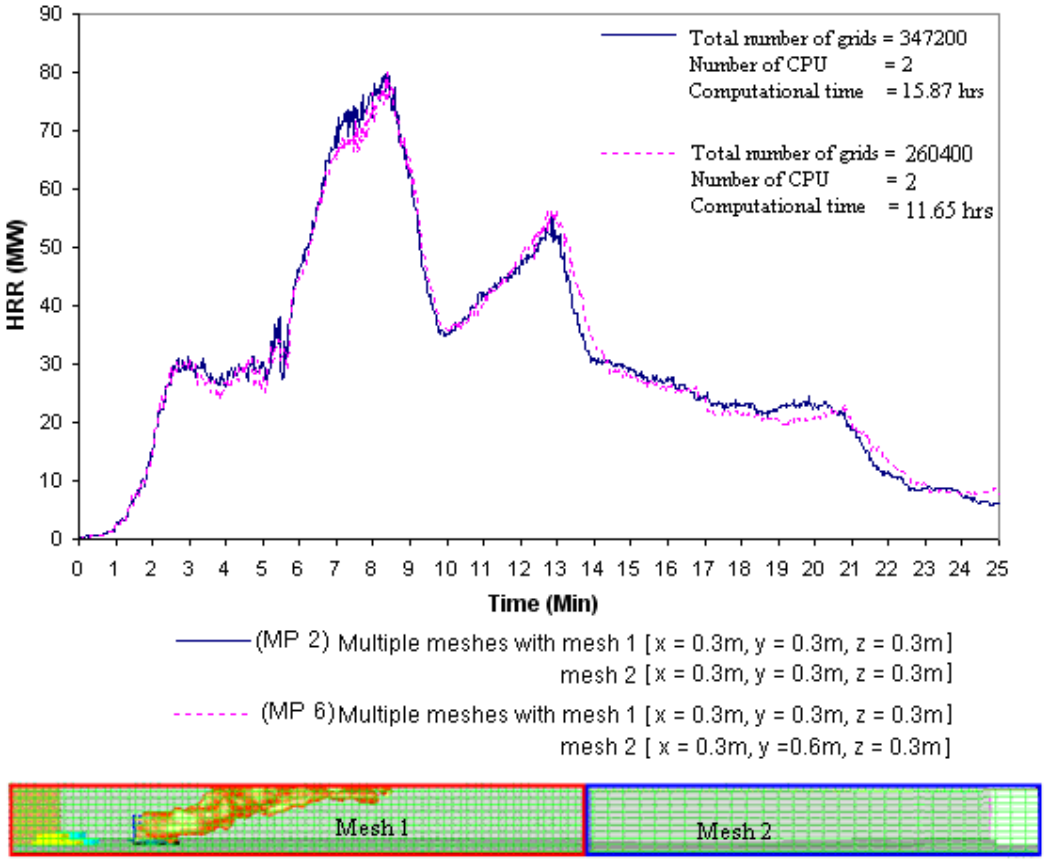

Figure 14.9: Using coarser grid at downstream of fire

14.6 Discussion

There is always a demand to solve larger and more complex tunnel fire problem through the use of CFD modelling. With the limitation in computation power on single computer system, using parallel processing for large simulation tasks has becomes an attractive option. The use of parallel processing applications will have an influence on fire engineering in terms of how fire engineers model and analyse their work. The arrangements of mesh partitions and the number of meshes used are dependent on the time frame needed for the analysis and the computational resources available. However, the work discussed in this chapter shows it is important to consider a number of factors when performing FDS4 simulations using parallel processing techniques. These factors include:

- Poor allocation of boundary meshes particularly at the fire location is not ideally suited when using parallel processing techniques in FDS4 simulations.

- The importance of identifying the minimum length required to capture all the flame extension and if at all possible to keep the fire source and flame extension within a single mesh.

- Given the effects of placing mesh boundaries at the fire location or through any flame extension, it is recommended that a simulation run on a single domain be performed before splitting the domains for subsequent simulation runs involving parallel processing.

Generally more processors speed up the computational time. However, the number of processors used for the parallel computation is limited by the mesh that computes the fire and flame extension. When performing simulations using parallel processing techniques within FDS4 it is preferable to arrange each mesh to have a similar quantity of grid cells in order to achieve optimal computational time. As demonstrated in MP7, the additional processors used for the simulation do not further reduce the computational time because most of the processors computing meshes are limited by the processor computing mesh 1 which has a larger domain size resulting in longer run time for the overall simulation. Clearly there are almost limitless ways in which a domain can be divided into meshes as the number of available processors increases thus users need to consider configurations that give more efficient computational times by balancing the computational domain into semi-uniform meshes. Using a coarser grid size at the downstream of the tunnel fire does not seem to affect the HRR value significantly and there is an advantage of having a shorter computational time.

14.7 Conclusion

This work provides an introduction on the use of parallel processing techniques in FDS4 simulation, particularly for vehicle fires in a tunnel. It discusses aspects concerning the verification of the parallel processing simulation results and computational run time. Although running FDS4 using multiple processors for fire analysis is more difficult compared to using a single computer processor due to the need for making connections between processors, the concept of parallel processing is promising, particularly for complex designs involving large computation domains where demands of the project require shorter computation time for fire analysis.

Chapter 15:
TUNNEL SIMULATION USING FDS 5.0.3

This chapter provides a brief introduction on the use of FDS 5.0.3 for tunnel simulation. The Runehamar tunnel fire experiment is used as an illustration for discussion purposes. This chapter will also be highlighting the available functions that are different in FDS 5 from previous FDS versions and future work required to improve the modelling approach used in this thesis.

15.1 Background

The Fire Dynamics Simulator (FDS version 1) public domain version has been around since February 2000. It has been widely used for smoke handling system design, sprinkler activation studies, residential and industrial fire reconstruction etc (McGrattan et al 2007). As part of a continual effort to improve the computation code, there have been several revision updates from NIST since the release of its first version. In March 2007, NIST launch the FDS 5 Beta version inviting FDS users to test the trial version. By October 2007, FDS 5.0.0 was officially available in the public domain. To-date, there have been a few sub-revision updates made by NIST to FDS 5.

This project commenced at the time where the FDS 4.07 was the latest FDS version available in the public domain. A substantial number of simulations had been performed since the commencement of this project. Although the research work in this project was conducted using FDS 4.07, the launch of FDS 5 has raised the subject if performing tunnel simulations using FDS 5. Considering the number of simulations involved, it is not the intent of this project to re-simulate all the scenarios previously studied using FDS 5. To address this concern, a preliminary simulation for the reconstruction of the Runehamar tunnel fire experiment was performed using similar modelling approach as discussed in chapter 10 with FDS 5.0.3. This is part of the simulation calibration process and laid down the foundation for future research work. The work was performed using FDS 5.0.3 because this was the latest version available at the time of this analysis work. The work in this chapter includes grid and domain analysis, using various fuel arrangement layouts and simplified cone curves to examine the sensitivity of the estimated heat release rate with the last section of this chapter discussing possible future work that can be carried out to enhance the modelling approach for tunnel simulation work.

15.2 FDS 5 differs from previous versions

According to McGrattan et al (2007), FDS 5 is different from past versions in its treatment of solid boundaries and gas phase combustion. The changes made in FDS 5 include multi-step combustion where previous FDS versions assumed only one gas phase reaction. The current version is able to model solid boundaries as multiple layers whereas previous versions do not have such function. There is a slight change in command line format, material and reaction parameters must also be specified in the input file. The method used to describe a device such as sprinkler, detector has changed. A pressure zones function is introduced to allow for the calculation of leakage and fan curves. The numerical mesh commands defining the numerical grid and computational domain have been merged into a single command line.

15.3 Runehamar tunnel fire reconstruction using FDS 5.0.3

The background of the Runehamar tunnel fire experiment will not be presented in this chapter as it has been covered in chapter 10 of this thesis. Material thermal properties and fuel geometry dimension as defined in chapter 10 with cone test data for wood and plastic incorporating surface burning factor is used in the simulation. Geometry of the Runehamar tunnel with installation of the fire board is included in the simulation to account for the effect of re-radiation. An air velocity of 3 m/s is introduced at one end of the tunnel with the opposite end open to the atmosphere. Figure 15.1 shows the model setup using FDS 5 and Smoke view.

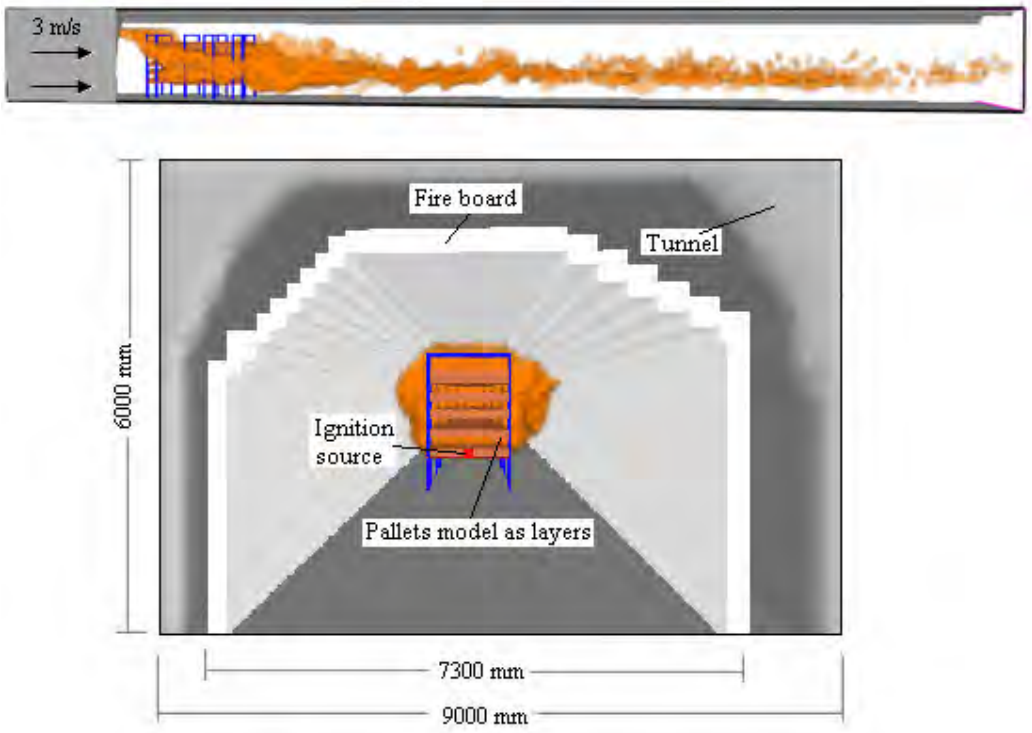

Figure 15.1: Runehamar tunnel fire reconstruction using FDS 5

15.4 Simulated Results

Based on the setup mention in section 15.3, the Runehamar tunnel fire experiment T1 was simulated using FDS 5.0.3. Grid and domain sensitivity were performed and varies fuel configurations were simulated. These results are presented in Figure 15.2, 15.3 and 15.4.

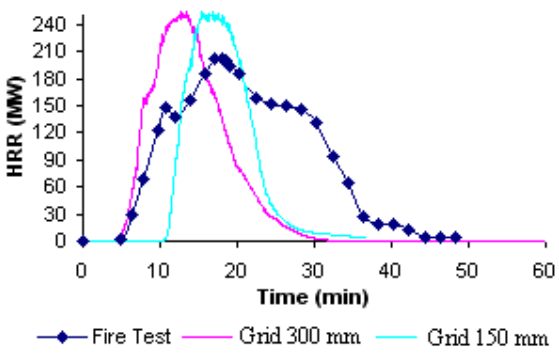

Figure 15.2: Grid sensitivity

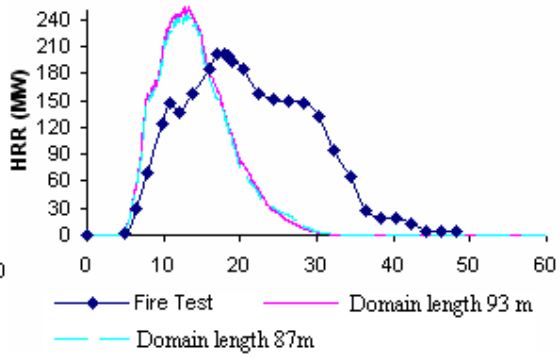

Figure 15.3: Domain sensitivity

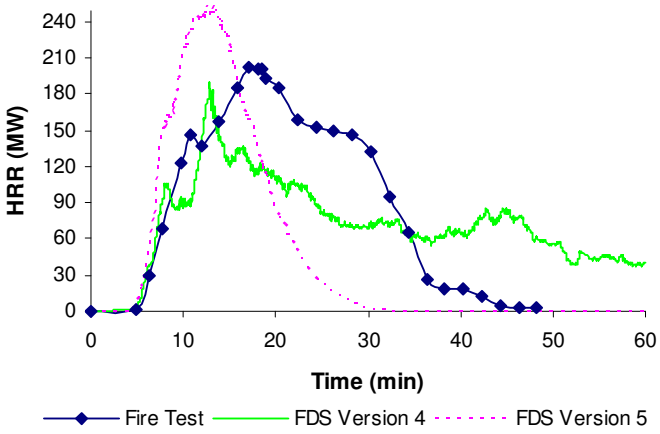

Figure 15.4: Comparing HRR computed using FDS version 4 and 5 with fire test

Heat release rate computed using FDS version 4 and 5 is presented in Figure 15.4. In these simulations, it has been observed that the peak heat release rate computed using FDS 4.07 has estimated a peak heat release rate of 190 MW as compared to the fire test of 201.9 MW which is around 6% different from the Runehamar tunnel fire experiment. Similar fire growth rate has been observed as compared with the fire experiment. However, the model is not able to predict the decay phase of the fire development partly because phenomena such as collapse of fuel package during the burning process was not captured in the simulation.

The simulation result computed using FDS 5.0.3 varies around 252 MW which is about 24% different from the peak HRR of the Runehamar tunnel fire experiment. The initial fire growth rate computed using FDS 5.0.3 was similar to the experimental value but shows signs of deviation as it reaches the peak HRR. Similar to FDS version 4, FDS version 5 is not able to predict the decay phase of the fire development partly because phenomena such as collapse of fuel package during burning cannot be captured in the simulation.

The deviation of the computed peak heat release rate with the experimental value can probably be attributed to the following reasons:

a) Although cone data used for the simulation were based on materials of similar type as the Runehamar fire experiment, the specimens used for the cone test data are not

directly taken from the fire experiment. This might indirectly affect the heat release rate estimate.

b) The fuel package (wood, plastic pallets and steel rack) burning in this experiment is made from 2 to 3 materials. The burning behaviour such as melting, flowing, forming pool of fires from the plastic material could not be captured in the simulation leaving out some details of the burning behaviour.

c) The way fuel load is arranged in the simulation. As it is seen in Figure 15.5 the fire growth behaviour can vary by changing the burning fuel arrangement configuration.

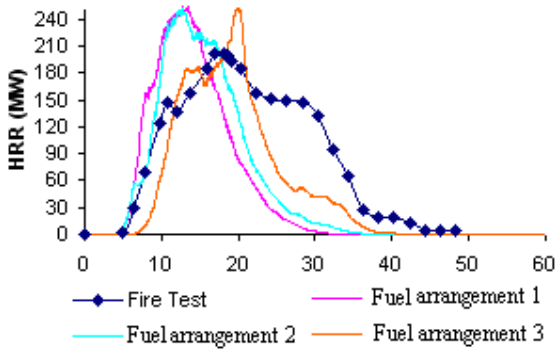

Figure 15.5: Different fuel arrangement

d) A particular material's heat release rate per unit area (HRRPUA) curve obtained from small scale fire test (e.g. Cone Calorimeter, LIFT apparatus) might not necessary produce the same HRRPUA results when these tests are repeatedly conducted a number of times. As the HRRPUA of material (from small-scale test) used for the simulation is a function of the predicted HRR, varying this input parameter would affect the overall heat release rate estimate. If sufficient cone data of the same material specimens are available, a sensitivity analysis can be performed which can be used as part of the calibration process to improve the simulation model.

15.5 Simplified Cone Curve

This section of the work continues to explore improvements that can be made on the calibration process and the effect of using different small scale fire data input on the global heat release rate estimate using FDS 5. As material thermal properties used for the simulations were taken from other research work, data on HRRPUA from small scale fire test is limited for the simulation. It is not possible to conduct a sensitivity analysis to improve the model calibration. Instead a simplified cone curve is used as an illustration. The work in this section does not form part of the calibration process. However, it opens up the scope for future research work to consider when using this approach to estimate heat release rate related to tunnel simulation.

In the Runehamar tunnel fire experiment T1, the total fuel load is made up of approximately 80 % wood pallets and 20 % plastic pallets. There are a total of 454 pallets burned in this experiment where 360 are 1.2 m x 0.8 m x 0.15 m wood pallets and 20 (1.2 m x 1 m x 0.15 m) wood pallets with the remaining fuel made up of 1.2 m x 0.8 m x 0.15 m plastic pallets. As mentioned in chapter 10, the dimensions of these pallets are different and the use of this simplified representation of wood and plastic pallets in the simulation would require a surface burning factor to account for the pallet's burning rate by ensuring the simulation burning area is the same as the actual fire experiment. The cone calorimeter curve base on the HRRPUA from cone test data incorporating surface burning factor is shown in Figure 15.6. These curves are simplified by creating a plateau in the curve but maintaining the same energy content (Figure 15.7) for the numerical simulation (Appendix P).

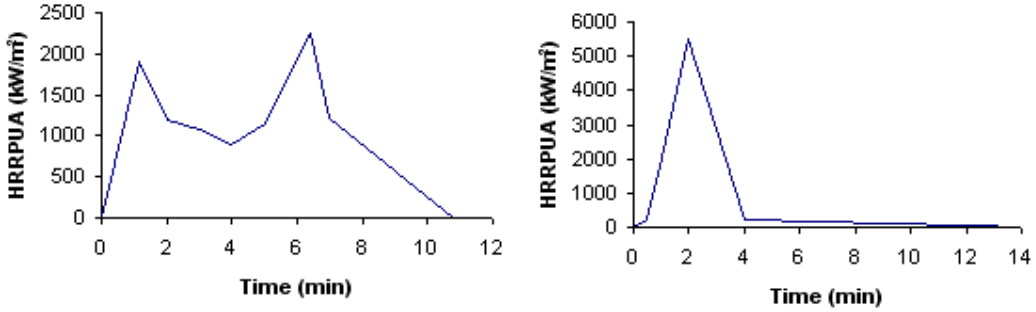

Wood *Polyethylene*

Figure 15.6: Exampleof HRRPUA curve incorporated surface burning factor

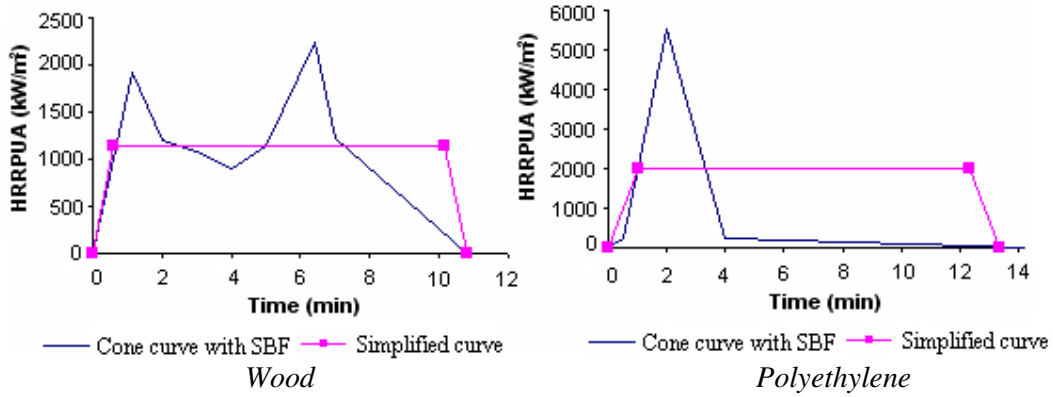

Wood *Polyethylene*

Figure 15.7: Example of simplified curve

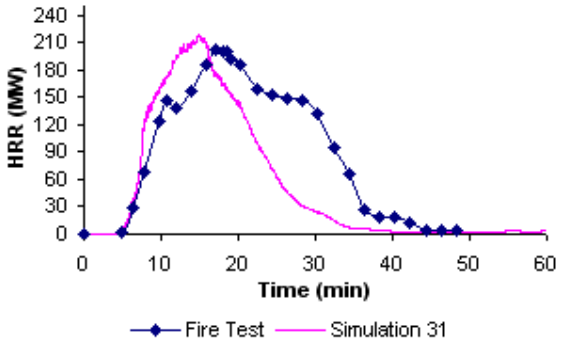

Figure 15.8: HRR of the Runehamar Tunnel fire experiment using simplified curve

Figure 15.8 shows the simulated result using a simplified HRRPUA curve. Comparing the simulation result in Figure 15.4 (based on cone test data incorporating SBF) with the result in Figure 15.8 (simplified from cone test data incorporating SBF), one can see the effect of HRRPUA parameter on the global heat release rate estimate. Unfortunately during the duration of this research project, a sensitivity analysis in the calibration of the FDS 5 model was not possible due to the lack of sufficient small scale fire test data. A better calibration could only be performed when such data is made available.

15.6 Conclusion

Simulating a fire scenario where the heat release rate is predicted rather than prescribed involves higher uncertainty. These include the lack of sufficient material fuel properties

data, the physical process of combustion, heat transfer is more complicated than the mathematical representation in FDS, the results of calculations are sensitive to both numerical and physical parameters. For these reasons modelling fire growth will always require a higher level of user skill and judgement (McGrattan et al, 2007). The work in this chapter has provided a brief discussion on some of these issues and highlights the need for more small-scale fire test data for heat release rate estimate.

Chapter 16:
CONCLUSION

16.1 Conclusion

A methodology using risk analysis and a deterministic approach (FDS) to establish the heat release rate in a road tunnel considering fuel load (traffic fleet, incident data such as vehicle fault, act of carelessness, intentional, collision), ventilation condition and tunnel geometry has been formulated. The important findings from various aspects of this research work include:

The recent fire tests programmes and research work carried out by various researchers in the area of tunnel fires have highlighted the importance of tunnel conditions such as tunnel geometry; ventilation condition; fuel load and location of fire ignition on the heat release rate.

From past tunnel fire incidents compiled in Appendix A and discussion in chapter 4, it has been found that a vehicle fault due to mechanical (engine fire, brake overheating, tyre fire, gear box and fuel tank leakage) or an electrical (motor fire, short circuits) from goods vehicles tend to have the largest share of vehicles involved in tunnel fires.

The implementation of Hazmat Transport Vehicle Tracking System (HTVTS) discussed in chapter 5 is an effective means to reduce tunnel fire risk. This is evident from the low number of tunnel fire incidents in the Singapore road tunnel network.

From this study, it is recognised that the number of fire scenarios in a tunnel can be numerous. It is not possible to design a smoke control system for every potential incident. The cost and practicality of designing for an extreme case is beyond what might be considered reasonable. Therefore, the selection of the design fire scenario has to be made on the basis of a risk analysis.

The risk analysis from chapter 8 showed that the highest fire risk that could occur in this tunnel project is due to a vehicle fault fire from a single light goods vehicle and the lowest fire risk occurs from multiple bus collision.

In chapter 10, re-construction of the Runehamar tunnel fire test using FDS 4.0.7 was performed. To enhance the confidence in using FDS to estimate the initial growth and peak heat release rate, work to develop a simplified representation of wood and plastic pallets burning in the tunnel was carried out. The simulated results showed that the model is able to capture a similar fire growth rate and a peak heat release rate.

It is found that when a single LGV or single HGV fire occurs in the tunnel, it is more likely to be fuel controlled rather than ventilation controlled due to the high flow rate generated by the tunnel ventilation fans.

The FDS simulation results presented in chapter 11 showed the following findings:

i) The heat release rate in this project varies from 54 MW to 88 MW for a single LGV fire and 75 MW to 193 MW for a single HGV fire. The fire size varies depending on factors such as tunnel geometry, ventilation condition and ignition location.

ii) The quantity of fuel load can significantly affect the fire size in the tunnel; an LGV would have a much lower heat release rate as compared with an HGV because the amount of goods carried is controlled by the laden weight of the goods vehicle.

iii) The ventilation condition in the tunnel could have a significant impact on the heat release rate. Generally, higher air velocity in the tunnel would result in a higher heat release rate.

iv) With the aid of the tunnel air flow (air flow movement from rear to the front of the vehicle), a fire ignited at the rear of the vehicle appears to spread faster as compared to a fire ignited at the front of the vehicle yielding higher heat release rate.

The effect of vehicle fire spreading from one vehicle to another is discussed in chapter 12. The simulation results showed a 160 m vehicle separate distance is generally required to prevent ignition considering the condition in this tunnel. This study provides an additional

source of information for the tunnel operator to strategise their emergency operating procedure if such situation arises.

A brief introduction on the use of an empirical probabilistic Bayesian approach and the approach using FDS to provide an estimate on the heat release rate in the road tunnel is covered in chapter 13. The work in this chapter further enhances the importance of tunnel ventilation condition when estimating heat release rate.

Chapter 14 presented the application of parallel processing to provide high performance computation CFD work. Findings from this study conclude that generally more processors do speed up computational time for the FDS simulation. However, it is critical to avoid placing mesh boundaries at the fire source or cutting through the flame extension as this will affect the accuracy of the computation results.

The recent launch of FDS 5 has suggested the use of this version to perform tunnel simulation work. Preliminary simulation for the reconstruction of the Runehamar tunnel fire experiment was performed. This formed part of the preliminary simulation work and laid down the foundation for future research activities.

The limitations of using FDS computational fluid dynamics model to estimate the heat release rate, specifically the peak heat release rate for tunnel ventilation smoke control design are discussed as follows:

i) The modelling approach in this research work uses the HRRPUA approach where the fuel considered in the FDS simulation is based on data taken from Cone Calorimeter HRRPUA curve. It assumed that the burning behaviour of materials in a tunnel fire is similar to a small-scale fire experiment e.g Cone Calorimeter. Depending on the simulation one is performing (simulating a free burning condition or enclosed environment), the selection of the appropriate heat flux cone data for the simulation is important as inappropriate selection of these cone data will result in over predicting or under predicting the heat release rate estimate in the simulation analysis.

ii) Comparing the FDS simulations results with the fire tests results discussed in chapter 9 and 10 shows that FDS is unable to predict the decay phase of the fire development accurately because phenomenon such as collapse of the fuel package during the burning process was not considered in the FDS code.

iii) A simple model (refer to page 26 Figure 3.2 of the FDS4 Technical Reference Guide) for flame extinction has been implemented in FDS to assess if combustion is allowed or not allowed to take place. When the gas environment falls within the "Burn" zone, combustion will commence. The state relations are no longer valid if the gas environment falls in the "No Burn" zone (McGrattan 2005). In this work, as HRRPUA approach is used and the ignition temperature is input based on each material properties. The surface of the object will start burning following the cone data which is different from the default assumption made in FDS.

iv) Although study from chapter 9 and 10 shows that similar growth rate history and peak heat release rate were produced from the FDS simulation when comparing with the fire tests, achieving grid independence in this study is a challenging task. It would be ideal if finer computational grid sizes could have been performed. Unfortunately this would have required substantial amount of computational power and simulation run time which was beyond the resources available of this work.

v) One of the limitations is that the calibration of the FDS model is based on the Runehamar tunnel fire test. It is not known whether this is the worst case scenario; as suggested by Beard (2008) the peak HRR in this test has been estimated to be around the 59^{th} percentile of possible results. However, if one examines the prescriptive codes such as NFPA 502, the recommendation for the fire size of an HGV makes reference to the Runehamar tunnel fire tests.

vi) Another limitation is the petrol in the fuel tank is not included in the simulation. In a vehicle collision, there is a possibility of a fuel tank rupture resulting in liquid fuel spilling onto the incident and neighbouring vehicle. The flow rate from the ruptured fuel tank can vary depending on the opening of the damaged fuel tank. When the flammable liquid fuel ignites, the heat release rate would vary depending on the diameter of the pool fire on the surface of the road tunnel. There are also

other factors such as gradient in the tunnel which can affect the direction and flow of the spillage from the ruptured fuel tank. When the liquid fuel burns, the flaming liquid fuel may be flowing down-slope and this is different from the approach used to model a solid material fire for this study.

vii) The gradient in the tunnel is another parameter which can affect the performance of the tunnel ventilation smoke control design. Gradient is not considered in this work mainly because the tunnel gradient for this study is insignificant (0 to 2%). However, it might be worth while to consider the gradient in the tunnel for other tunnel projects with steep gradient.

viii) The current study is based on a limited number of actual fire test data (e.g Cone Calorimeter, full scale fire tests) for the calibration of the FDS model to estimate the heat release in the tunnel. While using the HRRPUA with SBF approach, there is a need to perform more sensitivity analysis by using more cone test data input for the FDS calibrate with more full scale fire tests.

Through this work, this study highlights to stakeholders (e.g.: tunnel owner, relevant authority, tunnel ventilation designer, relevant engineers involved in the tunnel design) the impact of changing the ventilation design airflow, regulation on vehicle access right or traffic fleet in tunnel has on heat release rate. Changing these parameters would result in a change in fire risk level and re-evaluation on the heat release rate through the use of deterministic approach such as (FDS) is required. The analysis of the re-evaluation of the heat release rate in the tunnel will need to be agreed upon by the stakeholders.

A general schematic of the overall parameters that need to be considered when establishing the heat release rate in road tunnel is shown in Figure 16.1.

Lastly, it is to highlighted that the proposed method used to evaluate the heat release rate for road tunnel can only be treated as a case study for future consideration.

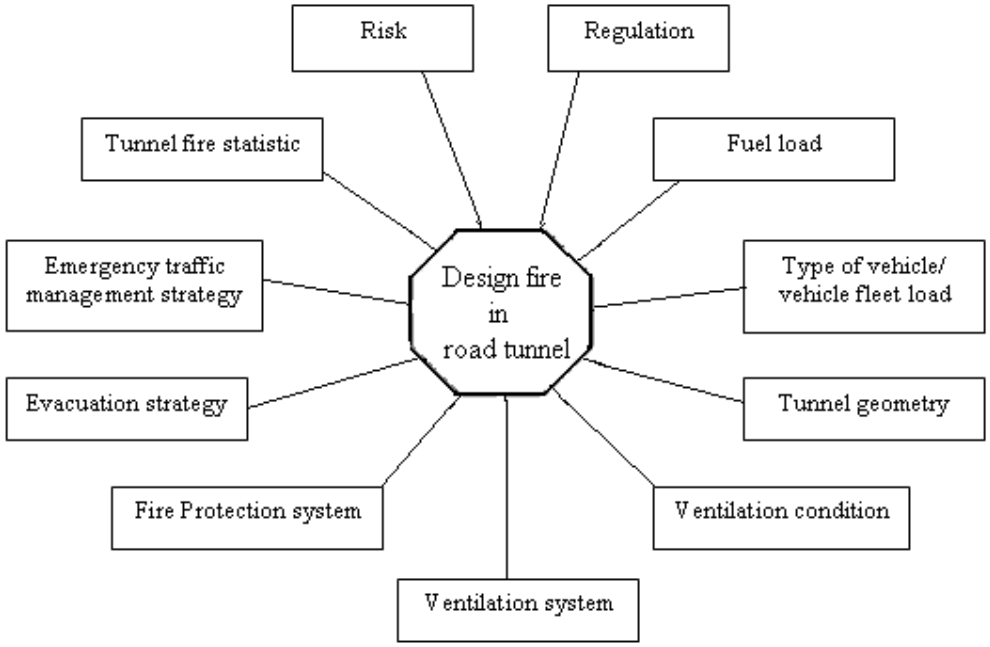

Figure 16.1: Parameters to consider when estimating HRR in road tunnel

16.2 Recommendations for future work

There are developments taking place in the area of fire and smoke control in tunnels such as large scale fire tests or the use of computational techniques to provide information to tunnel designers, relevant authorities and tunnel owners concerning safety in road tunnels. Considering that road tunnels are complex and dynamic in nature, each tunnel is unique by itself in terms of its tunnel layout, systems provision, incident management procedures, regulations from authority and traffic condition that could have an effect on the design fire. These conditions, particularly traffic condition in the tunnel might change over the life span of the tunnel and constant revisiting on the fire risk in the tunnel is suggested.

For future research work, there is a need to gather more thermal properties of components (seats, tyres, plastic panel) for vehicles such as motorcycles, cars and buses through small scale fire test for future FDS simulation. Although this will involve a substantial amount of work, this would allow for wider range of simulations to be performed for other vehicle types.

A new simulation approach considering fuel tank rupture resulting in a liquid fuel spill to the incident and neighbour vehicle can be examined.

The use of fire suppression systems on vehicle fire can be performed using the numerical approach to explore the effectiveness of these systems in road tunnel.

Another potential area where further research work is required is to establish a modelling approach in FDS to establish a heat release rate for a petrol tanker fire. This piece of work would be useful for tunnel design fire where there is no constraint in allowing dangerous vehicles such as a petrol tanker from entering their tunnel.

And last but not least, there is a need to validate the modelling results if the opportunity to carry out full-scale fire tests arises.

References

Abbott M B and Basco D R (1989), *Computational Fluid Dynamics – An Introduction for Engineers*, Longman Scientific & Technical.

AS/NZS 4360, 2004, "Standards for Risk Management AS/NZS 4360", Edition 2004, Standards New Zealand.

AS/NZ 4360, 2004a, "Risk Management Guidelines – Companion to AS/NZS 4360", Edition 2004, Standards New Zealand.

ASTRATA (2005), "Case study on ASTRATA group incorporated", Mapinfo, http://www.mapinfo.com/static/files/document/1117507061494/Astrata_CS.pdf., accessed 6 January 2007.

Atkinson G T and Wu Y (1996), "Smoke Control in Sloping Tunnels", Fire Safety Journal, Vol 27, Number 4, pp 335-341.

Babrauskas V and Grayson S J (1992), Heat Release In Fires, London; New York : Elsevier Applied Science.

Babrauskas V (2002), "Heat Release Rate", In *SFPE Handbook of Fire Protection Engineering*, 3rd Edition, National Fire Protection Association.

Babrauskas V (2003), Ignition handbook : principles and applications to fire safety engineering, fire investigation, risk management and forensic science, Issaquah, Wash. : Fire Science Publishers.

Barney B (2007), "Introduction to parallel computing", Training materials, High performance computing Lawrence Livermore National Laboratory.

Beard, A.N. (2008), "Tunnel Fire Safety: Prevention, Protection and Ventilation", *China Tunnel Summit-2008*, 20-21, Shanghai.

Beard A.N and Carvel R.O (2005), *The Handbook of Tunnel Fire Safety* , Edited by Beard A and Cavel R, Thomas Telford Publishing.

Bechtel and Brinckerhoff (1995), *Memorial Tunnel Fire Ventilation Test Program Test Report*, Massachusetts Highway Department and Bechtel/Parson Brinckerhoff.

BD (1999), BD 78/99 - Design manual for road and bridges volume 2 section 2 part 9, The Highways Agency London.

Bendelius, A. (2003), "Fire Protection for Road Tunnels", In *Fire Protection Handbook*, National Fire Protection Association (NFPA), Quincy MA, pp.14-127 to 14-144.

Bendelius, A. (2005), "Tunnel Ventilation –state of the art", In *The Handbook of Tunnel Fire Safety*, Thomas Telford Publishing, pp 127-143.

Beowulf (2007), website Beowulf overview, http://www.beowulf.org/overview/index.html, accessed December 2007.

Biollay H, Chasse P, Lacroix D, "Fire and Smoke Control in Road Tunnel", PIARC Committee on Road Tunnel (C5), 1999.

Bolland J, Weir D and Vincent M (2005), "Development of a New Zealand National Freight Matrix", Land Transport New Zealand Research Report 283.

Brekelmans J, Bosch R.V (2003), "Summary of large scale fire tests in the Runehamar tunnel in Norway", Published by: UPTUN, TNO, PROMAT.

Bryant R A, Ohlemiller T J, Johnsson EL, Hamins A, Grove B S, Guthrie W F, Maranghides A, Mulholland G H (2003), "The NIST 3 Megawatt Quantitative Heat Release Rate Facility", National Institute of Standards and Technology Special Publication 1007.

BRE (2008), the BRE website Fire research and consultancy, http://www.bre.co.uk/fire/page.jsp?id=286 , accessed March 2008.

Carvel R.O, Beard A.N, Jowitt P.W and Drydale D.D (2001), "Variation of heat release rate with forced longitudinal ventilation for vehicle firs in tunnels", *Fire Safety Journal*, v 36, pp 569-596.

Carvel R.O, Beard A.N and Jowitt P.W (2001). "A method for making realistic estimates of the heat release rate of a fire in a tunnel", Heriot-Watt University Fire Safety Engineering website www.civ.hw.ac.uk/research/structural/fire/pdfs/2001tunnelfire.pdf, accessed 1st December 2006.

Carvel R.O, Beard A.N, Jowitt P.W, Drysdale D.D (2005), "Fire Size and Fire Spread in Tunnels with Longitudinal Ventilation Systems", *Journal of Fire Sciences*, Vol 23, Number 6, pp 485-518.

Carvel R.O and Beard A.N and Jowitt P.W (2004a), "The influence of Tunnel Geometry and Ventilation on the Heat Release Rate of a Fire", *Fire Technology*, Vol 40, Number 1, January 2004, pp 5-26.

Carvel R.O and Beard A.N (2005), "The influence of tunnel ventilation on fire behaviour", In *The Handbook of Tunnel Fire Safety* , Edited by Beard A and Cavel R, Thomas Telford Publishing, pp 184-197.

Carvel R.O and Marlair G (2005), "A history of fire incidents in tunnels", In *The Handbook of Tunnel Fire Safety* , Edited by Beard A and Cavel R,Thomas Telford Publishing, pp 3-41.

Carvel et al (2004), "How longitudinal ventilation influences fire size in tunnels", *Tunnel Management International Journal*, Volume 7, Issue 1.

CFX (2008), website on ANSYS CFX, http://www.ansys.com/Products/cfx.asp, accessed March 2008.

Chanda M and Roy S K (1987), *Plastics Technology Handbook*, New York : M. Dekker, c1987.

Chen C J, Tsai M J, Ji B C, Wu C W (2005), "Burning Analysis of Motor Scooters", *8th International Symposium on Fire Safety Science*", Beijing, IAFSS.

Cheong M K and Lim L W (2005), "Preliminary Study on the Tunnel Ventilation System for Wodsville Vehicular Interchange", feasibility study report, Land Transport Authority, Mechanical and Electrical System.

Cholin J M (2003). "Wood and Wood-based Products", In *Fire Protection Handbook* 19th Edition. National Fire Protection Association.

Chuang Y J, Tang C H, Chen P H and Lin C Y (2007), "Experimental Investigation of Burning Scenario of Loaded 3.49-Ton Pickup Trucks", *Journal Applied Fire Science*, Vol 14(1), pp 27-46.

Cox G (1995), "Combustion Fundamentals of fire", Academic Press.

DiNenno P (2002), The SFPE Handbook of Fire Protection Engineering (3rd ed.), Appendix B, NFPA, Quincy, MA.

Donaldson I, Bach K and Frost T (2005), "International Fire Engineering Guidelines", Edition 2005, Australia Building Code Board.

Drysdale D (1998), *An Introduction to Fire Dynamics*, John Wiley & Sons Ltd.

Elms D G (2004), "Structural safety-issues and progress", *Progress in Structural Engineering and Materials*, 6:ll6-126, John Wiley & Sons Ltd.

EUREKA (1995), Fire in Transport Tunnels - Report on Full-Scale Tests (1995), *EUREKA-Project EU 499: FIRETUN*, Editor Studiengesellschaft Stahlanwendung e.V Dusseldorf.

FHA (1984), "Prevention and control of highway tunnel fires", Report no. FHWA/RD-83/032, U.S Department of Transportation.

FHWA (1980) Federal Highway Administration, Offices of Research and Development, Users Guide for the TUNVEN and Duct Programs, Report No FHWA-RD-78-187, Washington, DC.

Fleischmann C.M (2006), "Piloted ignition of solid materials under radiant expose", University of Canterbury.

Floyd J (2002), "Comparison of CFAST and FDS for Fire Simulation with the HDR T51 and T52 Tests", NISTIR 6866, National Institute of Standards and Technology, Gaithersburg, Maryland.

Fluent (2008), website on ANSYS Fluent, http://www.fluent.com/, accessed March 2008.

Forney G.P, McGrattan K. (2004), "User's Guide for Smokeview Version 4" , National Institute of Standards and Technology.

Grosshandler W L (1993), "RADCAL: A Narrow-Band Model for Radiation Calculations in a Combustion Environment", National Institute of Standards and Technology.

Goodfellow (2007), Website from Goodfellow – Material information, http://www.goodfellow.com/csp/active/gfHome.csp, access date: 21 June 2007.

Hall, R.C (2006), "Ventilation during road tunnel emergencies", Mott MacDonald http://www.ha-research.gov.uk/projects/projectdocuments.php?method=download&ID=76, accessed 2 December 2006.

Hack A (2002), "Fire and Safety", *Tunnelling and Underground Space Technology,* Vol 17 pp 117-127.

Hall J R (2006), "Probability Concepts", In *The SFPE handbook of Fire Protection Engineering*, Third Edition, NFPA, pp 1-182 – 1-192.

Heselden, A J M. (1978), "Studies of Fire and Smoke Behaviour relevant to Tunnels", Building Research Establishment.

Hietaniemi J, Hostikka S and Vaari J (2004), "FDS simulation of fire spread – comparison of model results with experimental data", VTT working papers no 4, VTT Building and Transport.

Holliday. S (2002), "Proposed Lane Cove Tunnel and Associated Road Improvements", Director-General's Report section 115C of environmental planning and assessment Act 1979.

Hostikka S and McGrattan K (2001), " Large Eddy Simulation of Wood Combustion", In *Proceedings of the Ninth International Interflam Conference*, Inter-science Communication, London, pp 755-762.

Hopkins Jr D and Quintiere J G (1996), "Material Fire Properties and Predictions for Thermoplastics", In *Fire Safety Journal,* 26:33, Page 241- 268.

HTVTS (2006), "Hazmat Transport Vehicles Tracking System (HTVTS)", http://www.chemindustry.org.sg/govern_rep.asp , accessed 23 June 2006.

IDA (2005) IDA Road Tunnel Ventilation Version 3.0, "Getting stated guide", EQUA Simulation AB.

Incropera F P and Dewitt D P (2002), *Fundamentals of Heat and Mass Transfer*, Fifth Edition, John Wiley and Sons.

Ismat A Abu-Isa (2000), "Thermal Properties of Automatic Polymers II Thermal Conductivity Measurements", SAE Technical Paper, *SAE 2000 World Congress*, Detroit Michigan, March 6-9.

ISO 13387-2. (1999), "Design fire scenarios and design fire", Technical Report ISO/TR 13387-2, First Edition 1999, International Organisation for Standardization.

ISO 5660-1 (2002), Reaction to fire Test Heat Release, Smoke Protection and Mass Loss Rate Part 1: Heat Release Rate (Cone Calorimeter Method).

Ingason H (2003), "Fire Development in Castastropic Tunnel Fires (CTF)", Proceeding of the International Symposium on *Catastrophic Tunnel Fires*, SP Swedish National Testing and Research Institute.

Ingason H (2005), "Fire dynamics in tunnels", In *The Handbook of Tunnel Fire Safety*, Thomas Telford Publishing, pp 231 – 266.

Ingason H(2006), "Fire testing in road and railway tunnels", *In Flammability Testing of Materials used in Construction*, Transport and Mining, Woodhead Publishing, pp 231-271.

Ingason (2006a), "Design fire in tunnels", Safe & Reliable Tunnels Innovative European Achievements, Second International Symposium, Lausanne.

Ingason H and Lonnermark A (2003), "Large-scale Fire Tests in the Runehamar tunnel – Heat release Rate (HRR), Proceeding of the International Symposium on *Catastrophic Tunnel Fires*, SP Swedish National Testing and Research Institute.

Ingason H and Lonnermark A (2003a), "Project description and planning of large-scale tests in Runehamar tunnel", SP Swedish National Testing and Research Institute.

Ingason H and Lonnermark A (2004), "Make the HGV freight compartment safer", in *Tunnel Management International Journal*, Vol 7 number 3.

Ingason H and Lonnermark A (2005), "Heat release rate from heavy goods vehicle trailer fires in tunnels" *Fire Safety Journal*, Vol 40, Issue 7, pp 646-668.

Ingason H, Gustavsson S and Dahlberg M (1994), Heat Release Rate Measurements in Tunnel Fires, SP report 1994:08, SP Swedish National Testing and Research Institute Fire Technology.

Jacques and Seynhaeve (2006), “Fire in the Cointe Tunnel: A Design Case Study”, http:// www.term.ucl.ac.be/reacherche/tunnels_%20routiers/vt1998apdf , accessed 23 November 2006.

Jagger and Grant (2005), "Use of tunnel ventilation for fire safety", In *The Handbook of Tunnel Fire Safety*, Thomas Telford Publishing, pp 144-183.

Johnson P and Barber D (2007), *Burnley Tunnel Fire – The Arup View,* Arup Fire, http:// www.fpaa.com.au/docs/burnley.pdf , accessed 23 November 2006.

Kashef A, Benichou N, Lougheed G and Debs A (2006), “Performance investigation of emergency ventilation strategies in a road tunnel”, http:// irc.nrc-cnrc.gc.ca/fulltext/nrcc48625/nrcc48625.pdf, accessed 24 December 2006.

Kashef A, Benichou N, Lougheed G.D and McCartney C (2002), “A Computational and Experimental Study of Fire Growth and Smoke Movement in Large Spaces. Technical Report NRCC-45201, National Research Council Canada.

Keey R B, (2000), “Management of Engineering Risk”, Centre for advanced Engineering, University of Canterbury.

Karlsson B and Quintiere J G (2000), *Enclosure Fire Dynamics*, CRC Press, Washington DC.

Kocsis R N (2002), “Arson: Exploring Motives and Possible Solutions – No 236”, *Trends and issues in crime and criminal justice,* Australian Institute of Criminology.

Kaiserkraft (2006), Pallets website, http://www.kaiserkraft.co.uk/section/320, accessed 29 November 2006.

Lee S C (2001), *Investigation of Motor Vehicle Fires*, Fourth Edition, Lee Books publisher, 4th edition (March 1, 2001).

Lonnermark, A (2005), "On the characteristics of Fire in Tunnels" PhD Thesis, University of Lund.

Lonnermark, A (2003), Presentation slide "Large-scale Fire Tests in the Runehamar tunnel", International Symposium on *Catastrophic Tunnel Fires*.

Lonnermark A and Ingason H (2003), "Large-scale Fire Tests in the Runehamar tunnel – Gas temperature and radiation, proceeding of the International Symposium on *Catastrophic Tunnel Fires*, SP Swedish National Testing and Research Institute.

Lönnermark A and Ingason H (2005), "Gas Temperatures in Heavy Goods Vehicle Fires in Tunnels", *Fire Safety Journal*, Vol 40, Issue 6, pp 506-527.

LTA (2006), Website from the Land Transport Authority of Singapore – Motor Vehicle Population in Singapore, http://www.lta.gov.sg/corp_info/index_corp_facts.htm, accessed 30 December 2006.

Lee S.R and Ryou H.S (2006), "A numerical study on smoke movement in longitudinal ventilation tunnel fires for different aspect ratio", Science direct *Building and environment 41* pp 719-725.

Lemaire and Kenyon (2006), "Large Scale Fire Tests in the Second Benelux Tunnel", *Fire Technology*, Vol 42, Number 4, pp 329-350.

Levy S.S, Sandzimier J.R, Rosenbluth E.M (2000), "Emergency operating mode analysis for the Ted Williams Tunnel", Proceedings of the third International Conference on *Tunnel Management Internationa, Australia*.

Liu Z G, Kashef A, Lougheed G, Kim A K (2007), "Challenges for use of fixed fire suppression systems in road tunnel fire protection", Suppression and detection research applications – A Technical Working Conference, Orlando, Florida, pp 1-10.

Luk E (2003). *Final Design Report on Tunnel Ventilation and Environmental Control System*. Parson Brinckerhoff Consultant Pte Ltd, Contract 4901, prepared for the Land Transport Authority of Singapore.

Luk E (2004), " Tunnel Ventilation Report for Fortcanning Tunnel – Final Design", Tyco Pte Ltd, prepared for the Land transport Authority of Singapore.

Mangs J & Keski-Rahkonen O (1994), "Characterization of the Fire Behaviour of a Burning Passenger Car. Part I: Car Fire Experiments", *Fire Safety Journal,* Vol 23, pp 17-35.

Mangs J & Keski-Rahkonen O (1994a), "Characterization of the Fire Behaviour of a Burning Passenger Car. Part II: Parametrization of measured rate of heat release curves" , *Fire Safety Journal*, Vol 23, pp 37-49.

McGrattan and Hamins (2002), "Numerical Simulation of the Howard Street Tunnel Fire, Baltimore, Maryland, July 2001", National Institute of Standards and Technology.

McGrattan K (2005), "Fire Dynamics Simulator (Version 4) Technical Reference Guide", National Institute of Standards and Technology.

McGrattan K, Hostikka S, Floyd J,Baum H, Rehm R, Mell W and McDermott R(2008), "Fire Dynamics Simulator (Version 5) Technical Reference Guide", National Institute of Standards and Technology.

McGrattan K and Forney G (2005), "Fire Dynamics Simulator (Version 4) User's Guide", National Institute of Standards and Technology.

McGrattan K (2001), "Computational Fluid Dynamics and Fire Modeling", National Institute of Standards and Technology, http://www.fire.nist.gov/fds/docs/fds_class_notes.pdf, accessed 25 February 2007.

McGrattan K, Bouldin C and Forney G (2005), Federal Building and Fire Safety Investigation of the World Trade Centre Disaster, "Computer Simulation of the Fires in the World Trade Centre Towers", NIST.

McGrattan K, Klein B, Hostikka S, Floyd J (2007), "Fire Dynamics Simulator (Version 5) User's Guide", National Institute of Standards and Technology.

McMurtrie C (2006), "UC Super computer facility – An Introduction", University of Canterbury, 26 October 2006.

Mitsubishi (2004), Body Builder's Drawings and Supporting Data for Mitsubishi FUSO Truck, Mitsubishi FUSO Truck of America, INC.

Nelson H.E and Frederick W.M (2002), "Emergency Movement" in *The SFPE Handbook of Fire Protection Engineering,* Third Edition, National Fire Protection Association.

NFPA 502. (2004), *Standards for Road Tunnels, Bridges and Other Limited Access Highways*, Edition 2004, National Fire Protection Association, Quincy, Massachusetts.

NFPA 502 (2008), *Standards for Road Tunnels, Bridges and Other Limited Access Highways* - Edition 2008, National Fire Protection Association, Quincy, Massachusetts.

Ng A and Gong N (2007), "Preliminary Design Report on Tunnel Ventilation and Environmental Control System – C461", Parson Brinckerhoff Consultant Pte Ltd, prepared for the Land Transport Authority of Singapore.

Nisted T (1991), "Flame Spread Experiments in Bench Scale" Project 5 of the EUREFIC fire research programme, Dantest *Fire Technology*.

NUREG (2007), "Verification and Validation of Selected Fire Models for Nuclear Power Plant Applications". NUREG 1824, United States Nuclear Regulatory Commission, Washington, DC.

OECD / PIARC (2006), "Transports of Dangerous Goods Through Road Tunnels" ,Technical report, page 4 – 13, http://www.oecd.org/dataoecd/22/43/1882046.pdf, accessed 7 July 2006

Paprzycki M and Stpiczynski P (2005), "A Brief Introduction to Parallel Computing", in *Handbook of Parallel Computing and Statistics*, Edited by E J Kontoghirghes, Chapman & Hall.

Parsons Brinckerhoff Quade and Douglas (1997), "Subway Environment Simulation (SES) Computer Program Version 4, Part 1: User's Manual", U.S. Department of Transportation.

Parson (2000), "Concept Design Submission Tunnel Ventilation System & Environmental Control System – C4901", Parson Brinckerhoff Consultant Pte Ltd, prepared for the Land Transport Authority of Singapore.

Parson (2003), "Final Design Report on Tunnel Ventilation and Environmental Control System – C4901", Parson Brinckerhoff Consultant Pte Ltd, prepared for the Land Transport Authority of Singapore.

Parson (2001), "Conceptual Design Report on Fire and Life Safety – C4901", Parson Brinckerhoff Consultant Pte Ltd, prepared for the Land Transport Authority of Singapore.

Phoenics (2008) website on PHOENICS, http://www.cham.co.uk/, accessed March 2008.

Philips (1991), "CTE Phase II M&E work O&M manual", Philips Pte Ltd, prepared for the Land Transport Authority of Singapore.

PIARC. (1987), Road Tunnels report of the committee to the XVIIIth World Road Congress Bussels, 1987 (ref 18.05E), *Permanent International Association of Road Congresses*.

PIARC. (1991), Road Tunnels report of the committee to the XIXth World Road Congress, Marrakesh, 1991 (ref 19.05B), *Permanent International Association of Road Congresses*.

PIARC. (1995), Road Tunnels report of the committee to the XXth World Road Congress, Montreal, 1995 (ref 20.05B), *Permanent International Association of Road Congresses.*

PIARC. (1999), Fire and Smoke Control in Road Tunnels,1999 (ref 05.05.B), *Permanent International Association of Road Congresses.*

Promat (2003), "Full Scale Fire Tests, Runehamar tunnel, Norway", Promat Tunnel Fire Protection, http://www.promat-tunnel.com/full-scale-fire5.htm, accessed 19 February 2007.

Promat (2007a), "Full Scale Fire Tests, Runehamar tunnel, Norway - Tests", Promat Tunnel Fire Protection, http://www.promat-tunnel.com/idprt001.htm, accessed 4 March 2007.

Promat (2007b), "Full Scale Fire Tests – Thermal protection boards, Runehamar tunnel, Norway", Promat Tunnel, http://www.promat-tunnel.com/en/thermal-protection-boards.aspx , accessed 19 February 2007.

Rein G, Abecassis Empis C and Carvel R.O. (2007), The Dalmarnock fire tests: Experiments and modelling, School of Engineering and Electronics, University of Edinburgh, ISBN 978-0-9557497-0-4.

Rew C and Deaves D (1999), "Fire spread and flame length in ventilated tunnels a model used in Channel Tunnel assessments", International conference on proceedings of tunnel fires and escape from tunnels, lyon, pg 397-406.

Rhodes N (2005), "CFD modelling of tunnel fires", In *The Handbook of Tunnel Fire Safety*, Edited by Beard A and Cavel R, Thomas Telford Publishing, pp 267- 283

Reilly (2005), "Fire engineering for UK highway tunnels", *Tunnel and Tunnelling International*, British Tunnelling Society, July 2005.

Riess et al (2001), "Smoke Extraction in Tunnels with Considerable Slope", *4th International Conference Safety in Road and Rail Tunnels*, Madrid.

Santrock J (2000), *Evaluation of Motor Vehicle Fire Initiation and Propagation / Part 3: Propagation of an Engine Compartment Fire in a 1996 Passenger Van*, General Motors Corporation.

Santrock J (2001), *Evaluation of Motor Vehicle Fire Initiation and Propagation / Part 4: Propagation of an Underbody Gasoline Pool Fire in a 1996 Passenger Van*, General Motors Corporation.

Santrock J (2001a), *Evaluation of Motor Vehicle Fire Initiation and Propagation / Part 6: Propagation of an Underbody Gasoline Pool Fire in a 1997 Rear Wheel Drive Passenger Car*, General Motors Corporation.

Santrock J (2002), *Evaluation of Motor Vehicle Fire Initiation and Propagation / Part 7: Propagation of an Engine Fire in a 1997 Rear Wheel Drive Passenger Car,* General Motors Corporation.

Santrock J (2002a), *Evaluation of Motor Vehicle Fire Initiation and Propagation / Part 9: Propagation of a Rear-Underbody Gasoline Pool Fire in a 1998 Sport Utility Vehicle*, General Motors Corporation.

Santrock J (2002b), *Evaluation of Motor Vehicle Fire Initiation and Propagation / Part 10: Propagation of a Mid-Underbody Gasoline Pool Fire in a 1998 Sport Utility Vehicle*, General Motors Corporation.

Santrock J (2003), *Evaluation of Motor Vehicle Fire Initiation and Propagation / Part 12: Propagation of a Underbody Gasoline Pool Fire in a 1998 Front-Wheel Drive Passenger Vehicle*, General Motors Corporation.

Santrock J (2003a), *Evaluation of Motor Vehicle Fire Initiation and Propagation / Part 13: Propagation of an Engine Compartment Fire in a 1998 Front-Wheel Drive Passenger Vehicle*, General Motors Corporation.

Scania (2005), "Dismantling information – Truck ", SCANIA CV AB 2005, Sweden.

SCDF (2005), " Requirement on road transportation of petroleum and flammable materials", Circular No 4, Singapore Civil Defence Force.

SCDF (2006), "Update on HAZMAT Tranport Vehicles Tracking System (HTVTS)", Singapore Civil Defence Force.

SCDF (2005a), "Fire Incident Statistics (January to December 2005)", Singapore Civil Defence Force, http://www.scdf.gov.sg/General/News/statistics.html, accessed 13 January 2007.

SCDF (2006a), "Fire Incident Statistics (January to December 2006)", Singapore Civil Defence Force, http://www.scdf.gov.sg/General/News/statistics.html, accessed 5 July 2007.

SCDF (2007), "Implementation of the Vehicle Immobiliser System in Phase II of the Hazmat Transport Vehicle Tracking System (HTVTS)", Singapore Civil Defence Force.

Shipp M and Spearpoint M (1995), "Measurement of the Severity of Fires Involving Private Motor Vehicles", *Fire and Materials*, Vol 19, issue 3, pp 143-151.

SFPE engineering guide (2002), SFPE engineering guide to piloted ignition of solid materials under radiant exposure, Society of Fire Protection Engineers.

SFPE (2005a), "SFPE Engineering Guide to Application of Risk Assessment in Fire Protection Design", Society of Fire Protection Engineers.

Straits Times (2005), "The Straits Time Newspaper" Singapore, Feb 23, 2005.

Singstat (2006), "Motor Vehicle Involved in Road Accident by Vehicle Type in Singapore", Traffic Police Department, Statistic Singapore, http://www.singstat.gov.sg/keystats/annual/yos/transport.pdf, accessed 30 December 2006.

Stroup, D.W.; DeLauter, L.A.; Lee, J.; Roadarmel, G.L, Report on "Passenger Minivan Fire Tests", National Institute of Standards and Technology.

Solvent (2008), web site from Solvent, http://www.tunnelfire.com/default.htm, accessed March 2008.

Tangram (2007), Material web site from Tangram Technology, http://www.tangram.co.uk/TI-Polymer-ABS.html#GP, accessed 21 June 2007.

Tan C S (2005), "The Singapore Experience in Managing the New Terrorism Threat", Singapore Civil Defence Force, http://ncdr.nat.gov.tw/iwerr/doc/pdf/keynote%20PDF/K5.pdf , accessed 30 June 2006.

Tewarson A (2006), "Generation of heat and chemical compound in fire", In *The SFPE handbook of Fire Protection Engineering*, Third Edition, NFPA, pp 3-82 – 3-161.

Thureson P (1991), "Eurific – Cone Calorimater Test Results Project 4 of the Eurefic fire research programme", SP Swedish National Testing and Research Institute Fire Technology.

Traffic Act (2006), Singapore gazette: road traffic act (Chapter 276, section 114 and 140) , road traffic (expressway traffic) rules.

UCSC – UC Supercomputer website, http://www.ucsc.canterbury.ac.nz/, accessed December 2007.

USFA (1999), "Fire in the United States 1987-1996", Eleventh Edition, Federal Emergency Management Agency United States Fire Administration National Fire Data Centre.

Vegvesen S (2006), "The Runehamar Test Tunnel", Norwegian Public Road Administration.

VTPL (2000), Pallets Specification Sheet – 800 x 1200, Virginia Tech Pallet Laboratory, http://www.intermost.ru/bureau/containers/euro.pdf, accessed 29 November 2006.

VTPL (2000a), Pallets Specification Sheet – 1000 x 1200, Virginia Tech Pallet Laboratory, www.iso.org/iso/en/commcentre/pdf/Pallets0008.pdf , accessed 29 November 2006.

Welburn and Nettancourt (2002), "El Azhar road tunnel – Cairo's new frontier", proceedings of ICE, Paper 12736, August 2002.

Watts J M (2003), "Probabilistic Fire Models", In *Fire Protection Handbook*, National Fire Protection Association (NFPA), Quincy MA, pp.3-97 to 3-103.

Watts J M and Hall J R (2006), "Introduction to Fire Risk Analysis", In *The SFPE handbook of Fire Protection Engineering*, Third Edition, NFPA, pp 5-1 – 5-7.

White M S et al (2000), "Pallets Move the World – The Need for International Pallets Standards" ,ISO Bulletin, Pallet & Container Research Laboratory, www.iso.org/iso/en/commcentre/pdf/Pallets0008.pdf, accessed 5 March 2007.

Wu Y (2007), "Control Smoke Flow in Tunnel During an Event of Fire", University of Sheffield, http://www.cufer21.re.kr/jboard/file_down.php?tid=11&file_name=521_1121669007.pdf, accessed 19 February 2007.

Yun Jiang (2006), "Decomposition, Ignition and Flame Spread on Furnishing Materials" PhD Thesis, Victoria University, Australia.

List of Personal Communication

Chuang Y J, National Taiwan University of Science and Technology, September 2007, personal email.

Ingason H, SP Swedish National Testing and research Institute, May 2007. By Email

LTA Veh Eng 2007, Land Transport Authority (vehicle engineering) , Higher Engineering Officer Leong Seng Fatt. By telephone call.

Nate Hoyt 2007,IDES support request reply from ChemPoint. 13 June 2007, By Email

SCDF 2006b, Singapore Civil Defence Force, Maj Yeo Geok Kuan of Ops Dept, January 2007. By Email

Wong C W, Parson Brinckerhoff Consultants Pte Ltd. By Email

APPENDIX A

Appendix A: Summary of fire in road tunnels

No	Years	Tunnel, length	Country	Vehicles at orgin of fire	Cause of fire	Duration	Consequences			Source
							People	Vehicles	Structural	
1	2007, 23 March	Burnley L = 3400 m	Australia	Collision between 2 truck	Collision	NA	3 dead 2 injured	3 trucks and 3 cars	NA	(Johnson and Barber 2007)
2	2005, 4 Jun	Frejus L = 12 900 m	France-Italy	1 HGV carrying tyres	Engine fire	NA	2 dead 21 injured	4 HGVs	10 km of equipment to be repaired	(Lonnermark 2005)
3	2004, 21 Feb	Frejus L = 12 900 m	France-Italy	HGV	Braking system caught fire	NA	none	HGV	closed for 2.5 h	(Carvel and Marlair 2005)
4	2004, 3 Feb	Kinkempois L = 600 m	Belgium	HGV	NA	NA	none	HGV	closed for a few days for cleaning and repair	(Carvel and Marlair 2005)
5	2004, 18 Jan	Dullin L = 1 500 m	France	Coach	Engine Compartment	NA	none	Coach	NA	(Carvel and Marlair 2005)
6	2003, 20 Dec	Golovec L = 700 m	Slovenia	Bus	NA	NA	None	Bus	None	(Carvel and Marlair 2005)
7	2003, 10 Nov	Floyfjell L = 3 100 m	Norway	Fire in car spread to the tunnel lining	Collision between car and wall	6 min	1 dead	1 car	NA	(Carvel and Marlair 2005)
8	2003, 25 July	Locica L = 800 m	Slovenia	1 HGV carrying a cargo of aluminium beams	HGV caught fire	NA	none	Cab and canvas destroyed	NA	(Carvel and Marlair 2005)
9	2002, 3 Nov	Homer L = 1 200 m	New Zealand	Coach	Flames coming from the motor at the rear of the vehicle	NA	3 treated for smoke inhalation	Coach	Coach wreckage blocked the tunnel	(Carvel and Marlair 2005)
10	2002, 19 May	Ted Williams L = 2 600 m	Boston, USA	Bus	Electrical compartment	NA	driver and passenger treated for smoke inhalation	Bus	None	(Carvel and Marlair 2005)
11	2002, 18 Jan	Tauern, 6 400 m	South-east of Salzburg, Austria	NA	Faulty Engine	NA	None	NA	NA	(Carvel and Marlair 2005)
12	2001, 24 Oct	St. Gotthard L = 16 900 m	Switzerland	Collision between 2 HGVs	Collision	2 days	11 dead	23 vehicles destroyed	Severe damage 250m	(Carvel and Marlair 2005) (Lonnermark 2005)
13	2001, 3 Sep	Gleinalim L = 8000 m	Graz, Austria	Coach	NA	NA	None	Coach	NA	(Carvel and Marlair 2005)

Appendix A

No	Years	Tunnel, length	Country	Vehicles at orgin of fire	Cause of fire	Duration	Consequences			Source
							People	Vehicles	Structural	
14	2001, 7 Aug	Gleinalim L = 8000 m	Graz, Austria	Car	Collision	NA	5 dead 4 injured	Car	NA	(Carvel and Marlair 2005)
15	2001, 10 Jul	Tauern, 6 400 m	South-east of Salzburg, Austria	Cars	Collision	NA	NA	NA	NA	(Carvel and Marlair 2005)
16	2001, 28 May	Prapontin	Italy	HGV	unknown	NA	14 treated for smoke inhalation	NA	NA	(Carvel and Marlair 2005)
17	2000, 27 Nov	Laerdal, 24 500 m	Norway	Bus (fire extinguished by driver)	NA	NA	NA	NA	NA	(Carvel and Marlair 2005)
18	2000, 24 Aug	Saukopftunnel = 2 700 m	Germany	Car at lay-by	NA	NA	none	1 car	NA	(Carvel and Marlair 2005)
19	2000, 14 Jul	Seljestad L = 1 300 m	Norway	Immediately after collision, 1 vehicle caught fire and spread to other vehicle	Multiple collision	NA	20 injuries	8 vehicles	NA	(Carvel and Marlair 2005)
20	2000, 29 May	Cross-harbour	Hong Kong	1 car caught fire	NA	30 mins	none	Car	tunnel reopen 1 hr later	(Carvel and Marlair 2005)
21	2000, 10 Jan	Tauern, 6 400 m	South-east of Salzburg, Austria	HGV	HGV	30 mins	NA	HGV	NA	(Carvel and Marlair 2005)
22	1999, 30 Aug	Munich, L = 252 m	Germany	Car	Car engine	NA	NA	NA	NA	(Carvel and Marlair 2005)
23	1999, 29 May	Tauern L = 6 400 m	South-east of Salzburg, Austria	HGV collide with stationary traffic	Multiple collision	15 h	8 dead	16 HGVs, 24 cars	NA	(Carvel and Marlair 2005)
24	1999, 24 Mar	Mont Blanc L = 11 600 m	France-Italy	HGV carrying a refrigeratored cargo of margarine and flour and car	diesel fuel leakage	53 h	39 dead	34 vehicles	Severe damageto the lining for 900 m, the tunnel closed for 3 years	(Carvel and Marlair 2005)
25	1998	Gleinalim L = 8 000m	Graz, Austria	Coach	Short Circuit	1 h	None	Coach	NA	(Carvel and Marlair 2005)
26	1997, 31 Oct	St. Gotthard L = 16 900 m	Switzerland	1 HGV loaded with cars	Engine overheated	3 h	1 injured	1 HGV with 8 cars it carry	Small damage	(Carvel and Marlair 2005)
27	1997, 17 Sep	St. Gotthard L = 16 900 m	Switzerland	Bus	Engine overheated	20 mins	None	Bus	NA	(Carvel and Marlair 2005)
28	1997, 13 Jan	Prapontin Tunnel = 4 900 m	Italy	1 HGV	Brakes oveheated	4 h	5 injured	1 HGV	spalling of concrete lining	(Carvel and Marlair 2005)

Appendix A

No	Years	Tunnel, length	Country	Vehicles at orgin of fire	Cause of fire	Duration	Consequences			Source
							People	Vehicles	Structural	
29	1996, 21 Aug	Ekeberg Tunnel = 1 500 m	Norway	Bus	Engine fire	2 h	none	Bus	NA	(Carvel and Marlair 2005)
30	1996, 18 Mar	Isola delle Femmine L = 150m	Sicilia, Italy	1 tanker with liquid gas and 1 little bus	Wet road collision of a bus with tanker (stopped because of previous collision), explosion	unknown	5 dead (by fire) 20 injured	1 tanker, 1 bus, 18 cars	Damage to the tunnel lining and lighting equipment	(PIARC 1995)
31	1995	Pfander L = 6719m	Austria	1 lorry, 1 van and 1 car	Collision	1 h	3 dead (by crash)	1 lorry, 1 van and 1 car	Serious damage to ceiling and equipment 50m, tunnel closed for 2.5 days	(PIARC 1995)
32	1995, 24 Jan	Hitra, L = 5 600 m	Norway	motor of mobile crane	Motor fire	2 h	none	Crane	NA	(Carvel and Marlair 2005)
33	1994, 15 Oct	Kingsway L = 2000m	UK, Liverpool	Bus	NA	1 h	NA	Bus	minior demage to tunnel	(Carvel and Marlair 2005)
34	1994	St. Gotthard L = 16 900 m	Goeschenen, Switzerland	1 lorry and trailer loaded with bikes wrapped in carton and plastic	Friction wheel/ loading bridge	2 h	none	1 lorry and trailer	Serious damage to ceiling, pavement and equipment 50m, tunnel closed for 2.5 days	(PIARC 1995)
35	1994, 14 Apr	Castellor L= 570 m	France	1 HGV loaded with waste paper	exploding tyres	NA	none	1 HGV	NA	(Carvel and Marlair 2005)
36	1994, 27 Feb	Huguenot L = 4 000 m	South Africa	Bus	Fire in gearbox	1 h	1 dead	bus	Damage to installations, tunnel reopen 4 day later	(Carvel and Marlair 2005)
37	1993, 13 June	Hovden L =1 300 m	Hoyanger, Norway	1 motor cycle, 2 cars	Front-rear collision	1 h 30 min	5 injured	1 motor cycle, 2 cars	significant tunnel demage	(Carvel and Marlair 2005)
38	1993	Serra a Ripoli L = 442m	Bologna, Italy	1 car and 1 lorry loaded with rolls of paper	Vehicle out of control and collision	2.5 h	4 dead 4 injured	4 lorries, 11 cars	Serious damage to lining	(PIARC 1995)

Appendix A

No	Years	Tunnel, length	Country	Vehicles at orgin of fire	Cause of fire	Duration	Consequences			Source
							People	Vehicles	Structural	
39	1983	Pecorila Galleria L = 662 m	Italy	Lorry with fish	Collision	NA	9 dead 22 injured	NA	NA	(Carvel and Marlair 2005)
40	1990, 19 Aug	Roldal L = 4 700 m	Norway	Transporter	Engine Overheating	NA	1 injured	Transporter	NA	(Carvel and Marlair 2005)
41	1990, 11 Jan	Mont Blanc L = 11 600m	France-Italy	HGV flame enter cab	NA	NA	2 injured	HGV	NA	(Carvel and Marlair 2005)
42	1988, 2 Sep	Mont Blanc L = 11 600 m	France-Italy	HGV	NA	NA	none	HGV	NA	(Carvel and Marlair 2005)
43	1987, 2 July	Tanzenberg = 2 400 m	Austria	1 car	Suicidal car crash into tunnel wall	NA	none	1 car	significant tunnel demage	(Carvel and Marlair 2005)
44	1987	Gumefens L = 340 m	Bern, Swizerland	1 lorry	mass collision on slippery road	2 h	2 dead	2 lorries and 1 van	slight demage	(PIARC 1995)
45	1986, 30 Dec	Herzogberg L = 2 000 m	Austria	HGV	Brakes overheating	20 mins	NA	NA	NA	(Carvel and Marlair 2005)
46	1986, 9 Sept	L'arme L = 1 100 m	France	Trailer and car	Collision	NA	3 dead 5 injured	Trailer and car	NA	(Carvel and Marlair 2005)
47	1984	Felbertauern L = 5 130 m	Austria	1 bus	blocking brakes	1 h 30 min	none	1 bus	Damage to ceiling and equipment for 100 m	(PIARC 1995)
48	1984, 2 Apr	St. Gotthard L = 16 321 m	Goeschenen, Switzerland	1 lorry loaded with rolls of plastic	fire in engine	24 min	none	1 lorry	Serious damage for 30m	(PIARC 1995)
49	1983	Frejus L = 12 858 m	Modane, France-Italy	1 lorry loaded with plastic materials	Gear box breaking	1 h 50 min	none	1 lorry	Serious damage for 200m	(PIARC 1995)
50	1982, 3 Nov	Salang	Afghanistan	Gas tanker	Tanker explosion	NA	> 176 dead	NA	NA	(Carvel and Marlair 2005)
51	1982	Caldecott L = 1 028 m	Oakland, USA	1 lorry, 1 coach and 1 car 33000 l of petrol	Front-back collision	2 h 40 min	7 dead 2 injured	3 lorries, 4 cars and 1 coach	Serious damage 580m	(PIARC 1995)
52	1981, 17 Sep	Mont Blanc L = 11 600 m	France-Italy	1 HGV - thick smoke from engine vehicle did not catch fire	Engine fire	NA	none	1 HGV	NA	(Carvel and Marlair 2005)
53	1980, 15 Jul	Sakai Tunnel L = 459 m	Japan	truck	Collision	3 h	5 dead 5 injured	10 vehicles	NA	(Carvel and Marlair 2005)
54	1980	Kajiwara L = 740m	Japan	1 truck (4 tons) with 3 600 l paint in 200 cans and 1 truck (10 tons)	Collision with side wall and over turning	NA	1 dead	1 truck (4 tons) and 1 truck (10 tons)	Damage for 280m	(PIARC 1995)

Appendix A

No	Years	Tunnel, length	Country	Vehicles at orgin of fire	Cause of fire	Duration	Consequences			Source
							People	Vehicles	Structural	
55	1979	Nihonzaka L = 2045m	Shizuoka, Japan	4 lorries and 2 cars	Front-back collision	4 days	7 dead 2 injured	127 lorries and 46 cars	Serious damage for 1 100m	(PIARC 1995)
56	1978	Velsen L = 770 m	Velsen Netherlands	2 lorries and 4 cars	Front-back collision	1 h 20 min	5 dead 5 injured	2 lorries and 4 cars	Serious damage for 30m	(PIARC 1995)
57	1978, 15 Apr	Mont Blanc L = 11 600 m	France-Italy	1 HGV	NA	NA	none	1 HGV	NA	(Carvel and Marlair 2005)
58	1978, 23 Mar	Baltimore Harbour	USA	Truck and fuel tanker	Collision	NA	NA	2 vehicle and 1 HGV	NA	(Carvel and Marlair 2005)
59	1976, 21 Sep	San Bernardino Tunnel L = 6 600 m	Switzerland	1 bus	NA	NA	none	1 bus	NA	(Carvel and Marlair 2005)
60	1976	B6 L = 430m	Paris - France	1 lorry with drums of 16 tons of polyster in bundles	unknown	1 h	12 slight injured smoke inhalation	1 lorry	Damage for 150m	(PIARC 1995)
61	1975, 14 Aug	Guadarrama L = 3 330m	Guadarrama, Spain	1 lorry loaded with tanks of pine resin	unknown	2 h 45 min	none	1 lorry	Serious damage for 210m	(PIARC 1995)
62	1974, 3 Apr	Chesapeake Bay	USA	1 HGV	exploding tyres	4 h	1 injured	1 HGV	NA	(Carvel and Marlair 2005)
63	1974, 28 Jan	Mont Blanc L = 11 600 m	France-Italy	HGV	NA	NA	NA	NA	NA	(Carvel and Marlair 2005)
64	1970	Wallace Tunnel L = 1 000 m	USA	1 camper truck	Engine fire	NA	none	1 camper truck	Little damage	(Carvel and Marlair 2005)
65	1968	Moorfleet L = 243 m	Hamburg, Germany	1 lorry trailer (14 tons of polyethene bags)	brakes overheating	1 h 30 min	none	1 trailer	Serious damage for 34m	(PIARC 1995)
66	1967, 6 Mar	Suzaka Tunnel L = 244m	Japan	1 truck (7 tons) loaded with about 600 polystyrene boxes and other combustible goods	Engine Compartment	11 h	2 injured	13 truck	NA	(Carvel and Marlair 2005)
67	1965	Blue Mountain L = 1300m	USA	1 truck carrying fish oil	Motor fire	NA	none	1 truck	NA	(Carvel and Marlair 2005)
68	1949, 13 May	Holland L = 2 550m	New York, USA	1 lorry loaded with 11 tons of carbon bisulfur	Load falling of HGV	4 h	66 injured smoke inhalation	10 lorries and 13 cars	Serious damage for 200m	(PIARC 1995)

APPENDIX B

Appendix B: Vehicles collision configuration for risk analysis approach for Chapter 8

Assumption made: Vehicles ignites at the same time and the vehicles collision heat release rate is the sum of the individual vehicle heat release rate taken from fire tests.

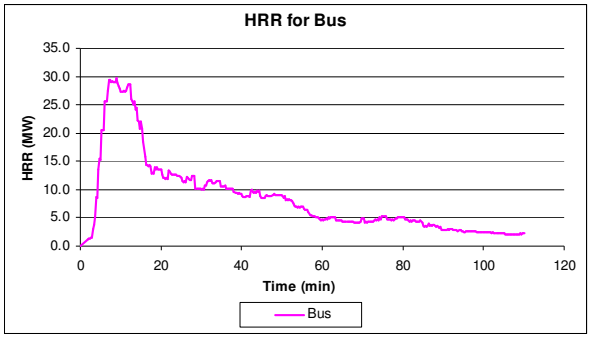

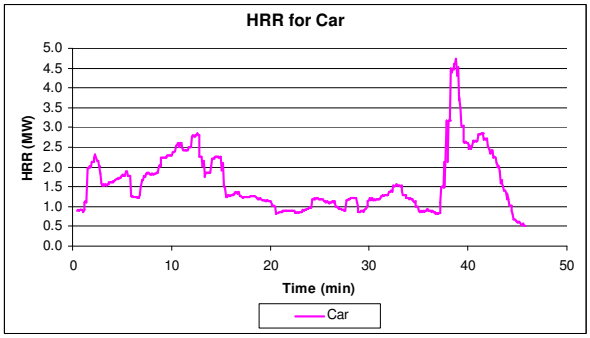

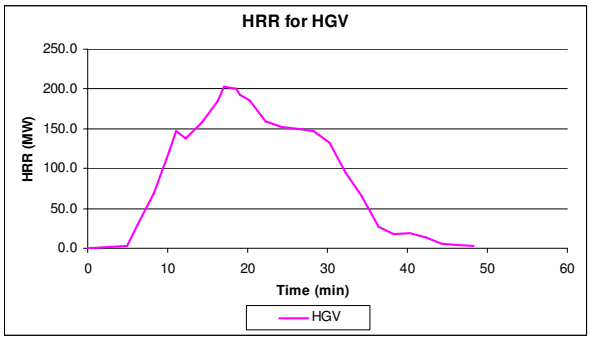

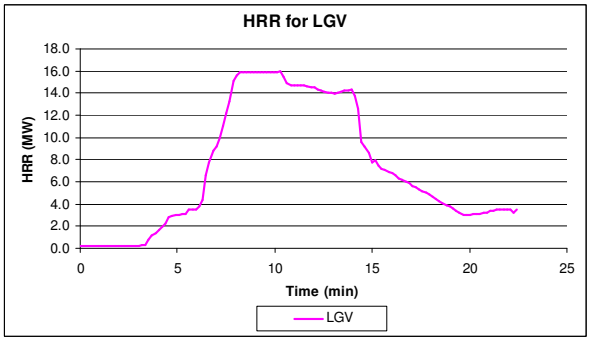

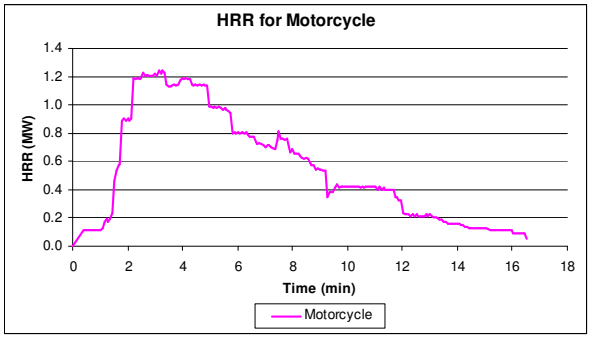

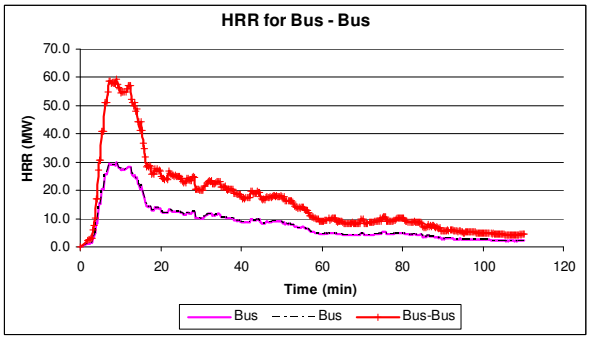

Appendix B

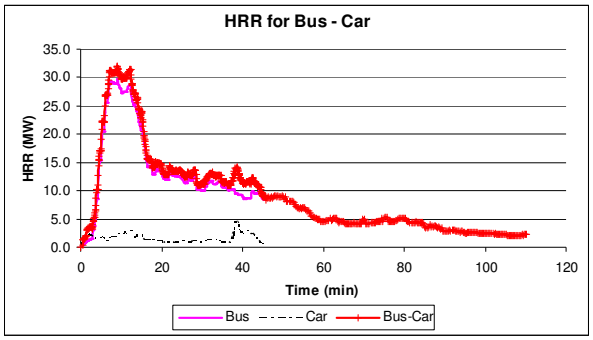
HRR for Bus - Car
HRR (MW)
Time (min)
Bus
Car
Bus-Car

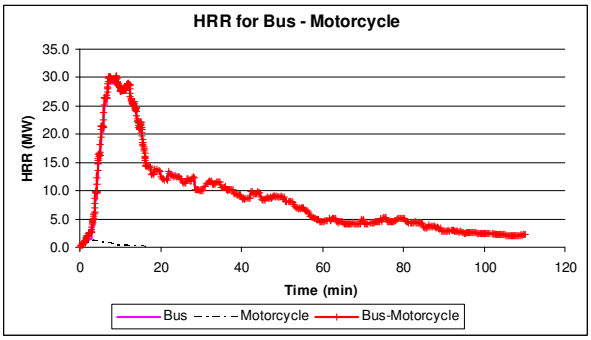
HRR for Bus - Motorcycle
HRR (MW)
Time (min)
Bus
Motorcycle
Bus-Motorcycle

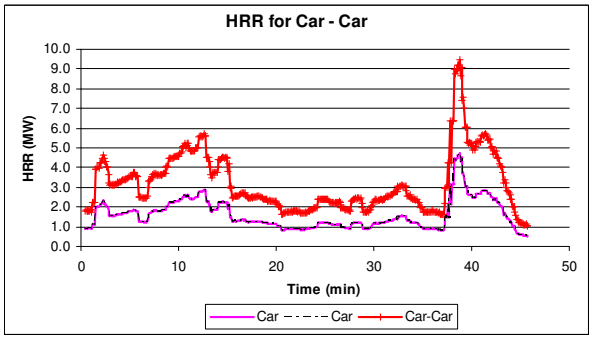
HRR for Car - Car
HRR (MW)
Time (min)
Car
Car
Car-Car

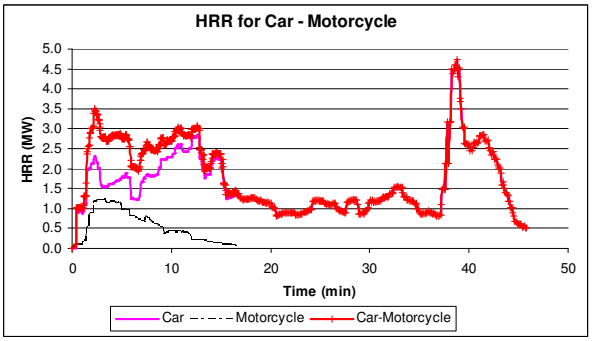
HRR for Car - Motorcycle
HRR (MW)
Time (min)
Car
Motorcycle
Car-Motorcycle

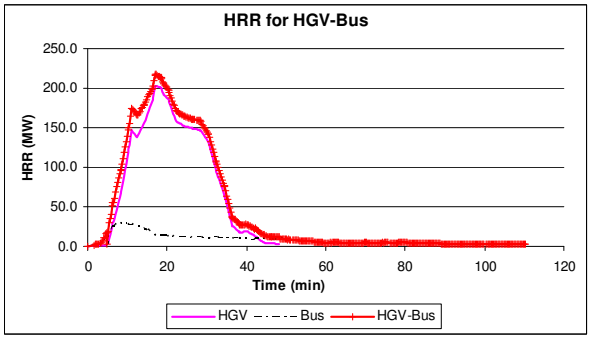
HRR for HGV-Bus
HRR (MW)
Time (min)
HGV
Bus
HGV-Bus

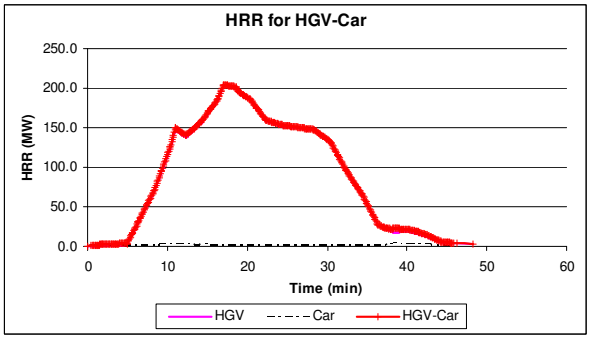
HRR for HGV-Car
HRR (MW)
Time (min)
HGV
Car
HGV-Car

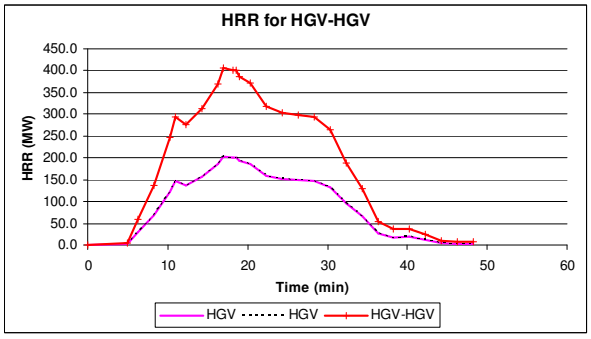
HRR for HGV-HGV
HRR (MW)
Time (min)
HGV
HGV
HGV-HGV

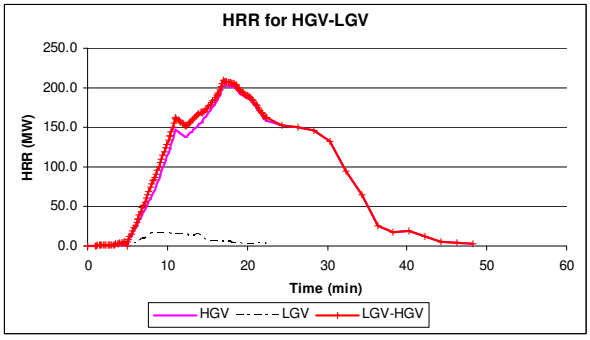
HRR for HGV-LGV
HRR (MW)
Time (min)
HGV
LGV
LGV-HGV

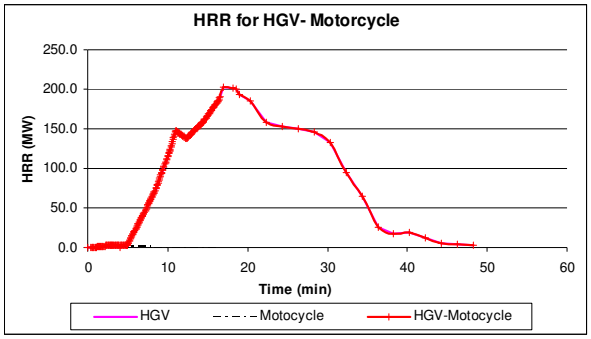
HRR for HGV- Motorcycle
HRR (MW)
250.0
200.0
150.0
100.0
50.0
0.0
0
10
20
30
40
50
60
Time (min)
HGV
Motocycle
HGV-Motocycle

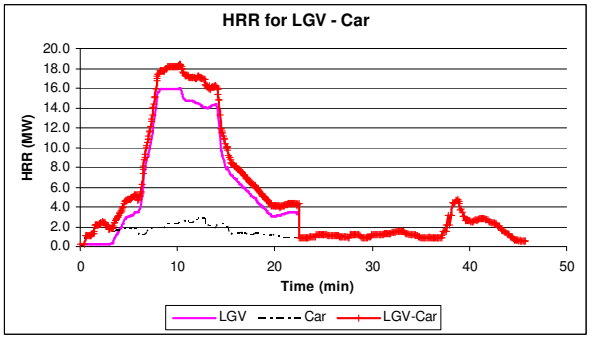
HRR for LGV - Car
HRR (MW)
20.0
18.0
16.0
14.0
12.0
10.0
8.0
6.0
4.0
2.0
0.0
0
10
20
30
40
50
Time (min)
LGV
Car
LGV-Car

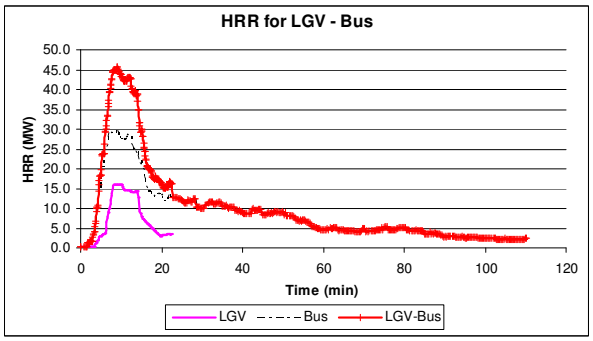
HRR for LGV - Bus
HRR (MW)
50.0
45.0
40.0
35.0
30.0
25.0
20.0
15.0
10.0
5.0
0.0
0
20
40
60
80
100
120
Time (min)
LGV
Bus
LGV-Bus

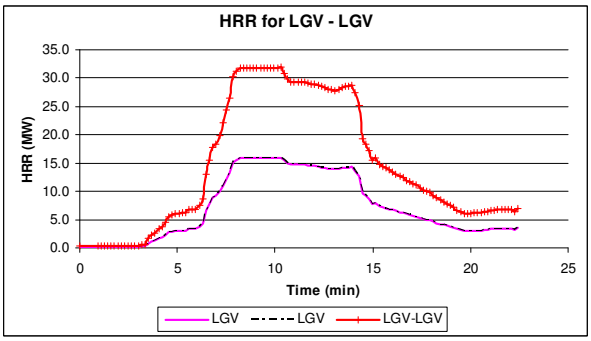
HRR for LGV - LGV
HRR (MW)
35.0
30.0
25.0
20.0
15.0
10.0
5.0
0.0
0
5
10
15
20
25
Time (min)
LGV
LGV
LGV-LGV

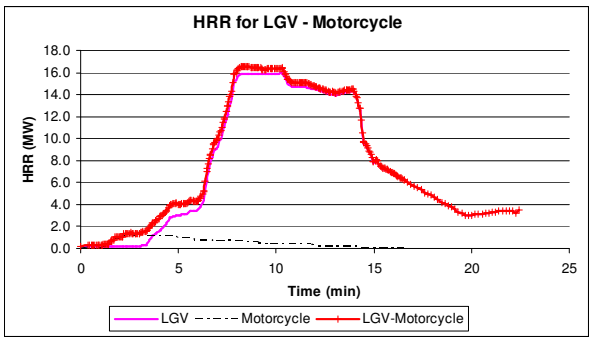
HRR for LGV - Motorcycle
HRR (MW)
18.0
16.0
14.0
12.0
10.0
8.0
6.0
4.0
2.0
0.0
0
5
10
15
20
25
Time (min)
LGV
Motorcycle
LGV-Motorcycle

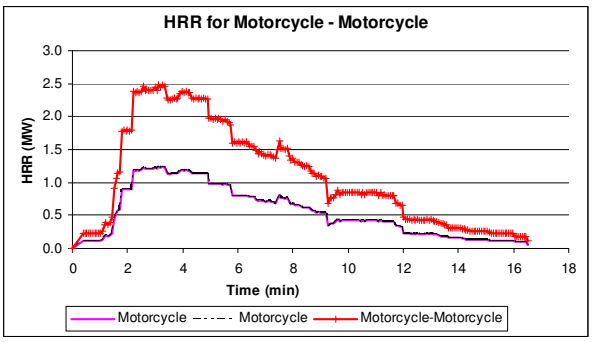
HRR for Motorcycle - Motorcycle
HRR (MW)
3.0
2.5
2.0
1.5
1.0
0.5
0.0
0
2
4
6
8
10
12
14
16
18
Time (min)
Motorcycle
Motorcycle
Motorcycle-Motorcycle

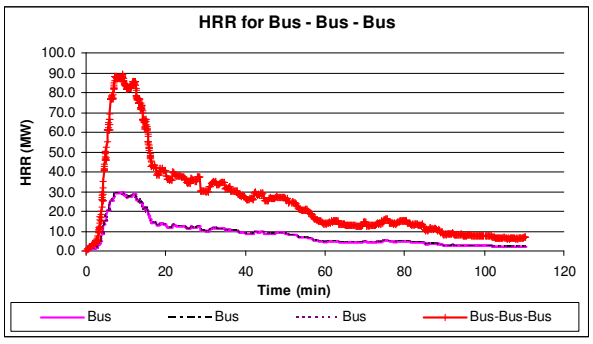
HRR for Bus - Bus - Bus
HRR (MW)
100.0
90.0
80.0
70.0
60.0
50.0
40.0
30.0
20.0
10.0
0.0
0
20
40
60
80
100
120
Time (min)
Bus
Bus
Bus
Bus-Bus-Bus

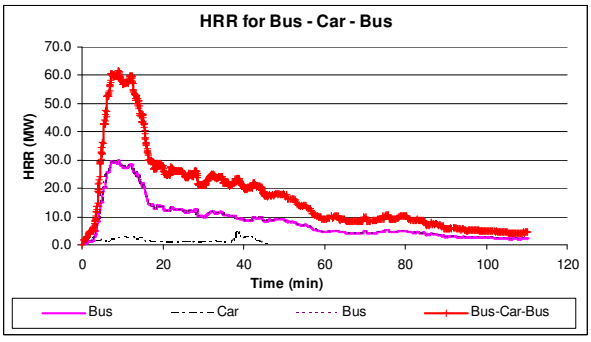
HRR for Bus - Car - Bus
HRR (MW)
70.0
60.0
50.0
40.0
30.0
20.0
10.0
0.0
0
20
40
60
80
100
120
Time (min)
Bus
Car
Bus
Bus-Car-Bus

Appendix B

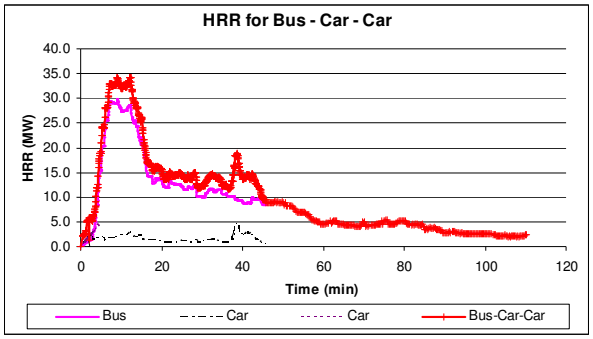
HRR for Bus - Car - Car
HRR (MW)
Time (min)
Bus
Car
Car
Bus-Car-Car

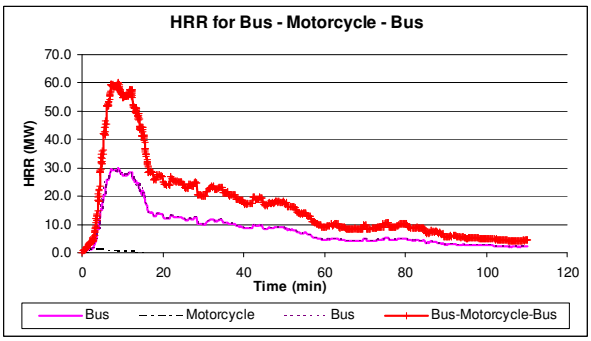
HRR for Bus - Motorcycle - Bus
HRR (MW)
Time (min)
Bus
Motorcycle
Bus
Bus-Motorcycle-Bus

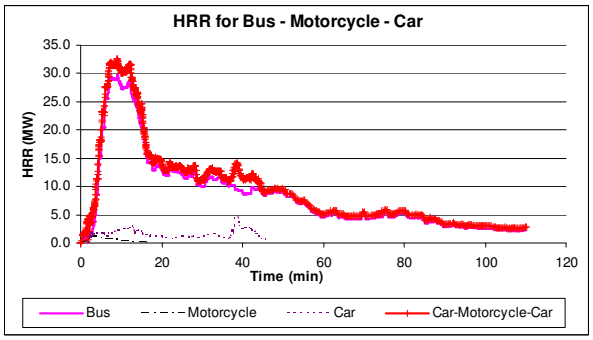
HRR for Bus - Motorcycle - Car
HRR (MW)
Time (min)
Bus
Motorcycle
Car
Car-Motorcycle-Car

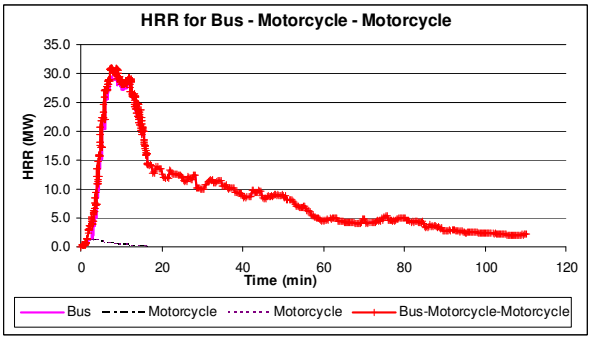
HRR for Bus - Motorcycle - Motorcycle
HRR (MW)
Time (min)
Bus
Motorcycle
Motorcycle
Bus-Motorcycle-Motorcycle

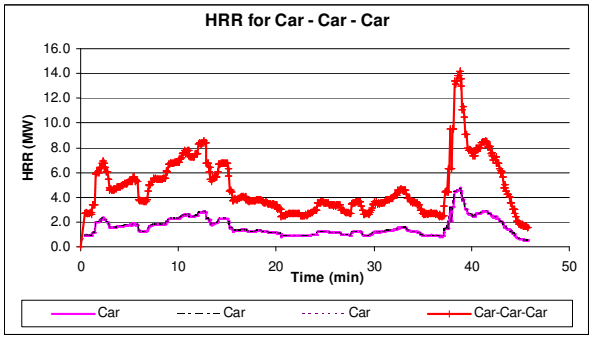
HRR for Car - Car - Car
HRR (MW)
Time (min)
Car
Car
Car
Car-Car-Car

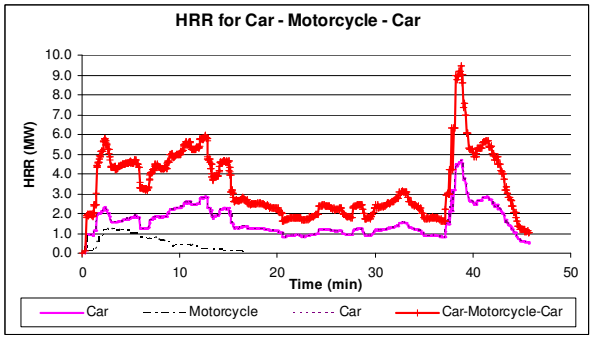
HRR for Car - Motorcycle - Car
HRR (MW)
Time (min)
Car
Motorcycle
Car
Car-Motorcycle-Car

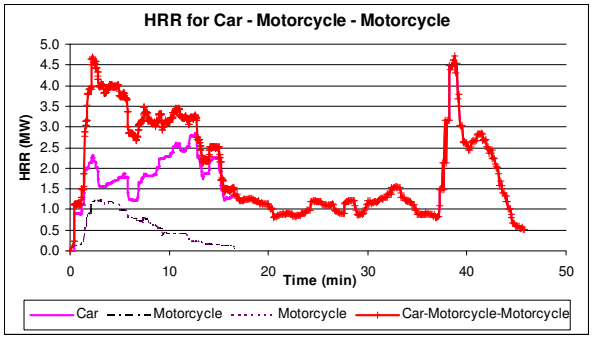
HRR for Car - Motorcycle - Motorcycle
HRR (MW)
Time (min)
Car
Motorcycle
Motorcycle
Car-Motorcycle-Motorcycle

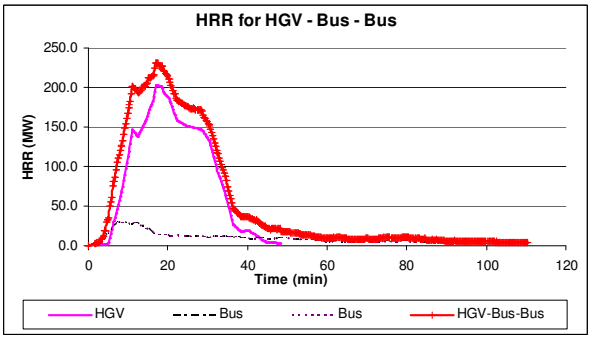
HRR for HGV - Bus - Bus
HRR (MW)
Time (min)
HGV
Bus
Bus
HGV-Bus-Bus

Appendix B

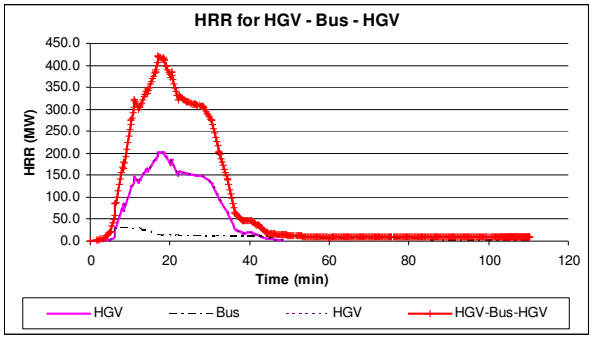
HRR for HGV - Bus - HGV
HRR (MW)
Time (min)
HGV
Bus
HGV
HGV-Bus-HGV

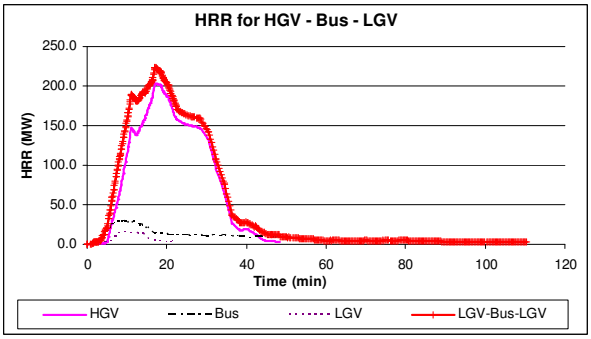
HRR for HGV - Bus - LGV
HRR (MW)
Time (min)
HGV
Bus
LGV
LGV-Bus-LGV

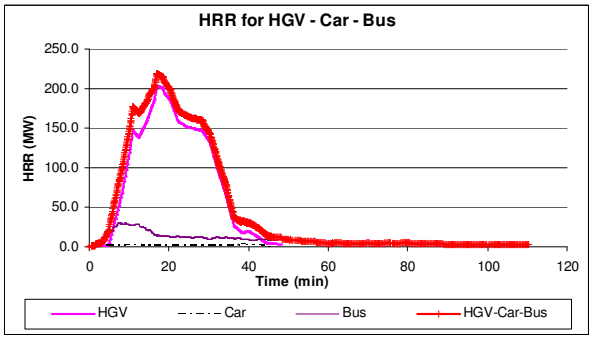
HRR for HGV - Car - Bus
HRR (MW)
Time (min)
HGV
Car
Bus
HGV-Car-Bus

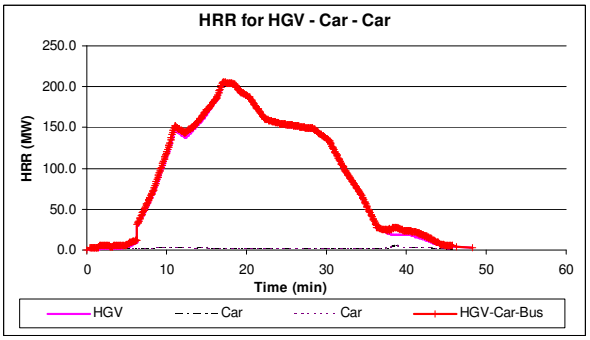
HRR for HGV - Car - Car
HRR (MW)
Time (min)
HGV
Car
Car
HGV-Car-Bus

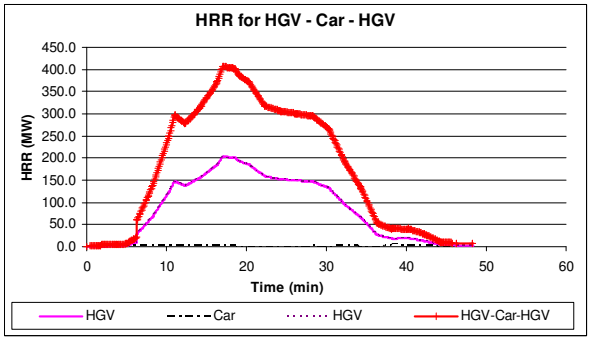
HRR for HGV - Car - HGV
HRR (MW)
Time (min)
HGV
Car
HGV
HGV-Car-HGV

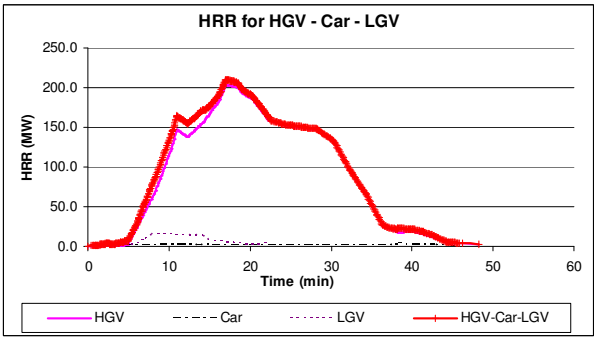
HRR for HGV - Car - LGV
HRR (MW)
Time (min)
HGV
Car
LGV
HGV-Car-LGV

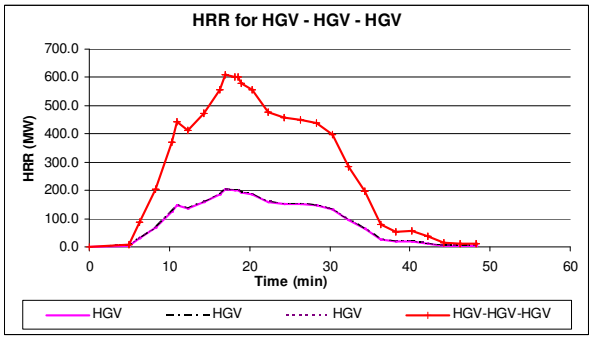
HRR for HGV - HGV - HGV
HRR (MW)
Time (min)
HGV
HGV
HGV
HGV-HGV-HGV

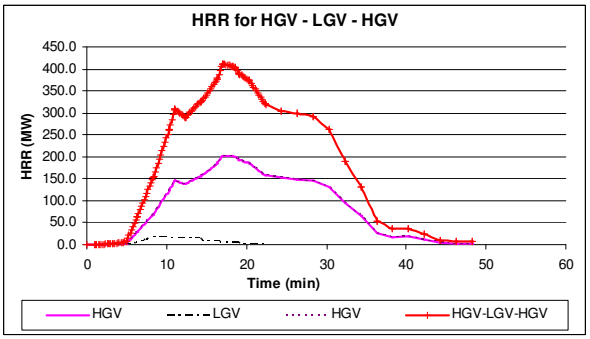
HRR for HGV - LGV - HGV
HRR (MW)
Time (min)
HGV
LGV
HGV
HGV-LGV-HGV

Appendix B

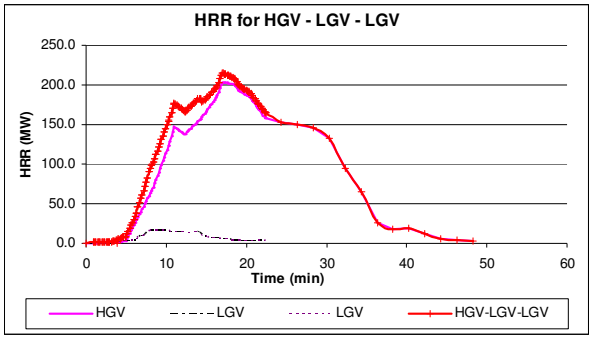
HRR for HGV - LGV - LGV
HRR (MW)
Time (min)
HGV
LGV
LGV
HGV-LGV-LGV

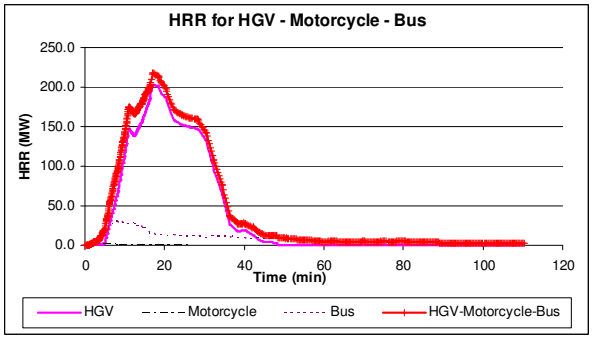
HRR for HGV - Motorcycle - Bus
HRR (MW)
Time (min)
HGV
Motorcycle
Bus
HGV-Motorcycle-Bus

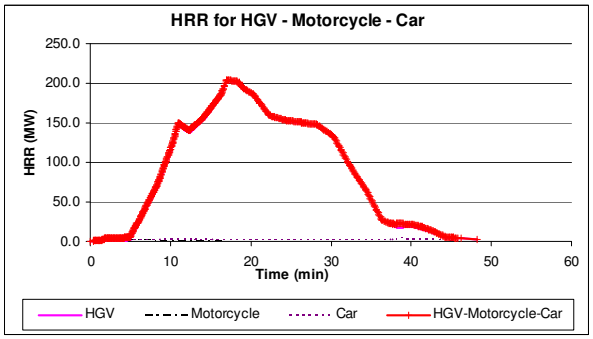
HRR for HGV - Motorcycle - Car
HRR (MW)
Time (min)
HGV
Motorcycle
Car
HGV-Motorcycle-Car

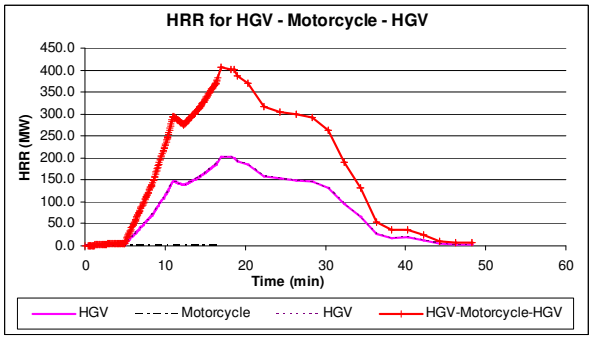
HRR for HGV - Motorcycle - HGV
HRR (MW)
Time (min)
HGV
Motorcycle
HGV
HGV-Motorcycle-HGV

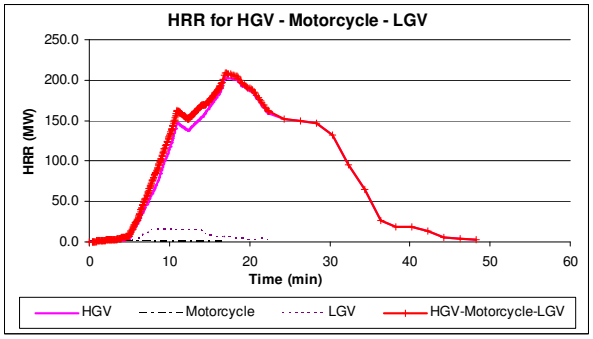
HRR for HGV - Motorcycle - LGV
HRR (MW)
Time (min)
HGV
Motorcycle
LGV
HGV-Motorcycle-LGV

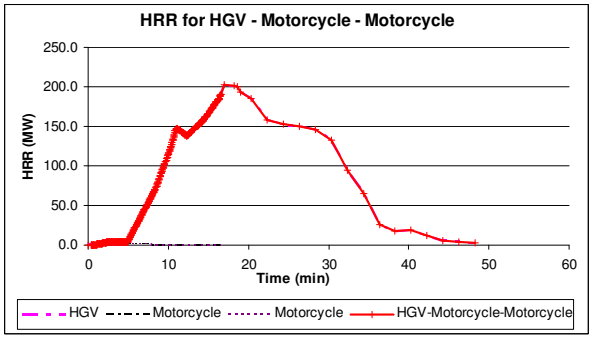
HRR for HGV - Motorcycle - Motorcycle
HRR (MW)
Time (min)
HGV
Motorcycle
Motorcycle
HGV-Motorcycle-Motorcycle

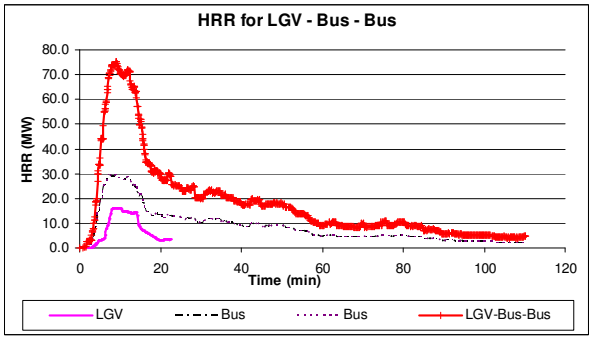
HRR for LGV - Bus - Bus
HRR (MW)
Time (min)
LGV
Bus
Bus
LGV-Bus-Bus

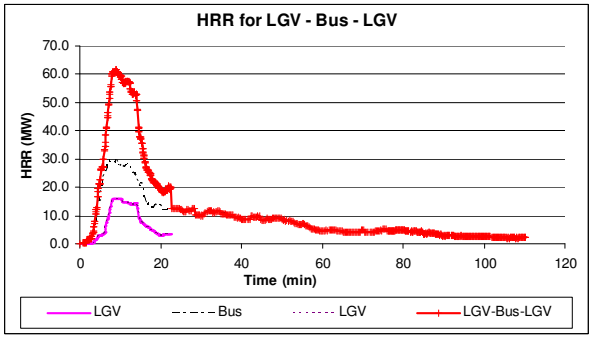
HRR for LGV - Bus - LGV
HRR (MW)
Time (min)
LGV
Bus
LGV
LGV-Bus-LGV

Appendix B

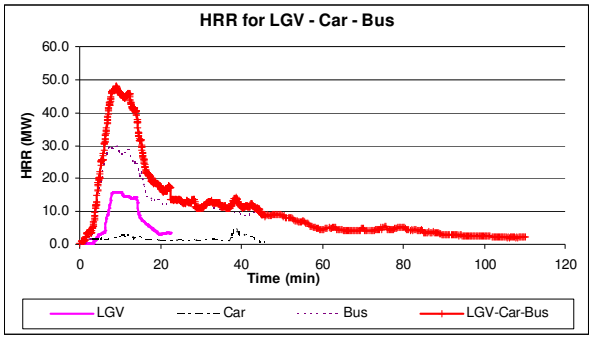
HRR for LGV - Car - Bus
HRR (MW)
Time (min)
LGV
Car
Bus
LGV-Car-Bus

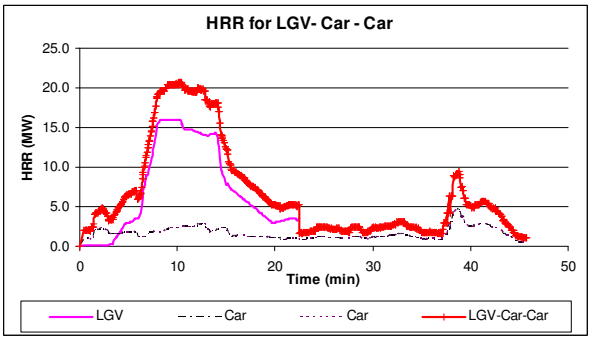
HRR for LGV- Car - Car
HRR (MW)
Time (min)
LGV
Car
Car
LGV-Car-Car

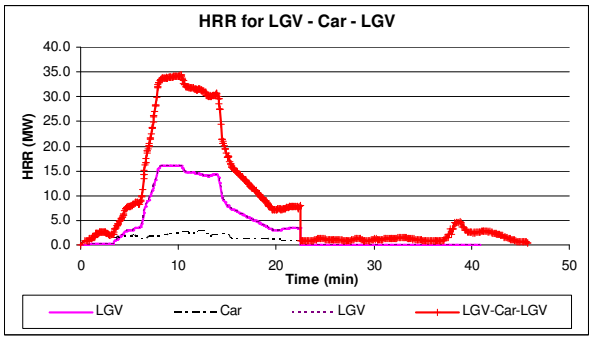
HRR for LGV - Car - LGV
HRR (MW)
Time (min)
LGV
Car
LGV
LGV-Car-LGV

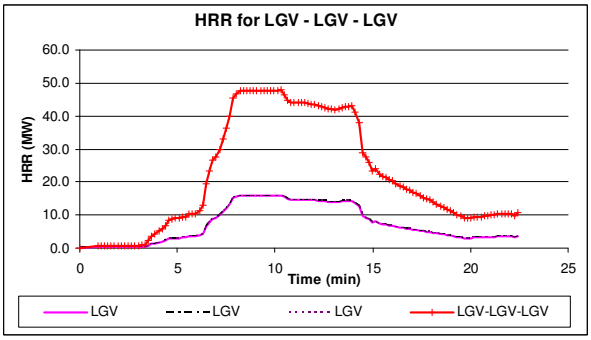
HRR for LGV - LGV - LGV
HRR (MW)
Time (min)
LGV
LGV
LGV
LGV-LGV-LGV

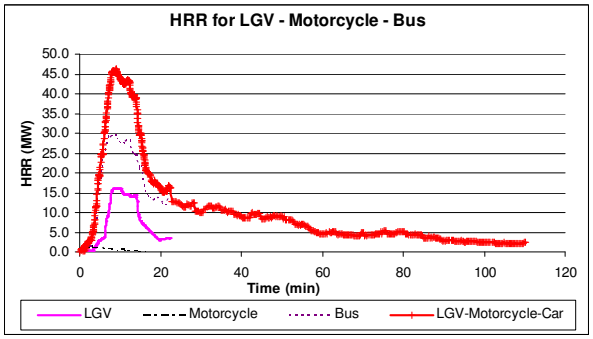
HRR for LGV - Motorcycle - Bus
HRR (MW)
Time (min)
LGV
Motorcycle
Bus
LGV-Motorcycle-Car

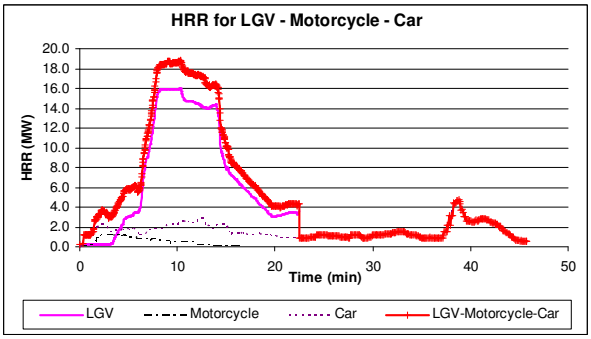
HRR for LGV - Motorcycle - Car
HRR (MW)
Time (min)
LGV
Motorcycle
Car
LGV-Motorcycle-Car

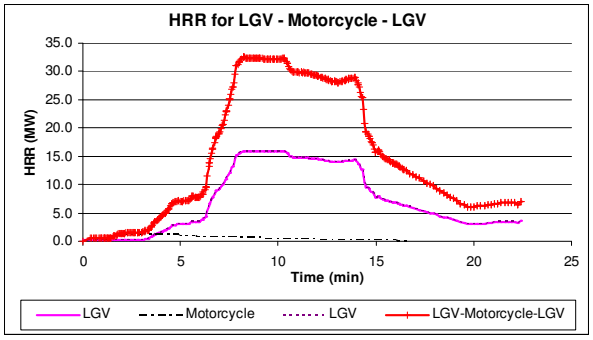
HRR for LGV - Motorcycle - LGV
HRR (MW)
Time (min)
LGV
Motorcycle
LGV
LGV-Motorcycle-LGV

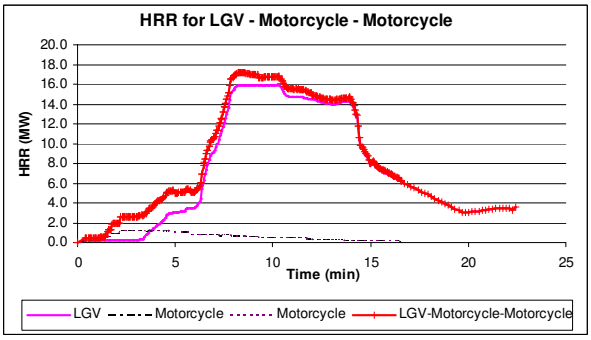
HRR for LGV - Motorcycle - Motorcycle
HRR (MW)
Time (min)
LGV
Motorcycle
Motorcycle
LGV-Motorcycle-Motorcycle

Appendix B

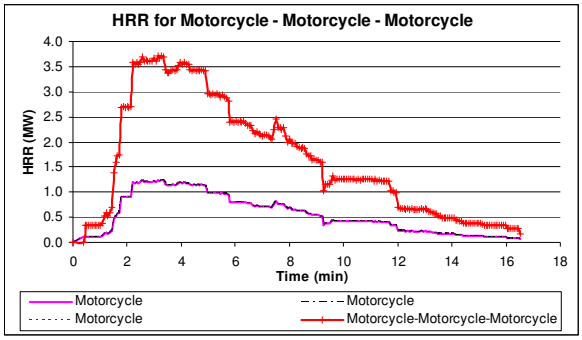
HRR for Motorcycle - Motorcycle - Motorcycle
HRR (MW)
Time (min)
Motorcycle
Motorcycle
Motorcycle
Motorcycle-Motorcycle-Motorcycle

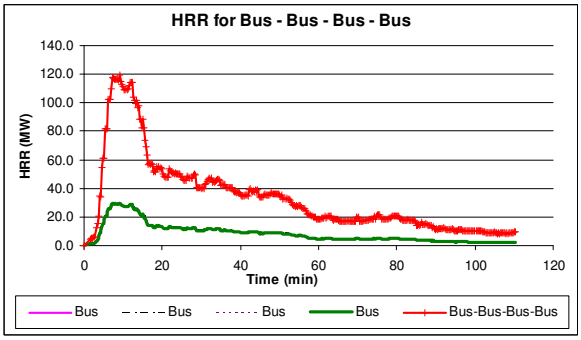
HRR for Bus - Bus - Bus - Bus
HRR (MW)
Time (min)
Bus
Bus
Bus
Bus
Bus-Bus-Bus-Bus

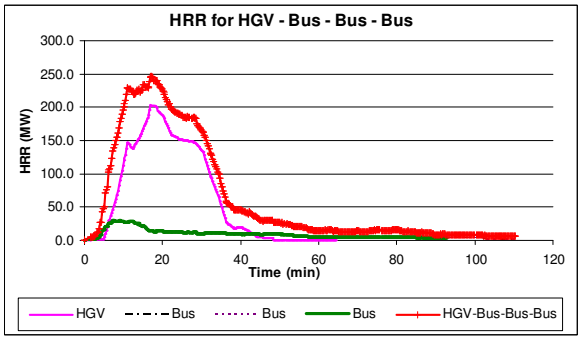
HRR for HGV - Bus - Bus - Bus
HRR (MW)
Time (min)
HGV
Bus
Bus
Bus
HGV-Bus-Bus-Bus

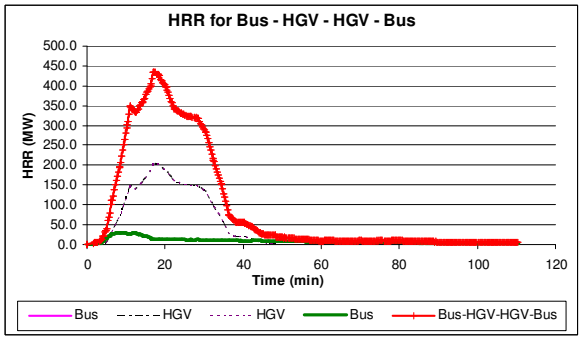
HRR for Bus - HGV - HGV - Bus
HRR (MW)
Time (min)
Bus
HGV
HGV
Bus
Bus-HGV-HGV-Bus

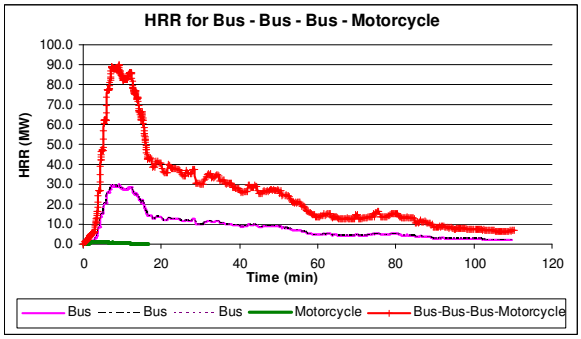
HRR for Bus - Bus - Bus - Motorcycle
HRR (MW)
Time (min)
Bus
Bus
Bus
Motorcycle
Bus-Bus-Bus-Motorcycle

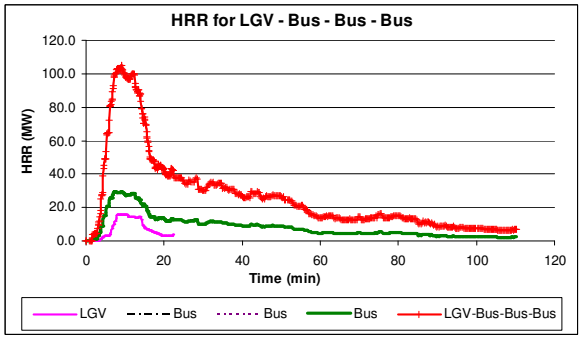
HRR for LGV - Bus - Bus - Bus
HRR (MW)
Time (min)
LGV
Bus
Bus
Bus
LGV-Bus-Bus-Bus

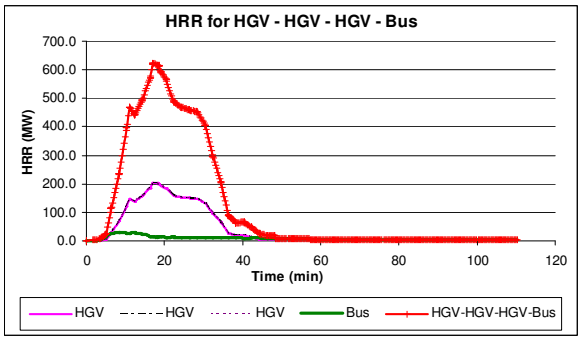
HRR for HGV - HGV - HGV - Bus
HRR (MW)
Time (min)
HGV
HGV
HGV
Bus
HGV-HGV-HGV-Bus

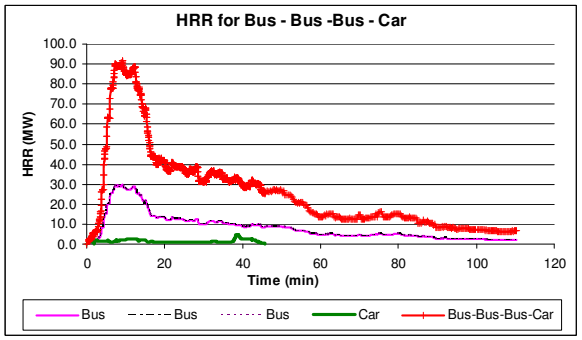
HRR for Bus - Bus -Bus - Car
HRR (MW)
Time (min)
Bus
Bus
Bus
Car
Bus-Bus-Bus-Car

Appendix B

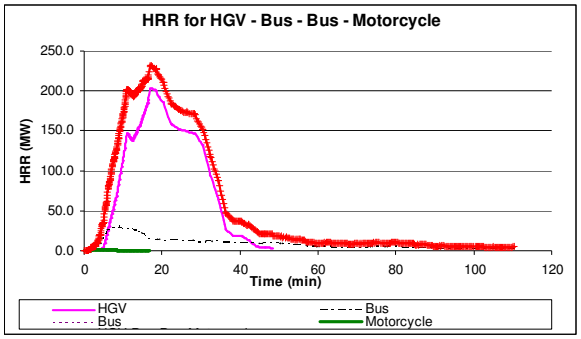
HRR for HGV - Bus - Bus - Motorcycle
HRR (MW)
Time (min)
HGV
Bus
Bus
Motorcycle

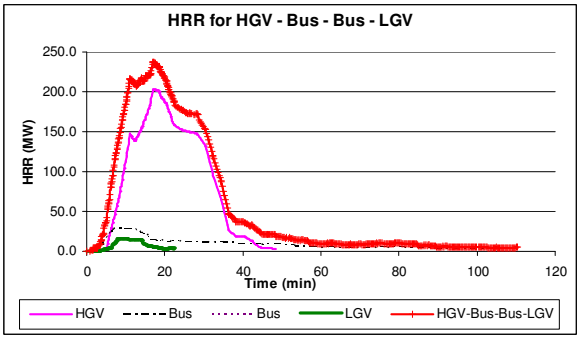
HRR for HGV - Bus - Bus - LGV
HRR (MW)
Time (min)
HGV
Bus
Bus
LGV
HGV-Bus-Bus-LGV

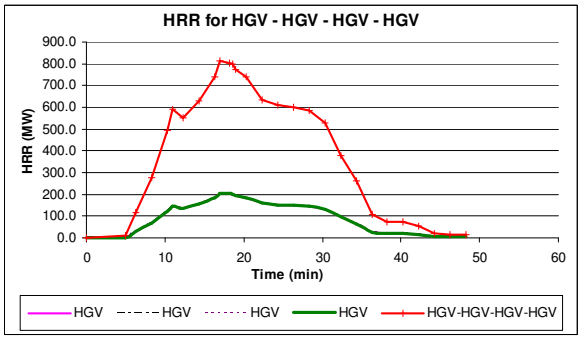
HRR for HGV - HGV - HGV - HGV
HRR (MW)
Time (min)
HGV
HGV
HGV
HGV
HGV-HGV-HGV-HGV

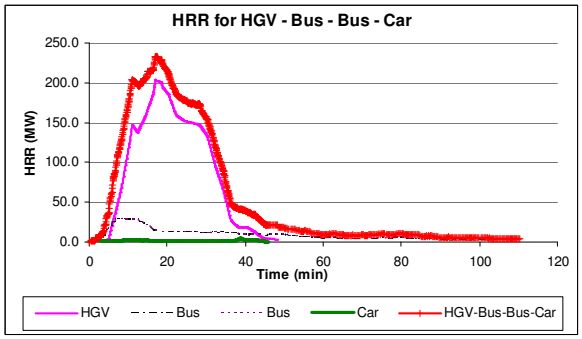
HRR for HGV - Bus - Bus - Car
HRR (MW)
Time (min)
HGV
Bus
Bus
Car
HGV-Bus-Bus-Car

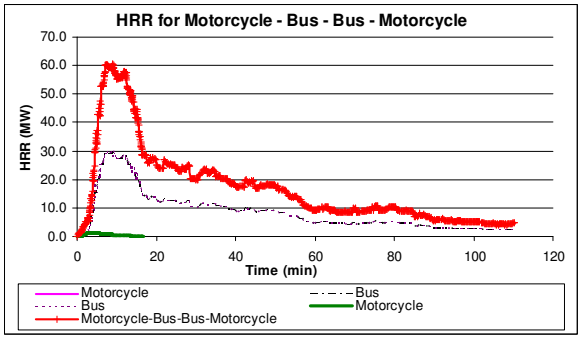
HRR for Motorcycle - Bus - Bus - Motorcycle
HRR (MW)
Time (min)
Motorcycle
Bus
Bus
Motorcycle
Motorcycle-Bus-Bus-Motorcycle

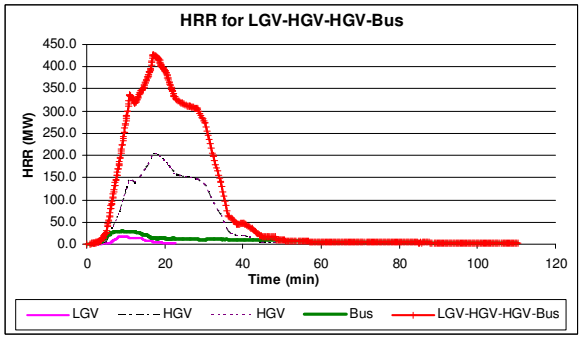
HRR for LGV-HGV-HGV-Bus
HRR (MW)
Time (min)
LGV
HGV
HGV
Bus
LGV-HGV-HGV-Bus

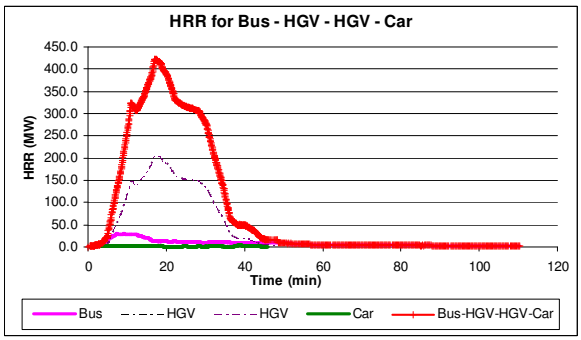
HRR for Bus - HGV - HGV - Car
HRR (MW)
Time (min)
Bus
HGV
HGV
Car
Bus-HGV-HGV-Car

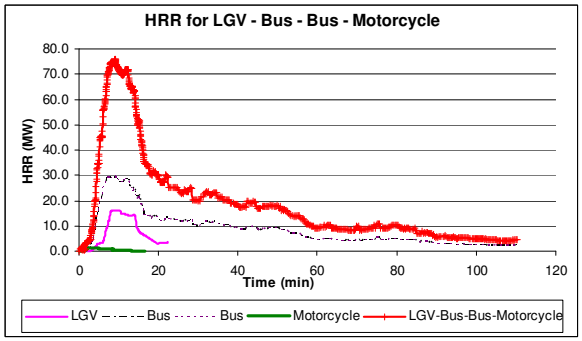
HRR for LGV - Bus - Bus - Motorcycle
HRR (MW)
Time (min)
LGV
Bus
Bus
Motorcycle
LGV-Bus-Bus-Motorcycle

Appendix B

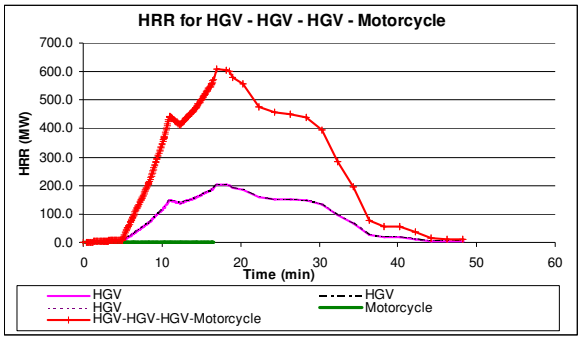
HRR for HGV - HGV - HGV - Motorcycle
HRR (MW)
Time (min)
HGV
HGV
HGV
Motorcycle
HGV-HGV-HGV-Motorcycle

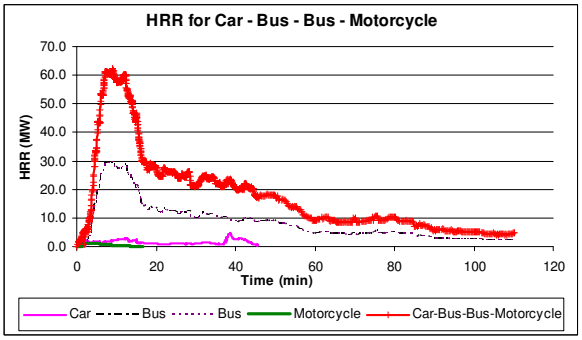
HRR for Car - Bus - Bus - Motorcycle
HRR (MW)
Time (min)
Car
Bus
Bus
Motorcycle
Car-Bus-Bus-Motorcycle

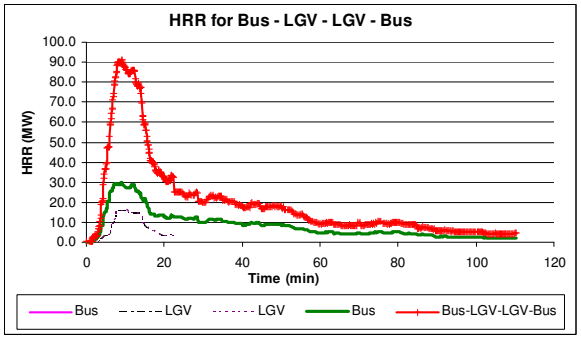
HRR for Bus - LGV - LGV - Bus
HRR (MW)
Time (min)
Bus
LGV
LGV
Bus
Bus-LGV-LGV-Bus

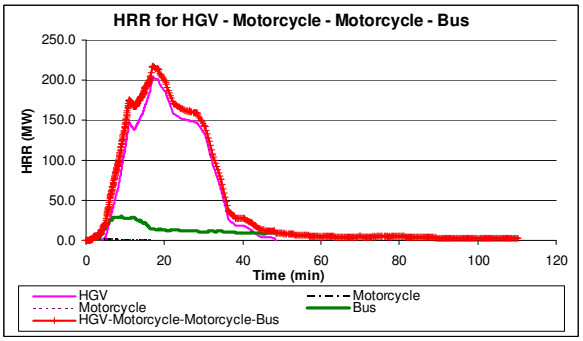
HRR for HGV - Motorcycle - Motorcycle - Bus
HRR (MW)
Time (min)
HGV
Motorcycle
Motorcycle
Bus
HGV-Motorcycle-Motorcycle-Bus

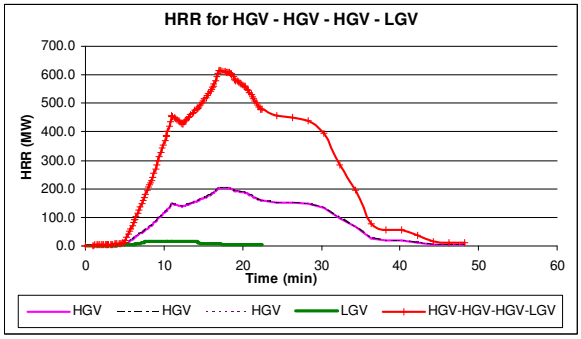
HRR for HGV - HGV - HGV - LGV
HRR (MW)
Time (min)
HGV
HGV
HGV
LGV
HGV-HGV-HGV-LGV

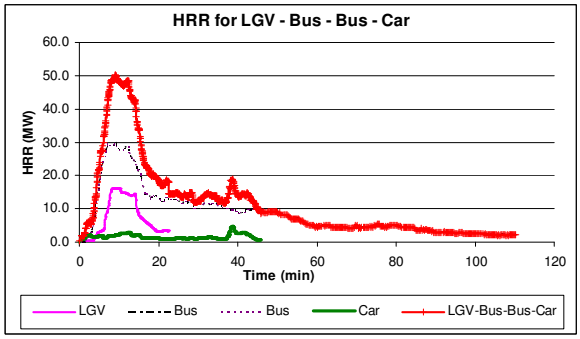
HRR for LGV - Bus - Bus - Car
HRR (MW)
Time (min)
LGV
Bus
Bus
Car
LGV-Bus-Bus-Car

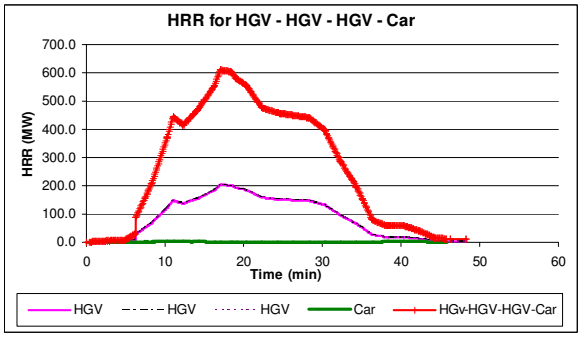
HRR for HGV - HGV - HGV - Car
HRR (MW)
Time (min)
HGV
HGV
HGV
Car
HGv-HGV-HGV-Car

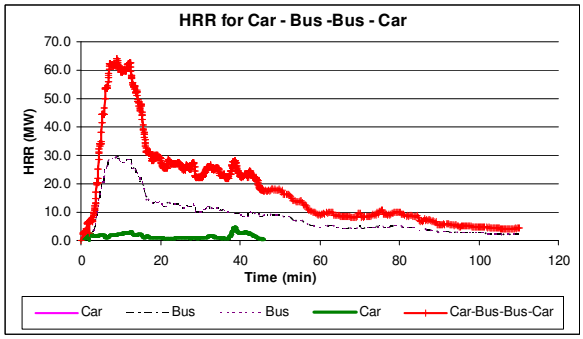
HRR for Car - Bus -Bus - Car
HRR (MW)
Time (min)
Car
Bus
Bus
Car
Car-Bus-Bus-Car

Appendix B

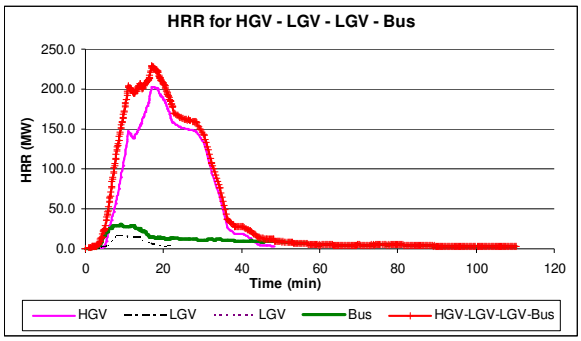
HRR for HGV - LGV - LGV - Bus
HRR (MW)
Time (min)
HGV
LGV
LGV
Bus
HGV-LGV-LGV-Bus

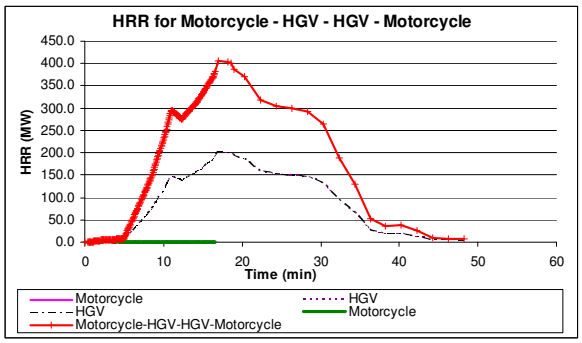
HRR for Motorcycle - HGV - HGV - Motorcycle
HRR (MW)
Time (min)
Motorcycle
HGV
HGV
Motorcycle
Motorcycle-HGV-HGV-Motorcycle

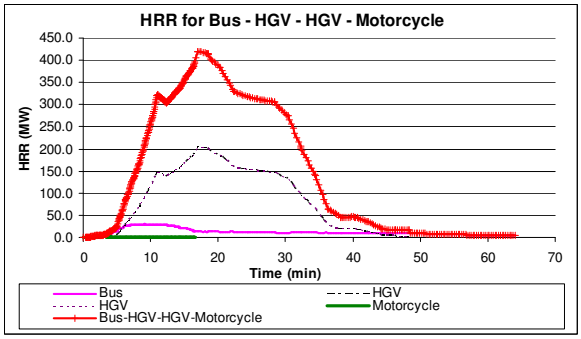
HRR for Bus - HGV - HGV - Motorcycle
HRR (MW)
Time (min)
Bus
HGV
HGV
Motorcycle
Bus-HGV-HGV-Motorcycle

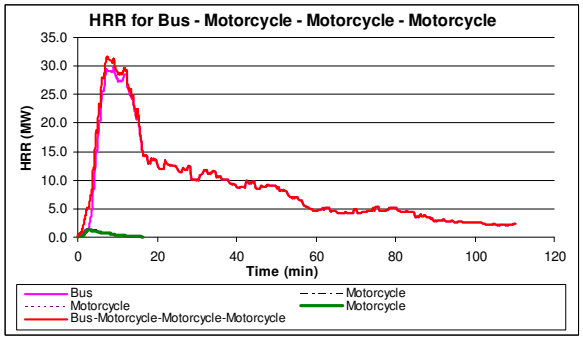
HRR for Bus - Motorcycle - Motorcycle - Motorcycle
HRR (MW)
Time (min)
Bus
Motorcycle
Motorcycle
Motorcycle
Bus-Motorcycle-Motorcycle-Motorcycle

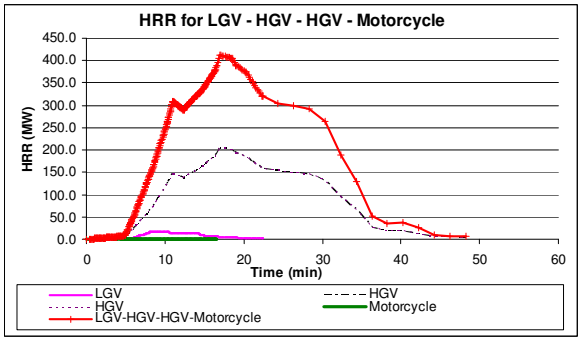
HRR for LGV - HGV - HGV - Motorcycle
HRR (MW)
Time (min)
LGV
HGV
HGV
Motorcycle
LGV-HGV-HGV-Motorcycle

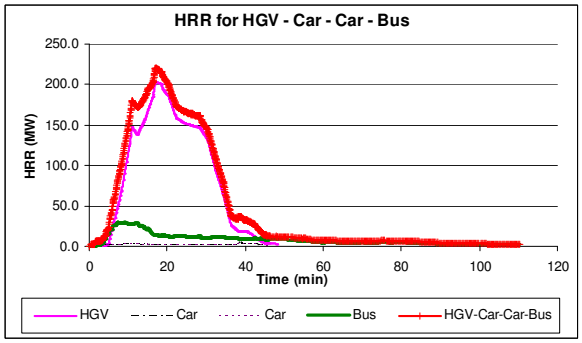
HRR for HGV - Car - Car - Bus
HRR (MW)
Time (min)
HGV
Car
Car
Bus
HGV-Car-Car-Bus

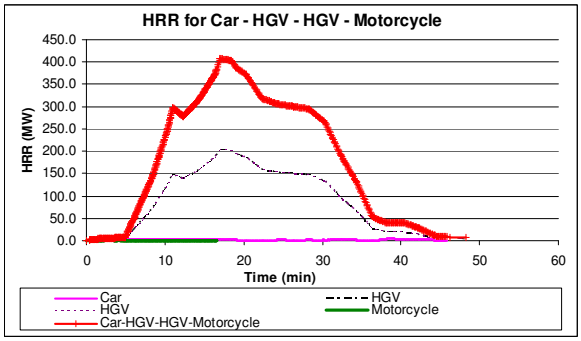
HRR for Car - HGV - HGV - Motorcycle
HRR (MW)
Time (min)
Car
HGV
HGV
Motorcycle
Car-HGV-HGV-Motorcycle

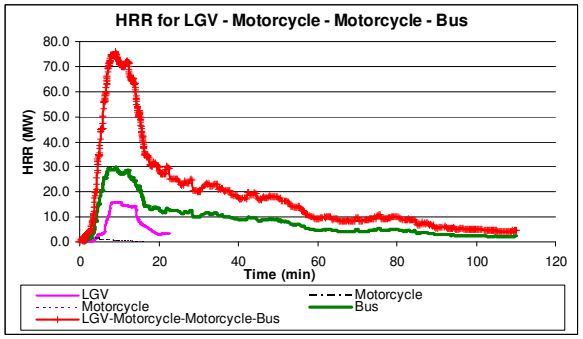
HRR for LGV - Motorcycle - Motorcycle - Bus
HRR (MW)
Time (min)
LGV
Motorcycle
Motorcycle
Bus
LGV-Motorcycle-Motorcycle-Bus

Appendix B

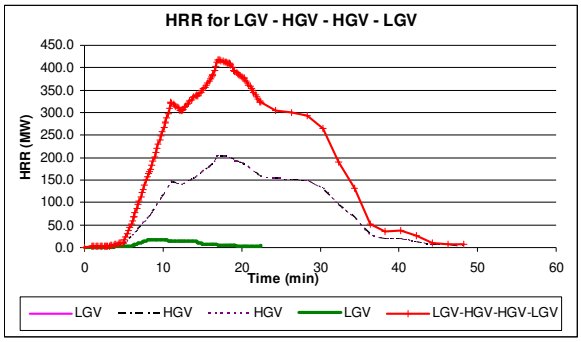
HRR for LGV - HGV - HGV - LGV
HRR (MW)
Time (min)
LGV
HGV
HGV
LGV
LGV-HGV-HGV-LGV

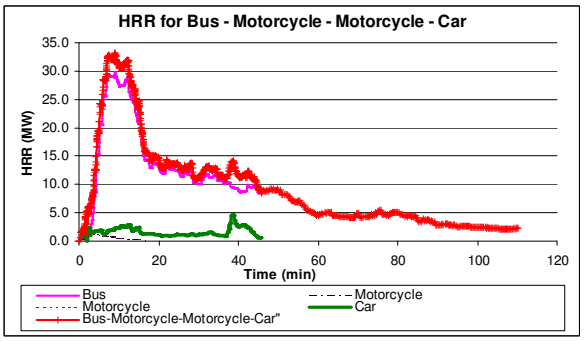
HRR for Bus - Motorcycle - Motorcycle - Car
HRR (MW)
Time (min)
Bus
Motorcycle
Motorcycle
Car
Bus-Motorcycle-Motorcycle-Car"

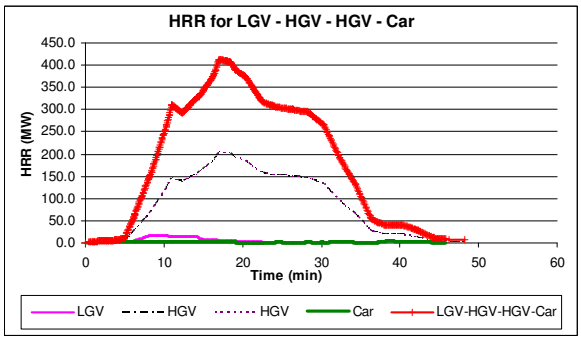
HRR for LGV - HGV - HGV - Car
HRR (MW)
Time (min)
LGV
HGV
HGV
Car
LGV-HGV-HGV-Car

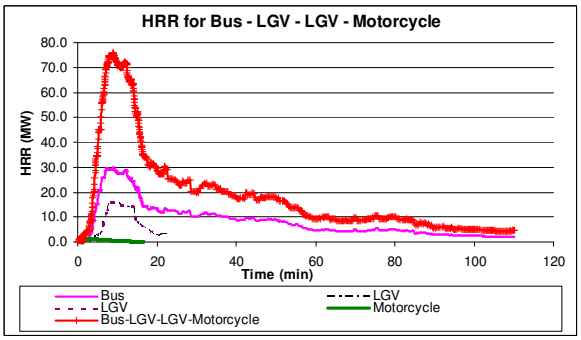
HRR for Bus - LGV - LGV - Motorcycle
HRR (MW)
Time (min)
Bus
LGV
LGV
Motorcycle
Bus-LGV-LGV-Motorcycle

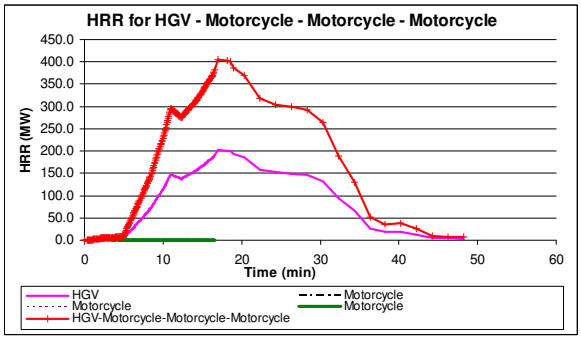
HRR for HGV - Motorcycle - Motorcycle - Motorcycle
HRR (MW)
Time (min)
HGV
Motorcycle
Motorcycle
Motorcycle
HGV-Motorcycle-Motorcycle-Motorcycle

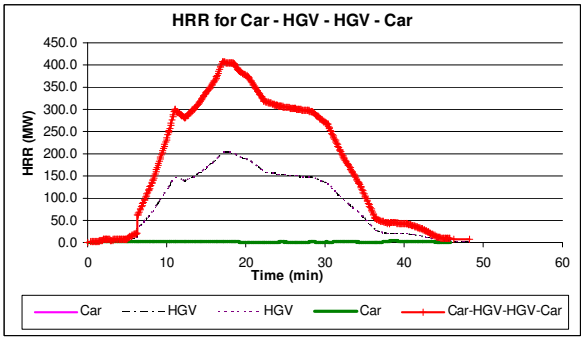
HRR for Car - HGV - HGV - Car
HRR (MW)
Time (min)
Car
HGV
HGV
Car
Car-HGV-HGV-Car

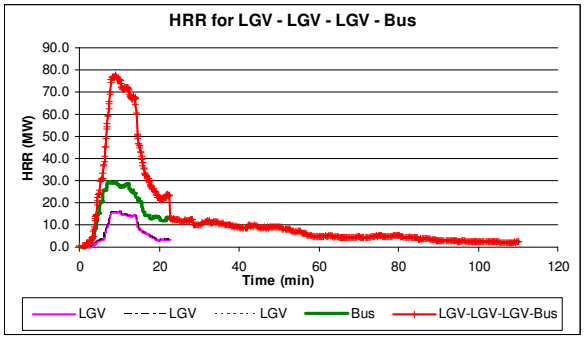
HRR for LGV - LGV - LGV - Bus
HRR (MW)
Time (min)
LGV
LGV
LGV
Bus
LGV-LGV-LGV-Bus

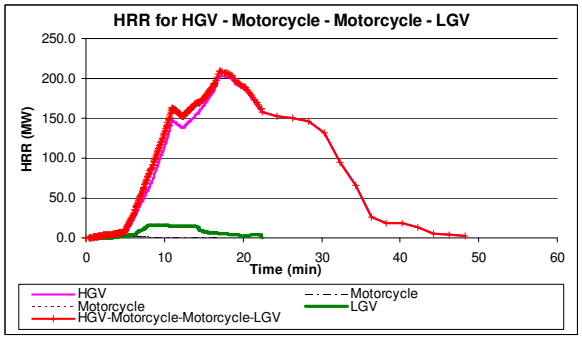
HRR for HGV - Motorcycle - Motorcycle - LGV
HRR (MW)
Time (min)
HGV
Motorcycle
Motorcycle
LGV
HGV-Motorcycle-Motorcycle-LGV

Appendix B

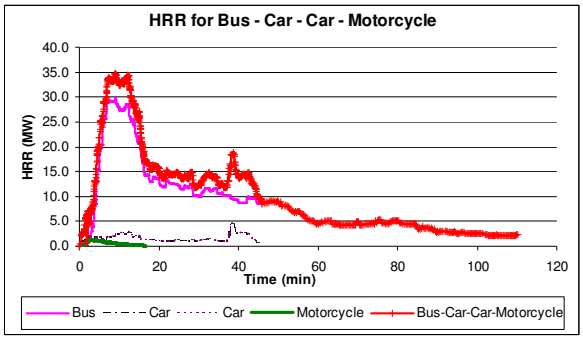
HRR for Bus - Car - Car - Motorcycle
HRR (MW)
Time (min)
Bus
Car
Car
Motorcycle
Bus-Car-Car-Motorcycle

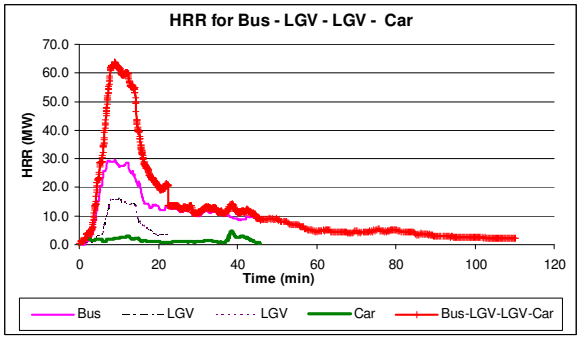
HRR for Bus - LGV - LGV - Car
HRR (MW)
Time (min)
Bus
LGV
LGV
Car
Bus-LGV-LGV-Car

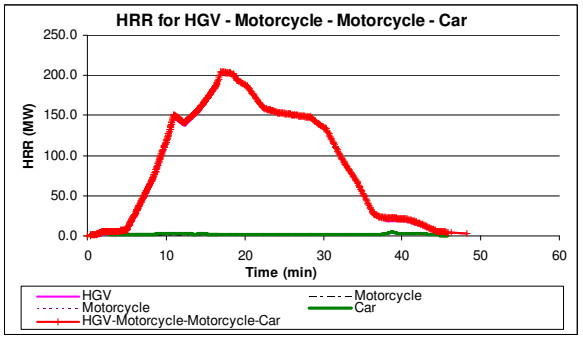
HRR for HGV - Motorcycle - Motorcycle - Car
HRR (MW)
Time (min)
HGV
Motorcycle
Motorcycle
Car
HGV-Motorcycle-Motorcycle-Car

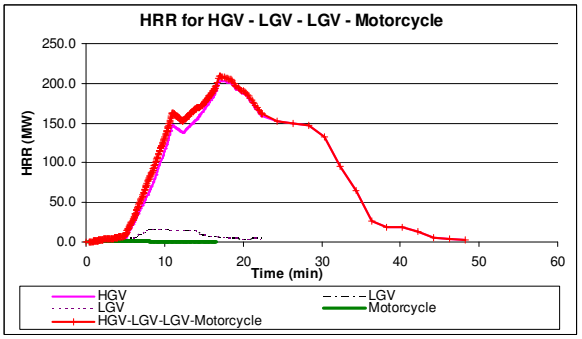
HRR for HGV - LGV - LGV - Motorcycle
HRR (MW)
Time (min)
HGV
LGV
LGV
Motorcycle
HGV-LGV-LGV-Motorcycle

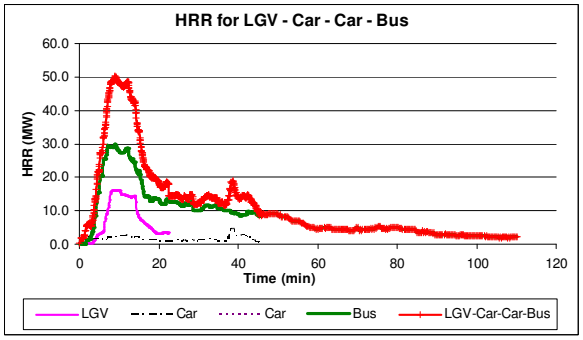
HRR for LGV - Car - Car - Bus
HRR (MW)
Time (min)
LGV
Car
Car
Bus
LGV-Car-Car-Bus

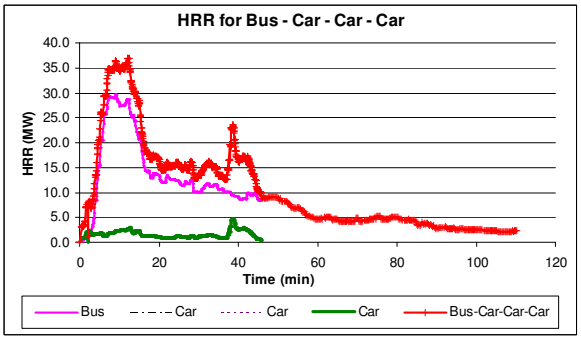
HRR for Bus - Car - Car - Car
HRR (MW)
Time (min)
Bus
Car
Car
Car
Bus-Car-Car-Car

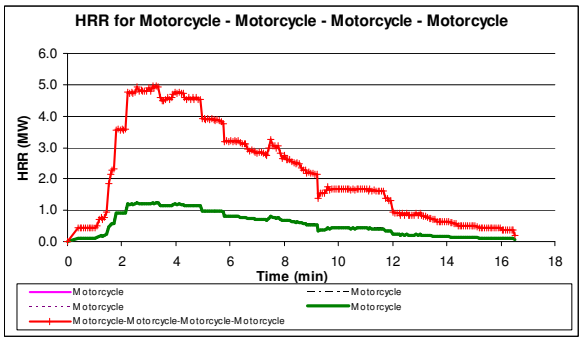
HRR for Motorcycle - Motorcycle - Motorcycle - Motorcycle
HRR (MW)
Time (min)
Motorcycle
Motorcycle
Motorcycle
Motorcycle
Motorcycle-Motorcycle-Motorcycle-Motorcycle

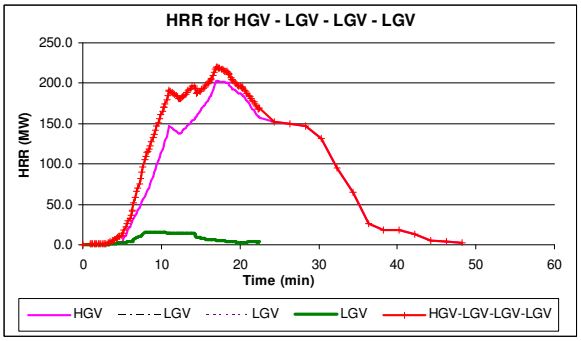
HRR for HGV - LGV - LGV - LGV
HRR (MW)
Time (min)
HGV
LGV
LGV
LGV
HGV-LGV-LGV-LGV

Appendix B

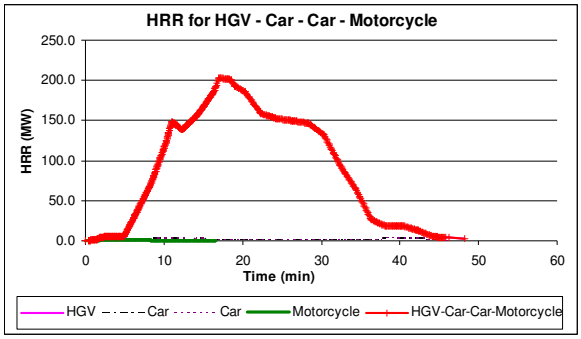
HRR for HGV - Car - Car - Motorcycle
HRR (MW)
Time (min)
HGV
Car
Car
Motorcycle
HGV-Car-Car-Motorcycle

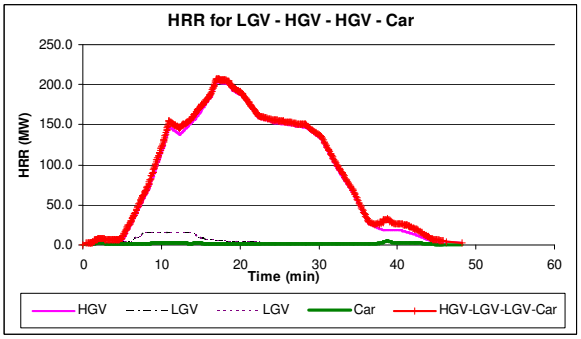
HRR for LGV - HGV - HGV - Car
HRR (MW)
Time (min)
HGV
LGV
LGV
Car
HGV-LGV-LGV-Car

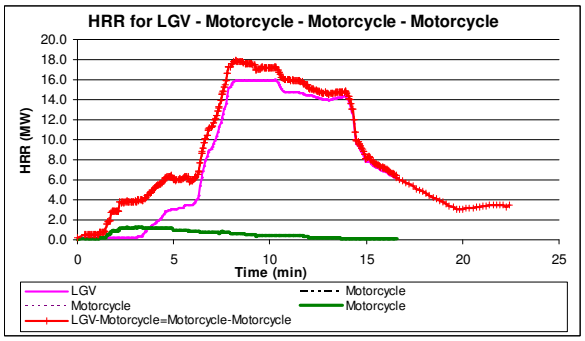
HRR for LGV - Motorcycle - Motorcycle - Motorcycle
HRR (MW)
Time (min)
LGV
Motorcycle
Motorcycle
Motorcycle
LGV-Motorcycle=Motorcycle-Motorcycle

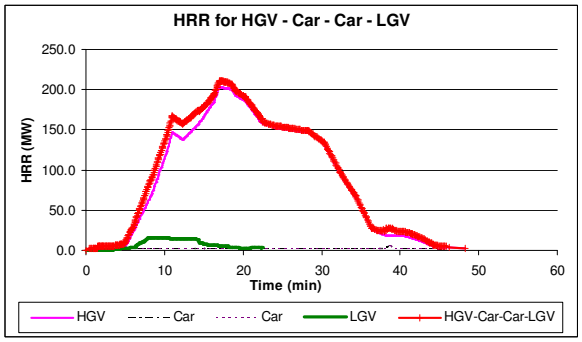
HRR for HGV - Car - Car - LGV
HRR (MW)
Time (min)
HGV
Car
Car
LGV
HGV-Car-Car-LGV

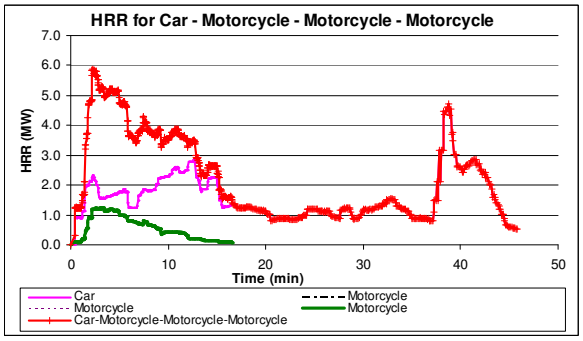
HRR for Car - Motorcycle - Motorcycle - Motorcycle
HRR (MW)
Time (min)
Car
Motorcycle
Motorcycle
Motorcycle
Car-Motorcycle-Motorcycle-Motorcycle

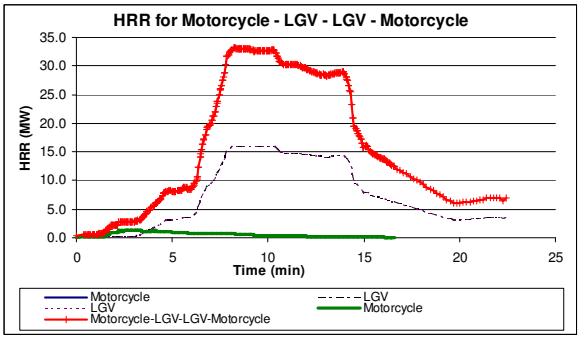
HRR for Motorcycle - LGV - LGV - Motorcycle
HRR (MW)
Time (min)
Motorcycle
LGV
LGV
Motorcycle
Motorcycle-LGV-LGV-Motorcycle

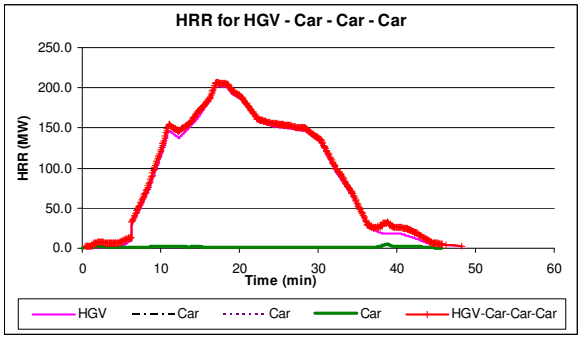
HRR for HGV - Car - Car - Car
HRR (MW)
Time (min)
HGV
Car
Car
Car
HGV-Car-Car-Car

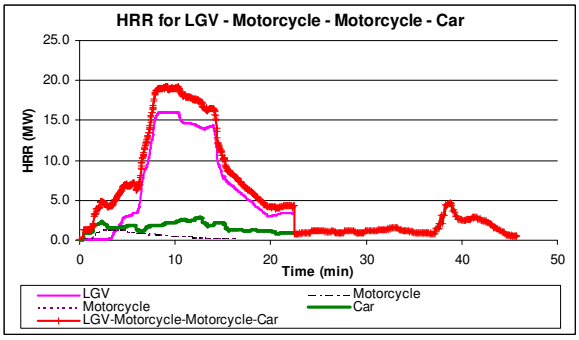
HRR for LGV - Motorcycle - Motorcycle - Car
HRR (MW)
Time (min)
LGV
Motorcycle
Motorcycle
Car
LGV-Motorcycle-Motorcycle-Car

Appendix B

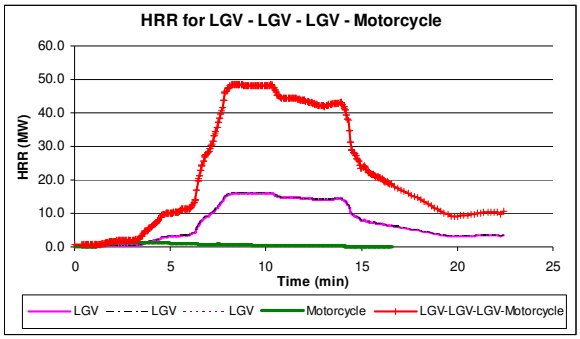
HRR for LGV - LGV - LGV - Motorcycle
HRR (MW)
Time (min)
LGV
LGV
LGV
Motorcycle
LGV-LGV-LGV-Motorcycle

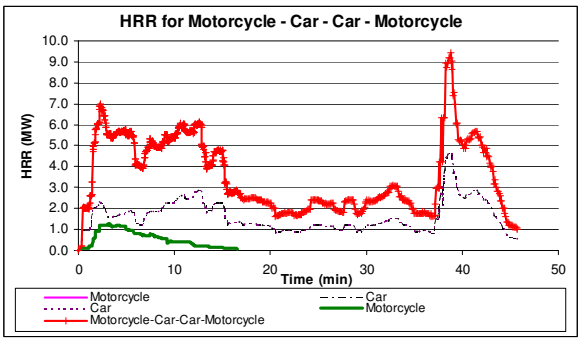
HRR for Motorcycle - Car - Car - Motorcycle
HRR (MW)
Time (min)
Motorcycle
Car
Car
Motorcycle
Motorcycle-Car-Car-Motorcycle

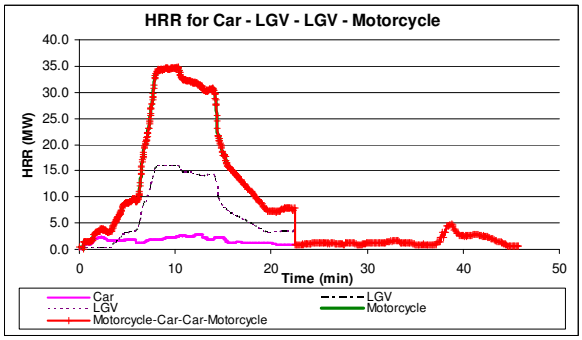
HRR for Car - LGV - LGV - Motorcycle
HRR (MW)
Time (min)
Car
LGV
LGV
Motorcycle
Motorcycle-Car-Car-Motorcycle

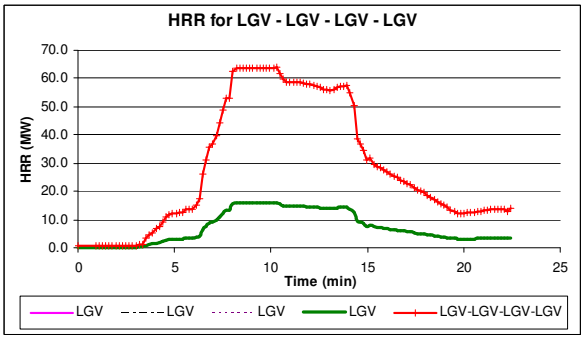
HRR for LGV - LGV - LGV - LGV
HRR (MW)
Time (min)
LGV
LGV
LGV
LGV
LGV-LGV-LGV-LGV

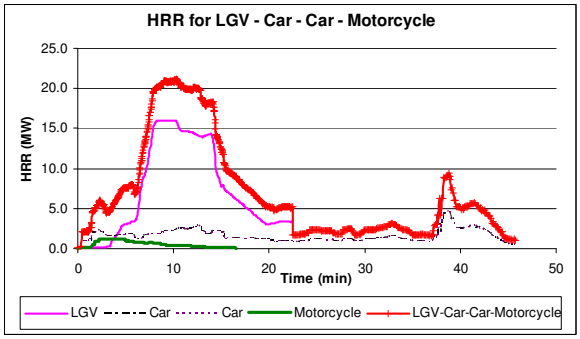
HRR for LGV - Car - Car - Motorcycle
HRR (MW)
Time (min)
LGV
Car
Car
Motorcycle
LGV-Car-Car-Motorcycle

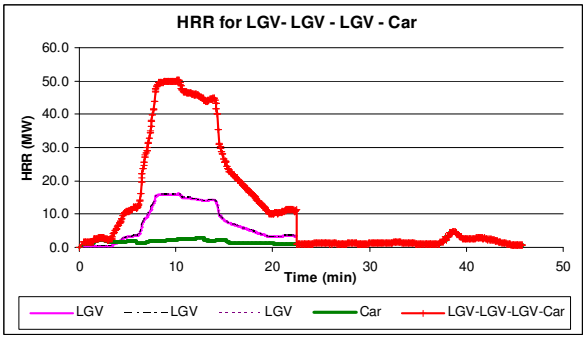
HRR for LGV- LGV - LGV - Car
HRR (MW)
Time (min)
LGV
LGV
LGV
Car
LGV-LGV-LGV-Car

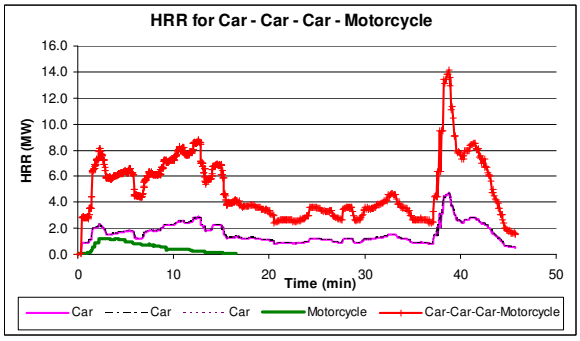
HRR for Car - Car - Car - Motorcycle
HRR (MW)
Time (min)
Car
Car
Car
Motorcycle
Car-Car-Car-Motorcycle

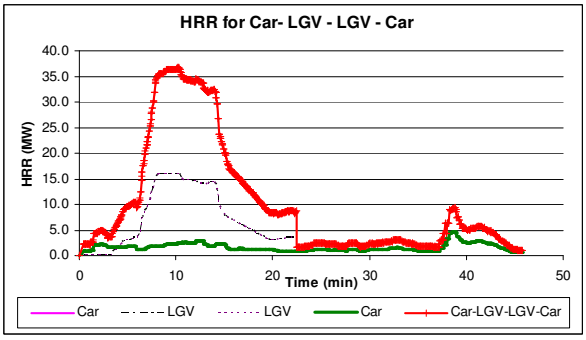
HRR for Car- LGV - LGV - Car
HRR (MW)
Time (min)
Car
LGV
LGV
Car
Car-LGV-LGV-Car

Appendix B

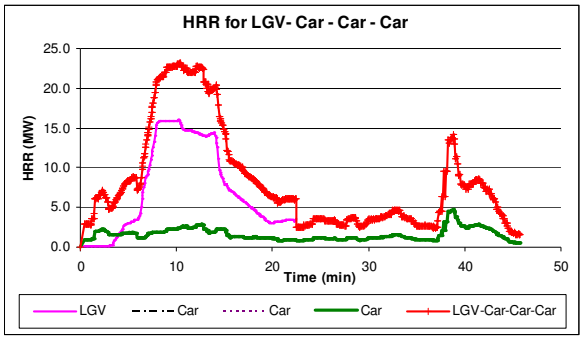
HRR for LGV- Car - Car - Car
HRR (MW)
Time (min)
LGV
Car
Car
Car
LGV-Car-Car-Car

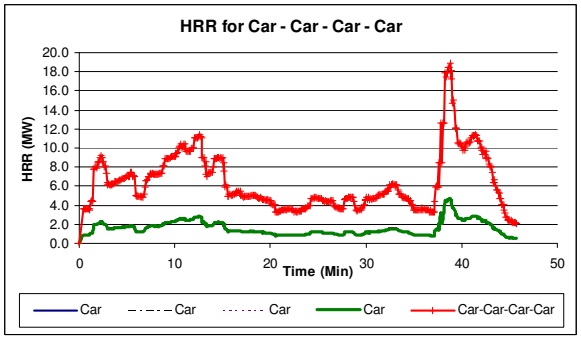
HRR for Car - Car - Car - Car
HRR (MW)
Time (Min)
Car
Car
Car
Car
Car-Car-Car-Car

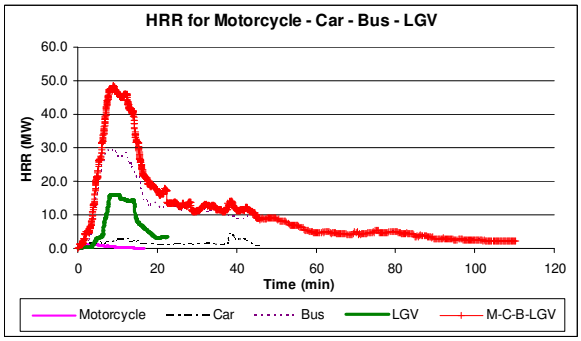
HRR for Motorcycle - Car - Bus - LGV
HRR (MW)
Time (min)
Motorcycle
Car
Bus
LGV
M-C-B-LGV

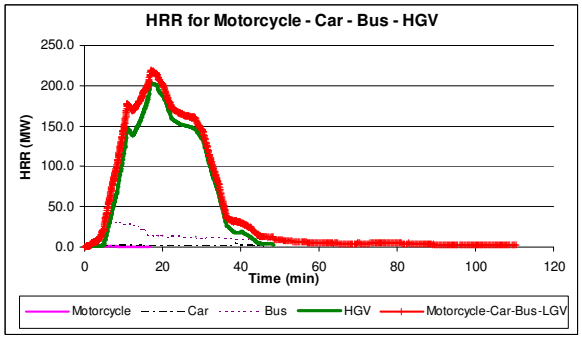
HRR for Motorcycle - Car - Bus - HGV
HRR (MW)
Time (min)
Motorcycle
Car
Bus
HGV
Motorcycle-Car-Bus-LGV

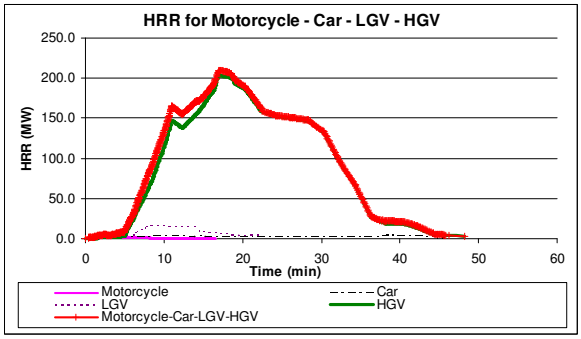
HRR for Motorcycle - Car - LGV - HGV
HRR (MW)
Time (min)
Motorcycle
Car
LGV
HGV
Motorcycle-Car-LGV-HGV

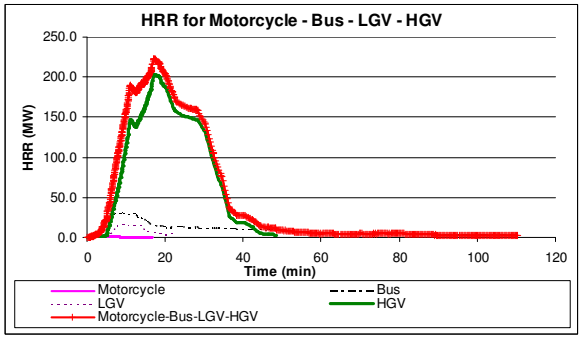
HRR for Motorcycle - Bus - LGV - HGV
HRR (MW)
Time (min)
Motorcycle
Bus
LGV
HGV
Motorcycle-Bus-LGV-HGV

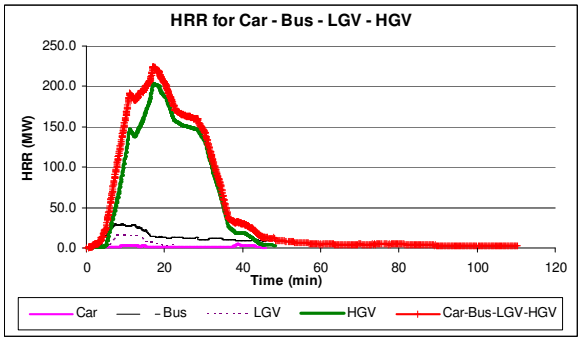
HRR for Car - Bus - LGV - HGV
HRR (MW)
Time (min)
Car
Bus
LGV
HGV
Car-Bus-LGV-HGV

APPENDIX C

Appendix C: Statistic data for vehicle fire incident in Singapore, road accident by vehicle type and traffic mix in a urban tunnel in Singapore

Motor Vehicle Population by Vehicle Type in Singapore

Year	1995	2000	2001	2002	2003	2004	2005	2006
Motorcycle/Scooters	129587	131937	131869	132318	135649	137029	139434	142736
Car and Taxi	363906	413545	426442	425695	427110	439877	462966	498051
Light Goods Vehicles (LGV)	69589	89484	92237	90597	89697	90579	91588	87805
Heavy Goods Vehicles (HGV)	55487	35370	35036	35334	35326	36130	36605	28983
Bus	10723	12569	12902	12992	12951	13173	13494	14120
Total vehicle population	629292	682905	698486	696936	700733	716788	744087	771695

*Note: Total vehicle population refer to the total vehicle population in Singapore that is allow to access the tunnel. Source: (*LTA, 2006)

Table C1: Motor Vehicle Population by Vehicle Type in Singapore

Vehicle Fire Statistic in Singapore

Vehicle fire due to act of carelessness, intentional and vehicle fault

Vehicle fires	**2004**	**2005**	**2006**
Overheating	55	62	59
Electrical	76	63	55
Incendiary (Arson)	56	59	54
Others*	32	21	24
Total	219	205	192

*Note: *Others include naked lights, spark, dropped lights and collision*
Source: (SCDF, 2006b)

Table C2: Vehicle Fire Statistic in Singapore

Traffic Mix in an Urban Tunnel in Singapore

Vehicle description	Traffic Mix %	Vehicle Category	% fleet by category
Motorcycle / Scooter	11.75	Motorcycle	11.75
Petrol Passenger Car	54.21	Car	56.76
Diesel Taxi	2.55		
Petrol Van	11.61	LGV	30.64
Diesel Van	16.79		
Diesel Light Goods	0.3		
Diesel Goods	1.94		
Diesel Medium Goods	0.18	HGV	0.75
Diesel Heavy Goods	0.57		
Diesel Omibus	0.03	Bus	0.1
Diesel School Bus	0.02		
Diesel double-decker Bus	0.04		
Diesel double-decker Bus	0.01		

Column 1 & 2 - Source: (Luk 2003)

Table C3: Traffic Mix

Motor Vehicle Involved in Road Accident by Vehicle Type in Singapore

Year	1995	2000	2001	2002	2003	2004	2005
Motorcycle/Scooters	3187	4541	4435	4194	3999	4297	4223
Car	3449	5251	5307	5262	4890	4943	4713
Light Goods Vehicles (LGV)	567	697	609	639	567	59	605
Heavy Goods Vehicles (HGV)	872	1137	1076	1020	887	1014	887
Bus	454	492	483	459	402	431	391

Source: (Statistic Singapore 2006)

Table C4: Motor Vehicle Involved in Road Accident by Vehicle Type in Singapore

Probability of Fire due to vehicle fault, act of carelessness and intentional

Please refer to section C1, C2 and C3 on calculation to establish probability of fire due to vehicle fault, act of carelessness and intentional.

Vehicles fires	2004	2005	2006	Average Value
Vehicle fault	1.828E-04	1.680E-04	1.477E-04	1.66E-04
Intentional (Arson)	7.813E-05	7.929E-05	6.998E-05	7.58E-05
Act of carelessness / collision	4.464E-05	2.822E-05	3.110E-05	3.47E-05

Table C5: Probability of Fire (vehicle fault, act of carelessness, collision and intentional)

Section C1: Probability calculation (Vehicle fault)

Sample calculation for year 2006:

From Equation C1.1

$$\Pr obability = \frac{Number\ of\ outcomes\ with\ "successful"\ result}{Total\ nmber\ of\ equally\ likely.outcomes} \qquad \text{Equation C1.1}$$

$$= \frac{Number\ of\ vehicle\ fire\ due\ to\ vehile\ fault}{Total\ vehicle\ population\ in\ Singapore} = \frac{Overheating + Electrical}{Total\ vehicle\ population\ in\ Singapore}$$

Where:

Overheating (Refer to Appendix C, Table C2)

Electrical (Refer to Appendix C, Table C2)

Total vehicle population (Refer to Appendix C, Table C1)

$$\Pr obability = \frac{59 + 55}{771695} = 0.0001477$$

Therefore the probability of vehicle fault resulting fire in year 2006 is 0.0001477

Similar calculation is performed for year 2004 and 2005.

The average value calculated from year 2004 to 2006 will be used for the analysis.

Therefore, the probability of vehicle fault is

$$\frac{0.0001828 + 0.0001680 + 0.0001477}{3} = 1.66E - 04$$

Section C2: Probability calculation (Intentional)

Sample calculation for year 2006:

From Equation C1.1

$$\Pr obability = \frac{Number\ of\ outcomes\ with\ "successful"\ result}{Total\ nmber\ of\ equally\ likely\ outcomes}$$

$$= \frac{Number\ of\ vehicle\ fire\ cause\ by\ \text{int}ential}{Total\ vehicle\ population\ in\ Singapore} = \frac{Incendiary}{Total\ vehicle\ population\ in\ Singapore}$$

Where:

Incendiary (Refer to Appendix C, Table C2)

Total vehicle population (Refer to Appendix C, Table C1)

$$\Pr obability = \frac{54}{771695} = 0.00006998$$

Therefore the probability of fire cause by intentional in year 2006 is 0.00006998

Similar calculation is performed for year 2004 and 2005.

The average value calculated from year 2004 to 2006 will be used for the analysis.

Therefore, the probability of fire cause by intentional is

$$\frac{0.00007813 + 0.00007929 + 0.00006998}{3} = 7.58E-05$$

Section B3: Probability calculation (Act of carelessness / collision)

Sample calculation for year 2006:

From Equation C1.1

$$\Pr obability = \frac{Number\ of\ outcomes\ with\ "successful"\ result}{Total\ number\ of\ equally\ likely\ outcomes}$$

$$= \frac{Number\ of\ vehicle\ fire\ result\ from\ act\ of\ carelessness}{Total\ vehicle\ population\ in\ Singapore} = \frac{Carelessness\ /\ collision}{Total\ vehicle\ population\ in\ Singapore}$$

Where:

Drop light (Refer to Appendix C, Table C2)

Total vehicle population (Refer to Appendix C, Table C1)

$$\Pr obability = \frac{24}{771695} = 0.00003110$$

Therefore the probability of fire cause by act of carelessness in year 2006 is 0.0000311

Similar calculation is performed for year 2004 and 2005.

The average value calculated from year 2004 to 2006 will be used for the analysis. Therefore, the probability of fire cause by act of carelessness is

$$\frac{0.00004464 + 0.00002822 + 0.00003110}{3} = 3.47E-05$$

Probability of accident rate by vehicle type in Singapore

Please refer to section C4, C5, C6, C7 and C8 on calculation to establish probability of accident rate by type in Singapore.

Year / Vehicle type	1995	2000	2001	2002	2003	2004	2005	Average Value
Motorcycle/Scooters	2.46E-02	3.44E-02	3.36E-02	3.17E-02	2.95E-02	3.14E-02	3.03E-02	3.08E-02
Cars	9.48E-03	1.27E-02	1.24E-02	1.24E-02	1.13E-02	1.12E-02	1.02E-02	1.14E-02
Bus	4.23E-02	3.91E-02	3.74E-02	3.53E-02	3.10E-02	3.27E-02	2.90E-02	3.53E-02
Light goods vehicle (LGV)	8.15E-03	7.79E-03	6.60E-03	7.05E-03	6.32E-03	6.60E-03	6.61E-03	7.02E-03
Heavy goods vehicle (HGV)	1.57E-02	3.21E-02	3.07E-02	2.89E-02	2.51E-02	2.81E-02	2.42E-02	2.64E-02

Table C6: Probability of accident rate by vehicle type in Singapore

Section C4: Probability calculation (Motorcycle accident)

Sample calculation for year 2005:

From Equation C1.1

$$\Pr obability = \frac{Number\ of\ outcomes\ with\ "successful"\ result}{Total\ number\ of\ equally\ likely\ outcomes}$$

$$= \frac{Number\ of\ motorcycle\ in\ 2005\ involved\ in\ accident\ at\ Singapore}{Total\ Singapore\ motorcycle\ population\ in\ 2005}$$

Where:

Number of motorcycle in year 2005 involved in accident (Refer Appendix C,Table C4)

Total Singapore motorcycle population in year 2005(Refer Appendix C, Table C1)

$$\Pr obability = \frac{4223}{139434} = 3.029E-02$$

Therefore the probability of motorcycle accident for year 2005 in Singapore is 3.029E-02

Similar calculation is performed for year 1995, 2000, 2001, 2002, 2003 and 2004.

The average value calculated from year 1995, 2000 to 2005 will be used for the analysis. Therefore, the probability of motorcycle accident in Singapore is

$$\frac{(0.02459)+(0.03442)+(0.03363)+(0.03170)+(0.02948)+(0.03136)+(0.03029)}{7} = 3.08E-02$$

Section C5: Probability calculation (Car accident)

Sample calculation for year 2005:

From Equation C1.1

$$\Pr obability = \frac{Number\ of\ outcomes\ with\ "successful"\ result}{Total\ nmber\ of\ equally\ likely\ outcomes}$$

$$= \frac{Number\ of\ car\ in\ 2005\ involved\ in\ accident\ at\ Singapore}{Total\ Singapore\ car\ population\ in\ 2005}$$

Where:

Number of car in year 2005 involved in accident (Refer Appendix C, Table C4)

Total Singapore car population in year 2005 (Refer Appendix C, Table C1)

$$\Pr obability = \frac{4713}{462966} = 1.02E-02$$

Therefore the probability of car accident for year 2005 in Singapore is 1.02E-02

Similar calculation is performed for year 1995, 2000, 2001, 2002, 2003 and 2004.

The average value calculated from year 1995, 2000 to 2005 will be used for the analysis. Therefore, the probability of car accident in Singapore is

$$\frac{(0.00948)+(0.0127)+(0.0124)+(0.0124)+(0.0113)+(0.0112)+(0.0102)}{7} = 1.14E-02$$

Section C6: Probability calculation (Bus accident)

Sample calculation for year 2005:

From Equation C1.1

$$\Pr obability = \frac{Number\ of\ outcomes\ with\ "successful"\ result}{Total\ number\ of\ equally\ likely\ outcomes}$$

$$= \frac{Number\ of\ bus\ in\ 2005\ involved\ in\ accident\ at\ Singapore}{Total\ Singapore\ bus\ population\ in\ 2005}$$

Where:

Number of bus in year 2005 involved in accident (Refer Appendix C, Table C4)

Total Singapore bus population in year 2005 (Refer Appendix C, Table C1)

$$\Pr obability = \frac{391}{13494} = 2.90E-02$$

Therefore the probability of bus accident for year 2005 in Singapore is 2.90E-02

Similar calculation is performed for year 1995, 2000, 2001, 2002, 2003 and 2004.

The average value calculated from year 1995, 2000 to 2005 will be used for the analysis. Therefore, the probability of bus accident in Singapore is

$$\frac{(0.0423)+(0.0391)+(0.0374)+(0.0353)+(0.0310)+(0.0327)+(0.0290)}{7} = 3.53E-02$$

Section C7: Probability calculation (LGV accident)

Sample calculation for year 2005:

From Equation C1.1

$$\Pr obability = \frac{Number\ of\ outcomes\ with\ "successful"\ result}{Total\ nmber\ of\ equally\ likely\ outcomes}$$

$$= \frac{Number\ of\ LGV\ in\ 2005\ involved\ in\ accident\ at\ Singapore}{Total\ Singapore\ LGV\ population\ in\ 2005}$$

Where:

Number of LGV in year 2005 involved in accident (Refer Appendix C, Table C4)

Total Singapore LGV population in year 2005 (Refer Appendix C, Table C1)

$$\Pr obability = \frac{605}{91588} = 6.61E-03$$

Therefore the probability of LGV accident for year 2005 in Singapore is 6.61E-03

Similar calculation is performed for year 1995, 2000, 2001, 2002, 2003 and 2004.

The average value calculated from year 1995, 2000 to 2005 will be used for the analysis. Therefore, the probability of LGV accident in Singapore is

$$\frac{(0.00815)+(0.00779)+(0.00660)+(0.00705)+(0.00632)+(0.00660)+(0.00661)}{7} = 7.02E-03$$

Section C8: Probability calculation (HGV accident)

Sample calculation for year 2005:

From Equation C1.1

$$\Pr obability = \frac{Number\ of\ outcomes\ with\ "successful"\ result}{Total\ number\ of\ equally\ likely\ outcomes}$$

$$= \frac{Number\ of\ .HGV\ in\ 2005\ involved\ in\ accident\ at\ Singapore}{Total\ Singapore\ HGV\ \ population\ in\ 2005}$$

Where:

Number of HGV in year 2005 involved in accident (Refer Appendix C, Table C4)

Total Singapore HGV population in year 2005 (Refer Appendix C, Table C1)

$$\Pr obability = \frac{887}{36605} = 2.42E-02$$

Therefore the probability of HGV accident for year 2005 in Singapore is 2.42E-02

Similar calculation is performed for year 1995, 2000, 2001, 2002, 2003 and 2004.

The average value calculated from year 1995, 2000 to 2005 will be used for the analysis. Therefore, the probability of HGV accident in Singapore is

$$\frac{(0.0157)+(0.0321)+(0.0307)+(0.0289)+(0.0251)+(0.0281)+(0.0242)}{7} = 2.64E-02$$

APPENDIX D

Appendix D: Event Tree – Fire in tunnel due to collision for Chapter 8

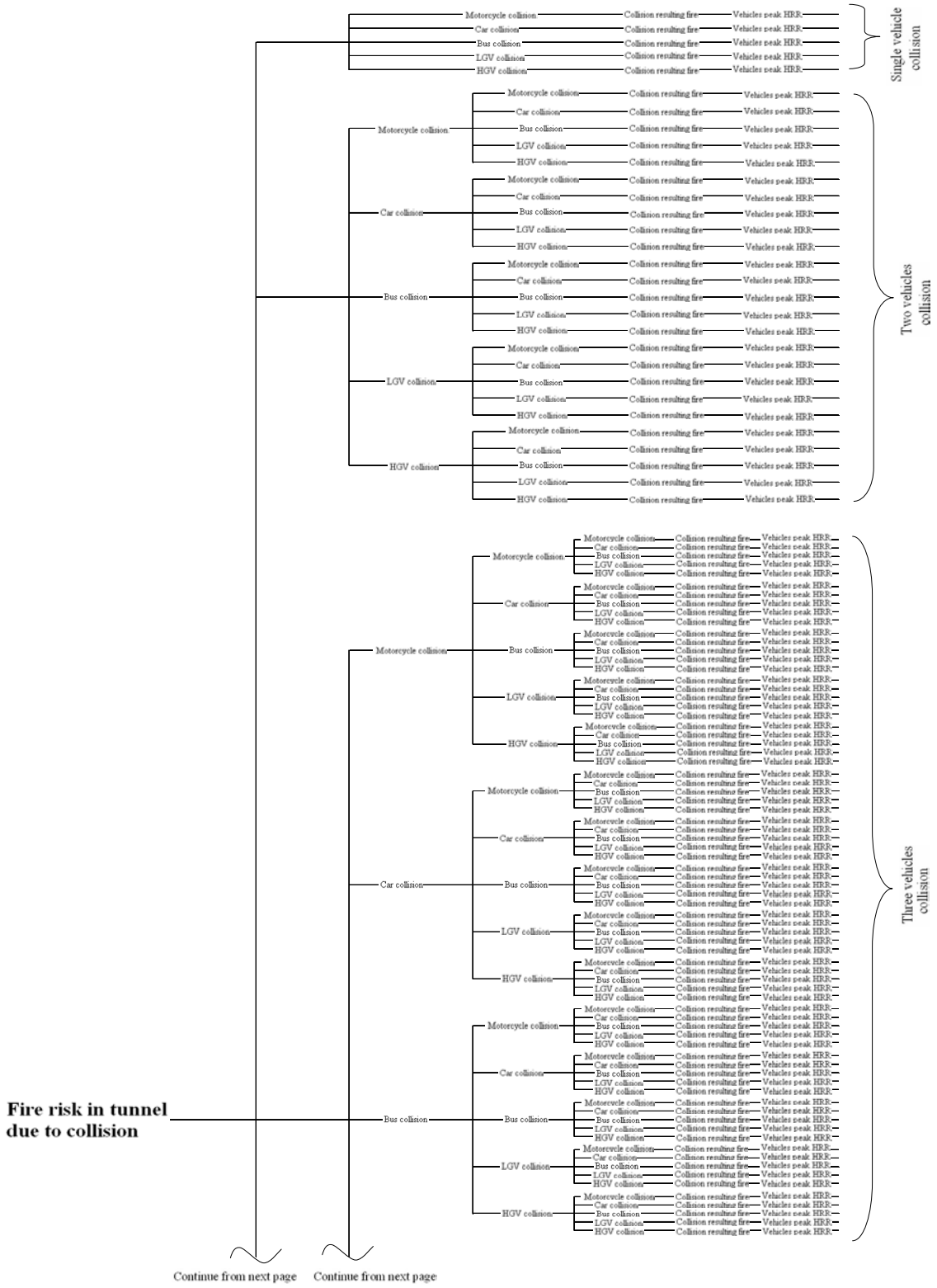

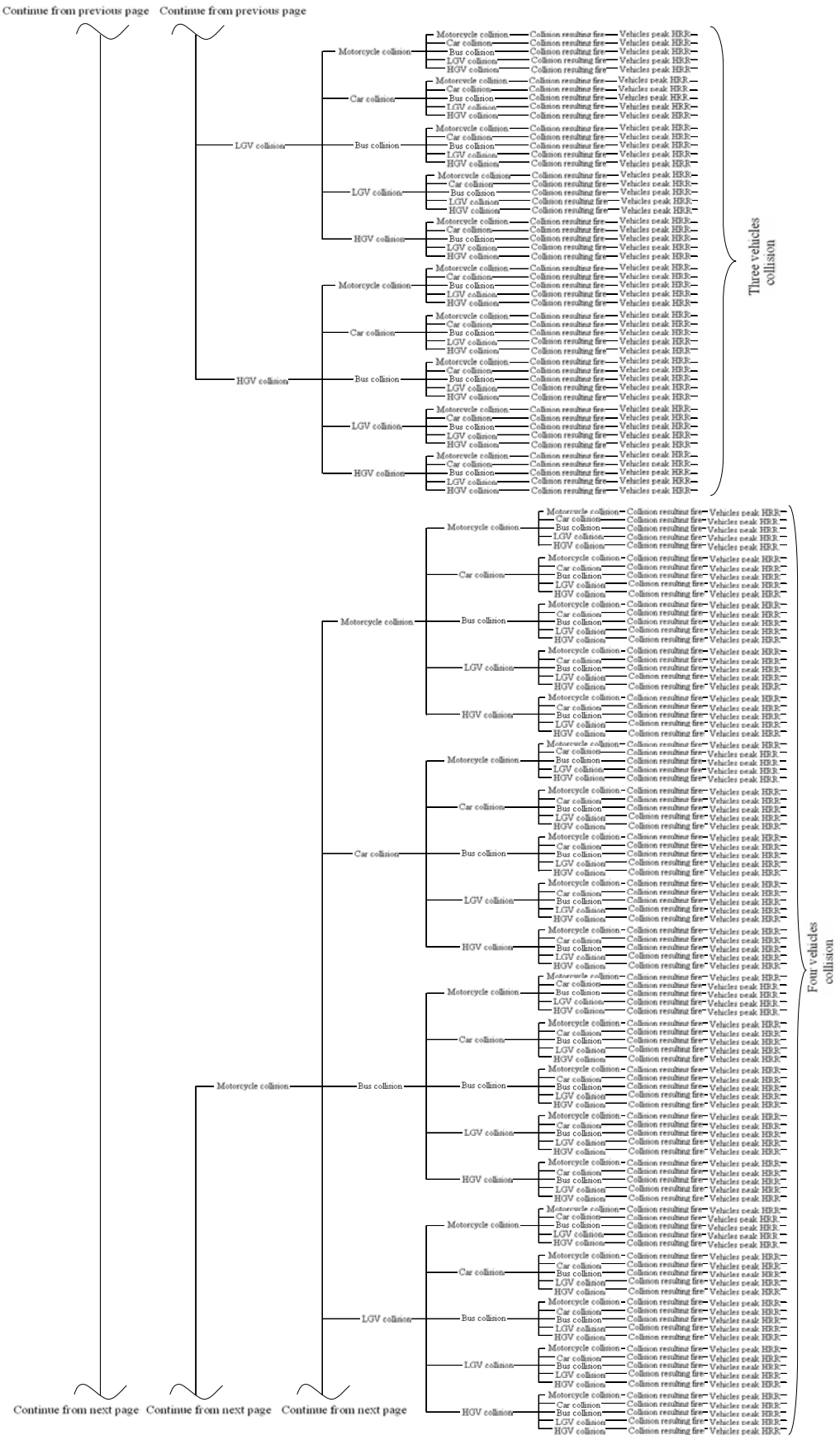
Continue from previous page
Continue from previous page
Motorcycle collision
Car collision
Bus collision
LGV collision
HGV collision
Collision resulting fire
Vehicles peak HRR
Three vehicles collision
Four vehicles collision
Continue from next page
Continue from next page
Continue from next page

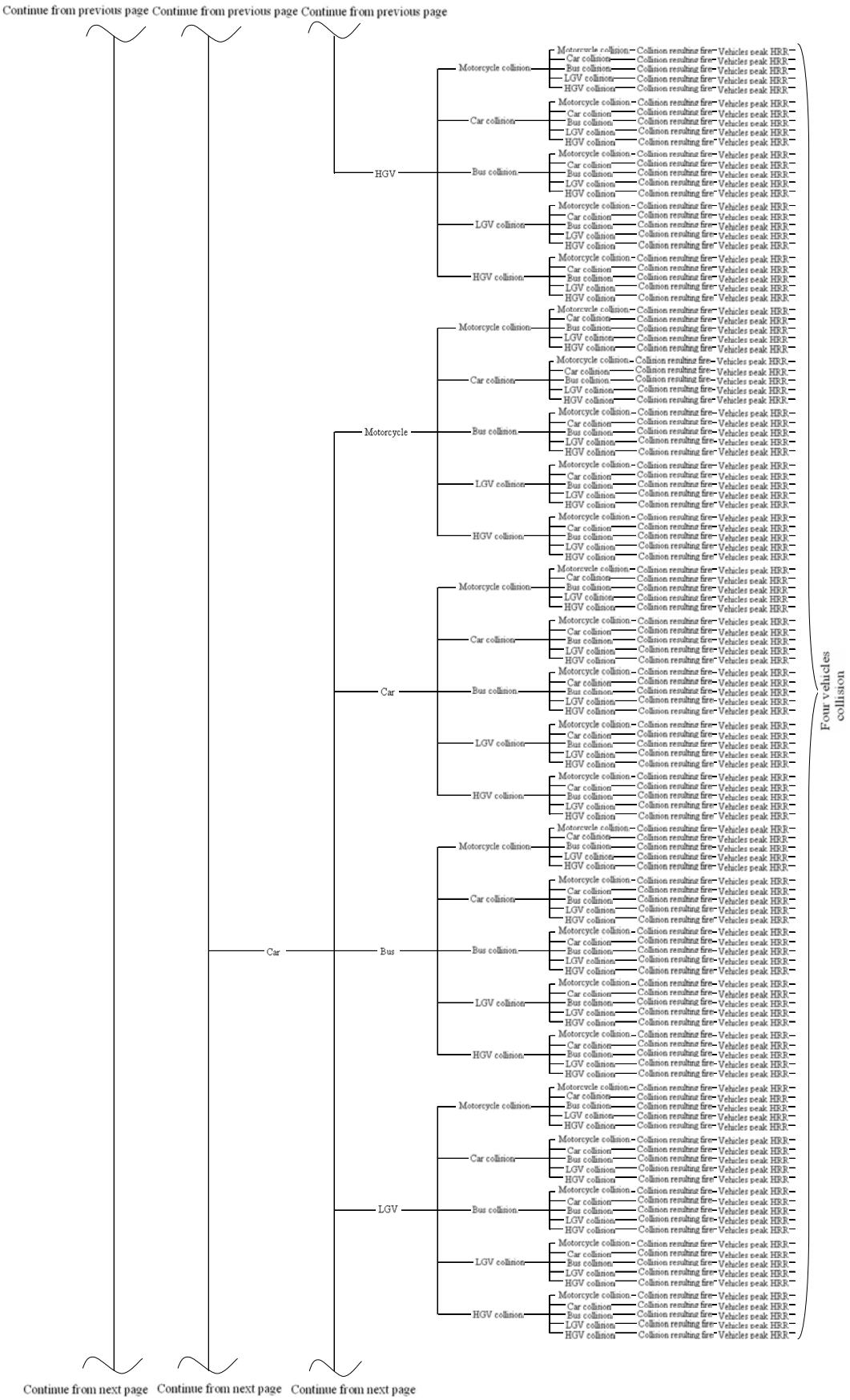
Continue from previous page
Continue from previous page
Continue from previous page
HGV
Motorcycle
Car
Bus
LGV
Motorcycle collision
Car collision
Bus collision
LGV collision
HGV collision
Motorcycle collision
Car collision
Bus collision
LGV collision
HGV collision
Collision resulting fire
Vehicles peak HRR
Four vehicles collision
Continue from next page
Continue from next page
Continue from next page

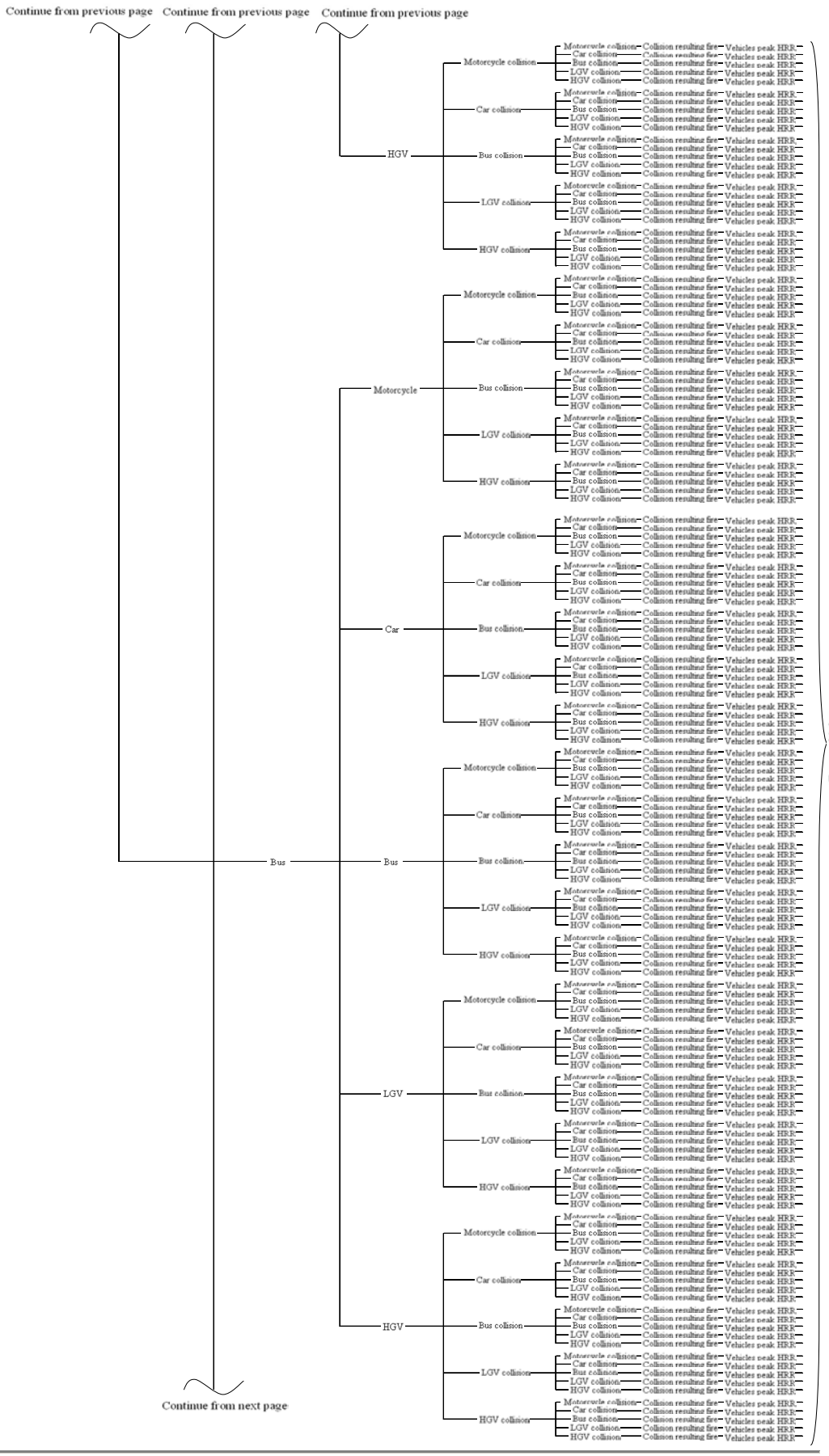
Continue from previous page
Continue from previous page
Continue from previous page
Bus
Bus
Motorcycle
Car
LGV
HGV
Motorcycle collision
Car collision
Bus collision
LGV collision
HGV collision
Motorcycle collision
Car collision
Bus collision
LGV collision
HGV collision
Collision resulting fire
Vehicles peak HRR
Four vehicles collision
Continue from next page

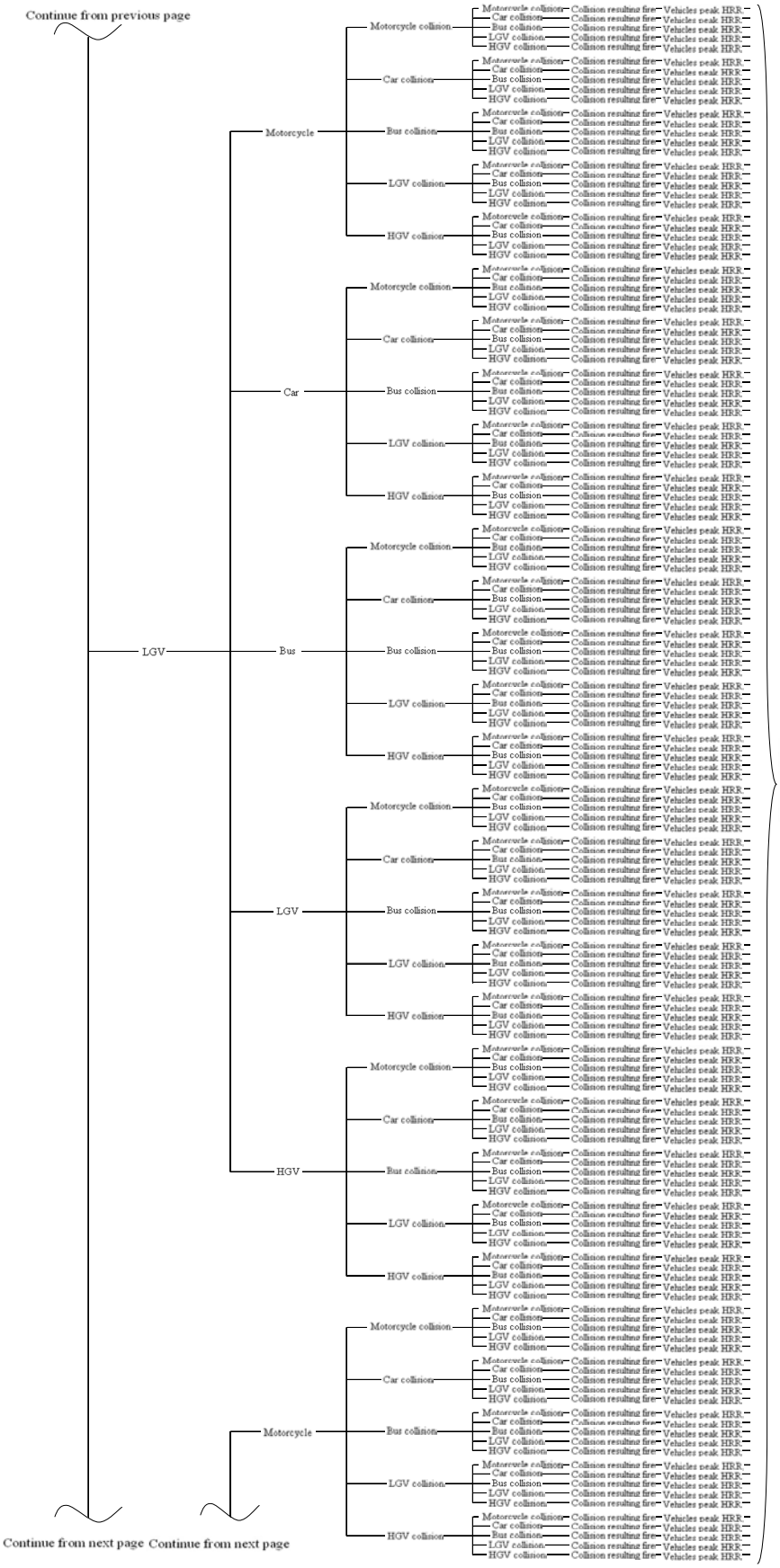
Continue from previous page
Four vehicles collision
LGV
Motorcycle
Car
Bus
LGV
HGV
Motorcycle collision
Car collision
Bus collision
LGV collision
HGV collision
Collision resulting fire
Vehicles peak HRR
Continue from next page
Continue from next page

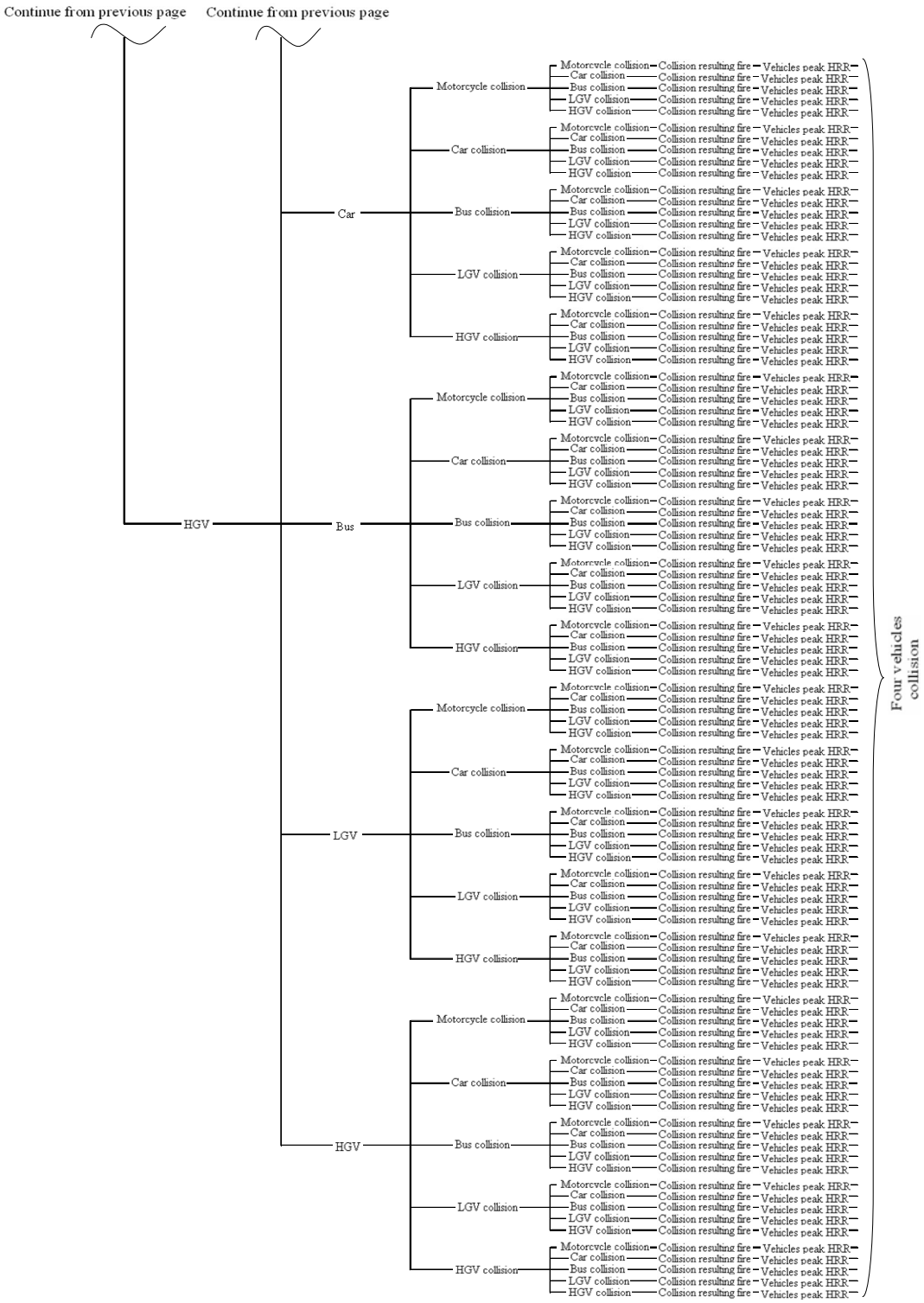
Continue from previous page
Continue from previous page
HGV
Car
Bus
LGV
HGV
Motorcycle collision
Car collision
Bus collision
LGV collision
HGV collision
Collision resulting fire
Vehicles peak HRR
Four vehicles collision

APPENDIX E

Appendix E: Simplified event tree – fire in tunnel due to collision for Chapter 8

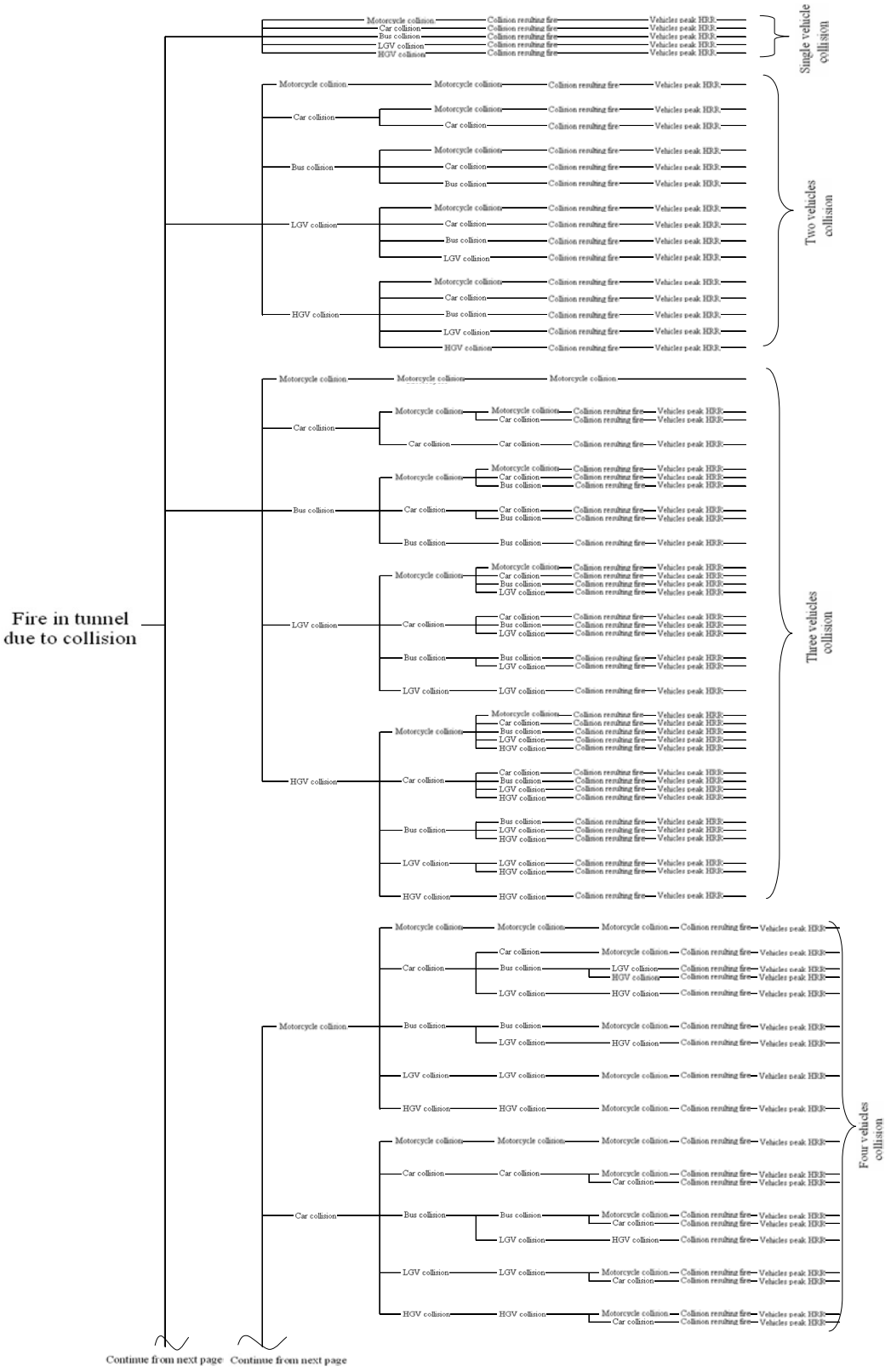

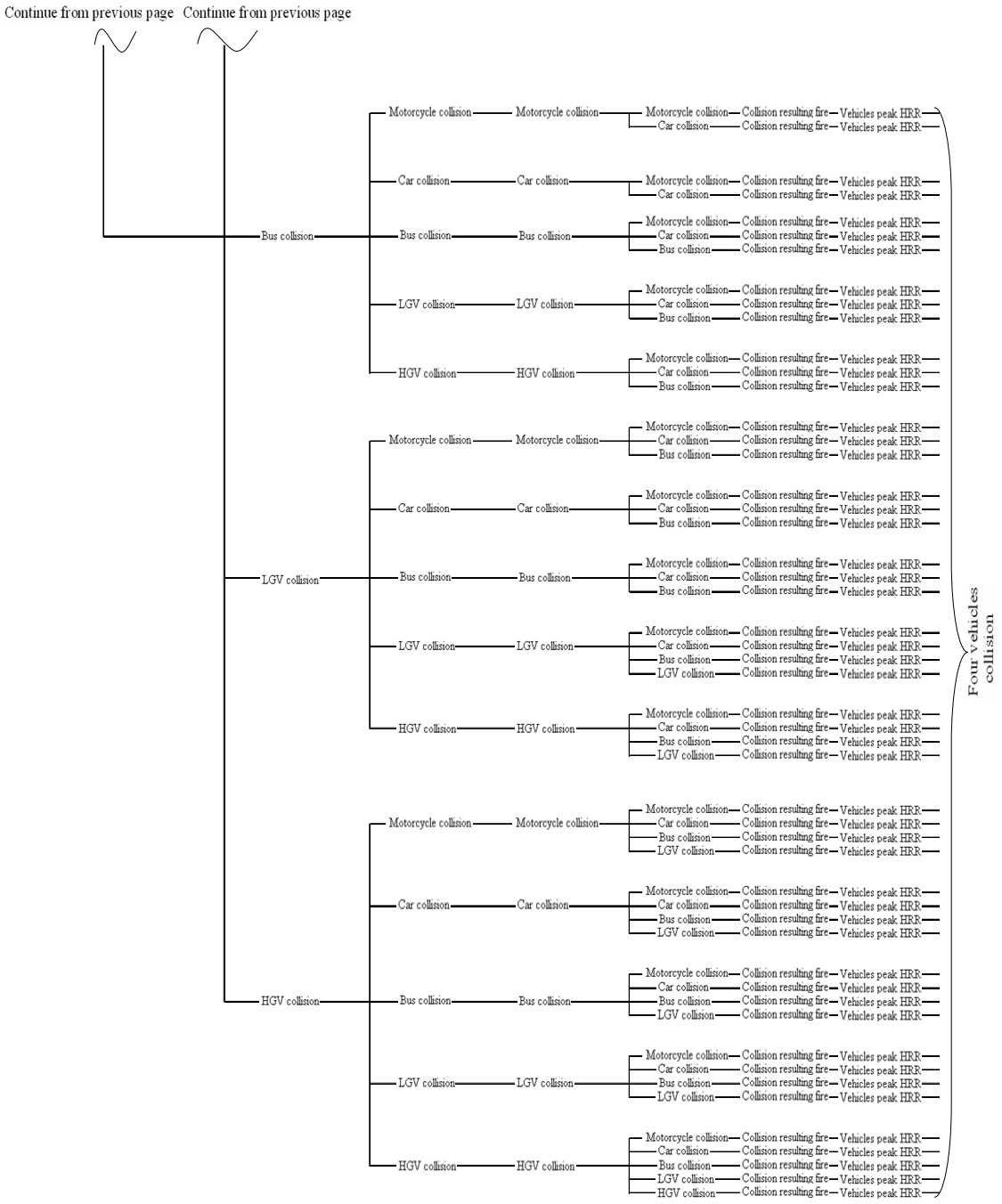
Continue from previous page
Continue from previous page
Bus collision
LGV collision
HGV collision
Motorcycle collision
Car collision
Bus collision
LGV collision
HGV collision
Collision resulting fire
Vehicles peak HRR
Four vehicles collision

APPENDIX F

Appendix F: Expose risk level due to vehicle collision for Chapter 8

Possible vehicle configuration				Vehicle 1		Vehicle 2		Vehicle 3		Vehicle 4		Probability	Peak HRR	Risk level
				Probability of vehicle 1 in tunnel	Probability of accidient rate	Probability of vehicle 2 in tunnel	Probability of accidient rate	Probability of vehicle 3 in tunnel	Probability of accidient rate	Probability of vehicle 4 in tunnel	Probability of accidient rate	collision resulting in fire	MW	
B				0.001	3.53E-02	0	0	0	0	0	0	3.47E-05	29.7	3.64E-08
C				0.5676	1.14E-02	0	0	0	0	0	0	3.47E-05	4.7	1.05E-06
HGV				0.0075	2.64E-02	0	0	0	0	0	0	3.47E-05	201.9	1.39E-06
LGV				0.3064	7.02E-03	0	0	0	0	0	0	3.47E-05	16.0	1.19E-06
M				0.1175	3.08E-02	0	0	0	0	0	0	3.47E-05	1.24	1.56E-07
B	B			0.001	3.53E-02	0.001	3.53E-02	0	0	0	0	3.47E-05	59.4	2.57E-12
B	C			0.001	3.53E-02	0.5676	1.14E-02	0	0	0	0	3.47E-05	32.0	2.53E-10
B	M			0.001	3.53E-02	0.1175	3.08E-02	0	0	0	0	3.47E-05	30.3	1.34E-10
C	C			0.5676	1.14E-02	0.5676	1.14E-02	0	0	0	0	3.47E-05	9.4	1.36E-08
C	M			0.5676	1.14E-02	0.1175	3.08E-02	0	0	0	0	3.47E-05	4.7	3.84E-09
HGV	B			0.0075	2.64E-02	0.001	3.53E-02	0	0	0	0	3.47E-05	217.2	5.27E-11
HGV	C			0.0075	2.64E-02	0.5676	1.14E-02	0	0	0	0	3.47E-05	204.3	9.08E-09
HGV	HGV			0.0075	2.64E-02	0.0075	2.64E-02	0	0	0	0	3.47E-05	403.8	5.50E-10
HGV	LGV			0.0075	2.64E-02	0.3064	7.02E-03	0	0	0	0	3.47E-05	208.8	3.09E-09
HGV	M			0.0075	2.64E-02	0.1175	3.08E-02	0	0	0	0	3.47E-05	203.1	5.05E-09
LGV	C			0.3064	7.02E-03	0.5676	1.14E-02	0	0	0	0	3.47E-05	18.6	8.98E-09
LGV	B			0.3064	7.02E-03	0.001	3.53E-02	0	0	0	0	3.47E-05	45.7	1.20E-10
LGV	LGV			0.3064	7.02E-03	0.3064	7.02E-03	0	0	0	0	3.47E-05	32.0	5.13E-09
LGV	M			0.3064	7.02E-03	0.1175	3.08E-02	0	0	0	0	3.47E-05	16.6	4.47E-09
M	M			0.1175	3.08E-02	0.1175	3.08E-02	0	0	0	0	3.47E-05	2.5	1.13E-09
B	B	B		0.001	3.53E-02	0.001	3.53E-02	0.001	3.53E-02	0	0	3.47E-05	89.1	1.36E-16
B	C	B		0.001	3.53E-02	0.5676	1.14E-02	0.001	3.53E-02	0	0	3.47E-05	61.7	1.72E-14
B	C	C		0.001	3.53E-02	0.5676	1.14E-02	0.5676	1.14E-02	0	0	3.47E-05	34.2	1.75E-12
B	M	B		0.001	3.53E-02	0.1175	3.08E-02	0.001	3.53E-02	0	0	3.47E-05	60.1	9.38E-15

Possible vehicle configuration				Vehicle 1		Vehicle 2		Vehicle 3		Vehicle 4		Probability	Peak HRR	Risk level
				Probability of vehicle 1 in tunnel	Probability of accidient rate	Probability of vehicle 2 in tunnel	Probability of accidient rate	Probability of vehicle 3 in tunnel	Probability of accidient rate	Probability of vehicle 4 in tunnel	Probability of accidient rate	collision resulting in fire	MW	
B	M	C		0.001	3.53E-02	0.1175	3.08E-02	0.5676	1.14E-02	0	0	3.47E-05	32.5	9.31E-13
B	M	M		0.001	3.53E-02	0.1175	3.08E-02	0.1175	3.08E-02	0	0	3.47E-05	30.9	4.96E-13
C	C	C		0.5676	1.14E-02	0.5676	1.14E-02	0.5676	1.14E-02	0	0	3.47E-05	14.1	1.32E-10
C	M	C		0.5676	1.14E-02	0.1175	3.08E-02	0.5676	1.14E-02	0	0	3.47E-05	9.5	4.95E-11
C	M	M		0.5676	1.14E-02	0.1175	3.08E-02	0.1175	3.08E-02	0	0	3.47E-05	4.7	1.39E-11
HGV	B	B		0.0075	2.64E-02	0.001	3.53E-02	0.001	3.53E-02	0	0	3.47E-05	231.4	1.98E-15
HGV	B	HGV		0.0075	2.64E-02	0.001	3.53E-02	0.0075	2.64E-02	0	0	3.47E-05	420.3	2.02E-14
HGV	B	LGV		0.0075	2.64E-02	0.001	3.53E-02	0.3064	7.02E-03	0	0	3.47E-05	223.0	1.16E-13
HGV	C	B		0.0075	2.64E-02	0.5676	1.14E-02	0.001	3.53E-02	0	0	3.47E-05	218.5	3.42E-13
HGV	C	C		0.0075	2.64E-02	0.5676	1.14E-02	0.5676	1.14E-02	0	0	3.47E-05	205.6	5.90E-11
HGV	C	HGV		0.0075	2.64E-02	0.5676	1.14E-02	0.0075	2.64E-02	0	0	3.47E-05	407.4	3.58E-12
HGV	C	LGV		0.0075	2.64E-02	0.5676	1.14E-02	0.3064	7.02E-03	0	0	3.47E-05	210.1	2.01E-11
HGV	HGV	HGV		0.0075	2.64E-02	0.0075	2.64E-02	0.0075	2.64E-02	0	0	3.47E-05	605.7	1.63E-13
HGV	LGV	HGV		0.0075	2.64E-02	0.3064	7.02E-03	0.0075	2.64E-02	0	0	3.47E-05	410.9	1.20E-12
HGV	LGV	LGV		0.0075	2.64E-02	0.3064	7.02E-03	0.3064	7.02E-03	0	0	3.47E-05	214.5	6.82E-12
HGV	M	B		0.0075	2.64E-02	0.1175	3.08E-02	0.001	3.53E-02	0	0	3.47E-05	217.2	1.91E-13
HGV	M	C		0.0075	2.64E-02	0.1175	3.08E-02	0.5676	1.14E-02	0	0	3.47E-05	204.3	3.28E-11
HGV	M	HGV		0.0075	2.64E-02	0.1175	3.08E-02	0.0075	2.64E-02	0	0	3.47E-05	406.2	2.00E-12
HGV	M	LGV		0.0075	2.64E-02	0.1175	3.08E-02	0.3064	7.02E-03	0	0	3.47E-05	208.8	1.12E-11
HGV	M	M		0.0075	2.64E-02	0.1175	3.08E-02	0.1175	3.08E-02	0	0	3.47E-05	203.1	1.83E-11
LGV	B	B		0.3064	7.02E-03	0.001	3.53E-02	0.001	3.53E-02	0	0	3.47E-05	75.4	7.00E-15
LGV	B	LGV		0.3064	7.02E-03	0.001	3.53E-02	0.3064	7.02E-03	0	0	3.47E-05	61.6	3.48E-13
LGV	C	B		0.3064	7.02E-03	0.5676	1.14E-02	0.001	3.53E-02	0	0	3.47E-05	47.9	8.15E-13
LGV	C	C		0.3064	7.02E-03	0.5676	1.14E-02	0.5676	1.14E-02	0	0	3.47E-05	20.7	6.46E-11
LGV	C	LGV		0.3064	7.02E-03	0.5676	1.14E-02	0.3064	7.02E-03	0	0	3.47E-05	34.3	3.56E-11
LGV	LGV	LGV		0.3064	7.02E-03	0.3064	7.02E-03	0.3064	7.02E-03	0	0	3.47E-05	48.0	1.66E-11

Possible vehicle configuration				Vehicle 1		Vehicle 2		Vehicle 3		Vehicle 4		Probability	Peak HRR	Risk level
				Probability of vehicle 1 in tunnel	Probability of accidient rate	Probability of vehicle 2 in tunnel	Probability of accidient rate	Probability of vehicle 3 in tunnel	Probability of accidient rate	Probability of vehicle 4 in tunnel	Probability of accidient rate	collision resulting in fire	MW	
LGV	M	B		0.3064	7.02E-03	0.1175	3.08E-02	0.001	3.53E-02	0	0	3.47E-05	46.2	4.40E-13
LGV	M	C		0.3064	7.02E-03	0.1175	3.08E-02	0.5676	1.14E-02	0	0	3.47E-05	18.8	3.28E-11
LGV	M	LGV		0.3064	7.02E-03	0.1175	3.08E-02	0.3064	7.02E-03	0	0	3.47E-05	32.5	1.88E-11
LGV	M	M		0.3064	7.02E-03	0.1175	3.08E-02	0.1175	3.08E-02	0	0	3.47E-05	17.2	1.68E-11
M	M	M		0.1175	3.08E-02	0.1175	3.08E-02	0.1175	3.08E-02	0	0	3.47E-05	3.7	6.11E-12
B	B	B	B	0.001	3.53E-02	0.001	3.53E-02	0.001	3.53E-02	0.001	3.53E-02	3.47E-05	118.8	6.39E-21
HGV	B	B	B	0.0075	2.64E-02	0.001	3.53E-02	0.001	3.53E-02	0.001	3.53E-02	3.47E-05	245.7	7.42E-20
B	HGV	HGV	B	0.001	3.53E-02	0.0075	2.64E-02	0.0075	2.64E-02	0.001	3.53E-02	3.47E-05	434.5	7.36E-19
B	B	B	M	0.001	3.53E-02	0.001	3.53E-02	0.001	3.53E-02	0.1175	3.08E-02	3.47E-05	89.8	4.95E-19
LGV	B	B	B	0.3064	7.02E-03	0.001	3.53E-02	0.001	3.53E-02	0.001	3.53E-02	3.47E-05	105.2	3.45E-19
HGV	HGV	HGV	B	0.0075	2.64E-02	0.0075	2.64E-02	0.0075	2.64E-02	0.001	3.53E-02	3.47E-05	623.4	5.93E-18
B	B	B	C	0.001	3.53E-02	0.001	3.53E-02	0.001	3.53E-02	0.5676	1.14E-02	3.47E-05	91.5	9.01E-19
HGV	B	B	M	0.0075	2.64E-02	0.001	3.53E-02	0.001	3.53E-02	0.1175	3.08E-02	3.47E-05	231.4	7.16E-18
HGV	B	B	LGV	0.0075	2.64E-02	0.001	3.53E-02	0.001	3.53E-02	0.3064	7.02E-03	3.47E-05	237.1	4.36E-18
HGV	HGV	HGV	HGV	0.0075	2.64E-02	0.0075	2.64E-02	0.0075	2.64E-02	0.0075	2.64E-02	3.47E-05	807.6	4.31E-17
HGV	B	B	C	0.0075	2.64E-02	0.001	3.53E-02	0.001	3.53E-02	0.5676	1.14E-02	3.47E-05	232.7	1.29E-17
M	B	B	M	0.1175	3.08E-02	0.001	3.53E-02	0.001	3.53E-02	0.1175	3.08E-02	3.47E-05	60.6	3.42E-17
LGV	HGV	HGV	B	0.3064	7.02E-03	0.0075	2.64E-02	0.0075	2.64E-02	0.001	3.53E-02	3.47E-05	426.0	4.40E-17
B	HGV	HGV	C	0.001	3.53E-02	0.0075	2.64E-02	0.0075	2.64E-02	0.5676	1.14E-02	3.47E-05	421.6	1.31E-16
LGV	B	B	M	0.3064	7.02E-03	0.001	3.53E-02	0.001	3.53E-02	0.1175	3.08E-02	3.47E-05	76.0	2.55E-17
HGV	HGV	HGV	M	0.0075	2.64E-02	0.0075	2.64E-02	0.0075	2.64E-02	0.1175	3.08E-02	3.47E-05	609.2	5.94E-16
C	B	B	M	0.5676	1.14E-02	0.001	3.53E-02	0.001	3.53E-02	0.1175	3.08E-02	3.47E-05	62.3	6.29E-17
B	LGV	LGV	B	0.001	3.53E-02	0.3064	7.02E-03	0.3064	7.02E-03	0.001	3.53E-02	3.47E-05	91.3	1.82E-17
HGV	M	M	B	0.0075	2.64E-02	0.1175	3.08E-02	0.1175	3.08E-02	0.001	3.53E-02	3.47E-05	217.2	6.89E-16
HGV	HGV	HGV	LGV	0.0075	2.64E-02	0.0075	2.64E-02	0.0075	2.64E-02	0.3064	7.02E-03	3.47E-05	615.0	3.56E-16
LGV	B	B	C	0.3064	7.02E-03	0.001	3.53E-02	0.001	3.53E-02	0.5676	1.14E-02	3.47E-05	50.1	3.01E-17

Possible vehicle configuration				Vehicle 1		Vehicle 2		Vehicle 3		Vehicle 4		Probability	Peak HRR	Risk level
				Probability of vehicle 1 in tunnel	Probability of accidient rate	Probability of vehicle 2 in tunnel	Probability of accidient rate	Probability of vehicle 3 in tunnel	Probability of accidient rate	Probability of vehicle 4 in tunnel	Probability of accidient rate	collision resulting in fire	MW	
HGV	HGV	HGV	C	0.0075	2.64E-02	0.0075	2.64E-02	0.0075	2.64E-02	0.5676	1.14E-02	3.47E-05	610.5	1.06E-15
C	B	B	C	0.5676	1.14E-02	0.001	3.53E-02	0.001	3.53E-02	0.5676	1.14E-02	3.47E-05	64.0	1.15E-16
HGV	LGV	LGV	B	0.0075	2.64E-02	0.3064	7.02E-03	0.3064	7.02E-03	0.001	3.53E-02	3.47E-05	228.7	2.56E-16
M	HGV	HGV	M	0.1175	3.08E-02	0.0075	2.64E-02	0.0075	2.64E-02	0.1175	3.08E-02	3.47E-05	406.2	7.23E-15
B	HGV	HGV	M	0.001	3.53E-02	0.0075	2.64E-02	0.0075	2.64E-02	0.1175	3.08E-02	3.47E-05	420.3	7.30E-17
B	M	M	M	0.001	3.53E-02	0.1175	3.08E-02	0.1175	3.08E-02	0.1175	3.08E-02	3.47E-05	31.7	1.84E-15
LGV	HGV	HGV	M	0.3064	7.02E-03	0.0075	2.64E-02	0.0075	2.64E-02	0.1175	3.08E-02	3.47E-05	411.9	4.36E-15
HGV	C	C	B	0.0075	2.64E-02	0.5676	1.14E-02	0.5676	1.14E-02	0.001	3.53E-02	3.47E-05	219.8	2.23E-15
C	HGV	HGV	M	0.5676	1.14E-02	0.0075	2.64E-02	0.0075	2.64E-02	0.1175	3.08E-02	3.47E-05	407.4	1.30E-14
LGV	M	M	B	0.3064	7.02E-03	0.1175	3.08E-02	0.1175	3.08E-02	0.001	3.53E-02	3.47E-05	76.0	2.62E-15
LGV	HGV	HGV	LGV	0.3064	7.02E-03	0.0075	2.64E-02	0.0075	2.64E-02	0.3064	7.02E-03	3.47E-05	417.6	2.63E-15
B	M	M	C	0.001	3.53E-02	0.1175	3.08E-02	0.1175	3.08E-02	0.5676	1.14E-02	3.47E-05	33.1	3.42E-15
LGV	HGV	HGV	C	0.3064	7.02E-03	0.0075	2.64E-02	0.0075	2.64E-02	0.5676	1.14E-02	3.47E-05	413.1	7.81E-15
B	LGV	LGV	M	0.001	3.53E-02	0.3064	7.02E-03	0.3064	7.02E-03	0.1175	3.08E-02	3.47E-05	76.0	1.55E-15
HGV	M	M	M	0.0075	2.64E-02	0.1175	3.08E-02	0.1175	3.08E-02	0.1175	3.08E-02	3.47E-05	406.2	1.32E-13
C	HGV	HGV	C	0.5676	1.14E-02	0.0075	2.64E-02	0.0075	2.64E-02	0.5676	1.14E-02	3.47E-05	408.7	2.32E-14
LGV	LGV	LGV	B	0.3064	7.02E-03	0.3064	7.02E-03	0.3064	7.02E-03	0.001	3.53E-02	3.47E-05	77.5	9.43E-16
HGV	M	M	LGV	0.0075	2.64E-02	0.1175	3.08E-02	0.1175	3.08E-02	0.3064	7.02E-03	3.47E-05	208.8	4.04E-14
B	C	C	M	0.001	3.53E-02	0.5676	1.14E-02	0.5676	1.14E-02	0.1175	3.08E-02	3.47E-05	34.7	6.43E-15
B	LGV	LGV	C	0.001	3.53E-02	0.3064	7.02E-03	0.3064	7.02E-03	0.5676	1.14E-02	3.47E-05	63.8	2.33E-15
HGV	M	M	C	0.0075	2.64E-02	0.1175	3.08E-02	0.1175	3.08E-02	0.5676	1.14E-02	3.47E-05	204.3	1.19E-13
HGV	LGV	LGV	M	0.0075	2.64E-02	0.3064	7.02E-03	0.3064	7.02E-03	0.1175	3.08E-02	3.47E-05	208.8	2.40E-14
LGV	C	C	B	0.3064	7.02E-03	0.5676	1.14E-02	0.5676	1.14E-02	0.001	3.53E-02	3.47E-05	50.1	5.51E-15
B	C	C	C	0.001	3.53E-02	0.5676	1.14E-02	0.5676	1.14E-02	0.5676	1.14E-02	3.47E-05	36.9	1.22E-14
M	M	M	M	0.1175	3.08E-02	0.1175	3.08E-02	0.1175	3.08E-02	0.1175	3.08E-02	3.47E-05	5.0	2.94E-14
HGV	LGV	LGV	LGV	0.0075	2.64E-02	0.3064	7.02E-03	0.3064	7.02E-03	0.3064	7.02E-03	3.47E-05	220.3	1.50E-14

Possible vehicle configuration				Vehicle 1		Vehicle 2		Vehicle 3		Vehicle 4		Probability	Peak HRR	Risk level
				Probability of vehicle 1 in tunnel	Probability of accidient rate	Probability of vehicle 2 in tunnel	Probability of accidient rate	Probability of vehicle 3 in tunnel	Probability of accidient rate	Probability of vehicle 4 in tunnel	Probability of accidient rate	collision resulting in fire	MW	
HGV	C	C	M	0.0075	2.64E-02	0.5676	1.14E-02	0.5676	1.14E-02	0.1175	3.08E-02	3.47E-05	203.1	2.11E-13
HGV	LGV	LGV	C	0.0075	2.64E-02	0.3064	7.02E-03	0.3064	7.02E-03	0.5676	1.14E-02	3.47E-05	206.8	4.25E-14
LGV	M	M	M	0.3064	7.02E-03	0.1175	3.08E-02	0.1175	3.08E-02	0.1175	3.08E-02	3.47E-05	17.9	6.31E-14
HGV	C	C	LGV	0.0075	2.64E-02	0.5676	1.14E-02	0.5676	1.14E-02	0.3064	7.02E-03	3.47E-05	211.3	1.30E-13
C	M	M	M	0.5676	1.14E-02	0.1175	3.08E-02	0.1175	3.08E-02	0.1175	3.08E-02	3.47E-05	5.9	6.22E-14
M	LGV	LGV	M	0.1175	3.08E-02	0.3064	7.02E-03	0.3064	7.02E-03	0.1175	3.08E-02	3.47E-05	33.1	6.95E-14
HGV	C	C	C	0.0075	2.64E-02	0.5676	1.14E-02	0.5676	1.14E-02	0.5676	1.14E-02	3.47E-05	206.8	3.84E-13
LGV	M	M	C	0.3064	7.02E-03	0.1175	3.08E-02	0.1175	3.08E-02	0.5676	1.14E-02	3.47E-05	19.2	1.21E-13
LGV	LGV	LGV	M	0.3064	7.02E-03	0.3064	7.02E-03	0.3064	7.02E-03	0.1175	3.08E-02	3.47E-05	48.4	6.04E-14
M	C	C	M	0.1175	3.08E-02	0.5676	1.14E-02	0.5676	1.14E-02	0.1175	3.08E-02	3.47E-05	9.5	1.79E-13
C	LGV	LGV	M	0.5676	1.14E-02	0.3064	7.02E-03	0.3064	7.02E-03	0.1175	3.08E-02	3.47E-05	34.8	1.30E-13
LGV	LGV	LGV	LGV	0.3064	7.02E-03	0.3064	7.02E-03	0.3064	7.02E-03	0.3064	7.02E-03	3.47E-05	64.0	4.75E-14
LGV	C	C	M	0.3064	7.02E-03	0.5676	1.14E-02	0.5676	1.14E-02	0.1175	3.08E-02	3.47E-05	21.2	2.39E-13
LGV	LGV	LGV	C	0.3064	7.02E-03	0.3064	7.02E-03	0.3064	7.02E-03	0.5676	1.14E-02	3.47E-05	50.3	1.12E-13
C	C	C	M	0.5676	1.14E-02	0.5676	1.14E-02	0.5676	1.14E-02	0.1175	3.08E-02	3.47E-05	14.2	4.80E-13
C	LGV	LGV	C	0.5676	1.14E-02	0.3064	7.02E-03	0.3064	7.02E-03	0.5676	1.14E-02	3.47E-05	36.7	2.46E-13
LGV	C	C	C	0.3064	7.02E-03	0.5676	1.14E-02	0.5676	1.14E-02	0.5676	1.14E-02	3.47E-05	23.2	4.67E-13
C	C	C	C	0.5676	1.14E-02	0.5676	1.14E-02	0.5676	1.14E-02	0.5676	1.14E-02	3.47E-05	18.9	1.14E-12
M	C	B	LGV	0.1175	3.08E-02	0.5676	1.14E-02	0.001	3.53E-02	0.3064	7.02E-03	3.47E-05	48.4	2.98E-15
M	C	B	HGV	0.1175	3.08E-02	0.5676	1.14E-02	0.001	3.53E-02	0.0075	2.64E-02	3.47E-05	218.5	1.24E-15
M	C	LGV	HGV	0.1175	3.08E-02	0.5676	1.14E-02	0.3064	7.02E-03	0.0075	2.64E-02	3.47E-05	210.1	7.26E-14
M	B	LGV	HGV	0.1175	3.08E-02	0.001	3.53E-02	0.3064	7.02E-03	0.0075	2.64E-02	3.47E-05	223.0	4.20E-16
C	B	LGV	HGV	0.5676	1.14E-02	0.001	3.53E-02	0.3064	7.02E-03	0.0075	2.64E-02	3.47E-05	224.2	7.56E-16
												Highest fire risk by collision	**HGV**	1.39E-06
												Lowest fire risk by collision	**B-B-B-B**	6.39E-21

APPENDIX G

Appendix G: Calculation of molecular weight and stoichiometry coefficient for wood

Molecular weight for wood

The chemical formula for wood is $C_{3.4}$ $H_{6.2}$ $O_{2.5.}$

Knowing the Atomic weights: C = 12; H = 1; O = 16

Molecular weight of wood ($C_{3.4}$ $H_{6.2}$ $O_{2.5}$)

= (3.4 x Atomic weight of C) + (6.2 x Atomic weight of H) + (2.5 x Atomic weight of O)

= (3.4 x 12) + (6.2 x 1) + (2.5 x 16) = 87

Stoichiometry coefficient for CO_2, H_2O, O_2

The stoichiometry equation is defined as follows:

$$Fuel[C,H,O] + Air \rightarrow \Pr oduct[CO_2 H_2 O, N_2] \qquad \text{Equation G1}$$

$$C_a H_b, O_c + d[O_2 + 3.76N_2] \rightarrow aCO_2 + \frac{b}{2} H_2 O + 3.76dN_2 \qquad \text{Equation G2}$$

where

$$d = a + \frac{b}{4} - \frac{c}{2} \qquad \text{Equation G3}$$

Knowing the chemical formula for wood is $C_{3.4}$ $H_{6.2}$ $O_{2.5.}$ The value for a, b, c and d is 3.4, 6.2, 2.5 and $d = 3.4 + \frac{6.2}{4} - \frac{2.5}{2} = 3.7$

By applying equation G2:

$$C_{3.4}H_{6.2}, O_{2.5} + 3.7[O_2 + 3.76N_2] \rightarrow 3.4CO_2 + \frac{6.2}{2} H_2 O + 3.76[3.7]N_2$$

$$C_{3.4}H_{6.2}, O_{2.5} + 3.7[O_2 + 3.76N_2] \rightarrow 3.4CO_2 + 3.1H_2 O + 13.9N_2$$

Reference: (Karlsson and Quintiere 2000)

APPENDIX H

Appendix H: Sample of FDS input file for simulating free burning pallets (FDS 4.0.7)

Define name of output files

****

```
&HEAD CHID='Pallets',TITLE='Free Burning of pallets'/
```

Define gird size and domain size

****

Grid size for tunnel

```
&GRID IBAR=18,JBAR=18,KBAR=50/  0.3 grids
```

Domain size

```
&PDIM XBAR0=0,XBAR=5.4,YBAR0=0,YBAR=5.4,ZBAR0=0,ZBAR=15/
```

Define simulation time

****

```
&TIME TWFIN=2100/ simulation time in second
```

Miscellaneous input parameters

****

```
&MISC DTCORE=200,SURF_DEFAULT='CONCRETE',REACTION='WOOD',TMPA=20/ Unless specific,
the default surface line applied to all SURF line is CONCRETE. The combustion stoichiometry defined as
WOOD is used. The ambient temperature used for the simulation is 20°C
```

Reaction input parameter

****

```
&REAC ID='WOOD'
     FYI='Ritchie, et al., 5th IAFSS, C_3.4 H_6.2 O_2.5'
     SOOT_YIELD = 0.01
     NU_O2          = 3.7
     NU_CO2         = 3.4
     NU_H2O         = 3.1
     MW_FUEL        = 87.
     EPUMO2         = 11020. / Calculation of molecular weight and stoichiometry coefficient for wood Refer to
                                Appendix G
```

Ignition of fire
****

Size of ignition source

```
&SURF ID='fire',HRRPUA=5500,RAMP_Q='INCfire' /
&RAMP ID='INCfire',T=0.0,F=1/
&RAMP ID='INCfire',T=300,F=1/
&RAMP ID='INCfire',T=301,F=0/
```

Location of ignition source

```
&OBST XB=1.8,2.1,2.6,2.9,1.2,1.5,RGB=1,0,0,SURF_ID6='INERT','INERT','INERT','INERT','INERT','fire'/
```

Flammability parameter based on HRRPUA
****

```
&SURF ID              = 'WOOD PALLETS 1.2 X 0.8'
    FYI               = 'PLYWOOD ordinary '
    KS                = 0.12
    DENSITY           = 600
    C_P               = 2.58
    DELTA             = 0.043
    BURN_AWAY         = .TRUE.
    TMPIGN            = 373
    BACKING           = 'INSULATED'
    HRRPUA            = 1064
    RAMP_Q            = 'GAP1'
&RAMP ID='GAP1',T= 0,F=0 /
&RAMP ID='GAP1',T= 30,F=1 / 266 x 4
&RAMP ID='GAP1',T= 60,F=0.63 /
&RAMP ID='GAP1',T= 90,F=0.5 /
&RAMP ID='GAP1',T= 150,F=0.38 /
&RAMP ID='GAP1',T= 210,F=0.38 /
&RAMP ID='GAP1',T= 270,F=0.5 /
&RAMP ID='GAP1',T= 330,F=0.69 /
&RAMP ID='GAP1',T= 390,F=0.94 /
&RAMP ID='GAP1',T= 450,F=0.31 /

&SURF ID              = 'WOOD PALLETS 1.2 X 1'
    FYI               = 'PLYWOOD ordinary '
    KS                = 0.12
    DENSITY           = 600
    C_P               = 2.58
    DELTA             = 0.037
    BURN_AWAY         = .TRUE.
    TMPIGN            = 373
    BACKING           = 'INSULATED'
    HRRPUA            = 1021.44
    RAMP_Q            = 'GAP2'
&RAMP ID='GAP2',T= 0.0,F=0 /
&RAMP ID='GAP2',T= 30,F=1 /266 x 3.84
&RAMP ID='GAP2',T= 60,F=0.63 /
&RAMP ID='GAP2',T= 90,F=0.5 /
&RAMP ID='GAP2',T= 150,F=0.38 /
```

```
&RAMP ID='GAP2',T= 210,F=0.38 /
&RAMP ID='GAP2',T= 270,F=0.5 /
&RAMP ID='GAP2',T= 330,F=0.69 /
&RAMP ID='GAP2',T= 390,F=0.94 /
&RAMP ID='GAP2',T= 450,F=0.31 /


&SURF ID              = 'PLASTIC PALLETS 1.2 X 0.8'
    FYI               = 'POLYETHYLENE '
    KS                = 0.64
    DENSITY           = 956
    C_P               = 3
    DELTA             = 0.048
    BURN_AWAY         = .TRUE.
    TMPIGN            = 323
    BACKING           = 'INSULATED'
    HRRPUA            = 9130
    RAMP_Q            = 'GAP3'
&RAMP ID='GAP3',T=   0.0,F=0.0 /
&RAMP ID='GAP3',T=   285,F=0.0 /
&RAMP ID='GAP3',T=   345,F=0.045 /
&RAMP ID='GAP3',T=   435,F=0.136 /
&RAMP ID='GAP3',T=   465,F=0.45 /
&RAMP ID='GAP3',T=   585,F=0.77 /
&RAMP ID='GAP3',T=   645,F=1 /1100 x 8.3
&RAMP ID='GAP3',T=   705,F=0.36 /
&RAMP ID='GAP3',T=   765,F=0 /
```

Material properties input parameters

```
***********************************

&SURF ID    = 'CONCRETE'
    FYI         = 'Quintiere, Fire Behavior'
    RGB         = 0.66,0.66,0.66
    C_P         = 0.88
    DENSITY=2100.
    KS          = 1.0
    DELTA    = 0.7 /


&SURF ID              = 'STEEL'
    RGB               = 0.20,0.20,0.20
    C_DELTA_RHO = 20
    DELTA             = 0.005 /
```

Boundary condition (free burning)

```
****************************

&VENT XB=0,5.4,0,0,0,15, SURF_ID='OPEN'/
&VENT XB=0,5.4,5.4,5.4,0,15, SURF_ID='OPEN'/
&VENT XB=0,0,0,5.4,0,15, SURF_ID='OPEN'/
&VENT XB=5.4,5.4,0,5.4,0,15, SURF_ID='OPEN'/
&VENT XB=0,5.4,0,5.4,15,15, SURF_ID='OPEN'/
```

Ground
****
&OBST XB=0,5.4,0,5.4,0,0.3,RGB=0.5,0.5,0.5/

Pallets Supports
****
&OBST XB=1.7,3.5,1.5,4.2,0.9,1.2,RGB=0.5,0.5,0.5/
&OBST XB=1.7,2,1.5,1.8,0.3,0.9,RGB=0.0,0.0,1,SURF_ID='STEEL'/
&OBST XB=1.7,2,3.9,4.2,0.3,0.9,RGB=0.0,0.0,1,SURF_ID='STEEL'/
&OBST XB=3.2,3.5,1.5,1.8,0.3,0.9,RGB=0.0,0.0,1,SURF_ID='STEEL'/
&OBST XB=3.2,3.5,3.9,4.2,0.3,0.9,RGB=0.0,0.0,1,SURF_ID='STEEL'/

Fuel package (wood and plastic pallets)
****

&OBST XB=2.1,3,1.8,4.2,2.4,2.7,RGB=0.8,0.6,0.4,SURF_IDS='WOOD PALLETS 1.2 X 0.8','WOOD PALLETS 1.2 X 0.8','WOOD PALLETS 1.2 X 0.8'/PALLET
&OBST XB=2.1,3,1.8,4.2,1.8,2.1,RGB=0.8,0.6,0.4,SURF_IDS='WOOD PALLETS 1.2 X 0.8','PLASTIC PALLETS 1.2 X 0.8','WOOD PALLETS 1.2 X 0.8'/PALLET
&OBST XB=2.1,3,1.8,4.2,1.2,1.5,RGB=0.8,0.6,0.4,SURF_IDS='WOOD PALLETS 1.2 X 1','WOOD PALLETS 1.2 X 0.8','WOOD PALLETS 1.2 X 0.8'/PALLET

Output from FDS
****

&ISOF QUANTITY='MIXTURE_FRACTION',VALUE(1)=0.148/
&SLCF PBY=2, QUANTITY='TEMPERATURE', DTSAM=1/

APPENDIX I

Appendix I: Calculation to define surface burning factor and thickness of fuel used in the Runehamar tunnel simulation

This section explains the necessary calculation required to establish the surface burning factor and thickness of the fuel used in the simulation. These parameters are critical as changes to these values will indirectly affect the heat release rate estimation by FDS.

Calculation to establish the surface burning factor and thickness for the Runehamar Tunnel fire experiment T1 are presented in the following section.

The dimension for a simulated truck is approximately 10.1 m (L) by 2.9m (W) by 2.8m (H) (Figure I1). In this fire experiment, a total of 454 pallets were burned and the fuel load is set up in the proportion by mass ratio of 80% wood and 20% plastic. The break down of the pallets size and the quantities used for this experiment is tabulated in Table I1.

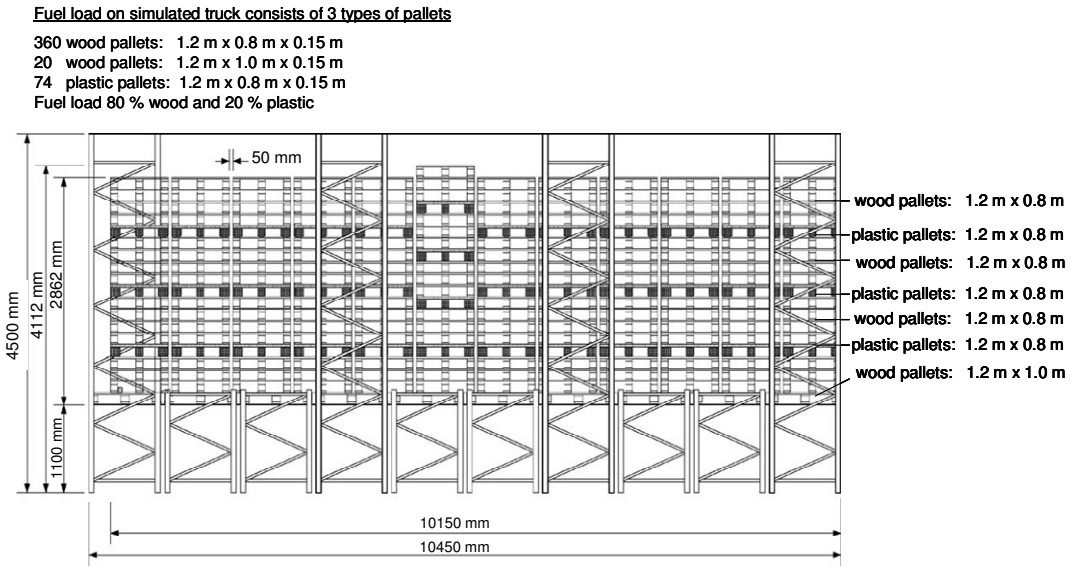

Figure I1: Dimension for simulated truck in Runehamar fire test 1

Description of pallets	Quantity
Wood pallets 1.2 m x 0.8 m x 0.15 m	360
Wood pallets 1.2 m x 1 m x 0.15 m	20
PE plastic pallets 1.2 m x 0.8 m x 0.15 m	74

Table I1: Dimensions of pallets and quantity of pallets

To simplify the modelling of wood and plastic pallets, these pallets are modelled as multiple layers in the simulation (Figure I1). The re-distribution of plastic and wood pallets for this simulation is modelled as follows (Table I2) & (Figure I2):

Layer	Pallet dimensions (Number of pallets)	Top SBF/Material/Thickness	Centre SBF/Material/Thickness	Bottom SBF/Material/Thickness
1	1.2 m x 0.8 m x 0.15 m (154 pallets)	10.24 / wood / 0.109 m	10.24 / wood / 0.109 m	10.24 / wood / 0.109 m
2	1.2 m x 0.8 m x 0.15 m (74 pallets)	5 / plastic / 0.03 m	5 / plastic / 0.03 m	7.27 / wood / 0.077 m
3	1.2 m x 0.8 m x 0.15 m (103 pallets)	7.27 / wood / 0.077 m	7.27 / wood / 0.077 m	7.27 / wood / 0.077 m
4	1.2 m x 0.8 m x 0.15 m (103 pallets)	5 / plastic / 0.03 m	7.27 / wood / 0.077 m	7.27 / wood / 0.077 m
5	1.2 m x 1.0 m x 0.15 m (20 pallets)	1.36 / wood / 0.013 m	1.36 / wood / 0.013 m	1.36 / wood / 0.013 m

Table I2: Re-distribution of plastic and wood pallets for FDS simulation

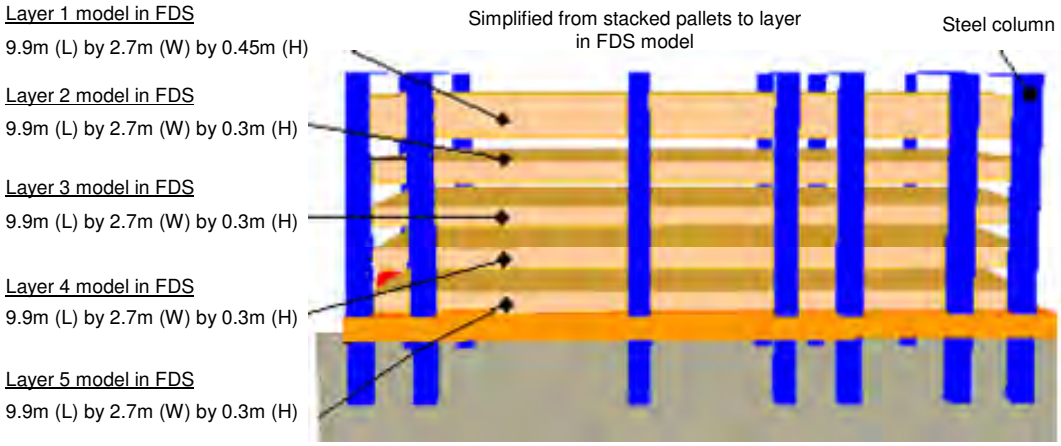

Figure I2: Representation of the fuel load pallets model for the Runehamar experiment

Calculations to determine thickness and surface burning factor for layer 1

Layer 1 – based on layer with 154 wood pallets

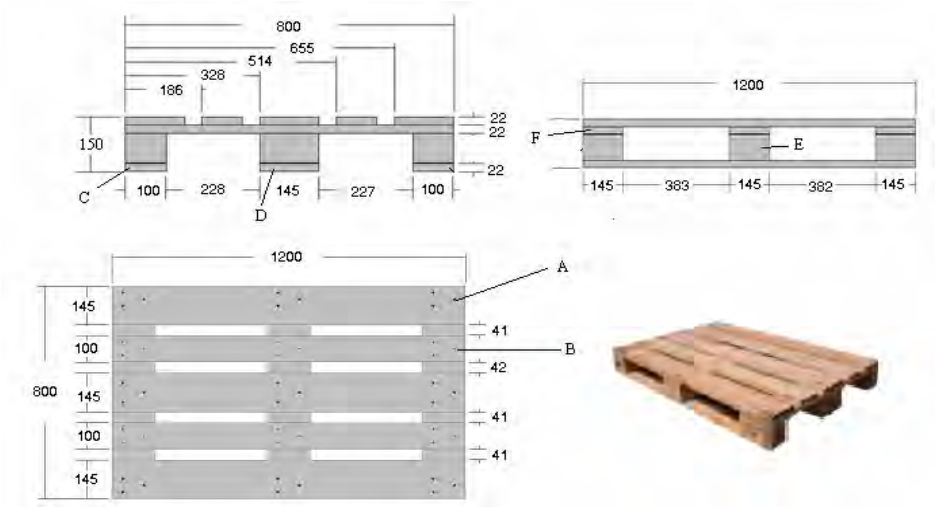

Figure I3:1.2m by 0.8m by 0.15m wood pallets

Plank	*Number of planks*	*Total area (m^2)*	*Total volume (m^3)*
A	*3*	*1.071*	*0.0115*
B	*2*	*0.594*	*0.0053*
C	*2*	*0.594*	*0.0035*
D	*1*	*0.407*	*0.0026*
E	*9*	*0.817*	*0.0159*
F	*3*	*0.821*	*0.0077*

Total area per pallet = 1.071 +0.594+0.594+0.407+0.817+0.821=4.31 m^2

Total volume per pallet =0.0115+0.0053+0.0035+0.0026+0.0159+0.0077=0.046 m^3

Volume per actual wood pallet (1.2m by 0.8m by 0.15m) is 0.046 m^3.

Total volume for 154 pallets is $154 \times 0.046 = 7.08$ m^3.

The total area model for layer 1 in the simulation is

$(9.9\text{m} \times 2.7\text{m} \times 2) + (9.9\text{m} \times 0.45\text{m} \times 2) + (2.7\text{m} \times 0.45\text{m} \times 2) = 64.8$ m^2.

Therefore the thickness used for the FDS simulation is $\frac{7.08}{64.8} = 0.109$ m.

Area per actual wood pallet (1.2m by 0.8m by 0.15m) is 4.31 m^2.

Actual total area for 154 pallets is $154 \times 4.31 = 663.7$ m^2.

Therefore the surface burning factor used for layer 1 is $\frac{663.7}{64.8} = 10.24$

Calculations to determine thickness and surface burning factor for layer 2

Layer 2 – based on layer with 74 plastic pallets

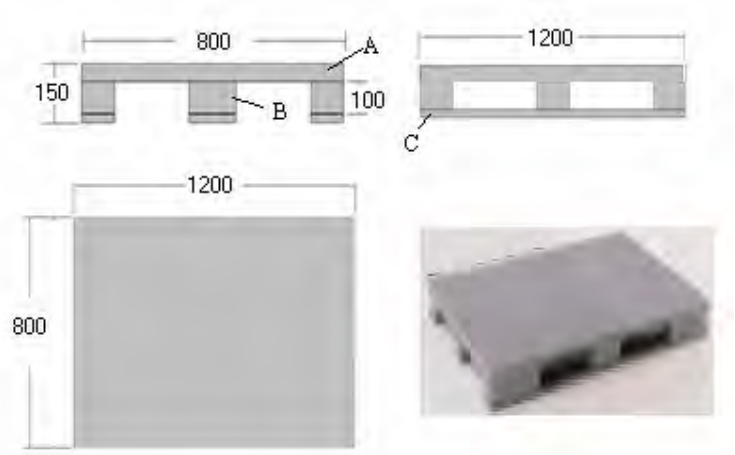

Figure I4:1.2m by 0.8m by 0.15m plastic pallets

Plank	*Number of planks*	*Total area (m^2)*
A	*1*	*2.02*
B	*9*	*1.037*
C	*2*	*0.598*
D	*1*	*0.428*

Total area per pallet = 2.02+1.037+0.598+0.428=4.1 m^2

Mass for 1 pallet of PE plastic is 23 kg. (kaiserkraft 2006)

Density for PE plastic is 956 kg/m^3. (Babrauskas 2003)

Volume per actual plastic pallet is $\frac{mass}{density} = \frac{23}{956} = 0.024\,\mathrm{m}^3$

Total volume for 74 actual pallets is 74 × 0.024 = 1.78 m^3.

The total area model for layer 2 in the simulation is

(9.9m × 2.7m × 2) + (9.9m × 0.3m × 2) + (2.7m × 0.3m × 2) = 61.02 m^2.

Therefore the thickness used for the FDS simulation is $\frac{1.78}{61.02} = 0.03$ m.

Area per actual plastic pallet (1.2m by 0.8m by 0.15m) is 4.1 m^2.

Actual total area for 74 pallets is 74 × 4.1 = 303.4 m^2.

Therefore the surface burning factor used for layer 2 is $\frac{303.4}{61.02} = 5$

Calculations to determine thickness and surface burning factor for type layer 3 or 4

Layer 3 or 4 – based on layer with 103 wood pallets

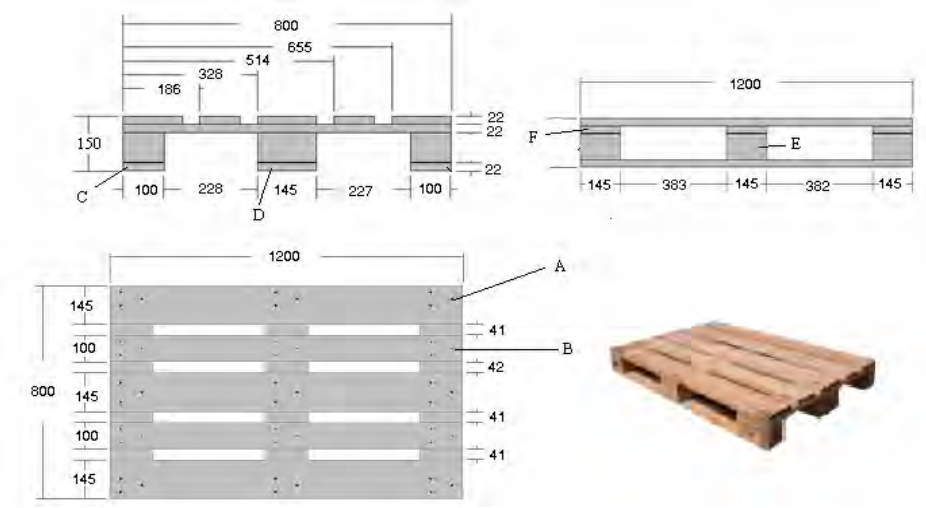

Figure I5:1.2m by 0.8m by 0.15m wood pallets

Plank	*Number of planks*	*Total area (m^2)*	*Total volume (m^3)*
A	*3*	*1.071*	*0.0115*
B	*2*	*0.594*	*0.0053*
C	*2*	*0.594*	*0.0035*
D	*1*	*0.407*	*0.0026*
E	*9*	*0.817*	*0.0159*
F	*3*	*0.821*	*0.0077*

Total area per pallet = 1.071 +0.594+0.594+0.407+0.817+0.821=4.31 m^2

Total volume per pallet =0.0115+0.0053+0.0035+0.0026+0.0159+0.0077=0.046 m^3

Volume per actual wood pallet (1.2m by 0.8m by 0.15m) is 0.046 m^3.

Total volume for 103 actual pallets is $103 \times 0.046 = 4.74$ m^3.

The total area model for layer 2 in the simulation is

$(9.9\text{m} \times 2.7\text{m} \times 2) + (9.9\text{m} \times 0.3\text{m} \times 2) + (2.7\text{m} \times 0.3\text{m} \times 2) = 61.02$ m^2.

Therefore the thickness used for the FDS simulation is $\frac{4.74}{61.02} = 0.077$ m.

Area per actual wood pallet (1.2m by 0.8m by 0.15m) is 4.31 m^2.

Actual total area for 103 pallets is $103 \times 4.31 = 443.93$ m^2

Therefore the surface burning factor used for layer 3 or 4 is $\frac{443.93}{61.02} = 7.27$

Calculations to determine thickness and surface burning factor for layer 5

Layer 5 – based on layer with 20 wood pallets

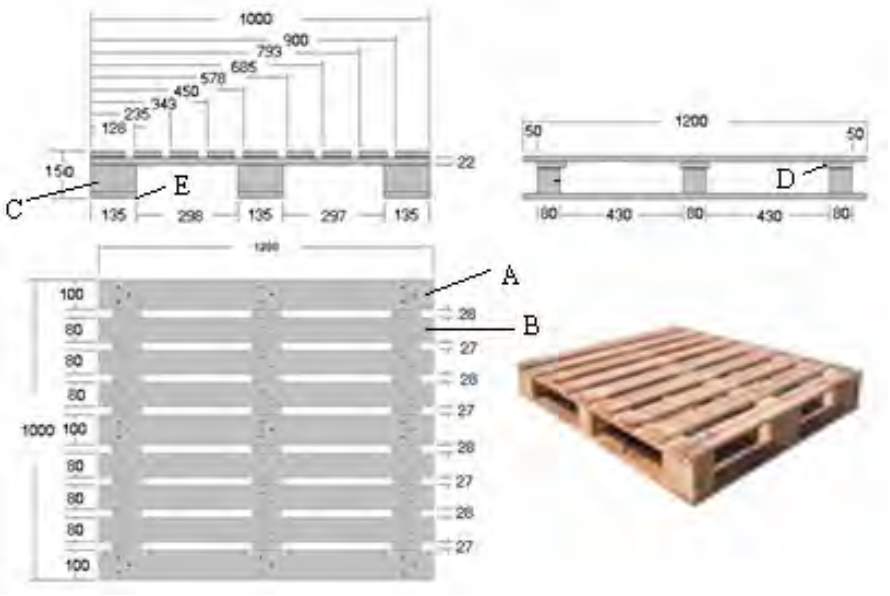

Figure I6:1.2m by 1m by 0.15m wood pallets

Plank	*Number of planks*	*Total area (m^2)*	*Total volume (m^3)*
A	*3*	*0.82*	*0.008*
B	*6*	*1.37*	*0.013*
C	*9*	*0.33*	*0.008*
D	*3*	*0.67*	*0.005*
E	*3*	*0.95*	*0.009*

Total area per pallet = 0.82+1.37+0.33+0.67+0.95=4.14 m^2

Total volume per pallet = 0.008+0.013+0.008+0.005+0.009=0.04 m^3

Volume per actual wood pallet (1.2m by 1.0m by 0.15m) is 0.04 m^3.

Total volume for 20 actual pallets is 20 × 0.04 =0.8 m^3.

The total area model for layer 5 in the simulation is

(9.9m × 2.7m × 2) + (9.9m × 0.3m × 2) + (2.7m × 0.3m × 2) = 61.02 m^2.

Therefore the thickness used for the FDS simulation is $\frac{0.8}{61.02} = 0.013$ m.

Area per actual wood pallet (1.2m by 1.0m by 0.15m) is 4.14 m^2.

Actual total area for 20 pallets is 20 × 4.14 = 82.8 m^2

Therefore the burning rate factor used for the FDS simulation is $\frac{82.8}{61.02} = 1.36$

APPENDIX J

Appendix J: Sample of FDS input file for simulating Runehamar tunnel (FDS 4.0.7)

Define name of output files

```
**************************
&HEAD CHID='Runehamar',TITLE='Runehamar Tunnel Fire Test 1'/
```

Define gird size and domain size single mesh

```
****************************************
Grid size for tunnel
-------------------------
&GRID IBAR=62,JBAR=620,KBAR=42/ 0.15 grids model
------------------------------
&PDIM XBAR0=0,XBAR=9.3,YBAR0=0,YBAR=93,ZBAR=6.3/
```

Define simulation time

```
**********************
&TIME TWFIN=3600/ simulation time in second
```

Miscellaneous input parameters

```
*******************************
&MISC DTCORE=200,SURF_DEFAULT='CONCRETE',REACTION='WOOD',TMPA=20/ Unless specific,
```

the default surface line applied to all SURF line is CONCRETE. The combustion stoichiometry defined as WOOD is used. The ambient temperature used for the simulation is 20^{o}C

Reaction input parameter

```
**************************
&REAC ID='WOOD'
     FYI='Ritchie, et al., 5th IAFSS, C_3.4 H_6.2 O_2.5'
     SOOT_YIELD = 0.01
     NU_O2       = 3.7
     NU_CO2    = 3.4
     NU_H2O    = 3.1
     MW_FUEL = 87
     EPUMO2    = 11020 /
```

Ignition of fire
****

Size of ignition source

```
&SURF ID='fire',HRRPUA=4500,RAMP_Q='INCfire' /
&RAMP ID='INCfire',T=0.0,F=1/
&RAMP ID='INCfire',T=3600,F=1/
```

Location of ignition source

```
&OBST XB=3.9,4.2,11.9,12.2,1.1,1.4,RGB=1,0,0,SURF_ID6='INERT','INERT','INERT','INERT',
'INERT','fire'/
&OBST XB=3.6,4.5,11.9,11.9,1.1,2,COLOR=INVISIBLE,T_REMOVE=360/ Tarpaulin cover burn off after
360s
```

Flammability parameter based on HRRPUA
****

Layer 1
****

```
&SURF ID              = 'WOOD PALLETS 1.2 X 0.8_0.45'
    FYI               = 'PLYWOOD ordinary '
    KS                = 0.12
    DENSITY           = 600
    C_P               = 2.58
    DELTA             = 0.109
    BURN_AWAY         = .TRUE.
    TMPIGN            = 373
    BACKING           = 'INSULATED'
    HRRPUA            = 3174.4
    RAMP_Q            = 'GAP1'
&RAMP ID='GAP1',T=0.0,F=0 /
&RAMP ID='GAP1',T=68.0,F=0.85/
&RAMP ID='GAP1',T=120.0,F=0.53 /
&RAMP ID='GAP1',T=180,F=0.48 /
&RAMP ID='GAP1',T=240,F=0.4 /
&RAMP ID='GAP1',T=300,F=0.64 /
&RAMP ID='GAP1',T=383,F=1/ [Surface burning factor × cone test peak HRRPUA=10.24 × 310=3174.4
                                    kW/m2]
&RAMP ID='GAP1',T= 420,F=0.54 /
```

Layer 2
****

```
&SURF ID              = 'PLASTIC PALLETS 1.2 X 0.8'
    FYI               = 'POLYETHYLENE (PE)'
    KS                = 0.64
    DENSITY           = 956
    C_P               = 3
    DELTA             = 0.03
    BURN_AWAY         = .TRUE.
    TMPIGN            = 323
    BACKING           = 'INSULATED'
    HRRPUA            = 14500
```

```
     RAMP_Q            = 'GAP2'
&RAMP ID='GAP2',T=0.0,F=0.0 /
&RAMP ID='GAP2',T=30,F=0.017 /
&RAMP ID='GAP2',T=60,F=0.14 /
&RAMP ID='GAP2',T=120,F=0.38 /
&RAMP ID='GAP2',T=180,F=1.0/[Surface burning factor × cone test peak HRRPUA = 5 × 2900=14500
                                        kW/m2]
&RAMP ID='GAP2',T=240,F=0.017 /
&RAMP ID='GAP2',T=870,F=0.0 /


Layer 3 or 4
*********
&SURF ID            = 'WOOD PALLETS 1.2 X 0.8'
     FYI            = 'PLYWOOD ordinary '
     KS             = 0.12
     DENSITY        = 600
     C_P            = 2.58
     DELTA          = 0.077
     BURN_AWAY      = .TRUE.
     TMPIGN         = 373
     BACKING        = 'INSULATED'
     HRRPUA         = 2253.7
     RAMP_Q         = 'GAP3'
&RAMP ID='GAP3',T=0.0,F=0 /
&RAMP ID='GAP3',T=68.0,F=0.85 /
&RAMP ID='GAP3',T=120.0,F=0.53 /
&RAMP ID='GAP3',T=180,F=0.48 /
&RAMP ID='GAP3',T=240,F=0.4 /
&RAMP ID='GAP3',T=300,F=0.64 /
&RAMP ID='GAP3',T=383,F=1/[Surface burning factor×cone test peak HRRPUA=7.27×310=2253.7 kW/m2]
&RAMP ID='GAP3',T= 420,F=0.54 /



Layer 5
*********
&SURF ID            = 'WOOD PALLETS 1.2 X 1'
     FYI            = 'PLYWOOD ordinary '
     KS             = 0.12
     DENSITY        = 600
     C_P            = 2.58
     DELTA          = 0.013
     BURN_AWAY      = .TRUE.
     TMPIGN         = 373
     BACKING        = 'INSULATED'
     HRRPUA         = 421.6
     RAMP_Q         = 'GAP4'
&RAMP ID='GAP4',T=0.0,F=0 /
&RAMP ID='GAP4',T=68.0,F=0.85 /
&RAMP ID='GAP4',T=120.0,F=0.53 /
&RAMP ID='GAP4',T=180,F=0.48 /
&RAMP ID='GAP4',T=240,F=0.4 /
&RAMP ID='GAP4',T=300,F=0.64 /
&RAMP ID='GAP4',T=383,F=1/[Surface burning factor×cone test peak HRRPUA=1.36×310=421.6 kW/m2]
&RAMP ID='GAP4',T= 420,F=0.54 /
```

Material properties input parameters
****

```
&SURF ID      = 'CONCRETE'
    FYI       = 'Quintiere, Fire Behaviour'
    RGB       = 0.66,0.66,0.66
    C_P       = 0.88
    DENSITY =2100
    KS        = 1.0
    DELTA     = 0.7 /

&SURF ID            = 'STEEL'
    RGB             = 0.20,0.20,0.20
    C_DELTA_RHO = 20
    DELTA           = 0.005 /

&SURF ID       = 'FIRE BOARD'
    FYI        = 'Quintiere, Fire Behavior'
    RGB        = 0.80,0.80,0.70
    HRRPUA   = 100
    RAMP_Q   = 'GB'
    KS         = 0.48
    C_P        = 0.84
    DENSITY = 1440
    DELTA     = 0.013
    TMPIGN   = 400. /
&RAMP ID='GB',T= 0.0,F=0.0 /
&RAMP ID='GB',T= 1.0,F=0.5 /
&RAMP ID='GB',T= 2.0,F=1.0 /
&RAMP ID='GB',T=10.0,F=1.0 /
&RAMP ID='GB',T=20.0,F=0.0 /
&RAMP ID='GB',T=30.0,F=0.0 /
```

Boundary condition (Ventilation in tunnel)
****

Tunnel fan operation at 3 m/s

```
&RAMP ID='FAN',T=0.0,F=1.0 / Fan operate at 3 m/s at time 0 seconds
&RAMP ID='FAN',T=3600,F=1.0 / Fan operate at 3 m/s at time 3600 seconds

&SURF ID='BOUNDARY CONDITION',VEL=-3, RAMP_V='FAN'/ 3 m/s airflow into tunnel
&VENT XB= 0,9.3,0,0,0.0,6.3, SURF_ID='BOUNDARY CONDITION'/
&VENT XB= 0,9.3,93,93,0.0,6.3, SURF_ID='OPEN'/
```

Tunnel geometry
****

TUNNEL GEOMETRY
****

```
&OBST XB=0.0,0.2,0,93,0,6.4,RGB=0.5,0.5,0.5,SAWTOOTH=.FALSE.,SURF_ID='CONCRETE'/
&OBST XB=0.2,0.4,0,93,3.2,6.4,RGB=0.5,0.5,0.5,SAWTOOTH=.FALSE.,SURF_ID='CONCRETE'/
&OBST XB=0.4,0.6,0,93,3.8,6.4,RGB=0.5,0.5,0.5,SAWTOOTH=.FALSE.,SURF_ID='CONCRETE'/
&OBST XB=0.6,0.8,0,93,4.4,6.4,RGB=0.5,0.5,0.5,SAWTOOTH=.FALSE.,SURF_ID='CONCRETE'/
&OBST XB=0.8,1.0,0,93,4.8,6.4,RGB=0.5,0.5,0.5,SAWTOOTH=.FALSE.,SURF_ID='CONCRETE'/
&OBST XB=1,1.2,0,93,5.2,6.4,RGB=0.5,0.5,0.5,SAWTOOTH=.FALSE.,SURF_ID='CONCRETE'/
```

```
&OBST XB=1.2,1.4,0,93,5.4,6.4,RGB=0.5,0.5,0.5,SAWTOOTH=.FALSE.,SURF_ID='CONCRETE'/
&OBST XB=1.4,1.6,0,93,5.6,6.4,RGB=0.5,0.5,0.5,SAWTOOTH=.FALSE.,SURF_ID='CONCRETE'/
&OBST XB=1.6,1.8,0,93,5.8,6.4,RGB=0.5,0.5,0.5,SAWTOOTH=.FALSE.,SURF_ID='CONCRETE'/
&OBST XB=1.8,7.4,0,93,6.0,6.4,RGB=0.5,0.5,0.5,SAWTOOTH=.FALSE.,SURF_ID='CONCRETE'/
&OBST XB=7.4,7.6,0,11,5.8,6.4,RGB=0.5,0.5,0.5,SAWTOOTH=.FALSE.,SURF_ID='CONCRETE'/
&OBST XB=7.6,7.8,0,11,5.6,6.4,RGB=0.5,0.5,0.5,SAWTOOTH=.FALSE.,SURF_ID='CONCRETE'/
&OBST XB=7.8,8.0,0,11,5.4,6.4,RGB=0.5,0.5,0.5,SAWTOOTH=.FALSE.,SURF_ID='CONCRETE'/
&OBST XB=8.0,8.2,0,11,5.2,6.4,RGB=0.5,0.5,0.5,SAWTOOTH=.FALSE.,SURF_ID='CONCRETE'/
&OBST XB=8.2,8.4,0,11,4.8,6.4,RGB=0.5,0.5,0.5,SAWTOOTH=.FALSE.,SURF_ID='CONCRETE'/
&OBST XB=8.4,8.6,0,11,4.4,6.4,RGB=0.5,0.5,0.5,SAWTOOTH=.FALSE.,SURF_ID='CONCRETE'/
&OBST XB=8.6,8.8,0,11,3.8,6.4,RGB=0.5,0.5,0.5,SAWTOOTH=.FALSE.,SURF_ID='CONCRETE'/
&OBST XB=8.8,9,0,11,3.2,6.4,RGB=0.5,0.5,0.5,SAWTOOTH=.FALSE.,SURF_ID='CONCRETE'/
&OBST XB=9.0,9.4,0,11,0,6.4,RGB=0.5,0.5,0.5,SAWTOOTH=.FALSE.,SURF_ID='CONCRETE'/
&OBST XB=7.4,7.6,11,93,5.8,6.4,COLOR=INVISIBLE,SAWTOOTH=.FALSE.,SURF_ID='CONCRETE'/
&OBST XB=7.6,7.8,11,93,5.6,6.4,COLOR=INVISIBLE,SAWTOOTH=.FALSE.,SURF_ID='CONCRETE'/
&OBST XB=7.8,8.0,11,93,5.4,6.4,COLOR=INVISIBLE,SAWTOOTH=.FALSE.,SURF_ID='CONCRETE'/
&OBST XB=8.0,8.2,11,93,5.2,6.4,COLOR=INVISIBLE,SAWTOOTH=.FALSE.,SURF_ID='CONCRETE'/
&OBST XB=8.2,8.4,11,93,4.8,6.4,COLOR=INVISIBLE,SAWTOOTH=.FALSE.,SURF_ID='CONCRETE'/
&OBST XB=8.4,8.6,11,93,4.4,6.4,COLOR=INVISIBLE,SAWTOOTH=.FALSE.,SURF_ID='CONCRETE'/
&OBST XB=8.6,8.8,11,93,3.8,6.4,COLOR=INVISIBLE,SAWTOOTH=.FALSE.,SURF_ID='CONCRETE'/
&OBST XB=8.8,9,11,93,3.2,6.4,COLOR=INVISIBLE,SAWTOOTH=.FALSE.,SURF_ID='CONCRETE'/
&OBST XB=9.0,9.4,11,93,0,6.4,COLOR=INVISIBLE,SAWTOOTH=.FALSE.,SURF_ID='CONCRETE'/

FIRE BOARD
**********
&OBST XB=0.7,1,0,93,0,3.4,RGB=1,1,1,SURF_ID='FIRE BOARD'/
&OBST XB=0.7,1.2,0,93,3.4,3.6,RGB=1,1,1,SAWTOOTH=.FALSE.,SURF_ID='FIRE BOARD'/
&OBST XB=1.0,1.4,0,93,3.6,4,RGB=1,1,1,SAWTOOTH=.FALSE.,SURF_ID='FIRE BOARD'/
&OBST XB=1.4,1.6,0,93,3.8,4.2,RGB=1,1,1,SAWTOOTH=.FALSE.,SURF_ID='FIRE BOARD'/
&OBST XB=1.6,1.8,0,93,4.0,4.4,RGB=1,1,1,SAWTOOTH=.FALSE.,SURF_ID='FIRE BOARD'/
&OBST XB=1.8,2.0,0,93,4.2,4.6,RGB=1,1,1,SAWTOOTH=.FALSE.,SURF_ID='FIRE BOARD'/
&OBST XB=2.0,2.2,0,93,4.4,4.8,RGB=1,1,1,SAWTOOTH=.FALSE.,SURF_ID='FIRE BOARD'/
&OBST XB=2.2,2.4,0,93,4.6,5,RGB=1,1,1,SAWTOOTH=.FALSE.,SURF_ID='FIRE BOARD'/
&OBST XB=2.4,2.6,0,93,4.8,5.2,RGB=1,1,1,SAWTOOTH=.FALSE.,SURF_ID='FIRE BOARD'/
&OBST XB=2.6,5.6,0,93,5,5.3,RGB=1,1,1,SAWTOOTH=.FALSE.,SURF_ID='FIRE BOARD'/
&OBST XB=5.6,6.0,0,11,4.8,5.2,RGB=1,1,1,SAWTOOTH=.FALSE.,SURF_ID='FIRE BOARD'/
&OBST XB=6.0,6.4,0,11,4.6,5,RGB=1,1,1,SAWTOOTH=.FALSE.,SURF_ID='FIRE BOARD'/
&OBST XB=6.4,6.8,0,11,4.4,4.8,RGB=1,1,1,SAWTOOTH=.FALSE.,SURF_ID='FIRE BOARD'/
&OBST XB=6.8,7.2,0,11,4.2,4.6,RGB=1,1,1,SAWTOOTH=.FALSE.,SURF_ID='FIRE BOARD'/
&OBST XB=7.2,7.6,0,11,4.0,4.4,RGB=1,1,1,SAWTOOTH=.FALSE.,SURF_ID='FIRE BOARD'/
&OBST XB=7.6,8.0,0,11,3.8,4.2,RGB=1,1,1,SAWTOOTH=.FALSE.,SURF_ID='FIRE BOARD'/
&OBST XB=7.7,8.0,0,11,0,4,RGB=1,1,1,SURF_ID='FIRE BOARD'/
&OBST XB=5.6,6.0,11,93,4.8,5.2,COLOR=INVISIBLE,SAWTOOTH=.FALSE.,SURF_ID='FIRE BOARD'/
&OBST XB=6.0,6.4,11,93,4.6,5,COLOR=INVISIBLE,SAWTOOTH=.FALSE.,SURF_ID='FIRE BOARD'/
&OBST XB=6.4,6.8,11,93,4.4,4.8,COLOR=INVISIBLE,SAWTOOTH=.FALSE.,SURF_ID='FIRE BOARD'/
&OBST XB=6.8,7.2,11,93,4.2,4.6,COLOR=INVISIBLE,SAWTOOTH=.FALSE.,SURF_ID='FIRE BOARD'/
&OBST XB=7.2,7.6,11,93,4.0,4.4,COLOR=INVISIBLE,SAWTOOTH=.FALSE.,SURF_ID='FIRE BOARD'/
&OBST XB=7.6,8.0,11,93,3.8,4.2,COLOR=INVISIBLE,SAWTOOTH=.FALSE.,SURF_ID='FIRE BOARD'/
&OBST XB=7.7,8.0,11,93,0,4,COLOR=INVISIBLE,SURF_ID='FIRE BOARD'/
```

Simulated truck frame
****

```
&OBST XB=2.6,5.5,12,22.55,1,1.1,RGB=1,0.5,0.0/ FLOOR
&OBST XB=2.6,2.7,12,12.2,0,4.5,RGB=0.0,0.0,1,SURF_ID='STEEL'/ FRAME
&OBST XB=5.4,5.5,12,12.2,0,4.5,RGB=0.0,0.0,1,SURF_ID='STEEL'/ FRAME
&OBST XB=2.6,5.5,12,12.2,4.4,4.5,RGB=0.0,0.0,1,SURF_ID='STEEL'/ FRAME
&OBST XB=2.6,2.7,13,13.2,0,4.5,RGB=0.0,0.0,1,SURF_ID='STEEL'/ FRAME
&OBST XB=5.4,5.5,13,13.2,0,4.5,RGB=0.0,0.0,1,SURF_ID='STEEL'/ FRAME
&OBST XB=2.6,5.5,13,13.2,4.4,4.5,RGB=0.0,0.0,1,SURF_ID='STEEL'/ FRAME
```

```
 &OBST XB=2.6,2.7,13,13.2,0,4.5,RGB=0.0,0.0,1,SURF_ID='STEEL'/ FRAME
&OBST XB=5.4,5.5,13,13.2,0,4.5,RGB=0.0,0.0,1,SURF_ID='STEEL'/ FRAME
&OBST XB=2.6,5.5,13,13.2,4.4,4.5,RGB=0.0,0.0,1,SURF_ID='STEEL'/ FRAME
&OBST XB=2.6,2.7,16,16.2,0,4.5,RGB=0.0,0.0,1,SURF_ID='STEEL'/ FRAME
&OBST XB=5.4,5.5,16,16.2,0,4.5,RGB=0.0,0.0,1,SURF_ID='STEEL'/ FRAME
&OBST XB=2.6,5.5,16,16.2,4.4,4.5,RGB=0.0,0.0,1,SURF_ID='STEEL'/ FRAME
&OBST XB=2.6,2.7,18,18.2,0,4.5,RGB=0.0,0.0,1,SURF_ID='STEEL'/ FRAME
&OBST XB=5.4,5.5,18,18.2,0,4.5,RGB=0.0,0.0,1,SURF_ID='STEEL'/ FRAME
&OBST XB=2.6,5.5,18,18.2,4.4,4.5,RGB=0.0,0.0,1,SURF_ID='STEEL'/ FRAME
&OBST XB=2.6,2.7,19,19.2,0,4.5,RGB=0.0,0.0,1,SURF_ID='STEEL'/ FRAME
&OBST XB=5.4,5.5,19,19.2,0,4.5,RGB=0.0,0.0,1,SURF_ID='STEEL'/ FRAME
&OBST XB=2.6,5.5,19,19.2,4.4,4.5,RGB=0.0,0.0,1,SURF_ID='STEEL'/ FRAME
&OBST XB=2.6,2.7,21,21.2,0,4.5,RGB=0.0,0.0,1,SURF_ID='STEEL'/ FRAME
&OBST XB=5.4,5.5,21,21.2,0,4.5,RGB=0.0,0.0,1,SURF_ID='STEEL'/ FRAME
&OBST XB=2.6,5.5,21,21.2,4.4,4.5,RGB=0.0,0.0,1,SURF_ID='STEEL'/ FRAME
&OBST XB=2.6,2.7,22,22.2,0,4.5,RGB=0.0,0.0,1,SURF_ID='STEEL'/ FRAME
&OBST XB=5.4,5.5,22,22.2,0,4.5,RGB=0.0,0.0,1,SURF_ID='STEEL'/ FRAME
&OBST XB=2.6,5.5,22,22.2,4.4,4.5,RGB=0.0,0.0,1,SURF_ID='STEEL'/ FRAME
```

Fuel load (wood and plastic pallets)

```
**********
```

```
&OBST XB=2.7,5.4,12.2,22.1,3.5,3.95,RGB=0.8,0.6,0.4,SURF_IDS='WOOD PALLETS 1.2 X
0.8_0.45','WOOD PALLETS 1.2 X 0.8_0.45','WOOD PALLETS 1.2 X 0.8_0.45'/ Layer 1
&OBST XB=2.7,5.4,12.2,22.1,2.9,3.2,RGB=0.8,0.6,0.4,SURF_IDs='PLASTIC PALLETS 1.2 X
0.8','PLASTIC PALLETS 1.2 X 0.8','WOOD PALLETS 1.2 X 0.8'/ Layer 2
&OBST XB=2.7,5.4,12.2,22.1,2.3,2.6,RGB=0.8,0.6,0.4,SURF_IDS='WOOD PALLETS 1.2 X 0.8','WOOD
PALLETS 1.2 X 0.8','WOOD PALLETS 1.2 X 0.8'/ Layer 3
&OBST XB=2.7,5.4,12.2,22.1,1.7,2,RGB=0.8,0.6,0.4,SURF_IDS='PLASTIC PALLETS 1.2 X 0.8','WOOD
PALLETS 1.2 X 0.8','WOOD PALLETS 1.2 X 0.8'/ Layer 4
&OBST XB=2.7,5.4,12.2,22.1,1.1,1.4,RGB=0.8,0.6,0.4,SURF_IDS='WOOD PALLETS 1.2 X 1','WOOD
PALLETS 1.2 X 1','WOOD PALLETS 1.2 X 1'/ Layer 5
```

Output from FDS

```
******************
```

```
&ISOF QUANTITY='MIXTURE_FRACTION',VALUE(1)=0.148, VALUE(2)=0.001/
&SLCF PBY=2, QUANTITY='TEMPERATURE', DTSAM=1./
&SLCF PBY=13, QUANTITY='TEMPERATURE', DTSAM=1./
&SLCF PBY=21, QUANTITY='TEMPERATURE', DTSAM=1./
&SLCF PBY=35, QUANTITY='TEMPERATURE', DTSAM=1./
&SLCF PBX=8, QUANTITY='TEMPERATURE', DTSAM=1./
&SLCF PBx=8, QUANTITY='VELOCITY',VECTOR=.TRUE./
```

APPENDIX K

Appendix K: Calculation to determine surface burning factor and thickness used in simulation (LGV)

The deck dimensions (allowable cargo space) for a LGV is approximately 3.1 m (L) by 1.69 m (W) by 2.4 m (H). LGV of this size is able to carry around 60 pallets and by using a mass ratio of 80 % wood and 20 % plastic, the fuel load used for the FDS simulation for a LGV will consist of 48 wood pallets (1.2 m × 1 m × 0.15 m) and 12 plastic pallets (1.2 m × 0.8 m × 0.15 m) (Figure K1).

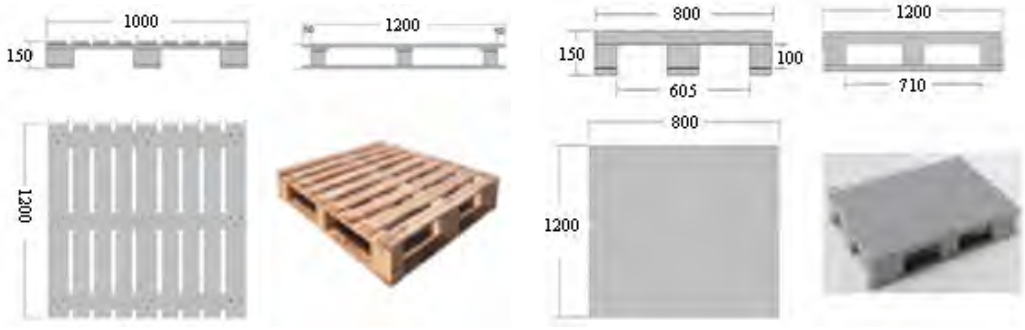

1.2m by 1.0m by 0.15m wood pallets (reproduced from (Pallet 2000a))

1.2m by 0.8m by 0.15m plastic pallets (reproduced from (kaiserkraft 2006))

Figure K1: Wood and plastic pallets dimensions

To simplify the modelling of wood and plastic pallets, these pallets are modelled as multiple layers in the simulation (Figure K2). The re-distribution of plastic and wood pallets for the HGV simulation model is as follows:

LGV simulation

Layer	Pallet dimensions (Number of pallets)	Top	Centre	Bottom
		SBF/Material/Thickness	SBF/Material/Thickness	SBF/Material/Thickness
1	1.2 m x 0.80 m x 0.15 m (16 pallets)	4.5 / plastic / 0.026	6.3 / wood / 0.067 m	6.3 / wood / 0.067 m
2	1.2 m x 0.8 m x 0.15 m (16 pallets)	6.3 / wood / 0.067 m	6.3 / wood / 0.067 m	6.3 / wood / 0.067 m
3	1.2 m x 0.8 m x 0.15 m (12 pallets)	4.5 / plastic / 0.026	4.5 / plastic / 0.026	6.3 / wood / 0.067 m
4	1.2 m x 0.8 m x 0.15 m (16 pallets)	6.3 / wood / 0.067 m	6.3 / wood / 0.067 m	6.3 / wood / 0.067 m

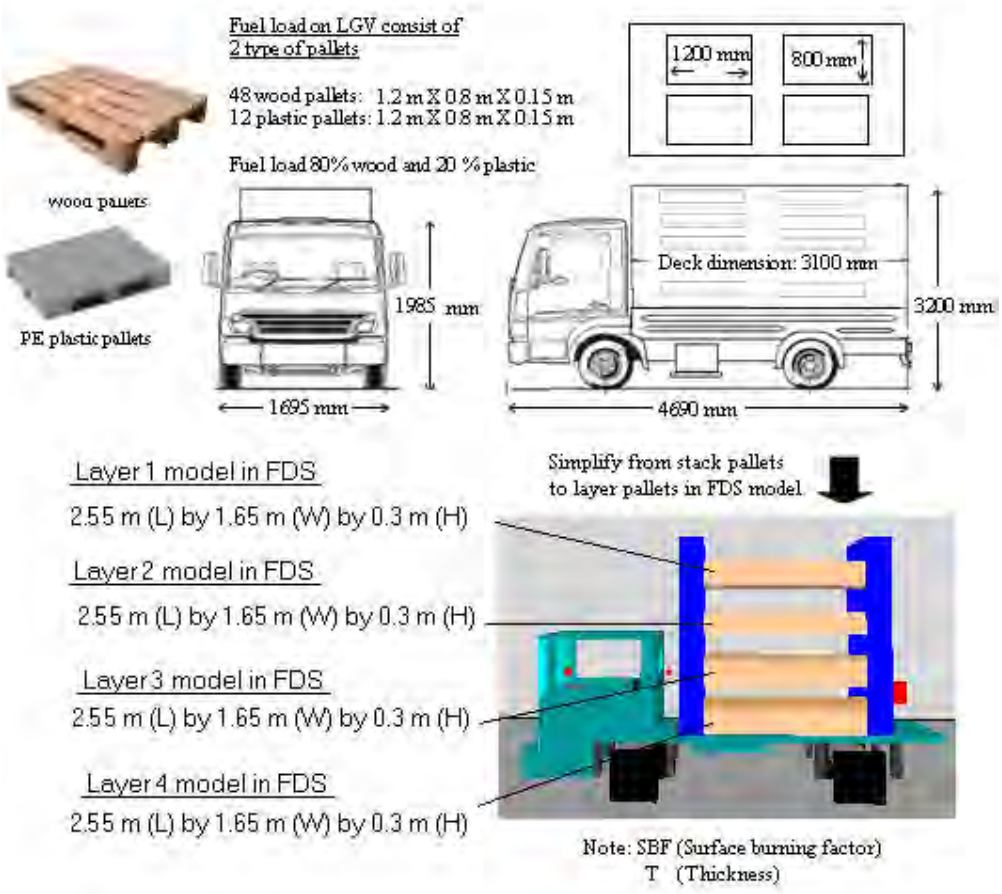

Figure K2: Dimension for light goods vehicle (LGV)

Calculations to determine thickness and surface burning factor for layer 1 pallets (LGV)

Layer 1 – based on layer with 16 pallets

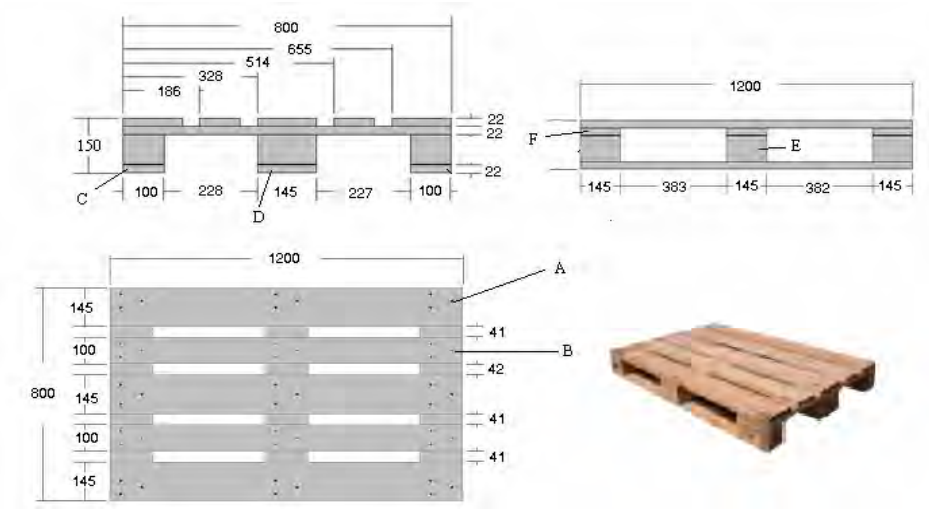

Figure K3:1.2m by 0.8m by 0.15m wood pallets

Plank	*Number of planks*	*Total area (m^2)*	*Total volume (m^3)*
A	*3*	*1.071*	*0.0115*
B	*2*	*0.594*	*0.0053*
C	*2*	*0.594*	*0.0035*
D	*1*	*0.407*	*0.0026*
E	*9*	*0.817*	*0.0159*
F	*3*	*0.821*	*0.0077*

Total area per pallet = 1.071 +0.594+0.594+0.407+0.817+0.821=4.31 m^2

Total volume per pallet =0.0115+0.0053+0.0035+0.0026+0.0159+0.0077=0.046 m^3

Volume per actual wood pallet (1.2m by 0.8m by 0.15m) is 0.046 m^3.

Total volume for 16 actual pallets is $16 \times 0.046 = 0.736$ m^3.

The total area model for layer 1 in the simulation is

$(2.55\text{m} \times 1.65\text{m} \times 2)+(2.55\text{m} \times 0.3\text{m} \times 2)+(1.65\text{m} \times 0.3\text{m} \times 2) = 10.94$ m^2.

Therefore the thickness used for the FDS simulation is $\frac{0.736}{10.94} = 0.067$ m.

Area per actual wood pallet (1.2m by 0.8m by 0.15m) is 4.31 m^2.

Actual total area for 16 pallets is $16 \times 4.31 = 68.96$ m^2

Therefore the burning rate factor used for the FDS simulation is $\frac{68.96}{10.94} = 6.3$

Calculations to determine thickness and surface burning factor for layer 2 pallets (LGV)

Layer 2 – based on layer with 16 pallets

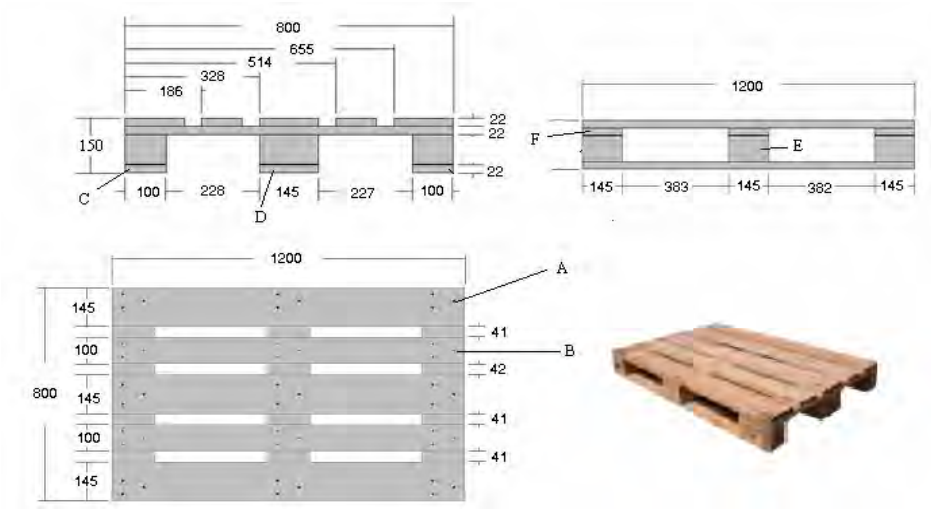

Figure K3:1.2m by 0.8m by 0.15m wood pallets

Plank	*Number of planks*	*Total area (m^2)*	*Total volume (m^3)*
A	*3*	*1.071*	*0.0115*
B	*2*	*0.594*	*0.0053*
C	*2*	*0.594*	*0.0035*
D	*1*	*0.407*	*0.0026*
E	*9*	*0.817*	*0.0159*
F	*3*	*0.821*	*0.0077*

Total area per pallet = 1.071 +0.594+0.594+0.407+0.817+0.821=4.31 m^2

Total volume per pallet =0.0115+0.0053+0.0035+0.0026+0.0159+0.0077=0.046 m^3

Volume per actual wood pallet (1.2m by 0.8m by 0.15m) is 0.046 m^3.

Total volume for 16 actual pallets is $16 \times 0.046 = 0.736$ m^3.

The total area model for layer 1 in the simulation is

$(2.55\text{m} \times 1.65\text{m} \times 2)+(2.55\text{m} \times 0.3\text{m} \times 2)+(1.65\text{m} \times 0.3\text{m} \times 2) = 10.94$ m^2.

Therefore the thickness used for the FDS simulation is $\frac{0.736}{10.94} = 0.067$ m.

Area per actual wood pallet (1.2m by 0.8m by 0.15m) is 4.31 m^2.

Actual total area for 16 pallets is $16 \times 4.31 = 68.96$ m^2

Therefore the burning rate factor used for the FDS simulation is $\frac{68.96}{10.94} = 6.3$

Calculations to determine thickness and surface burning factor for layer 3 pallets (LGV)

Layer 3 – based on layer with 12 pallets

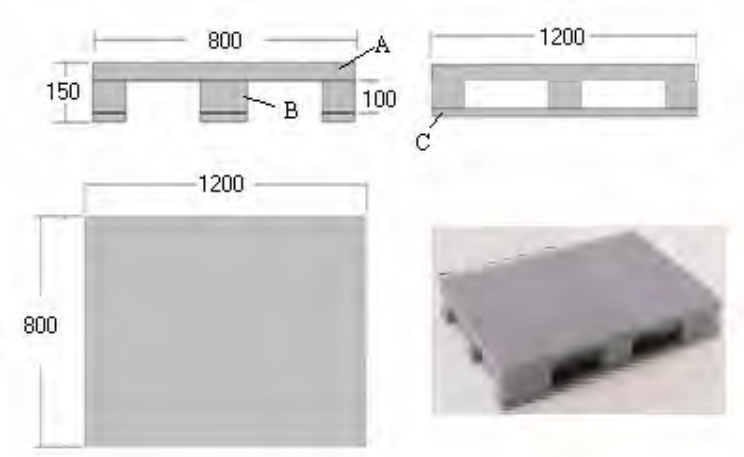

Figure K4:1.2m by 0.8m by 0.15m plastic pallets

Plank	*Number of planks*	*Total area (m^2)*
A	*1*	*2.02*
B	*9*	*1.037*
C	*2*	*0.598*
D	*1*	*0.428*

Total area per pallet = 2.02+1.037+0.598+0.428=4.1 m^2

Mass for 1 pallet of PE plastic is 23 kg. (kaiserkraft 2006)

Density for PE plastic is 956 kg/m^3. (Babrauskas 2003)

Volume per actual plastic pallet is $\frac{mass}{density} = \frac{23}{956} = 0.024\,\mathrm{m}^3$

Total volume for 12 actual pallets is $12 \times 0.024 = 0.288$ m^3.

The total area model for layer 3 in the simulation is

$(2.55\mathrm{m} \times 1.65\mathrm{m} \times 2)+(2.55\mathrm{m} \times 0.3\mathrm{m} \times 2)+(1.65\mathrm{m} \times 0.3\mathrm{m} \times 2) = 10.94$ m^2.

Therefore the thickness used for the FDS simulation is $\frac{0.288}{10.94} = 0.026$ m.

Area per actual plastic pallet (1.2m by 0.8m by 0.15m) is 4.1 m^2.

Actual total area for 12 pallets is $12 \times 4.1 = 49.2$ m^2.

Therefore the surface burning factor used for layer 3 is $\frac{49.2}{10.94} = 4.5$

Calculations to determine thickness and surface burning factor for layer 4 pallets (LGV)

Layer 4 – based on layer with 16 pallets

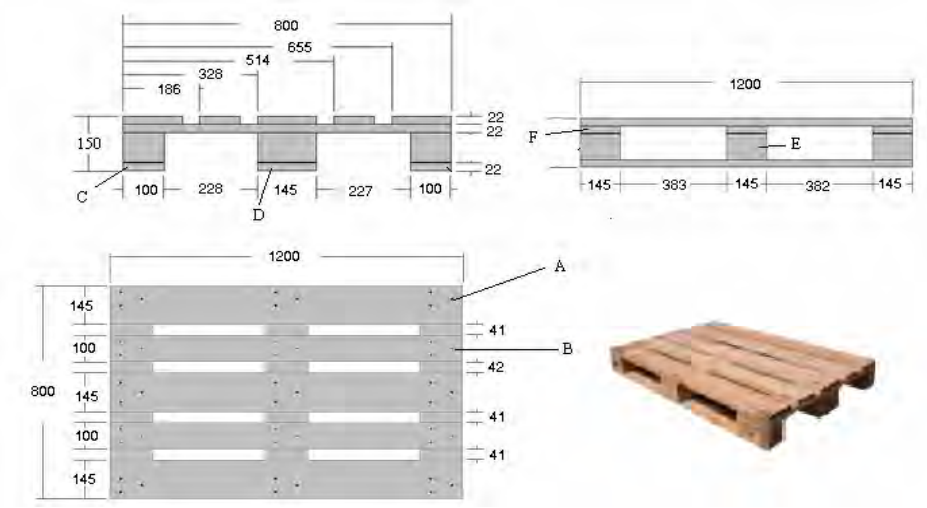

Figure K3:1.2m by 0.8m by 0.15m wood pallets

Plank	*Number of planks*	*Total area (m^2)*	*Total volume (m^3)*
A	*3*	*1.071*	*0.0115*
B	*2*	*0.594*	*0.0053*
C	*2*	*0.594*	*0.0035*
D	*1*	*0.407*	*0.0026*
E	*9*	*0.817*	*0.0159*
F	*3*	*0.821*	*0.0077*

Total area per pallet = 1.071 +0.594+0.594+0.407+0.817+0.821=4.31 m^2

Total volume per pallet =0.0115+0.0053+0.0035+0.0026+0.0159+0.0077=0.046 m^3

Volume per actual wood pallet (1.2m by 0.8m by 0.15m) is 0.046 m^3.

Total volume for 16 actual pallets is $16 \times 0.046 = 0.736$ m^3.

The total area model for layer 1 in the simulation is

$(2.55\text{m} \times 1.65\text{m} \times 2)+(2.55\text{m} \times 0.3\text{m} \times 2)+(1.65\text{m} \times 0.3\text{m} \times 2) = 10.94$ m^2.

Therefore the thickness used for the FDS simulation is $\frac{0.736}{10.94} = 0.067$ m.

Area per actual wood pallet (1.2m by 0.8m by 0.15m) is 4.31 m^2.

Actual total area for 16 pallets is $16 \times 4.31 = 68.96$ m^2

Therefore the burning rate factor used for the FDS simulation is $\frac{68.96}{10.94} = 6.3$

APPENDIX L

Appendix L: Material schedule for vehicles

Heavy goods vehicle (HGV)

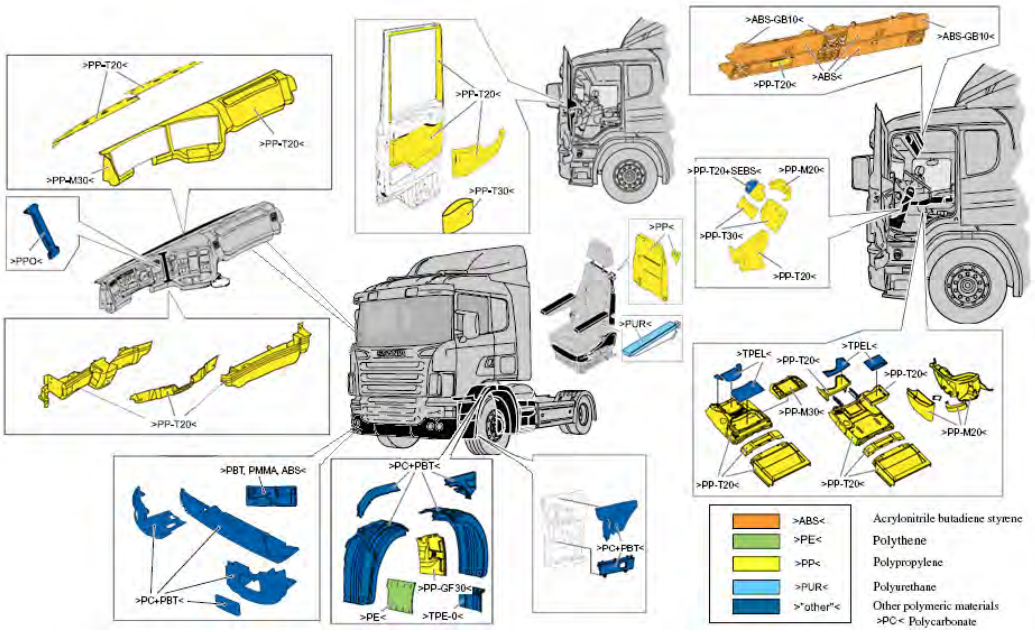

Figure K1: Material used in a heavy goods vehicle construction (Scania 2005)

HGV material schedule used in FDS simulation

Parts Description	Material	Thickness (mm)[a]
Vehicle seat	PUR - Polyurethane	50
Storage compartment	ABS - Acrylonitrile butadiene styrene	3
Cabin internal panel trim	PP - Polypropylene	3
Instrument panel	PP - Polypropylene	3
Bumper cover	PC - Polycarbonate	5
Tyres	EPDM – Ethylene propylene diene rubber	45
Mud Guard	PC - Polycarbonate	5

Note - a: measure value from a heavy goods vehicle

Light goods vehicle (LGV)

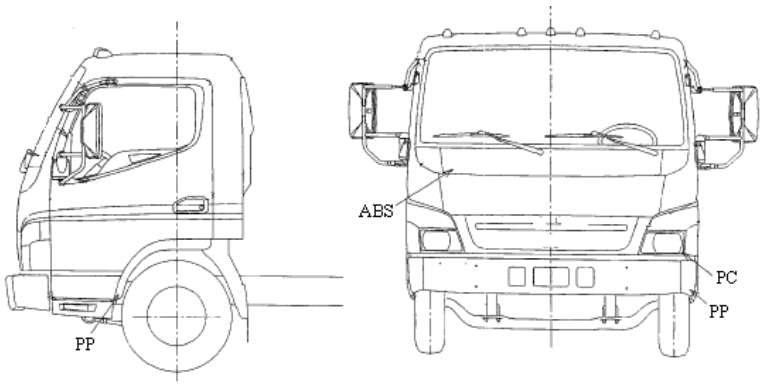

Figure J2: Material used in a light goods vehicle construction (Mitsubishi 2004)

LGV material schedule used in FDS simulation

Parts Description	Material	Thickness (mm)[a]
Vehicle seat	PUR – Polyurethane	50
Instrument panel	PP – Polypropylene	3
Bumper cover	PP - Polypropylene	3
Tyres	EPDM – Ethylene propylene diene rubber	15
Mud Guard	PP - Polypropylene	3
Front Cover	ABS - Acrylonitrile butadiene styrene	3
Head lump	PC - Polycarbonate	3

Note - a: measure value from a light goods vehicle

APPENDIX M

Appendix M: Calculation for Ignition Temperature (EPDM)

Material: EPDM (Ethylene propylene diene rubber)

To find the ignition temperature for EPDM, the time of ignition for EPDM taken from cone test experiment involving different heat flux were plotted in term of t_{ig}^{-1} versus q''_e, $t_{ig}^{(-1/5)}$ versus q''_e and $t_{ig}^{(-1/2)}$ versus q''_e.

The experiment results taken from (Babrauskas and Grayson 1992) are tabulated in Table L1.

Heat Flux (kW/m^2)	Time (sec)	t_{ig}^{-1} (sec t_{ig}^{-1})	$t_{ig}^{-1/1.5}$ (sec $t_{ig}^{-1.5}$)	$t_{ig}^{-1/2}$ (sec $t_{ig}^{-1/2}$)
20	486	0.0021	0.0162	0.0454
40	68	0.0147	0.0600	0.1213
70	36	0.0278	0.0917	0.1667

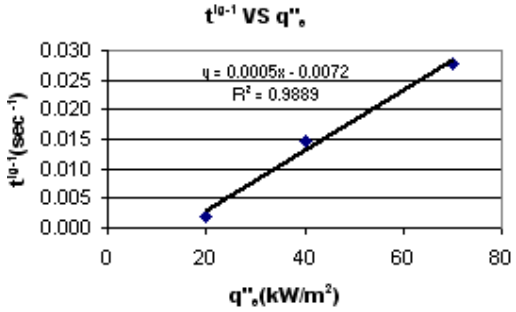

Graph 1

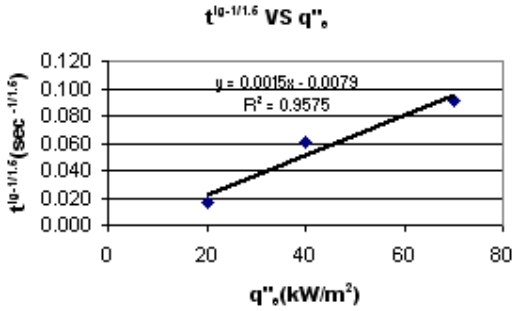

Graph 2

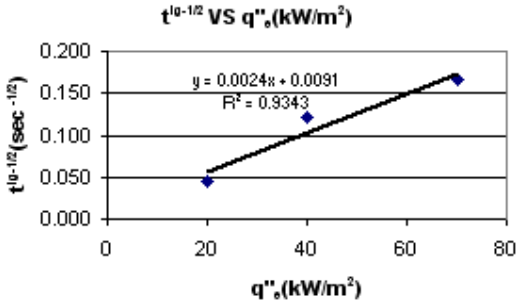

Graph 3

Figure L1: Plot for EPDM

To find critical heat flux q''_{crit} used equation M1

$$\dot{q}''_{crit} = \frac{-\text{int}\,ercept}{slope} \quad \text{---------- [M1]}$$

The plot result in graph 1 to 3 for EPDM , graph 1 has the slope of the best fit line (R-square value = 0.9889) as compare to the other two graph. The observation suggested that the critical heat flux q"$_{crit}$ obtained from t_{ig}^{-1} versus q"$_e$ is more realistic. Using equation M1, the q"$_{crit}$ is 14.4 kW/m^2.

Knowing the critical heat flux q"$_{crit}$, the ignition temperature T_{ig} can be estimated from steady state energy balance at the surface (equation M2).

$$\dot{q}''_{crit} = \varepsilon\sigma(T_{ig}^4 - T_\infty^4) + h_c(T_{ig} - T_0) \quad \text{---------- [M2]}$$

Where:

$\dot{q}''_{crit}$ = critical heat flux (kW/m^2)

ε = emissivity

σ = Stefan-Boltzmann constant (5.67×10^{-11} kW/m^{2}K)

h_c = Convective coefficient (kW/m^{2}K)

T_{ig} = Ignition Temperature (K)

T_0 = Ambient Temperature (K)

Knowing $\dot{q}''_{crit}$ = 14.4 kW/m^2, ε = 1, h_c =0.015 kW/m^{2}K, T_0 =293 K. By trial and error the value for EPDM T_{ig} is 642 K or 369^{o}C.

APPENDIX N

Appendix N: Sample of FDS input file for simulating a LGV fire in tunnel (FDS 4.0.7)

Define name of output files
****

```
&HEAD CHID='tunnel ',TITLE='Tunnel - LGV'/
```

Define gird size and domain size
****

Select only one geometry (Slip road or main tunnel) for simulation

Slip road geometry

Select only one type of grid size (Slip road)

```
GRID IBAR=31,JBAR=280,KBAR=20/  0.3m x 0.3m x 0.3 m grids size
GRID IBAR=62,JBAR=560,KBAR=40/  0.15m x 0.15m x 0.15 m grids size
```

Domain size for Slip road

```
PDIM XBAR0=0,XBAR=9.3,YBAR0=0,YBAR=84,ZBAR=6/
```

Main tunnel geometry

Select only one type of grid size (Main tunnel)

```
&GRID IBAR=50,JBAR=280,KBAR=20/  0.3m x 0.3m x 0.3 m grids size
 GRID IBAR=100,JBAR=560,KBAR=40/  0.15m x 0.15m x 0.15 m grids size
```

Domain size for Main tunnel

```
 &PDIM XBAR0=0,XBAR=15,YBAR0=0,YBAR=84,ZBAR=6/
```

Define simulation time
****

```
&TIME TWFIN=3600/ simulation time in second
```

Miscellaneous input parameters
****

&MISC DTCORE=200,SURF_DEFAULT='CONCRETE',REACTION='WOOD',TMPA=32/ Unless specific, the default surface line applied to all SURF line is CONCRETE. The combustion stoichiometry defined as WOOD is used. The ambient temperature used for the simulation is 32^{o}C

Reaction input parameter
****

```
&REAC ID='WOOD'
     FYI='Ritchie, et al., 5th IAFSS, C_3.4 H_6.2 O_2.5'
     SOOT_YIELD = 0.01
     NU_O2      = 3.7
     NU_CO2     = 3.4
     NU_H2O     = 3.1
     MW_FUEL    = 87
     EPUMO2     = 11020 /
```

Ignition of fire
****

Size of ignition source

```
-----------------------------
&SURF ID='fire',HRRPUA=4800,RAMP_Q='INCfire' /
&RAMP ID='INCfire',T=0.0,F=1/
&RAMP ID='INCfire',T=3600,F=1/
```

Location of ignition source (select only one location – model setup base on main tunnel)

```
---------------------------------------------------------------------
&OBST  XB=7.7,8,14.6,14.3,1.1,1.4,RGB=1,0,0,SURF_ID6='INERT','INERT','INERT','fire','INERT','INERT'
/Rear of light goods vehicle

OBST XB=7.7,8,17.45,17.15,1.1,1.4,RGB=1,0,0,SURF_ID6='INERT','INERT','INERT','INERT','INERT','fire'
/  Front of light goods vehicle
```

Flammability parameter based on HRRPUA

```
*****************************************

*******WOOD PALLETS 1.2 X 0.8*******
&SURF ID              = 'LWOOD 1'
    FYI               = 'PLYWOOD ordinary '
    KS                = 0.12
    DENSITY           = 600
    C_P               = 2.58
    DELTA             = 0.067
    BURN_AWAY         = .TRUE.
    TMPIGN            = 373
    BACKING           = 'INSULATED'
    HRRPUA            = 1953
     RAMP_Q           = 'GAP1'
&RAMP ID='GAP1',T=  0.0,F=0 /
&RAMP ID='GAP1',T=  68.0,F=0.85 /
&RAMP ID='GAP1',T=  120.0,F=0.53 /
&RAMP ID='GAP1',T= 180,F=0.48 /
&RAMP ID='GAP1',T= 240,F=0.4 /
&RAMP ID='GAP1',T= 300,F=0.64 /
&RAMP ID='GAP1',T= 383,F=1/[Surface burning factor × cone test peak HRRPUA =6.3×310= 1953 kW/m2]
&RAMP ID='GAP1',T= 420,F=0.54 /

********PLASTIC PALLETS 1.2 X 0.8********
&SURF ID              = 'LPE'
    FYI               = 'POLYETHYLENE (PE) '
    KS                = 0.64
    DENSITY           = 956
    C_P               = 3
    DELTA             = 0.026
    BURN_AWAY         = .TRUE.
    TMPIGN            = 323
    BACKING           = 'INSULATED'
    HRRPUA            = 13050
    RAMP_Q            = 'GAP2'
&RAMP ID='GAP2',T=   0.0,F=0.0 /
&RAMP ID='GAP2',T=   30,F=0.017 /
&RAMP ID='GAP2',T=   60,F=0.14 /
&RAMP ID='GAP2',T=   120.0,F=0.38 /
&RAMP ID='GAP2',T=180.0,F=1.0/ [Surface burning factor  × cone test peak HRRPUA =4.5 × 2900= 13050
                                        kW/m2]
&RAMP ID='GAP2',T=   240.0,F=0.017 /
&RAMP ID='GAP2',T=   870.0,F=0.0 /


********VEHICLE PLASTIC ********
&SURF ID              = 'LABS'
    FYI               = 'ACRYLONITRILE BUTADIENCE STYRENE (ABS) '
    KS                = 0.17
    DENSITY           = 1050
    C_P               = 1.48
    DELTA             = 0.003
    BURN_AWAY         = .TRUE.
    TMPIGN            = 414
    BACKING           = 'INSULATED'
    HRRPUA            = 1280
    RAMP_Q            = 'GAP3'
&RAMP ID='GAP3',T=0.0,F=0.0 /
&RAMP ID='GAP3',T=30,F=0.44 /
```

```
&RAMP ID='GAP3',T=60,F=0.59 /
&RAMP ID='GAP3',T=90,F=0.69 /
&RAMP ID='GAP3',T=132,F=0.75 /
&RAMP ID='GAP3',T=150,F=0.88 /
&RAMP ID='GAP3',T=174,F=1 /
&RAMP ID='GAP3',T=210,F=0.03 /

********VEHICLE PLASTIC ********
&SURF ID              = 'LPP'
    FYI               = 'POLYPROPYLENE (PP) '
    KS                = 0.38
    DENSITY           = 900
    C_P               = 6.27
    DELTA             = 0.003
    BURN_AWAY         = .TRUE.
    TMPIGN            = 305
    BACKING           = 'INSULATED'
    HRRPUA            = 2700
    RAMP_Q            = 'GAP4'
&RAMP ID='GAP4',T=   0.0,F=0.0 /
&RAMP ID='GAP4',T=   30,F=0.15 /
&RAMP ID='GAP4',T=   60,F=0.31 /
&RAMP ID='GAP4',T=   90,F=0.37 /
&RAMP ID='GAP4',T=   120,F=0.44 /
&RAMP ID='GAP4',T=   150,F=0.65 /
&RAMP ID='GAP4',T=   165,F=1 /
&RAMP ID='GAP4',T=   180,F=0.57 /
&RAMP ID='GAP4',T=   210,F=0.04 /

********VEHICLE PLASTIC ********
&SURF ID              = 'LPU'
    FYI               = 'POLYURETHANE (PUR)'
    KS                = 0.034
    DENSITY           = 20
    C_P               = 1.4
    DELTA             = 0.05
    BURN_AWAY         = .TRUE.
    TMPIGN            = 272
    BACKING           = 'INSULATED'
    HRRPUA            = 1300
    RAMP_Q            = 'GAP4'
&RAMP ID='GAP4',T=   0,F=0.0 /
&RAMP ID='GAP4',T=   9,F=0.3 /
&RAMP ID='GAP4',T=   15,F=0.43 /
&RAMP ID='GAP4',T=   19,F=1 /
&RAMP ID='GAP4',T=   23,F=0.92 /
&RAMP ID='GAP4',T=   26,F=0.09 /
&RAMP ID='GAP4',T=   30,F=0.03 /
&RAMP ID='GAP4',T=   39,F=0 /

********VEHICLE PLASTIC ********
&SURF ID              = 'LEPDM'
    FYI               = 'Ethylene propylene diene rubber (EPDM) '
    KS                = 0.3
    DENSITY           = 860
    C_P               = 2.18
    DELTA             = 0.015
    BURN_AWAY         = .TRUE.
    TMPIGN            = 369
    BACKING           = 'INSULATED'
```

```
     HRRPUA          = 1240
     RAMP_Q          = 'GAP5'
&RAMP ID='GAP5',T=   0.0,F=0.0 /
&RAMP ID='GAP5',T=   30,F=0.51 /
&RAMP ID='GAP5',T=   60,F=0.61 /
&RAMP ID='GAP5',T=   90,F=0.65 /
&RAMP ID='GAP5',T=   120,F=0.71 /
&RAMP ID='GAP5',T=   150,F=0.77 /
&RAMP ID='GAP5',T=   180,F=0.87 /
&RAMP ID='GAP5',T=   195,F=1 /
&RAMP ID='GAP5',T=   210,F=0.9 /
&RAMP ID='GAP5',T=   240,F=0.32 /
&RAMP ID='GAP5',T=   270,F=0.03 /
&RAMP ID='GAP5',T=   300,F=0 /

********VEHICLE PLASTIC ********
&SURF ID            = 'LPC'
     FYI            = 'POLYCARBONATE (PC)'
     KS             = 0.2
     DENSITY        = 1190
     C_P            = 2.06
     DELTA          = 0.003
     BURN_AWAY      = .TRUE.
     TMPIGN         = 497
     BACKING        = 'INSULATED'
     HRRPUA         = 360
     RAMP_Q         = 'GAP6'
&RAMP ID='GAP6',T=   0.0,F=0.0 /
&RAMP ID='GAP6',T=   120,F=1 /
&RAMP ID='GAP6',T=   180,F=0.28 /
&RAMP ID='GAP6',T=   240,F=0.19 /
&RAMP ID='GAP6',T=   360,F=0.17 /
&RAMP ID='GAP6',T=   660,F=0.28 /
&RAMP ID='GAP6',T=   720,F=0.22 /
&RAMP ID='GAP6',T=   840,F=0.22 /
&RAMP ID='GAP6',T=   1800,F=0 /
```

Material properties input parameters

```
************************************

&SURF ID    = 'CONCRETE'
     FYI        = 'Quintiere, Fire Behavior'
     RGB        = 0.66,0.66,0.66
     C_P        = 0.88
     DENSITY =2100.
     KS   = 1.0
     DELTA = 0.7 /

&SURF ID     = 'GLASS'
     FYI        = 'Quintiere, An Introduction to Fire Dynamics TABLE 2.1'
     RGB        = 1.0,1.0,0.75
     DELTA      = 0.003
     KS         = 0.76
     C_P        = 0.84
     DENSITY = 2700.
     BACKING= 'EXPOSED' /

&SURF ID            = 'STEEL'
```

```
RGB             = 0.20,0.20,0.20
C_DELTA_RHO = 20.
DELTA           = 0.005 /
```

Boundary condition (Tunnel ventilation fans operation mode)

```
**************************************************************

Tunnel fan operation mode – normal to emergency for 0 to 3.1m/s main tunnel (select only one mode)
-------------------------------------------------------------------------------------------------------------------

&RAMP ID='FAN',T=0.0,F=0.0 / Fans off at 0 seconds
&RAMP ID='FAN',T=300.0,F=0.0/ Fans start at 301 seconds
&RAMP ID='FAN',T=360.0,F=1.0/ Fans operating at emergency mode, full operating speed at 360 seconds
&RAMP ID='FAN',T=3600.0,F=1.0 / Fans operating at emergency mode, full operating speed at 3600 seconds

&SURF ID=' Airflow ',VEL=-3.1, RAMP_V='FAN'/ Supply 0 – 3.1 m/s airflow into tunnel
&VENT XB=0,15,0,0,0.0,6,SURF_ID='Airflow'/ Air velocity varies with scenarios see table 12.6
&VENT XB=0,15,84,84,0.0,6, SURF_ID='OPEN'/

Tunnel fan operation mode–congestion to emergency for 3.5 to 3.1m/s main tunnel (select only one mode)
-------------------------------------------------------------------------------------------------------------------

RAMP ID='FAN',T=0.0,F=1.0 / Fans operating at congestion mode, full operating speed at 0 seconds
RAMP ID='FAN',T=300.0,F=1.0/ Fans operating at congestion mode, full operating speed at 300 seconds
RAMP ID='FAN',T=330.0,F=0.0/ Fans stop and start operating at emergency mode at 330 seconds
RAMP ID='FAN',T=390.0,F=0.89/ Fans operating at emergency mode, full operating speed at 390 seconds
RAMP ID='FAN',T=3600.0,F=0.89/ Fans operating at emergency mode, full operating speed at 3600 seconds

SURF ID='BOUNDARY CONDITION',VEL=-3.5, RAMP_V='FAN'/ Supply 3.5– 3.1 m/s airflow into tunnel
VENT XB=0,15,0,0,0.0,6,SURF_ID='Airflow'/ Air velocity varies scenarios see table 12.6
VENT XB=0,15,84,84,0.0,6, SURF_ID='OPEN'/
```

Walkway

```
**********

&OBST XB=0,1.2,0,84,0,0.6,RGB=0.5,0.5,0.5/ walkway
&OBST XB=13.8,15,0,84,0,0.6,RGB=0.5,0.5,0.5/ walkway
```

Simulated LGV truck

```
*********************
HEAT DETECTOR
&HEAT XYZ=7.8,18.6,1.5,RTI=100,ACTIVATION_TEMPERATURE=380,LABEL='HEAT1'/ Glass break
&HEAT XYZ=7.8,17.3,1.5,RTI=100,ACTIVATION_TEMPERATURE=380,LABEL='HEAT2'/ Glass break

&OBST XB=7.1,8.8,18.75,18.85,1.3,1.95,RGB=0,1,1,SURF_ID='GLASS',HEAT_REMOVE='HEAT1'/
Truck cabin front window
&OBST XB=7.1,8.8,18.8,18.85,1.12,1.3,RGB=0,0.5,0.5,SURF_ID='LABS'/ Truck cabin
&OBST XB=7.1,8.8,18.8,18.85,1.12,0.77,RGB=0,0.5,0.5,SURF_ID='STEEL'/ Truck cabin
&OBST XB=7.4,8.5,18.8,18.85,0.6,0.77,RGB=0,0.5,0.5,SURF_ID='STEEL'/ Truck cabin
&OBST XB=7.1,7.4,18.8,18.85,0.6,0.77,RGB=0,1,1,SURF_ID='LPC'/Head lamp right
&OBST XB=8.5,8.8,18.8,18.85,0.6,0.77,RGB=0,1,1,SURF_ID='LPC'/ Head lamp left
&OBST XB=7.1,8.8,19.05,18.85,0.3,0.6,RGB=0,0.5,0.5,SURF_ID6='LPP','LPP','STEEL','STEEL','STEEL',
'STEEL' / Bumper
```

```
&OBST XB=7.1,8.8,18.85,17.41,1.95,2,RGB=0,0.5,0.5,SURF_ID='STEEL'/ Truck cabin
&OBST XB=7.1,7.15,18.85,18.65,0.8,2,RGB=0,0.5,0.5,SURF_ID='STEEL'/ Truck cabin
&OBST XB=8.8,8.75,18.85,18.65,0.8,2,RGB=0,0.5,0.5,SURF_ID='STEEL'/ Truck cabin
&OBST XB=7.1,8.8,17.41,17.42,1.8,2,RGB=0,0.5,0.5,SURF_ID='STEEL'/ Truck cabin
&OBST XB=8.2,8.8,17.41,17.42,1.5,1.8,RGB=0,0.5,0.5,SURF_ID='STEEL'/ Truck cabin
&OBST XB=7.1,7.6,17.41,17.42,1.5,1.8,RGB=0,0.5,0.5,SURF_ID='STEEL'/ Truck cabin
&OBST XB=7.1,8.8,17.41,17.42,0.8,1.5,RGB=0,0.5,0.5,SURF_ID='STEEL'/ Truck cabin
&OBST XB=7.6,8.2,17.41,17.42,1.5,1.8,RGB=0,1,1,SURF_ID='GLASS',HEAT_REMOVE='HEAT2'/
Truck cabin back window
&OBST XB=7.1,8.8,18.85,18.25,0.3,0.31,RGB=0,0.5,0.5,SURF_ID='STEEL'/ Truck cabin floor
&OBST XB=7.1,8.8,18.25,18.2,0.31,0.8,RGB=0,0.5,0.5,SURF_ID='STEEL'/ Truck cabin
&OBST XB=7.1,8.8,18.25,14,0.7,0.8,RGB=0,0.5,0.5,SURF_ID='STEEL'/ Truck cabin floor
&OBST XB=7.4,8.5,18.75,18.45,1.3,1.0,RGB=0.4,0.4,0.4,SURF_ID='LPP'/ Vehicle instrument panel
&OBST XB=7.4,8.5,18.25,17.75,0.8,1.05,RGB=0.1,0.1,0.1,SURF_ID='LPU'/ Vehicle seat
&OBST XB=7.4,8.5,17.75,17.55,0.8,1.4,RGB=0.1,0.1,0.1,SURF_ID='LPU'/ Vehicle seat
&OBST XB=7.1,7.15,18.85,17.61,0.8,1.36,RGB=0,0.5,0.5,SURF_ID6='STEEL','LPP','STEEL','STEEL',
'STEEL','STEEL'/ Vehicle door
&OBSTXB=7.1,7.15,18.85,18.15,0.8,0.3,RGB=0,0.5,0.5,SURF_ID6='STEEL','LPP','STEEL','STEEL',
'STEEL', 'STEEL'/ Vehicle door
&OBST XB=8.8,8.75,18.85,17.61,0.8,1.36,RGB=0,0.5,0.5,SURF_ID6='LPP','STEEL','STEEL','STEEL',
'STEEL','STEEL'/ Vehicle door
&OBST XB=8.8,8.75,18.85,18.15,0.8,0.3,RGB=0,0.5,0.5,SURF_ID6='LPP','STEEL','STEEL','STEEL',
'STEEL','STEEL'/ Vehicle door
&OBST XB=7.1,7.15,17.61,17.41,0.8,2,RGB=0,0.5,0.5,SURF_ID='STEEL'/ Truck cabin
&OBST XB=8.8,8.75,17.61,17.41,0.8,2,RGB=0,0.5,0.5,SURF_ID='STEEL'/ Truck cabin
&OBST XB=8.8,8.42,17,16,0.4,0.8,RGB=0,0.5,0.5,SURF_ID='STEEL'/ Truck equipment
&OBST XB=7.1,7.3,18.2,18.1,0.3,0.7,RGB=0.2,0.2,0.2,SURF_ID='LPP'/ Truck mud guard
&OBST XB=7.1,7.3,17.2,17.3,0.3,0.7,RGB=0.2,0.2,0.2,SURF_ID='LPP'/ Truck mud guard
&OBST XB=7.1,7.3,18,17.4,0,0.6,RGB=0,0,0,SURF_ID6='STEEL','STEEL','LEPDM','LEPDM','LEPDM',
'LEPDM'/ Truck front wheel
&OBST XB=8.6,8.8,18.2,18.1,0.3,0.7,RGB=0.2,0.2,0.2,SURF_ID='LPP'/ Truck mud guard
&OBST XB=8.6,8.8,17.2,17.3,0.3,0.7,RGB=0.2,0.2,0.2,SURF_ID='LPP'/ Truck mud guard
&OBST XB=8.6,8.8,18,17.4,0,0.6,RGB=0,0,0,SURF_ID6='STEEL','STEEL','LEPDM','LEPDM','LEPDM',
'LEPDM'/ Truck front wheel
&OBST XB=8.6,7.3,17.6,17.9,0.3,0.6,RGB=0.5,0.5,0.5,SURF_ID='STEEL'/ Truck front axial
&OBST XB=7.1,7.3,15.5,15.4,0.3,0.7,RGB=0.2,0.2,0.2,SURF_ID='LPP'/ Truck mud guard
&OBST XB=7.1,7.3,14.5,14.6,0.3,0.7,RGB=0.2,0.2,0.2,SURF_ID='LPP'/ Truck mud guard
&OBST XB=7.1,7.3,15.3,14.7,0,0.6,RGB=0,0,0,SURF_ID6='STEEL','STEEL','LEPDM','LEPDM','LEPDM',
'LEPDM'/Truck back wheel
&OBST XB=8.6,8.8,15.5,15.4,0.3,0.7,RGB=0.2,0.2,0.2,SURF_ID='LPP'/ Truck mud guard
&OBST XB=8.6,8.8,14.5,14.6,0.3,0.7,RGB=0.2,0.2,0.2,SURF_ID='LPP'/ Truck mud guard
&OBST XB=8.6,8.8,15.3,14.7,0,0.6,RGB=0,0,0,SURF_ID6='STEEL','STEEL','LEPDM','LEPDM','LEPDM',
'LEPDM'/ Truck back wheel
&OBST XB=8.6,7.3,14.9,15.2,0.3,0.6,RGB=0.5,0.5,0.5,SURF_ID='STEEL'/ Truck back axial
&OBST XB=7.1,7.15,14.6,14.9,0.8,3.2,RGB=0.0,0.0,1,SURF_ID='STEEL'/ Cargo frame
&OBST XB=8.75,8.8,14.6,14.9,0.8,3.2,RGB=0.0,0.0,1,SURF_ID='STEEL'/ Cargo frame
&OBST XB=7.1,8.8,14.6,14.9,3.15,3.2,RGB=0.0,0.0,1,SURF_ID='STEEL'/ Cargo frame
&OBST XB=7.1,7.15,16.85,17.15,0.8,3.2,RGB=0.0,0.0,1,SURF_ID='STEEL'/ Cargo frame
&OBST XB=8.75,8.8,16.85,17.15,0.8,3.2,RGB=0.0,0.0,1,SURF_ID='STEEL'/ Cargo frame
&OBST XB=7.1,8.8,16.85,17.15,3.15,3.2,RGB=0.0,0.0,1,SURF_ID='STEEL'/ Cargo frame
```

Fuel cargo in LGV (wood and plastic pallets)
```
****************************************

&OBST XB=7.15,8.8,14.6,17.15,0.8,1.1,RGB=0.8,0.6,0.4,SURF_IDS='LWOOD 1','LWOOD 1','LWOOD 1'/
&OBST XB=7.15,8.8,14.6,17.15,1.4,1.7,RGB=0.8,0.6,0.4,SURF_IDs='LPE','LPE','LWOOD 1'/
&OBST XB=7.15,8.8,14.6,17.15,2,2.3,RGB=0.8,0.6,0.4,SURF_IDS='LWOOD 1','LWOOD 1','LWOOD 1'/
&OBST XB=7.15,8.8,14.6,17.15,2.6,2.9,RGB=0.8,0.6,0.4,SURF_IDS='LPE','LWOOD 1','LWOOD 1'/
```

Vehicles (Cars)
```
****************
&OBST XB=3.4,5.1,1.5,4,0.9,1.5,RGB=0,1.0,1.0,SURF_ID='STEEL'/ Upper part of vehicle 1
&OBST XB=3.4,5.1,1,5.5,0.3,0.9,RGB=0,1.0,1.0,SURF_ID='STEEL'/ Lower part of vehicle 1
&OBST XB=3.4,5.1,1.5,1.8,0.0,0.3,RGB=0.0,0.0,0.0/  Rear vehicle wheel
&OBST XB=3.4,5.1,4.8,5,0.0,0.3,RGB=0.0,0.0,0.0/  Front vehicle wheel
&HOLE XB=3.6,4.9,0.8,5.6,0,0.3/


&OBST XB=7.3,9,1.5,4,0.9,1.5,RGB=1.0,1.0,0.0,SURF_ID='STEEL'/ Upper part of vehicle 2
&OBST XB=7.3,9,1,5.5,0.3,0.9,RGB=1.0,1.0,0.0,SURF_ID='STEEL'/ Lower part of vehicle 2
&OBST XB=7.3,9,1.5,1.8,0.0,0.3,RGB=0.0,0.0,0.0/  Rear vehicle wheel
&OBST XB=7.3,9,4.8,5,0.0,0.3,RGB=0.0,0.0,0.0/  Front vehicle wheel
&HOLE XB=7.5,8.8,0.8,5.6,0,0.3/

&OBST XB=10.8,12.5,1.5,4,0.9,1.5,RGB=0.0,1.0,0.0,SURF_ID='STEEL'/ Upper part of vehicle 3
&OBST XB=10.8,12.5,1,5.5,0.3,0.9,RGB=0.0,1.0,0.0,SURF_ID='STEEL'/ Lower part of vehicle 3
&OBST XB=10.8,12.5,1.5,1.8,0.0,0.3,RGB=0.0,0.0,0.0/  Rear vehicle wheel
&OBST XB=10.8,12.5,4.8,5,0.0,0.3,RGB=0.0,0.0,0.0/  Front vehicle wheel
&HOLE XB=11.0,12.3,0.8,5.6,0,0.3/
```

Output from FDS
```
******************
&ISOF QUANTITY='MIXTURE_FRACTION',VALUE(1)=0.148, VALUE(2)=0.001/
&SLCF PBY=2, QUANTITY='TEMPERATURE', DTSAM=1/
&SLCF PBY=13, QUANTITY='TEMPERATURE', DTSAM=1/
&SLCF PBY=21, QUANTITY='TEMPERATURE', DTSAM=1/
&SLCF PBY=35, QUANTITY='TEMPERATURE', DTSAM=1/
&SLCF PBX=8, QUANTITY='TEMPERATURE', DTSAM=1/
&SLCF PBX=8, QUANTITY='VELOCITY',VECTOR=.TRUE./
```

APPENDIX O

Appendix O: Sample of FDS input file for simulating a HGV fire in tunnel (FDS 4.0.7)

Define name of output files
****

```
&HEAD CHID='Tunnel ',TITLE='Tunnel - HGV'/
```

Define gird size and domain size
****

Select only one geometry (Slip road or main tunnel) for simulation

Slip road geometry
Select only one type of grid size (Slip road)

```
---------------------------------------------------

  &GRID IBAR=31,JBAR=280,KBAR=20/  0.3m x 0.3m x 0.3 m grids size
  GRID IBAR=62,JBAR=560,KBAR=40/  0.15m x 0.15m x 0.15 m grids size

Domain size for Slip road
---------------------------------

  &PDIM XBAR0=0,XBAR=9.3,YBAR0=0,YBAR=84,ZBAR=6/
```

Main tunnel geometry
Select only one type of grid size (Main tunnel)

```
-----------------------------------------------------------

   GRID IBAR=50,JBAR=280,KBAR=20/  0.3m x 0.3m x 0.3 m grids size
   GRID IBAR=100,JBAR=560,KBAR=40/  0.15m x 0.15m x 0.15 m grids size

Domain size for Main tunnel
-----------------------------------
   PDIM XBAR0=0,XBAR=15,YBAR0=0,YBAR=84,ZBAR=6/
```

Define simulation time
****

```
&TIME TWFIN=3600/ simulation time in second
```

Miscellaneous input parameters
****

```
&MISC DTCORE=200,SURF_DEFAULT='CONCRETE',REACTION='WOOD',TMPA=32/ Unless specific,
the default surface line applied to all SURF line is CONCRETE. The combustion stoichiometry defined as
WOOD is used. The ambient temperature used for the simulation is 32°C
```

Reaction input parameter

```
**************************

&REAC ID='WOOD'
     FYI='Ritchie, et al., 5th IAFSS, C_3.4 H_6.2 O_2.5'
     SOOT_YIELD = 0.01
     NU_O2          = 3.7
     NU_CO2         = 3.4
     NU_H2O         = 3.1
     MW_FUEL        = 87
     EPUMO2         = 11020 /
```

Ignition of fire

```
***************

Size of ignition source
-----------------------------
&SURF ID='fire',HRRPUA=4800,RAMP_Q='INCfire' /
&RAMP ID='INCfire',T=0.0,F=1/
&RAMP ID='INCfire',T=3600,F=1/

Location of ignition source (select only one location)
----------------------------------------------------------------------
&OBST XB=4.3,4.6,14,14.3,1.4,1.7,RGB=1,0,0,SURF_ID6='INERT','INERT','INERT','fire','INERT','INERT' /
Rear of heavy goods vehicle

OBST XB=4.3,4.6,22.05,22.35,1.4,1.7,RGB=1,0,0,SURF_ID6='INERT','INERT','INERT','INERT','INERT',
'fire'/  Front of heavy goods vehicle
```

Flammability parameter based on HRRPUA

```
*****************************************

*******WOOD PALLETS 1.2 X 1*******
&SURF ID             = 'HWOOD 1'
     FYI             = 'PLYWOOD ordinary'
     KS              = 0.12
     DENSITY         = 600
     C_P             = 2.58
     DELTA           = 0.043
     BURN_AWAY       = .TRUE.
     TMPIGN          = 373
     BACKING         = 'INSULATED'
     HRRPUA          = 1398.1
      RAMP_Q         = 'GAP1'
&RAMP ID='GAP1',T=   0.0,F=0 /
&RAMP ID='GAP1',T=  68.0,F=0.85 /
&RAMP ID='GAP1',T=  120.0,F=0.53 /
&RAMP ID='GAP1',T= 180,F=0.48 /
&RAMP ID='GAP1',T= 240,F=0.4 /
&RAMP ID='GAP1',T= 300,F=0.64 /
&RAMP ID='GAP1',T=383,F=1/[Surface burning factor×cone test peak HRRPUA=4.51×310=1398.1 kW/m2]
&RAMP ID='GAP1',T= 420,F=0.54 /
```

```
********WOOD PALLETS 1.2 X 1_0.45********
&SURF ID              = 'HWOOD 2'
    FYI               = 'PLYWOOD ordinary '
    KS                = 0.12
    DENSITY           = 600
    C_P               = 2.58
    DELTA             = 0.059
    BURN_AWAY         = .TRUE.
    TMPIGN            = 373
    BACKING           = 'INSULATED'
    HRRPUA            = 1897.2
    RAMP_Q            = 'GAP2'
&RAMP ID='GAP2',T=0.0,F=0 /
&RAMP ID='GAP2',T=68.0,F=0.85 /
&RAMP ID='GAP2',T=120.0,F=0.53 /
&RAMP ID='GAP2',T=180,F=0.48 /
&RAMP ID='GAP2',T=240,F=0.4 /
&RAMP ID='GAP2',T=300,F=0.64 /
&RAMP ID='GAP2',T=383,F=1/[Surface burning factor×cone test peak HRRPUA=6.12×310=1897.2 kW/m2]
&RAMP ID='GAP2',T= 420,F=0.54 /

********PLASTIC PALLETS 1.2 X 0.8********
&SURF ID             = 'HPE'
    FYI              = 'POLYETHYLENE (PE)'
    KS               = 0.64
    DENSITY          = 956
    C_P              = 3
    DELTA            = 0.029
    BURN_AWAY        = .TRUE.
    TMPIGN           = 323
    BACKING          = 'INSULATED'
    HRRPUA           = 14500
    RAMP_Q           = 'GAP3'
&RAMP ID='GAP3',T=0,F=0.0 /
&RAMP ID='GAP3',T=30,F=0.017 /
&RAMP ID='GAP3',T=60,F=0.14 /
&RAMP ID='GAP3',T=120,F=0.38 /
&RAMP ID='GAP3',T=180,F=1/ [Surface burning factor × cone test peak HRRPUA=5×2900=1906.5 kW/m2]
&RAMP ID='GAP3',T=240,F=0.017 /
&RAMP ID='GAP3',T=870,F=0.0 /

********VEHICLE PLASTIC ********
&SURF ID             = 'HABS'
    FYI              = 'ACRYLONITRILE BUTADIENCE STYRENE (ABS)'
    KS               = 0.17
    DENSITY          = 1050
    C_P              = 1.48
    DELTA            = 0.003
    BURN_AWAY        = .TRUE.
    TMPIGN           = 414
    BACKING          = 'INSULATED'
    HRRPUA           = 1280
    RAMP_Q           = 'GAP4'
&RAMP ID='GAP4',T= 0, F=0.0 /
&RAMP ID='GAP4',T=30,F=0.44 /
&RAMP ID='GAP4',T=60,F=0.59 /
&RAMP ID='GAP4',T=90,F=0.69 /
&RAMP ID='GAP4',T=132,F=0.75 /
&RAMP ID='GAP4',T=150,F=0.88 /
```

```
&RAMP ID='GAP4',T=170,F=1 /
&RAMP ID='GAP4',T=210,F=0.03 /

********VEHICLE PLASTIC ********
&SURF ID             = 'HPP'
     FYI             = 'POLYPROPYLENE (PP) '
     KS              = 0.38
     DENSITY         = 900
     C_P             = 6.27
     DELTA           = 0.003
     BURN_AWAY       = .TRUE.
     TMPIGN          = 305
     BACKING         = 'INSULATED'
     HRRPUA          = 2700
     RAMP_Q          = 'GAP5'
&RAMP ID='GAP5',T=0.0,F=0.0 /
&RAMP ID='GAP5',T=30,F=0.15 /
&RAMP ID='GAP5',T=60,F=0.31 /
&RAMP ID='GAP5',T=90,F=0.37 /
&RAMP ID='GAP5',T=120,F=0.44 /
&RAMP ID='GAP5',T=150,F=0.65 /
&RAMP ID='GAP5',T=165,F=1 /
&RAMP ID='GAP5',T=180,F=0.57 /
&RAMP ID='GAP5',T=210,F=0.04 /

********VEHICLE PLASTIC ********
&SURF ID             = 'HPU'
     FYI             = 'POLYURETHANE  (PUR)'
     KS              = 0.034
     DENSITY         = 20
     C_P             = 1.4
     DELTA           = 0.05
     BURN_AWAY       = .TRUE.
     TMPIGN          = 272
     BACKING         = 'INSULATED'
     HRRPUA          = 1300
     RAMP_Q          = 'GAP6'
&RAMP ID='GAP6',T=0,F=0.0 /
&RAMP ID='GAP6',T=9,F=0.3 /
&RAMP ID='GAP6',T=15,F=0.43 /
&RAMP ID='GAP6',T=19,F=1 /
&RAMP ID='GAP6',T=23,F=0.92 /
&RAMP ID='GAP6',T=26,F=0.09 /
&RAMP ID='GAP6',T=30,F=0.03 /
&RAMP ID='GAP6',T=39,F=0 /

********VEHICLE PLASTIC ********
&SURF ID             = 'HEPDM'
     FYI             = 'Ethylene propylene diene rubber (EPDM) '
     KS              = 0.3
     DENSITY         = 860
     C_P             = 2.18
     DELTA           = 0.045
     BURN_AWAY       = .TRUE.
     TMPIGN          = 369
     BACKING         = 'INSULATED'
     HRRPUA          = 1240
     RAMP_Q          = 'GAP7'
&RAMP ID='GAP7',T=0.0,F=0.0 /
&RAMP ID='GAP7',T=30,F=0.51 /
```

```
&RAMP ID='GAP7',T=60,F=0.61 /
&RAMP ID='GAP7',T=90,F=0.65 /
&RAMP ID='GAP7',T=120,F=0.71 /
&RAMP ID='GAP7',T=150,F=0.77 /
&RAMP ID='GAP7',T=180,F=0.87 /
&RAMP ID='GAP7',T=195,F=1 /
&RAMP ID='GAP7',T=210,F=0.9 /
&RAMP ID='GAP7',T=240,F=0.32 /
&RAMP ID='GAP7',T=270,F=0.03 /
&RAMP ID='GAP7',T=300,F=0 /

********VEHICLE PLASTIC ********
&SURF ID              = 'HPC'
    FYI                = 'POLYCARBONATE (PC) '
    KS                 = 0.2
    DENSITY            = 1190
    C_P                = 2.06
    DELTA              = 0.005
    BURN_AWAY    = .TRUE.
    TMPIGN             = 497
    BACKING            = 'INSULATED'
    HRRPUA             = 360
    RAMP_Q             = 'GAP8'
&RAMP ID='GAP8',T=0.0,F=0.0 /
&RAMP ID='GAP8',T=120,F=1 /
&RAMP ID='GAP8',T=180,F=0.28 /
&RAMP ID='GAP8',T=240,F=0.19 /
&RAMP ID='GAP8',T=360,F=0.17 /
&RAMP ID='GAP8',T=660,F=0.28 /
&RAMP ID='GAP8',T=720,F=0.22 /
&RAMP ID='GAP8',T=840,F=0.22 /
&RAMP ID='GAP8',T=1800,F=0 /
```

Material properties input parameters

```
************************************

&SURF ID     = 'CONCRETE'
    FYI          = 'Quintiere, Fire Behavior'
    RGB          = 0.66,0.66,0.66
    C_P          = 0.88
    DENSITY =2100
    KS           = 1.0
    DELTA     = 0.7 /

&SURF ID       = 'GLASS'
    FYI            = 'Quintiere, An Introduction to Fire Dynamics TABLE 2.1'
    RGB            = 1.0,1.0,0.75
    DELTA      = 0.003
    KS             = 0.76
    C_P            = 0.84
    DENSITY  = 2700
    BACKING = 'EXPOSED' /

&SURF ID               = 'STEEL'
    RGB                = 0.20,0.20,0.20
    C_DELTA_RHO = 20
    DELTA              = 0.005 /
```

Boundary condition (Tunnel ventilation fans operation mode)
****

Tunnel fan operation mode – normal to emergency for 0 to 2.9m/s scenario slip road
(select only one mode)

&RAMP ID='FAN',T=0.0,F=0.0 / Fans off at 0 seconds
&RAMP ID='FAN',T=300.0,F=0.0/ Fans start at 300 seconds
&RAMP ID='FAN',T=360.0,F=1.0/ Fans operating at emergency mode, full operating speed at 360 seconds
&RAMP ID='FAN',T=3600.0,F=1.0 / Fans operating at emergency mode, full operating speed at 3600 seconds

&SURF ID=' Airflow ',VEL=-2.9, RAMP_V='FAN'/ Supply 0 – 2.9 m/s airflow into tunnel
&VENT XB= XB=0,9.3,0,0,0.0,6,SURF_ID='Airflow'/ Air velocity varies with scenarios see Table 12.6
&VENT XB= 0,9.3,84,84,0.0,6, SURF_ID='OPEN'/

Tunnel fan operation mode – congestion to emergency for 5.6 to 2.9 m/s scenario slip road
(select only one mode)

RAMP ID='FAN',T=0.0,F=1.0 / Fans operating at congestion mode, full operating speed at 0 seconds
RAMP ID='FAN',T=300.0,F=1.0/ Fans operating at congestion mode, full operating speed at 300 seconds
RAMP ID='FAN',T=330.0,F=0.0/ Fans stop and start operating at emergency mode at 330 seconds
RAMP ID='FAN',T=390.0,F=0.88/ Fans operating at emergency mode, full operating speed at 390 seconds
RAMP ID='FAN',T=3600.0,F=0.88/ Fans operating at emergency mode, full operating speed at 3600 seconds

SURF ID='BOUNDARY CONDITION',VEL=-5.6, RAMP_V='FAN'/ Supply 5.6-2.9 m/s airflow into tunnel
VENT XB=0,9.3,0,0,0.0,6,SURF_ID='Airflow'/ Varies air velocity scenarios see Table 12.6
VENT XB=0,9.3,84,84,0.0,6, SURF_ID='OPEN'/

Walkway
****

&OBST XB=0,1.2,0,84,0,0.6,RGB=0.5,0.5,0.5,SURF_ID='CONCRETE'/ walkway
&OBST XB=8.1,9.3,0,84,0,0.6,RGB=0.5,0.5,0.5,SURF_ID='CONCRETE'/walkway

Simulated HGV truck
****

HEAT DETECTOR
&HEAT XYZ=4,23.9,2.16,RTI=100,ACTIVATION_TEMPERATURE=380,LABEL='HEAT1'/ Glass break
&HEAT XYZ=5.1,22.9,2.16,RTI=100,ACTIVATION_TEMPERATURE=380,LABEL='HEAT2'/Glass break
&HEAT XYZ=3.3,22.9,2.16,RTI=100,ACTIVATION_TEMPERATURE=380,LABEL='HEAT3'/Glass break
&HEAT XYZ=4.2,22.3,2.3,RTI=100,ACTIVATION_TEMPERATURE=380,LABEL='HEAT4'/ Glass break

&OBST XB=3,5.4,23.96,24.06,1.83,2.49,RGB=0,1,1,SURF_ID='GLASS',HEAT_REMOVE='HEAT1'/
Truck cabin front window
&OBST XB=5.3,5.4,22.65,22.95,1.83,2.49,RGB=0,1,1,SURF_ID='GLASS',HEAT_REMOVE='HEAT2'/
Truck cabin side window
&OBST XB=3,3.1,22.65,22.95,1.83,2.49,RGB=0,1,1,SURF_ID='GLASS',HEAT_REMOVE='HEAT3'/
Truck cabin side window
&OBST XB=3,5.4,23.96,24.06,2.49,2.8,RGB=0,0.4,0,SURF_ID='STEEL'/ Truck cabin
&OBST XB=3,5.4,23.66,23.96,2.49,2.8,RGB=0,0.4,0,SURF_ID='HABS'/ Truck cabin
&OBST XB=3,5.4,23.96,24.06,0.8,1.83,RGB=0,0.4,0,SURF_ID='STEEL'/ Truck cabin
&OBST XB=3,5.4,23.96,24.06,0.4,0.8,RGB=0,0.4,0,SURF_ID='HPC'/ Truck cabin
&OBST XB=3,5.4,22.35,24.06,2.7,2.8,RGB=0,0.4,0,SURF_ID='STEEL'/ Truck cabin
&OBST XB=3,5.4,22.35,22.45,2.49,2.8,RGB=0,0.4,0,SURF_ID='STEEL'/ Truck cabin
&OBST XB=3,3.9,22.35,22.45,2.04,2.49,RGB=0,0.4,0,SURF_ID='STEEL'/ Truck cabin

```
&OBST XB=4.5,5.4,22.35,22.45,2.04,2.49,RGB=0,0.4,0,SURF_ID='STEEL'/ Truck cabin
&OBST XB=3,5.4,22.35,22.45,1.2,2.04,RGB=0,0.4,0,SURF_ID='STEEL'/ Truck cabin
&OBST XB=3.9,4.5,22.35,22.45,2.04,2.49,RGB=0,1,1,SURF_ID='GLASS',HEAT_REMOVE='HEAT4'/
Truck cabin back window
&OBST XB=3,5.4,22.35,24.06,1.1,1.2,RGB=0,0.4,0,SURF_ID='STEEL'/ Truck cabin floor
&OBST XB=3.8,4.6,22.45,23.96,1.2,1.36,RGB=0.4,0.4,0.4,SURF_ID='HPP'/ Truck cabin internal
&OBST XB=3.8,4.6,22.45,23.3,1.36,1.66,RGB=0.4,0.4,0.4,SURF_ID='HPP'/ Truck cabin internal
&OBST XB=3.4,5.2,23.63,23.96,1.5,1.83,RGB=0.4,0.4,0.4,SURF_ID='HPP'/ Vehicle instrument panel
&OBST XB=4.6,5.1,23.15,22.45,1.5,1.72,RGB=0.1,0.1,0.1,SURF_ID='HPU'/ Vehicle seat
&OBST XB=4.6,5.1,22.45,22.65,1.72,2.4,RGB=0.1,0.1,0.1,SURF_ID='HPU'/ Vehicle seat
&OBST XB=4.6,5.1,23.15,22.45,1.5,1.2,RGB=0.4,0.4,0.4,SURF_ID='STEEL'/ Truck cabin
&OBST XB=3.8,3.3,23.15,22.45,1.5,1.72,RGB=0.1,0.1,0.1,SURF_ID='HPU'/ Vehicle seat support
&OBST XB=3.8,3.3,22.45,22.65,1.72,2.4,RGB=0.1,0.1,0.1,SURF_ID='HPU'/ Vehicle seat support
&OBST XB=3.8,3.3,23.15,22.45,1.5,1.2,RGB=0,0.4,0,SURF_ID='STEEL'/ Truck cabin
&OBST XB=3,3.1,23.26,24.06,0.4,1.2,RGB=0,0.4,0,SURF_ID='HPC'/ Truck cabin
&OBST XB=5.3,5.4,23.26,24.06,0.4,1.2,RGB=0,0.4,0,SURF_ID='HPC'/ Truck cabin
&OBST XB=5.3,5.4,22.35,24.06,1.2,1.83,RGB=0,0.4,0,SURF_ID6='HPP','STEEL','STEEL','STEEL',
'STEEL', 'STEEL'/ Vehicle door
&OBST XB=3,3.1,22.35,24.06,1.2,1.83,RGB=0,0.4,0,SURF_ID6='STEEL','HPP','STEEL','STEEL',
'STEEL','STEEL'/ Vehicle door
&OBST XB=5.3,5.4,23.76,24.06,1.83,2.79,RGB=0,0.4,0,SURF_ID='STEEL'/ Truck cabin
&OBST XB=3,3.1,23.76,24.06,1.83,2.79,RGB=0,0.4,0,SURF_ID='STEEL'/ Truck cabin
&OBST XB=5.3,5.4,22.65,22.35,1.83,2.79,RGB=0,0.4,0,SURF_ID='STEEL'/ Truck cabin
&OBST XB=3,3.1,22.65,22.35,1.83,2.79,RGB=0,0.4,0,SURF_ID='STEEL'/ Truck cabin
&OBST XB=5.3,5.4,22.65,23.76,2.49,2.79,RGB=0,0.4,0,SURF_ID='STEEL'/ Truck cabin
&OBST XB=3,3.1,22.65,23.76,2.49,2.79,RGB=0,0.4,0,SURF_ID='STEEL'/ Truck cabin
&OBST XB=4.7,5.4,20.7,22,0.3,1.0,RGB=0,0.4,0,SURF_ID='STEEL'/  Truck equipment
&OBST XB=4.9,5.4,23.36,23.46,0.4,1.0,RGB=0.2,0.2,0.2,SURF_ID='HPC'/ Truck mud guard
&OBST XB=4.9,5.4,23.36,22.06,0.9,1.0,RGB=0.2,0.2,0.2,SURF_ID='HPC'/ Truck mud guard
&OBST XB=4.9,5.4,22.07,22.06,0.4,1.0,RGB=0.2,0.2,0.2,SURF_ID='HPC'/ Truck mud guard
&OBST XB=5.1,5.4,22.2,23.2,0,1,RGB=0,0,0,SURF_ID6='STEEL','STEEL','HEPDM','HEPDM',
'HEPDM','HEPDM'/ Truck front wheel
&OBST XB=3,3.5,23.36,23.46,0.4,1.0,RGB=0.2,0.2,0.2,SURF_ID='HPC'/ Truck mud guard
&OBST XB=3,3.5,23.36,22.06,0.9,1.0,RGB=0.2,0.2,0.2,SURF_ID='HPC'/ Truck mud guard
&OBST XB=3,3.5,22.07,22.06,0.4,1.0,RGB=0.2,0.2,0.2,SURF_ID='HPC'/ Truck mud guard
&OBST XB=3,3.5,22.2,23.2,0,1,RGB=0,0,0,SURF_ID6='STEEL','STEEL','HEPDM','HEPDM',
'HEPDM','HEPDM'/ Truck front wheel
&OBST XB=3.4,5,22.6,22.9,0.36,0.72,RGB=0.5,0.5,0.5,SURF_ID='STEEL'/ Truck front axial
&OBST XB=4.9,5.4,17.86,17.96,0.4,1.0,RGB=0.2,0.2,0.2,SURF_ID='HPC'/ Truck mud guard
&OBST XB=4.9,5.4,16.56,17.86,0.9,1.0,RGB=0.2,0.2,0.2,SURF_ID='HPC'/ Truck mud guard
&OBST XB=4.9,5.4,16.57,16.56,0.4,1.0,RGB=0.2,0.2,0.2,SURF_ID='HPC'/ Truck mud guard
&OBST XB=5.1,5.4,16.7,17.7,0,1,RGB=0,0,0,SURF_ID6='STEEL','STEEL','HEPDM','HEPDM',
'HEPDM','HEPDM'/ Truck back wheel
&OBST XB=3,3.5,17.86,17.96,0.4,1.0,RGB=0.2,0.2,0.2,SURF_ID='HPC'/ Truck mud guard
&OBST XB=3,3.5,16.56,17.86,0.9,1.0,RGB=0.2,0.2,0.2,SURF_ID='HPC'/ Truck mud guard
&OBST XB=3,3.5,16.57,16.56,0.4,1.0,RGB=0.2,0.2,0.2,SURF_ID='HPC'/ Truck mud guard
&OBST XB=3,3.3,16.7,17.7,0,1,RGB=0,0,0,SURF_ID6='STEEL','STEEL','HEPDM','HEPDM',
'HEPDM','HEPDM'/ Truck back wheel
&OBST XB=3.4,5,17.1,17.4,0.36,0.72,RGB=0.5,0.5,0.5,SURF_ID='STEEL'/ Truck back axial
&OBST XB=3,5.4,14,23.76,1,1.1,RGB=0,0.4,0,SURF_ID='STEEL'/ Truck floor
&OBST XB=3,3.1,14,14.3,1.1,4.5,RGB=0.0,0.0,1,SURF_ID='STEEL'/ Cargo frame
&OBST XB=5.3,5.4,14,14.3,1.1,4.5,RGB=0.0,0.0,1,SURF_ID='STEEL'/ Cargo frame
&OBST XB=3,5.4,14,14.3,4.4,4.5,RGB=0.0,0.0,1,SURF_ID='STEEL'/ Cargo frame
&OBST XB=3,3.1,16,16.2,1.1,4.5,RGB=0.0,0.0,1,SURF_ID='STEEL'/ Cargo frame
&OBST XB=5.3,5.4,16,16.2,1.1,4.5,RGB=0.0,0.0,1,SURF_ID='STEEL'/ Cargo frame
&OBST XB=3,5.4,16,16.2,4.4,4.5,RGB=0.0,0.0,1,SURF_ID='STEEL'/ Cargo frame
&OBST XB=3,3.1,18,18.2,1.1,4.5,RGB=0.0,0.0,1,SURF_ID='STEEL'/ Cargo frame
&OBST XB=5.3,5.4,18,18.2,1.1,4.5,RGB=0.0,0.0,1,SURF_ID='STEEL'/ Cargo frame
&OBST XB=3,5.4,18,18.2,4.4,4.5,RGB=0.0,0.0,1,SURF_ID='STEEL'/ Cargo frame
&OBST XB=3,3.1,19,19.2,1.1,4.5,RGB=0.0,0.0,1,SURF_ID='STEEL'/ Cargo frame
```

```
&OBST XB=5.3,5.4,19,19.2,1.1,4.5,RGB=0.0,0.0,1,SURF_ID='STEEL'/ Cargo frame
&OBST XB=3,5.4,19,19.2,4.4,4.5,RGB=0.0,0.0,1,SURF_ID='STEEL'/ Cargo frame
&OBST XB=3,3.1,21,21.2,1.1,4.5,RGB=0.0,0.0,1,SURF_ID='STEEL'/ Cargo frame
&OBST XB=5.3,5.4,21,21.2,1.1,4.5,RGB=0.0,0.0,1,SURF_ID='STEEL'/ Cargo frame
&OBST XB=3,5.4,21,21.2,4.4,4.5,RGB=0.0,0.0,1,SURF_ID='STEEL'/ Cargo frame
&OBST XB=3,3.1,22,22.2,1.1,4.5,RGB=0.0,0.0,1,SURF_ID='STEEL'/ Cargo frame
&OBST XB=5.3,5.4,22,22.2,1.1,4.5,RGB=0.0,0.0,1,SURF_ID='STEEL'/ Cargo frame
&OBST XB=3,5.4,22,22.2,4.4,4.5,RGB=0.0,0.0,1,SURF_ID='STEEL'/ Cargo frame
```

Fuel cargo in HGV (wood and plastic pallets)

```
**********************************************

&OBST XB=3.1,5.15,14.3,22.05,1.1,1.4,RGB=0.8,0.6,0.4,SURF_IDS='HWOOD 1','HWOOD 1','HWOOD 1'/
&OBST XB=3.1,5.15,14.3,22.05,1.7,2,RGB=0.8,0.6,0.4,SURF_IDS='HPE','HWOOD 1','HWOOD 1'/
&OBST XB=3.1,5.15,14.3,22.05,2.3,2.6,RGB=0.8,0.6,0.4,SURF_IDS='HWOOD 1','HWOOD 1','HWOOD 1'/
&OBST XB=3.1,5.15,14.3,22.05,2.9,3.2,RGB=0.8,0.6,0.4,SURF_IDs='HPE','HPE','HWOOD 1'/
&OBST XB=3.1,5.15,14.3,22.05,3.5,3.95,RGB=0.8,0.6,0.4,SURF_IDS='HWOOD 2','HWOOD 2','HWOOD 2'/
```

Vehicles (Cars)

```
**********

&OBST XB=2.1,3.8,1.5,4,0.9,1.5,RGB=0,1.0,1.0,SURF_ID='STEEL'/  Upper part of vehicle 1
&OBST XB=2.1,3.8,1,5.5,0.3,0.9,RGB=0,1.0,1.0,SURF_ID='STEEL'/ Lower part of vehicle 1
&OBST XB=2.1,3.8,1.5,1.8,0.0,0.3,RGB=0.0,0.0,0.0/  Rear vehicle wheel
&OBST XB=2.1,3.8,4.8,5,0.0,0.3,RGB=0.0,0.0,0.0/  Front vehicle wheel
&HOLE XB=2.3,3.6,0.8,5.6,0,0.3/


&OBST XB=5.7,7.4,1.5,4,0.9,1.5,RGB=1.0,1.0,0.0,SURF_ID='STEEL'/ Upper part of vehicle 2
&OBST XB=5.7,7.4,1,5.5,0.3,0.9,RGB=1.0,1.0,0.0,SURF_ID='STEEL'/ Lower part of vehicle 2
&OBST XB=5.7,7.4,1.5,1.8,0.0,0.3,RGB=0.0,0.0,0.0/  Rear vehicle wheel
&OBST XB=5.7,7.4,4.8,5,0.0,0.3,RGB=0.0,0.0,0.0/  Front vehicle wheel
&HOLE XB=5.9,7.2,0.8,5.6,0,0.3/
```

Output from FDS

```
******************

&ISOF QUANTITY='MIXTURE_FRACTION',VALUE(1)=0.148, VALUE(2)=0.001/
&SLCF PBY=2, QUANTITY='TEMPERATURE', DTSAM=1/
&SLCF PBY=13, QUANTITY='TEMPERATURE', DTSAM=1/
&SLCF PBY=21, QUANTITY='TEMPERATURE', DTSAM=1/
&SLCF PBY=35, QUANTITY='TEMPERATURE', DTSAM=1/
&SLCF PBX=8, QUANTITY='TEMPERATURE', DTSAM=1/
&SLCF PBX=8, QUANTITY='VELOCITY',VECTOR=.TRUE./
```

APPENDIX P

Appendix P: Sample of FDS data file for simulating Runehamar tunnel using simplify cone curves (FDS 5.0.3)

Define name of output files

```
**************************

&HEAD CHID='Runehamar',TITLE='Runehamar Tunnel Fire Test 1'/
```

Define gird size and domain size single mesh

```
****************************************

Grid size for tunnel
------------------------

&MESH IJK=31,310,21, XB=0,9.3,0,93,0,6.3 / 0.3 grids model
```

Define simulation time

```
**********************

&TIME TWFIN=3600/ simulation time in second
```

Miscellaneous input parameters

```
*******************************

&MISC SURF_DEFAULT='CONCRETE',TMPA=20/
```

Reaction input parameter

```
***************************

&REAC ID='WOOD'
     FYI='Ritchie, et al., 5th IAFSS, C_3.4 H_6.2 O_2.5'
     SOOT_YIELD = 0.01
     C      = 3.4
     H      = 6.2
     O      = 2.5
     EPUMO2 = 11020. /
```

Ignition of fire
****

Size of ignition source

```
&SURF ID='fire',HRRPUA=380,RAMP_Q='INCfire' /
&RAMP ID='INCfire',T=0.0,F=1/
&RAMP ID='INCfire',T=3600,F=1/
```

Location of ignition source

```
&OBSTXB=3.9,4.2,11.9,12.2,1.1,1.4,RGB=255,0,0,SURF_ID6='INERT','INERT','INERT','INERT','INERT','fire'
/
&OBST XB=3.6,4.5,11.9,11.9,1.1,2,RGB=255,0,0,DEVC_ID='TIME 1'/ Tarpaulin cover burn off after 360s
&DEVC XYZ=3.6,12,1.2, ID='TIME 1', SETPOINT=360, QUANTITY='TIME',INITIAL_STATE=.TRUE./
```

Flammability parameter based on HRRPUA
****

```
&MATL ID                ='WOOD PALLETS 1.2 X 0.8_0.45A'
    SPECIFIC_HEAT    = 2.58
    DENSITY          = 600
    CONDUCTIVITY     = 0.12/

&SURF ID                          = 'WOOD PALLETS 1.2 X 0.8_0.45'
    MATL_ID                       = 'WOOD PALLETS 1.2 X 0.8_0.45A'
    FYI                           = 'PLYWOOD ordinary'
    THICKNESS                     = 0.109
    IGNITION_TEMPERATURE = 373
    BACKING                       = 'INSULATED'
    HRRPUA                        = 1730
    RAMP_Q                        = 'GAP1'
&RAMP ID='GAP1',T=   0.0,F=0 /
&RAMP ID='GAP1',T=  44.0,F=1/
&RAMP ID='GAP1',T=  536.0,F=1 /
&RAMP ID='GAP1',T=  580.0,F=0 /

&MATL ID                ='PLASTIC PALLETS 1.2 X 0.8A'
    SPECIFIC_HEAT    = 3
    DENSITY          = 956
    CONDUCTIVITY     = 0.64/

&SURF ID                          = 'PLASTIC PALLETS 1.2 X 0.8'
    MATL_ID                       = 'PLASTIC PALLETS 1.2 X 0.8A'
    FYI                           = 'PE PLASTIC'
    THICKNESS                     = 0.03
    IGNITION_TEMPERATURE = 323
    BACKING                       = 'INSULATED'
    HRRPUA                        = 2000
    RAMP_Q                        = 'GAP2'
&RAMP ID='GAP2',T=   0.0,F=0.0 /
&RAMP ID='GAP2',T=   60.0,F=1 /
&RAMP ID='GAP2',T=   740.0,F=1 /
&RAMP ID='GAP2',T=   800.0,F=0 /
```

```
&MATL ID                ='WOOD PALLETS 1.2 X 0.8A'
    SPECIFIC_HEAT    = 2.58
    DENSITY          = 600
    CONDUCTIVITY     = 0.12/


&SURF ID                          = 'WOOD PALLETS 1.2 X 0.8'
    MATL_ID                       = 'WOOD PALLETS 1.2 X 0.8A'
    FYI                           = 'PLYWOOD ordinary'
    THICKNESS                     = 0.077
    IGNITION_TEMPERATURE = 373
    BACKING                       = 'INSULATED'
    HRRPUA                        = 1140
    RAMP_Q                        = 'GAP3'
&RAMP ID='GAP3',T=   0.0,F=0 /
&RAMP ID='GAP3',T=  36.0,F=1 /
&RAMP ID='GAP3',T=  610.0,F=1 /
&RAMP ID='GAP3',T= 647,F=0 /


&MATL ID                ='WOOD PALLETS 1.2 X 1A'
    SPECIFIC_HEAT        = 2.58
    DENSITY              = 600
    CONDUCTIVITY         = 0.12/


&SURF ID                          = 'WOOD PALLETS 1.2 X 1'
    MATL_ID                       = 'WOOD PALLETS 1.2 X 1A'
    FYI                           = 'PLYWOOD ordinary'
    THICKNESS                     = 0.013
    IGNITION_TEMPERATURE = 373
    BACKING                       = 'INSULATED'
    HRRPUA                        = 150
    RAMP_Q                        = 'GAP4'
&RAMP ID='GAP4',T=   0.0,F=0 /
&RAMP ID='GAP4',T=  29.0,F=1 /
&RAMP ID='GAP4',T=  1621.0,F=1 /
&RAMP ID='GAP4',T=  1630.0,F=0 /
```

Material properties input parameters

```
************************************

&MATL ID         ='CONCRETE1'
    SPECIFIC_HEAT= 0.88
    DENSITY      = 2100.
    CONDUCTIVITY = 1.0/


&SURF ID      ='CONCRETE'
    MATL_ID  ='CONCRETE1'
    COLOR    = GRAY
    FYI      ='Quintiere, Fire Behaviour'
    THICKNESS= 0.7 /
```

```
&MATL ID          ='STEEL1'
    SPECIFIC_HEAT= 0.48
    DENSITY      = 8055.
    CONDUCTIVITY = 15.1/

&SURF ID      ='STEEL'
    MATL_ID  ='STEEL1'
    FYI      ='AISI 302 STEELS FUNDAMENTAL OF HEAT AND MASS TRANSFER'
    THICKNESS= 0.005 /

&MATL ID                ='FIRE BOARD1'
    SPECIFIC_HEAT       = 0.48
    DENSITY             = 1440
    CONDUCTIVITY        = 0.48/


&SURF ID               = 'FIRE BOARD'
    MATL_ID                = 'FIRE BOARD1'
    FYI             = 'FIRE BOARD1'
    THICKNESS        = 0.013
    IGNITION_TEMPERATURE = 400
    BACKING                = 'INSULATED'
    HRRPUA           = 100
    RAMP_Q           = 'GB'
&RAMP ID='GB',T= 0.0,F=0.0 /
&RAMP ID='GB',T= 1.0,F=0.5 /
&RAMP ID='GB',T= 2.0,F=1.0 /
&RAMP ID='GB',T=10.0,F=1.0 /
&RAMP ID='GB',T=20.0,F=0.0 /
&RAMP ID='GB',T=30.0,F=0.0 /
```

Boundary condition (Ventilation in tunnel)

```
*****************************************

Tunnel fan operation at 3 m/s
-------------------------------------
&RAMP ID='FAN',T=0.0,F=1.0 / Fan operate at 3 m/s at time 0 seconds
&RAMP ID='FAN',T=3600,F=1.0 / Fan operate at 3 m/s at time 3600 seconds

&SURF ID='BOUNDARY CONDITION',VEL=-3, RAMP_V='FAN'/ 3 m/s airflow into tunnel
&VENT XB= 0,9.3,0,0,0.0,6.3, SURF_ID='BOUNDARY CONDITION'/
&VENT XB= 0,9.3,93,93,0.0,6.3, SURF_ID='OPEN'/
```

Tunnel geometry
****

TUNNEL GEOMETRY
****
&OBST XB=0.0,0.2,0,93,0,6.4,RGB=128,128,128,SAWTOOTH=.FALSE.,SURF_ID='CONCRETE'/ &OBST XB=0.2,0.4,0,93,3.2,6.4,RGB=128,128,128,SAWTOOTH=.FALSE.,SURF_ID='CONCRETE'/ &OBST XB=0.4,0.6,0,93,3.8,6.4,RGB=128,128,128,SAWTOOTH=.FALSE.,SURF_ID='CONCRETE'/ &OBST XB=0.6,0.8,0,93,4.4,6.4,RGB=128,128,128,SAWTOOTH=.FALSE.,SURF_ID='CONCRETE'/ &OBST XB=0.8,1.0,0,93,4.8,6.4,RGB=128,128,128,SAWTOOTH=.FALSE.,SURF_ID='CONCRETE'/ &OBST XB=1,1.2,0,93,5.2,6.4,RGB=128,128,128,SAWTOOTH=.FALSE.,SURF_ID='CONCRETE'/ &OBST XB=1.2,1.4,0,93,5.4,6.4,RGB=128,128,128,SAWTOOTH=.FALSE.,SURF_ID='CONCRETE'/ &OBST XB=1.4,1.6,0,93,5.6,6.4,RGB=128,128,128,SAWTOOTH=.FALSE.,SURF_ID='CONCRETE'/
&OBST XB=1.6,1.8,0,93,5.8,6.4,RGB=128,128,128,SAWTOOTH=.FALSE.,SURF_ID='CONCRETE'/ &OBST XB=1.8,7.4,0,93,6.0,6.4,RGB=128,128,128,SAWTOOTH=.FALSE.,SURF_ID='CONCRETE'/
&OBST XB=7.4,7.6,0,11,5.8,6.4,RGB=128,128,128,SAWTOOTH=.FALSE.,SURF_ID='CONCRETE'/ &OBST XB=7.6,7.8,0,11,5.6,6.4,RGB=128,128,128,SAWTOOTH=.FALSE.,SURF_ID='CONCRETE'/ &OBST XB=7.8,8.0,0,11,5.4,6.4,RGB=128,128,128,SAWTOOTH=.FALSE.,SURF_ID='CONCRETE'/ &OBST XB=8.0,8.2,0,11,5.2,6.4,RGB=128,128,128,SAWTOOTH=.FALSE.,SURF_ID='CONCRETE'/ &OBST XB=8.2,8.4,0,11,4.8,6.4,RGB=128,128,128,SAWTOOTH=.FALSE.,SURF_ID='CONCRETE'/ &OBST XB=8.4,8.6,0,11,4.4,6.4,RGB=128,128,128,SAWTOOTH=.FALSE.,SURF_ID='CONCRETE'/ &OBST XB=8.6,8.8,0,11,3.8,6.4,RGB=128,128,128,SAWTOOTH=.FALSE.,SURF_ID='CONCRETE'/ &OBST XB=8.8,9,0,11,3.2,6.4,RGB=128,128,128,SAWTOOTH=.FALSE.,SURF_ID='CONCRETE'/
&OBST XB=9.0,9.4,0,11,0,6.4,RGB=128,128,128,SAWTOOTH=.FALSE.,SURF_ID='CONCRETE'/
&OBST XB=7.4,7.6,11,93,5.8,6.4,COLOR=INVISIBLE,SAWTOOTH=.FALSE.,SURF_ID='CONCRETE'/
&OBST XB=7.6,7.8,11,93,5.6,6.4,COLOR=INVISIBLE,SAWTOOTH=.FALSE.,SURF_ID='CONCRETE'/
&OBST XB=7.8,8.0,11,93,5.4,6.4,COLOR=INVISIBLE,SAWTOOTH=.FALSE.,SURF_ID='CONCRETE'/
&OBST XB=8.0,8.2,11,93,5.2,6.4,COLOR=INVISIBLE,SAWTOOTH=.FALSE.,SURF_ID='CONCRETE'/
&OBST XB=8.2,8.4,11,93,4.8,6.4,COLOR=INVISIBLE,SAWTOOTH=.FALSE.,SURF_ID='CONCRETE'/
&OBST XB=8.4,8.6,11,93,4.4,6.4,COLOR=INVISIBLE,SAWTOOTH=.FALSE.,SURF_ID='CONCRETE'/
&OBST XB=8.6,8.8,11,93,3.8,6.4,COLOR=INVISIBLE,SAWTOOTH=.FALSE.,SURF_ID='CONCRETE'/
&OBST XB=8.8,9,11,93,3.2,6.4,COLOR=INVISIBLE,SAWTOOTH=.FALSE.,SURF_ID='CONCRETE'/
&OBST XB=9.0,9.4,11,93,0,6.4,COLOR=INVISIBLE,SAWTOOTH=.FALSE.,SURF_ID='CONCRETE'/

FIRE BOARD
****
&OBST XB=0.7,1,0,93,0,3.4,RGB=255,255,255,SURF_ID='FIRE BOARD'/
&OBST XB=0.7,1.2,0,93,3.4,3.6,RGB=255,255,255,SURF_ID='FIRE BOARD'/
&OBST XB=1.0,1.4,0,93,3.6,4,RGB=255,255,255,SURF_ID='FIRE BOARD'/
&OBST XB=1.4,1.6,0,93,3.8,4.2,RGB=255,255,255,SURF_ID='FIRE BOARD'/
&OBST XB=1.6,1.8,0,93,4.0,4.4,RGB=255,255,255,SURF_ID='FIRE BOARD'/
&OBST XB=1.8,2.0,0,93,4.2,4.6,RGB=255,255,255,SURF_ID='FIRE BOARD'/
&OBST XB=2.0,2.2,0,93,4.4,4.8,RGB=255,255,255,SURF_ID='FIRE BOARD'/
&OBST XB=2.2,2.4,0,93,4.6,5,RGB=255,255,255,SURF_ID='FIRE BOARD'/
&OBST XB=2.4,2.6,0,93,4.8,5.2,RGB=255,255,255,SURF_ID='FIRE BOARD'/
&OBST XB=2.6,5.6,0,93,5,5.3,RGB=255,255,255,SURF_ID='FIRE BOARD'/
&OBST XB=5.6,6.0,0,11,4.8,5.2,RGB=255,255,255,SURF_ID='FIRE BOARD'/
&OBST XB=6.0,6.4,0,11,4.6,5,RGB=255,255,255,SURF_ID='FIRE BOARD'/
&OBST XB=6.4,6.8,0,11,4.4,4.8,RGB=255,255,255,SURF_ID='FIRE BOARD'/
&OBST XB=6.8,7.2,0,11,4.2,4.6,RGB=255,255,255,SURF_ID='FIRE BOARD'/
&OBST XB=7.2,7.6,0,11,4.0,4.4,RGB=255,255,255,SURF_ID='FIRE BOARD'/
&OBST XB=7.6,8.0,0,11,3.8,4.2,RGB=255,255,255,SURF_ID='FIRE BOARD'/
&OBST XB=7.7,8.0,0,11,0,4,RGB=255,255,255,SURF_ID='FIRE BOARD'/
&OBST XB=5.6,6.0,11,93,4.8,5.2,RGB=255,255,255,SURF_ID='FIRE BOARD'/
&OBST XB=6.0,6.4,11,93,4.6,5,RGB=255,255,255,SURF_ID='FIRE BOARD'/
&OBST XB=6.4,6.8,11,93,4.4,4.8,RGB=255,255,255,SURF_ID='FIRE BOARD'/
&OBST XB=6.8,7.2,11,93,4.2,4.6,RGB=255,255,255,SURF_ID='FIRE BOARD'/
&OBST XB=7.2,7.6,11,93,4.0,4.4,RGB=255,255,255,SURF_ID='FIRE BOARD'/
&OBST XB=7.6,8.0,11,93,3.8,4.2,RGB=255,255,255,SURF_ID='FIRE BOARD'/
&OBST XB=7.7,8.0,11,93,0,4,RGB=255,255,255,SURF_ID='FIRE BOARD'/

Simulated truck frame
****

```
&OBST XB=2.6,5.5,12,22.55,1,1.1,RGB=165,42,42/TRUCK FLOOR
&OBST XB=2.6,2.7,12,12.2,0,4.5,RGB=0,0,255,SURF_ID='STEEL'/TRUCK FRAME
&OBST XB=5.4,5.5,12,12.2,0,4.5,RGB=0,0,255,SURF_ID='STEEL'/TRUCK FRAME
&OBST XB=2.6,5.5,12,12.2,4.4,4.5,RGB=0,0,255,SURF_ID='STEEL'/TRUCK FRAME
&OBST XB=2.6,2.7,13,13.2,0,4.5,RGB=0,0,255,SURF_ID='STEEL'/TRUCK FRAME
&OBST XB=5.4,5.5,13,13.2,0,4.5,RGB=0,0,255,SURF_ID='STEEL'/TRUCK FRAME
&OBST XB=2.6,5.5,13,13.2,4.4,4.5,RGB=0,0,255,SURF_ID='STEEL'/TRUCK FRAME
&OBST XB=2.6,2.7,13,13.2,0,4.5,RGB=0,0,255,SURF_ID='STEEL'/TRUCK FRAME
&OBST XB=5.4,5.5,13,13.2,0,4.5,RGB=0,0,255,SURF_ID='STEEL'/TRUCK FRAME
&OBST XB=2.6,5.5,13,13.2,4.4,4.5,RGB=0,0,255,SURF_ID='STEEL'/TRUCK FRAME
&OBST XB=2.6,2.7,16,16.2,0,4.5,RGB=0,0,255,SURF_ID='STEEL'/TRUCK FRAME
&OBST XB=5.4,5.5,16,16.2,0,4.5,RGB=0,0,255,SURF_ID='STEEL'/TRUCK FRAME
&OBST XB=2.6,5.5,16,16.2,4.4,4.5,RGB=0,0,255,SURF_ID='STEEL'/TRUCK FRAME
&OBST XB=2.6,2.7,18,18.2,0,4.5,RGB=0,0,255,SURF_ID='STEEL'/TRUCK FRAME
&OBST XB=5.4,5.5,18,18.2,0,4.5,RGB=0,0,255,SURF_ID='STEEL'/TRUCK FRAME
&OBST XB=2.6,5.5,18,18.2,4.4,4.5,RGB=0,0,255,SURF_ID='STEEL'/TRUCK FRAME
&OBST XB=2.6,2.7,19,19.2,0,4.5,RGB=0,0,255,SURF_ID='STEEL'/TRUCK FRAME
&OBST XB=5.4,5.5,19,19.2,0,4.5,RGB=0,0,255,SURF_ID='STEEL'/TRUCK FRAME
&OBST XB=2.6,5.5,19,19.2,4.4,4.5,RGB=0,0,255,SURF_ID='STEEL'/TRUCK FRAME
&OBST XB=2.6,2.7,21,21.2,0,4.5,RGB=0,0,255,SURF_ID='STEEL'/TRUCK FRAME
&OBST XB=5.4,5.5,21,21.2,0,4.5,RGB=0,0,255,SURF_ID='STEEL'/TRUCK FRAME
&OBST XB=2.6,5.5,21,21.2,4.4,4.5,RGB=0,0,255,SURF_ID='STEEL'/TRUCK FRAME
&OBST XB=2.6,2.7,22,22.2,0,4.5,RGB=0,0,255,SURF_ID='STEEL'/TRUCK FRAME
&OBST XB=5.4,5.5,22,22.2,0,4.5,RGB=0,0,255,SURF_ID='STEEL'/TRUCK FRAME
&OBST XB=2.6,5.5,22,22.2,4.4,4.5,RGB=0,0,255,SURF_ID='STEEL'/TRUCK FRAME
```

Fuel load (wood and plastic pallets)
****

```
&OBST XB=2.7,5.4,12.2,22.1,3.5,3.95,RGB=160,82,45,SURF_IDS='WOOD PALLETS 1.2 X
0.8_0.45','WOOD PALLETS 1.2 X 0.8_0.45','WOOD PALLETS 1.2 X 0.8_0.45'/ Layer 1
&OBST XB=2.7,5.4,12.2,22.1,2.9,3.2,RGB=160,82,45,SURF_IDs='PLASTIC PALLETS 1.2 X 0.8','PLASTIC
PALLETS 1.2 X 0.8','WOOD PALLETS 1.2 X 0.8'/ Layer 2
&OBST XB=2.7,5.4,12.2,22.1,2.3,2.6,RGB=160,82,45,SURF_IDS='WOOD PALLETS 1.2 X 0.8','WOOD
PALLETS 1.2 X 0.8','WOOD PALLETS 1.2 X 0.8'/ Layer 3
&OBST XB=2.7,5.4,12.2,22.1,1.7,2,RGB=160,82,45,SURF_IDS='PLASTIC PALLETS 1.2 X 0.8','WOOD
PALLETS 1.2 X 0.8','WOOD PALLETS 1.2 X 0.8'/ Layer 4
&OBST XB=2.7,5.4,12.2,22.1,1.1,1.4,RGB=160,82,45,SURF_IDS='WOOD PALLETS 1.2 X 1','WOOD
PALLETS 1.2 X 1','WOOD PALLETS 1.2 X 1'/ Layer 5


&OBST XB=2.7,5.4,12.2,22.1,3.5,3.95,RGB=0.8,0.6,0.4,SURF_IDS='WOOD PALLETS 1.2 X
0.8_0.45','WOOD PALLETS 1.2 X 0.8_0.45','WOOD PALLETS 1.2 X 0.8_0.45'/ Layer 1
&OBST XB=2.7,5.4,12.2,22.1,2.9,3.2,RGB=0.8,0.6,0.4,SURF_IDs='PLASTIC PALLETS 1.2 X 0.8','PLASTIC
PALLETS 1.2 X 0.8','WOOD PALLETS 1.2 X 0.8'/ Layer 2
&OBST XB=2.7,5.4,12.2,22.1,2.3,2.6,RGB=0.8,0.6,0.4,SURF_IDS='WOOD PALLETS 1.2 X 0.8','WOOD
PALLETS 1.2 X 0.8','WOOD PALLETS 1.2 X 0.8'/ Layer 3
&OBST XB=2.7,5.4,12.2,22.1,1.7,2,RGB=0.8,0.6,0.4,SURF_IDS='PLASTIC PALLETS 1.2 X 0.8','WOOD
PALLETS 1.2 X 0.8','WOOD PALLETS 1.2 X 0.8'/ Layer 4
&OBST XB=2.7,5.4,12.2,22.1,1.1,1.4,RGB=0.8,0.6,0.4,SURF_IDS='WOOD PALLETS 1.2 X 1','WOOD
PALLETS 1.2 X 1','WOOD PALLETS 1.2 X 1'/ Layer 5
```

Output from FDS
****

```
&ISOF QUANTITY='MIXTURE_FRACTION',VALUE(1)=0.149, VALUE(2)=0.001/
&SLCF PBY=2, QUANTITY='TEMPERATURE'/
&SLCF PBY=13, QUANTITY='TEMPERATURE'/
&SLCF PBY=21, QUANTITY='TEMPERATURE'/
&SLCF PBY=35, QUANTITY='TEMPERATURE'/
&SLCF PBX=8, QUANTITY='TEMPERATURE'/
&SLCF PBX=8, QUANTITY='VELOCITY',VECTOR=.TRUE./


&TAIL /
```